COURS ENSTA M306

Option: Dynamique des Fluides et Modélisation Numérique

Modélisation Physique des Ecoulements Turbulents Incompressibles



Marie Farge

LMD-CNRS, ENS, Paris
CMLA, ENS, Cachan

1. INTRODUCTION ET RAPPELS

Définition et historique de la turbulence

Transition laminaire - turbulent et nombre de Reynolds

Equations d'Euler et de Navier-Stokes

Lois de conservation

Référentiels Eulérien et Lagrangien

Théorèmes d'Helmholtz et de Kelvin

Effets de paroi et couches limites

Moyennes, distributions de probabilité et fonctions de corrélation

Transformée de Fourier et transformée en ondelettes

Fonction de densité de probabilité

Moments statistiques

Fonctions de structure

TURBULENT FLOWS

Fluids — mobile and deformable media / $\ell \gg \delta$ molecule mean free path
$\Rightarrow$ continuous fields

Turbulent flows — Turbo, inis: vortices
Turba, ae: crowd
$\Rightarrow$ crowd of vortices
Rotational motions

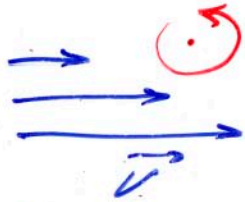

$$\vec{\omega} = \vec{\nabla} \times \vec{v}$$

If incompressible fluid no divergent motions

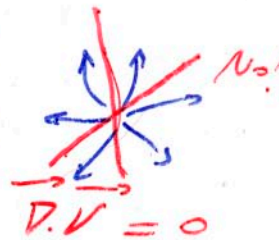

Reynolds number $Re \gg 1$

$$Reynolds = \frac{\text{N.L. Advection}}{\text{L. Dissipation}} = \frac{U^2}{L} \Big/ \frac{\nu U}{L^2} = \frac{UL}{\nu}$$

$$\frac{\partial \vec{\omega}}{\partial t} + \underbrace{(\vec{v}\cdot\vec{\nabla})\vec{\omega} - (\vec{\omega}\cdot\vec{\nabla})\vec{v}}_{\text{N.L. Advection}} - \underbrace{\nu \nabla^2 \vec{\omega}}_{\text{Dissipation}} = \vec{\nabla} \times \vec{F}$$

$$Re = \frac{UL}{\nu} = \frac{U}{L}\,\frac{L^2}{\nu} = \frac{\text{temps dissipation}}{\text{temps advection}}$$

$$= \frac{U}{\nu} L = \frac{\text{échelle d'advection}}{\text{échelle de dissipation}}$$

PROPERTIES OF TURBULENT FLOWS

LAMINAR FLOWS (lamina, ae: thin sheet)

- Dissipative due to viscosity

Viscosity is a property of fluids which generates frictional forces reacting on the fluid in motion and which, in absence of external forces, leads it to rest

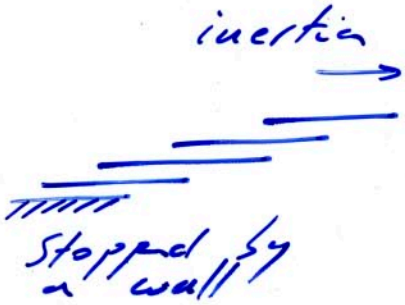

- Non diffusive, transport by (molecular) forces, microscopic fluctuations



- Non chaotic, thanks to their evolution is predictible

linear dynamics

TURBULENT FLOWS (turbo, inis: gyroscope)

- Dissipative due to "turbulent viscosity"

"turbulent viscosity" is a property of flows, not of fluid, due to the instabilities which develop during their motion

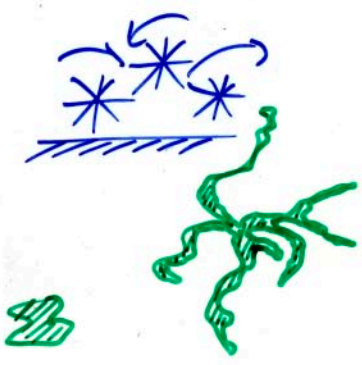

- Diffusive, transport by macroscopic fluctuations
- Chaotic ⇒ unpredictible

Nonlinear dynamics

UNPREDICTABICITY

1. Laminar flow — Perturbations are damped by viscous effects

$Re \sim 1$

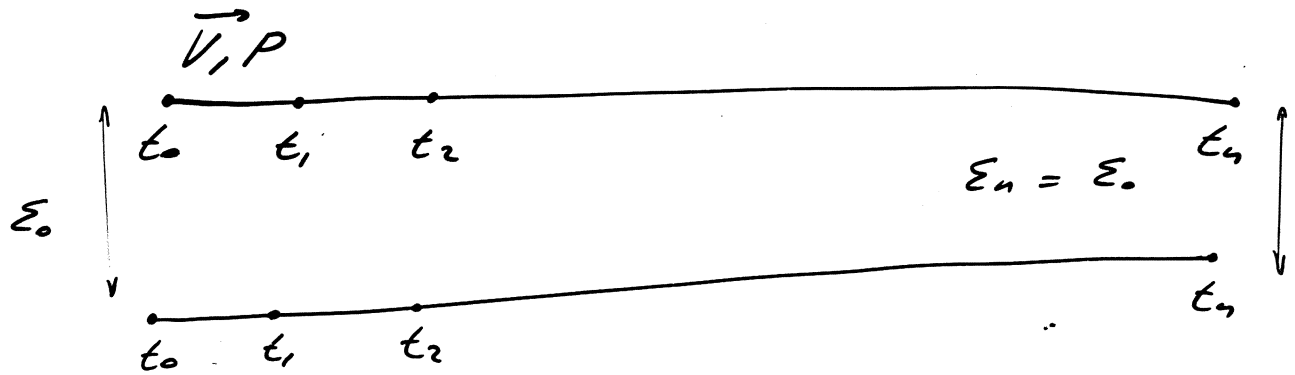

$(\vec{V}, P) \pm \varepsilon$

Non sensitivity to initial conditions
$\Rightarrow$ the flow dynamics is predictible

2. Turbulent flow — Perturbations are amplified by non linear effects

$Re \gg 1$

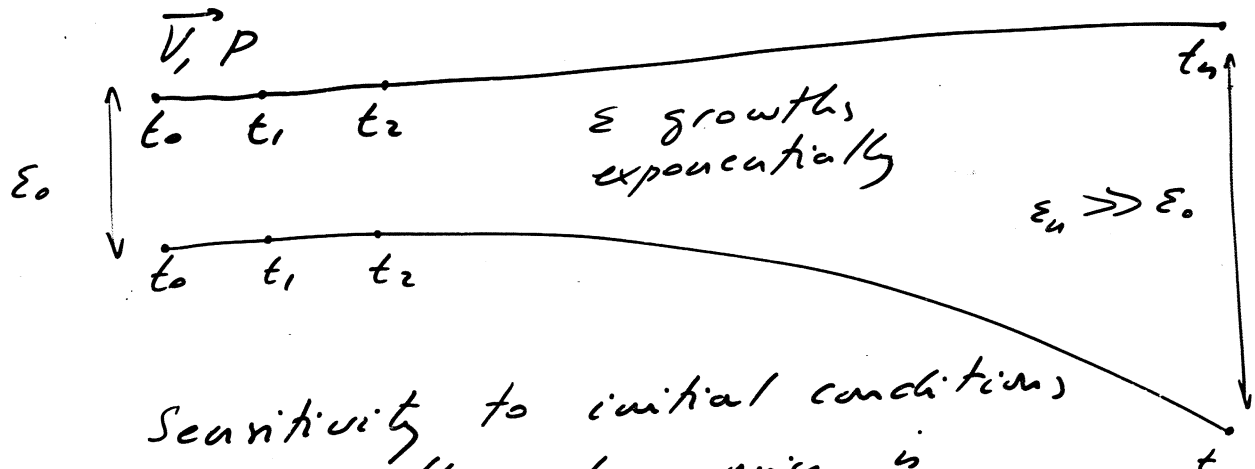

Sensitivity to initial conditions
$\Rightarrow$ the flow dynamics is unpredictible (Ex. meteorology)

EQUATION FONDAMENTALE DE LA MECANIQUE DES FLUIDES

Fluide → soit état liquide ⇒ incompressible $\nabla \cdot \vec{V} = 0$,

→ soit état gazeux ⇒ compressible $\nabla \cdot \vec{V} \neq 0$ équation d'état

Equation de Navier-Stokes :

$$\frac{\partial \vec{V}}{\partial t} + \vec{V} \cdot \nabla \vec{V} + \frac{1}{\rho} \nabla P = \nu \nabla^2 \vec{V} + \vec{F}$$

Conditions initiales

conditions aux limites

si pas Equation d'Euler

$$\frac{\partial \vec{\omega}}{\partial t} + (\vec{V} \cdot \nabla)\vec{\omega} - (\vec{\omega} \cdot \nabla)\vec{V} = \nu \nabla^2 \omega + \nabla \times \vec{F}$$

$$\vec{\omega} = \nabla^2 \vec{\psi} \qquad \vec{\psi} \,/\, \vec{V} = \nabla \times \vec{\psi}$$

→ Biot-Savart $\vec{V} = \nabla \times \nabla^{-2} \vec{\omega}$

cas 2D :  $\Rightarrow (\vec{\omega} \cdot \nabla)\vec{V} = 0$

$$\frac{\partial \omega}{\partial t} + (\vec{V} \cdot \nabla)\omega = \nu \nabla^2 \omega + \nabla \times F$$

Advection non linéaire = diffusion + Forçage

ETIREMENT DES TUBES DE VORTICITE PAR LES GRADIENTS DE VITESSE

$(\vec{\omega} \cdot \nabla)\vec{V}$

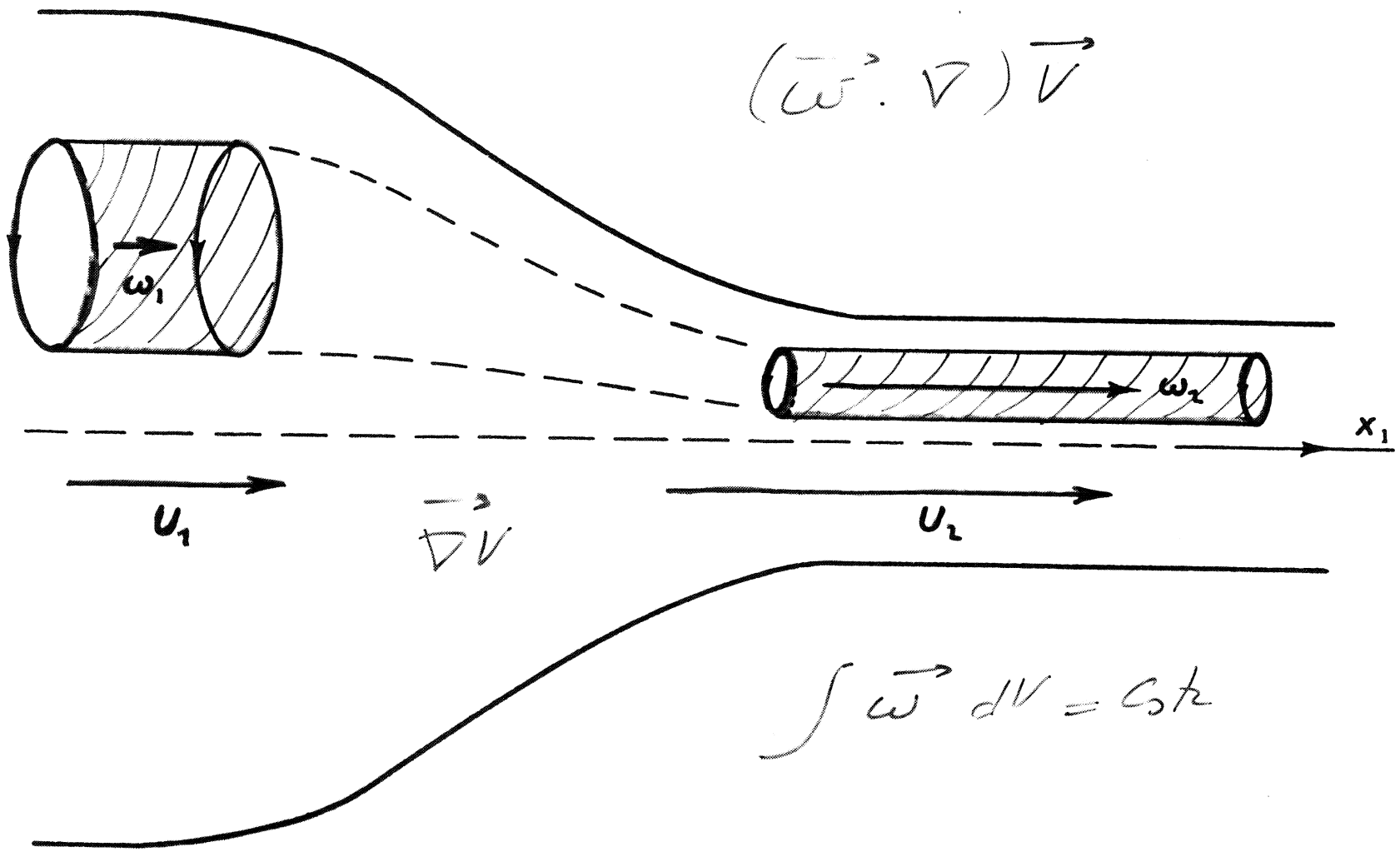

$\int \vec{\omega}\, dV = Cte$

ÉQUATIONS DE NAVIER-STOKES EN TERME DE VECTEUR DE LAMB

Vecteur de Lamb :

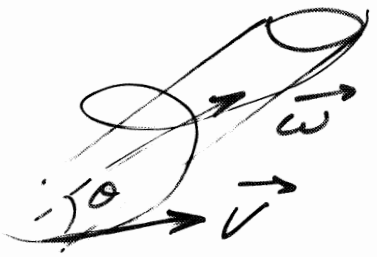

$$\vec{\ell} = \vec{\omega} \times \vec{V}$$

$$\Rightarrow |\vec{\ell}_{max}| \text{ si } \vec{\omega} \perp \vec{V}$$

$$|\vec{\ell}_{min}| \text{ si } \vec{\omega} \parallel \vec{V}$$

Hélicité :

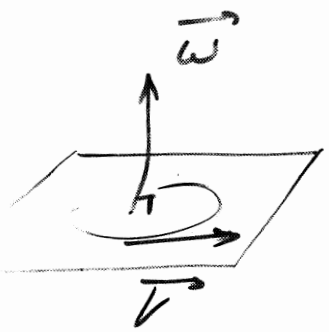

$$h = \frac{\vec{\omega} \cdot \vec{V}}{|\vec{\omega}||\vec{V}|} = \cos\theta$$

$$\Rightarrow h = 0 \text{ si } \vec{\omega} \perp \vec{V}$$

$$h_{max} \text{ si } \vec{\omega} \parallel \vec{V}$$

Navier-Stokes :

$$\frac{\partial \vec{V}}{\partial t} + \vec{\ell} = -\nabla\left(P + \frac{\vec{V}^2}{2}\right) + \nu \nabla^2 \vec{V}$$

$$\nabla \cdot \vec{V} = 0$$

ou encore

$$\frac{\partial \vec{\omega}}{\partial t} + \nabla \times \vec{\ell} = \nu \nabla^2 \vec{\omega}$$

$$\vec{V} = \nabla \times \nabla^{-2} \vec{\omega}$$

DEFINITIONS OF TURBULENCE

George K. BATCHELOR, 1953
The theory of homogeneous turbulence, Cambridge University Press

It is a well-known fact that under certain conditions, which normally amount to a requirement that the kinematic viscosity ν be sufficiently small, some of the motions are such that the velocity at any given time and position in the fluid is not found to be the same when it is measured several times under seemingly identical conditions. In these motions the velocity takes random values which are not determined by the obstacles, or controllable, or 'macroscopic', data of the flow, although we believe that the average properties of the motion are determined uniquely by the data. Fluctuating motions of this kind are said to be turbulent.

Peter BRADSHAW, 1972
An introduction to turbulence
and its measurement
Pergamon

Turbulence is a three-dimensional time-dependent motion in which vortex stretching causes velocity fluctuations to spread to all wavelengths between a minimum determined by viscous forces and a maximum determined by the boundary conditions of the flow. It is the usual state of fluid motion except at low Reynolds numbers.

Alexandre J. CHORIN, 1975
Lectures on turbulence theory
Publish or Perish, Berkeley

The distinguishing feature of turbulent flow is that its velocity field appears to be random and varies unpredictably. The flow, however, satisfies a set of differential equations, the Navier-Stokes equations, which are not random. This contrast is the source of much of what is interesting in turbulence theory.

Hans W. LIEPMANN, 1979
The rise and fall of ideas
in turbulence,
American Scientist, 67, p. 221

Turbulence can be defined by
a statement of impotence
reminiscent of the second laws
of thermodynamics: flows at
a sufficiently high Reynolds
number cannot be calculated
to rest in a steady fashion.
The calculation always produces
vorticity, and the resulting
vortex interactions are apparently
so sensitive to the initial condi-
tions that the resulting flow
pattern changes in time and
usually in stochastic fashion.

Philip G. SAFFMAN, 1978
Problems and progress in
the theory of turbulence
in: Structure and mechanics
of turbulence I, ed. H. Fiedler,
Springer, p. 276

We should not altogether
neglect the possibility that
there is no such thing as
'turbulence'. That is to say,
it is not meaningful to
talk of the properties of
a turbulent flow indepen-
dently of the physical situa-
tion in which it arises.
In searching for a theory of
turbulence, perhaps we are
looking for a chimera.

Richard P. FEYNMAN, 1964
The Feynman Lectures on physics I
Addison-Wesley, p. 41

The next great era of awaking
of human intellect may well
produce a method of understanding
the qualitative content of equations.
Today we cannot see that the
wake flow equations contain such
thing as the Barber pole structure of
turbulence that one sees between
rotating cylinders. Today we cannot
see whether Schrödinger's equation
contains frogs, musical composers,
or morality — or whether it does
not. We cannot say whether
something beyond like God is needed,
or not. And we can all hold
strong opinions either way.

Sir Horace LAMB

quoted by Sydney Goldstein, 1969,
Annual Reviews of Fluid Mech.,
Vol. 1, p. 23

I am an old man now,
and when I die and go to
Heaven there are two matters
on which I hope enlightenment.
One is quantum electrodynamics
and the other is turbulence of
fluids. About the former I
am rather optimistic.

HISTOIRE DE LA MECANIQUE DES FLUIDES

Indépendamment Navier en 1822 et Poisson en 1826, à partir de considérations contestables sur les actions des molécules du fluide les unes sur les autres obtiennent les équations de Navier-Stokes.

Sir Gabriel Stokes en 1845 et Adhémar Barré de Saint-Venant en 1846 ont montré qu'elles pouvaient être basées sur une seule hypothèse physique très simple : le tenseur des forces de frottement visqueux est proportionnel au tenseur des vitesses de déformation du fluide.

Bien que l'échec principal des solutions des équations de Navier-Stokes soit toujours d'actualité par la présence de termes non linéaires, on trouve tout de suite des solutions élémentaires pour quelques cas simples, par exemple l'écoulement permanent dans un tuyau cylindrique. Or la comparaison avec les mesures très approximatives faites par les ingénieurs hydrauliciens des 17e et 18e siècles donnaient des ports de choux

mesurées 10 à 100 fois
plus grandes que celles prévues.
La situation se compliqua encore lorsque
Henri Poiseuille en 1842 trouva
un accord exaltant (au 1/1000 près)
en opérant sur des tubes capillaires
d'un diamètre de 0.01 à 0.1 mm).

Pour résumer l'ambiance à l'époque:
'La question se complique et s'obscurcit donc davantage à mesure que des
expériences plus nombreuses et plus
précises paraissent devoir y jeter
un plus grand lumière' Darcy et Bazin
1865
ou encore:
'L'hydraulique est une désespérante
énigme' Saint-Venant 1872

C'est Jean Boussinesq en 1872 qui
introduisit un peu d'ordre dans ce
chaos en distinguant deux régimes
d'écoulement bien différents: le
premier 'bien continu' et le second
'tumultueux et tourbillonnant'.

C'est Osborne Reynolds en 1883
qui visualisa ces deux types d'écoulement 'direct' et 'sinueux' et montra
que leur réalisation dépendait du Re.

BIBLIOGRAPHIE
HISTOIRE de la Mécanique des fluides

C. L. M. H. Navier 1822
Mémoire sur les Lois du mouvement des fluides
Mem. Acad. Sci., VI

S. D. Poisson 1829
Mémoire sur les Equations générales de l'Equilibre et des Mouvements des Corps solides élastiques et des Fluides
Journal de l'Ecole Polytechnique, XIII

G. G. Stokes 1845
On the Theories of the Internal Friction of Fluids in Motion
Cambridge Transactions, VIII

Darcy et H. Bazin 1865
Recherches d'Hydraulique
Mem. Acad. Sci., XIX

A. Barré de Saint Venant 1872
Sur l'Hydrodynamique des cours d'eau
Compte-Rendus Acad. Sci. Paris, 74

J. Boussinesq 1872
Essai sur la théorie des eaux courantes

Rec. Savants Etrangers
Acad. Sciences Paris, 26

O. Reynolds 1883
An experimental investigation of the circumstances which determine whether the motion of water shall be direct or sinuous, and the law of resistance in parallel channels
Phil. Trans. Roy. Soc. London, 174, 935-982

O. Reynolds 1894
On the dynamical theory of incompressible viscous fluids and the determination of the criterion
Phil. Trans. Roy. Soc. London, 186, 123-161

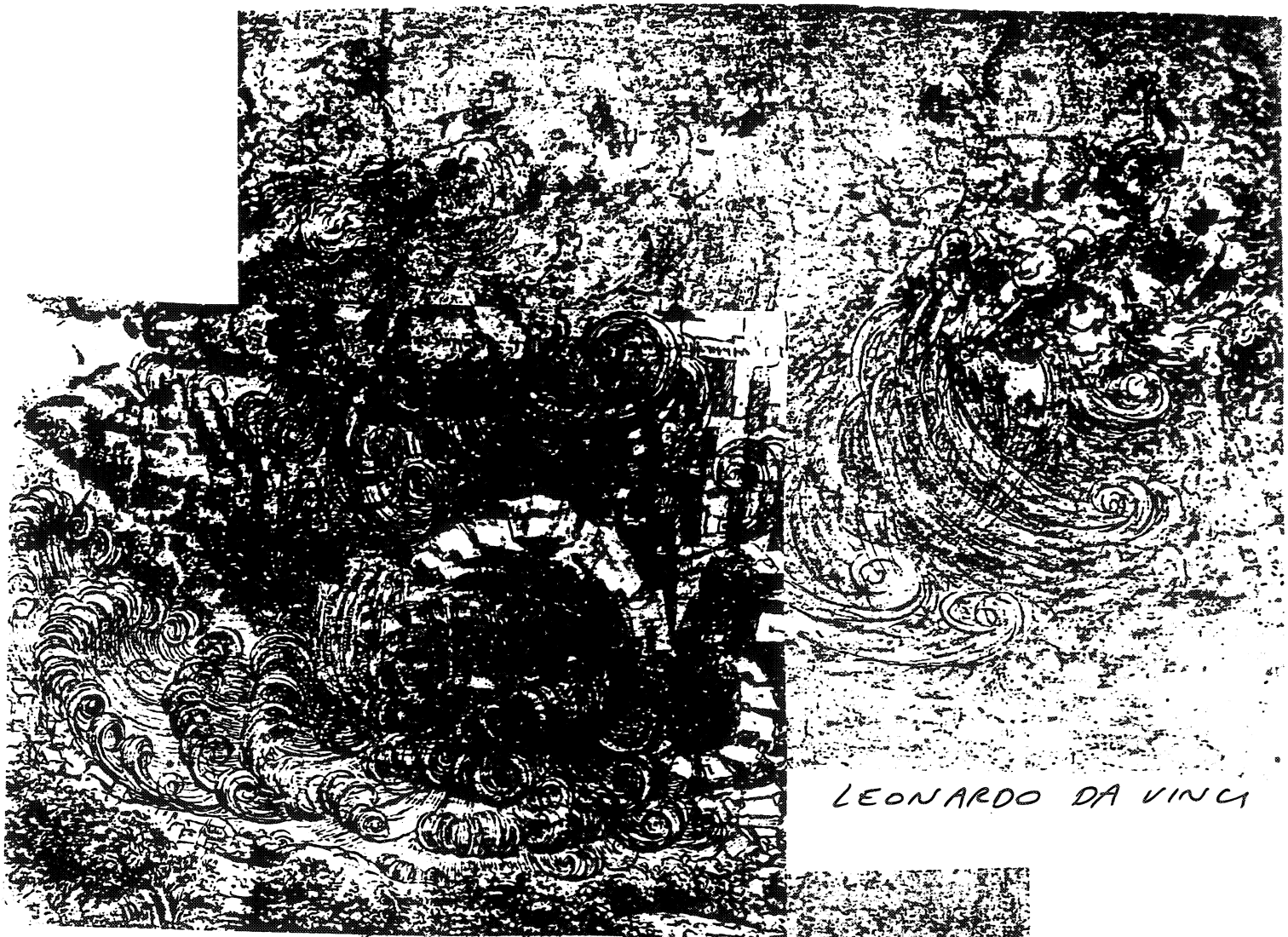

LEONARDO DA VINCI



Dove la turbolenza dellacqua rigenera,

Dove la turbolenza dellacqua rimantiene plugha,

Dove la turbolenza dellacqua riposa.

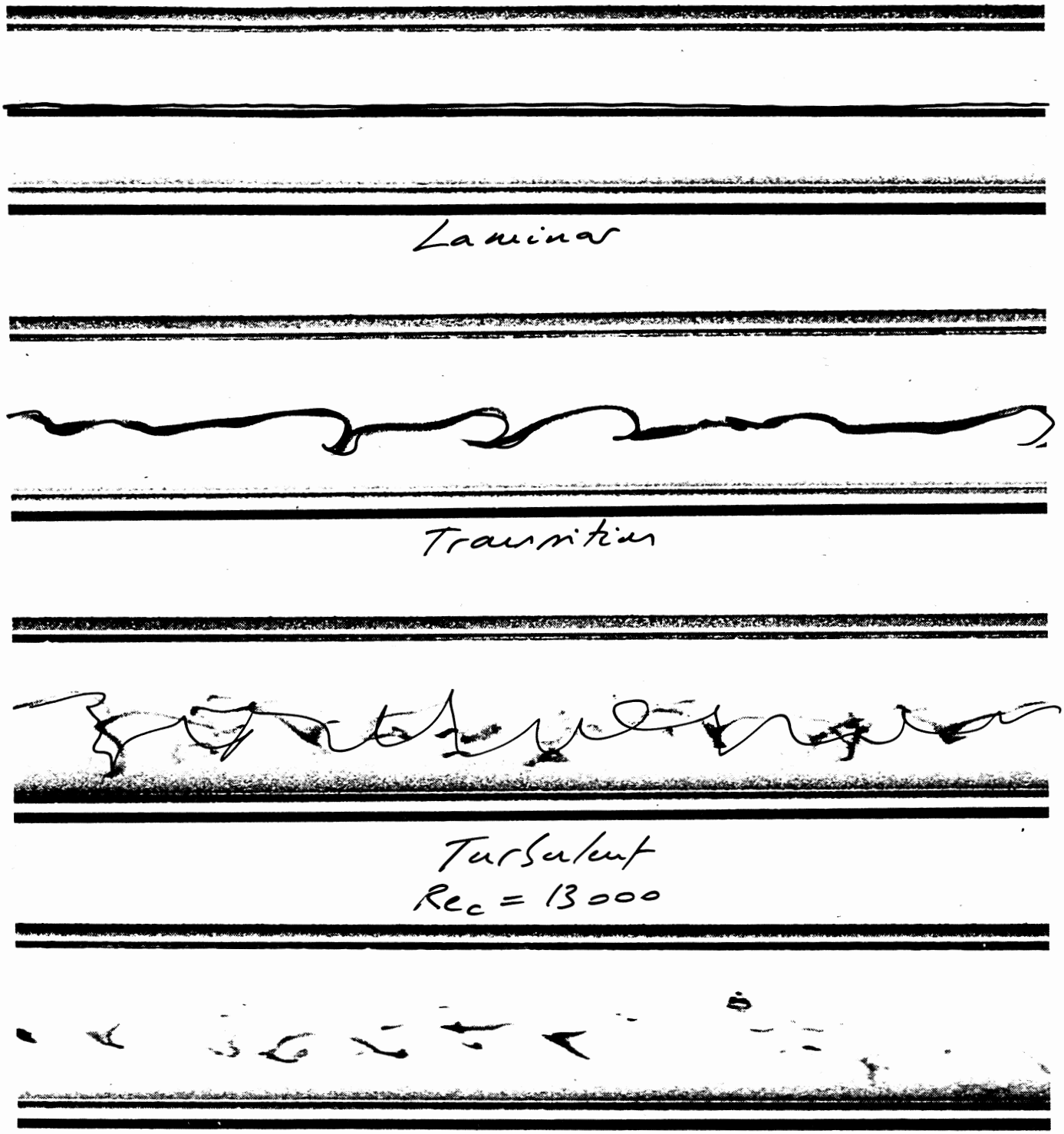

103. Repetition of Reynolds' dye experiment. Osborne Reynolds' celebrated 1883 investigation of stability of flow in a tube was documented by sketches rather than photography. However the original apparatus has survived at the University of Manchester. Using it a century later, N. H. Johannesen and C. Lowe have taken this sequence of photographs. In laminar flow a filament of colored water introduced at a bell-shaped entry extends undisturbed the whole length of the glass tube. Transition is seen in the second of the photographs as the speed is increased; and the last two photographs show fully turbulent flow. Modern traffic in the streets of Manchester made the critical Reynolds number lower than the value 13,000 found by Reynolds.

OSBORN REYNOLDS
Manchester, 1883

Problems to be solved

	Reynolds Number
Industrial flows (pipes, ships ...)	10^4
Airplanes (Wings, engine ...)	10^6
Space Shuttle	10^9
Meteorology, Ocean	10^{10}
Astrophysics	10^{12}

Direct Numerical Simulation
State of the art

2D	512^2	$\Rightarrow Re \sim 10^2$
3D	256^3	

THE PROBLEM IN TURBULENCE

Often, people in some unjustified fear of physics say you can't write an equation for life. Well, perhaps we can. As a matter of fact, we very possibly already have the equation to a sufficient approximation when we write the equation of quantum mechanics:

$$H\Psi = -\frac{h}{i}\frac{\partial \Psi}{\partial t}.$$

The next great era of awakening of human intellect may well produce a method of understanding the *qualitative* content of equations. Today we cannot. Today we cannot see that the water flow equations contain such things as the barber pole structure of turbulence that one sees between rotating cylinders. Today we cannot see whether Schrödinger's equation contains frogs, musical composers, or morality —or whether it does not. We cannot say whether something beyond it like God is needed, or not. And so we can all hold strong opinions either way.

Richard Feynman
Lecture Notes in
Physics,
1964

This is the same with turbulence: we have Navier-Stokes, the fundamental equation of fluid mechanics. We are sure it adequately describes the turbulent flow dynamics and yet we are unable to integrate it for most cases of interest. But we do not have yet understood turbulence in order to have adequate model equations based on first principles, namely without having to fit ad hoc parameters from experimental data.

INADEQUACY OF OUR TOOLS

The theory of fully-developed turbulence is a challenge for mathematicians & physicists.

It is yet unsolved and sadly understood because our present conceptual and technical tools are indeed inadequate.

Fully developed turbulent flows are:

dissipative $\Rightarrow$ irreversible,
present a very large number of degrees of freedom,
are highly nonlinear,
bounded, externally or internally,
and initial conditions are not C^∞.

'It is desesperate physics!'
as Wolfgang Pauli was stating.

WHERE DO WE COME FROM?

1. Dynamical approach

German school

1840-1940 Helmholtz, Kirchoff, Prandtl, Sommerfeld

→ 1940 Von Karman emigrated to Caltech

Dutch school

1920-1950 → Burgers emigrated to John Hopkins

1940-1997 Caltech school

Von Karman, Liepmann, Saffman

Roshko, Dimotakis, Gharib, Leonard

2. Statistical approach

1883 Reynolds 1920 Burgers 1920-1940 Taylor

Lorentz Ehrenfest Wiener

Hopf

3. Prosaicist approach

1940-1980 Russian school

Kolmogorov, Obukhov, Taylor

→ 1980 Novikov emigrated to San Diego

Cambridge school

1940-1970 Batchelor

→ 1970 Saffman emigrated to Caltech

4. Computational approach

deterministic Stanford school

1970-1997 Buaraman, Reynolds, Ferziger, Moin

Leonard moved to Caltech

stochastic

WHERE DO WE STAND TODAY?

1. Mathematical approach

   Existence and unicity of Navier-Stokes

   Finite time singularities

   We are unable to compute Navier-Stokes for large Reynolds flows

   Physical problems are bounded in (x,t)

   Initial and boundary conditions $\Rightarrow f \in C^\infty$

2. Theoretical approach

   21. Phenomenological

   Limit $Re \to \infty$ fully-developed

   Stationarity, homogeneity, isotropy

   grid turbulence

   Far from vorticity production regions

   22. Dynamical

   Limit $Re \to 1$ transition

   $\eta \propto Re^{9/4}$

   wakes, shear flows, mixing layers

   We do not have any fundamental law derived from first principles

3. Observational approach

   31. Laboratory experiments

   Point measures, many realizations

   32. Computational experiments

   Global measures, one realization

   We do not know how to measure vorticity

HOW DO WE PROCEED?

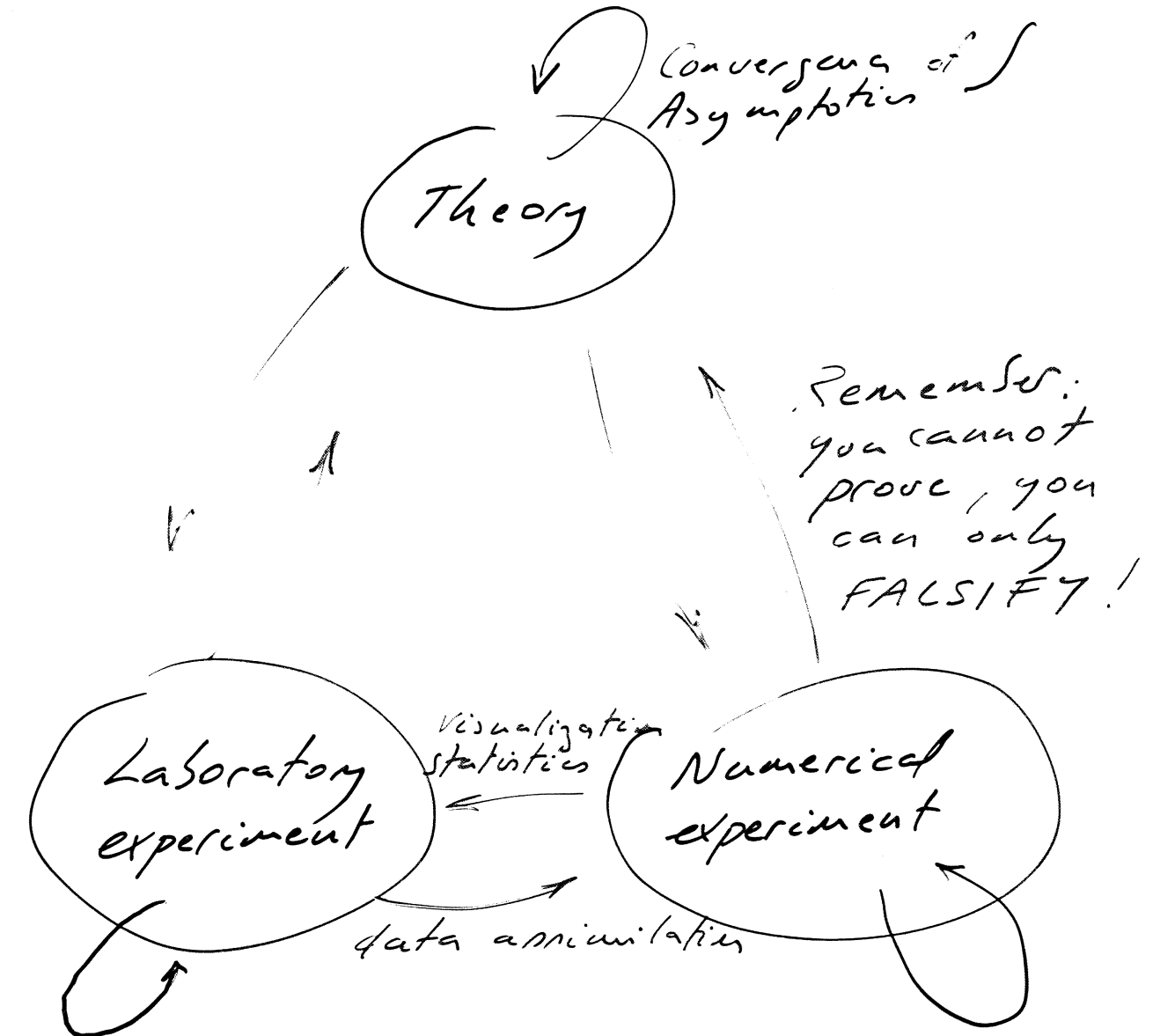

cf. Marie Farge, 1983
L'approche numérique
en physique
Fondements Scientifiques

RAPPELS

- Bernoulli equation
- Euler equations
- Navier-Stokes equations
- Velocity vector
- Vorticity vector
- Helmholtz's law
- Circulation
- Kelvin's theorem
- Rate of strain tensor
- Eulerian and Lagrangian frames
- Visualization of velocity, vorticity and stream function

BERNOULLI EQUATION
1738

Ecoulement irrotationnel,
incompressible,
de densité homogène,
stationnaire

Son mouvement est
décrit par l'équation:

$$\frac{1}{2} V^2 + \Phi + \frac{P}{\rho} = Cte$$

Φ potentiel des forces
extérieures $\vec{F} = -\nabla \Phi$

⟹ pour un fluide parfait

$$\Delta P = \frac{1}{2} \rho V^2$$

EULER EQUATIONS

Conservation of mass and momentum in an ideal fluid moving in the presence of an external force $\vec{F}$ per unit mass:

$$\rho_t + \vec{v}\cdot\vec{\nabla}\rho + \rho\,\vec{\nabla}\cdot\vec{v} = 0 \qquad (1)$$

$$\vec{v}_t + \vec{v}\cdot\vec{\nabla}\vec{v} = -\left(\frac{1}{\rho}\right)\vec{\nabla}p + \vec{F} \qquad (2)$$

We take curl of (2) and employ the relation: $\vec{v}\cdot\vec{\nabla}\vec{v} = \vec{\nabla}\left(\frac{1}{2}v^2\right) - \vec{v}\times\vec{\omega}$
This gives the evolution equation of $\vec{\omega}$:

$$\vec{\omega}_t + \vec{v}\cdot\vec{\nabla}\vec{\omega} = (\vec{\omega}\cdot\vec{\nabla})\vec{v} - \vec{\omega}(\vec{\nabla}\cdot\vec{v}) + \left(\frac{1}{\rho^2}\right)\vec{\nabla}\rho\times\vec{\nabla}p + \vec{\nabla}\times\vec{F}$$

If the fluid is barotropic, namely ρ is only a function of p, then the isopycnics (surfaces $\rho = \text{const}$) are parallel to the isobars ($p = \text{const}$) $\Rightarrow \vec{\nabla}\rho\times\vec{\nabla}p = 0$ and we obtain Helmholtz's equation:

$$\vec{\omega}_t + \vec{v}\cdot\vec{\nabla}\vec{\omega} = (\vec{\omega}\cdot\vec{\nabla})\vec{v} - \vec{\omega}(\vec{\nabla}\cdot\vec{v})$$

This equation is responsible for the

deep importance of vorticity, because pressure is absent and the rate of change of vorticity depends only on the instantaneous local values of $\vec{v}$ and $\vec{\omega}$ alone:

$$\frac{D}{Dt}\left(\frac{\vec{\omega}}{\rho}\right) \equiv \left(\frac{\partial}{\partial t} + \vec{v}\cdot\vec{\nabla}\right)\frac{\vec{\omega}}{\rho} = \left(\frac{\vec{\omega}}{\rho}\cdot\vec{\nabla}\right)\vec{v}$$

gives the rate of change of $\frac{\vec{\omega}}{\rho}$ following a fluid particle in terms of its instantaneous value and the local velocity gradient.

In contrast, the pressure field for a uniform fluid of constant density is given by Poisson's equation and is therefore non local:

$$\nabla^2 p = -\rho \frac{\partial^2 v_i v_j}{\partial x_i \partial x_j}$$

with not completely certain boundary conditions (Neumann in the bulk of the flow or Dirichlet on the walls).

NAVIER-STOKES EQUATIONS

Newton's second law of dynamics applied to a fluid particle which is:

property of the fluid { incompressible, of constant density; Newtonian }

$$m\vec{\gamma} = \sum \vec{F}$$

conservation of momentum per unit volume

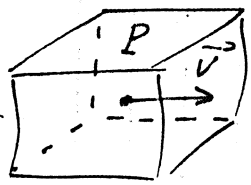

$$\Rightarrow \rho \frac{\partial \vec{V}}{\partial t} + \rho \vec{V} \cdot \vec{\nabla} \vec{V} + \vec{\nabla} P = \mu \nabla^2 \vec{V} + \vec{F}$$

Newtonian means that the stress tensor $\bar{\bar{\tau}}$ and the rate of strain tensor $\bar{\bar{S}}$ are linearly related therefore $\bar{\bar{\tau}} = \mu \nabla^2 \vec{V}$ or put $\nu = \frac{\mu}{\rho}$ kinematic viscosity

$$\underbrace{\frac{\partial \vec{V}}{\partial t} + \vec{V} \cdot \vec{\nabla} \vec{V}}_{\text{inertial force}} + \underbrace{\frac{1}{\rho} \vec{\nabla} P}_{\substack{\text{volume force} \\ \text{(internal)}}} = \underbrace{\nu \nabla^2 \vec{V}}_{\substack{\text{surface force} \\ \text{(Stress)}}} + \underbrace{\frac{1}{\rho} \vec{F}}_{\substack{\text{volume force} \\ \text{(external)}}}$$

Conservation of mass

$\Rightarrow$ Continuity equation $\frac{\partial \rho}{\partial t} + \vec{\nabla} \cdot (\rho \vec{V}) = 0$

VELOCITY VECTOR

For incompressible fluids the velocity field is solenoidal:

$$\underset{div}{\vec{\nabla}.\vec{V}} = 0$$

Incompressibility means that the material derivative of density is constant:

$$\frac{D\rho}{Dt} \equiv \frac{\partial \rho}{\partial t} + \vec{V}.\vec{\nabla}\rho = 0$$

It is not necessary that the fluid is homogeneous $\rho = cte$.

$\vec{\nabla} \times \vec{V} = \vec{\omega} \Rightarrow \nabla^2 \vec{V} = -\vec{\nabla} \times \vec{\omega}$ Poisson equation

To invert $\vec{V}$ from $\vec{\omega}$, we need the following conditions:

1. V_n, normal component of $\vec{V}$, is given on all bounding surfaces S,
2. $\vec{V}$ vanishes at ∞ when fluid is unbounded,
3. ω_n, normal component of $\vec{\omega}$ vanishes on S
4. vorticity field is compact,

then:

$$\vec{V}(\vec{x},t) = \vec{V}_{sol}(\vec{x},t) + \vec{\nabla}\Phi$$

$$\vec{\nabla} \cdot \vec{V}_{sol} = \text{curl } \vec{V}_{sol} = \vec{\omega}$$

where solenoidal vector potential component

$$\vec{V}_{sol} = -\frac{1}{4\pi} \int \vec{\omega}(\vec{x}', t) \times \vec{\nabla} \frac{1}{|\vec{x}' - \vec{x}|} d\vec{x}'$$

and irrotational scalar component

$$\nabla^2 \Phi = 0 \quad \text{with} \quad \frac{\partial \Phi}{\partial n} = V_n - \vec{V}_{sol} \cdot \vec{n}$$

$\nabla\Phi$ is the irrotational solenoidal field which can be added to satisfy a surface boundary condition V_n on S. If there is no bounding surface S, then $\Phi = 0$.

Vector identities which are used in the demonstration

$$\text{div}(\vec{a} \times \vec{b}) = \vec{b} \cdot \text{curl}\, \vec{a} - \vec{a} \cdot \text{curl}\, \vec{b}$$

$$\text{curl}(\vec{a} \times \vec{b}) = \vec{a}\, \text{div}\, \vec{b} - \vec{b}\, \text{div}\, \vec{a} - (\vec{a} \cdot \vec{\nabla})\vec{b} + (\vec{b} \cdot \vec{\nabla})\vec{a}$$

We also use the following results of generalized function theory:

$$\text{curl}\ \text{grad}\left(\frac{1}{r}\right) = 0$$

$$\nabla^2\left(\frac{1}{r}\right) = -4\pi\, \delta(\vec{x} - \vec{x}')$$

VORTICITY VECTOR

It is the curl of velocity:

$$\vec{\omega}(\vec{X}, t) = \omega_i \equiv \vec{\nabla} \times \vec{V} = \varepsilon_{ijk} \frac{\partial v_k}{\partial x_j}$$

$$= \left\{ \left(\frac{\partial v_3}{\partial x_2} - \frac{\partial v_2}{\partial x_3} \right), \left(\frac{\partial v_1}{\partial x_3} - \frac{\partial v_3}{\partial x_1} \right), \left(\frac{\partial v_2}{\partial x_1} - \frac{\partial v_1}{\partial x_2} \right) \right\}$$

Vorticity is solenoidal:

$$\vec{\nabla} \cdot \vec{\omega} = \frac{\partial \omega_i}{\partial x_i} = 0$$

$$\operatorname{div} \vec{\omega} =$$

Helmholtz laws 1858

(Crelles J. 55)

If: 1. viscosity is negligible,
2. fluid barotropic ($\rho = f(P)$),
3. external forces conservative,

then: 1. fluid particles originally free of vorticity remain free of vorticity,

2. vortex lines and tubes move with the fluid,

3. the strength of a vortex tube does not vary with time during the motion of the fluid.

1st law ⇒ Lagrange's theorem on the persistance of irrotational motion. If no vorticity (spin of the canoe) at $t=0$, it will remain so along the trajectory.

2nd law

$$\left(\frac{d}{dt}\left(\frac{\vec{\omega}}{\rho}\right)\right)_g = \frac{D}{Dt}\left(\frac{\vec{\omega}}{\rho}\right) = \left(\frac{\vec{\omega}}{\rho}\right)\cdot\vec{\nabla}\vec{V}$$

Lagrangian frame — Eulerian frame $= \overrightarrow{S_{ij}}\cdot\frac{\omega_j}{\rho}$

with $\overrightarrow{S_{ij}} = \frac{1}{2}\left(\frac{\partial V_i}{\partial x_j} + \frac{\partial V_j}{\partial x_i}\right)$ rate of strain tensor.

Therefore the rate of change of vorticity following a fluid particle is proportional to the local rate of strain tensor and does not explicitly depend on the local vorticity or rotation tensor. Material lines remain vortex lines and in this sense the vortex lines are said to move with the fluid.

3rd law Strength of axisymmetrical tubes is constant and therefore that of a tube of arbitrary size.

CIRCULATION SCALAR

Circulation $\Gamma(t)$ around a closed material curve $C(t)$ lying entirely in the fluid:

$$\Gamma(t) = \oint_{C(t)} \vec{V} \cdot d\vec{S} = \oint \vec{V}_\sigma \cdot \frac{\partial \vec{S}_\sigma}{\partial \sigma} d\sigma$$

$$= \int_D \omega(\vec{x})\, d\vec{x}$$



Kelvin's circulation theorem 1868

('On vortex motion', trans. Roy. Soc. Edinburgh)

If 1. fluid is barotropic,
2. external forces irrotational,
then 3. fluid ideal,
circulation around a material circuit is an invariant of the motion. $\frac{d\Gamma}{dt} = 0$

Assumptions: $\vec{V}$ is continuous,
the circuit $C(t)$ is being deformed smoothly.

Both conditions may be violated in flows of physical significance, leading to the creation of circulation.

Klein's Kaffeelöffel experiment 1910

(Zeit. für Math. und Phys. 59)

The question arises whether vorticity can be created without violating Kelvin's

and Helmholtz's theorems, and without invoking viscosity, non-conservative forces or baroclinic effects. The conclusion is that Helmholtz and Kelvin theorems preclude the generation of piece-wise continuous vorticity but do not prevent the formation of vortex sheets or the generation of circulation.

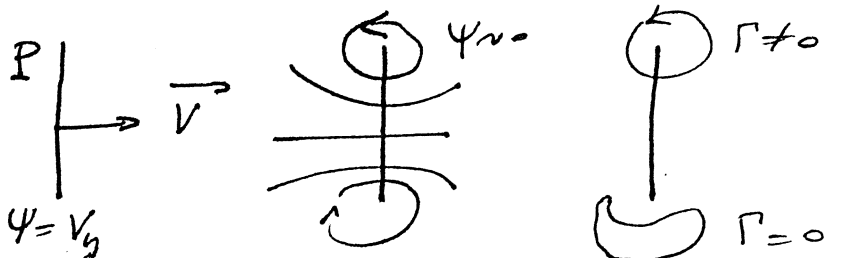

Klein argued that if the plate P is removed (by pulling out the cotter spoon or dissolving it), then a vortex sheet is left in the fluid and circulation has been created. There is no contradiction with Helmholtz and Kelvin's theorems, because no fluid particle has acquired vorticity and no circulation has been created - just closed lines. The new contours were not closed beforehand, they enclosed the body.

⇒ Vorticity has been created as a sheet (singular distribution) by changing the topology of the flow.

RATE OF STRAIN TENSOR

The relative velocity δV_i of two fluid particles separated by δX_i can be written:

$$\delta V_i = S_{ij} \cdot \delta X_j + \Omega_{ij} \cdot \delta X_j$$

where S_{ij} = rate of strain tensor

$$S_{ij} = \frac{1}{2}\left(\frac{\partial V_i}{\partial X_j} + \frac{\partial V_j}{\partial X_i}\right) \quad (1)$$

and Ω_{ij} = rate of rotation tensor

$$\Omega_{ij} = \frac{1}{2}\left(\frac{\partial V_i}{\partial X_j} - \frac{\partial V_j}{\partial X_i}\right) \quad (2)$$

$$= -\frac{1}{2}\varepsilon_{ijk}\,\omega_k$$

Conversely: $\omega_i = -\varepsilon_{ijk}\,\Omega_{jk}$.

(1) Pure straining motion
Line elements or spheres are extended or contracted with principal axes along those of the rate of strain tensor S_{ij}.

(2) Rigid body rotation
Line elements stay of constant length and spheres remain spheres while rotating with angular velocity

$$\Omega = \frac{1}{2}\omega$$

$\omega = 0$ irrotational flow
$\omega \neq 0$ rotational flow

Newtonian fluids are such that the stress tensor $\overrightarrow{\overrightarrow{\tau}}$ and the rate of strain tensor $\overrightarrow{\overrightarrow{S}}$ are linearly related.

Remarks

- Solid particles do in general rotate when suspended in fluid in irrotational motion, even if the fluid is ideal ($\nu = 0$). This is because a body of general shape is subject to a torque when suspended in irrotational flow of an ideal fluid.
- In a 2D irrotational flow, a square or cross will not rotate when carried along with the flow, but a rod or diagonal cross or ellipse will.
- In a 3D irrotational flow, the torque vanishes for non-spherical bodies with rotational symmetry about 3 perpendicular axes (e.g. cubes) but does not vanish for general shape.
- Part of the deformation by S_{ij} extends the vortex line and part rotates it.
- Separate consideration of rotation and extension may break up the vorticity field into non-solenoidal components.

EULERIAN FRAME

The observer remains fixed while the fluid moves (the fisherman sitting on the bench of the river).

$\theta(\vec{x}, t)$ field variable in Eulerian frame

The time derivative of θ moving with the fluid is:

$$\frac{D\theta}{Dt} = \frac{\partial \theta}{\partial t} + \vec{v} \cdot \vec{\nabla} \theta \quad \text{Eulerian frame}$$

$$= \frac{d\theta_0}{dt} \quad \text{Lagrangian frame}$$

Remark

$\theta(\vec{x}, t)$ is the Eulerian frame.

$\theta(t)$ is the Lagrangian frame.

To keep distinct the two representations we shall use $\frac{d}{dt}$ for the time differentiation in the Lagrangian frame, even if it is strictly a partial derivative with $\vec{x}$ and $\vec{v}$ fixed, and use $\frac{D}{Dt}$ as shorthand for the derivative following the flow in the Eulerian frame.

LAGRANGIAN FRAME

The idea of a fluid particle, material line and the concept of moving with the fluid are attached to the notion of trajectory $\vec{X}(t)$:

$$\frac{d\vec{X}}{dt} = \vec{U}(\vec{X}, t) \quad \text{with} \quad \vec{X}(0) = X_0$$

The description of the fluid motion contained in the set of trajectories $\vec{X}(t)$ or pathlines is called a Lagrangian representation.

- The velocity of the fluid at time t and position $\vec{X}$ is $\frac{d\vec{X}}{dt}$ and is a function of t and $\vec{X}_0$, instead of in terms of the current position $\vec{X}$ as in Eulerian representation.

- A material line is a curve $\vec{X}(t, \sigma)$ for constant t and varying $\vec{X}_0$ (cause) where σ is a Lagrangian particle specifying position along the original position of the line $X_0(\sigma) =$ $\vec{X}(t, \sigma)$

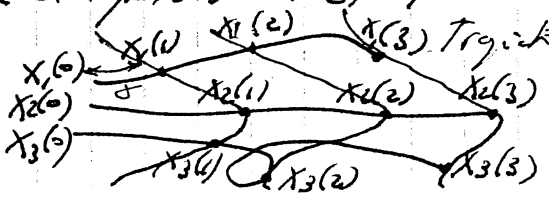

N.B. We shall use $\frac{d}{dt}$ in Lagrangian representation, even if it is strictly a partial derivative with σ and $\tau = t$.

A streakline is the locus of particles released from a fixed point $\vec{x}_0$ during the time interval t. It is obtained from the integration of:

$$\frac{d\vec{x}}{dt}(t,\tau) = \vec{v}(\vec{x},t) \quad \text{with} \quad \vec{x}(t,\tau) = \vec{x}_0$$

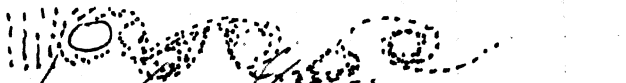

- In shady flows
streaklines ≡ pathlines ≡ streamlines.

Streamlines are the curves tangent to the instantaneous velocity.



- In unsteady flows great care must be exercised in the interpretation of streakline patterns from experiments employing flow visualization techniques. They may show apparent roll-up into vortices where no concentration of vorticity has occured. Vice-versa, there can be vortices which are not seen in the streamlines.

Let $\theta(\vec{x},t)$ be a field variable. The values on a material line is by

$$\theta_\sigma(t) = \theta(\vec{x}(t,\sigma),t)$$

$\theta(\vec{x},t)$ Eulerian representation, $\theta_\sigma(t)$ Lagrangian

CHOIX DES MODES DE REPRESENTATION

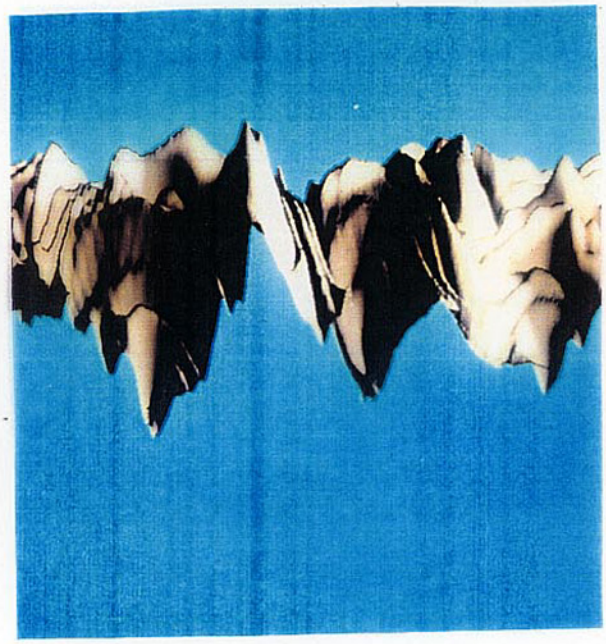

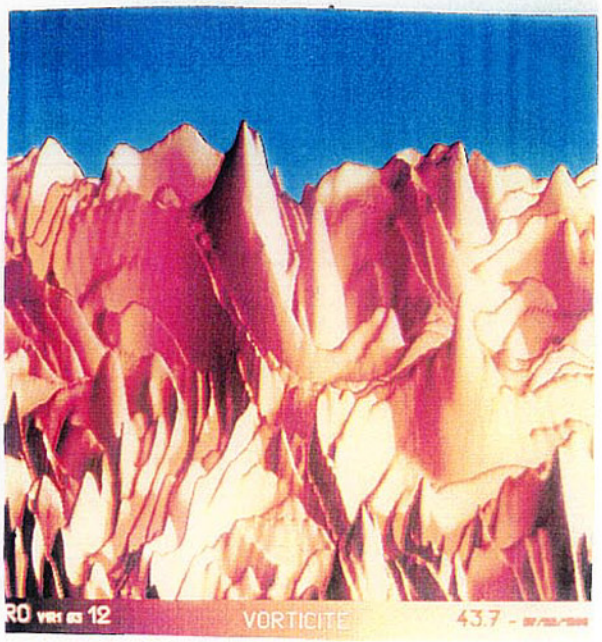



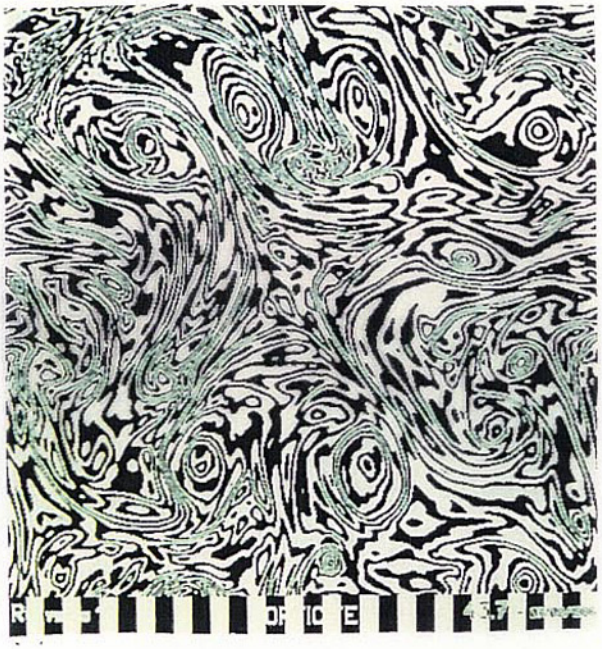





Le même champ de vorticité est visualisé avec différents représentations

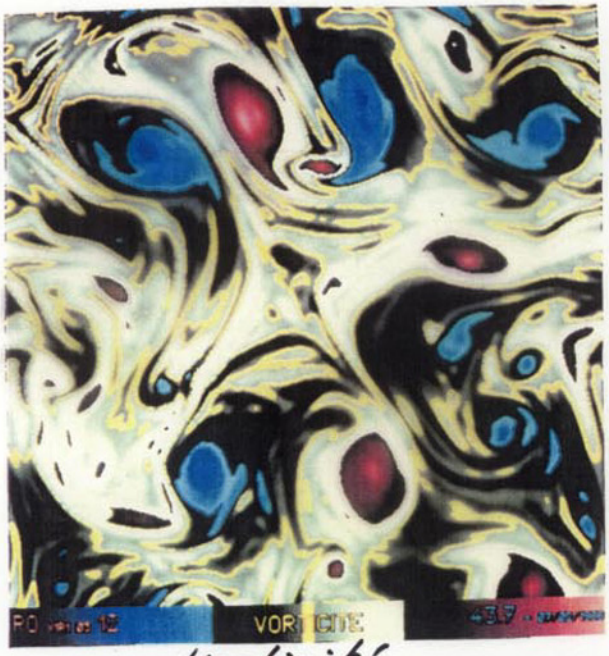

Vorticité



Divergence

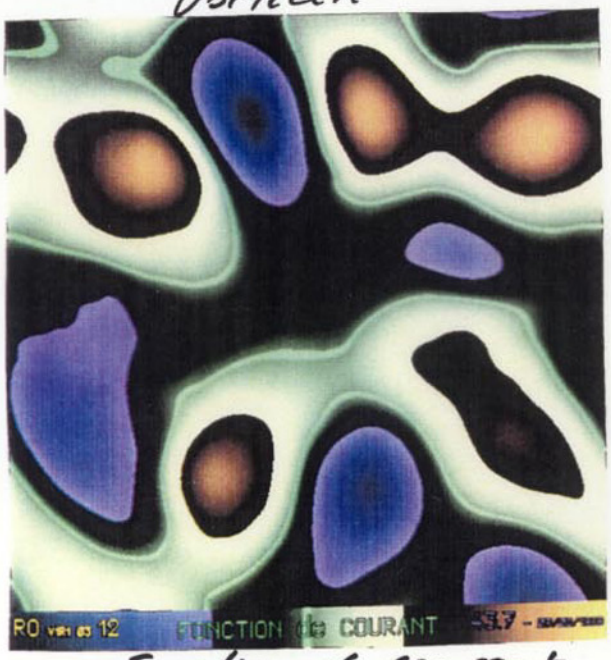

Fonction de courant

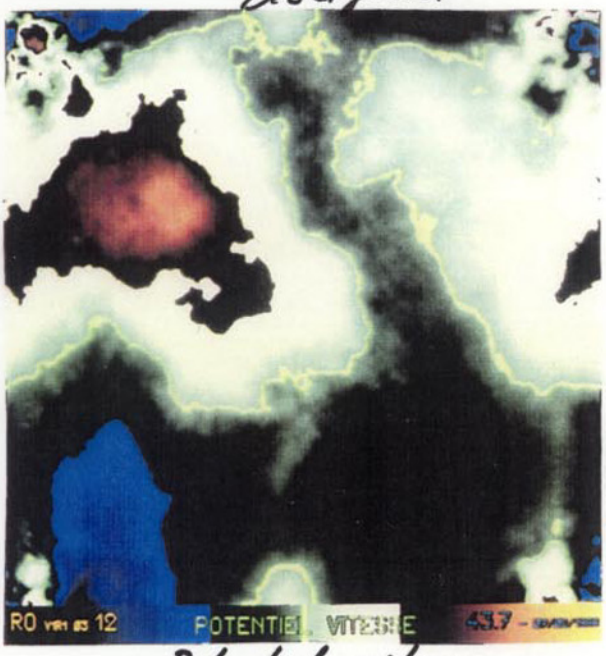

Potentiel vitesse

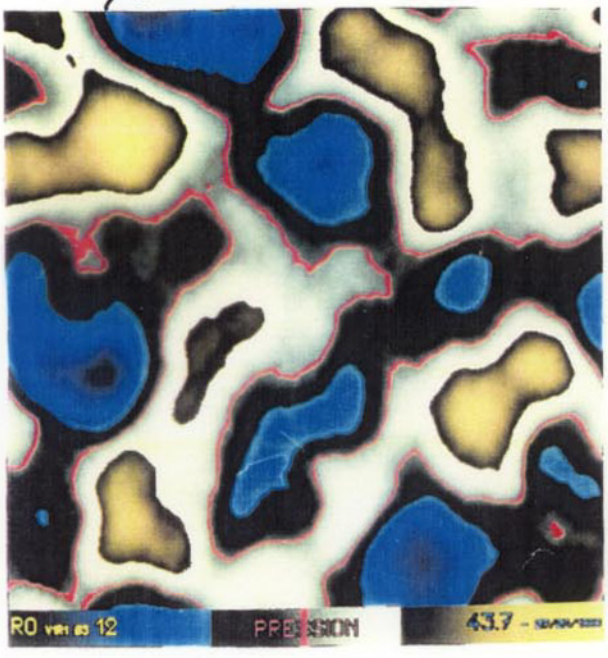

Pression

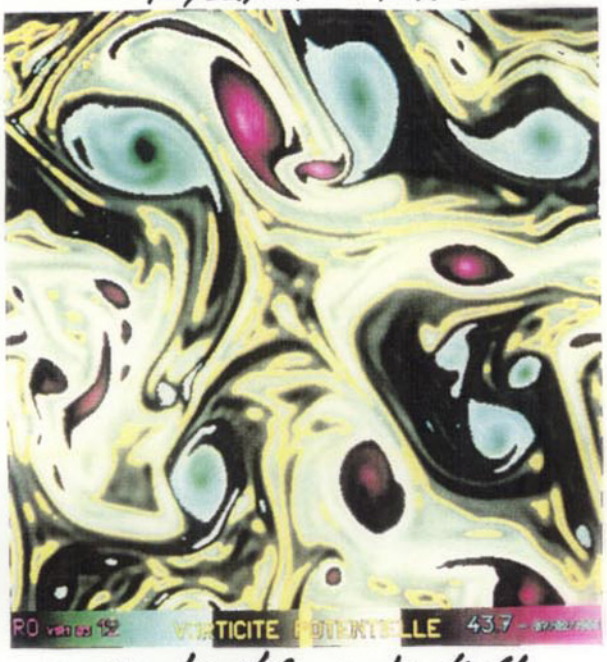

Vorticité potentielle

SOLUTION DES EQUATIONS
DE SAINT-VENANT (Fary, JFM, 1989)

TYPICAL FLOWS IN LAMINAR AND TURBULENT REGIMES

- Pipe flow (Poiseuille / Prandtl)
- Flow past a cylinder (Von Karman)
- Boundary layer:
  - Laminar
  - Turbulent
  - Wall law

PIPE FLOW

Henri POISEUILLE, 1840

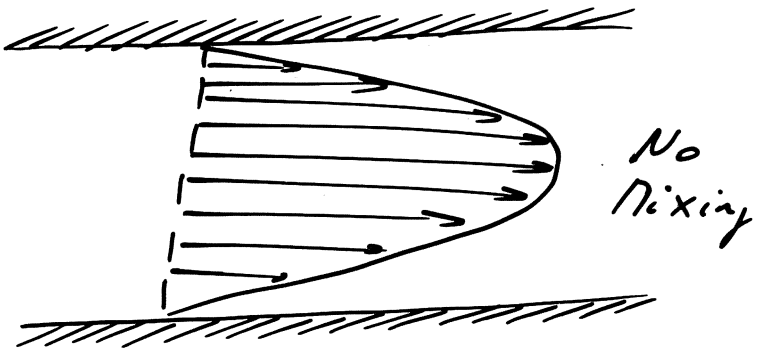

Laminar flow
Parabolic velocity profile

Critical Reynolds
$Re = 2300$

Ludwig PRANDTL, 1904
Boundary layer theory

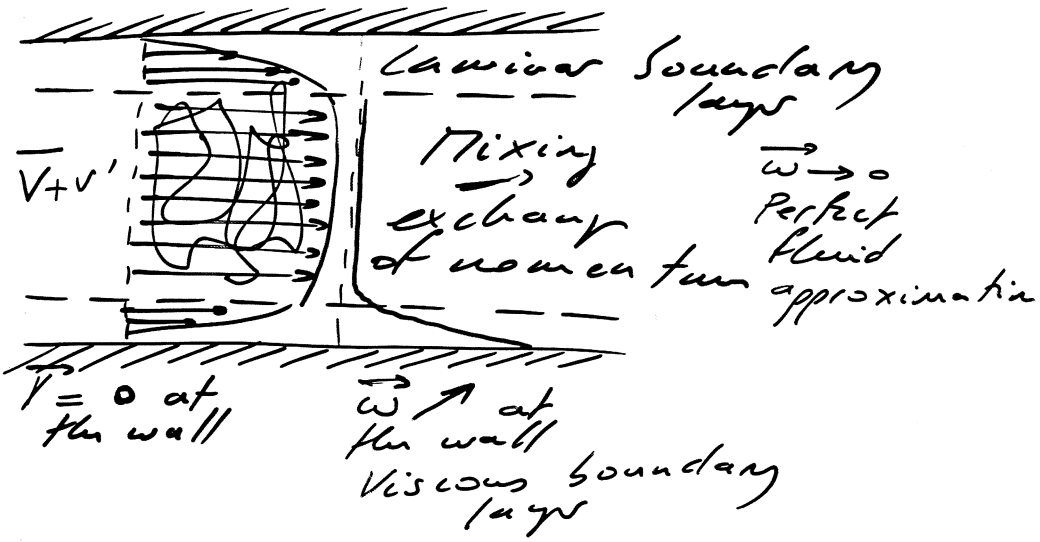

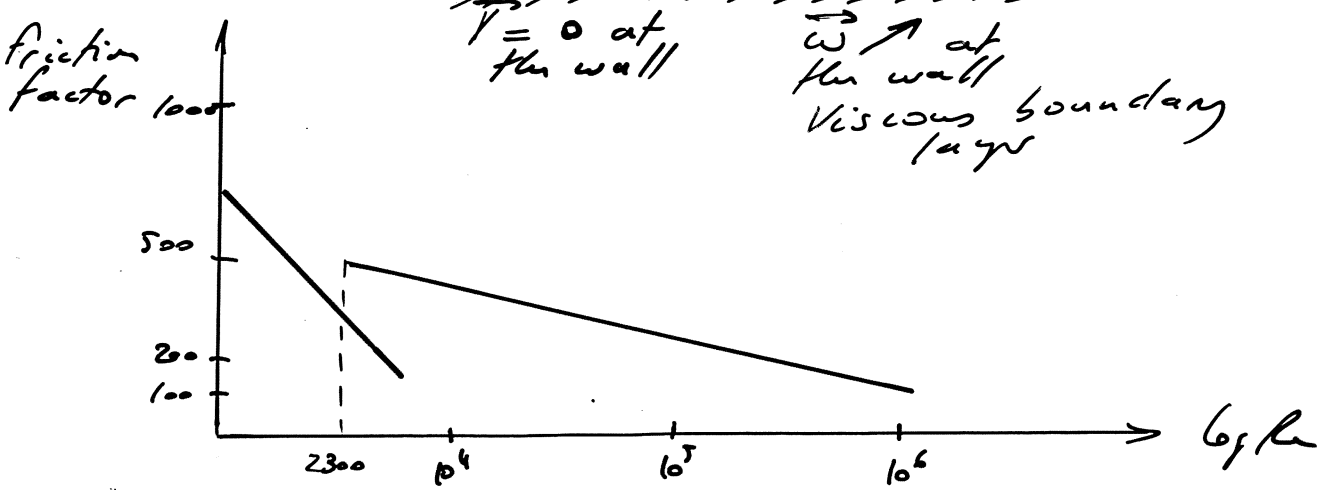

FLOW PAST A CYLINDER

Theodor VON KARMAN, 1921

$Re = 1$

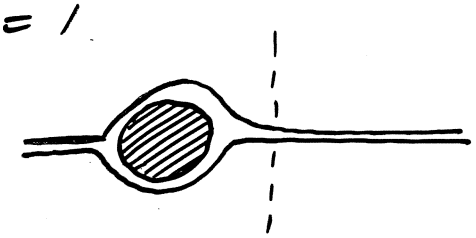

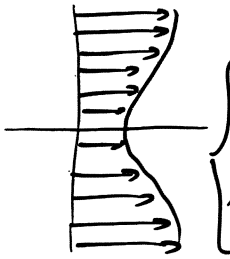

No wake

No recirculation

$Re = 5$

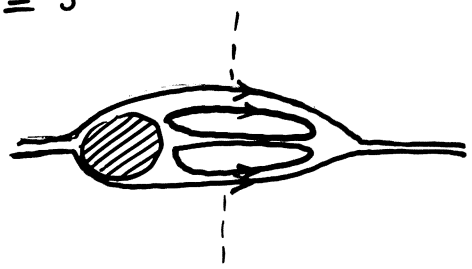

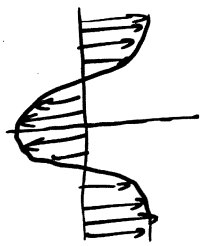

No wake

Recirculation attached to the body

$Re = 40$



Wake

Steady vortex shedding at Strouhal frequency

$Re = 200$

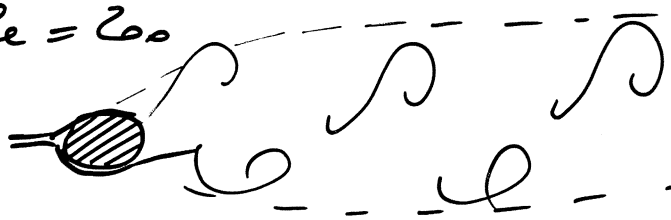

Unsteady vortex shedding with several frequencies

$Re = 10\,000$



Laminar boundary layer

Turbulent wake

$Re = 400\,000$

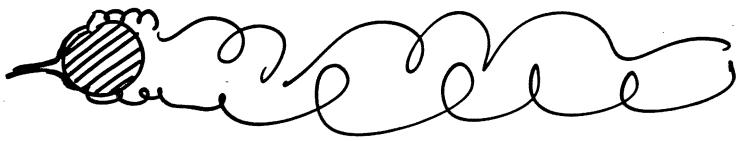

Turbulent boundary layer

Turbulent wake

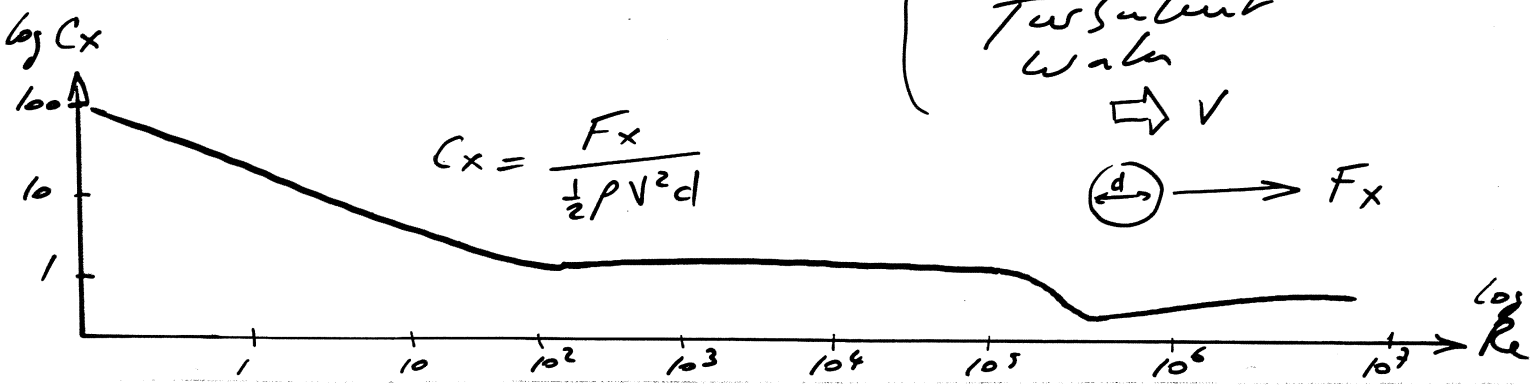

$$C_x = \frac{F_x}{\frac{1}{2}\rho V^2 d}$$

TANEDA, 1955
LAMINAR Re < 40

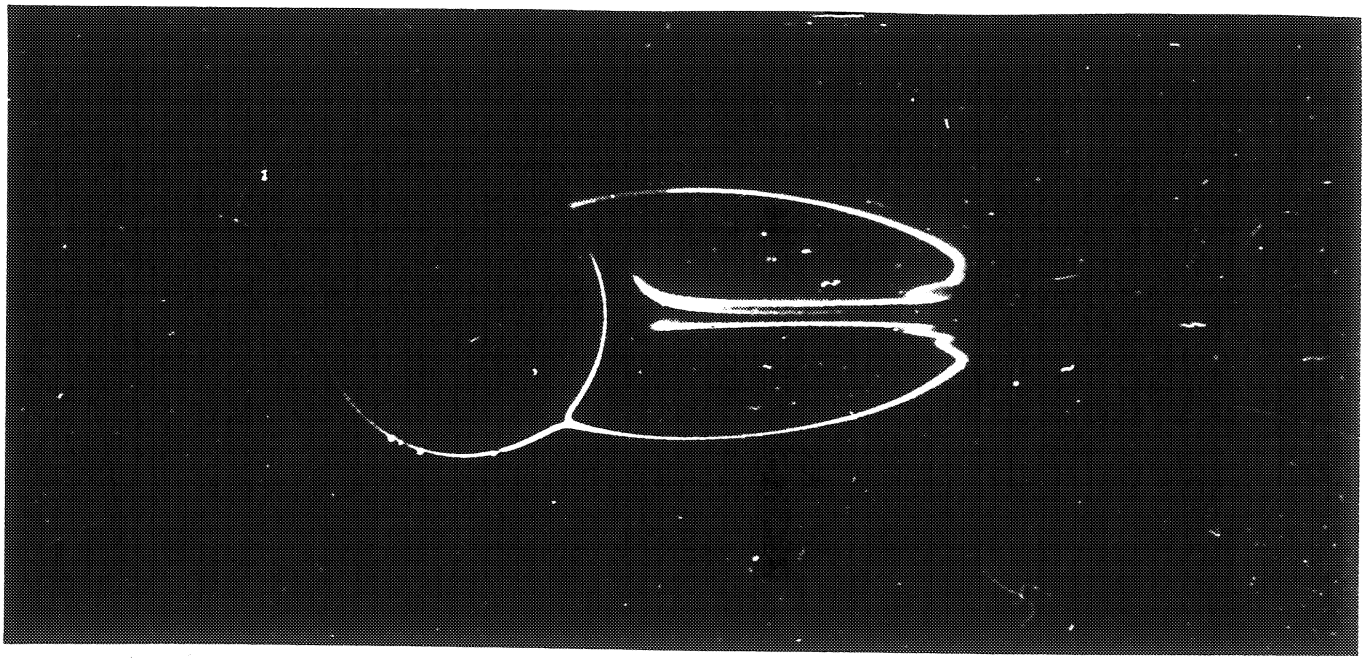

45. **Circular cylinder at $R=28.4$.** Here just the boundary of the recirculating region has been made visible by coating the cylinder with condensed milk and setting it in motion through water. *Taneda 1955*

Steady laminar flow with recirculation
Re = 28.4

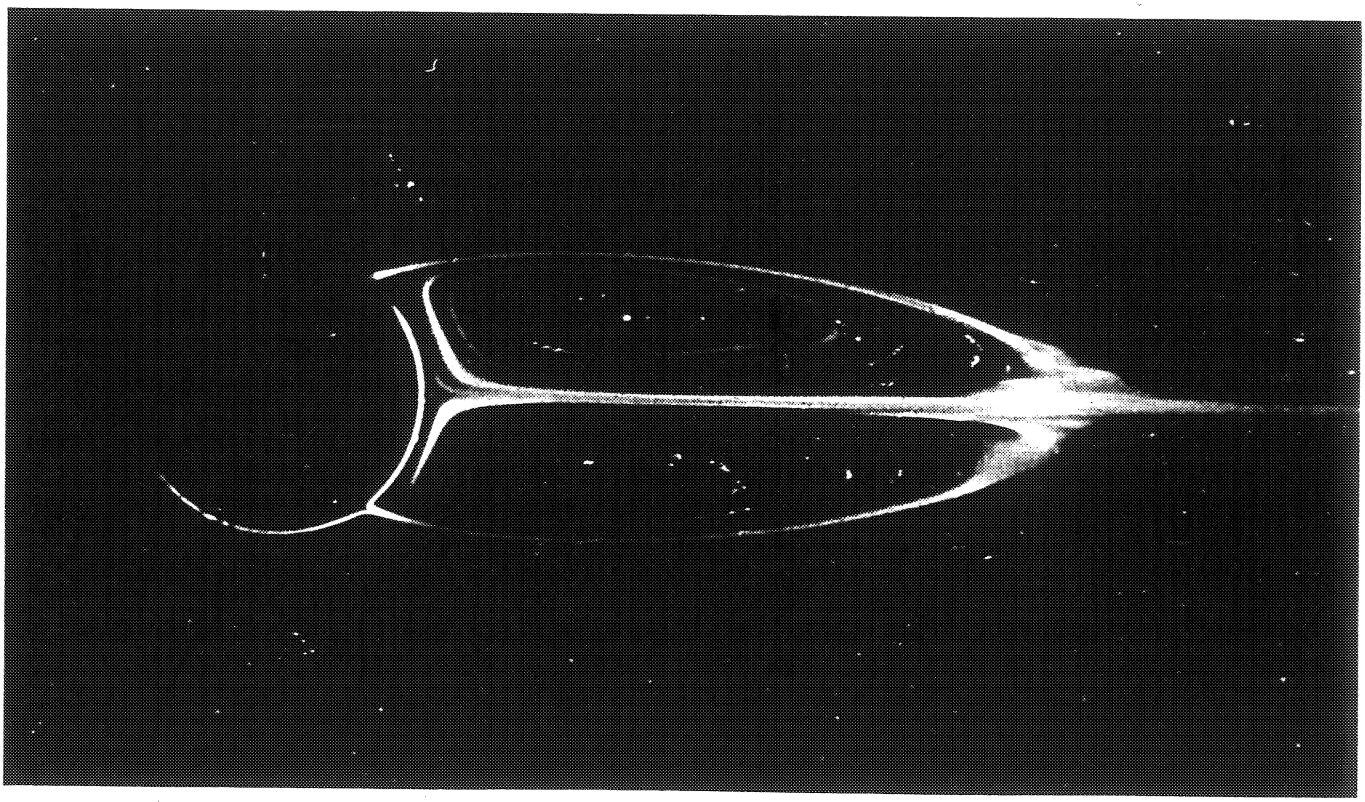

46. **Circular cylinder at $R=41.0$.** This is the approximate upper limit for steady flow. Far downstream the wake has already begun to oscillate sinusoidally. Tiny irregular gathers are appearing on the boundary of the recirculating region, but dying out as they reach its downstream end. *Taneda 1955*

Onset of unsteady oscillation on the boundary of the recirculation
Re = 41.0

TANEDA, 1955
TRANSITION
40 < Re < 200

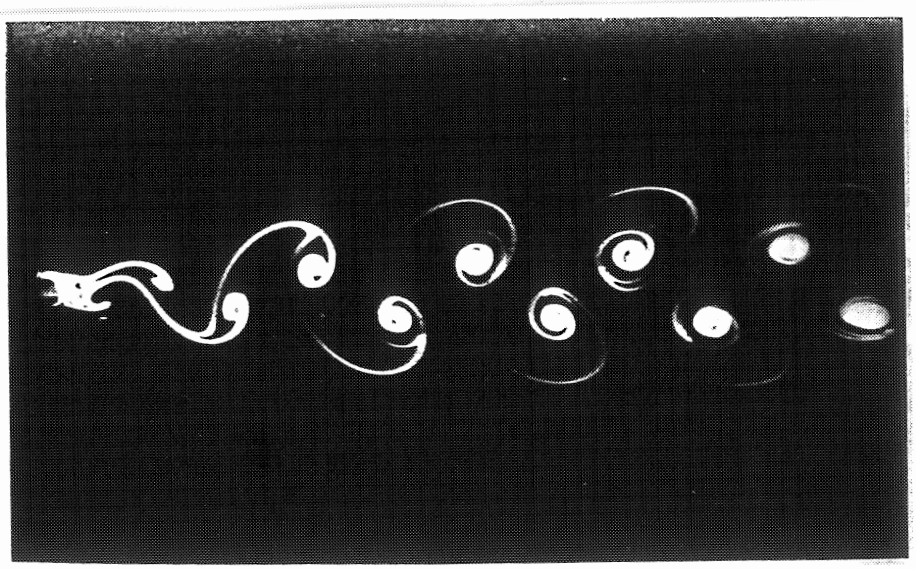

96. Kármán vortex street behind a circular cylinder at R=105. The initially spreading wake shown opposite develops into the two parallel rows of staggered vortices that von Kármán's inviscid theory shows to be stable when the ratio of width to streamwise spacing is 0.28. Streaklines are shown by electrolytic precipitation in water. *Photograph by Sadatoshi Taneda*

Stasb
Von Karman
Vortices
Re = 105
Strouhal frequency

Eulerian Frame

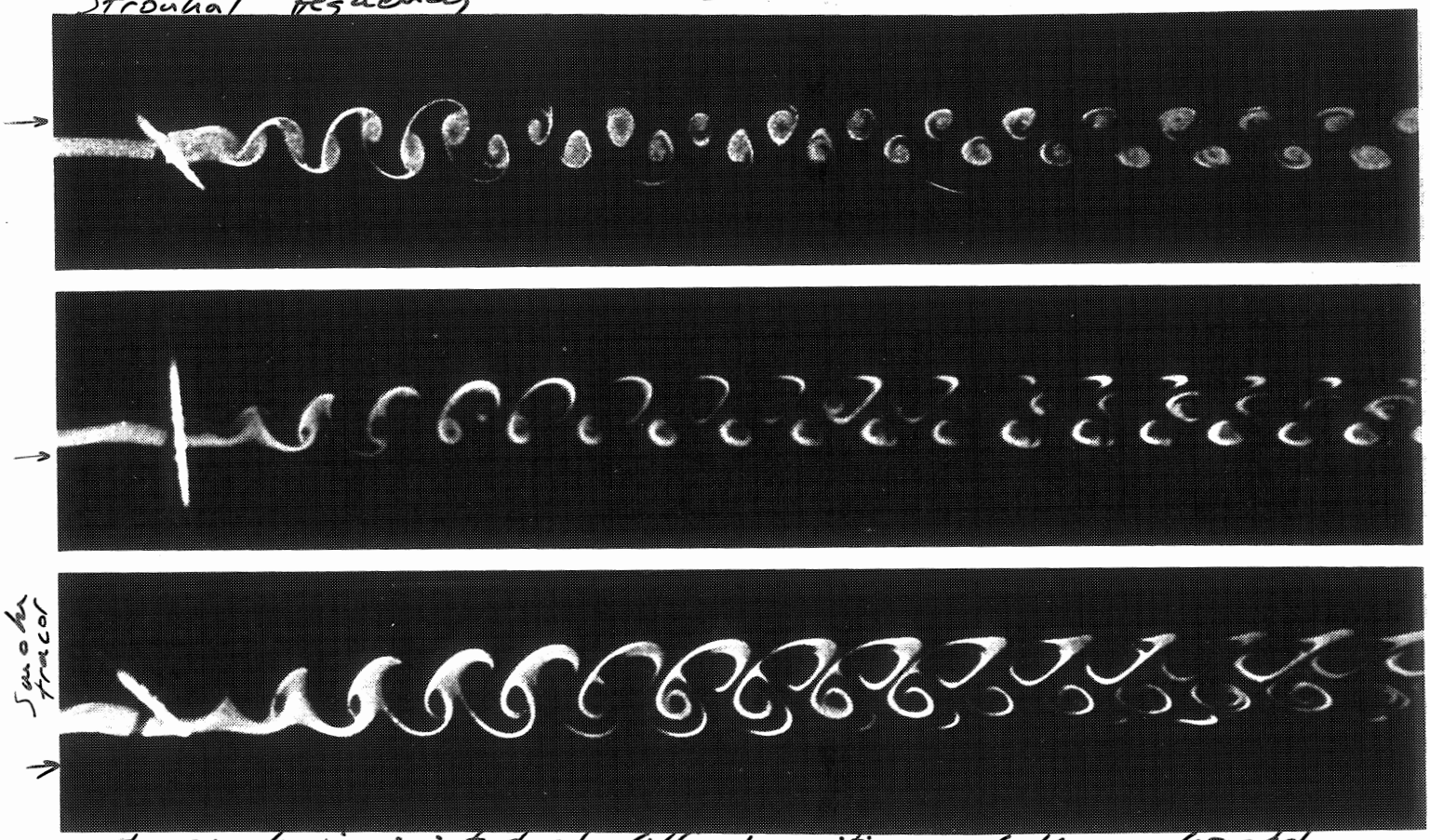

Smoke tracer

The smoke is injected at different position and then advected

97. Smoke at various levels in a vortex street. A smoke filament in air shows, at a Reynolds number of 100, both shear layers (top photographs), only one shear layer (middle), and the irrotational flow below the wake (bottom). *Zdravkovich 1969* ⇒ STREAKLINES

Lagrangian Frame



98. Kármán vortices in absolute motion. Here the camera moves with the vortices rather than the cylinder. The streamline pattern closely resembles the inviscid one calculated by von Kármán. The flow is visualized by particles floating on water. *Photograph by R. Wille, from Werlé 1973. Reproduced, with permission, from the* Annual Review of Fluid Mechanics, *Volume 5, © 1973 by Annual Reviews Inc.*

Camera moves with the vortices ⇒ STREAMLINES

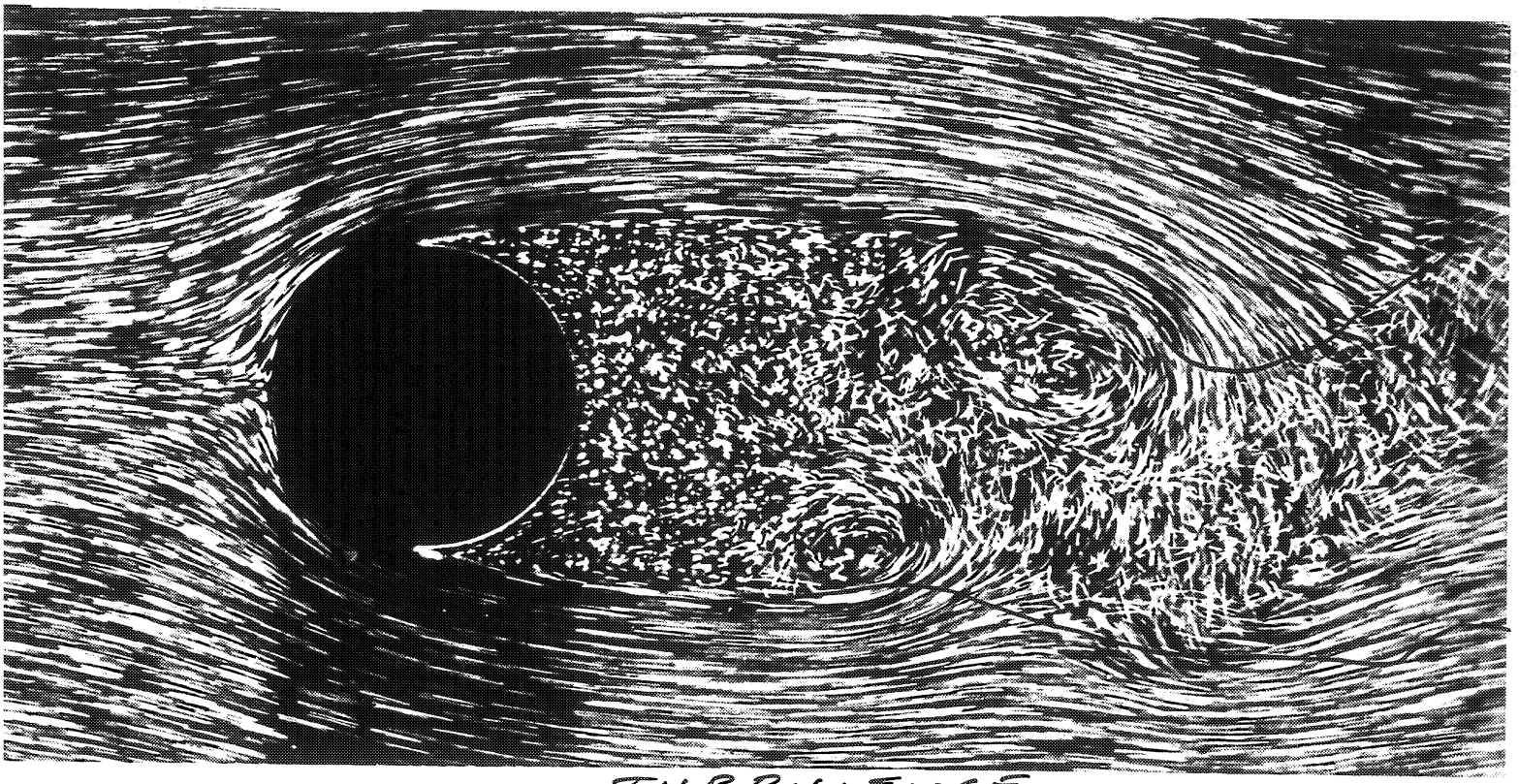

TURBULENCE

47. Circular cylinder at R=2000. At this Reynolds number one may properly speak of a boundary layer. It is laminar over the front, separates, and breaks up into a turbulent wake. The separation points, moving forward as the Reynolds number is increased, have now attained their upstream limit, ahead of maximum thickness. Visualization is by air bubbles in water. *ONERA photograph, Werlé & Gallon, 1972*

Laminar boundary layer separates and breaks into a turbulent wake ↑
Re = 2000 Separation → Drag

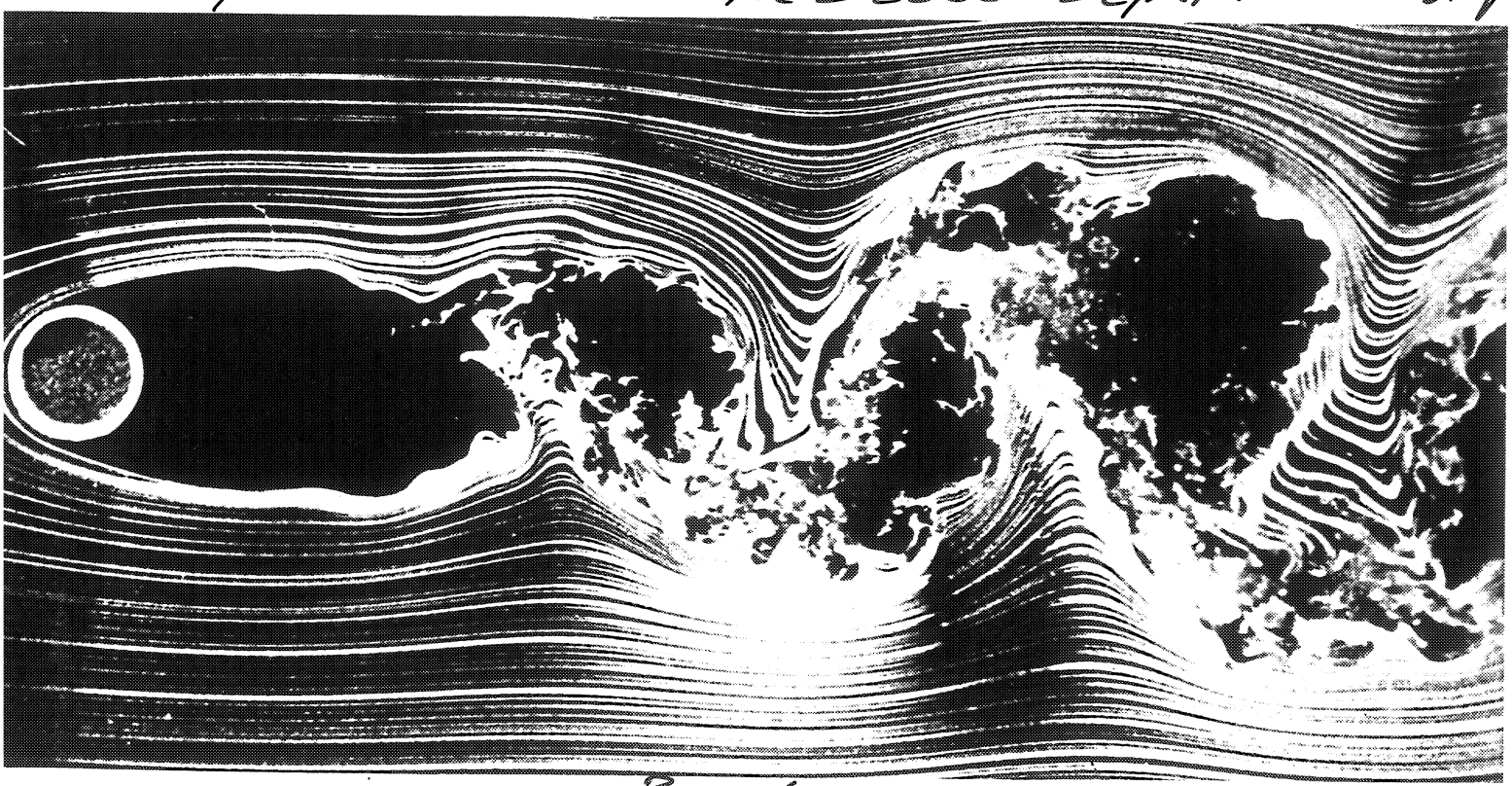

Re = 10 000

48. Circular cylinder at R=10,000. At five times the speed of the photograph at the top of the page, the flow pattern is scarcely changed. The drag coefficient consequently remains almost constant in the range of Reynolds number spanned by these two photographs. It drops later when, as in figure 57, the boundary layer becomes turbulent at separation. *Photograph by Thomas Corke and Hassan Nagib*

WERLE, 1972
CORKE & NAGIB, 1982

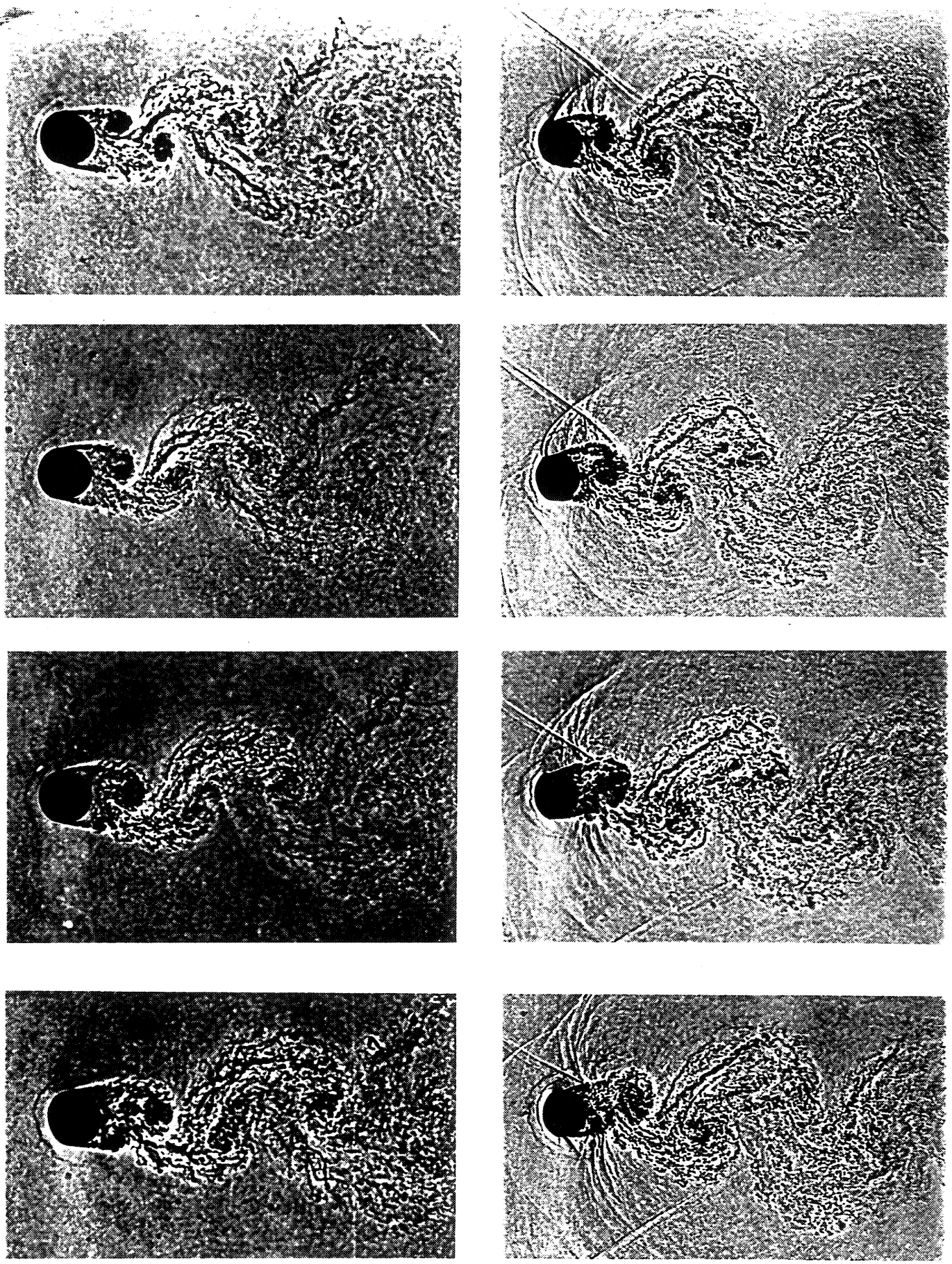

221. Vortex street behind a cylinder. Multiple-spark shadowgraphs taken at the rate of 30,000 per second show one-third of a period of vortex shedding from a circular cylinder. On the left is purely subsonic flow at free-stream Mach number 0.45 and Reynolds number 110,000; on the right is intermittently supercritical flow at M=0.64 and R=1.35 million. The cylinder is slightly distorted by parallax. *Dyment, Gryson & Ducruet 1980*

Re = 110 000
Ma = 0.45

Re = 1 350 000
Ma = 0.64

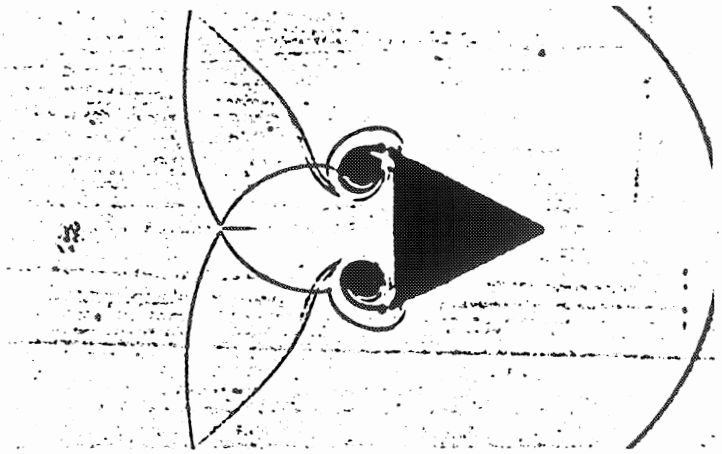

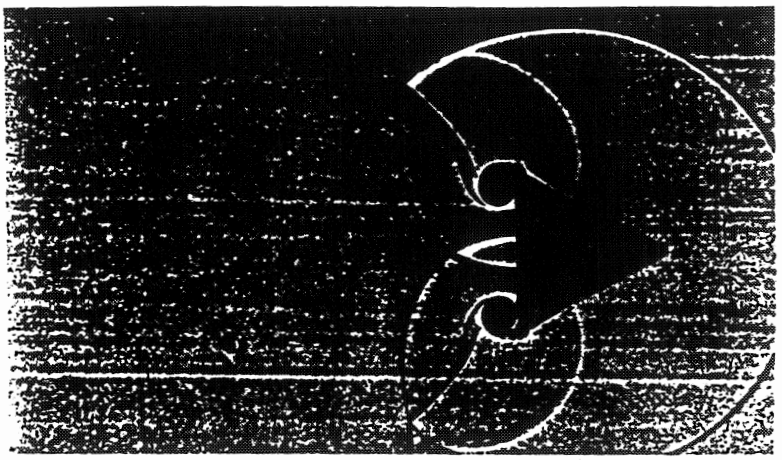

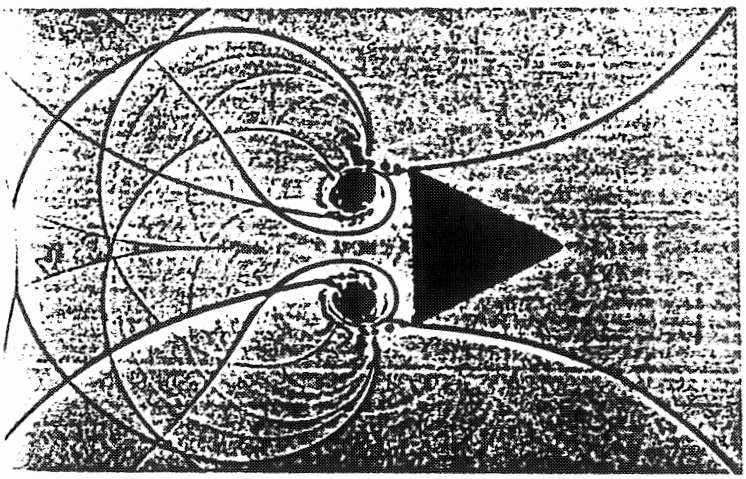

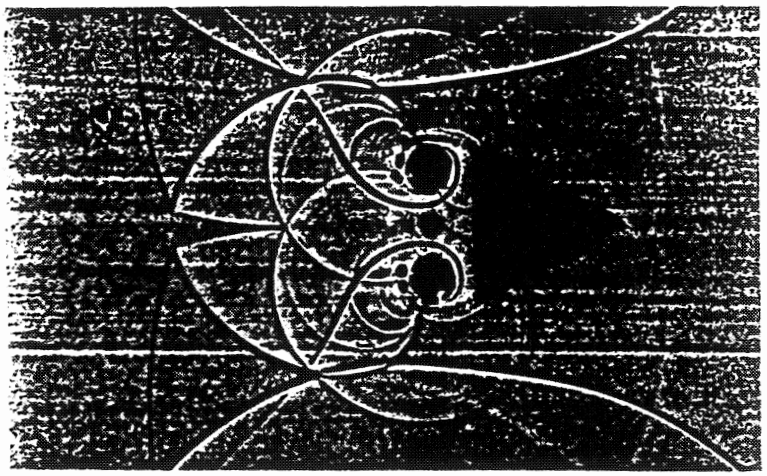

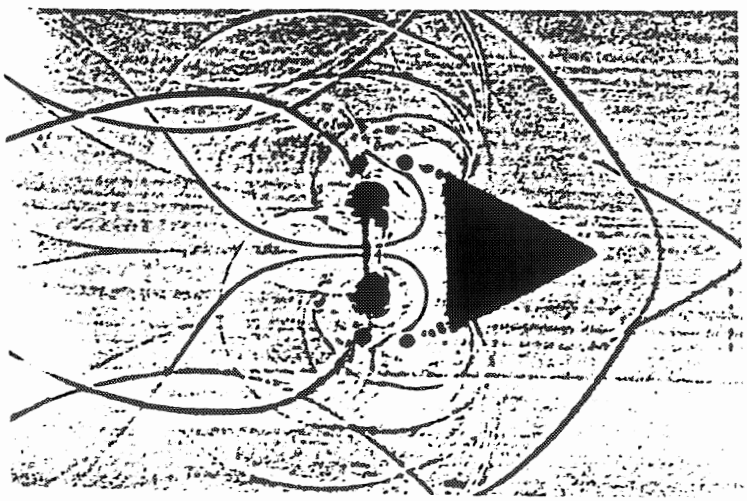

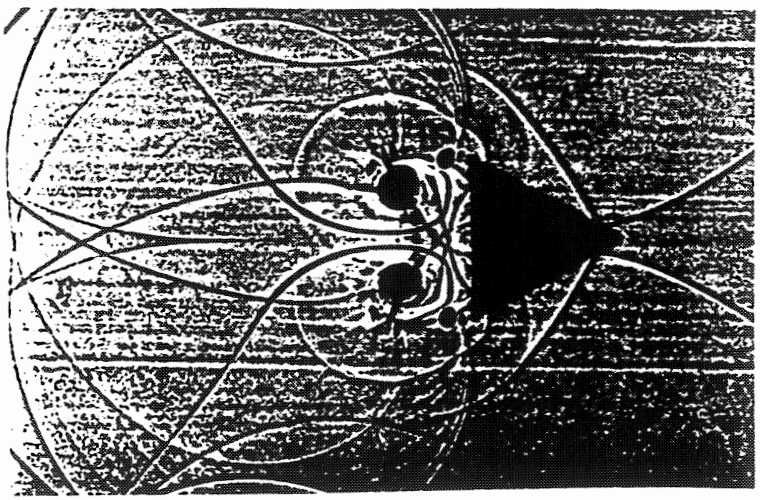

Diffraction of
a shock wave by
a finite wedge.
Flow separation
and vortex emission

BOUNDARY LAYER THEORY

Lamb, 1932
'The motion of a solid in a liquid endowed with vorticity is a problem of considerable interest, but is unfortunately not very tractable.'

Boundary layer theory is treated as a strong interaction between the convection by external flow fields and its own self-induced velocity of the vorticity produced by viscous diffusion from a wall.

Boundary layer separation is the highly non trivial matter of determining when and under what conditions vorticity is convected away from boundaries.

Küchemann, 1965
'Vortices are the sinews and muscles of fluid motions.' Keith Moffatt uses this remark in the title of one of his papers.

LAMINAR BOUNDARY LAYERS

$$Re = \frac{UL}{\nu} = \frac{U^2/L}{\nu U/L^2} = \frac{\text{inertia term}}{\text{viscous term}}$$

$\Rightarrow$ viscous term $\ll$ inertia term for large Re.

But it is impossible to neglect the viscous term everywhere in the flow due to boundary conditions and/or initial conditions.

In particular a laminar boundary layer has to exist in the flow along a solid surface to satisfy the no-slip condition: $\vec{v}_p = 0$.

Laminar boundary layer

In the vicinity of boundaries the flow becomes laminar, i.e. such that $\frac{U^2}{L} \sim \frac{\nu U}{\ell^2}$

ℓ being the thickness of the laminar boundary layer which is related to L such that

$$\ell \sim \left(\frac{\nu}{UL}\right)^{1/2} L = Re^{-1/2} L$$

This length is a transverse length scale

which characterizes the molecular diffusion of momentum deficit across the flow away from the boundary.

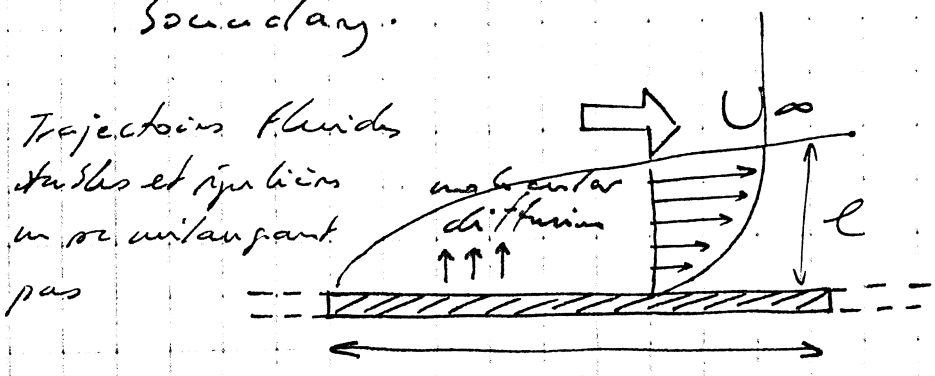

L → caractéristique boundary layer thickness at the end of the plate.

$\ell \sim Re_L^{-1/2} L$

⇒ large Re at constant L smaller ℓ

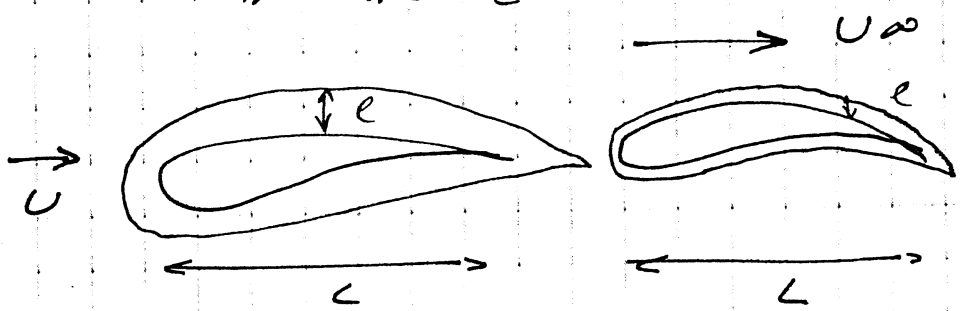

Drag per unit span = total rate of loss of momentum

$$C_D \equiv \frac{\text{diffusive loss of momentum}}{\text{total momentum}} = \frac{\rho U^2 \ell}{\frac{1}{2}\rho U^2 L} \sim 2\frac{\ell}{L} \sim 2Re_L^{-1/2}$$

WALL LAW

Turbulent boundary layer

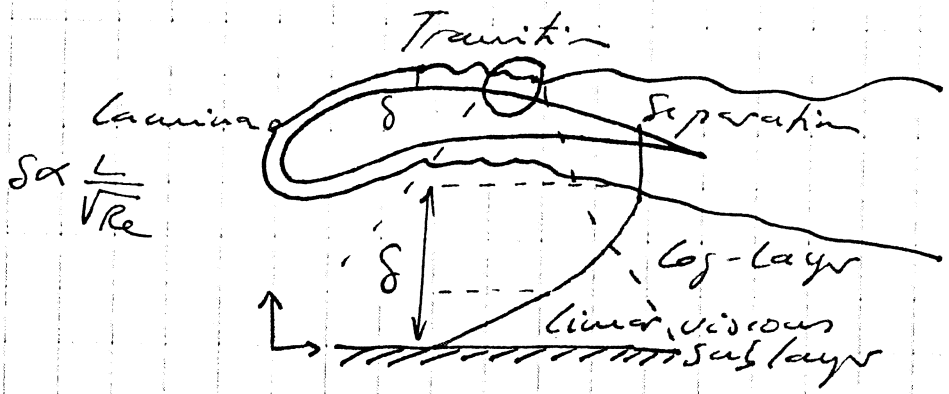

Experiments show some universality in the behaviour of <u>turbulent attached boundary layers</u>. The wall-law fails as soon as there is detachment.

Wall variable

$$U(x) = \lim_{T \to \infty} \frac{1}{T} \int_0^T u(x,t)$$

time averaged velocity

Wall velocity (nondimensional)

$$u^* = \sqrt{\nu \left.\frac{\partial U_1}{\partial x_2}\right|_{x_2=0}}$$

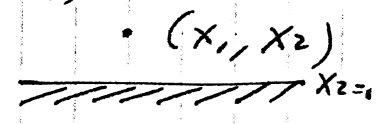

$$u^+ = \frac{U}{u^*}$$

Distance to the wall in wall units (nondimensional)

$$y^* = \frac{\nu}{u^*} \qquad y^+ = \frac{y}{y^*}$$

(1) Remark: If is necessary to verify a posteriori that:

$$20\sqrt{\nu\left|\frac{\partial u}{\partial n}\right|^{-1}} \leq \delta < 100\sqrt{\nu\left|\frac{\partial u}{\partial n}\right|^{-1}}$$

logarithmic layer

Experiments show that when $20 \leq y^+ \leq 100$, in the logarithmic layer, there is a universal formula for the scaled mean flow u^+ is:

$$u^+ = \frac{1}{C_k}\log y^+ + \beta$$

$C_k = 0.41$ Von Karman constant.

$\beta = 5.5$

Viscous sub layer

Near to the wall for $0 \leq y^+ \leq 20$ the scaled mean flow u^+ is almost linear in y^+:

$$u^+ = y^+$$

Application

These formulae are nonlinear relations between u and $\frac{\partial u}{\partial n}$. Our solves N.S. equations with the following boundary conditions, called a wall-law:

$$\left.\begin{aligned} \frac{u.t}{\sqrt{\nu\left|\frac{\partial u}{\partial n}\right|}} - \frac{1}{C_k}\log\left(\delta\sqrt{\frac{1}{\nu}\left|\frac{\partial u}{\partial n}\right|}\right) + \beta = 0 \\ u.n = 0 \end{aligned}\right\} (1)$$

TURBULENT BOUNDARY LAYERS

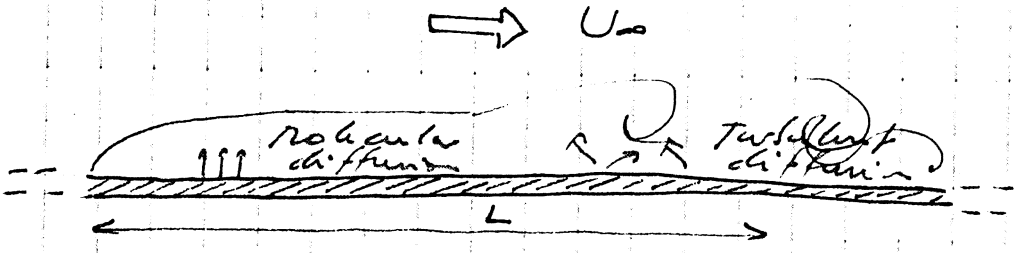

Couche limite laminaire

Transition $Re \sim 10^6$

Couche limite turbulente

$\ell \sim Re^{-1/2} L$

Trajectoires fluides stables et régulières

$\vec{V}, P$

$\ell \sim \frac{v'}{U} L$

Trajectoires fluides instationnaires et irrégulières

$\vec{V} + v', \ \vec{P} + p'$

La décélération des fluides près de la paroi produit le phénomène de décollement ou séparation de la couche limite qui affecte l'écoulement dans son ensemble.

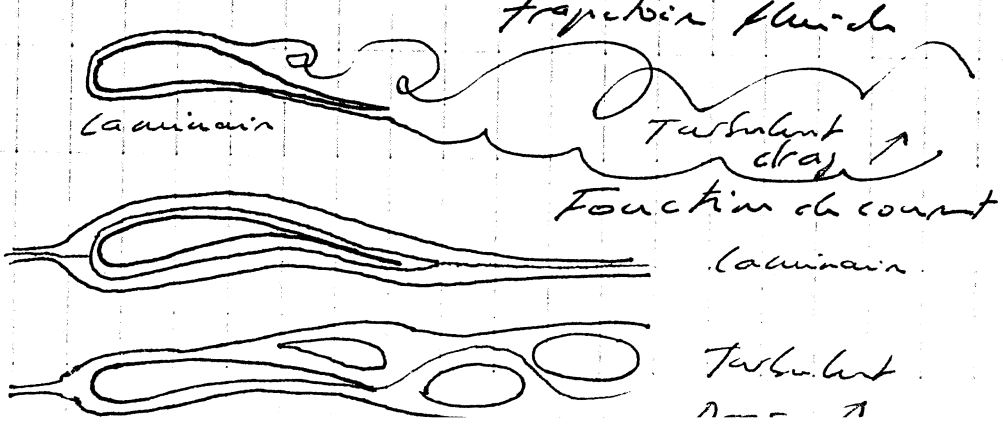

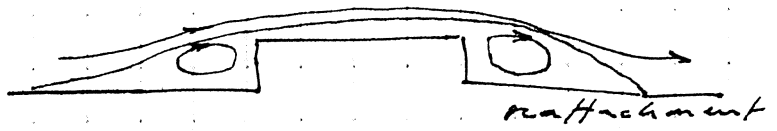

Pour $Re \gg 1$ le calcul de l'écoulement autour d'un profil se décompose en 2 problèmes :

1. le problème extérieur où l'on suppose le fluide idéal ($\nu \to 0, l \to 0$)
   $V_n = 0$ et $\vec{V}$ tangent à la paroi,
2. le problème intérieur de la couche limite où le fluide est visqueux et $\vec{V}_1 = (V_n, V_t) = \vec{0}$, tandis que la vitesse à la limite extérieure de la couche est donnée par la résolution du problème 1.

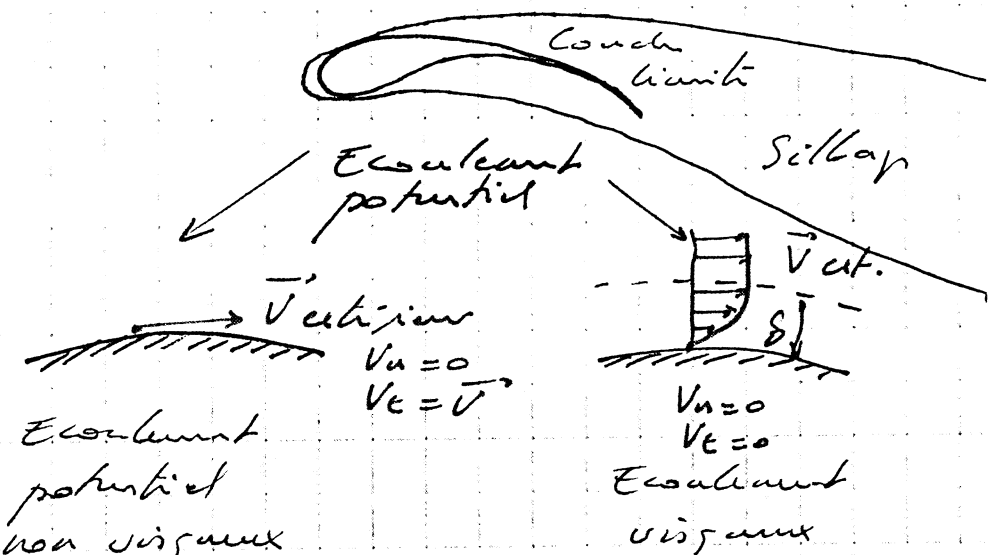

C'est dans la couche limite que vont se développer les processus de création, de transport et de destruction de la turbulence qui influencent le transport de quantité de mouvement global.

STATISTICAL TOOLS

(RAPPELS)

- Fourier transform
- Statistical moments
- Autocorrelation function
- Wavelet transform
- Probability Density Function
- Skewness, Flatness
- Gaussian distribution
- Structure functions

TRANSFORMEE DE FOURIER

Fourier Transform

Definition

$$f(x) = \frac{1}{\sqrt{2\pi}} \int_{-\infty}^{+\infty} \hat{f}(k)\, e^{ikx}\, dk \quad \text{TF synthèse inverse } (e^+)$$

$$\hat{f}(k) = \frac{1}{\sqrt{2\pi}} \int_{-\infty}^{+\infty} f(x)\, e^{-ikx}\, dx \quad \text{TF analyse directe } (e^-)$$

Properties

similarity dilatation $\quad \widehat{f(\lambda x)} = \frac{1}{\lambda} \hat{f}\left(\frac{k}{\lambda}\right)$

modulation, homogeneity in k $\quad \widehat{e^{i\pi x}} = \delta\left(k - \frac{1}{2}\right)$

$$\widehat{f(x)\cos x} = \frac{1}{2}\left[\hat{f}\left(k - \tfrac{1}{2}\right) + \hat{f}\left(k + \tfrac{1}{2}\right)\right]$$

translation, homogeneity in x $\quad \widehat{\delta\left(x - \tfrac{1}{2}\right)} = e^{-i\frac{1}{2}k}$

$$\widehat{f(x - x_0)} = e^{-ix_0 k}\, \hat{f}(k)$$

linearity, Addition

$$\widehat{f(x) + g(x)} = \hat{f}(k) + \hat{g}(k)$$

Duality physical / spectral spaces

Average of $f(x)$ $\quad \int_{-\infty}^{+\infty} f(x)\, dx = \hat{f}(0)$

Smoothness

The smoother $f(x)$, as measured by the number of continuous derivatives it has, the more compact its transform $\hat{f}(k)$, that is the faster it decays when $k \to \infty$.

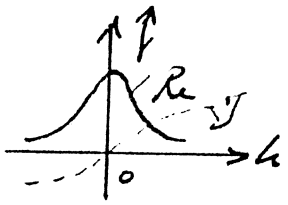

TF of real signals

If $f(x) \in \mathbb{R}$, then $\hat{f}(k) \in \mathbb{C}$ is Hermitian

namely / $Re[\hat{f}(k)]$ is even (pair) and / $\hat{f}(k) = \hat{f}^*(-k)$

$Im[\hat{f}(k)]$ is odd (impair) / autoconjugaison.

Remark

La transformée de Fourier permet de passer de l'algèbre de convolution à l'algèbre des produit de manière encore plus aisé.

Derivation $\widehat{\frac{\partial^m}{\partial x^m} f(x)} = (ik)^m \hat{f}(k)$

Moments $\widehat{x^m f(x)} = i^m \frac{\partial^m}{\partial k^m} \hat{f}(k)$

Parity pair (even) $f(-x) = f(x)$ cos $\hat{f}(-k) = \hat{f}(k)$

impair (odd) $f(-x) = -f(x)$ sin $\hat{f}(-k) = -\hat{f}(k)$

Reality $f(x)$ real $\longrightarrow$ $\hat{f}(k) = \hat{f}^*(-k)$ even

$f(x)$ imagin. $\longrightarrow$ $\hat{f}(k) = -\hat{f}^*(-k)$ odd

Rotation in $\mathbb{R}^n$ it is conserved $R[\hat{f}(x)] = R[\hat{f}(k)]$

Différentes écritures de la Transformée de Fourier

En traitement du signal $\quad f(x) \xrightarrow{\mathcal{F}} \hat{f}(k)$

ex: $e^{-\pi x^2} \longrightarrow e^{-\pi k^2}$

$$\hat{f}(k) = \int_{-\infty}^{+\infty} f(x)\, e^{-2i\pi k x}\, dx \qquad \mathcal{F}$$

k wavenumber in cycles/unit length

$$f(x) = \int_{-\infty}^{+\infty} \hat{f}(k)\, e^{+2i\pi k x}\, dk \qquad \mathcal{F}$$

$$\int |f(x)|^2 dx = \int |\hat{f}(k)|^2 dk \qquad \widehat{f(x) * g(x)} = \hat{f}(k) \cdot \hat{g}(k)$$

$$f(x) = \mathcal{F}^{-1}\mathcal{F}(f(x)) \qquad \widehat{\frac{\partial^n f(x)}{\partial x^n}} = (2i\pi k)^n \hat{f}(k)$$

$$\langle x^2 \rangle \langle k^2 \rangle \geq \frac{1}{8\pi^2}$$

En analyse harmonique $\quad f\left(\frac{x}{\sqrt{2\pi}}\right) \xrightarrow{\mathcal{F}} \hat{f}\left(\frac{k}{\sqrt{2\pi}}\right)$

ex: $e^{-\frac{x^2}{2}} \longrightarrow e^{-\frac{k^2}{2}}$

$$\hat{f}(k) = \frac{1}{\sqrt{2\pi}} \int_{-\infty}^{+\infty} f(x)\, e^{-ikx}\, dx \qquad \mathcal{F}$$

$$f(x) = \frac{1}{\sqrt{2\pi}} \int_{-\infty}^{+\infty} \hat{f}(k)\, e^{+ikx}\, dk \qquad \mathcal{F}^{-1}$$

$$\int |f(x)|^2 dx = \int |\hat{f}(k)|^2 dk \qquad \widehat{f(x) * g(x)} = \frac{1}{\sqrt{2\pi}} \hat{f}(k) \cdot \hat{g}(k)$$

$$f(x) = \mathcal{F}^{-1}\mathcal{F}(f(x)) \qquad \widehat{\frac{\partial^n f(x)}{\partial x^n}} = (ik)^n \hat{f}(k)$$

$$\langle x^2 \rangle \langle k^2 \rangle \geq \frac{1}{2}$$

En théorie des groupes $\quad f(x) \xrightarrow{\mathcal{F}} \hat{f}\left(\frac{k}{2\pi}\right)$

ex: $e^{-\pi x^2} \longrightarrow e^{-\frac{k^2}{4\pi}}$

$$\hat{f}(k) = \int_{-\infty}^{+\infty} f(x)\, e^{-ikx}\, dx \qquad \mathcal{F}$$

k wavenumber in radians/unit length

$$f(x) = \frac{1}{2\pi} \int_{-\infty}^{+\infty} f(k)\, e^{+ikx}\, dk \qquad \mathcal{F}^{-1}$$

$$\int |f(x)|^2 dx = \int \frac{1}{2\pi} |\hat{f}(k)|^2 dk$$

$$f(x) = \mathcal{F}^{-1}\mathcal{F}[f(x)]$$

$$\langle x^2 \rangle \langle k^2 \rangle \geq \frac{1}{2}$$

$$\widehat{f(x) * g(x)} = \hat{f}(k) \cdot \hat{g}(k)$$

$$\widehat{\frac{\partial^n f(x)}{\partial x^n}} = (ik)^n \hat{f}(k)$$

En mécanique quantique

$$\bar{\psi}(p) = \frac{1}{\sqrt{2\pi\hbar}} \int_{-\infty}^{+\infty} e^{-\frac{ipx}{\hbar}} \psi(x)\, dx$$

$$\psi(x) = \frac{1}{\sqrt{2\pi\hbar}} \int_{-\infty}^{+\infty} e^{\frac{ipx}{\hbar}} \bar{\psi}(p)\, dp$$

with $\hbar = \frac{h}{2\pi} \approx 1.05\ 10^{-34}$ J.s Planck constant

$$\int |f(x)|^2 dx = \int |\hat{f}(p)|^2 dp$$

$$f(x) = \mathcal{F}^{-1}\mathcal{F}[f(x)]$$

$$\langle x^2 \rangle \langle p^2 \rangle \geq \frac{\hbar}{2}$$

$$\widehat{f(x) * g(x)} = \frac{1}{\sqrt{2\pi\hbar}} \hat{f}(p) \cdot \hat{g}(p)$$

$$\widehat{\frac{\partial^n f(x)}{\partial x^n}} = \left(\frac{ip}{\hbar}\right)^n \hat{f}(p)$$

Moments

Zeroth moment

$$M_0 = \int_{-\infty}^{+\infty} f(x)\,dx = \hat{f}(0)$$

The mean value of $f(x)$ is given by the central ordinate of $\hat{f}(0)$.

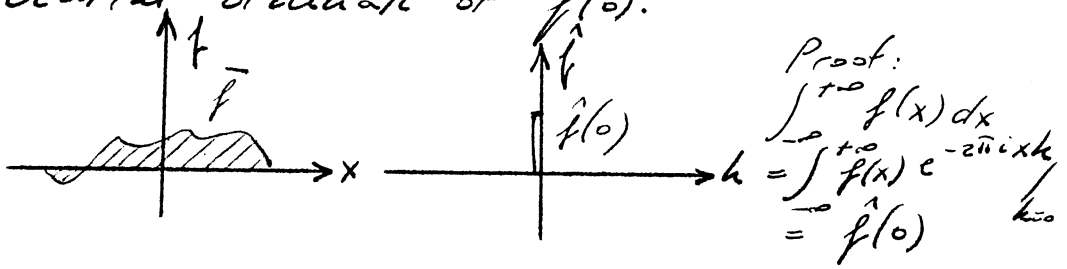

Proof:

$$\int_{-\infty}^{+\infty} f(x)\,dx = \int_{-\infty}^{+\infty} f(x)\,e^{-2\pi i x k}\Big|_{k=0} = \hat{f}(0)$$

First moment — notation used in TF on $e^{2\pi i k x}$: $\frac{-1}{2\pi i} \to i$

$$M_1 = \int_{-\infty}^{+\infty} x\,f(x)\,dx = \frac{-\hat{f}'(0)}{2\pi i}$$

The moment of a mass distribution along a line is given by the slope of $\hat{f}(0)$.

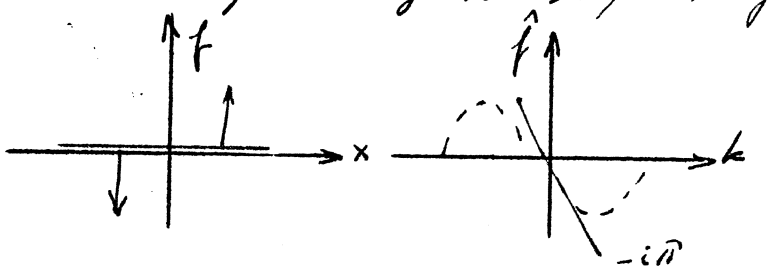

Proof: each impulse has moment $1/4$

$$M_1 = \frac{1}{2} = \frac{-i\pi}{-2\pi i}$$

Centroid

$$\langle x \rangle = \frac{M_1}{M_0} = \frac{-\hat{f}'(0)}{2\pi i \hat{f}(0)}$$

It tells us where the function $f(x)$ is mainly concentrated.

$$x_G = \frac{\int_{-\infty}^{+\infty} x\,[f(x)]^2\,dx}{\int_{-\infty}^{+\infty} [f(x)]^2\,dx}$$

Center of gravity

It is the centroid of $|f(x)|^2$. This avoids the risk of divergence we have with $\int_{-\infty}^{+\infty} f(x)\,dx \to \infty$

Second moment or moment of inertia

$$m_2 = \int_{-\infty}^{+\infty} x^2 f(x)\,dx = \frac{-\hat{f}''(0)}{4\pi^2}$$

The moment of inertia of $f(x)$ is given by the downward curvature of $\hat{f}(0)$.
The behavior of $f(x)$ for large x $(x \to \infty)$ corresponds to the behavior of $\hat{f}(k)$ for low k $(k \to 0)$.

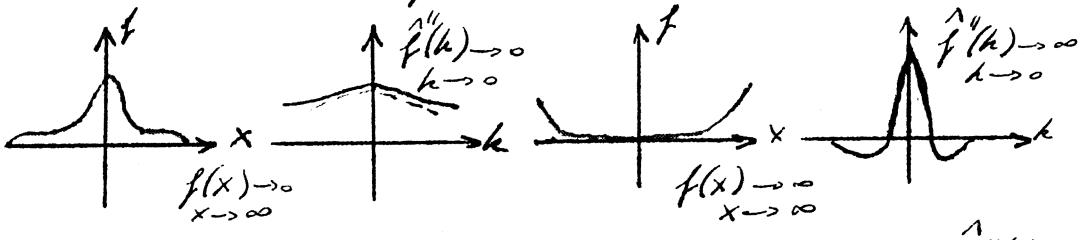

Mean square width

$$\langle x^2 \rangle = \frac{m_2}{m_0} = \frac{-\hat{f}''(0)}{4\pi^2 \hat{f}(0)}$$

Variance

$$\sigma^2 = \langle (x - \langle x \rangle)^2 \rangle = \frac{-\hat{f}''(0)}{4\pi^2 \hat{f}(0)} + \frac{[\hat{f}'(0)]^2}{4\pi^2 [\hat{f}(0)]^2}$$

nth moments

$$m_n = \int_{-\infty}^{+\infty} x^n f(x)\,dx = \frac{\hat{f}^{(n)}(0)}{(-2\pi i)^n}$$

If $f(x) \sim |x|^{-n}$ for $x \to \infty$, then only the first n moments exist. There will be a discontinuity of the $(n+1)^{th}$ order for $\hat{f}(0)$ in $k = 0$.

Moment Theorem for the Fourier transform

Property $\widehat{x^m f(x)} = i^m \frac{\partial^m}{\partial k^m} \hat{f}(k)$

Proof. $\frac{\partial^m}{\partial k^m} \hat{f}(k) = \frac{\partial^m}{\sqrt{2\pi}\partial k^m} \int e^{-ikx} f(x)\,dx$

$= \frac{1}{\sqrt{2\pi}} \int \frac{\partial^m}{\partial k^m} e^{-ikx} f(x)\,dx = \frac{1}{\sqrt{2\pi}} \int (-ix)^m e^{-ikx} f(x)\,dx$

$= \frac{(-i)^m}{\sqrt{2\pi}} \int e^{-ikx} x^m f(x)\,dx = (-i)^m \widehat{x^m f(x)}$

The Fourier transform exchanges derivatives and moments.

If $f(x)$ scales as $|x|^{-m}$ for large $|x|$, then only the first m moments will exist and there will be a discontinuity of the $(m+1)^{th}$ order at $k=0$.

Example

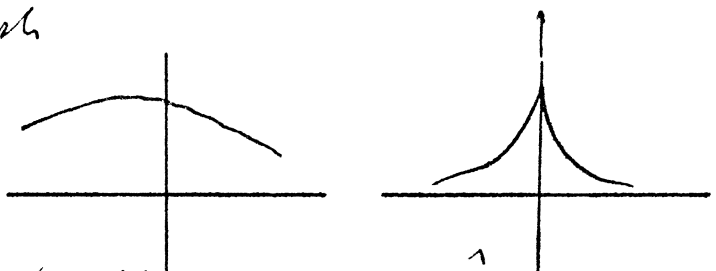

$\int x^2 f(x) \to \infty$ $\qquad$ $\frac{\partial}{\partial k} \hat{f}(k)$ diverges for $k=0$

Autocorrelation function

Definition

$$f * f = \int_{-\infty}^{+\infty} f(x') f^*(x'-x)\,dx' = \int_{-\infty}^{+\infty} f^*(x') f(x'+x)\,dx'$$

$f * f$ is an even function which differs from the self-convolution $f * f = \int_{-\infty}^{\infty} f(x') f(x-x')\,dx'$

In general we normalize it by dividing by the central value, which gives:

$$\gamma(x) = \frac{\int_{-\infty}^{+\infty} f^*(x') f(x'+x)\,dx'}{\int_{-\infty}^{+\infty} f(x') f^*(x')\,dx'}$$

Therefore $\gamma(0) = 1$ and $0 \leq |\gamma(x)| \leq 1$

Remark

In computing γ we have lost the original phases, therefore autocorrelation is not a reversible process and it is not possible to recover the original function from which it was derived. Autocorrelation thus involves a loss of information.

Theorem Wiener-Khintchine

If $f(x) = f(k)$ then its autocorrelation function $\int_{-\infty}^{+\infty} f^*(x') f(x'+x)\,dx'$ has the FT $|f(k)|^2$, in short $f(x) * f^*(-x) = |f(k)|^2$.

'In the last decade we have experienced a conceptual shift in our view of turbulence. For flows with strong velocity shear... or other organizing characteristics, many now feel that ***the spectral description has inhibited fundamental progress****. The next "El Dorado" lies in the* ***mathematical understanding of coherent structures*** *in weakly dissipative fluids: the formation, evolution and interaction of metastable vortex-like solutions of nonlinear partial differential equations...'*

Norman Zabusky, 1984

TRANSFORMEE EN ONDELETTES

MOTIVATIONS

Citation
Jean Ville
Théorie et applications de la notion de signal analytique, C&T, 2ième an. n°1, 1948
(Cables et Transmissions)

Si nous considérons en effet un morceau de musique contenant plusieurs mesures (ce qui est le moins que l'on puisse demander) et qu'une note, la par exemple, figure une fois dans le morceau, l'analyse harmonique nous présentera la fréquence correspondante avec une certaine amplitude et une certaine phase, sans localiser le la dans le temps. Or, il est évident qu'au cours du morceau il est des instants où l'on n'entends pas le la. La représentation de Fourier est néanmoins mathématiquement correcte parce que les phases des notes voisines du la sont agencées de manière à détruire cette note par interférence lorsqu'on ne l'entend pas et à la renforcer, également par interférence, lorsqu'on l'entend; mais s'il y a dans cette conception une habileté qui honore l'analyse mathématique, il ne faut pas se dissimuler qu'il y a également une défiguration de la réalité: en effet, quand on n'entend pas le la, la raison véritable est que le la n'est pas émis.

Citation
Jean Ville
(suite)

Il est souhaitable de rechercher pour un signal une définition mixte, dans l'esprit de celle préconisée par Gabor : à chaque instant se présentent un certain nombre de fréquences, donnant la hauteur et la finesse du son tel qu'on l'entend ; à chaque fréquence est associée une certaine répartition dans le temps qui définit les intervalles pendant lesquels la note correspondante est émise. On est ainsi conduit à la définition d'un spectre instantané, fonction du temps, donnant la structure d'un signal à un instant donné ; le spectre du signal, au sens usuel du terme, qui donne la structure en fréquences du signal pendant toute sa durée d'émission, s'obtient alors en cumulant tous les spectres instantanés (d'une manière précise, en les intégrant relativement au temps). D'une manière corrélative, on est amené à une répartition des fréquences dans le temps. En intégrant ces répartitions, on reconstitue le signal.

Citation Roger Balian
CRAS 1981

Un principe d'incertitude lort en théorie du signal

On peut avoir intérêt, en théorie des communications, à représenter un signal oscillant par une superposition d'oscillations élémentaires, dont chacune possède à la fois une fréquence et une localisation dans le temps assez bien définies.

L'information utile est en effet souvent véhiculée à la fois par les fréquences émises et par la structure temporelle du signal (l'exemple de la musique est caractéristique).

La représentation d'un signal comme fonction du temps exhibe mal le spectre de fréquences en jeu, alors qu'au contraire son analyse de Fourier masque l'instant d'émission et la durée de chacun des éléments du signal.

Une représentation adéquate devrait combiner les avantages de ces deux descriptions complémentaires, tout en présentant un caractère devant adapté à la théorie des communications.

Citation article
Annual Rev. of Fluid Mech.
Marie Farge, 1992

'Wavelet transforms are recent mathematical techniques, based on group theory and square integrable representations, which allows one to unfold a signal, or a field, into both space and scale, and possibly directions.
They use analyzing functions, called wavelets, which are localized in space. The scale decomposition is obtained by dilating or contracting the chosen analyzing wavelet before convoluting it with the signal. The limited spatial support of wavelets is important because then the behavior of the signal at infinity does not play any role. Therefore the wavelet analysis or synthesis can be performed locally on the signal, as opposed to the Fourier transform which is inherently non local due to the space-filling nature of the Fourier trigonometric functions.

INTEGRAL TRANSFORM PRINCIPLE

Analysis $T_f(k) = \int f(\vec{x})\, \psi_k(\vec{x})\, d\vec{x}$

Synthesis $f(\vec{x}) = \frac{1}{c} \int T_f(k)\, \psi_x(k)\, d\mu(k)$

$\Delta x \cdot \Delta k \geq \text{Cost}$

Shannon:

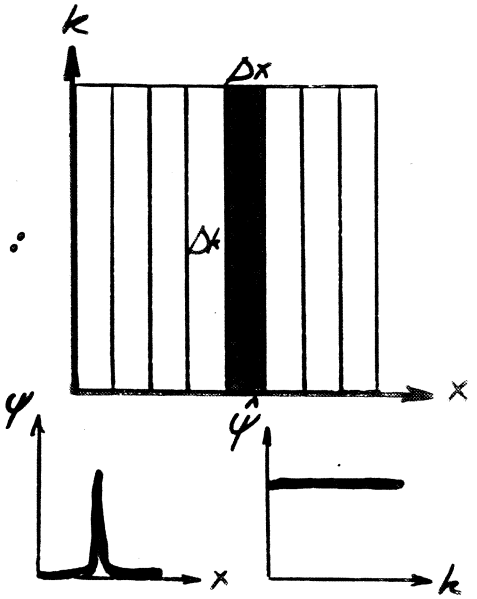

Fourier: (1807)

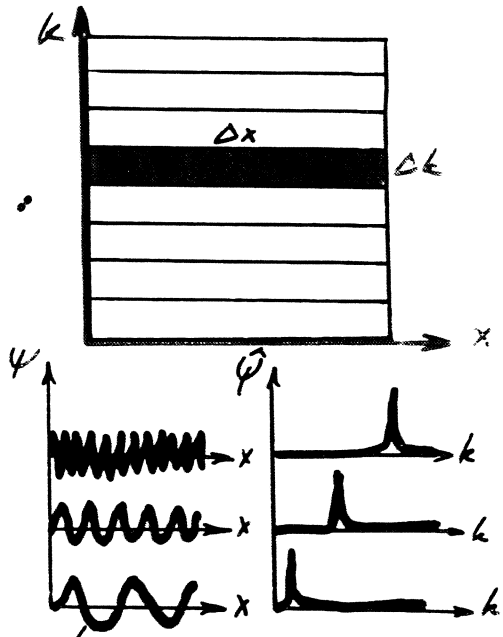

Gabor: (1946)

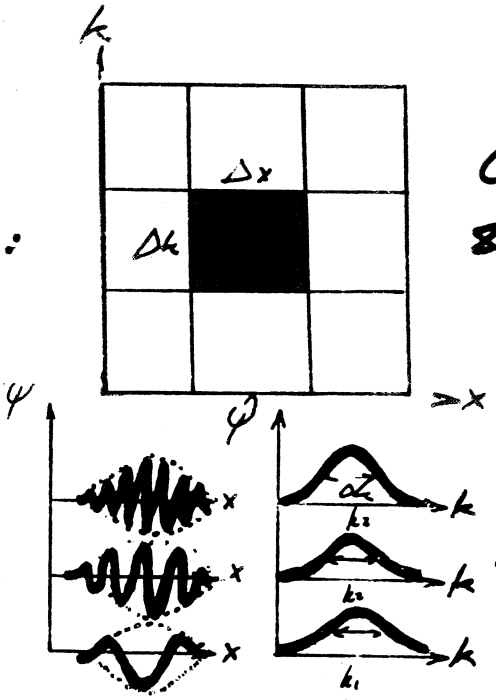

Grossmann & Morlet: (1981)

Balian's construction (1981)

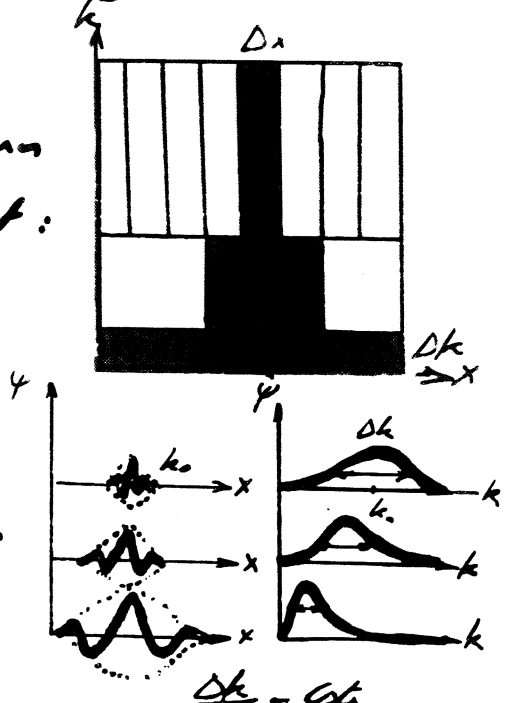

Morlet

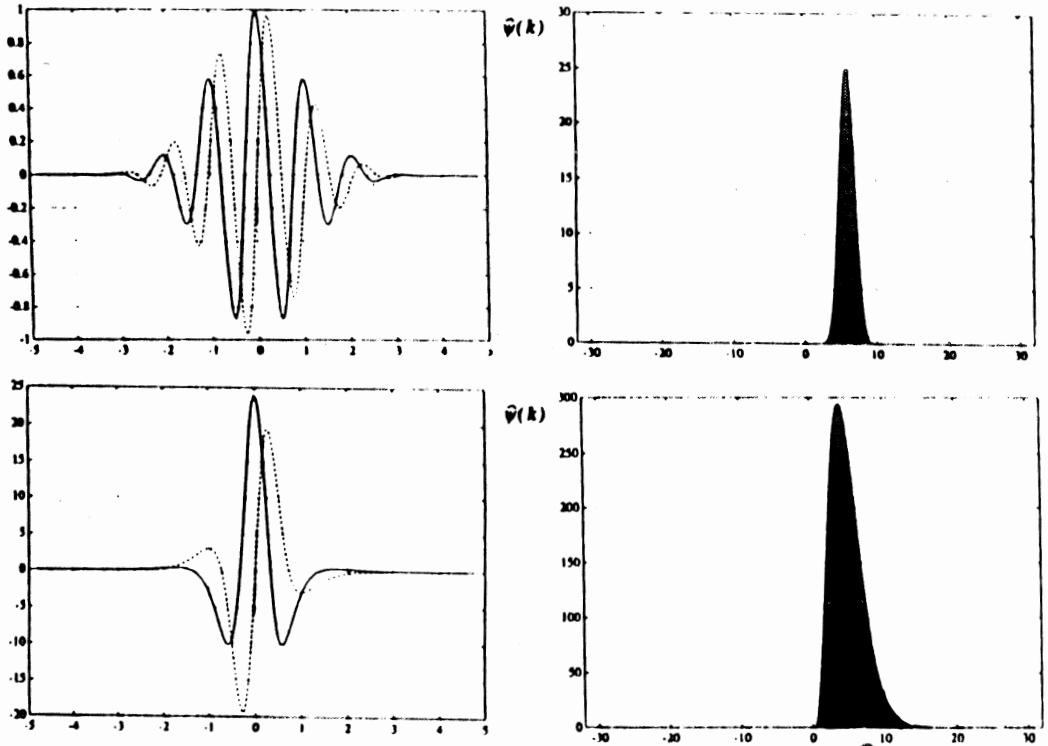

ψ $\hat{\psi}$

Paul

Complex-valued wavelets

Derivatives of a Gaussian

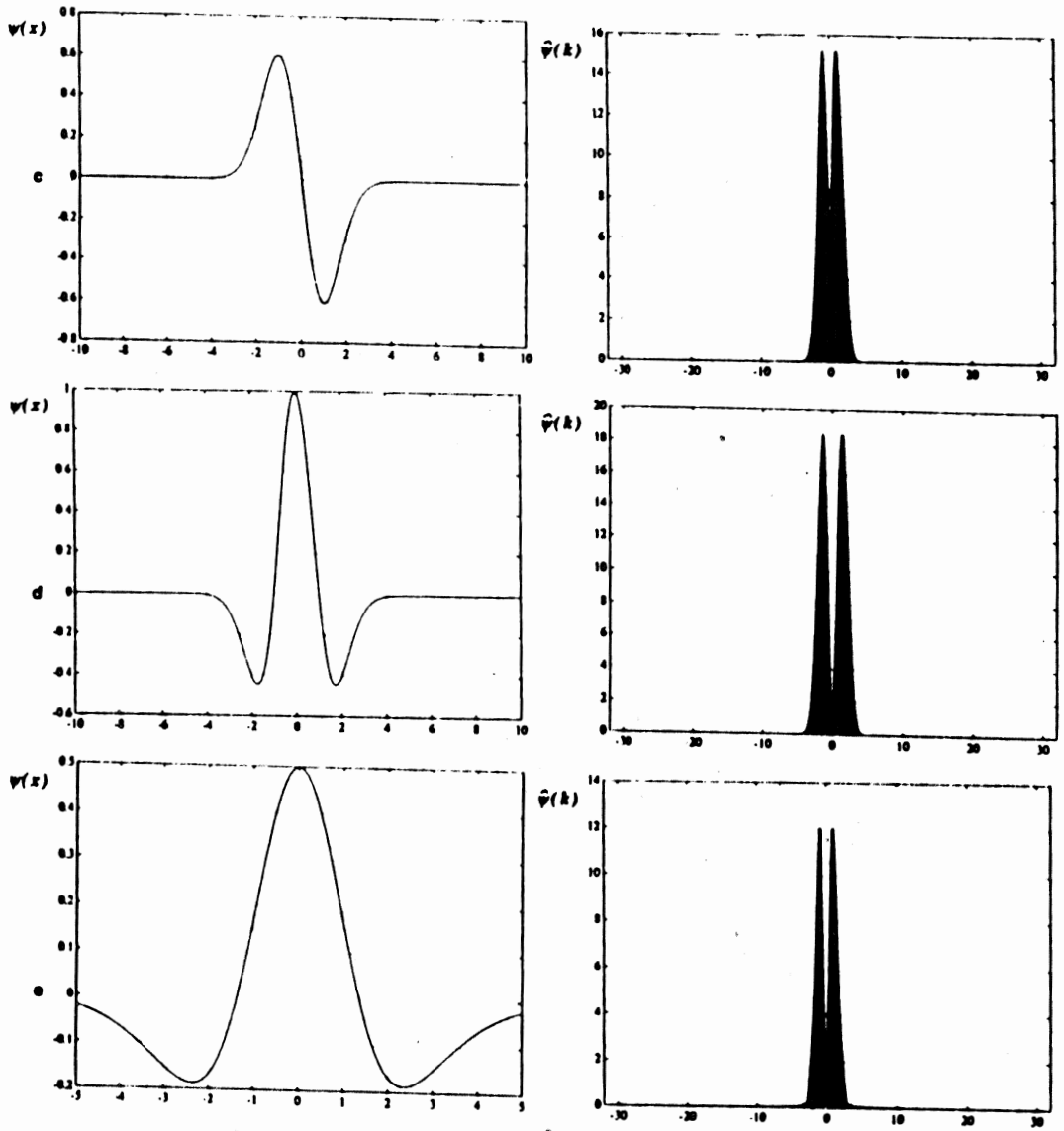

Difference of two Gaussians

ψ $\hat{\psi}$

Real-valued wavelets

N-DIMENSIONAL CONTINUOUS WAVELET TRANSFORM

Choice of the 'mother wavelet'

$$C_\psi = (2\pi)^N \int_{-\infty}^{+\infty} \cdots \int |\hat{\psi}(\vec{k})|^2 \frac{d^N\vec{k}}{|\vec{k}|^N} < \infty$$

Generation of the 'wavelet family'

Euclidean Group with dilation { by translation (vector $\vec{s}$), dilation (parameter $a>0$) and rotation (operator r).

$$\psi_{a,r,\vec{s}}(\vec{x}) = a^{-N/2}\psi(a^{-1}r^{-1}(\vec{x}-\vec{s}))$$

Analysis

$$\tilde{f}(a,r,\vec{s}) = a^{-N/2}\int \overline{\psi}_{a,r,\vec{s}}(\vec{x})\, f(\vec{x})\, d^N\vec{x}$$

Synthesis

$$f(\vec{x}) = \frac{1}{C_\psi}\iiint \psi_{a,r,\vec{s}}(\vec{x})\tilde{f}(a,r,\vec{s})\frac{da\,dr\,d^N\vec{s}}{a^{N+1}}$$

$\frac{da\,dr\,d^N\vec{s}}{a^{N+1}}$: Haar measure

Parseval

$$\int |f(\vec{x})|^2 d^N\vec{x} = \frac{1}{C_\psi}\iiint |\tilde{f}(a,r,\vec{s})|^2 \frac{da\,dr\,d^N\vec{s}}{a^{N+1}}$$

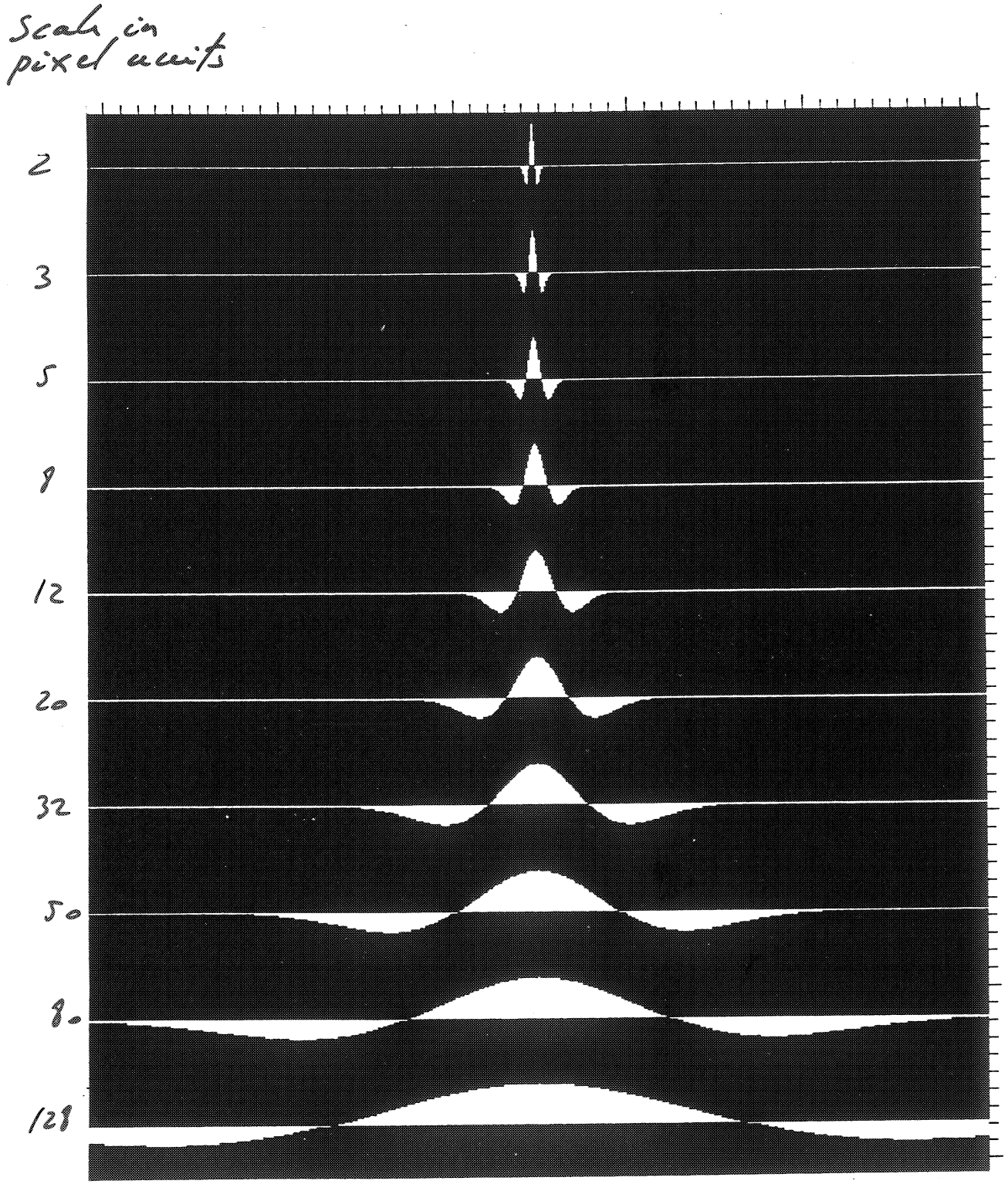

Mexican hat wavelet

$$\psi(x) = -\frac{d^2}{dx^2} e^{-\frac{x^2}{2}} = (1-x^2) e^{-\frac{x^2}{2}}$$

$\psi \in \mathbb{R}$

scale in pixel units

L signal duration

k_{max} Nyquist cut-off frequency

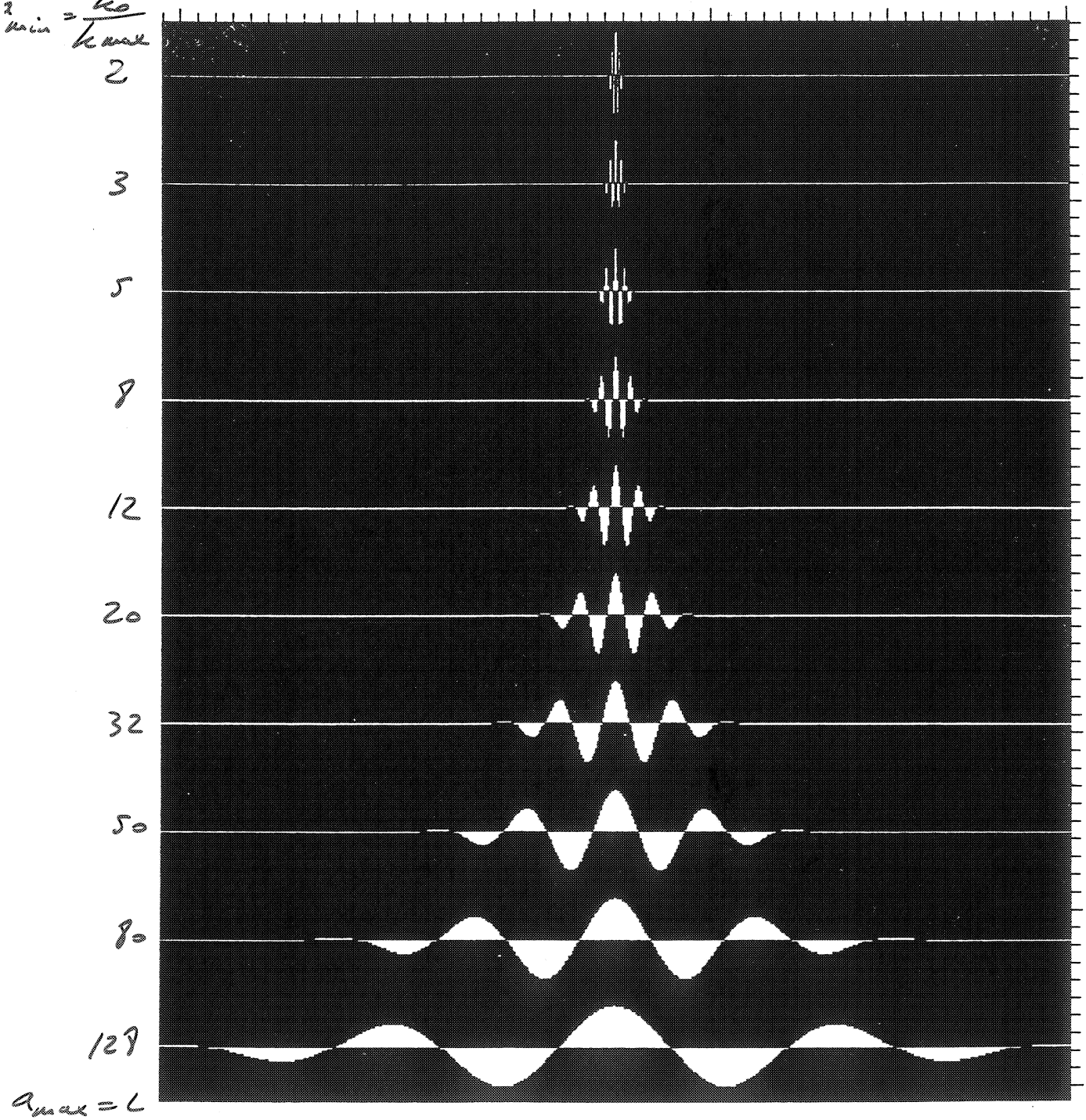

Morlet Wavelet

$$\psi(x) = e^{-ik_0 x} e^{-\frac{x^2}{2}}$$

$$\psi \in \mathbb{C}$$

CONTINUOUS WAVELET TRANSFORM

Choice of the 'mother wavelet'

Admissibility condition:

$$\int |\hat{\psi}(k)|^2 \frac{dk}{|k|} < \infty \Rightarrow \hat{\psi}(0) = 0 \quad \text{i.e.} \int \psi(x)\,dx = 0$$

And, if possible:

Good space (/time) localization,

$$|\psi(x)| < \frac{1}{1+|x|^n}$$

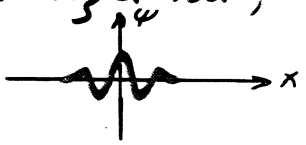

Good scale (/frequency) localization,

$$|\hat{\psi}(k)| < \frac{1}{1+|k-k_0|^n}$$

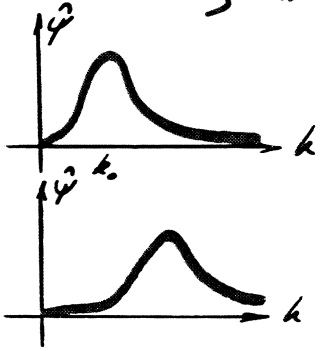

Zero high order moments,

$$\int \psi(x)\, x^n\, dx = 0$$

$$= \left(\frac{d}{dk}\right)^n \hat{\psi}(k)$$

Generation of the 'wavelet family'

Affine group { by translation (parameter s) and dilation (parameter a):

$$\psi_{s,a}(x) = \frac{1}{\sqrt{a}}\,\psi\left(\frac{x-s}{a}\right)$$

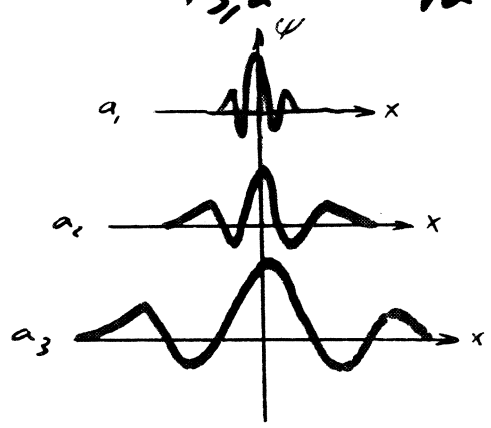

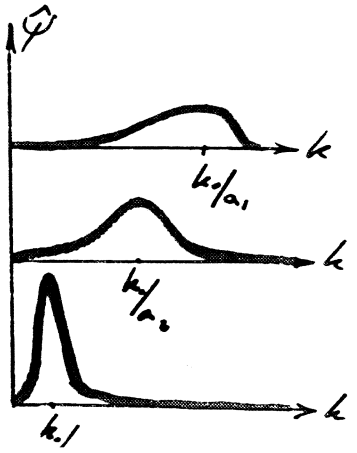

ANALYSIS/SYNTHESIS

Analysis:

$$\tilde{f}(b,a) = \int \overline{\psi_{a,b}}(x)\, f(x)\, dx$$

$$= \frac{1}{\sqrt{a}} \int_{-\infty}^{+\infty} \bar{\psi}\left(\frac{x-b}{a}\right) f(x)\, dx$$

$$= \frac{1}{\sqrt{a}} \int_{-\infty}^{+\infty} \underbrace{\hat{\bar{\psi}}(ak)\, e^{ibk}\, \hat{f}(k)\, dk}_{\text{Filter with } \frac{\Delta k}{|k|} = C^{st}}$$

The wavelet coefficients are defined on the open half-plane $(b,a) \in \mathbb{R} \times \mathbb{R}^+$

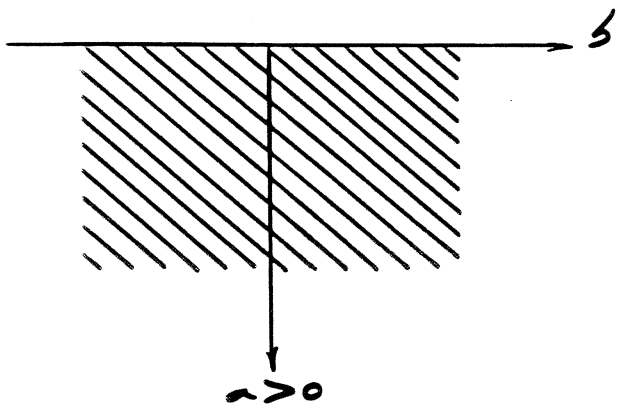

Synthesis

$$f(x) = \frac{1}{C} \iint \psi_{a,b}(x)\, \tilde{f}(b,a)\, \frac{da\,db}{a^2}$$

$$= \frac{1}{C} \int_0^{+\infty} \frac{1}{\sqrt{a}} \int_{-\infty}^{+\infty} \bar{\psi}\left(\frac{x-b}{a}\right) \tilde{f}(b,a)\, \frac{da\,db}{a^2}$$

avec $C = 2\pi \int_{-\infty}^{+\infty} |\hat{\psi}(k)|^2 \frac{dk}{|k|}$

Energy conservation (Parseval):

$$\int |f(x)|^2\, dx = \frac{1}{C} \iint |\tilde{f}(b,a)|^2\, \underbrace{\frac{da\,db}{a^2}}_{\text{Haar Measure}}$$

TeO : EXEMPLES

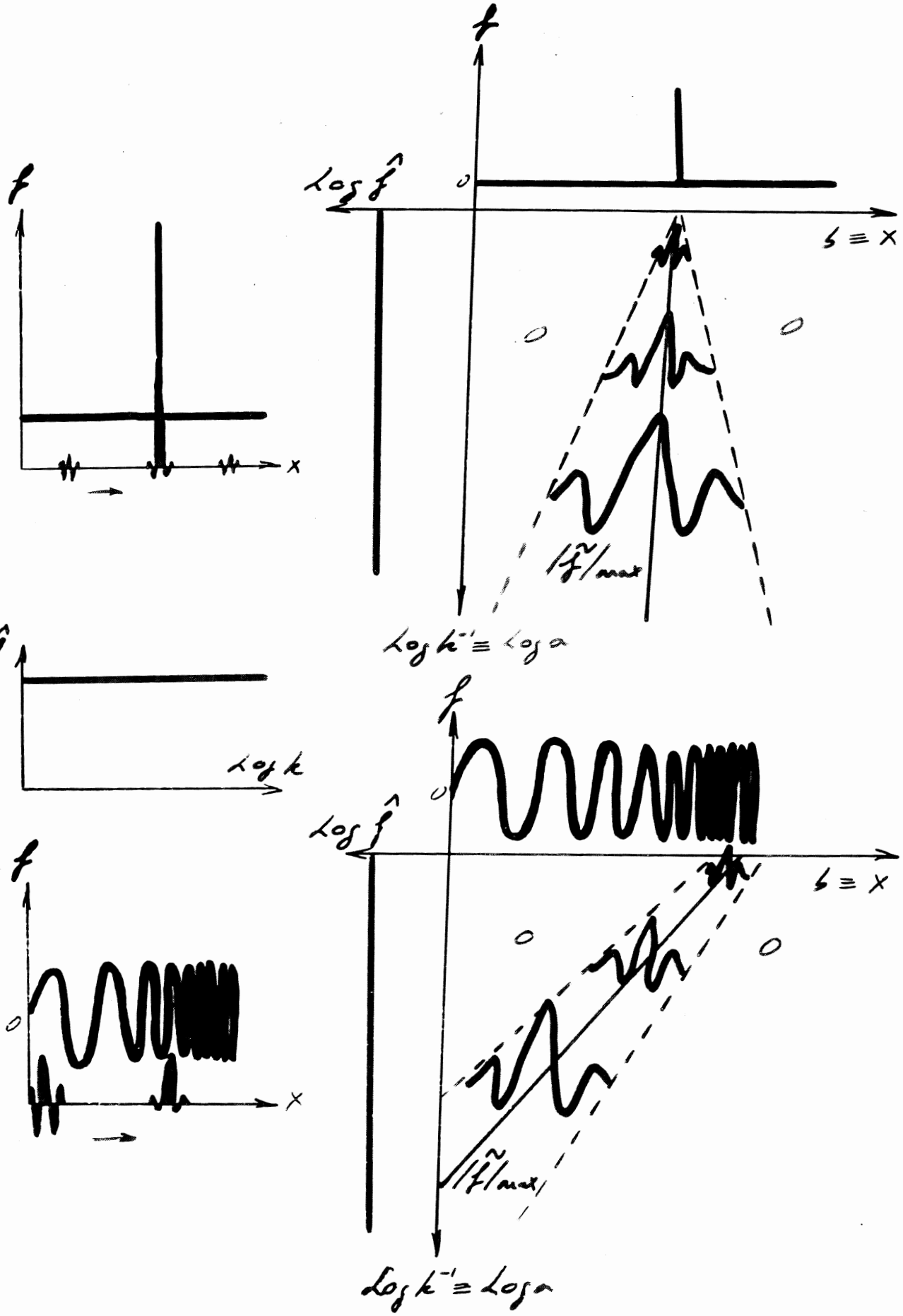

ELEMENTARY PROPERTIES

Linearity $\alpha f_1 + \beta f_2 \longrightarrow \alpha \tilde{f}_1 + \beta \tilde{f}_2$

Covariance

by translation $f(x - x_0) \longrightarrow \tilde{f}(s - x_0, a)$

by dilation $f\left(\frac{x}{a_0}\right) \longrightarrow \frac{1}{a_0} \tilde{f}\left(\frac{s}{a_0}, \frac{a}{a_0}\right)$

Locality

Influence cone of x_0 $\Rightarrow$ locality of the synthesis

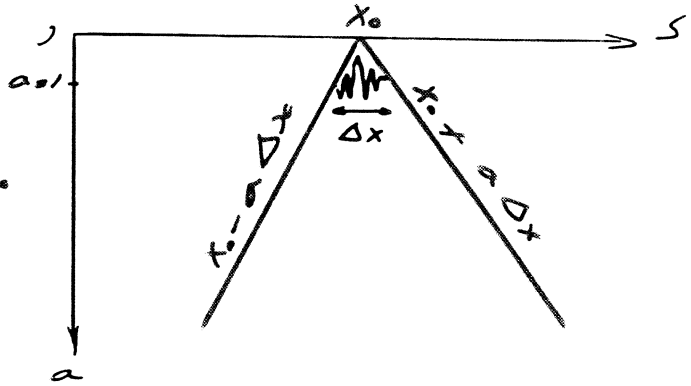

Characterization of the local regularity of a function

If $f(x_0) \in C^\alpha(x_0)$ then

$$\tilde{f}(x_0, a) \underset{a \to 0}{\propto} a^\alpha$$

Ex: f regular in x_0 $\alpha \geq 1$

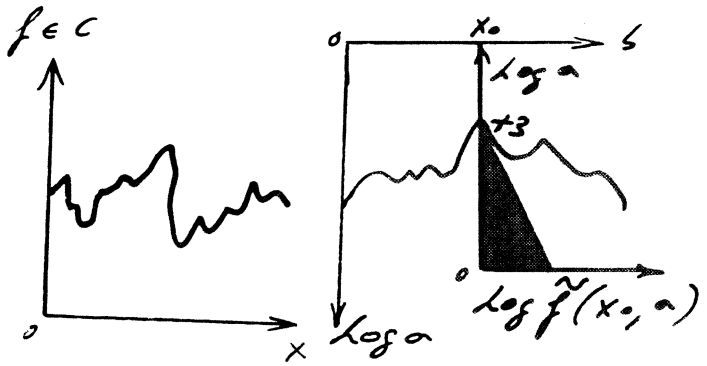

f Lipschitz $\alpha \in]-1, 1[$

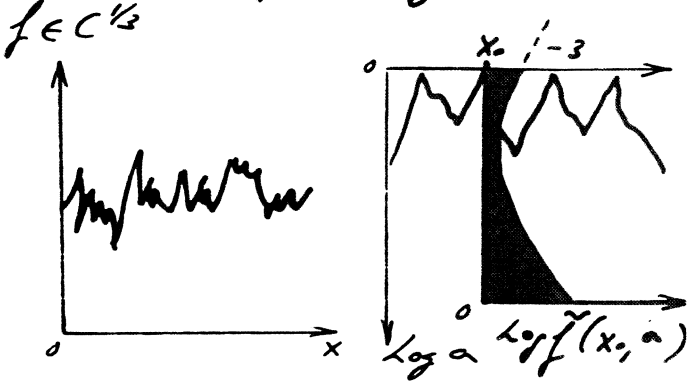

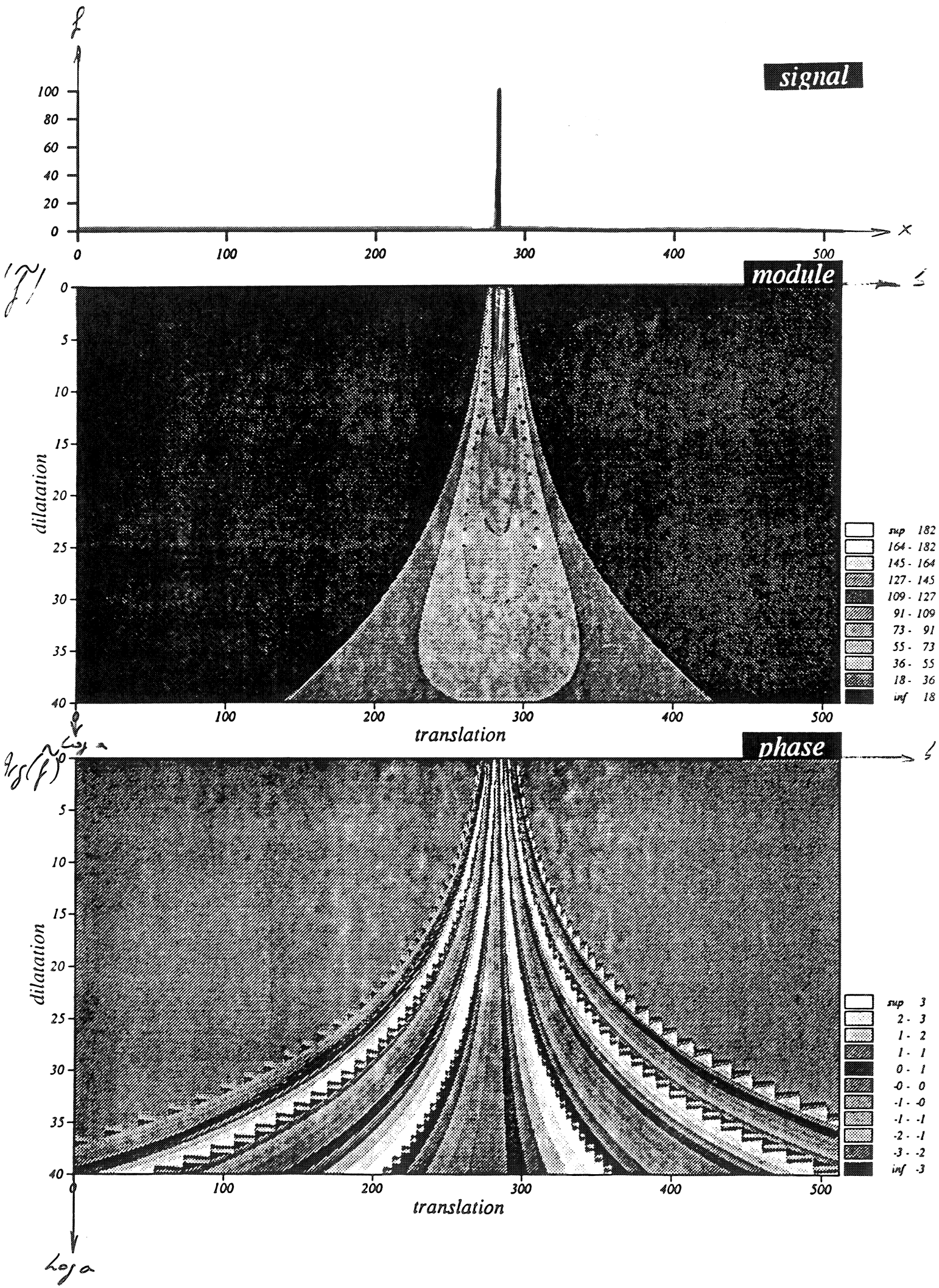
signal
f
x
0
100
200
300
400
500
0
20
40
60
80
100
module
dilatation
translation
0
5
10
15
20
25
30
35
40
sup 182
164 - 182
145 - 164
127 - 145
109 - 127
91 - 109
73 - 91
55 - 73
36 - 55
18 - 36
inf 18
phase
dilatation
translation
sup 3
2 - 3
1 - 2
1 - 1
0 - 1
-0 - 0
-1 - -0
-1 - -1
-2 - -1
-3 - -2
inf -3

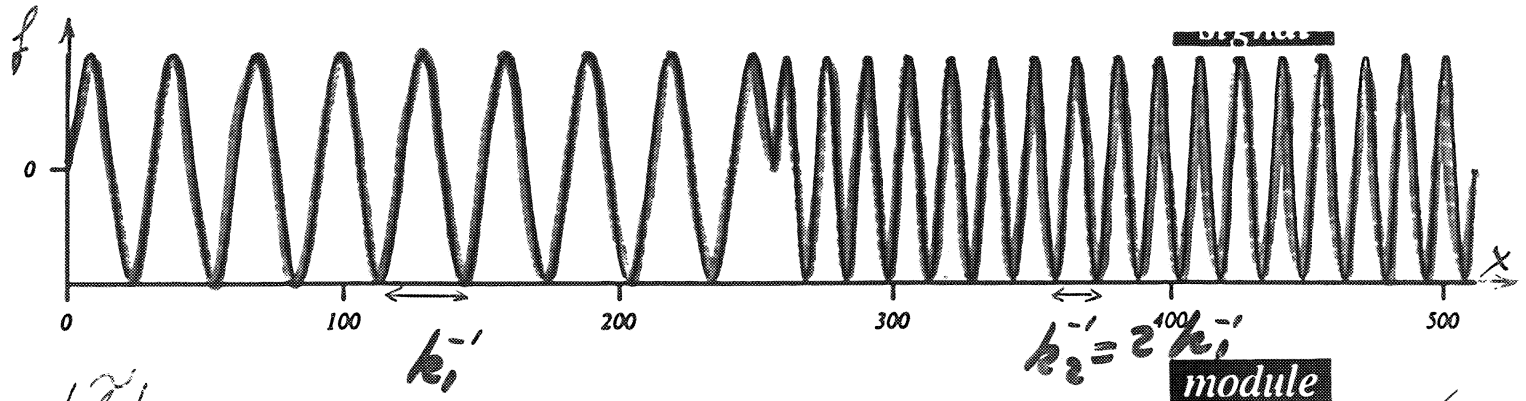
f
0
x
0
100
200
300
400
500
k_1^{-1}
$k_2^{-1} = 2^2 k_1^{-1}$

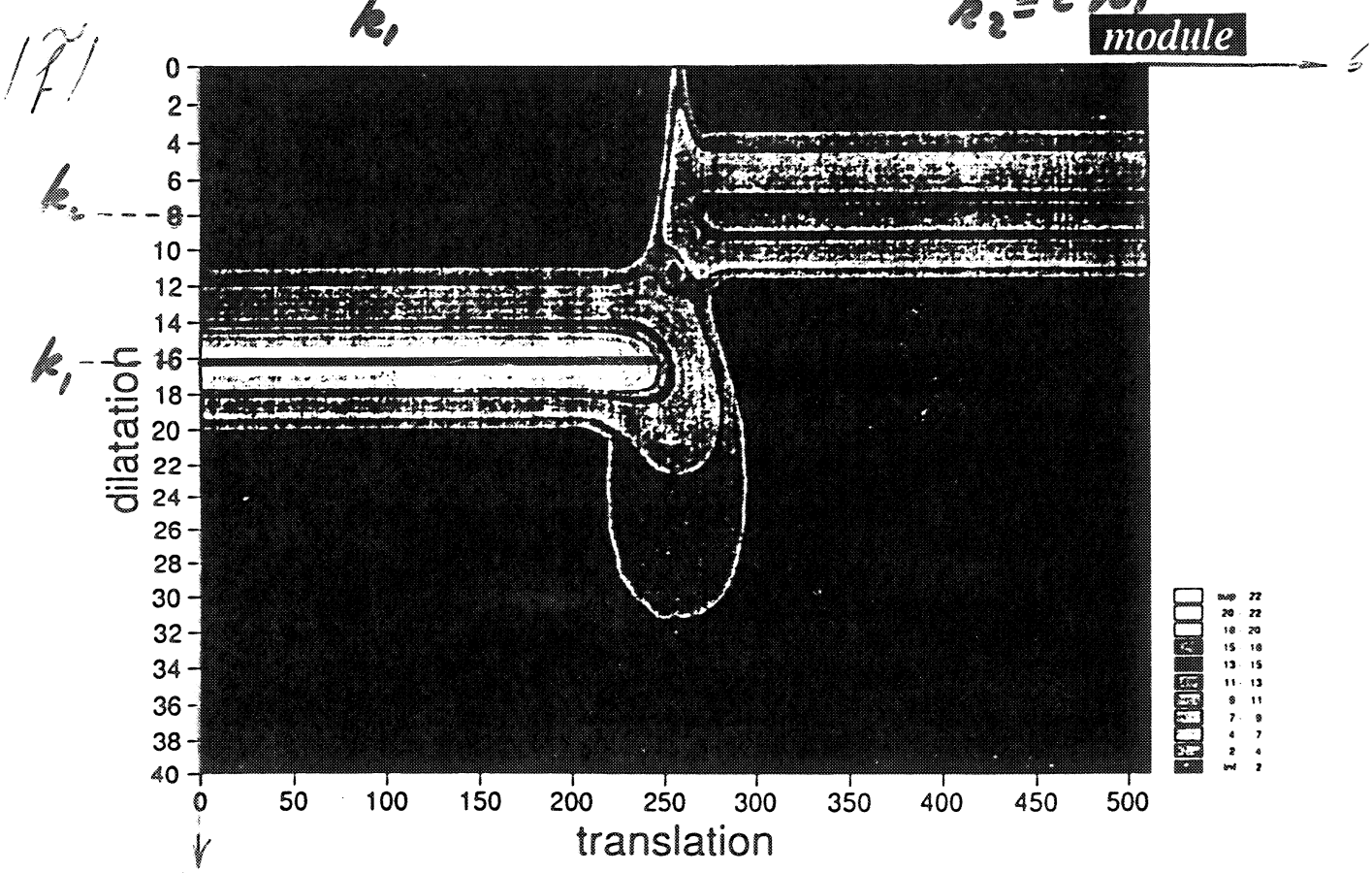
$|\tilde{f}|$
module
s
k_2
k_1
dilatation
translation
0
50
100
150
200
250
300
350
400
450
500
Log a

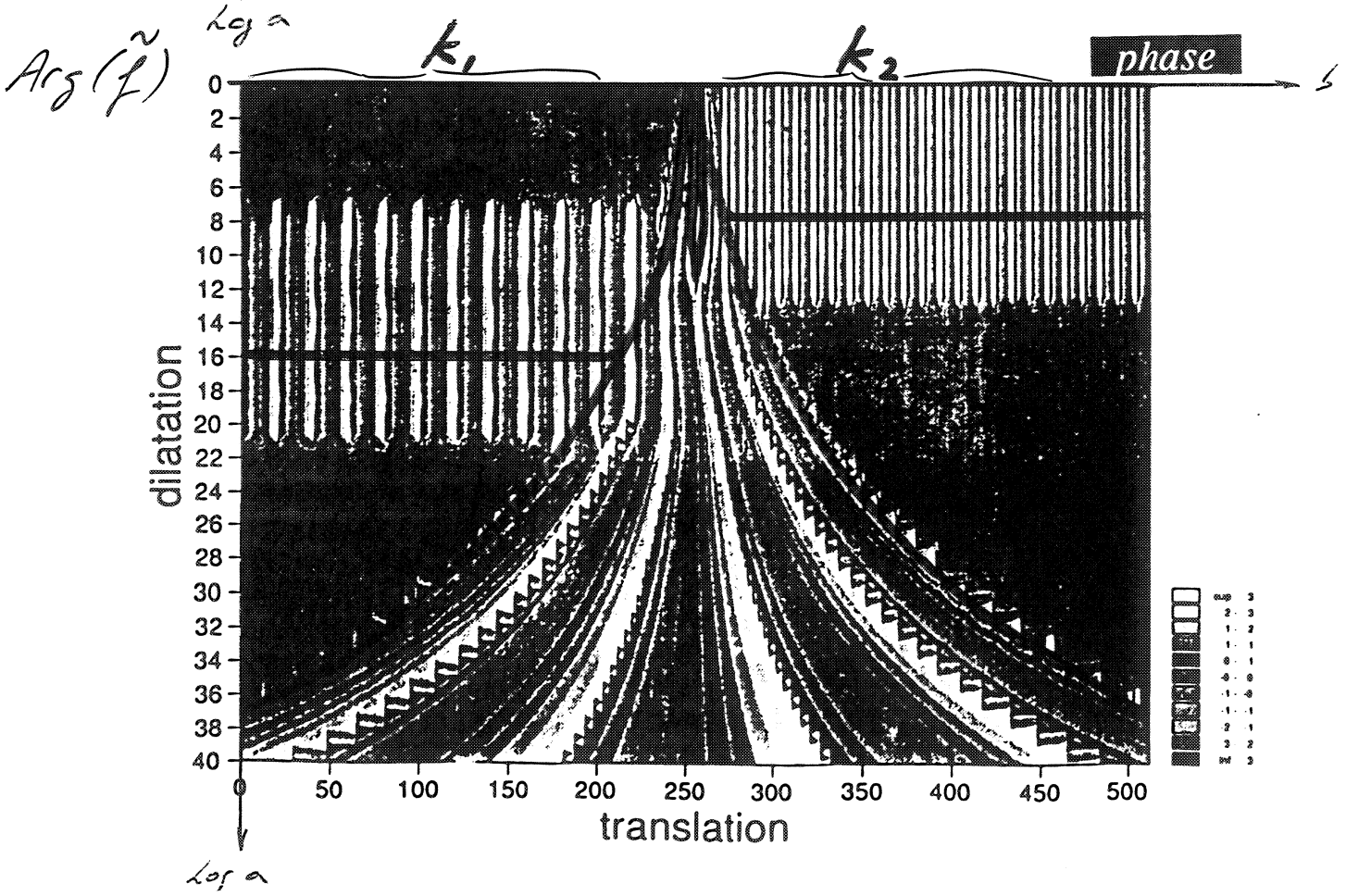
$Arg(\tilde{f})$
phase
s
k_1
k_2
dilatation
translation
0
50
100
150
200
250
300
350
400
450
500
Log a

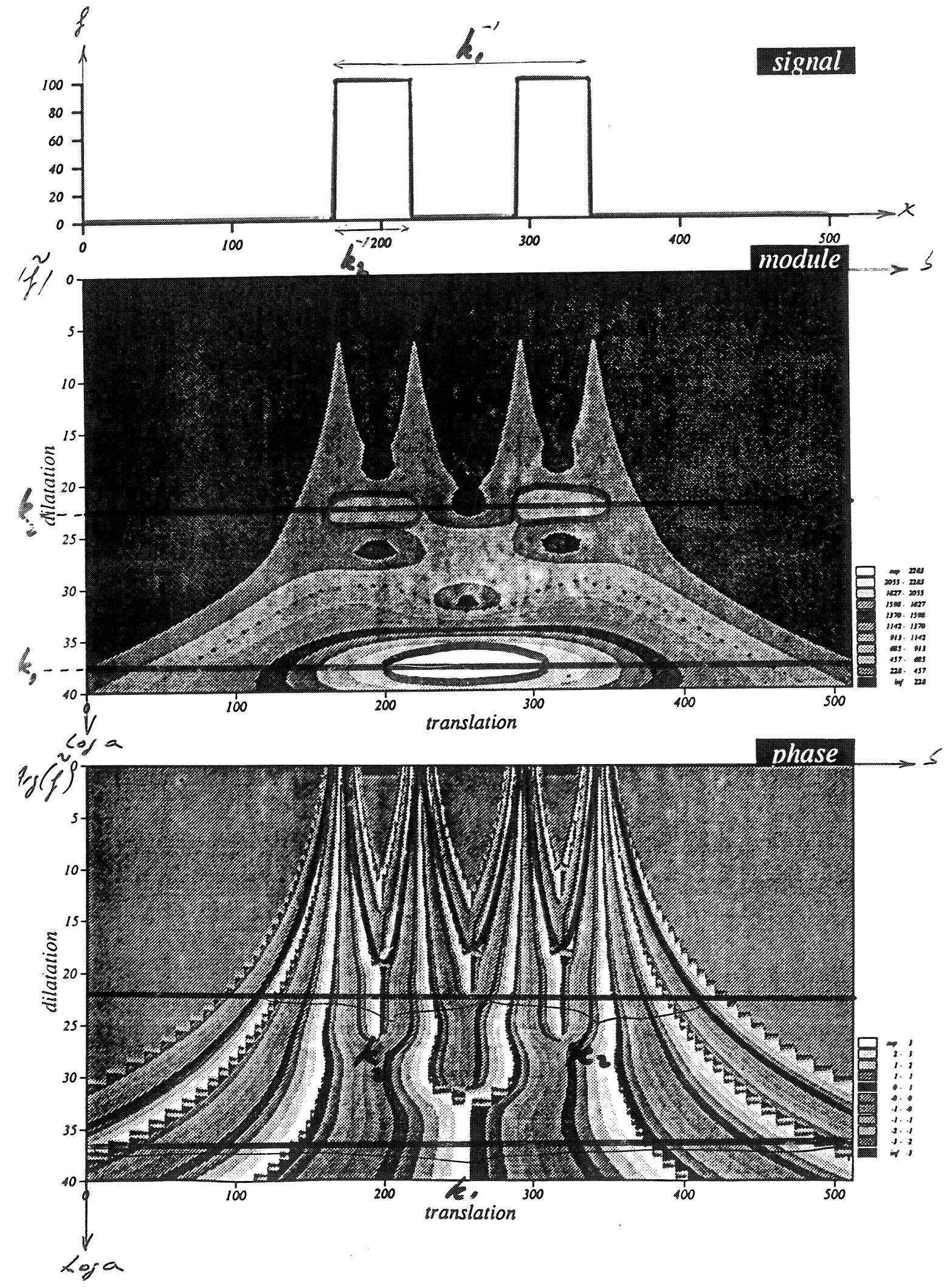

signal
module
phase
dilatation
translation
Log a

ANALYSE EN ONDELETTES d'une coupe du champ de vorticité d'une simulation numérique

$\omega = \vec{\nabla} \times \vec{V}$

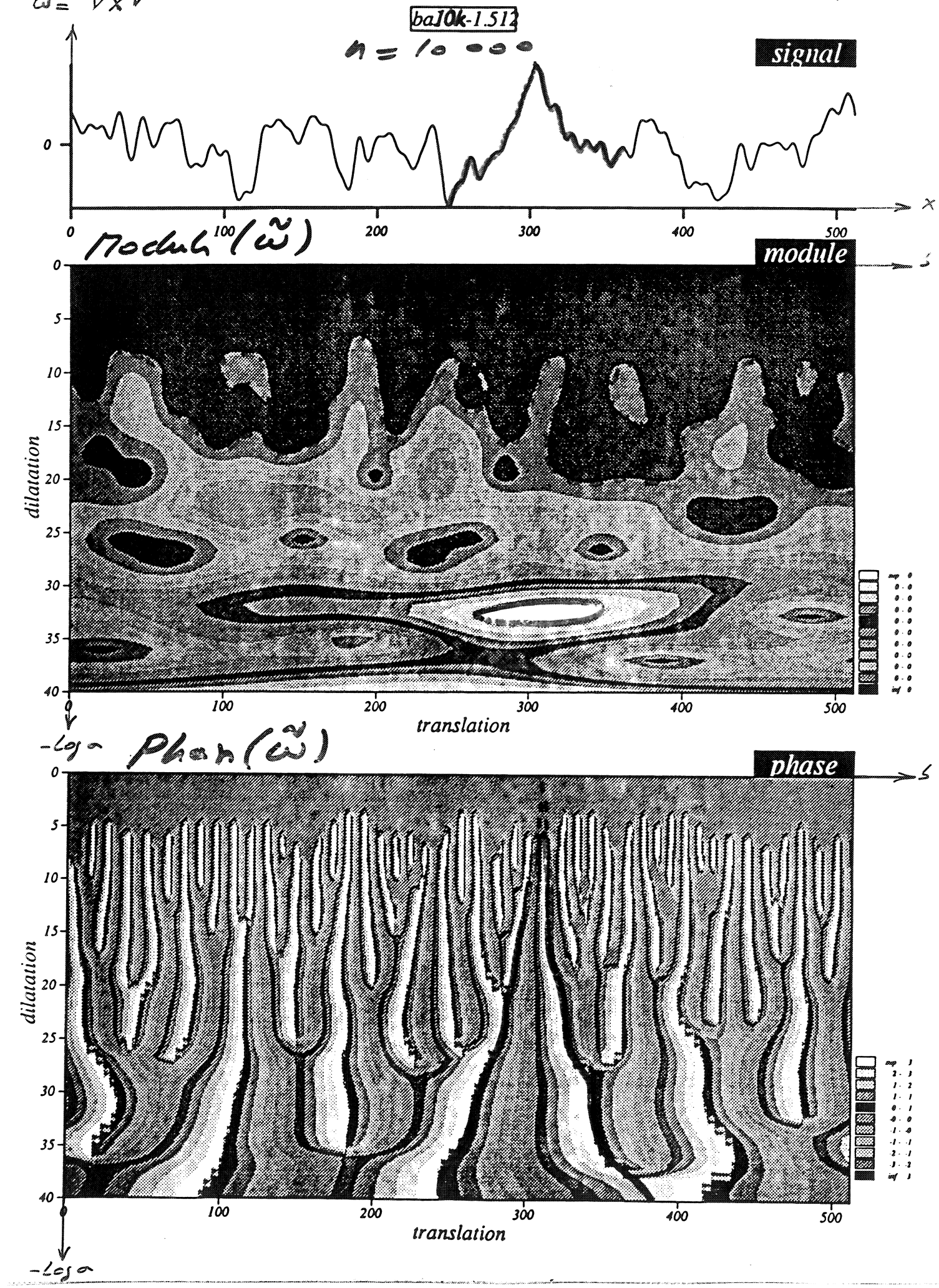

$n = 40\,000$

ba40k-1.512

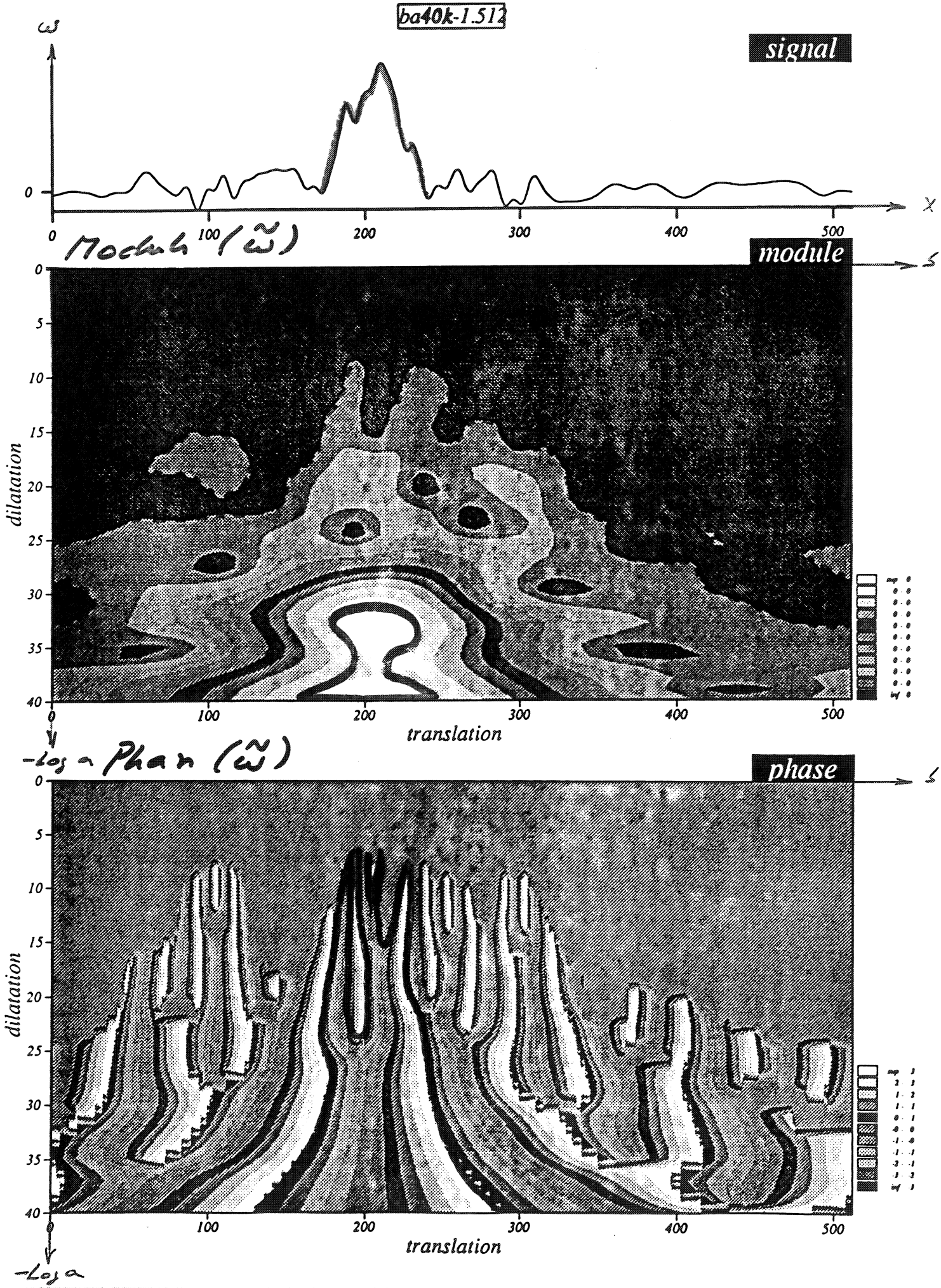

$n = 90\,000$

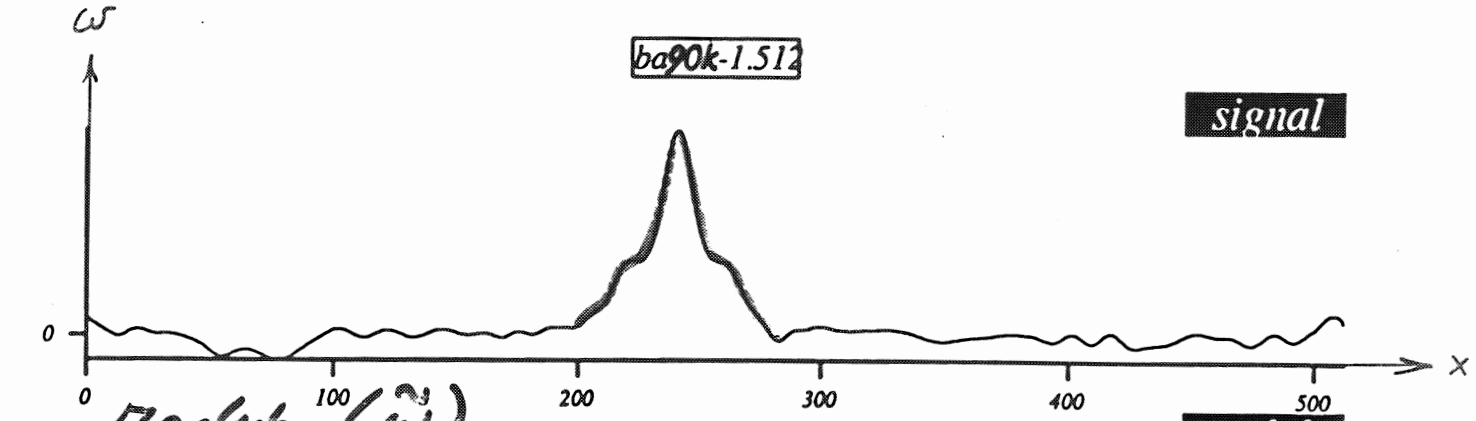

Module $(\tilde{\omega})$

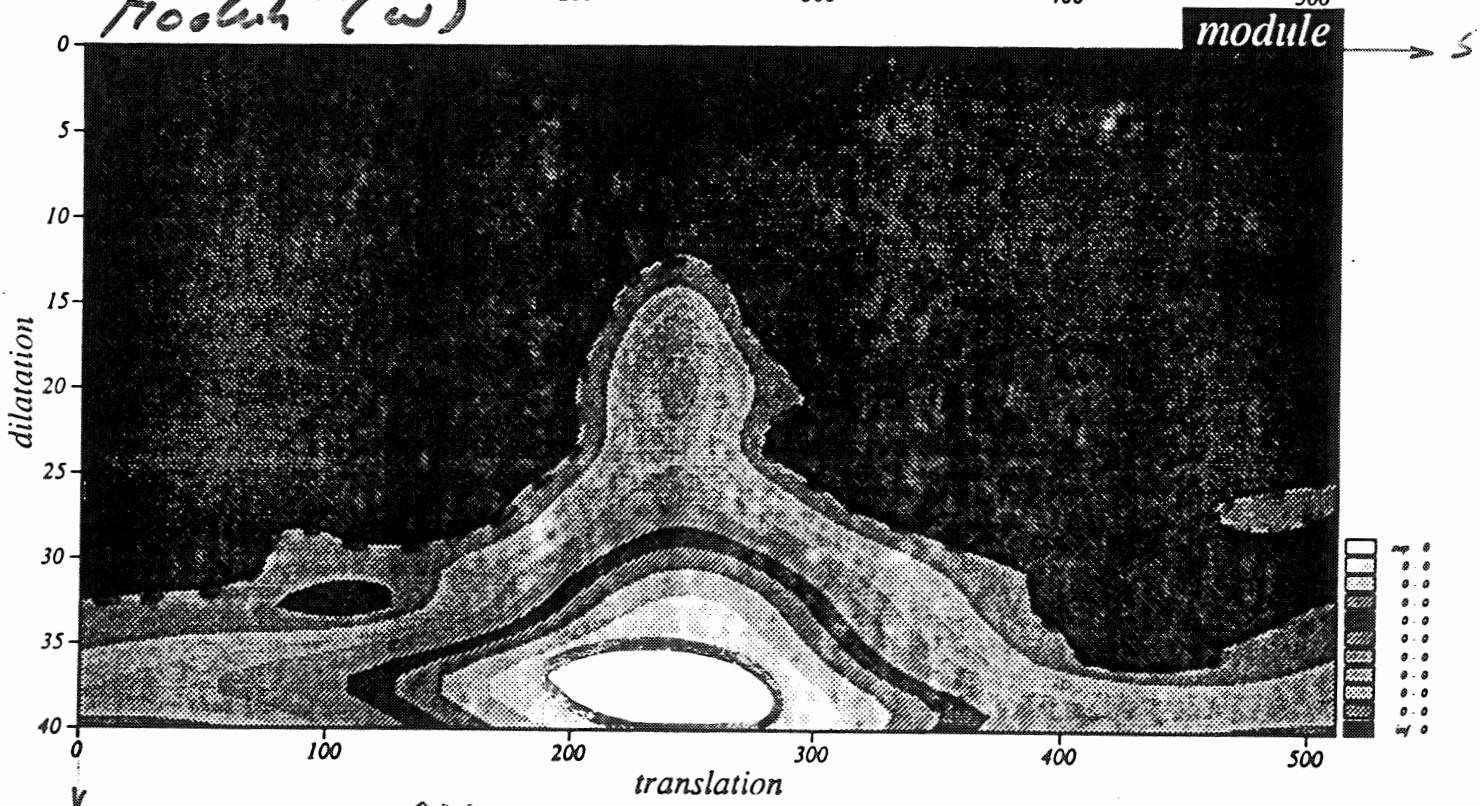

$-\log a$ Phase $(\tilde{\omega})$

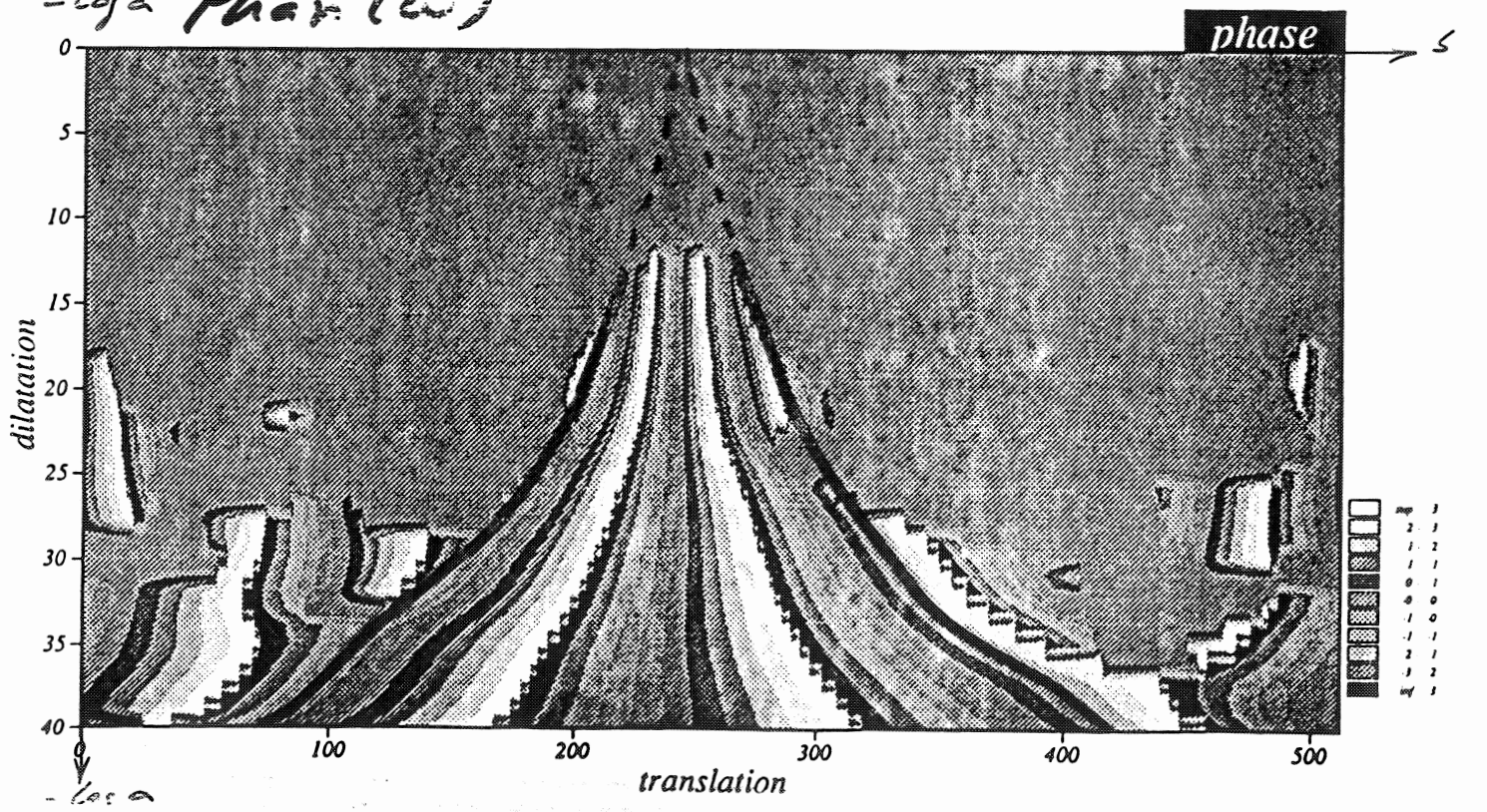

Topological Fluid Dyn., 1913
Farge, Holschneider & Glowna

2D Wavelet Analysis of Vorticity

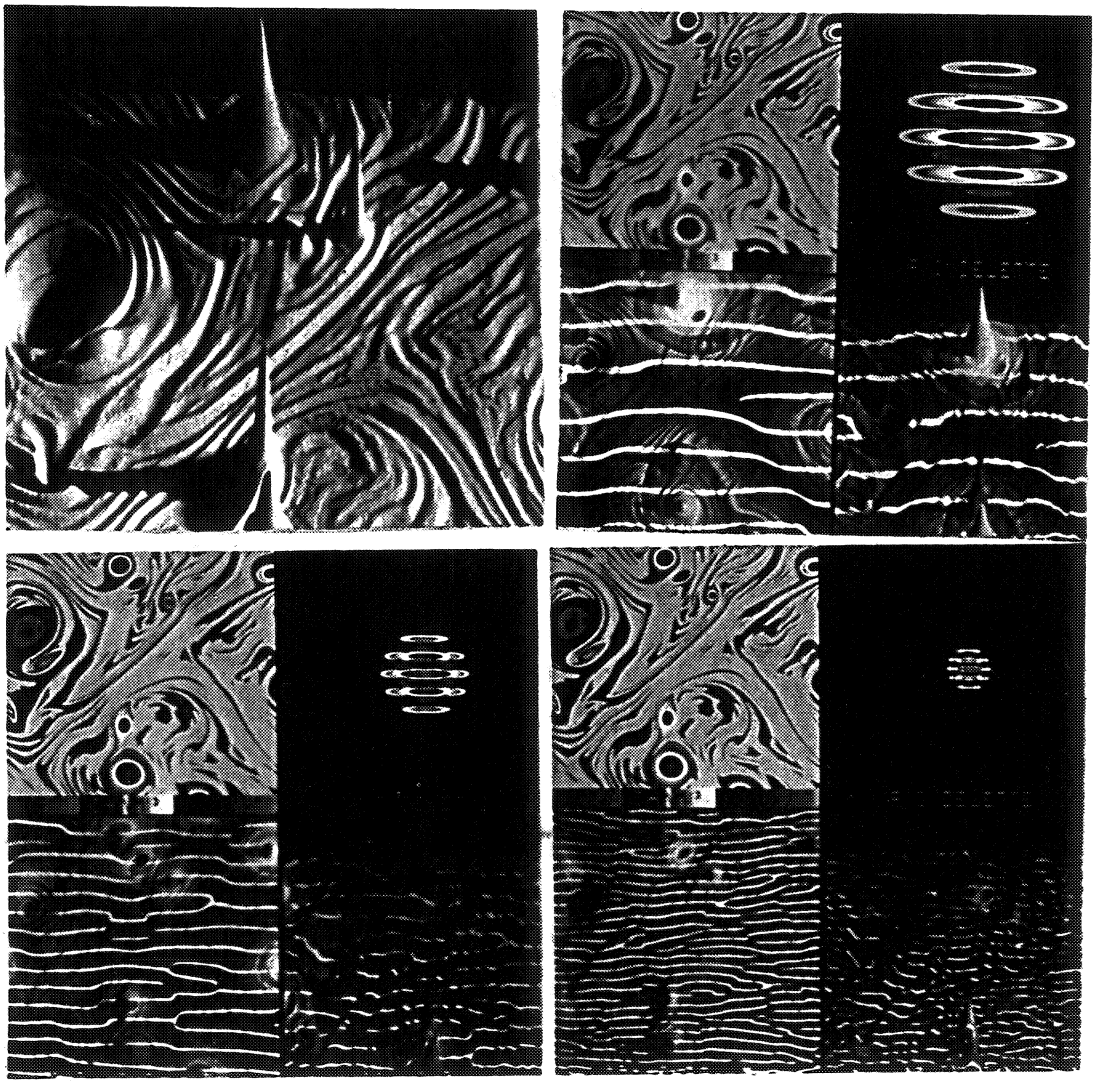

Strong wavelet coefficients correspond to coherent structures
Weak wavelet coefficients correspond to background flow

Analyses en ondelettes de champs turbulents

La transformée en ondelettes est une nouvelle technique d'analyse de signal, et nous avons été les premiers à l'utiliser pour étudier la turbulence. Nous avons écrit le premier code de transformée en ondelettes bidimensionnelles et nous l'avons utilisé pour analyser les sttructures cohérentes dans les écoulements turbulents, à deux et trois dimensions, résultats qui ont fait l'objet d'une dizaine de publications.

Sur la figure est représentée l'analyse en ondelettes de Morlet bidimensionnelles (montrées en haut à droite de chaque vue) d'un champ turbulent (montré en haut à gauche) à trois échelles différentes. Pour cela nous avons superposé le champ (en vue cavalière), le module des coefficients d'ondelettes (en couleur) et leur phase (l'isoligne blanche correspondant à la phase zéro).

Coherent structures condensate enstrophy ($\langle \omega^2 \rangle$) on a wide range of scales

(Farge, Holschneider, Gbaua
1989)



Transformée en ondelettes
d'un champ de vorticité
solution numérique des équa-
tions de Navier-Stokes 2D

Le champ de vorticité
est visualisé par la surface,
le module des coefficients
d'ondelette est donné par la couleur,
la phase ($\theta = 0$) des coefficients d'on-
delettes est donnée par les lignes grises.

Analyse en ondelettes d'un champ
turbulent bidimensionnel

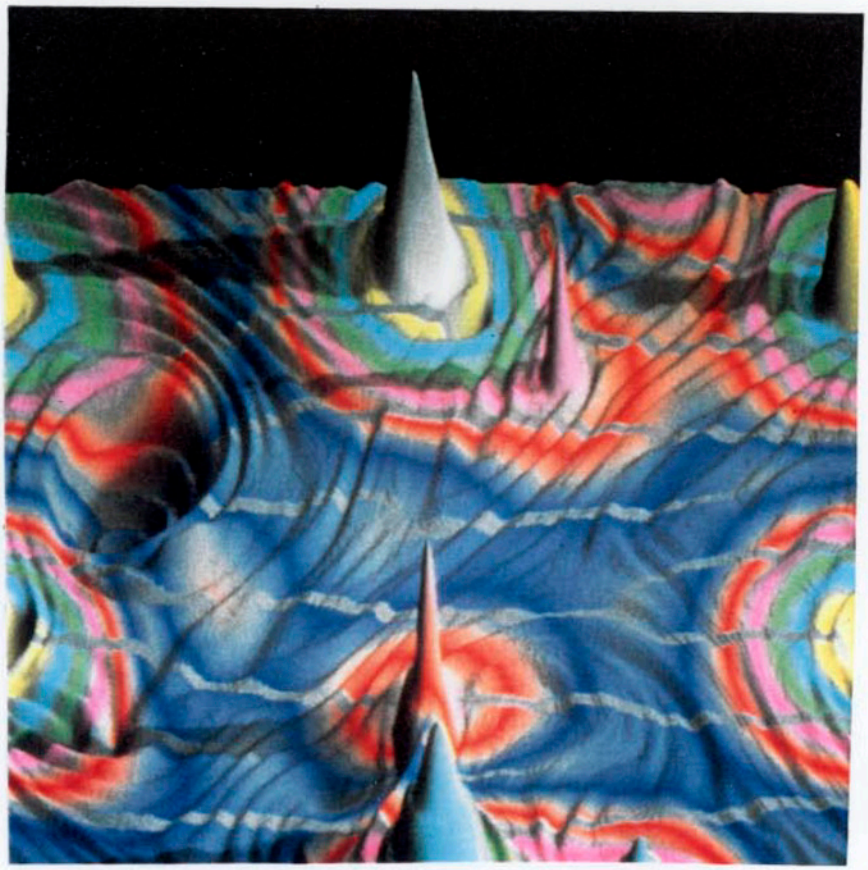

à grande échelle

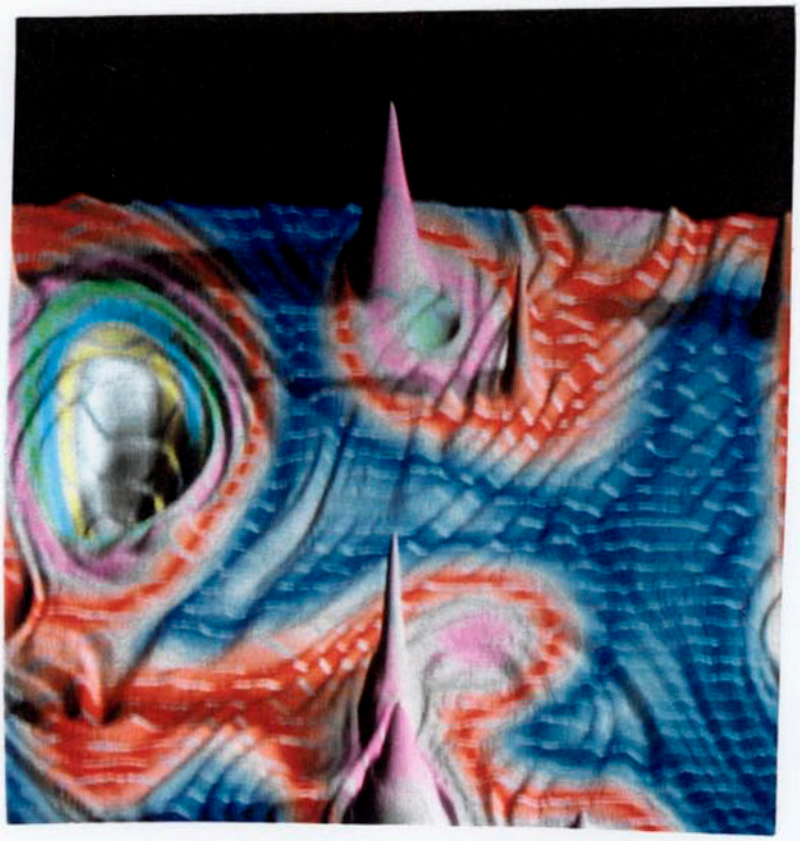

à petite échelle

Théorème des moments

Soit une distribution de probabilité $p(f)$ inconnue de la mesure de probabilité f

$$\Pi_p = \int_{-\infty}^{+\infty} f^p p(f)\, df = \frac{d^p}{dk^p} \frac{\hat{p}(k)}{(-2\pi i)^p}\Big|_{k=0}$$

$\hat{p}(k) = TF[p(f)]$ appelé fonction caractéristique

Echantillons statistiques

objet	continu
$f_1, f_2 \dots f_N$	$f(x_1), f(x_2) \dots f(x_N)$

Skewness $\quad S = \dfrac{\Pi_3}{\Pi_2^{3/2}}$

Flatness $\quad F = \dfrac{\Pi_4}{\Pi_2^2}$

Gaussian distribution

$$p(x) = \frac{1}{\sqrt{2\pi\sigma^2}} e^{-\frac{x^2}{2\sigma^2}}$$

$\Pi_2 = 3\sigma$
$\Pi_4 = -3\sigma^4$
$\Pi_6 = 15\sigma^6$

$S = 0$, $F = 3$

Pairs (even)

$\Pi_1 = \Pi_3 = \dots = 0$ impair (odd)

$$\frac{d^n}{dk}\hat{p}(k) = (n+1)\frac{d^{n-2}}{dk^{n-2}}\hat{p}(k)\Big|_{k=0}$$

STRUCTURE FUNCTIONS

Two-point structure function

$$S_2(x) = \int |f(x'+x) - f(x')|^2 dx'$$

Relation with the correlation function

$$S_2(x) = \int [f(x'+x)^2 + f(x')^2 - 2 f(x'+x) f(x')] dx'$$

$$= \int f(x'+x)^2 dx' + \int f(x')^2 dx' - 2 \int f(x'+x) f(x') dx'$$

$$= 2 \int f(x')^2 dx' - 2 \int f(x'+x) f(x') dx'$$

$$= 2R(0) - 2R(x) \quad \text{car} \quad R(x) = \int_{-\infty}^{+\infty} f(x') f(x'+x) dx'$$

Relation with the energy

Wiener-Khinchin

$$\int_{-\infty}^{+\infty} R(x) e^{-ikx} dx = |\hat{f}(k)|^2 = E(k)$$

$$\Rightarrow R(x) = TF^{-1}(E(k)) = \int_{-\infty}^{+\infty} E(k) e^{+ikx} dk$$

$$S_2(x) = 2R(0) - 2R(x)$$

$$= 2 \int E(k) dk - 2 \int E(k) e^{ikx} dk$$

$$= 2 \int^{+\infty} (1 - e^{ikx}) E(k) dk$$

One record of a turbulent signal sampled at 5 kHz

at t

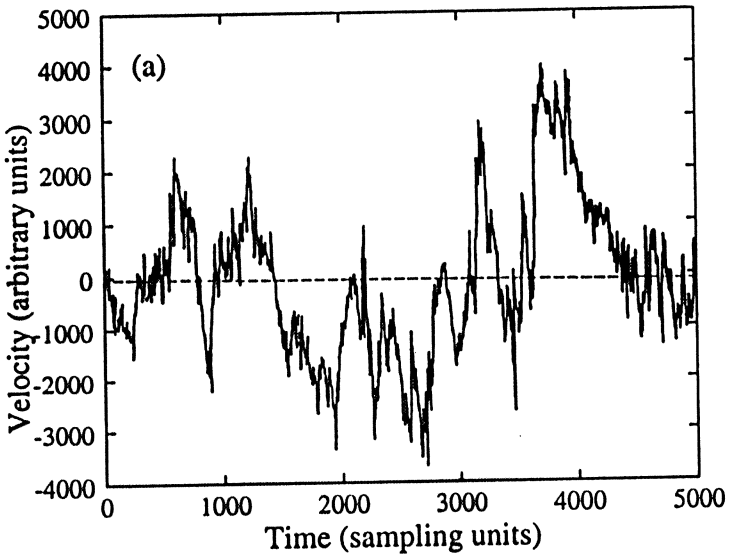

at $t+4\rho$

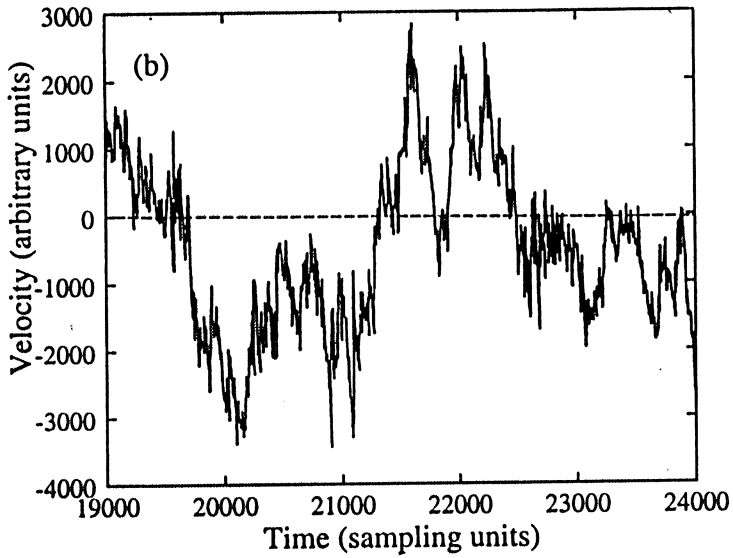

at t

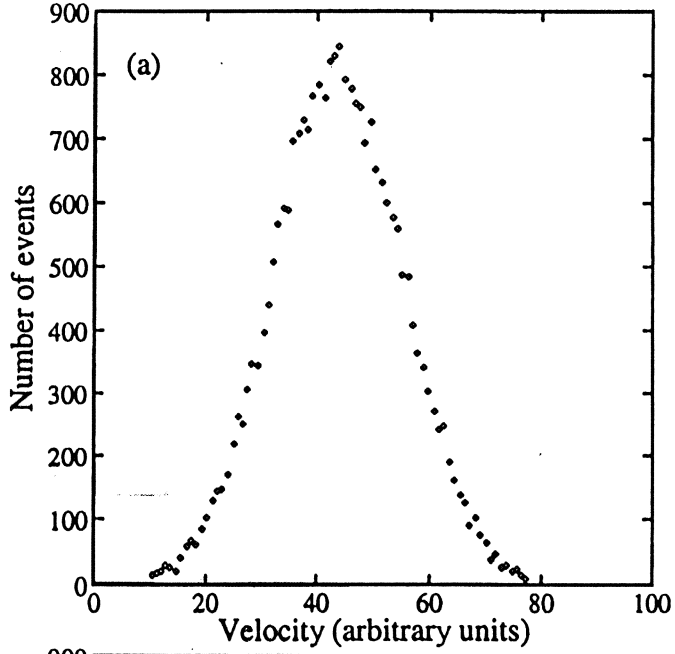

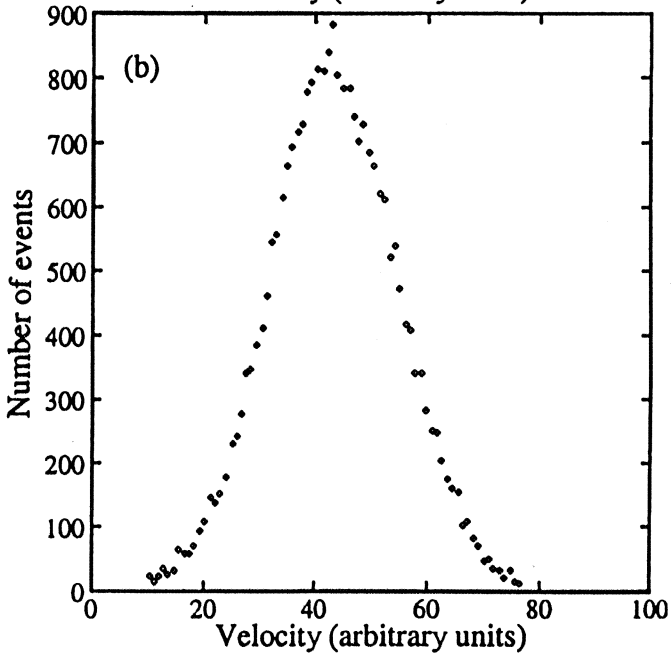

at $t+4s$

cf. Gagne and Hopfinger
ONERA, Modane

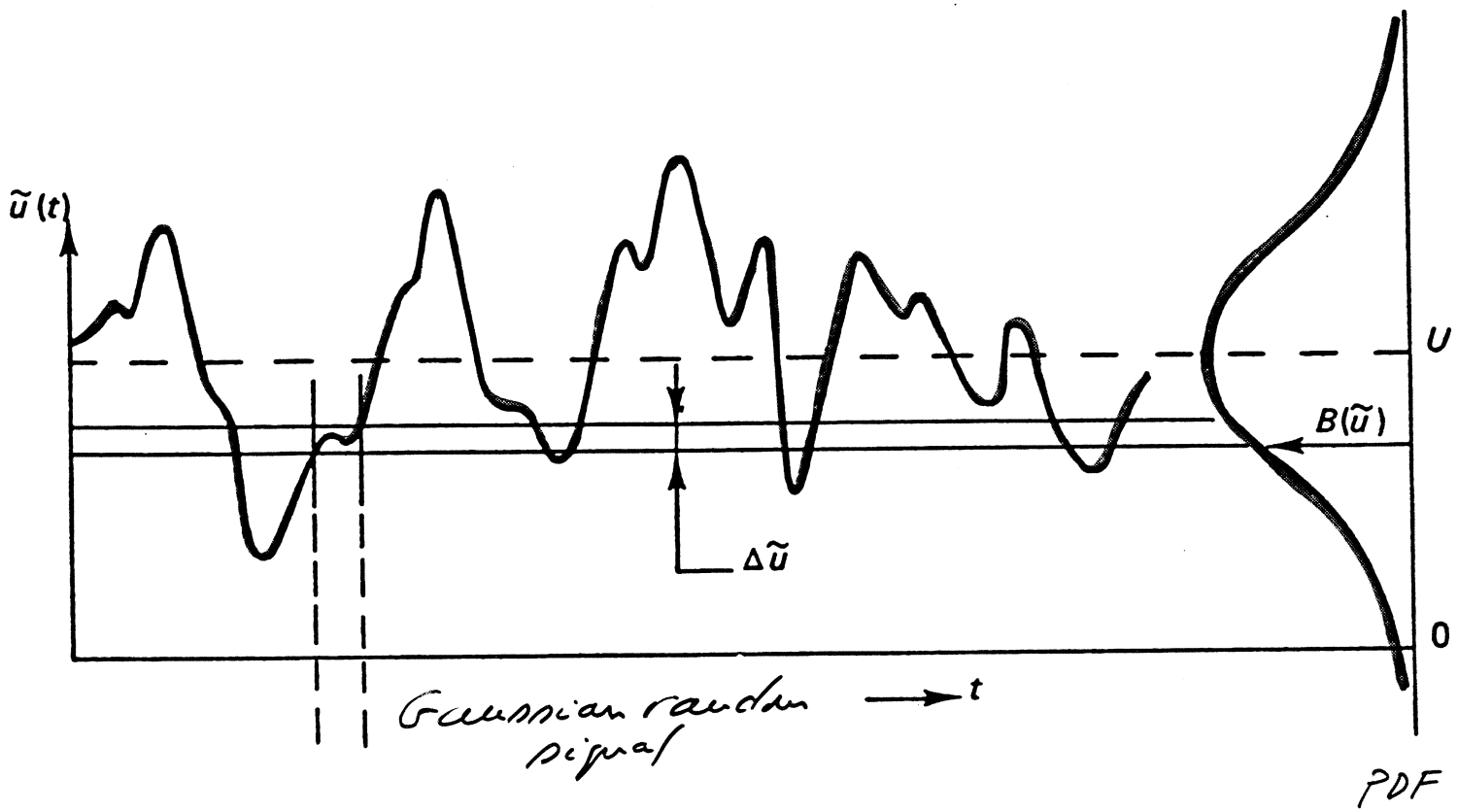
ũ(t)
U
B(ũ)
Δũ
0
t
Gaussian random signal
PDF

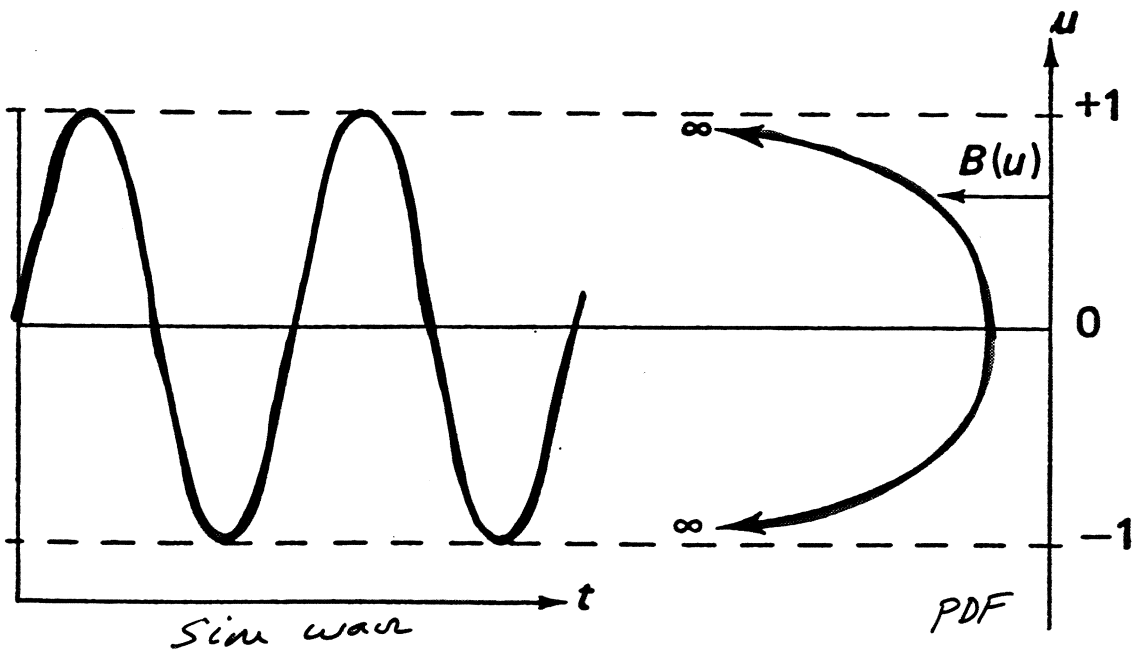
u
+1
∞
B(u)
0
∞
−1
t
Sine wave
PDF

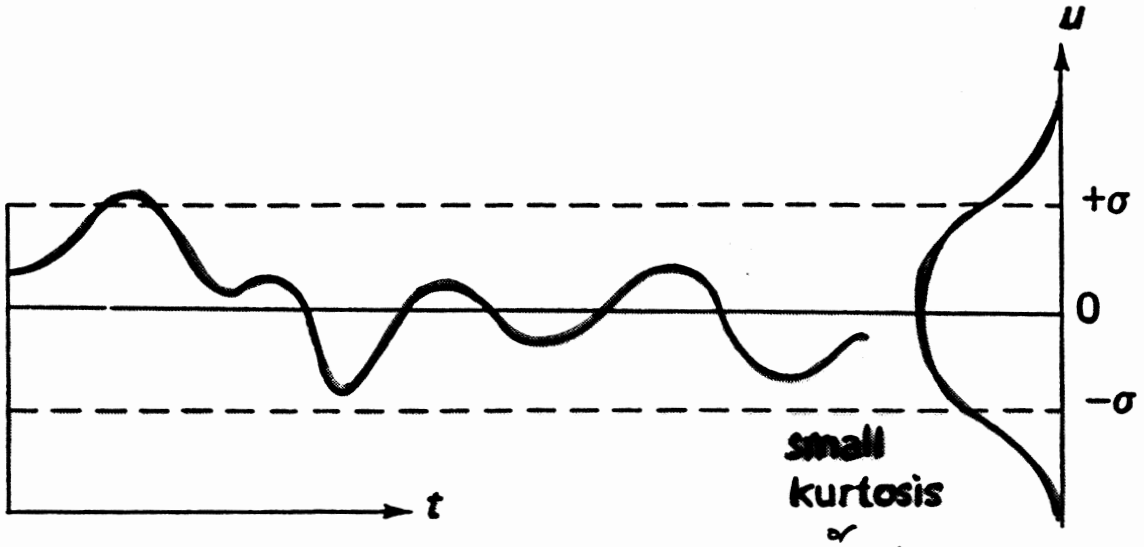

small kurtosis
or
small flatness

$F \equiv \frac{\Pi_4}{\Pi_2^2}$

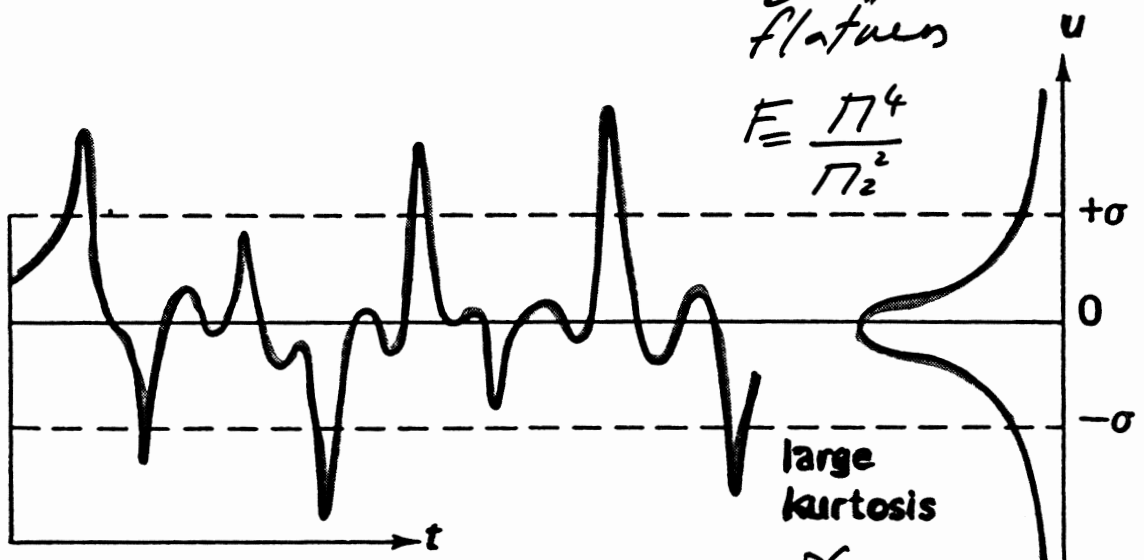

large kurtosis
or
large flatness

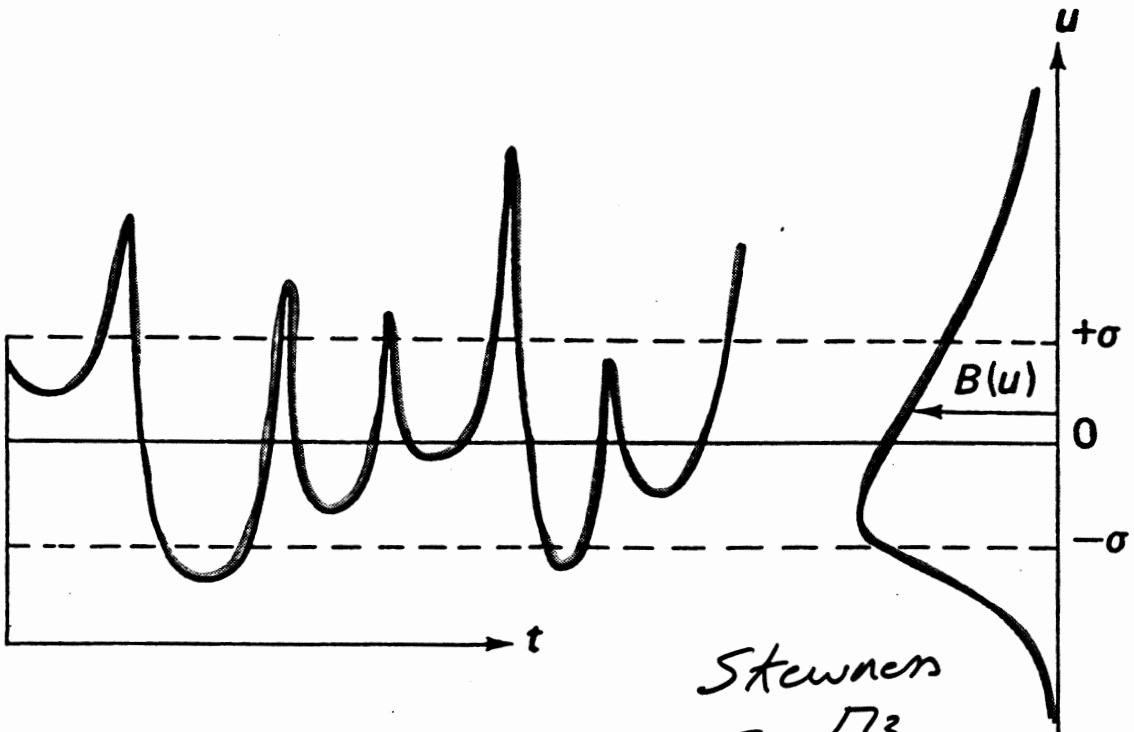

Skewness

$S = \frac{\Pi_3}{\Pi_2^{3/2}}$

AUTO-CORRELATION

$$C(\tau) = \frac{\int u(t)\, u(t+\tau)\, dt}{\int u^2(t)\, dt}$$

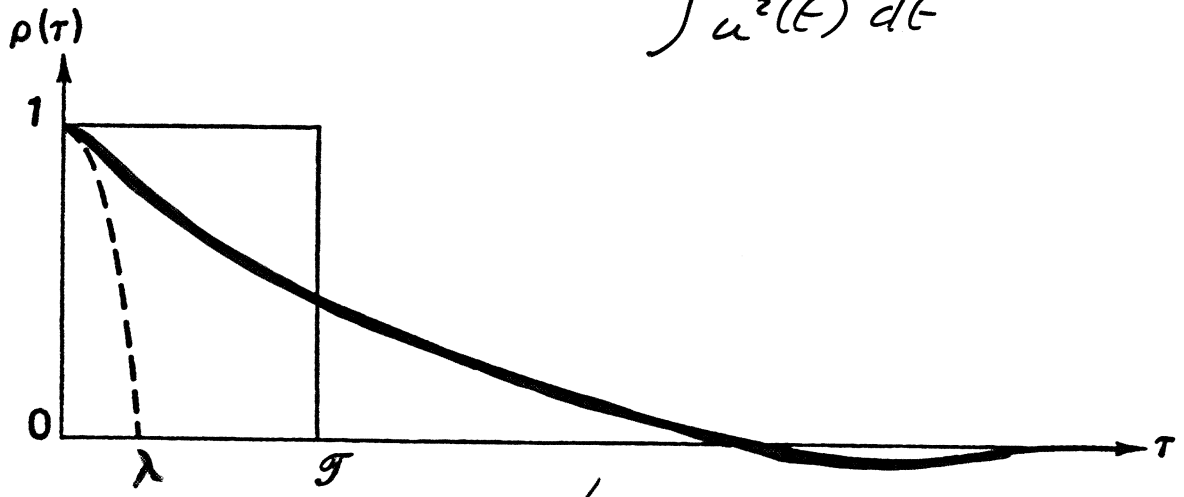

Taylor microscale given by the curvature of the autocorrelation function at $\tau = 0$

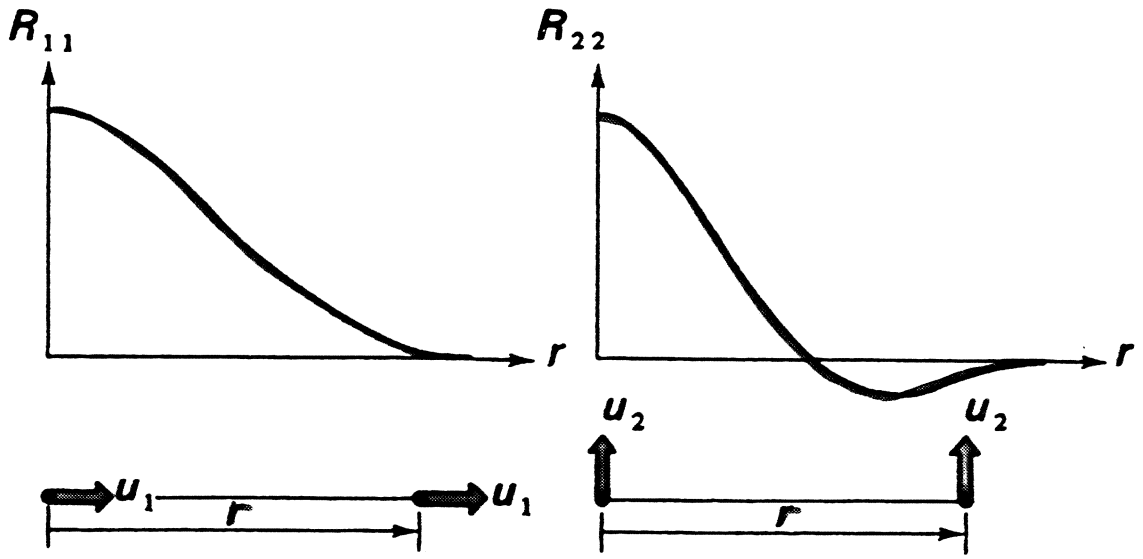

Longitudinal Correlation

$$R_{11}(r) = \frac{\int u_1(x)\, u_1(x+r)\, dx}{\int u_1^2(x)\, dx}$$

Transverse Correlation

$$R_{22}(r) = \frac{\int u_2(x)\, u_2(x+r)\, dx}{\int u_2^2(x)\, dx}$$

CROSS-CORRELATION

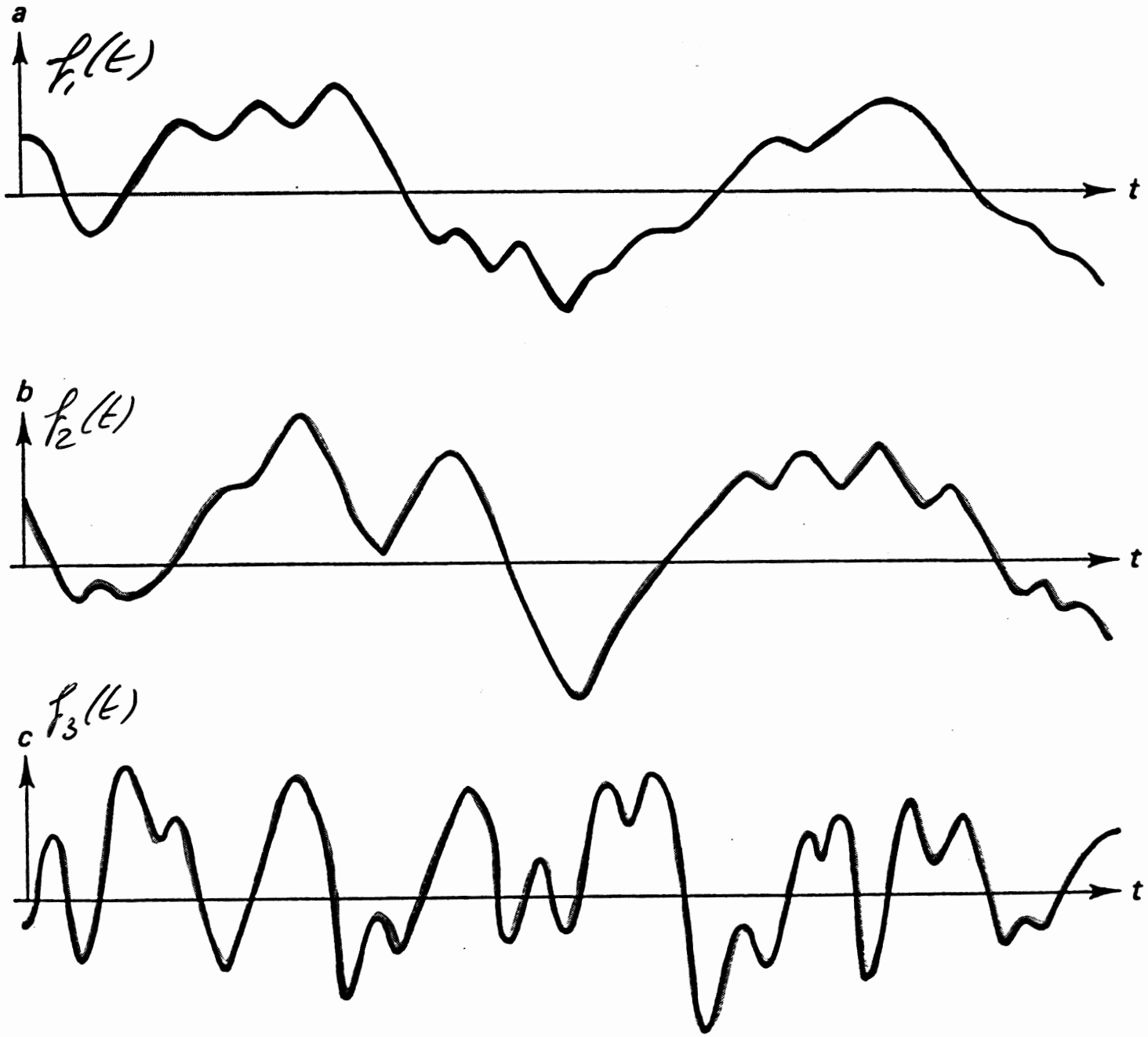

$f_1(t)$ and $f_2(t)$ are correlated $\quad \overline{f_1 f_2} > 0$

$f_3(t)$ and $f_1(t)$ or $f_2(t)$ are uncorrelated $\quad \overline{f_1 f_3} \simeq 0$ and $\overline{f_2 f_3} \simeq 0$

CROSS-CORRELATION

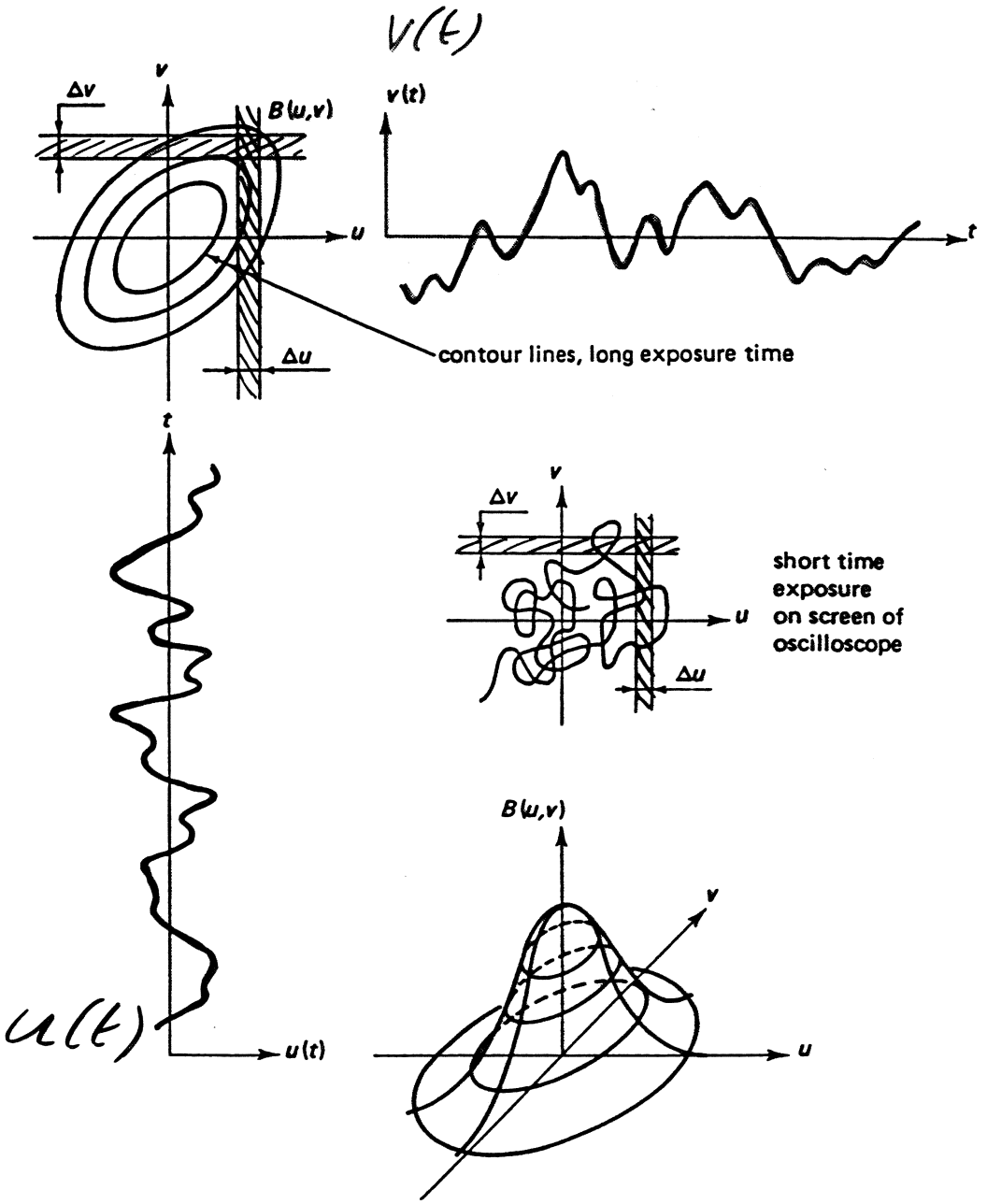

$\overline{uv} < 0$ $\overline{uv} = 0$ $\overline{uv} > 0$

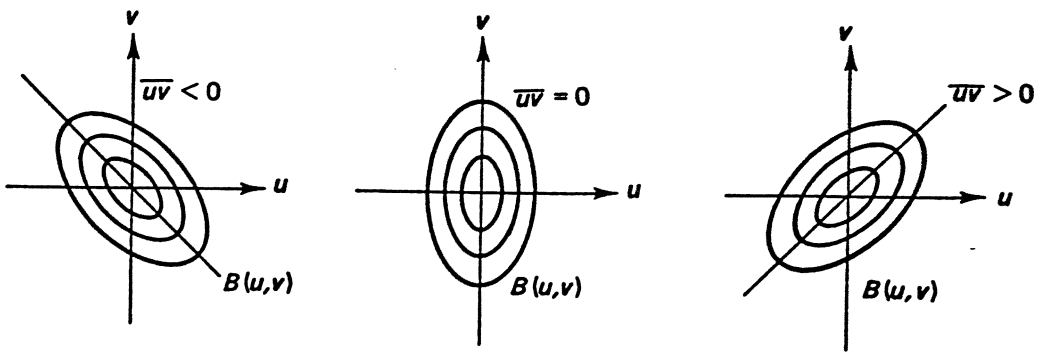

Anticorlatd Uncorlatd Corlatd

CLASSIFICATION OF SIGNALS

STATIONARY (HOMOGENEOUS) ≡ Translation invariant

NON STATIONARY (INHOMOGENEOU

NON INTERMITTENT (FRACTAL)

$\int p(x)\,dx = 1$

Mean $m_1 = \frac{1}{N}\sum_i f_i \simeq \int f\,p(f)\,df$

Variance $m_2 = \frac{1}{N}\sum_i |f_i|^2 \simeq \int f^2 p(f)\,df$

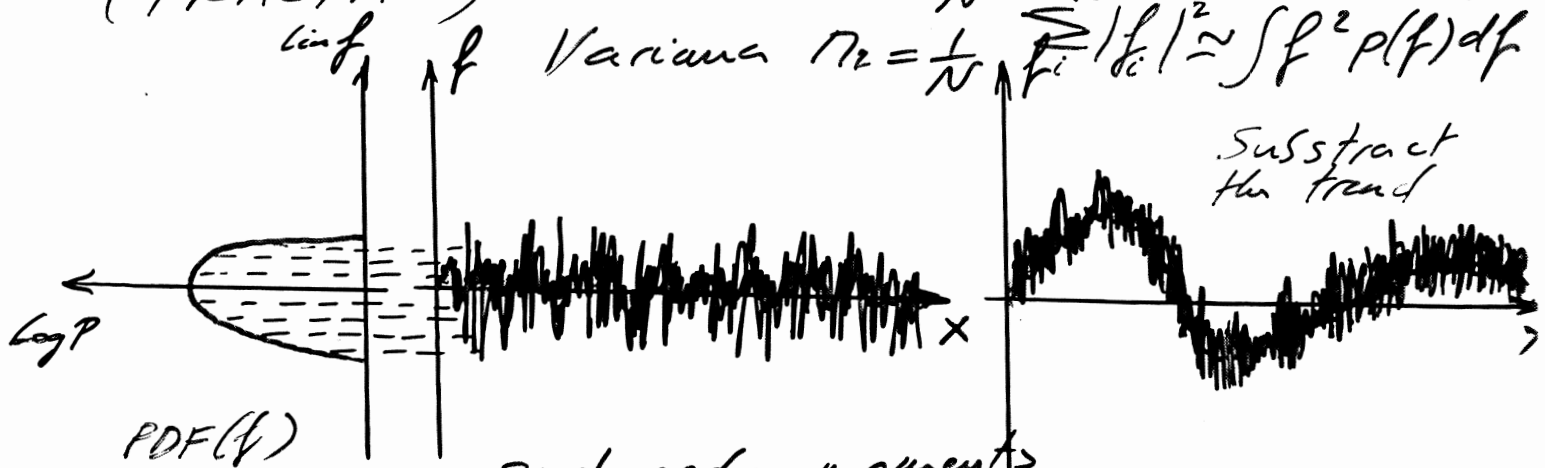

Small variance ≡ clean events

2nd order moments

$m_2 = \frac{1}{N}\sum_i |f_i|^2 \simeq \int x^2 p(x)\,dx$

Correlation of m_2 ⇒ spectrum

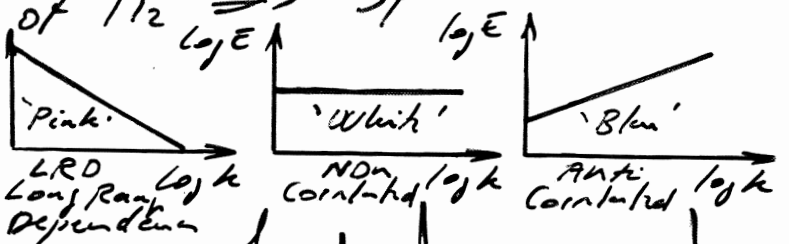

INTERMITTENT (MULTIFRACTAL)

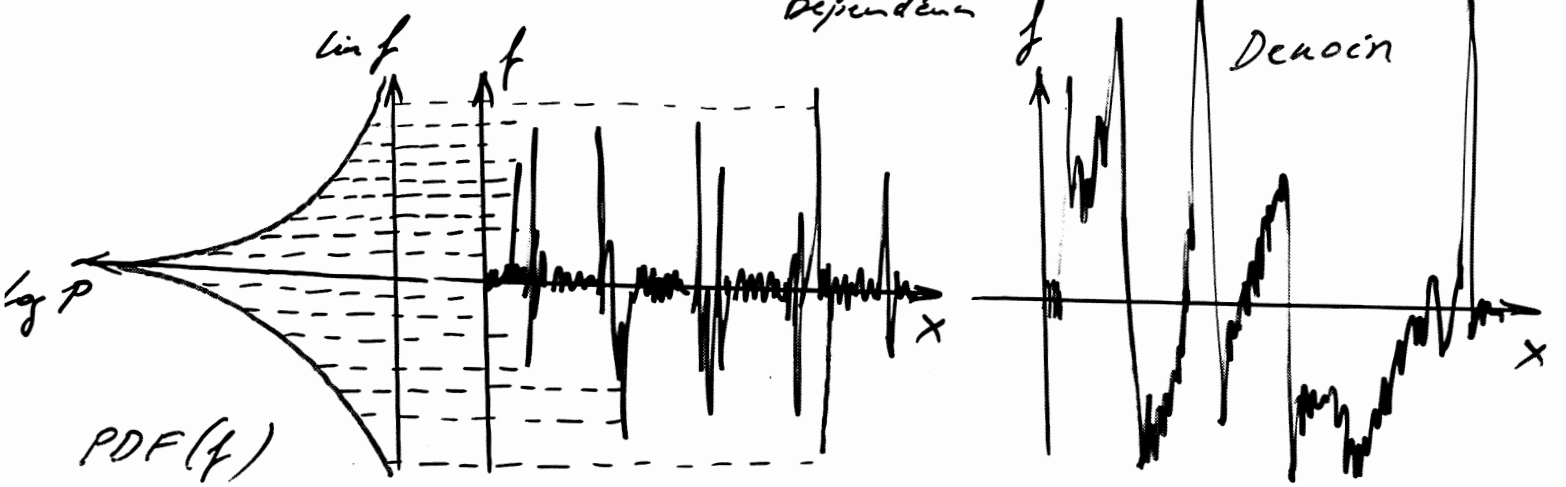

Large variance ≡ rare events

High order moments

$m_p = \frac{1}{N}\sum_i f^p \simeq \int f^p p(f)\,df$

SELF-SIMILARITY

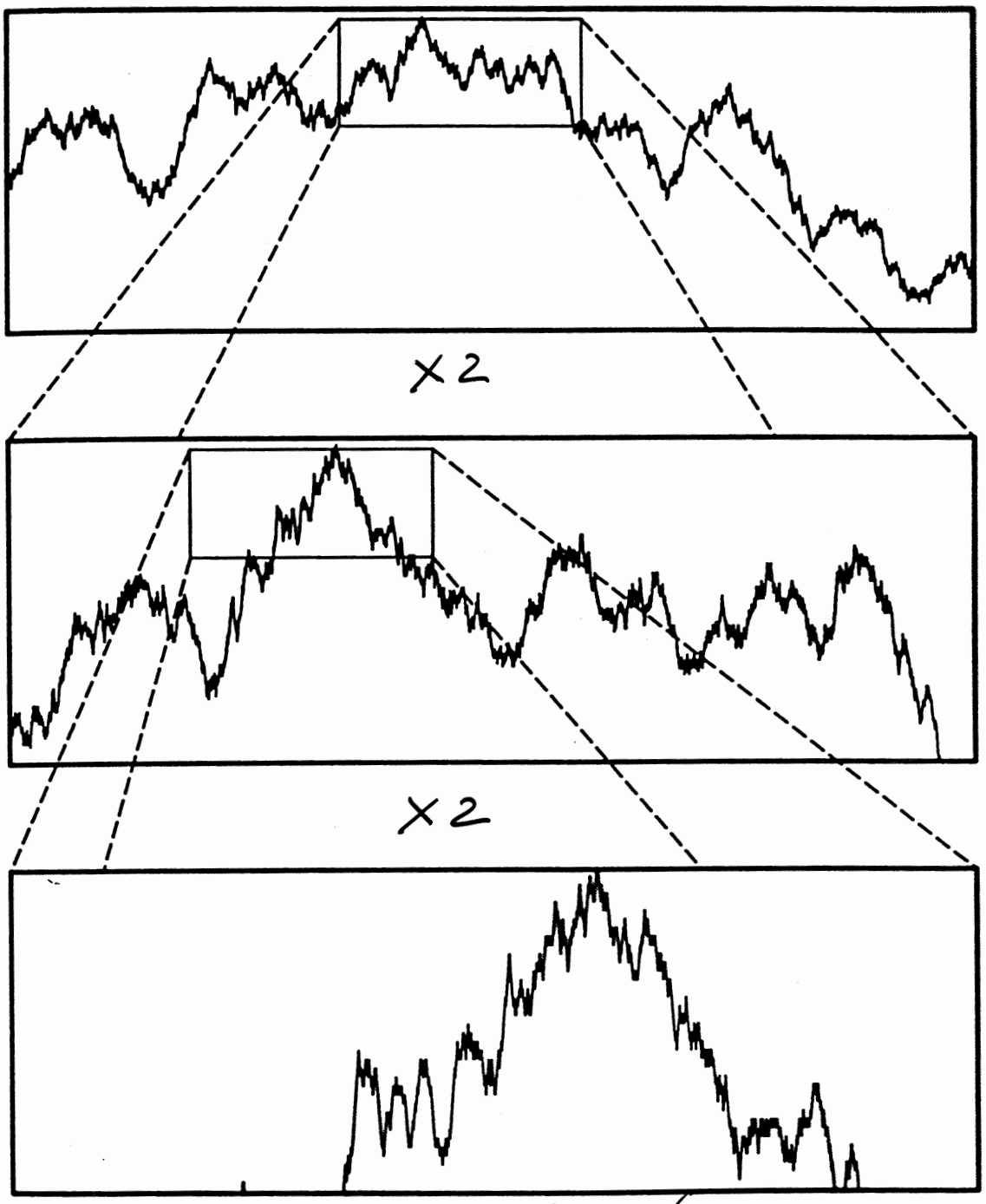

One realization of a Brownian motion

2. ECOULEMENTS TURBULENTS TRIDIMENSIONNELS INCOMPRESSIBLES

Turbulence dans les écoulements industriels (aérodynamique et hydrodynamique)

Ecoulements typiques (le long d'une paroi, en aval d'un obstacle, d'une grille, couche de mélange, jet, dans un canal) : observés dans des expériences de laboratoire et des expériences numériques effectuées par simulation directe

Théorie phénoménologique de la couche limite

Théorie statistique de la turbulence tridimensionnelle homogène et isotrope

Intermittence et structures cohérentes tridimensionnelles

NAVIER-STOKES EQUATIONS

$$\begin{cases} \frac{\partial \vec{v}}{\partial t} + \vec{v} \cdot \vec{\nabla} \vec{v} + \frac{1}{\rho} \vec{\nabla} p = \nu D^2 \vec{v} + \vec{F} \\ \vec{\nabla} \cdot \vec{v} = 0 \\ \text{C. I.} \\ \text{B. C.} \end{cases}$$

$\vec{v}$ velocity

p pressure

ρ density

ν kinematic viscosity

$Re \longrightarrow \infty \quad \nu \longrightarrow 0$

irreversibility

$\nu = 0$ Euler equation

reversibility

We take the curl

$$\begin{cases} \partial_t \vec{\omega} + (\vec{v}\cdot\vec{\nabla})\vec{\omega} = \\ (\vec{\omega}\cdot\vec{\nabla})\vec{v} + \nu \nabla^2 \vec{\omega} + \vec{\nabla}\times\vec{F} \\ \omega = -\nabla^2 \psi \end{cases}$$

$\omega = \vec{\nabla}\times\vec{v}$ vorticity

ψ $\begin{cases} u = \partial_y \psi \\ v = -\partial_x \psi \end{cases}$ streamfunction in 2D (which becomes a 2-form in 3D)

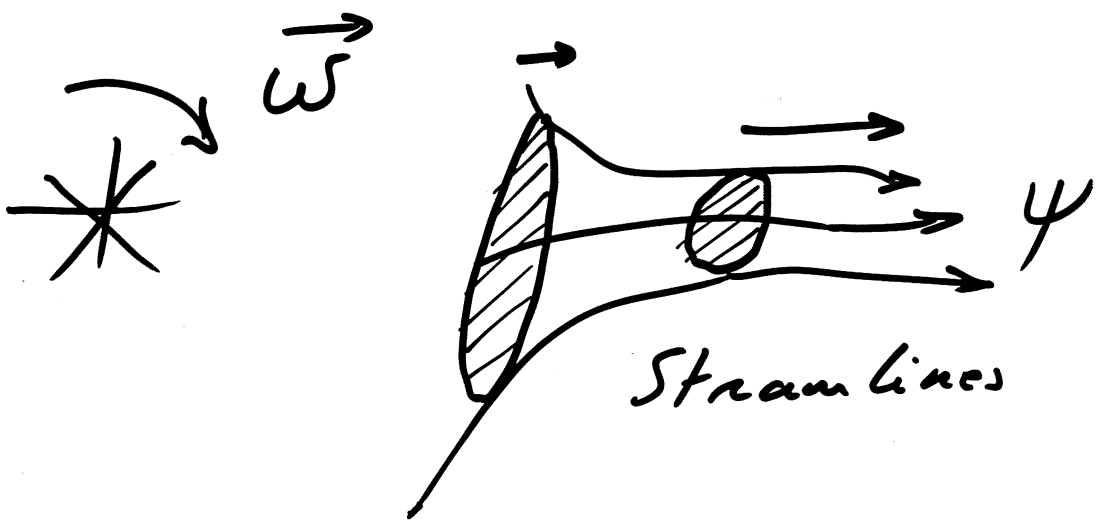

PROPERTIES IN 3D

If statistical steady stat

$$\vec{D} \times \vec{F} = \nu D^2 \vec{\omega}$$

$$\frac{d\vec{\omega}}{dt} = (\vec{\omega} \cdot \vec{D}) \vec{V}$$

vortex stretching which transfers energy $\langle v^2 \rangle$ from large scales to small scales.

PROPERTIES IN 2D

$\vec{\omega} = (0, 0, \omega) \perp \vec{V}$

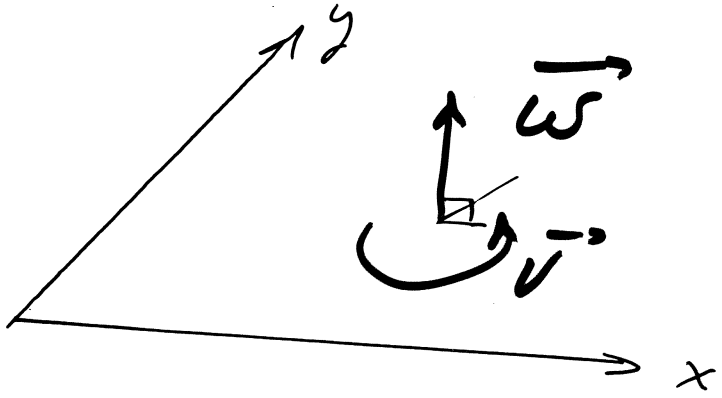

$$\frac{d\vec{\omega}}{dt} = 0$$

Lagrangian conservation of vorticity

$$d\frac{\vec{\nabla}\omega}{dt} = -(\vec{\nabla}\omega \cdot \vec{\nabla})\vec{V}$$

Vortex gradient stretching which transfers enstrophy $\langle \omega^2 \rangle$ from large scales to small scales

INVARIANTS OF EULER EQUATIONS

In three dimensions

Mean energy

$$E \equiv \frac{1}{2} \int |\vec{v}(\vec{x})|^2 \, d^3\vec{x}$$

Mean helicity

$$H \equiv \frac{1}{2} \int \vec{v}(\vec{x}) \cdot \vec{\omega}(\vec{x}) \, d^3\vec{x}$$

Mean vortical helicity

$$H_\omega \equiv \frac{1}{2} \int \vec{\omega}(\vec{x}) \cdot \vec{\xi}(\vec{x}) \, d^3\vec{x}$$

with $\vec{\xi} = \vec{\nabla} \times \vec{\omega}$ divorticity

In two dimensions

Mean energy

$$E \equiv \frac{1}{2} \int |\vec{v}(\vec{x})|^2 \, d^2\vec{x}$$

Mean enstrophy

$$Z \equiv \frac{1}{2} \int |\omega(\vec{x})|^2 \, d^2\vec{x}$$

BUDGETS FOR 2D NAVIER-STOKES

Enstrophy balance:

$$\eta \equiv \frac{dZ}{dt} = 2\nu P$$

with η enstrophy dissipation

and palinstrophy

$$P \equiv \frac{1}{2}\int |\xi(\vec{x})|^2 \, d^2\vec{x}$$

$$\Rightarrow$$

Enstrophy input
governs the generation
of vorticity gradients
and therefore palinstrophy
in 2D flows of
viscous fluids

BUDGETS FOR 3D NAVIER-STOKES

Energy Balance:

$$\mathcal{E} \equiv -\frac{d}{dt} E = 2\nu \mathcal{Z}$$

with $\mathcal{E}$ energy dissipation
and $\mathcal{Z}$ enstrophy

$\Rightarrow$

Energy input governs the
generation of vorticity
and therefore enstrophy
in 3D flows of viscous fluids

Helicity Balance:

$$-\frac{dH}{dt} = 2\nu H_\omega \Rightarrow$$

Helicity input governs the
generation of magnetic field
in 3D flows of conducting viscous fluids

ENERGY BUDGET IN K-SPACE

Parseval's formula:

$$\langle f g \rangle = \int f(\vec{x})\, g(\vec{x})\, d\vec{x} = \sum_{\vec{k}} \hat{f}(\vec{k})\, \hat{g}(-\vec{k})$$

Energy equation:

$$\int \vec{V}(\vec{x}) \left[N.S. \right] d\vec{x} = \int \vec{V}(\vec{k}) \widehat{\left[N.S. \right]}\, d\vec{k}$$

Energy budget through $k = |\vec{k}|$:

$$\underbrace{\frac{d}{dt} E_k}_{\text{Budget}} + \underbrace{T_k}_{\text{Transfers}} = \underbrace{-2\nu Z_k}_{\text{Dissipation}} + \underbrace{F_k}_{\text{Production}}$$

with $E_k = \frac{1}{2} \sum_{k \le K} |\hat{V}(\vec{k})|^2$ with $k = |\vec{k}|$

$$T_k = \int \vec{V}_k^{<}(\vec{x}) \cdot \left[\vec{V}_k^{<}(\vec{x}) \cdot \vec{\nabla} \vec{V}_k^{>}(\vec{x}) \right] d\vec{x} + \int \vec{V}_k^{<}(\vec{x}) \cdot \left[\vec{V}_k^{>}(\vec{x}) \cdot \vec{\nabla} \vec{V}_k^{>}(\vec{x}) \right]$$

with $\vec{V}_k^{<}$ Low-pass filtred velocity

$\vec{V}_k^{>}$ High-pass filtred velocity

$$Z_k = \frac{1}{2} \sum_{k \le K} |\hat{\omega}(\vec{k})|^2 = \frac{1}{2} \sum_{k \le K} k^2 |\hat{V}(\vec{k})|^2$$

$$F_k = \int \vec{F}_k^{<}(\vec{x}) \cdot \vec{V}_k^{<}(\vec{x})\, d\vec{x} = \sum_{k \le K} \hat{F}(\vec{k}) \cdot \hat{V}(-\vec{k})$$

with $\vec{F}_k^{<}$ Low-pass filtred forcing

CLASSIFICATION OF SHEAR FLOWS

1. Boundary layers

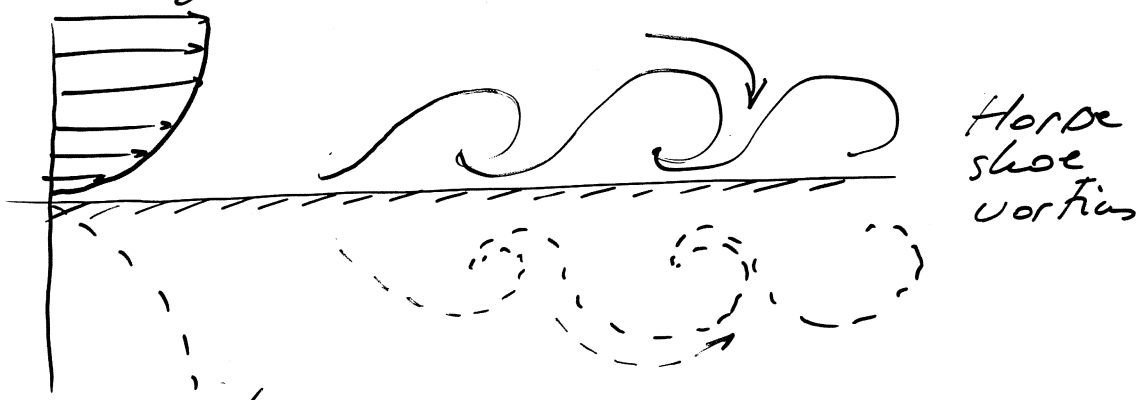

2. Mixing layers

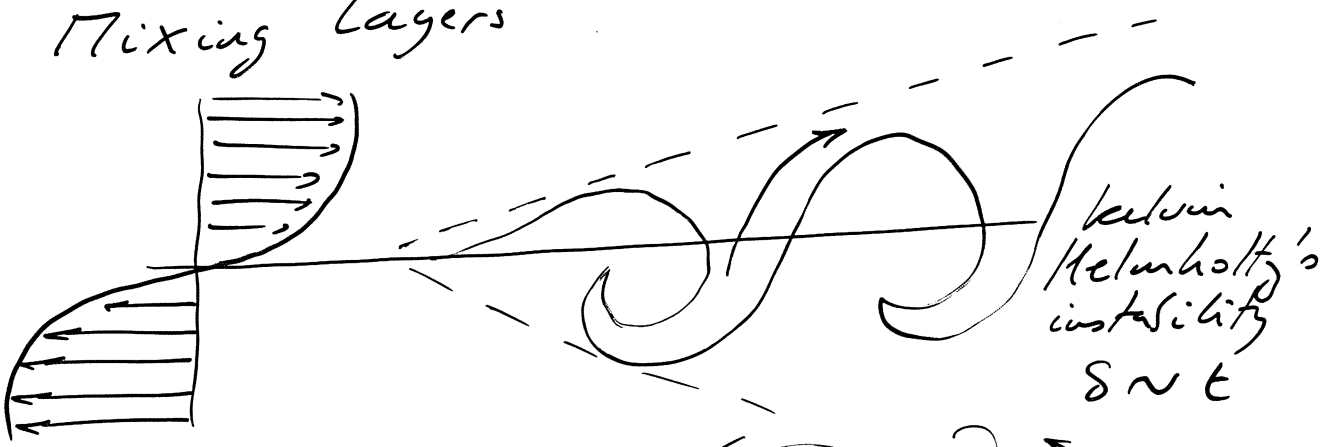

3. Plane jets

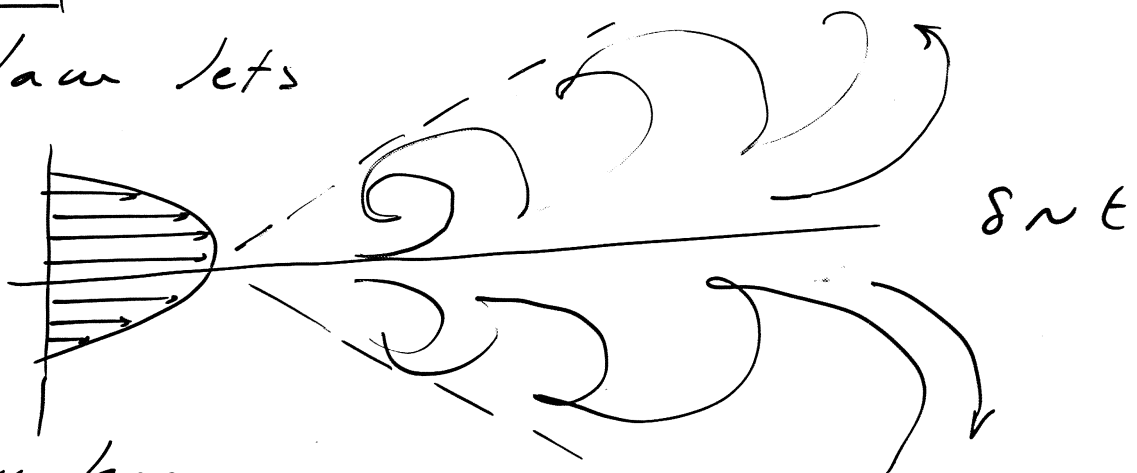

4. Wakes

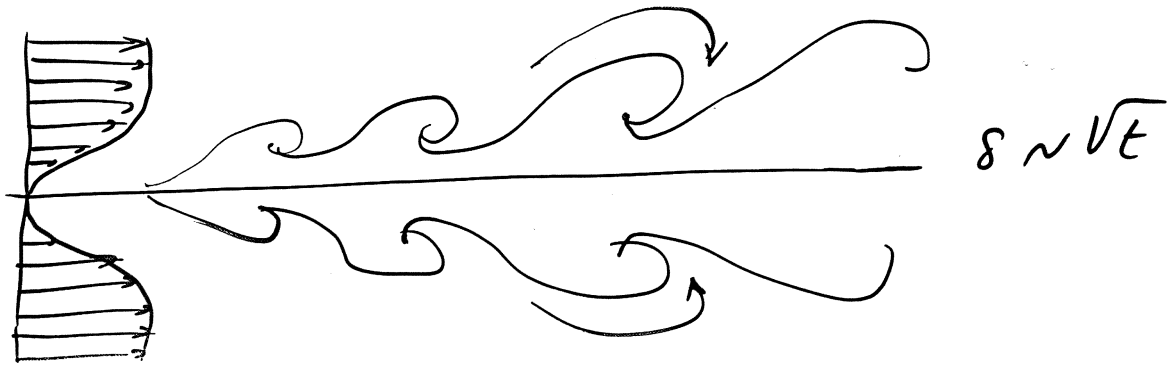

BOUNDARY LAYER

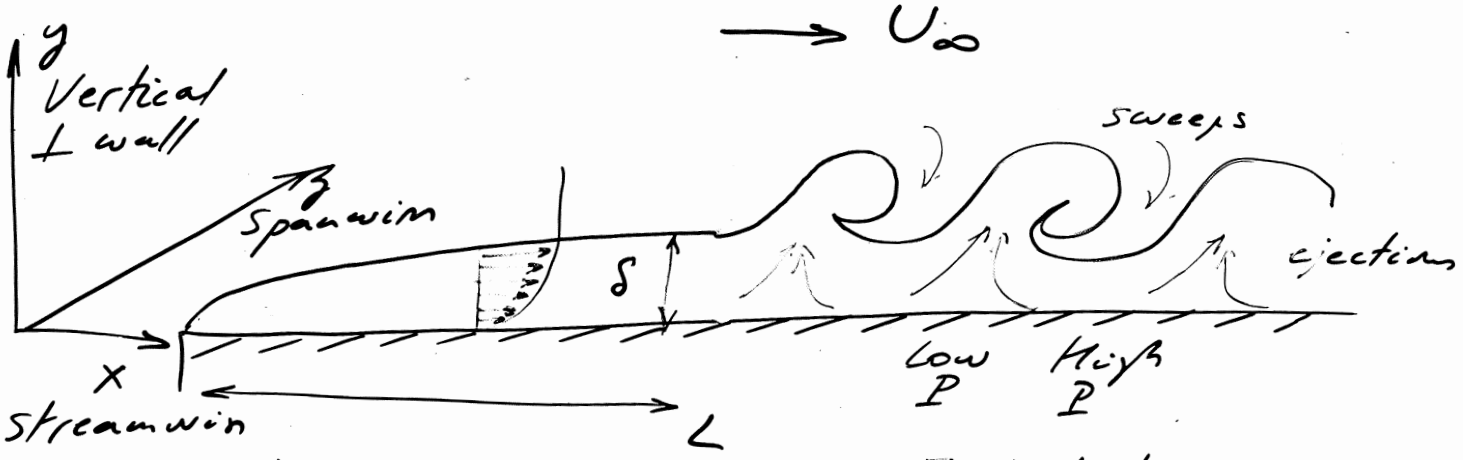

Laminar Boundary layer

$\delta \sim \frac{L}{\sqrt{Re}}$

$Re = \frac{U_\infty L}{\nu}$

10^4

Turbulent Boundary layer

$\delta \sim \frac{(\langle u'^2 \rangle)^{1/2}}{U_\infty} L$

Steady and smooth fluid trajectories, Attached Boundary layer.

Unsteady and random fluid trajectories, Detached Boundary layer.

Prandtl 1904's hypothesis

To solve large Re turbulent flow, one can split the problem into 2, supposing that the boundary layer remains attached:

1. Outer potential flow } Euler equations

$\nu \to 0$ $V_n = 0$

$\delta \to 0$ $V_t = V_0$ on the wall

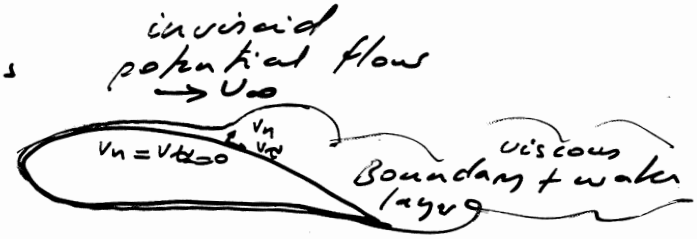

2. Inner Boundary layer } Prandtl equations

$\nu \neq 0$ $V_n = V_t = 0$ on the wall

But matching problem at the interface involving singular perturbation problem $\varepsilon = \frac{\delta}{L} = \frac{1}{\sqrt{Re}}$

THE WALL LAW

Von Karman, 1930

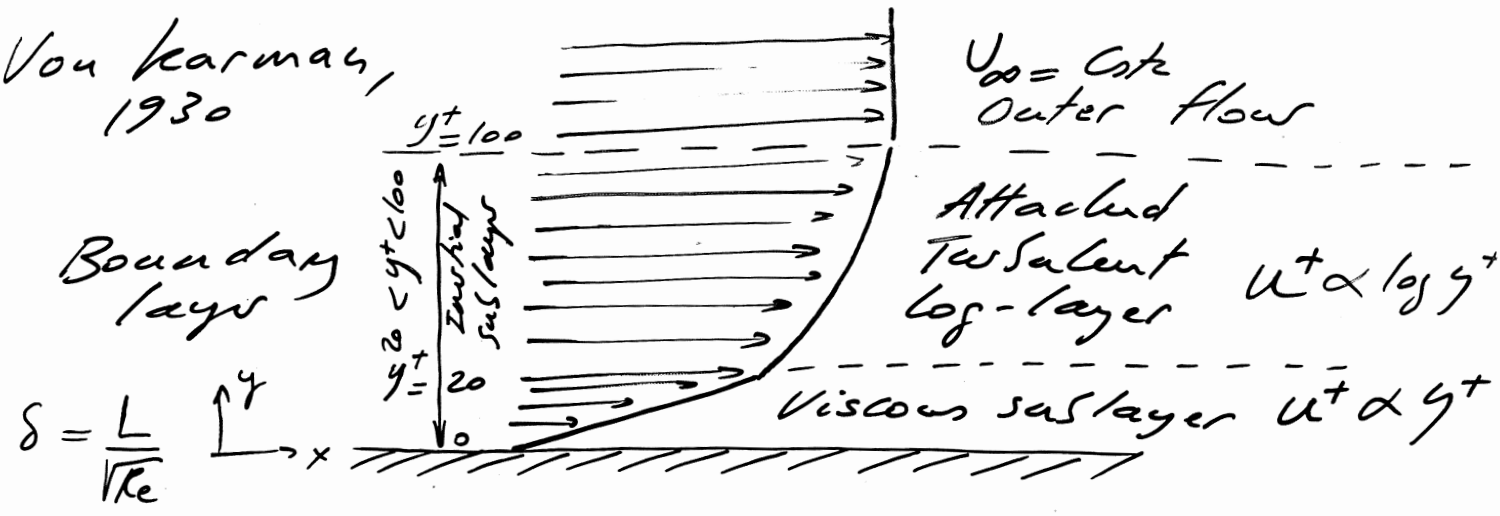

Laboratory experiments show some universal behaviour of attached turbulent boundary layers → wall law.

But the wall law fails as soon as there is detachment & does not account for wall roughness.

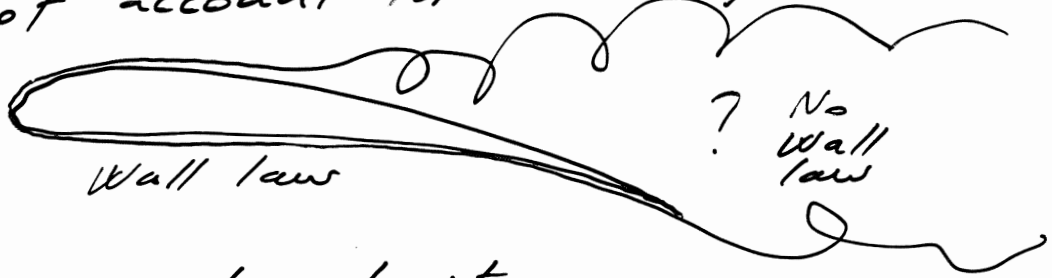

Time averaged velocity:

$$U(x) = \lim_{T\to\infty} \frac{1}{T} \int_0^T u(x,t)$$

$\vec{V}(u,v)$ $v \ll u$

Velocity in wall unit: $u^+ = \dfrac{U}{\left(\nu \dfrac{\partial U}{\partial y}\Big|_{y=0}\right)^{1/2}}$

Distance in wall unit (non dimensional): $y^+ = \dfrac{y\left(\nu \dfrac{\partial U}{\partial y}\Big|_{y=0}\right)^{1/2}}{\nu}$

$\Rightarrow$ the scaled mean flow u^+ is:

$$u^+ = \frac{1}{C_k} \log y^+ + \beta \quad \text{with} \quad \begin{cases} C_k = 0.41 & \text{Von Karman} \\ \beta = 5.5 & \text{Constant} \end{cases}$$

EXPERIMENTAL CHECK OF THE LOGARITHTIC LAW AT THE WALL

$$u^+ = \frac{U}{\left(\nu \left.\frac{\partial U}{\partial y}\right|_{y=0}\right)^{1/2}} \qquad u^+ = 2.5 \ln y^+ + 5.5$$

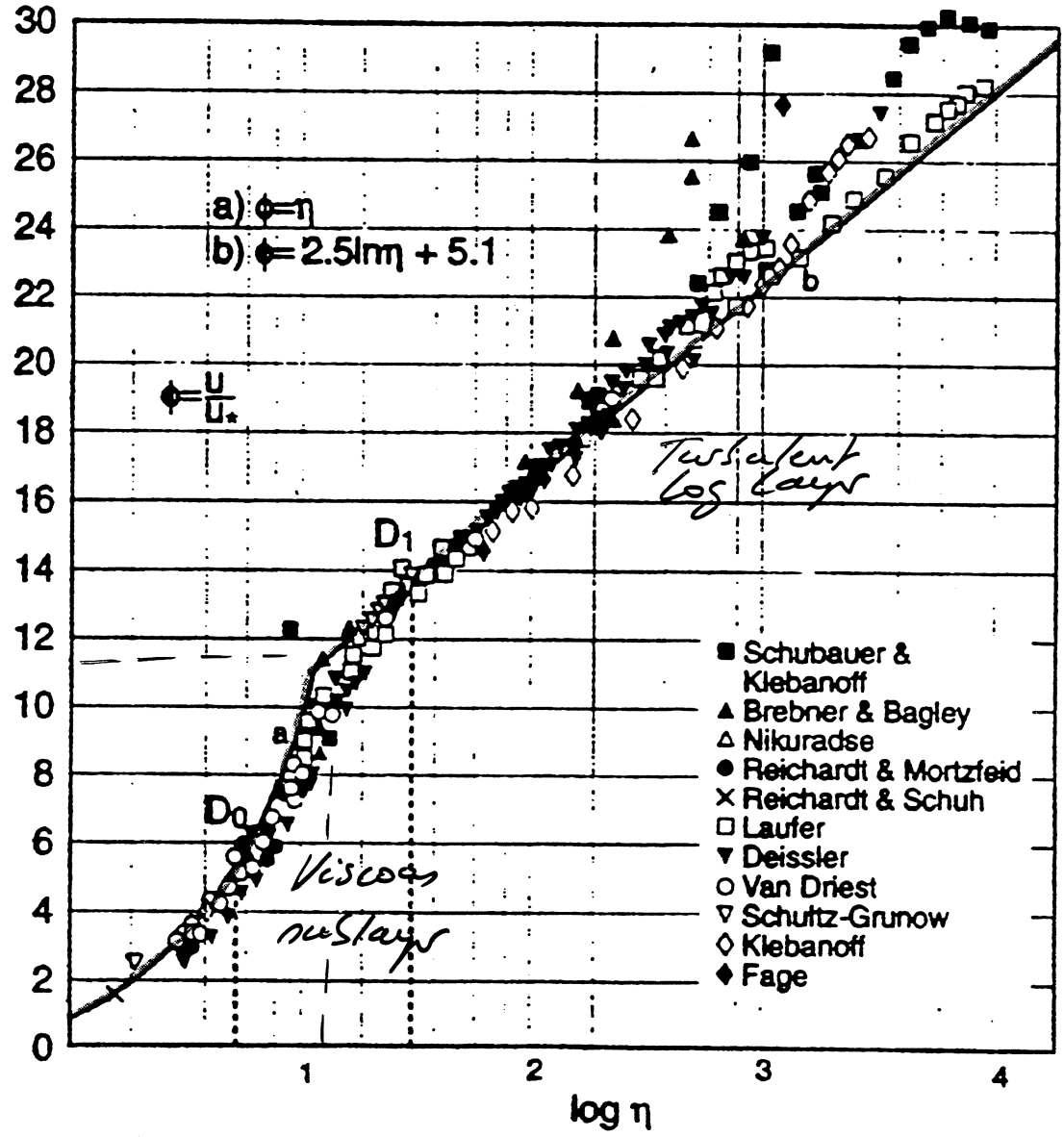

Fig 3. Comparison of the universal logarithmic law with experiment (after Monin and Yaglom [29])

$$\log y^+ = \log \left[\frac{y \left(\nu \left.\frac{\partial U}{\partial y}\right|_{y=0}\right)^{1/2}}{\nu} \right]$$



EXPERIMENTAL CHECK OF THE CHORIN-BARENBLATT LAW AT THE WALL

u^+ $u^+ = f(y^+, Re)$

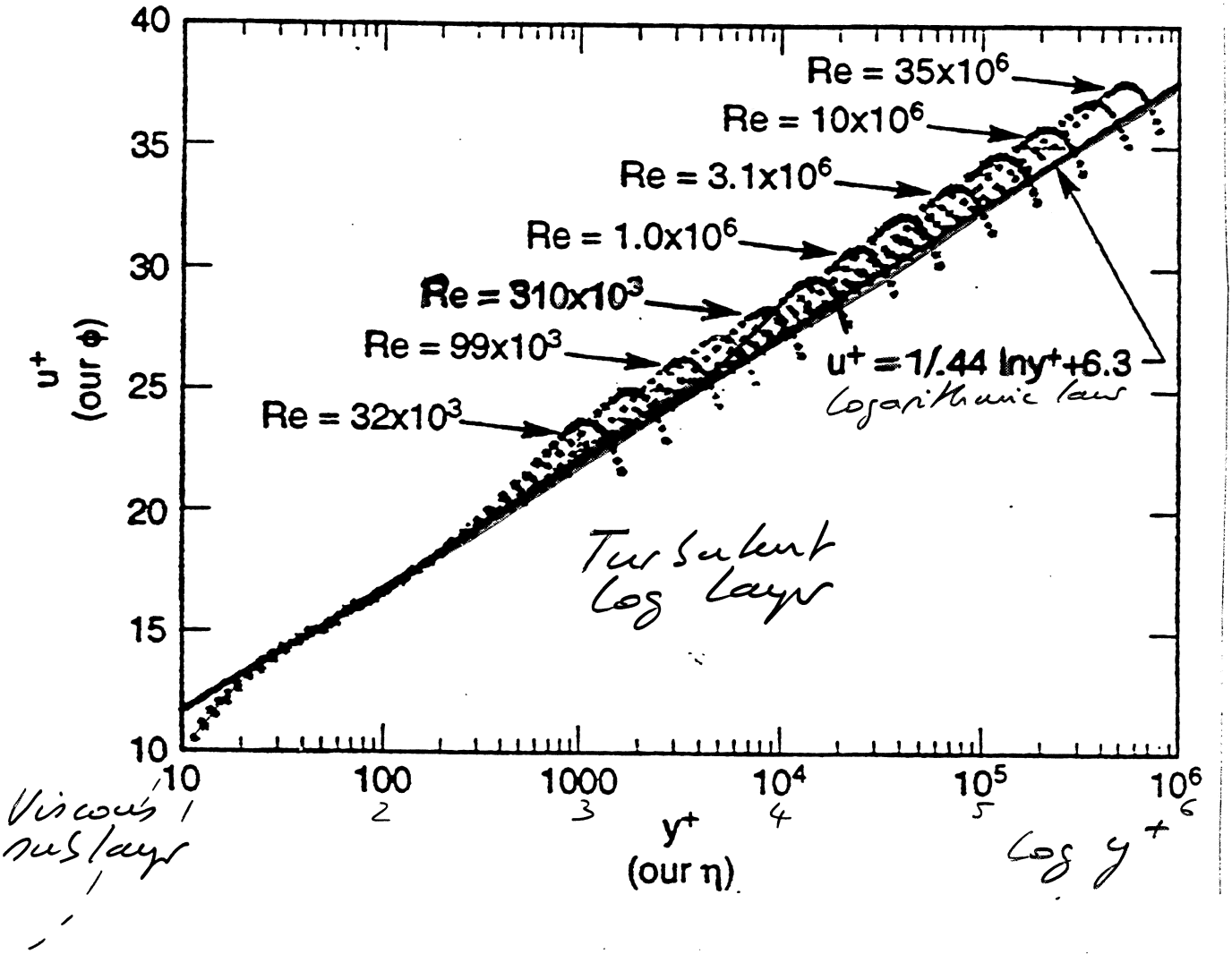

Fig 15. Princeton data [38] obtained in a high-pressure pipe confirm the splitting of the experimental data according to their Reynolds numbers and the predicted chevron-like velocity distribution in the (lnη, ϕ)-plane. The splitting and chevron-like form of the velocity profile agree with the scaling law, and are incompatible with the universal logarithmic law. (Reproduced with permission from [38]).

— Rough pipe
— Smooth pipe

log(100λ)

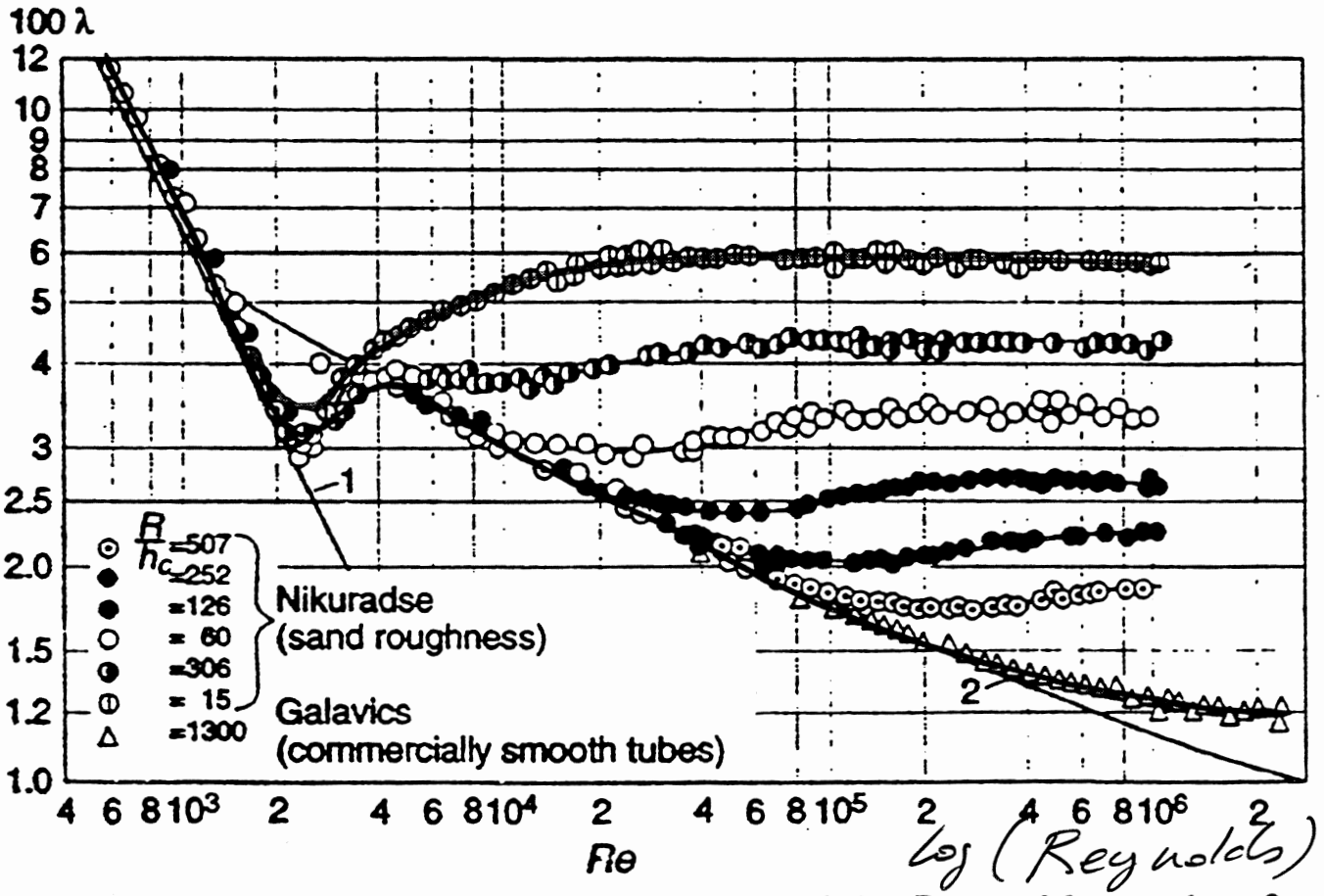

Fig 20. Drag coefficient λ as a function of the Reynolds number for pipes of various roughness (after Monin and Yaglom [29]). (1) Laminar flow, (2) law for smooth pipes.

DRAG COEFFICIENT
λ AS A FUNCTION
OF REYNOLDS NUMBER
$Re = 10^3$ to 10^6

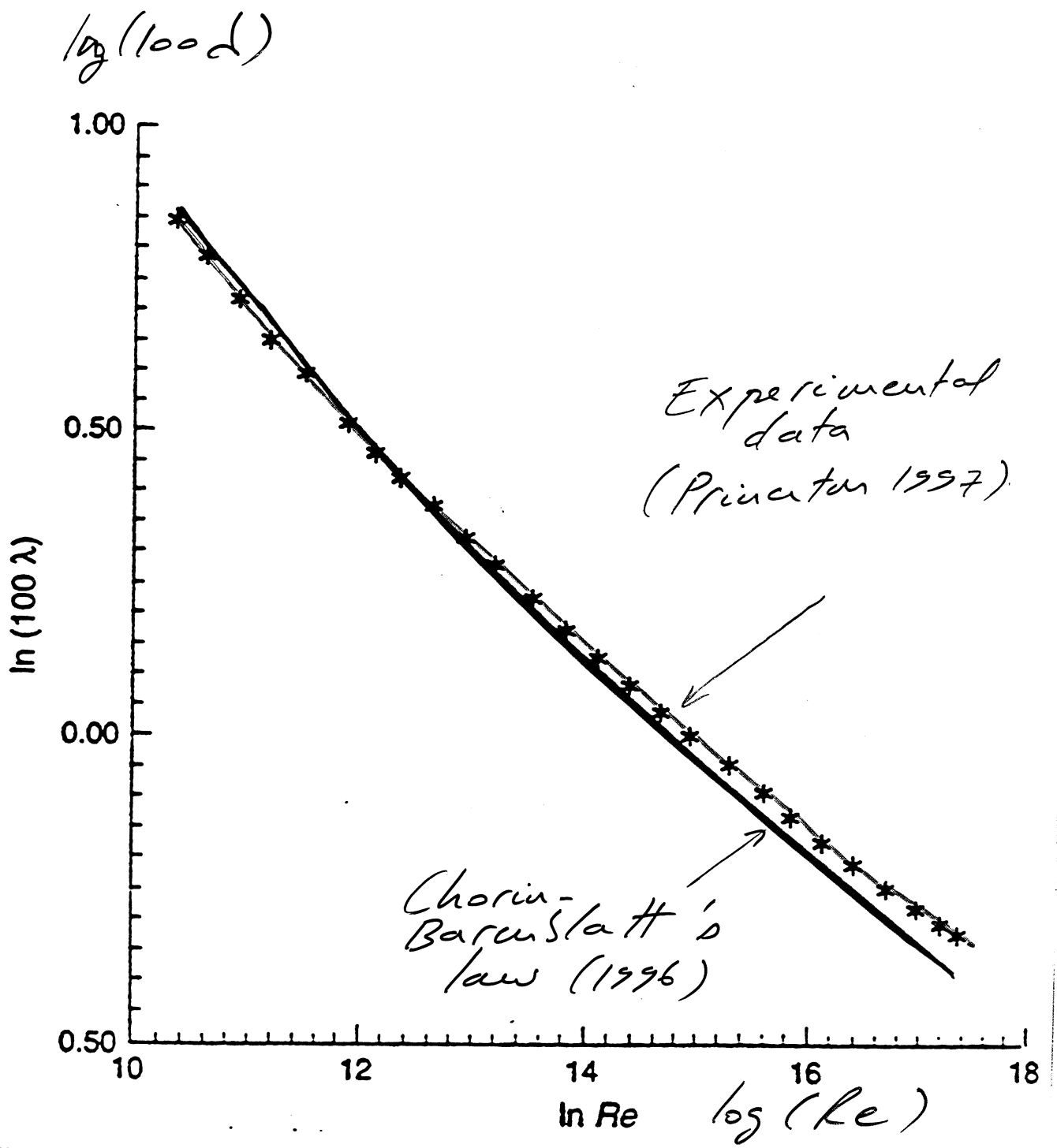

Fig 21. Drag coefficient λ as a function of the Reynolds number for the Princeton data. *- Princeton data; the continuous line is the law for smooth pipes.

DRAG COEFFICIENT
λ AS A FUNCTION
OF REYNOLDS NUMBER
$Re = 10^{10}$ to 10^{18}

HOW TO COMPUTE FLUID INTERACTION WITH WALLS OR OBSTACLES?

1. Euler equation ($\nu = 0$)
+ slip boundary conditions ($V_{wall} \neq 0$):

The solution is modified in the boundary layer using Prandtl's wall law.
This method fails when the boundary layer detaches (large Re).

2. Navier-Stokes equation ($\nu \neq 0$)
+ no-slip boundary conditions ($V_{wall} = 0$):

The solution is computed using finite differences, finite elements, Chebyshev polynomials or wavelets on the interval.
This method requires $\Delta x << \delta \propto Re^{-1/2}$ to have enough resolution in the boundary layer of thickness δ.

3. Penalisation method:
- either add an appropriate body force to simulate the obstacle (Peskin 77) but no error estimation,
- or suppose that the fluid is a porous medium described by d'Arcy equation (Brinkman & Fabrie 1997) with error estimation.

PENALISATION BY ARTIFICIAL POROSITY

The interaction of the fluid with the obstacle or the wall is approximated by

$$\frac{\partial \vec{V}}{\partial t} + \vec{V}.\nabla\vec{V} + \frac{1}{\rho}\nabla P = \nu\nabla^2\vec{V} + \nu\frac{\Pi}{\varepsilon}\vec{V}$$

therefore in the limit $\varepsilon \to 0$

the mask $\Pi(\vec{X})$ is

$\Pi(\vec{X}) = 1 \Rightarrow \dfrac{\Pi(\vec{X})}{\varepsilon} \to \infty$

$\Rightarrow \infty$ porosity in the solid,

$\Pi(\vec{X}) = 0 \Rightarrow \dfrac{\Pi(\vec{X})}{\varepsilon} \to 0$

$\Rightarrow$ no porosity in the fluid.

It has been demonstrated (Bruneau & Fabrie 1997) that the error of this approximation decreases like $\varepsilon^{3/4}$.

DRAG AND LIFT

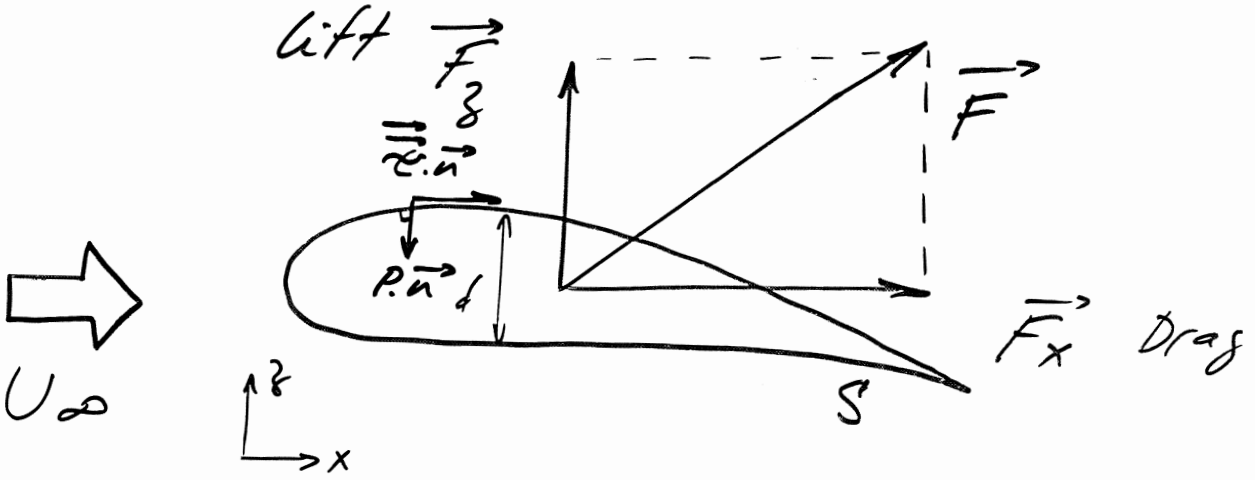

Total force by length unit $\vec{F}$ exerted by the fluid on the body:

$$\vec{F} = -\int_S (P.\vec{n})\,dS + \int_S (\vec{\tau}.\vec{n})\,dS$$

$$= -\int_S \begin{matrix}\text{normal}\\ \text{component}\\ \text{of the stress}\\ \text{at the wall}\end{matrix} + \int_S \begin{matrix}\text{tangential}\\ \text{component}\\ \text{of the stress}\\ \text{at the wall}\end{matrix}$$

with P pressure
$\vec{\tau}$ viscous stress tensor
S surface of the body
ρ density

⇒ Drag C_x and lift C_z are adimensional numbers:

$$C_x = \frac{F_x}{\frac{1}{2}\rho U_\infty^2 d} = F(Re)$$

same for C_z

2D NAVIER-STOKES USING A FOURIER CODE WITH THE PENALISATION METHOD

Network of cylinders at Re=200, α =45°

(joint work with Nicholas Kevlahan)

McMaster, Canada et Kai SCHNEIDER, Karlsruhe, Allemagne, 1999

t= 18

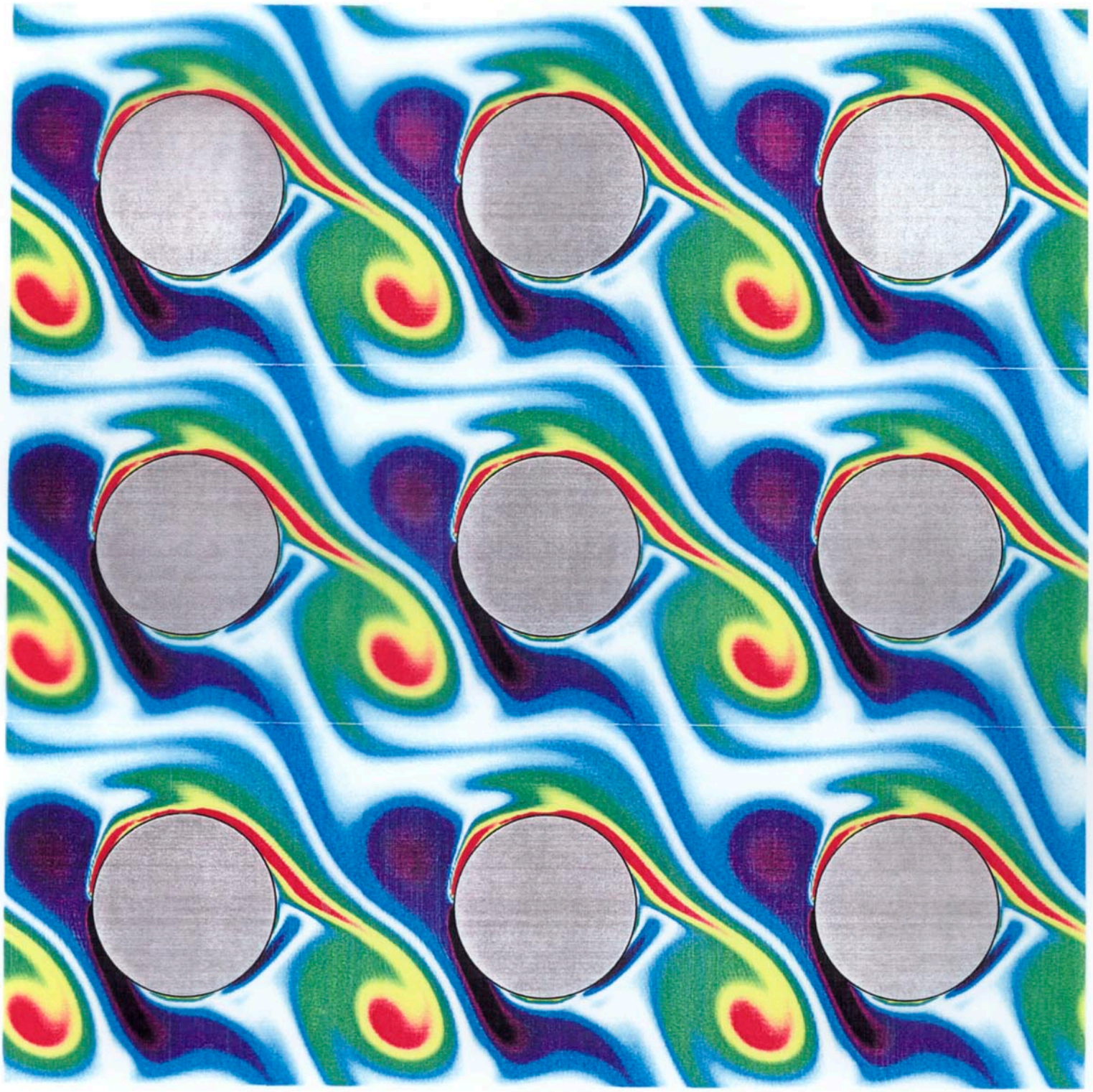

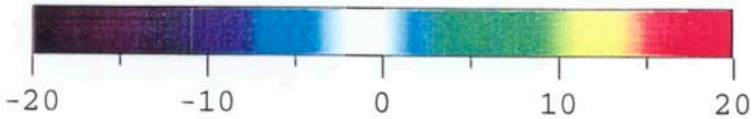

Vorticity

2 x 2 (256 x256)
Pseudo-spectral method
with penalization (η =1.e-3)

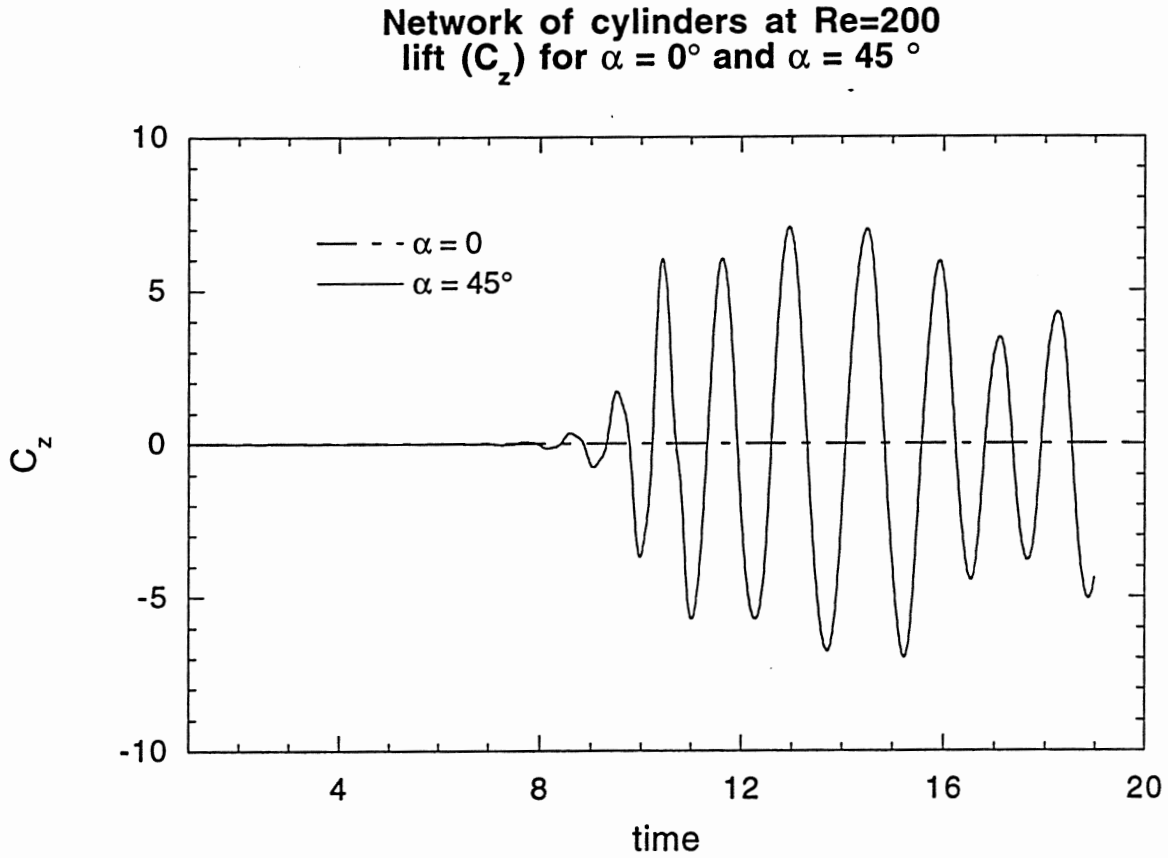
Network of cylinders at Re=200
lift (C_z) for α = 0° and α = 45 °
10
5
0
-5
-10
C_z
$\alpha = 0$
$\alpha = 45°$
4
8
12
16
20
time

Network of cylinders at Re=200
drag C_x for $\alpha = 0°$ and $\alpha = 45°$

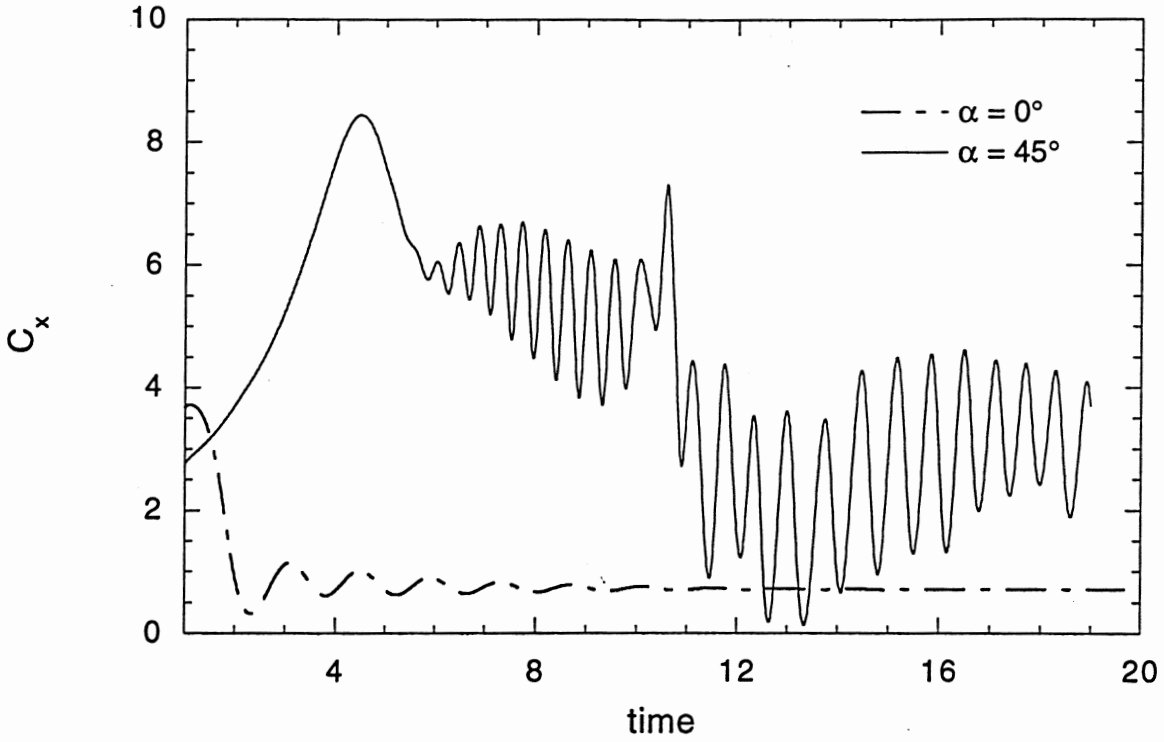

Network of cylinders at Re=200
rms-vorticity for $\alpha = 0°$ and $\alpha = 45°$

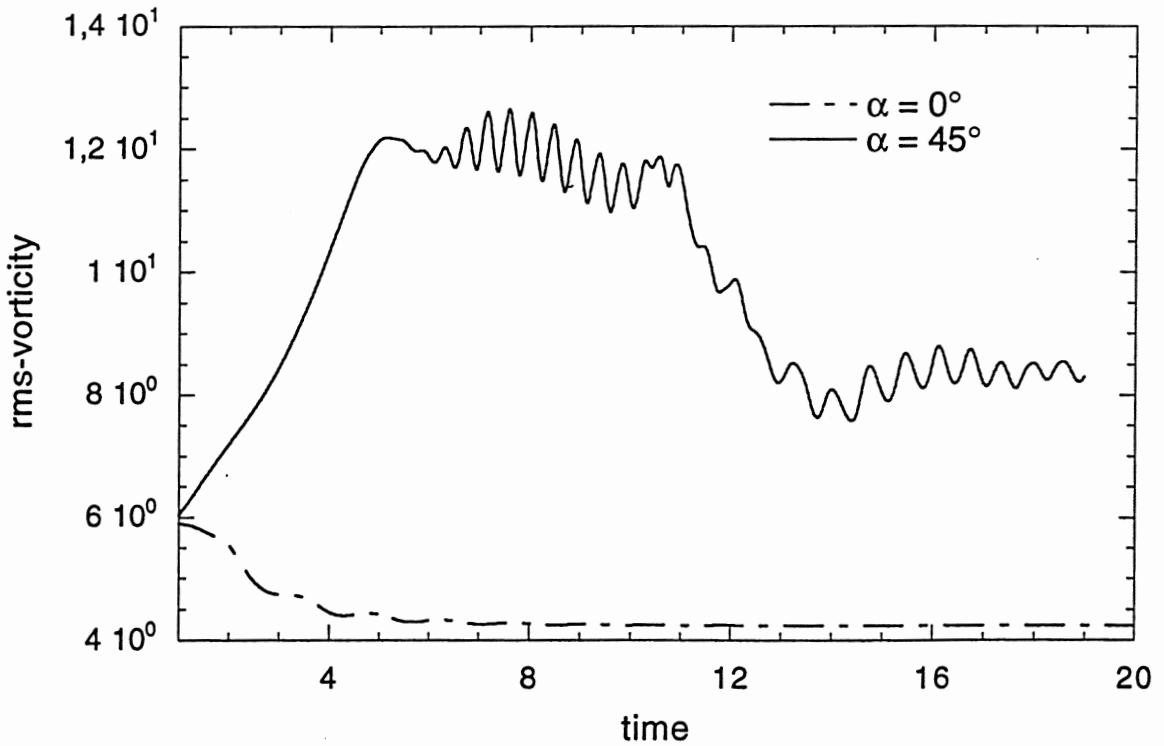

Network of cylinders at t=10, Re=1000, α =0°

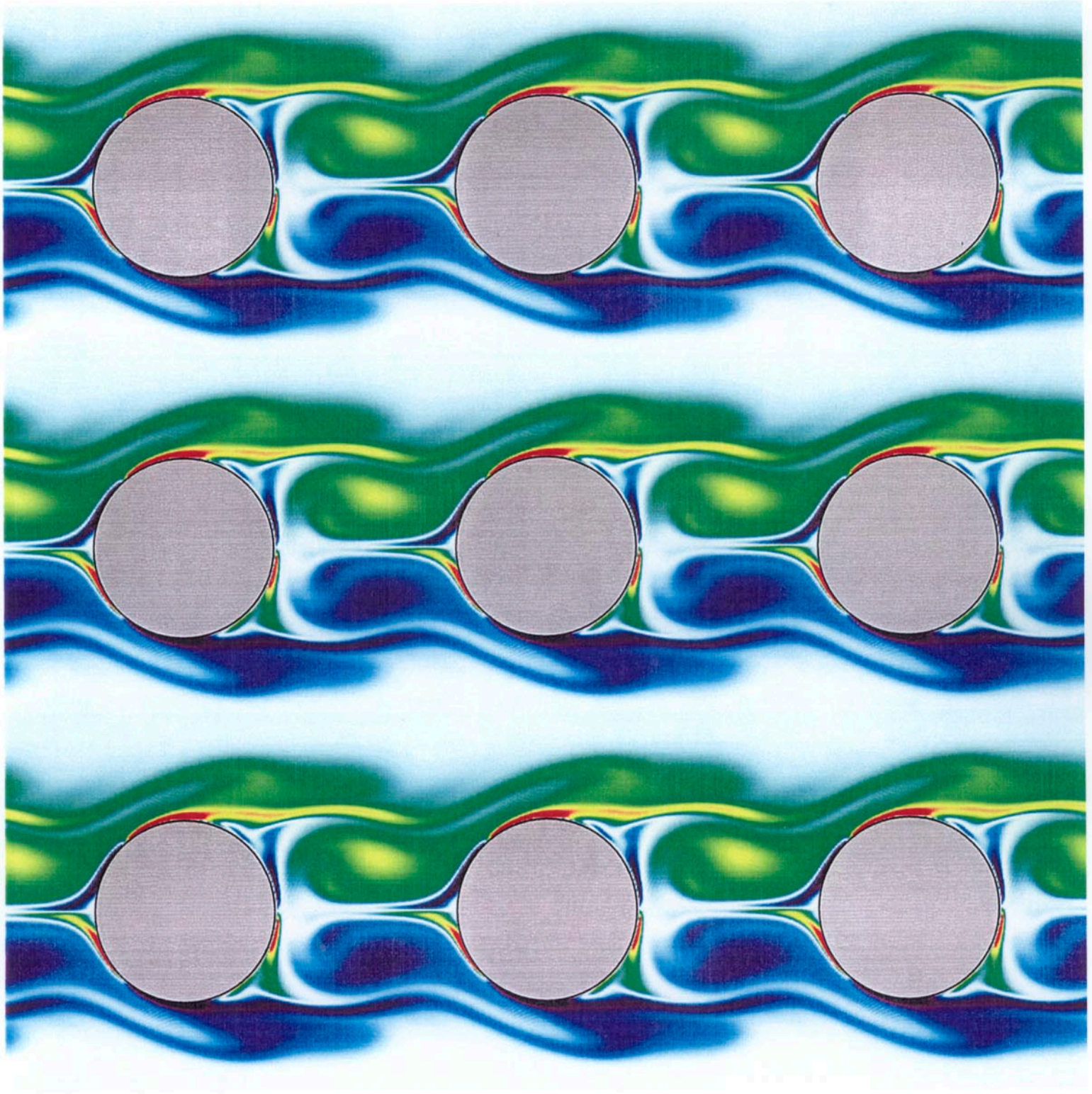

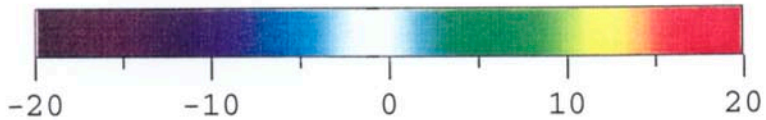

Vorticity

2 x 2 (512 x 512)
Pseudo-spectral method
with penalization (η =1.e-3)

(joint work with Nicholas Kevlahan)

Network of cylinders at t= 6, Re=1000, α =45°

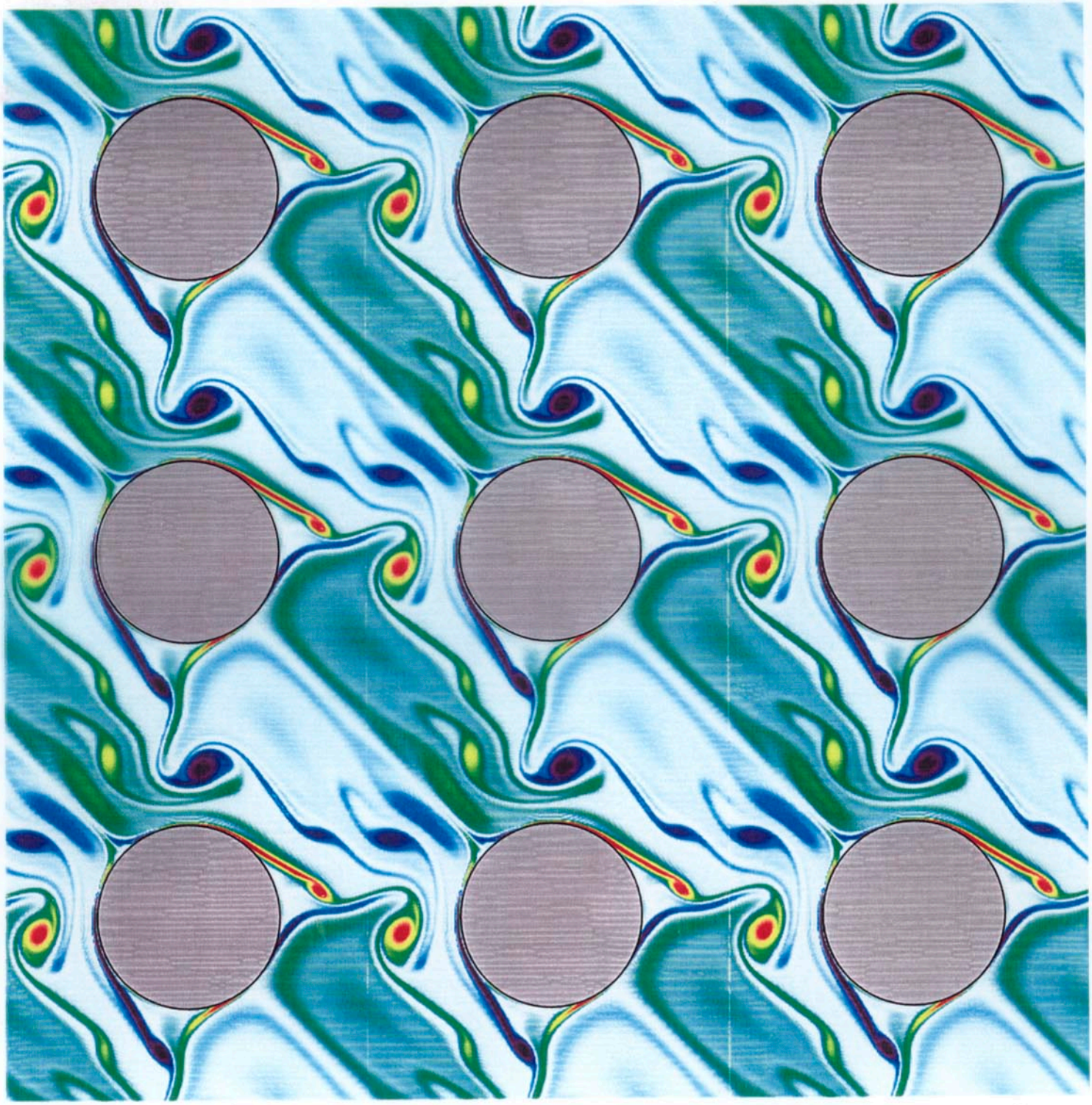

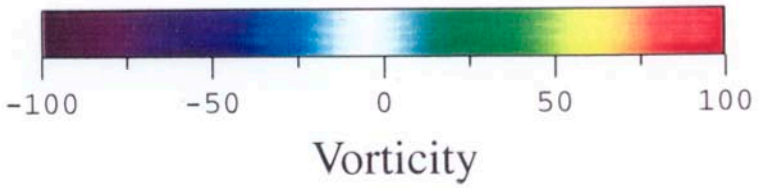

2 x 2 (512 x 512)
Pseudo-spectral method
with penalization (η =1.e-3)

(joint work with Nicholas Kevlahan)

Ecoulement derrière un réseau de cylindres en quinconce à Reynolds 1000

Champ de vorticité instantané

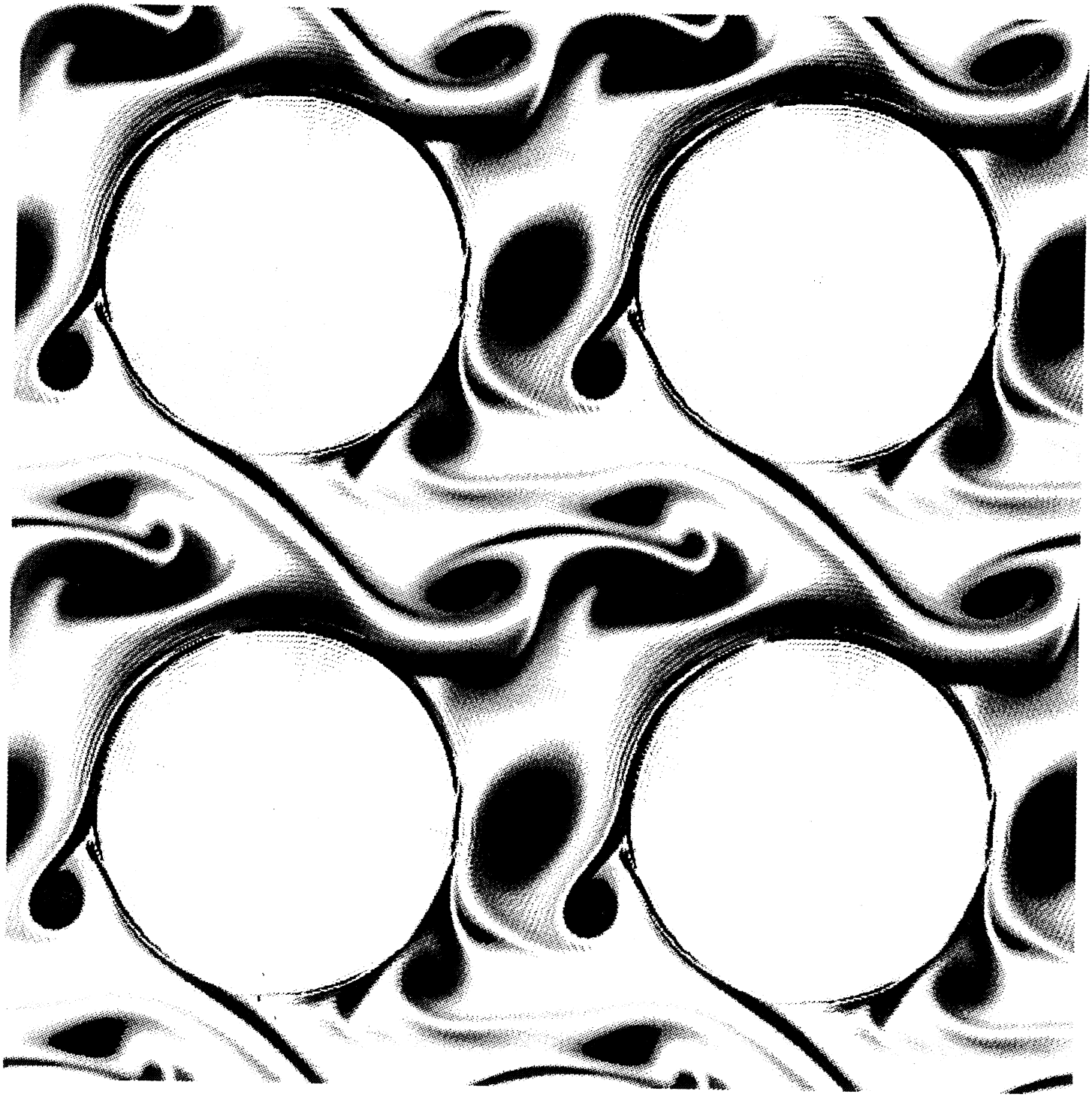

Re = 1000, no smoothing, rotated square array, 288x288, t=10

Nichlolas Kevlahan, Juin 1998

Ecoulement derrière un cylindre à Reynolds 200

Evolution temporelle de la portance

portance Cz

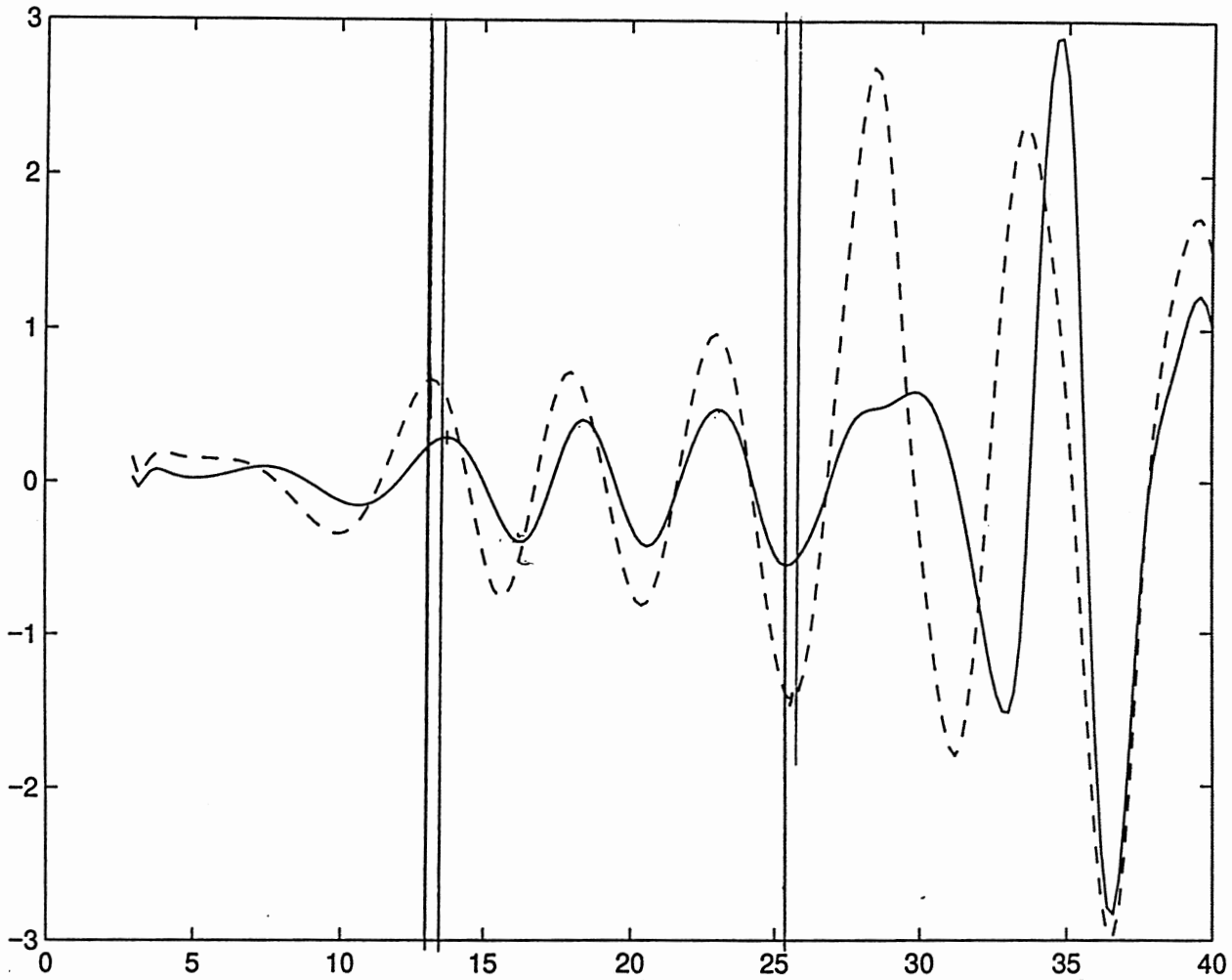

temps

Avec paroi lisse (traits pleins)
on obtient une fréquence de Strouhal de 0.218
Avec paroi rugueuse (traits pointillés)
on obtient une fréquence de Strouhal de 0.200

Williamson (1989) a mesuré en laboratoire
une fréquence de Strouhal de 0.195

Nichlolas Kevlahan, Juin 1998

Ecoulement derrière un cylindre à Reynolds 200

Evolution temporelle de la trainée

traînée Cx

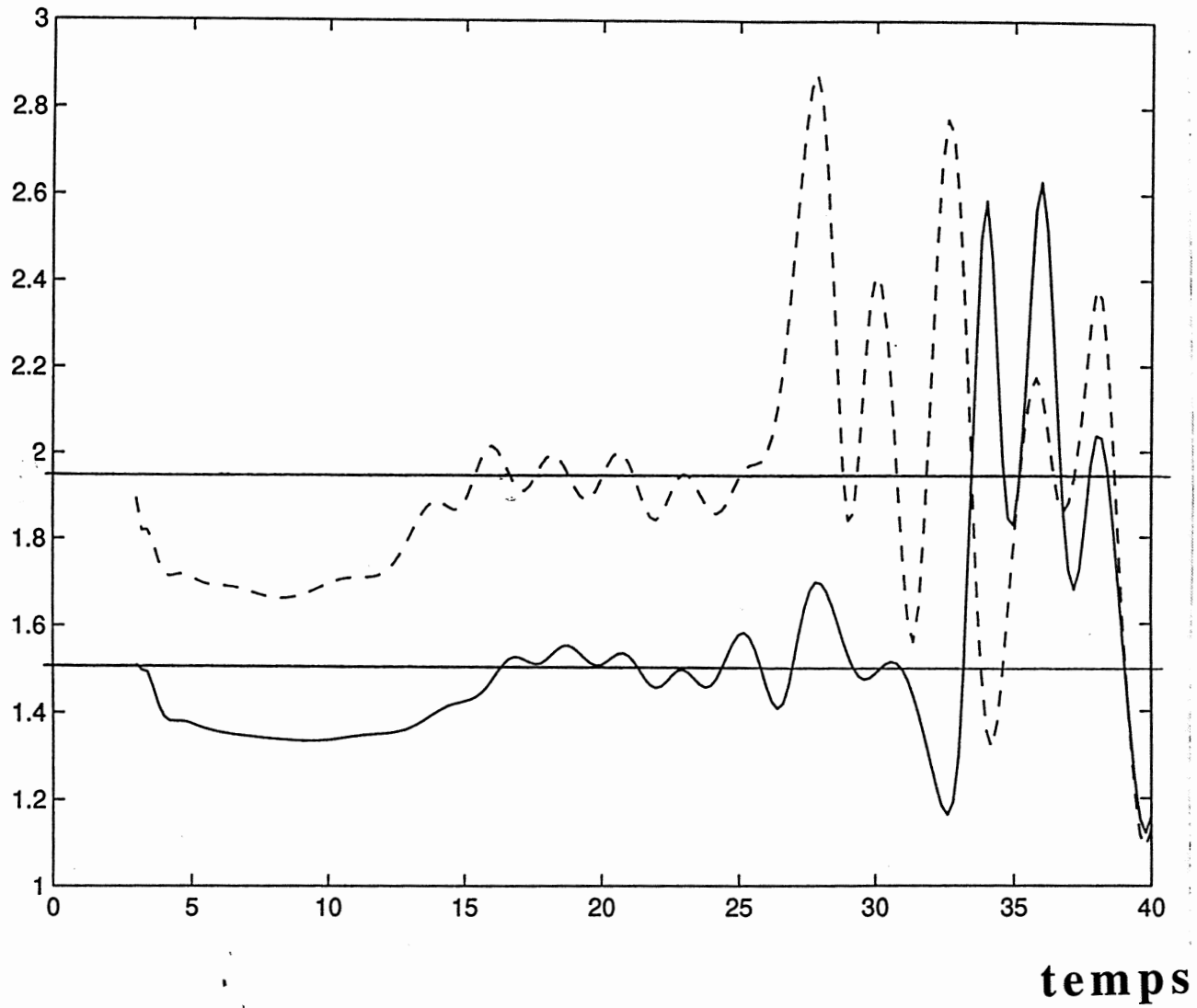

Avec paroi lisse (traits pleins)
Avec paroi rugueuse (traits pointillés)

Khadra et al. (1998) ont observé dans leurs expériences numériques une trainée de 1.40

Nichlolas Kevlahan, Juin 1998

THE WALL PROBLEM

'Un ensemble de molécules constituant un gaz ou un liquide cesse, en général, près des parois, d'avoir les propriétés d'un fluide, et, comme voie de conséquence, l'hydrodynamique classique cesse de lui être applicable !

Yves ROCARD, 1932
L'Hydrodynamique
et la théorie
cinétique des gaz
Gauthier-Villars



Germs for hydrodynamical instability ⇒ vortex generation

HAIRPIN VORTICES IN THE TURBULENT BOUNDARY LAYER

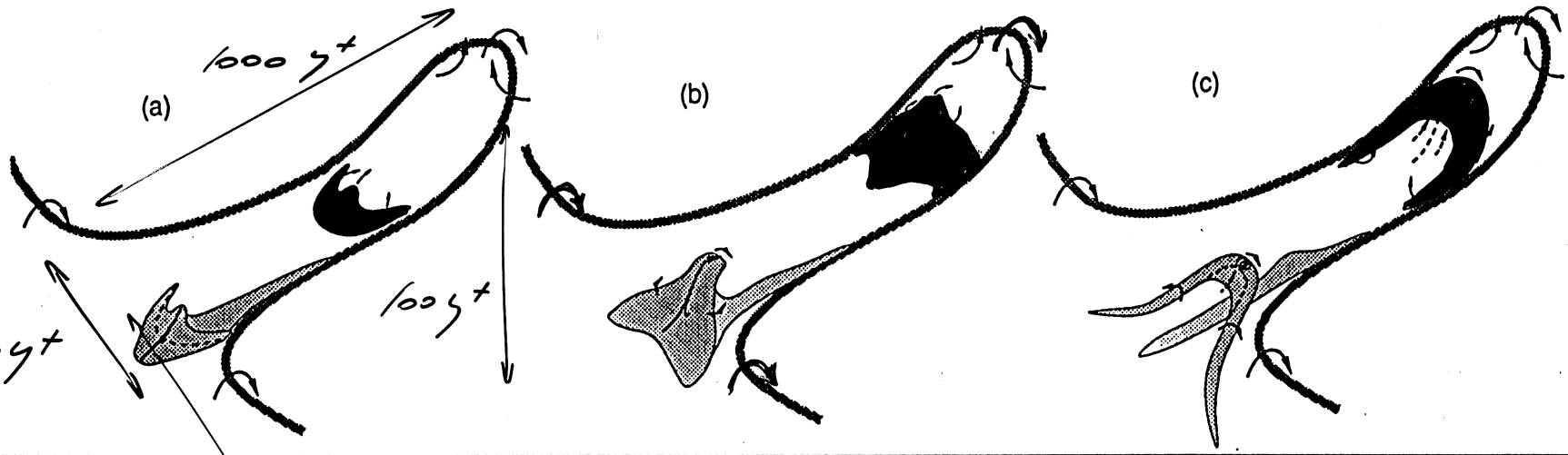

Spacing between hairpin vortices

The Reynolds shear stress $\langle u'v' \rangle$ is produced at the wall in a very intermittent fashion by bursting.

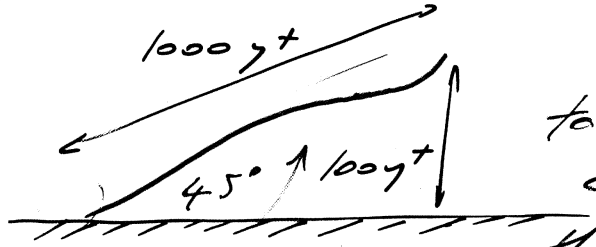

Bursting ⟹

45° to maximize $\langle u'v' \rangle$ the Reynolds Stress

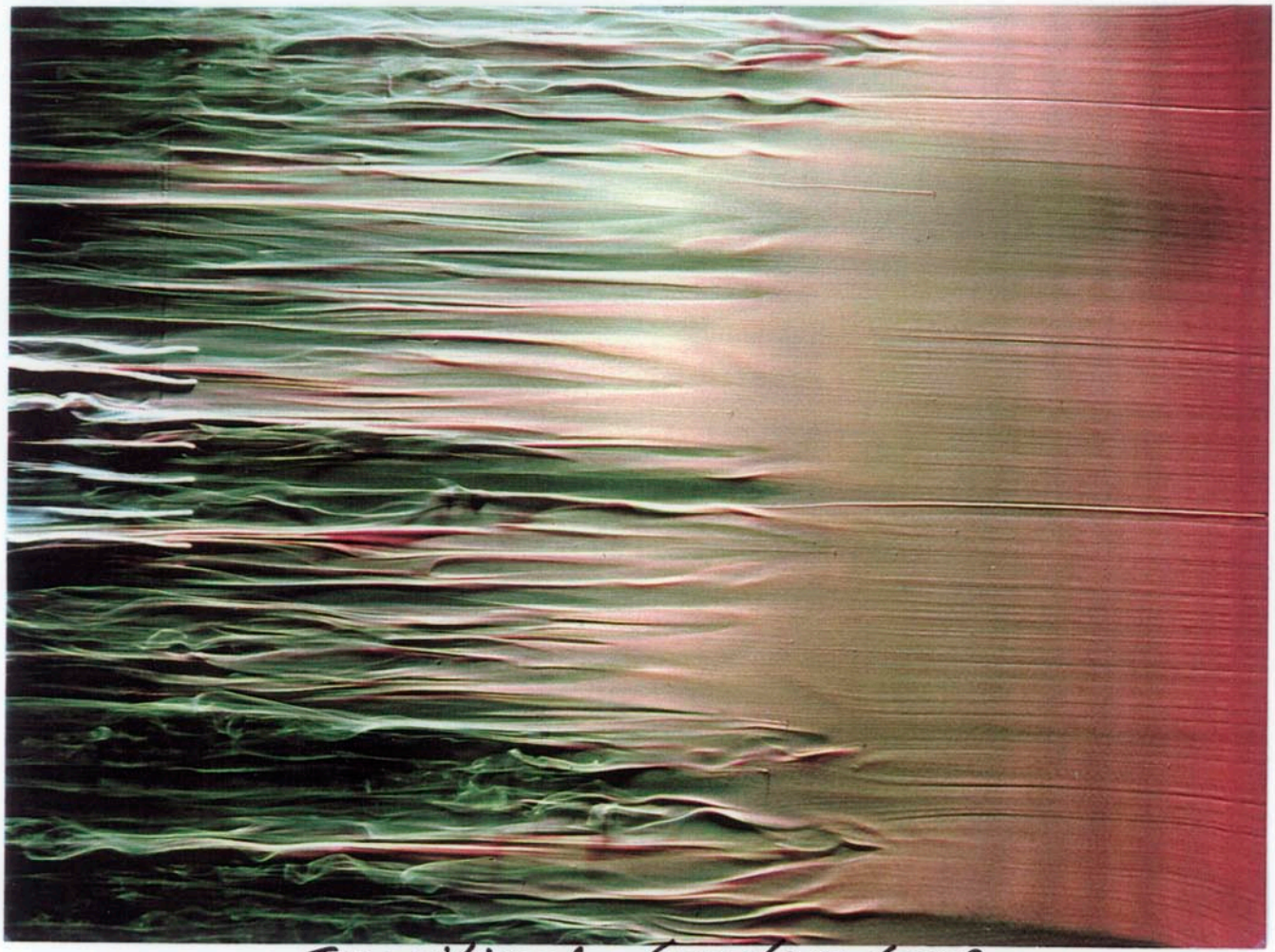

Transitional boundary layer

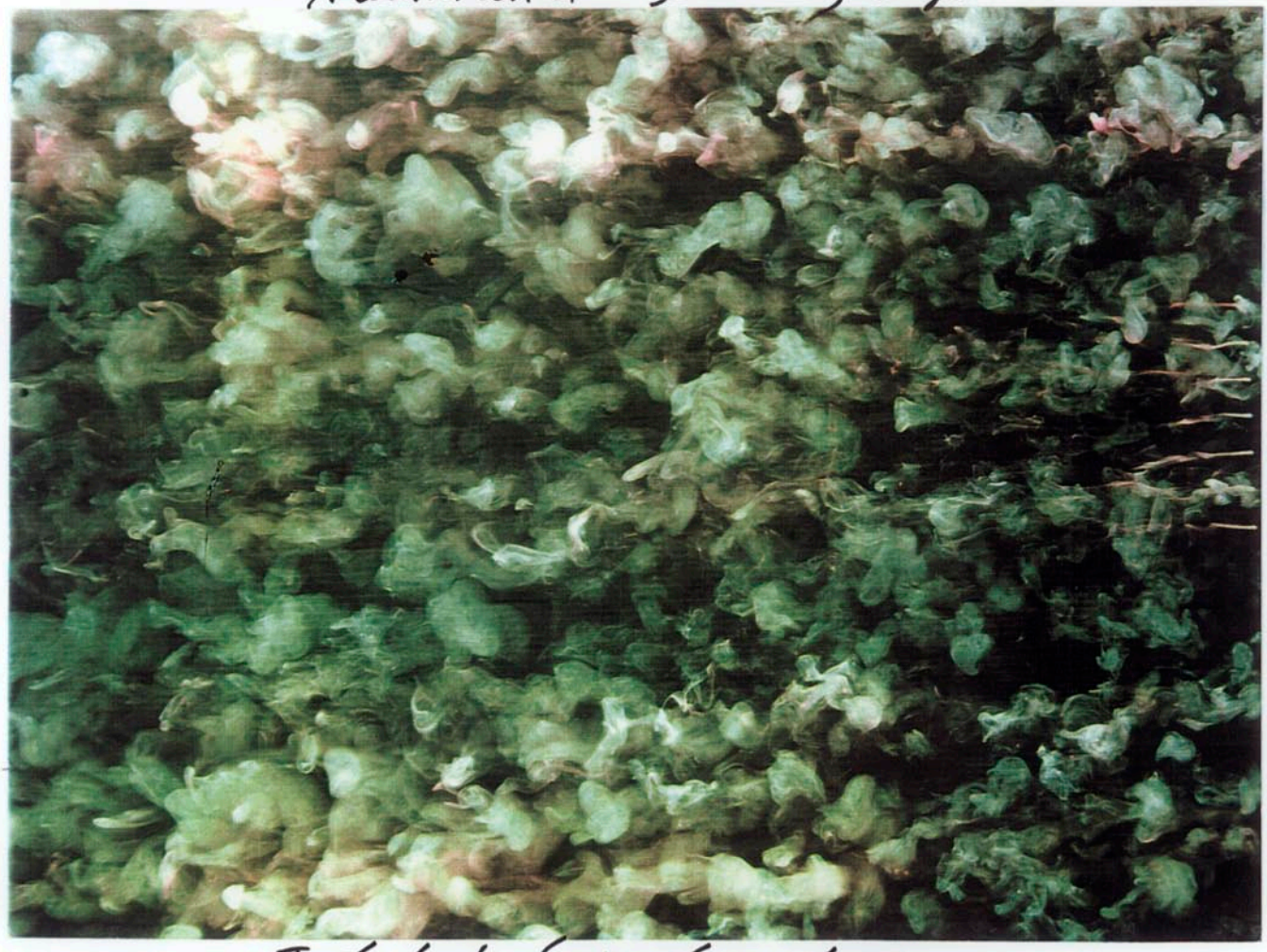

Turbulent boundary layer

LABORATORY EXPERIMENT
BY Henri WERLE

TURBULENT WALL FLOW



Henri WERLE, ONERA — Laboratory experiment

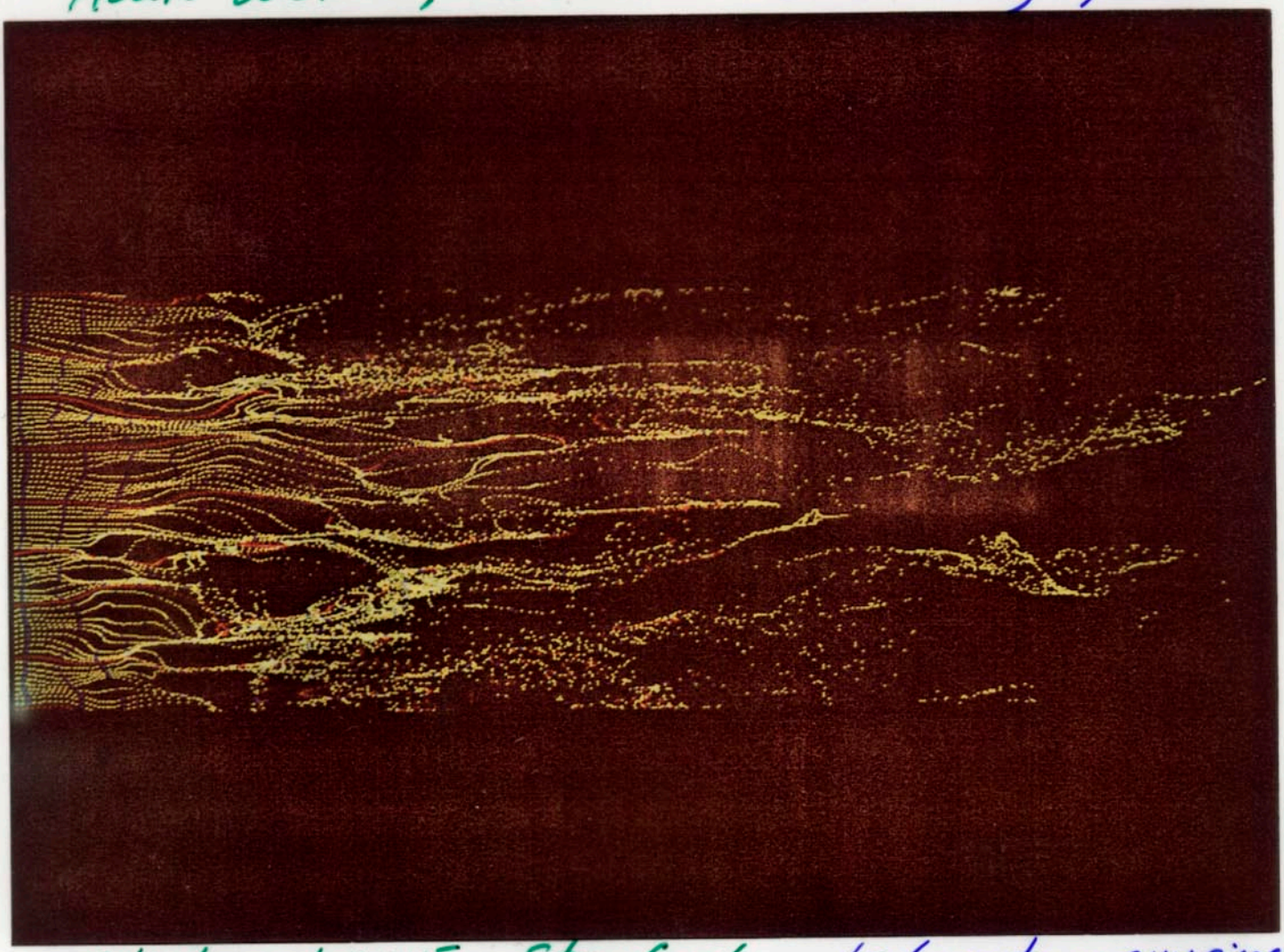

Stephen KLINE, Stanford — Laboratory experiment

MIXING LAYER

Anatol ROSHKO
Aeronautic Laboratory
Caltech

Santa Barbara Workshop, FEB. 97

- Reynolds number may not be as important as we think, because we observe the same features whatever the Reynolds number. It does not seem to affect the large scale structures!

- The mean velocity profile is a tricky concept, because it never exists!

- Turbulence is driven by instabilities and very small stochastic forcing (e.g. irregularity of the wall) changes their growth from linear to nonlinear!

- Spots are better building blocks for boundary layers than Tollmien-Schlichting waves!

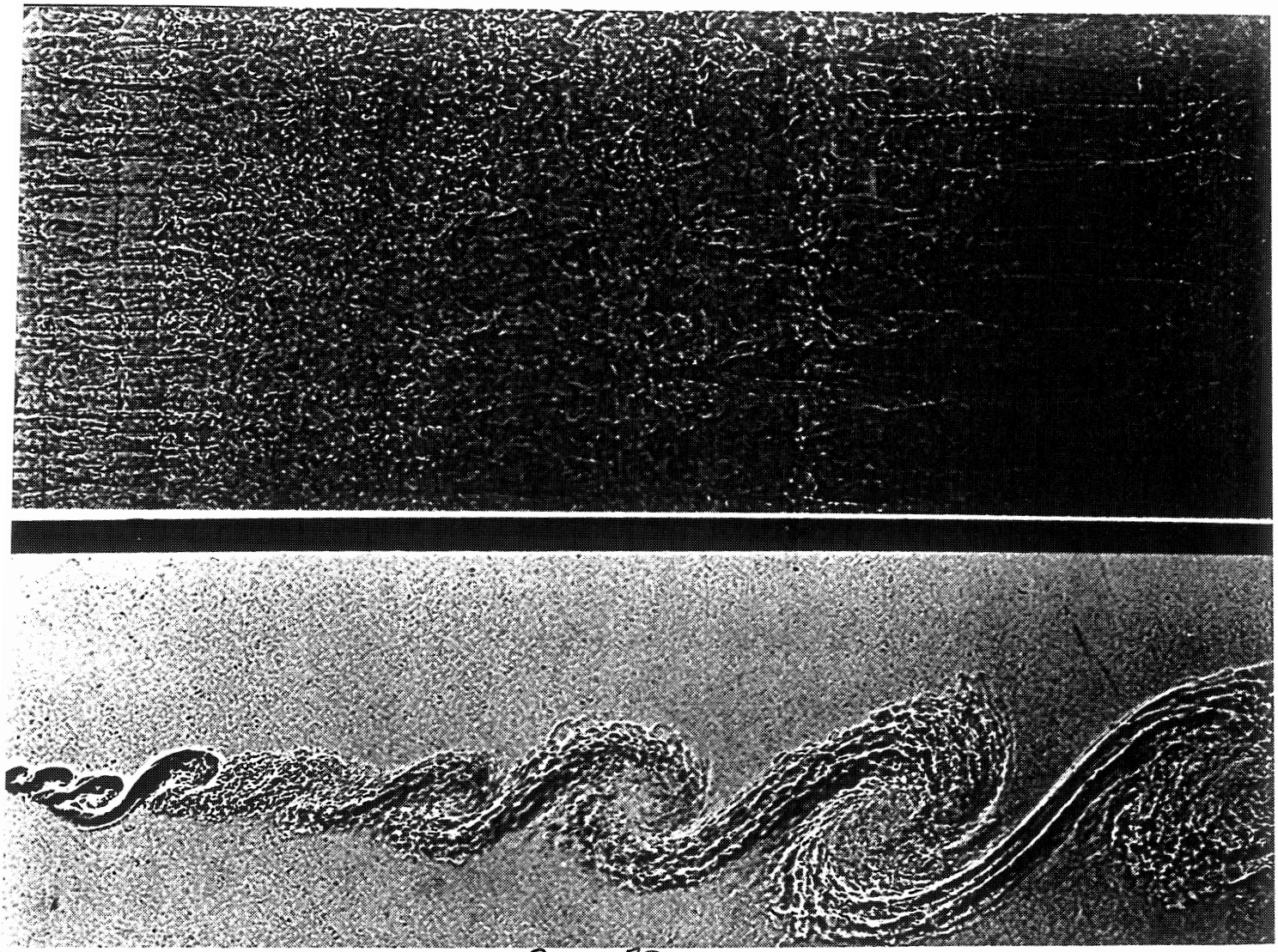

Re = 850 000

176. Large-scale structure in a turbulent mixing layer. Nitrogen above flowing at 1000 cm/s mixes with a helium-argon mixture below at the same density flowing at 380 cm/s under a pressure of 4 atmospheres. Spark shadow photography shows simultaneous edge and plan views, demonstrating the spanwise organization of the large eddies. The streamwise streaks in the plan view (of which half the span is shown) correspond to a system of secondary vortex pairs oriented in the streamwise direction. Their spacing at the downstream side of the layer is larger than near the beginning. *Photograph by J. H. Konrad, Ph.D. thesis, Calif. Inst. of Tech., 1976.*

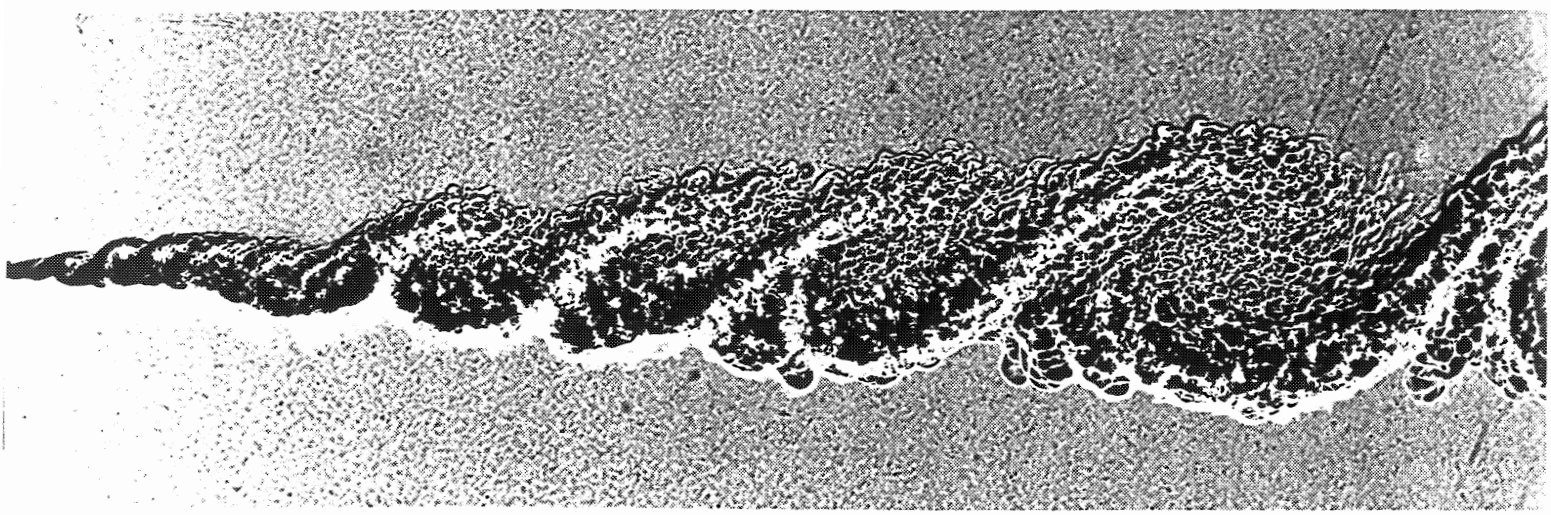

177. Coherent structure at higher Reynolds number. This flow is as above but at twice the pressure. Doubling the Reynolds number has produced more small-scale structure without significantly altering the large-scale structure. *M. R. Rebollo, Ph.D. thesis, Calif. Inst. of Tech., 1976; Brown & Roshko 1974*

Re = 1 700 000
coherent structur remain at large Re

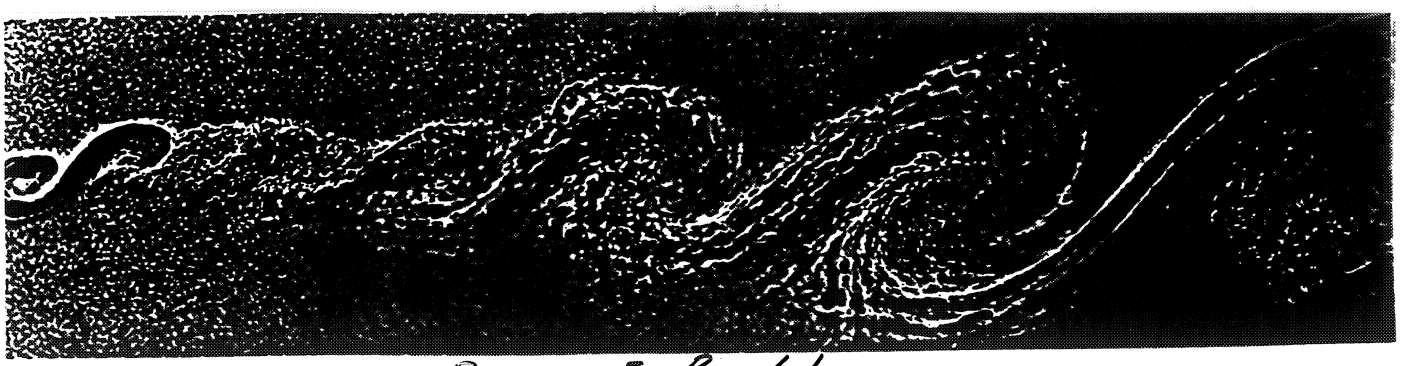

Brown & Roshko
1974



$Re = 850\,000$



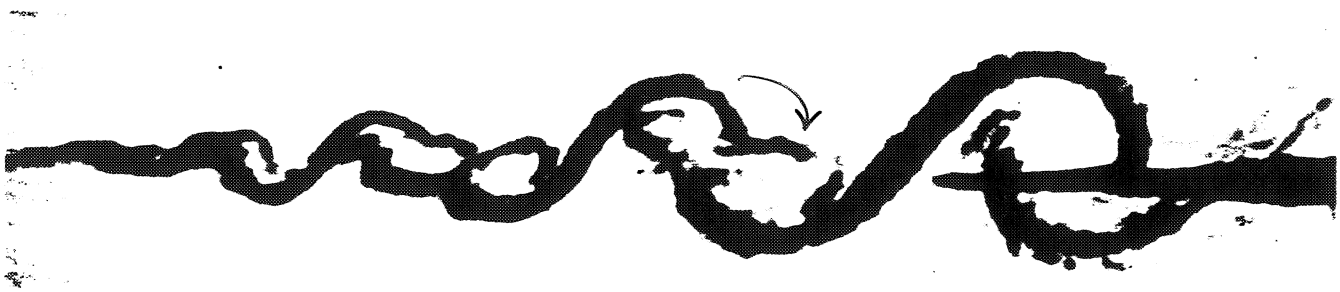





Vortex merging

(Kai Schneider, Karlsruhe University, 1997)

Vortex line: $\omega(x,y,t=0) = A * EXP(-((X-X0)^{**}2)/S^{**}2)$
with A = PI, S = 0.1 * 1.e0/PI, X0= PI + 0.05 * (n -0.5), n ~ U(0,1)
NX=NY=256, nu= 5.e-5 dt= 2.5e-3, t=0, 12.5, 25, 37.5

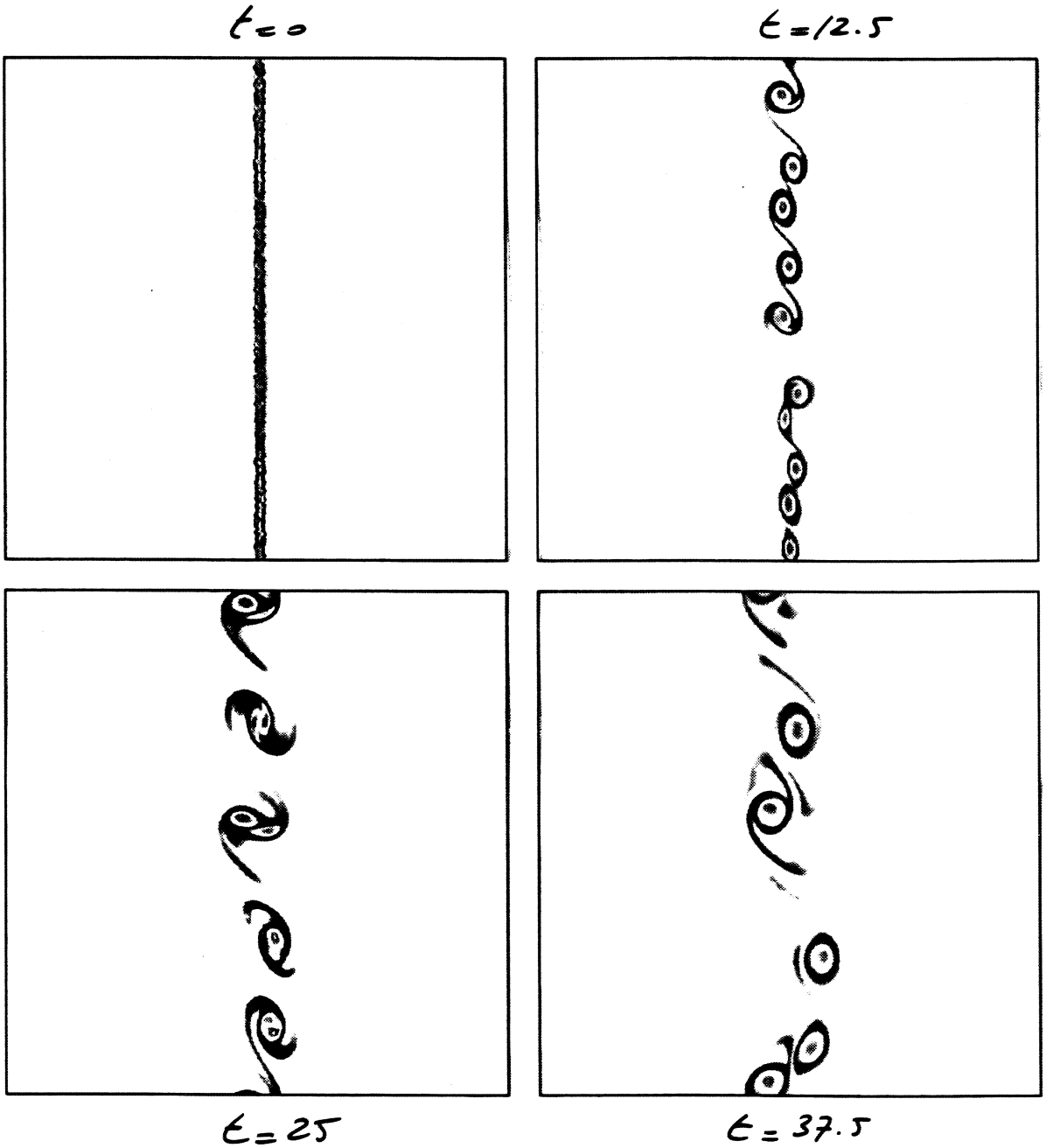

Mixing Layer
2D Direct Numerical Simulation
256^2
pseudo-spectral
code

Figure IV.4.a

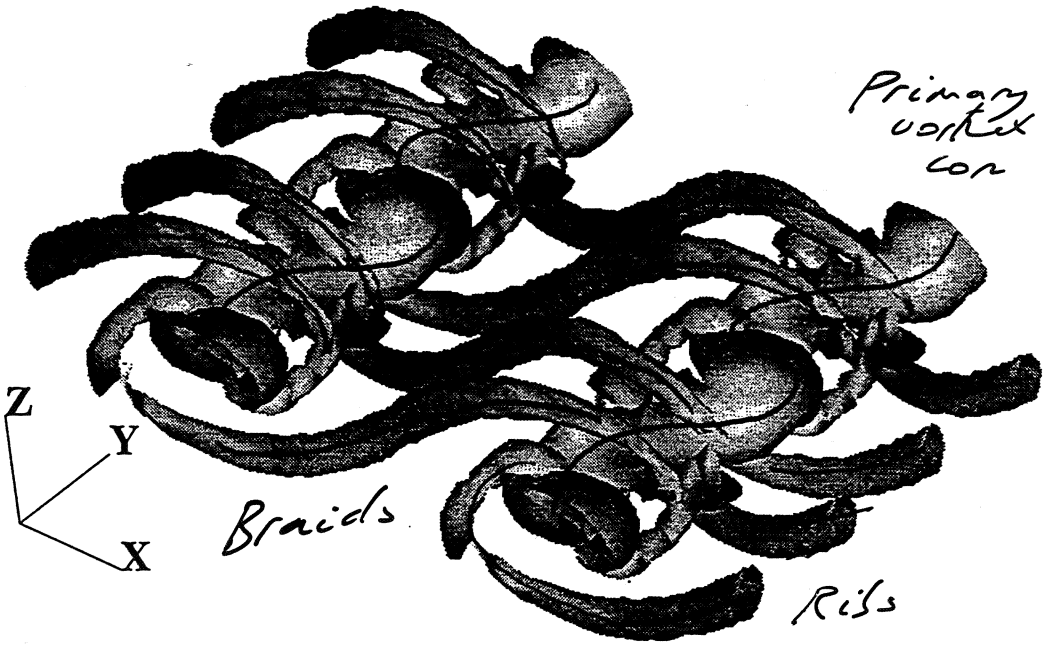

MIXING LAYER
3D Numerical Simulation

Figure IV.4.b

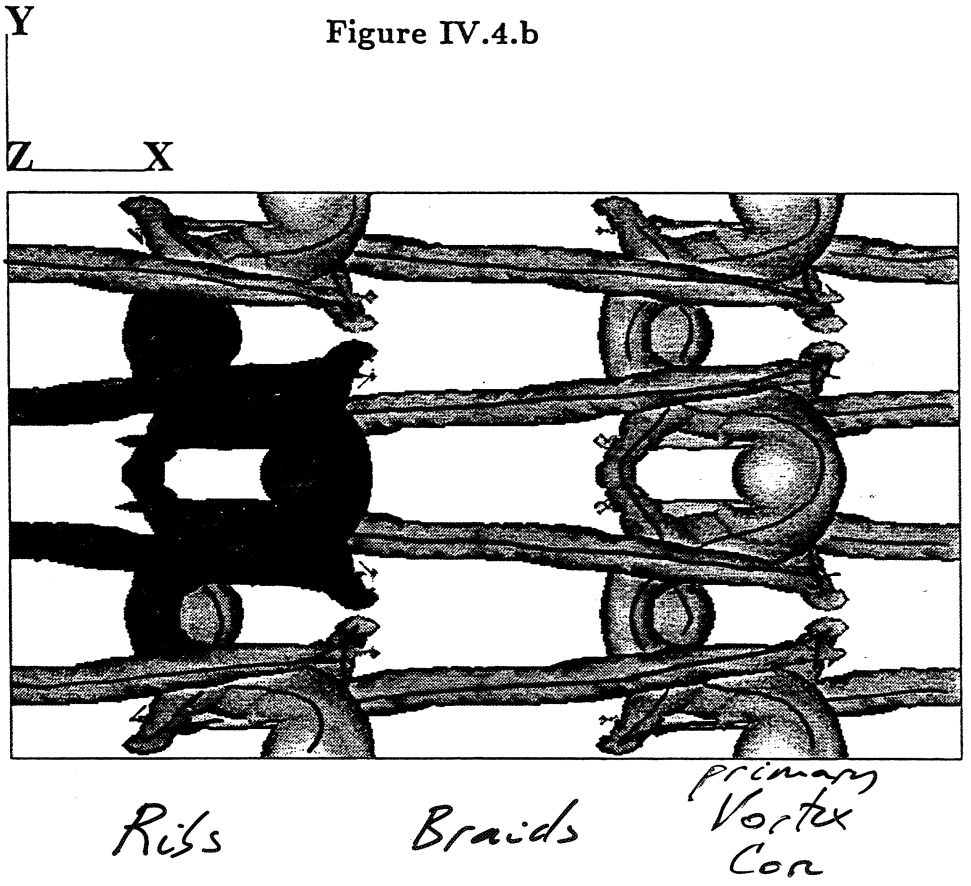

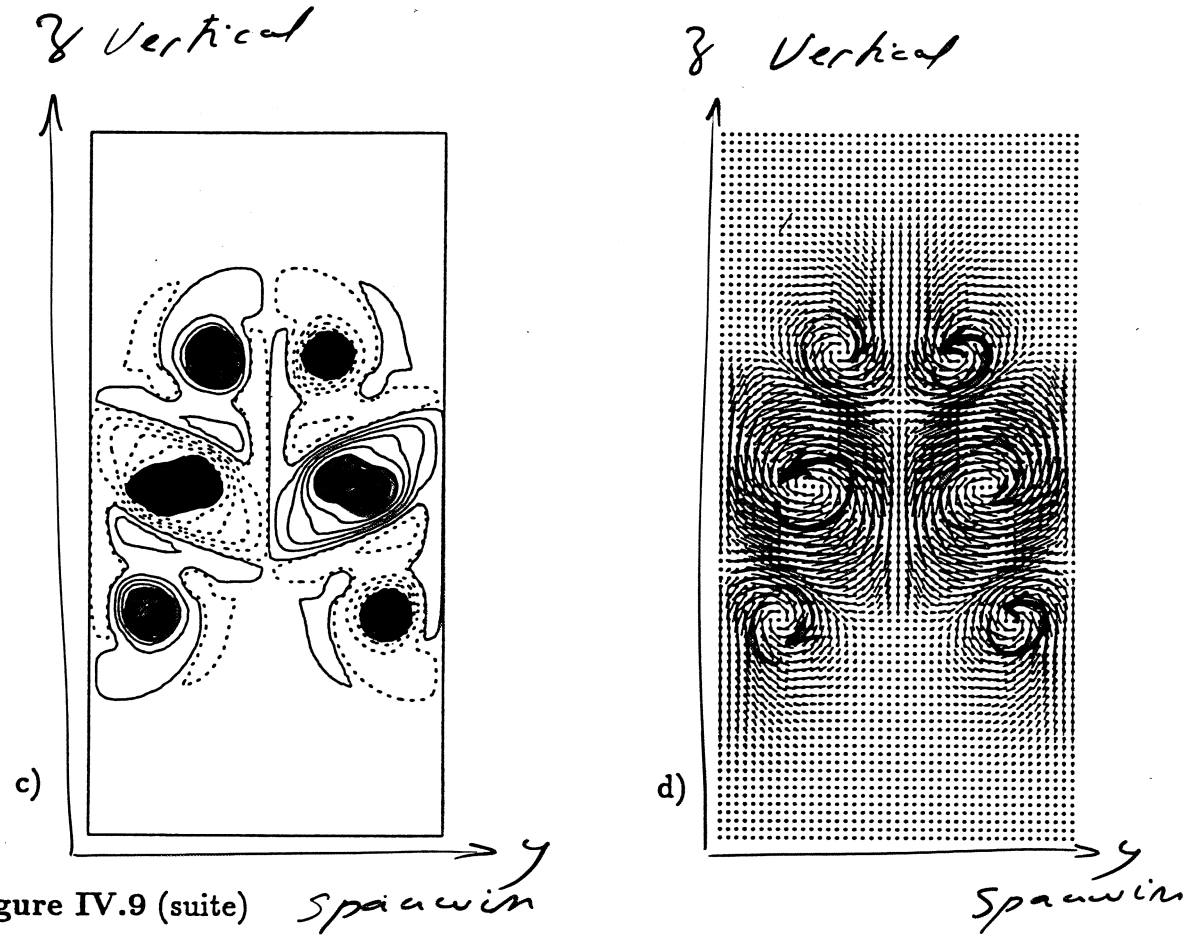

Figure IV.9 (suite)

c) cas 3D: iso-courbes du champ de vorticité ω_x au temps t=12 dans une coupe plane (y, z) dans la région du rouleau $(x = L_x/2)$.

d) cas 3D: champ du vecteur vitesse au temps t=12 projeté sur un plan de coupe (y, z) dans la région du rouleau $(x = L_x/2)$.

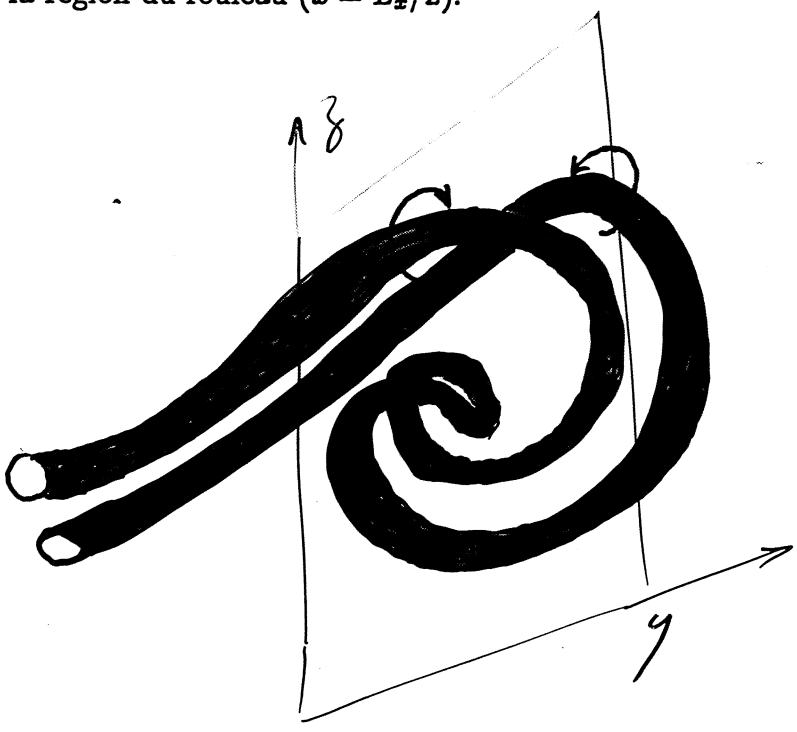

VORTEX TUBE
REGNNECTION

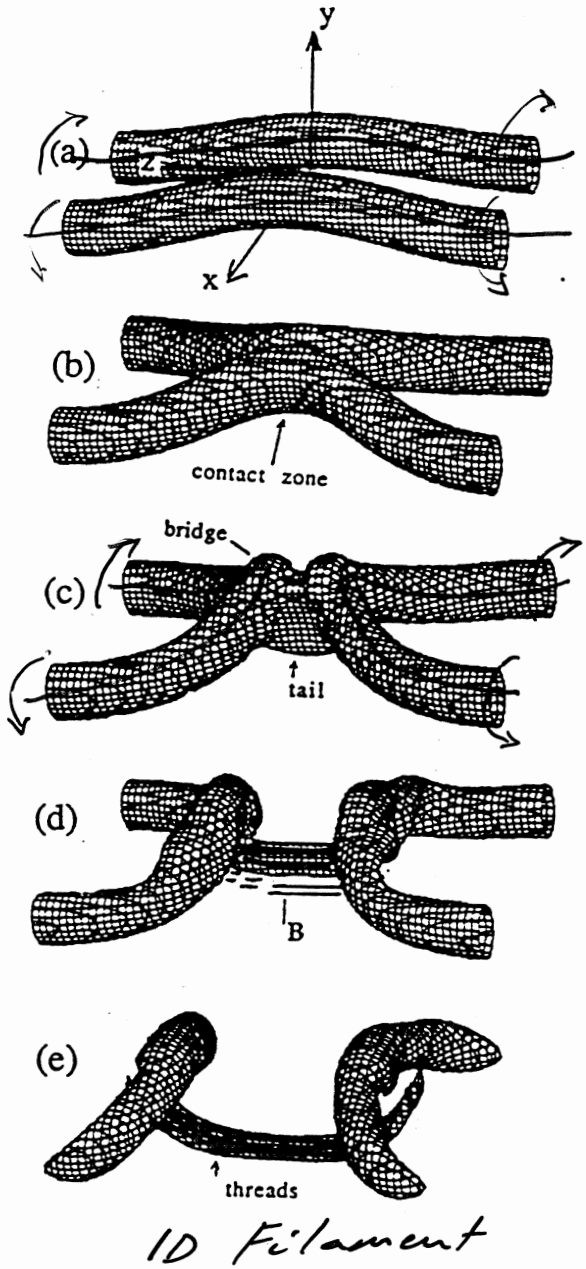

1D Filament

Figure 1. |ω| surface at 30% of the initial peak. (a) t=0; (b) t=2.25; (c) t=3.5; (d) t=4.75; (e) t=6.0

VORTICITY
NODULUS

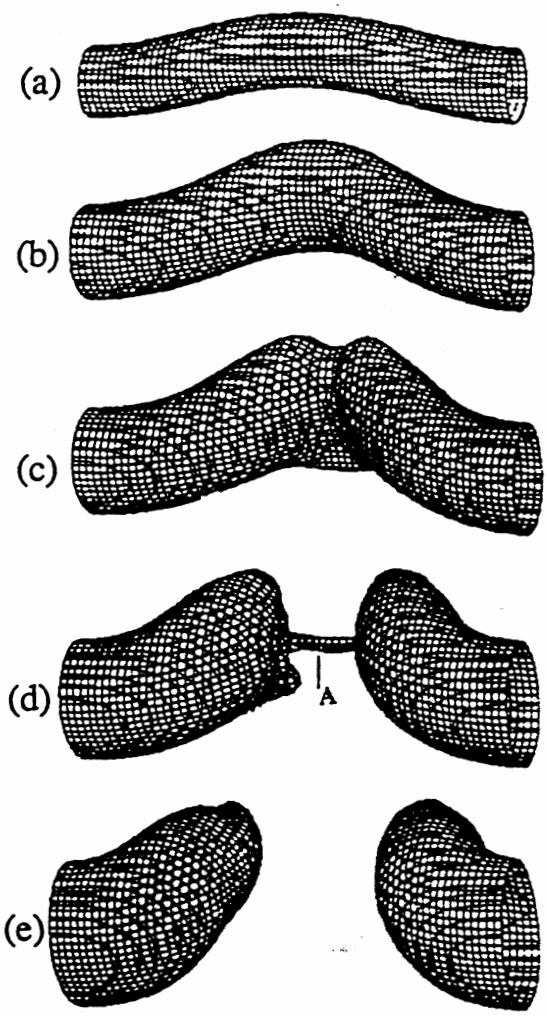

Figure 2. Scalar at 5% of the initial peak. (a) t=0; (b) t=2.25; (c) t=3.5; (d) t=4.75; (e) t=6.0

PASSIVE
SCALAR

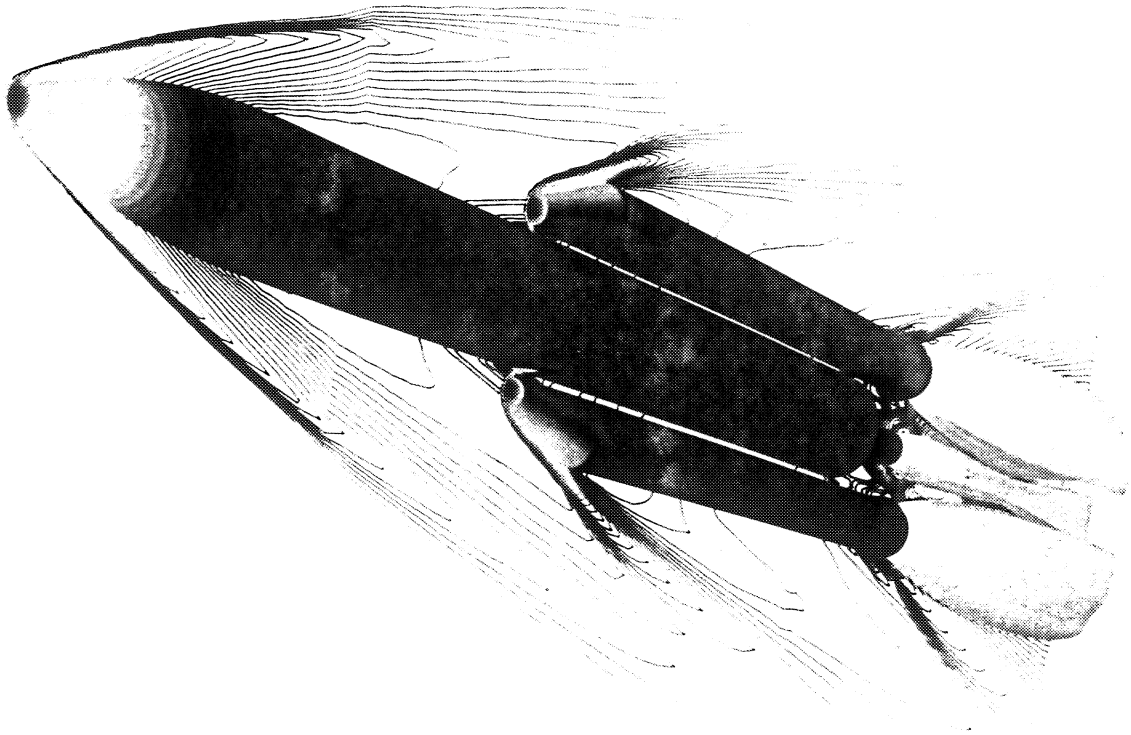

Mixing layer instability and coherent vortex formation in the boosters of Ariane V

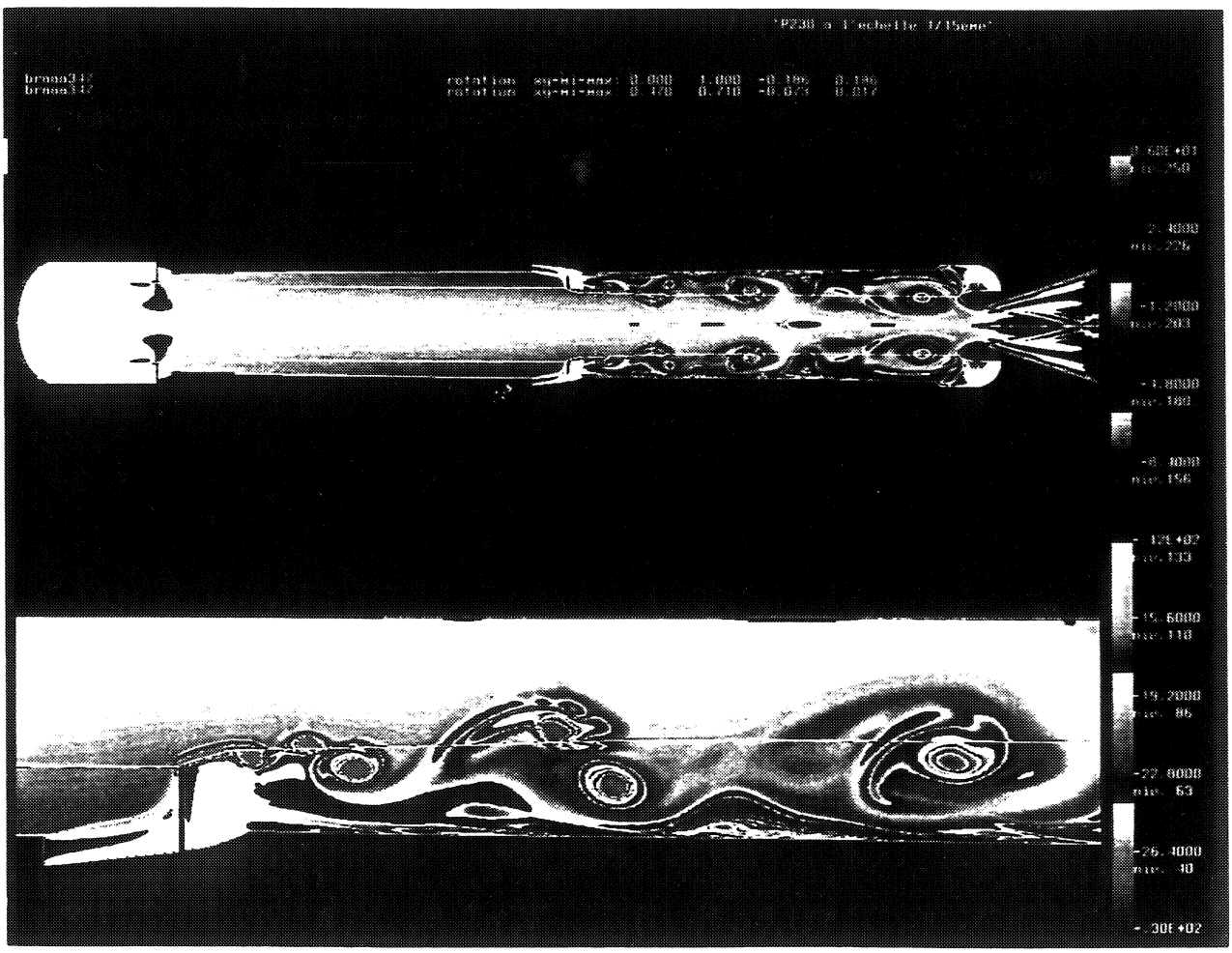

2D Numerical experiment (Soura ONERA)

Premiers résultats du code Navier-Stokes 2D pseudo-spectral avec pénalisation
écrit par Nicholas Kevlahan
lors de son séjour au CMLA,
ENS-Cachan, dans le cadre de la collaboration M3F

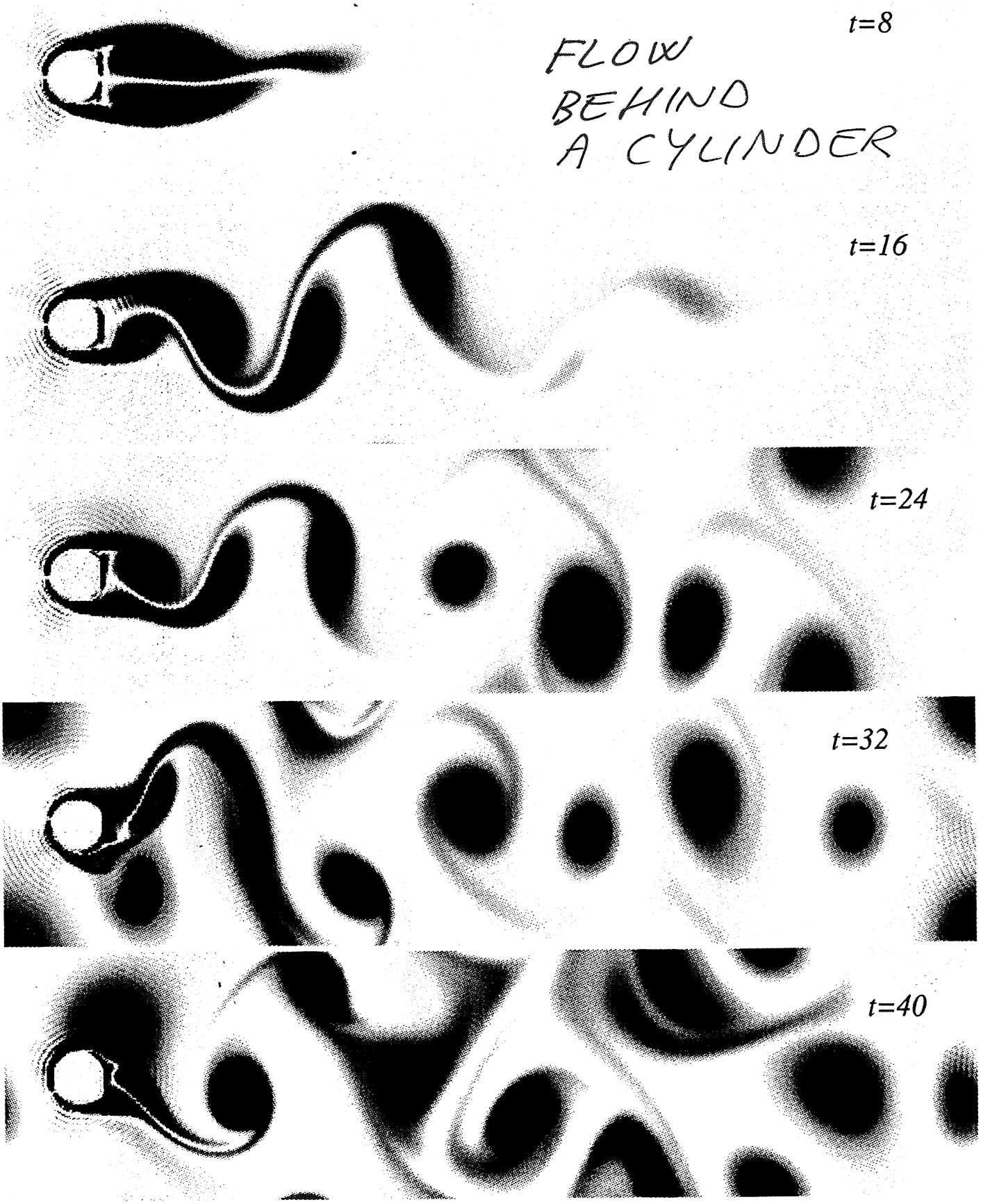

Re = 200 20x5 (512x128) with smoothing

Ecoulement derrière un cylindre à Reynolds 200
Evolution temporelle de la vorticité

TURBULENT WAKE

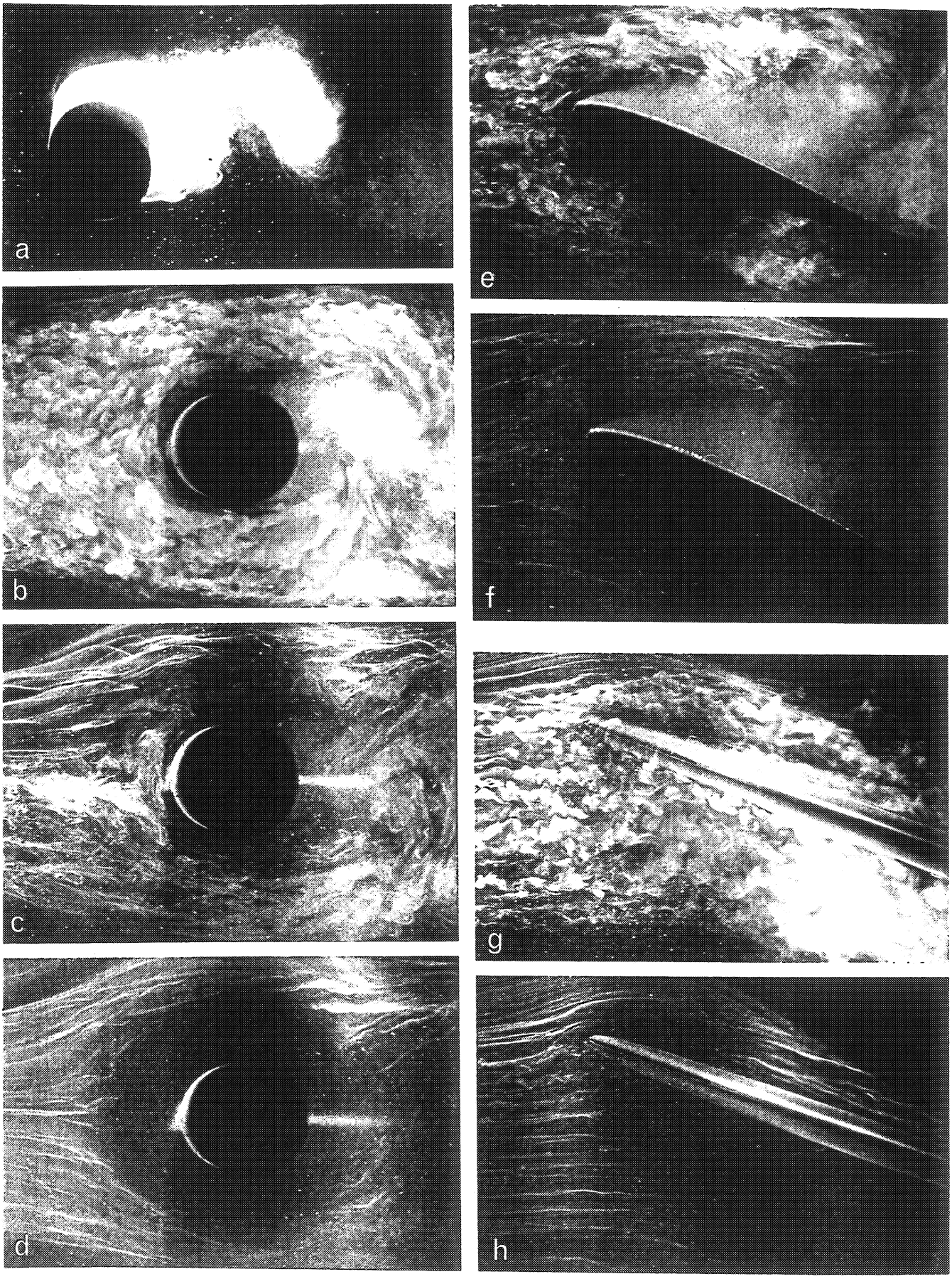

Henri WERLE
ONERA
1982

TURBULENT WAKE

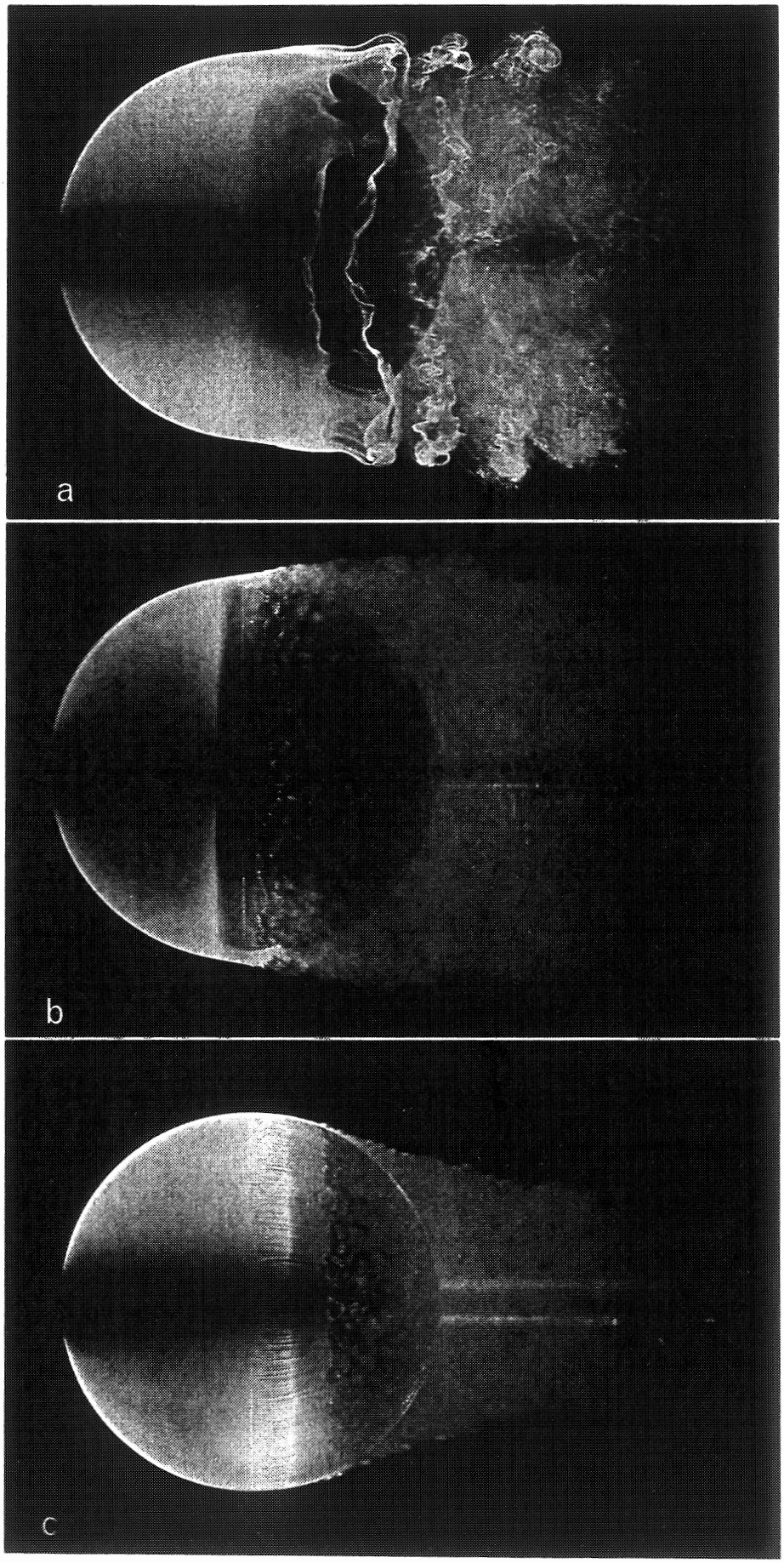

Re = 20 000
Laminar
boundary
layer
Turbulent
wake

Detachment
of the
boundary
layer
→
Drag ↗

Re = 200 000
Transition
boundary
layer
Turbulent
wake

Re = 300 000
Turbulent
boundary
layer
Turbulent
wake

Tendency
towards
Reattach-
ment
→
Drag ↘

Henri WERLÉ, 1987

Re = 20 000

TURBULENT WAKE
Henri WERLE, 1987

Behind a splur

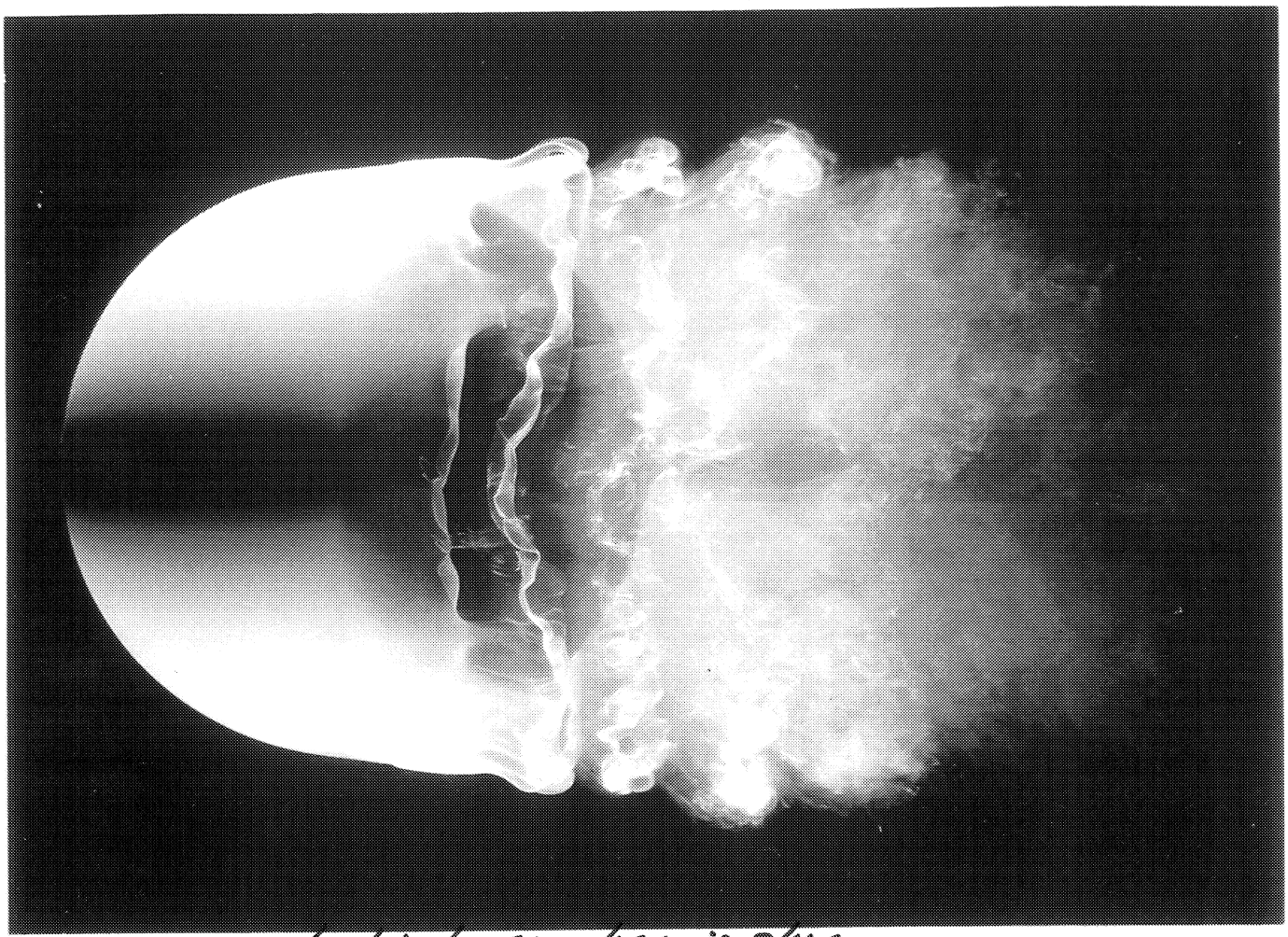

behind an hemisphere

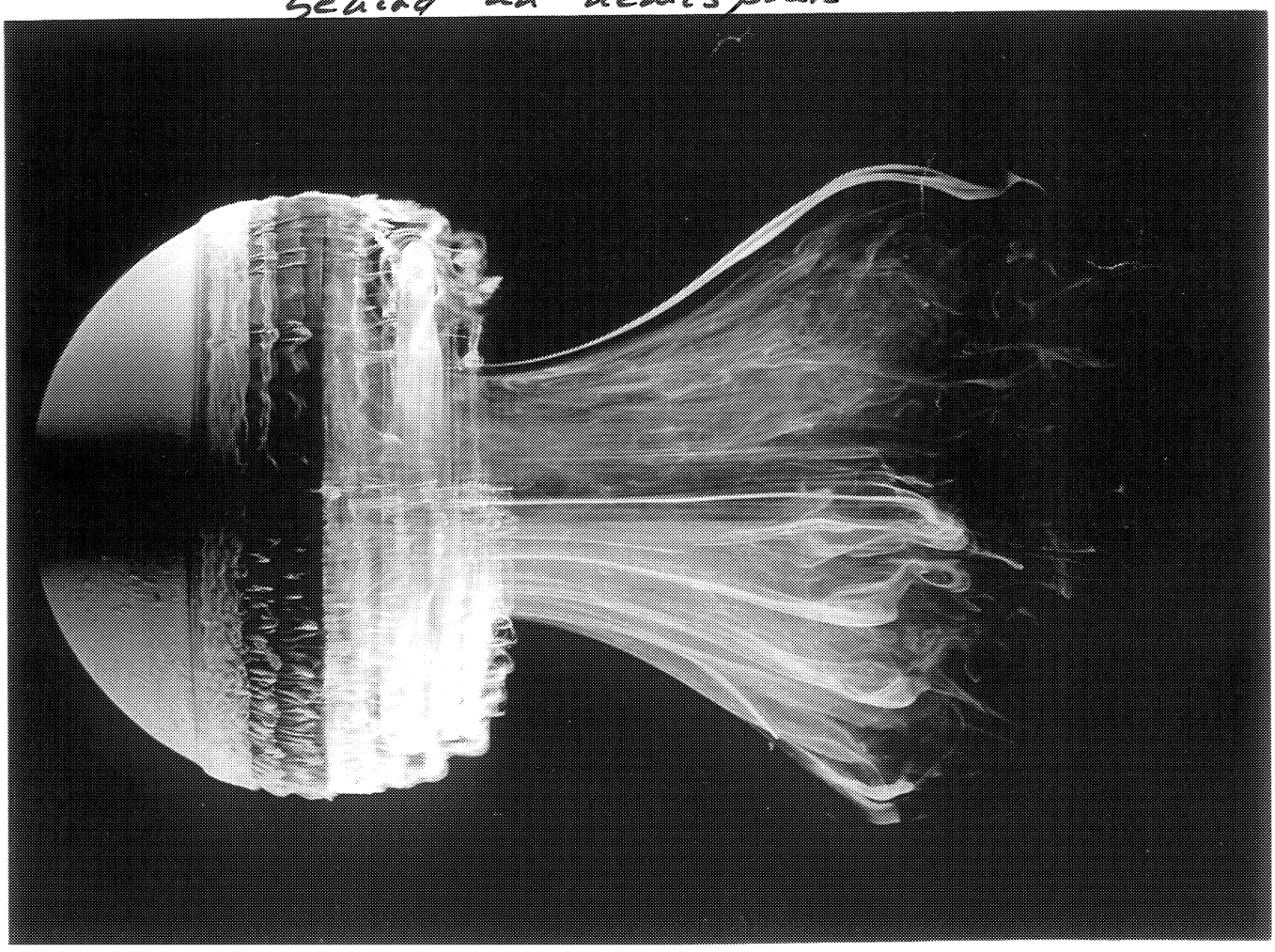

FLOW AROUND A STRAIGHT WING

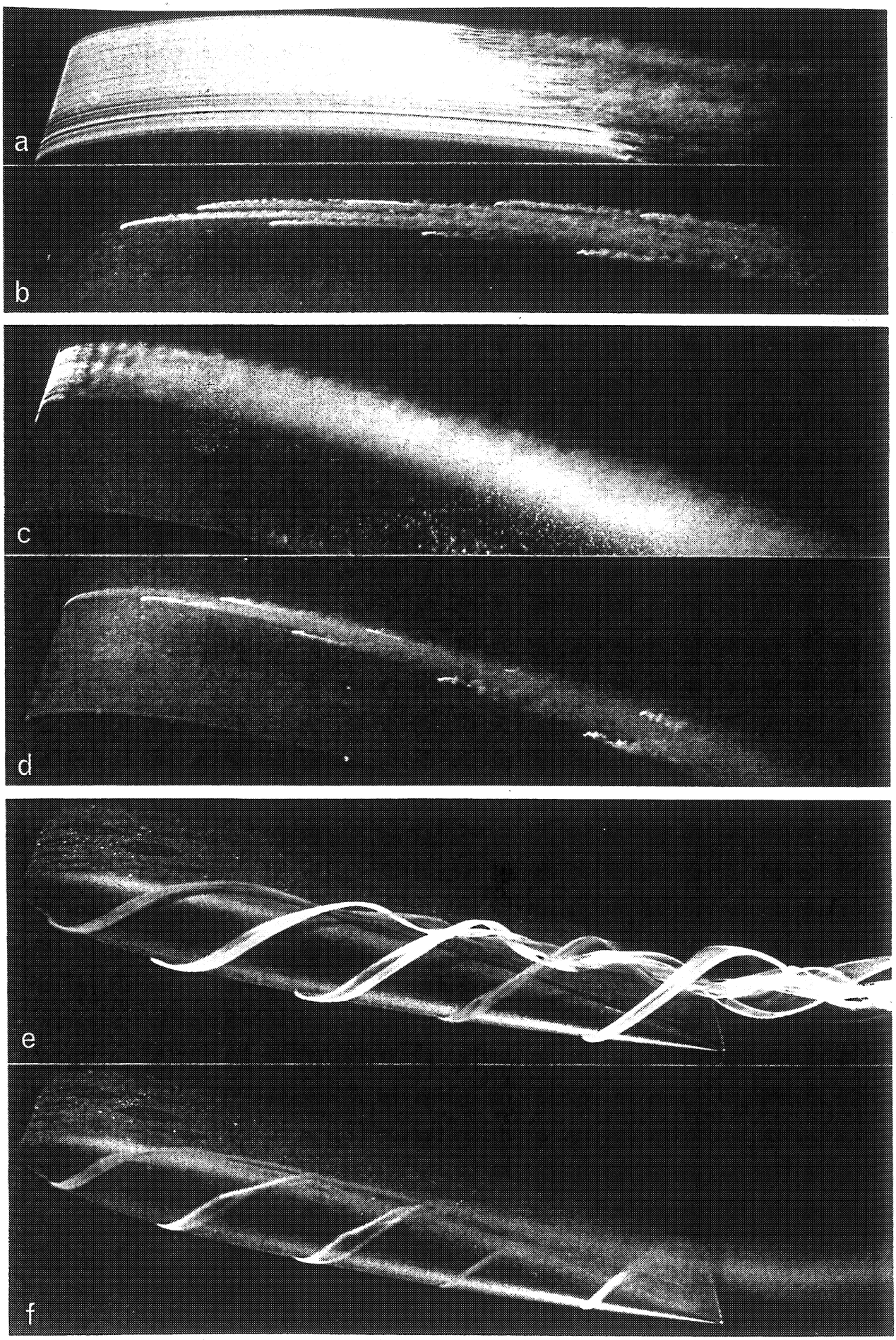

$\alpha = 0°$
$Re =$
300 000

$\alpha = 15°$
$Re =$
300 000

$\alpha = 15°$
$Re =$
20 000

$\alpha = 15°$
$Re =$
200 000

Henri WERLE, 1987

TRAILING VORTICES BEHIND AN A320

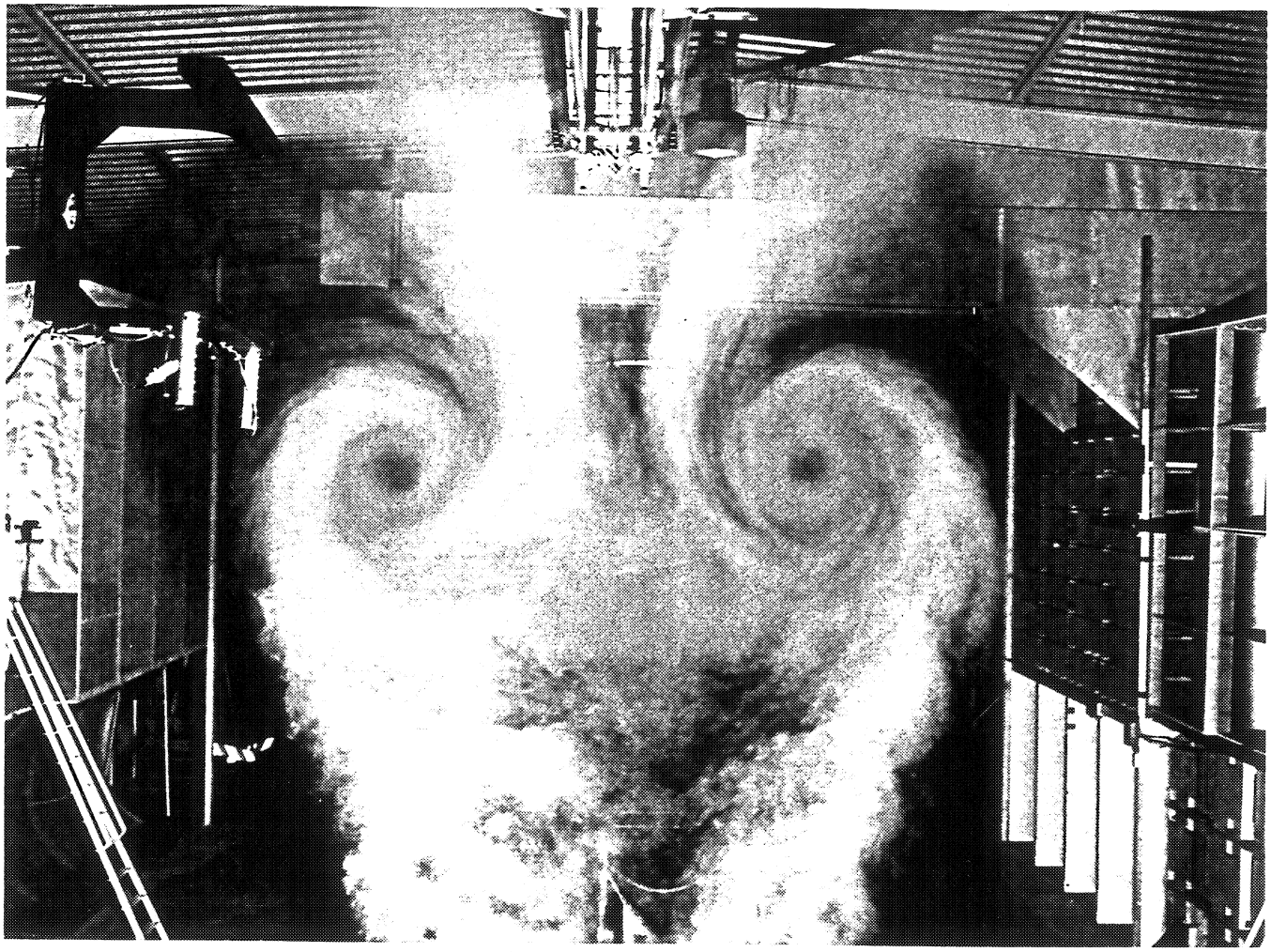

Airbus A320

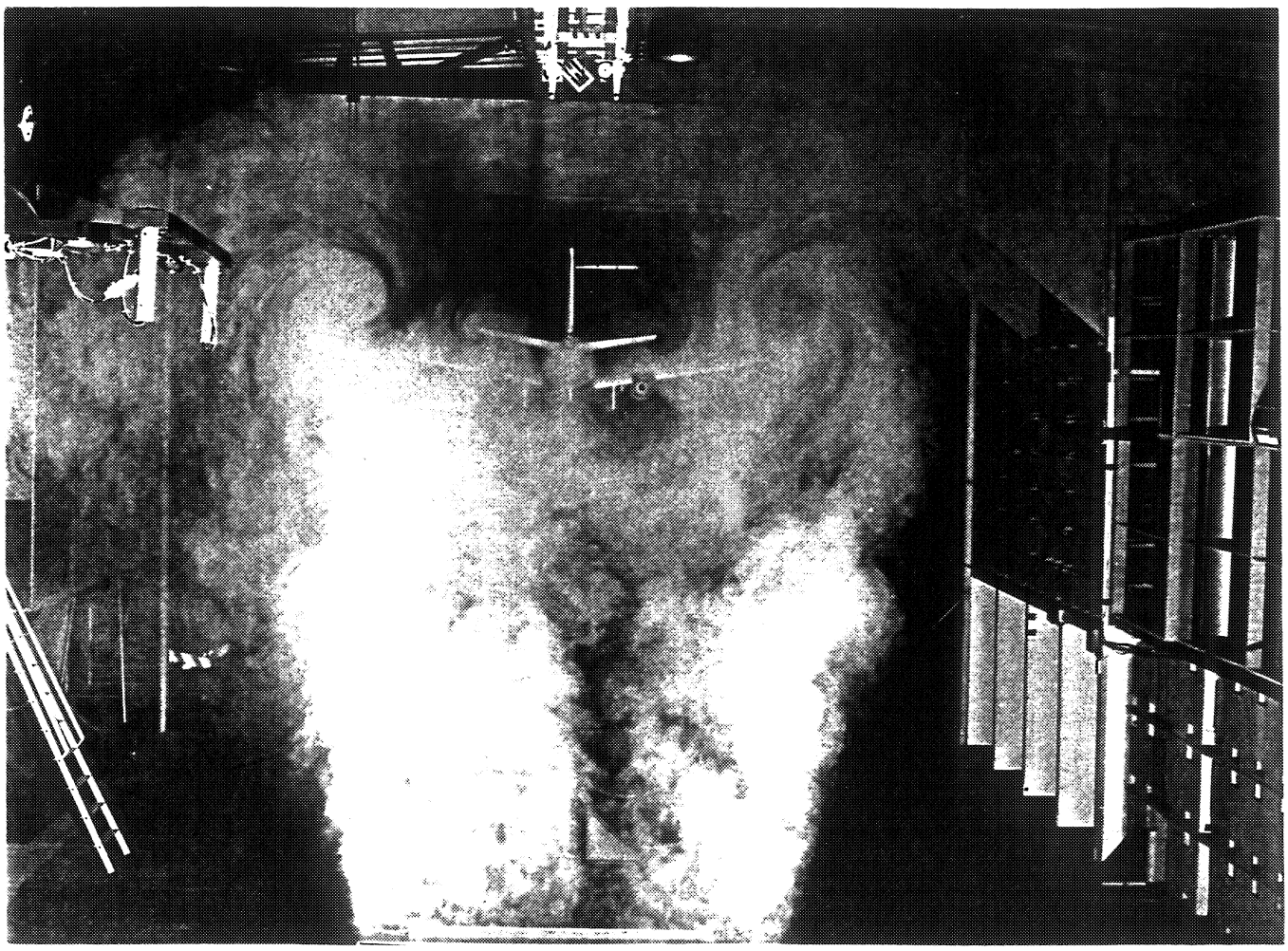

(Sowa ONERA)

TRAILING VORTICES (Sous ONERA)

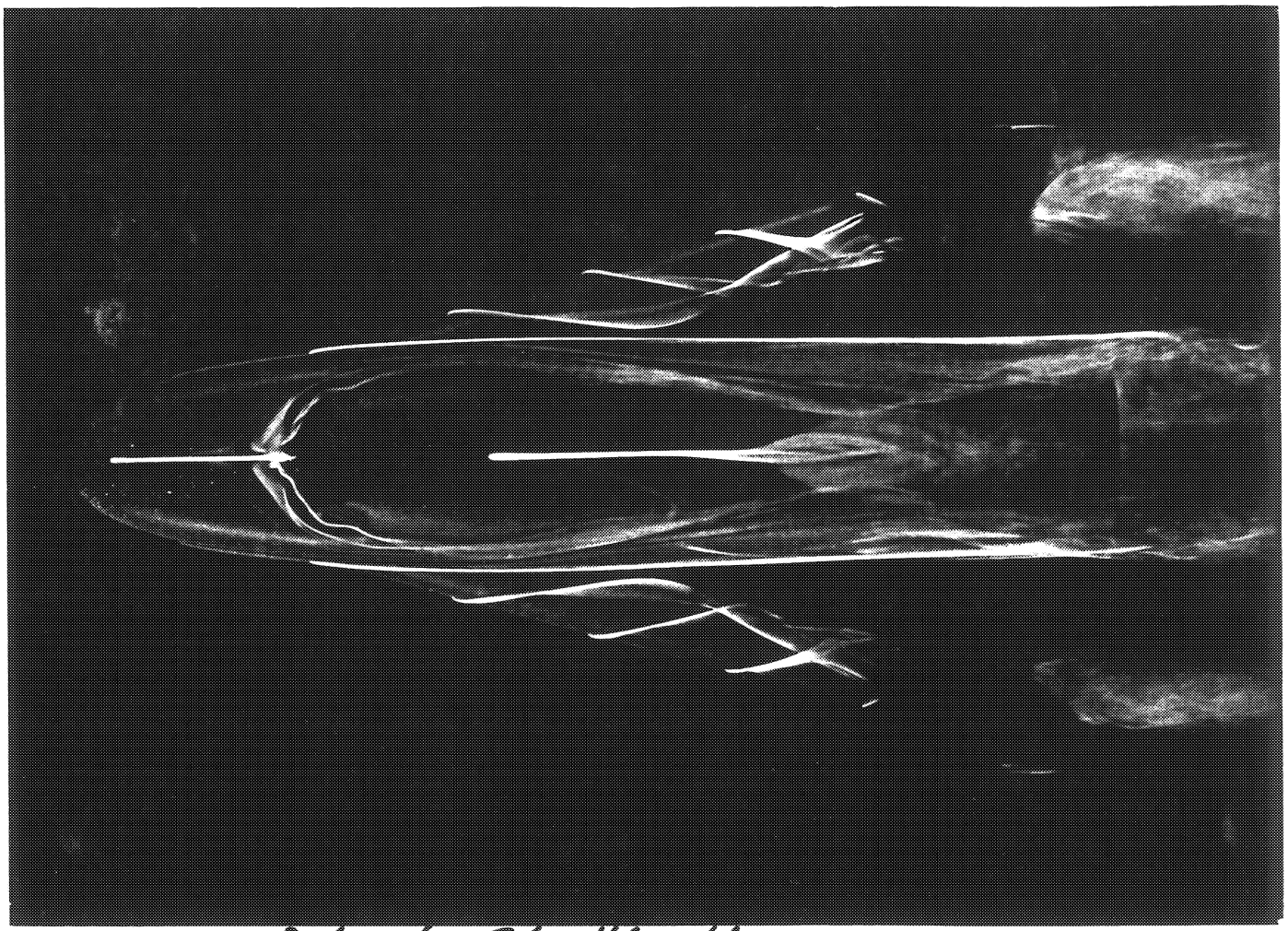

Behind Shuttle Hermes

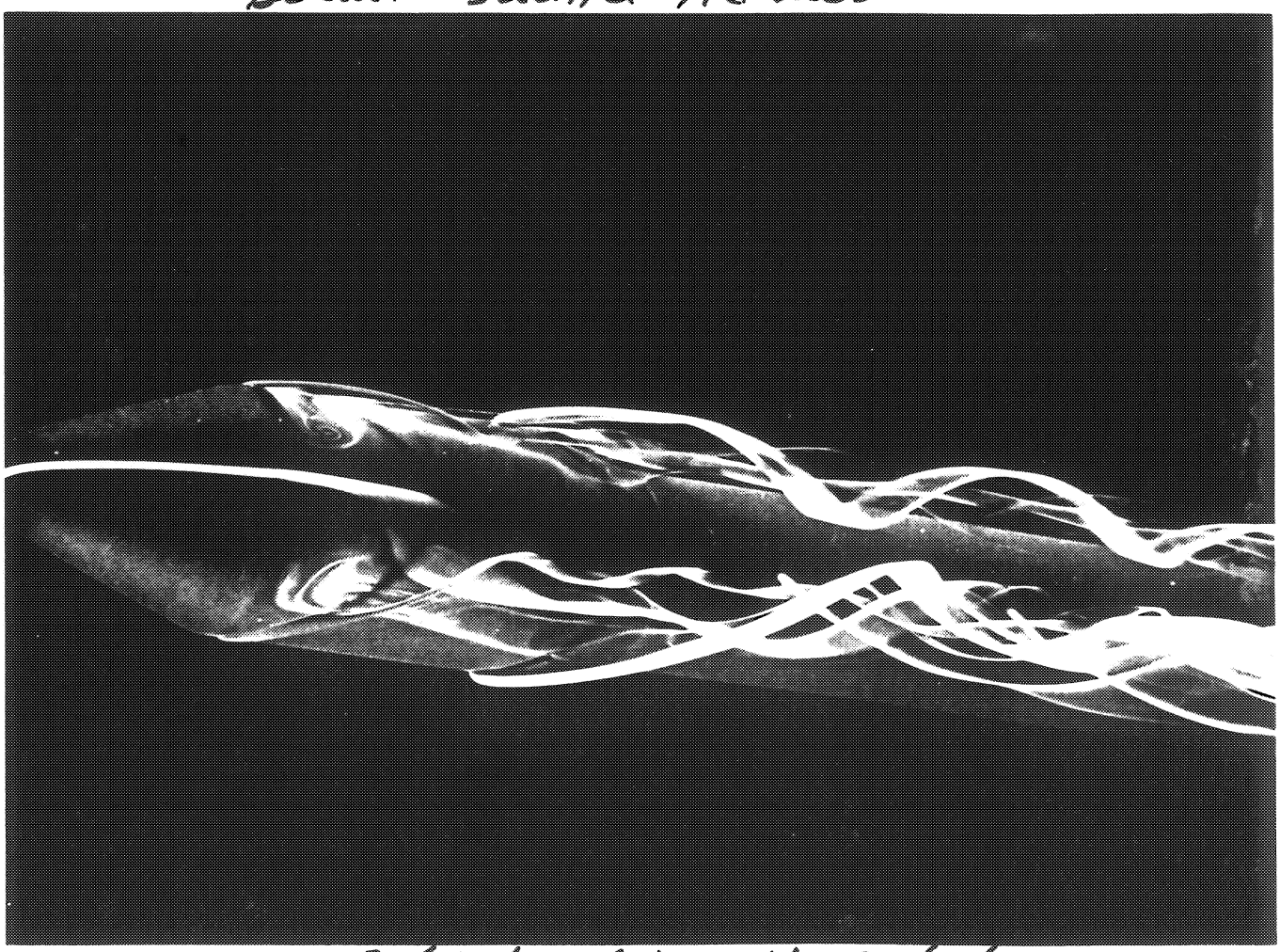

Behind Ariane V rocket

TRAILING VORTEX BEHIND A WING

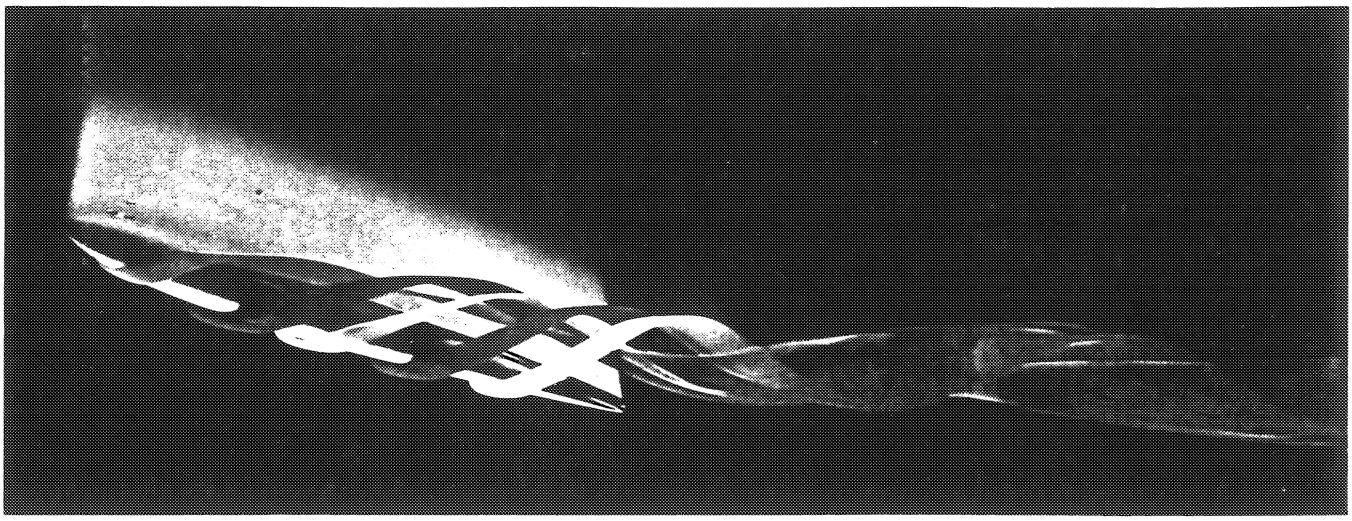

HORSESHOE VORTEX IN FRONT OF A CYLINDER

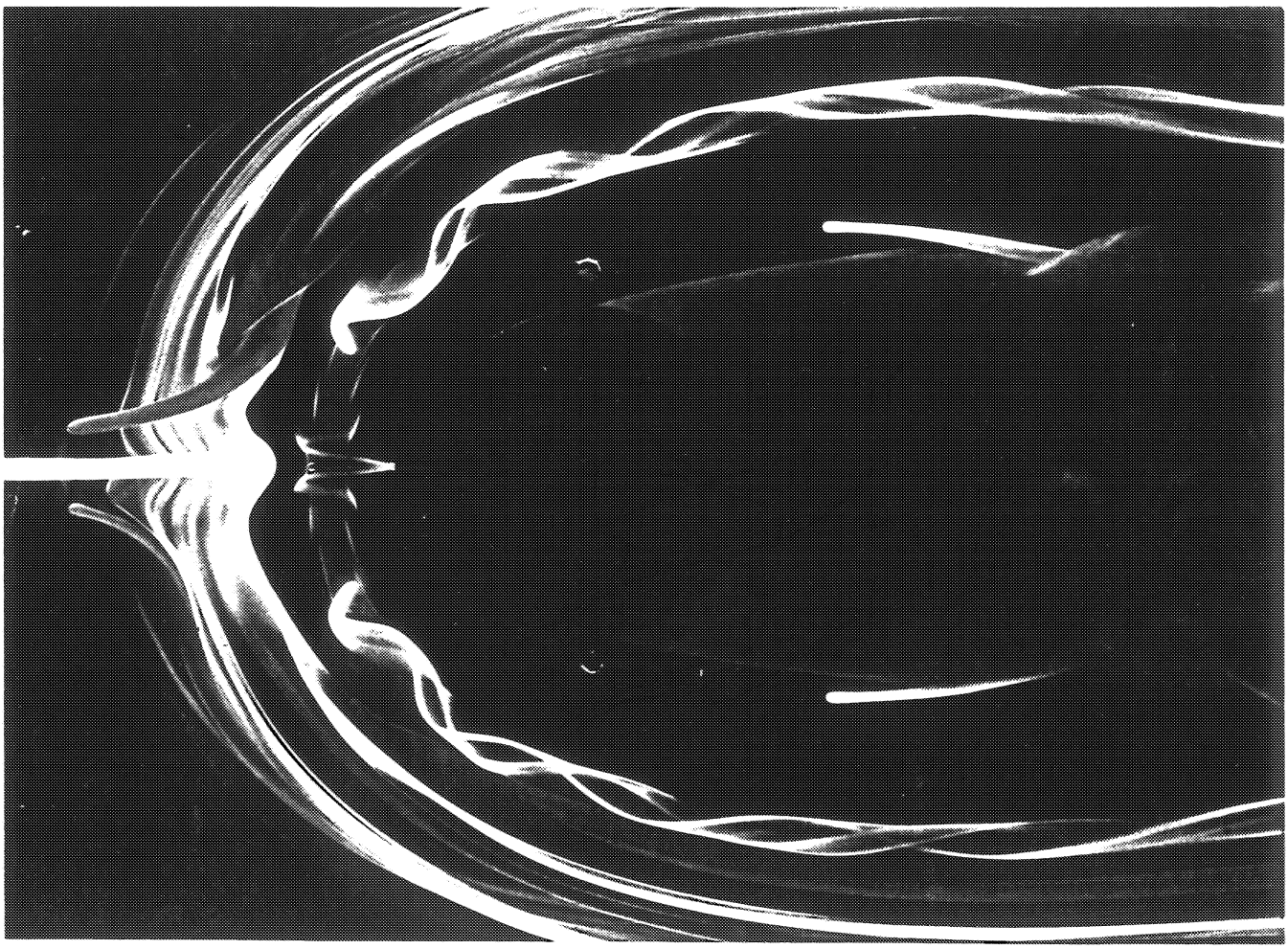

(Source ONERA)

Laboratory experiment
by Henri Werlé

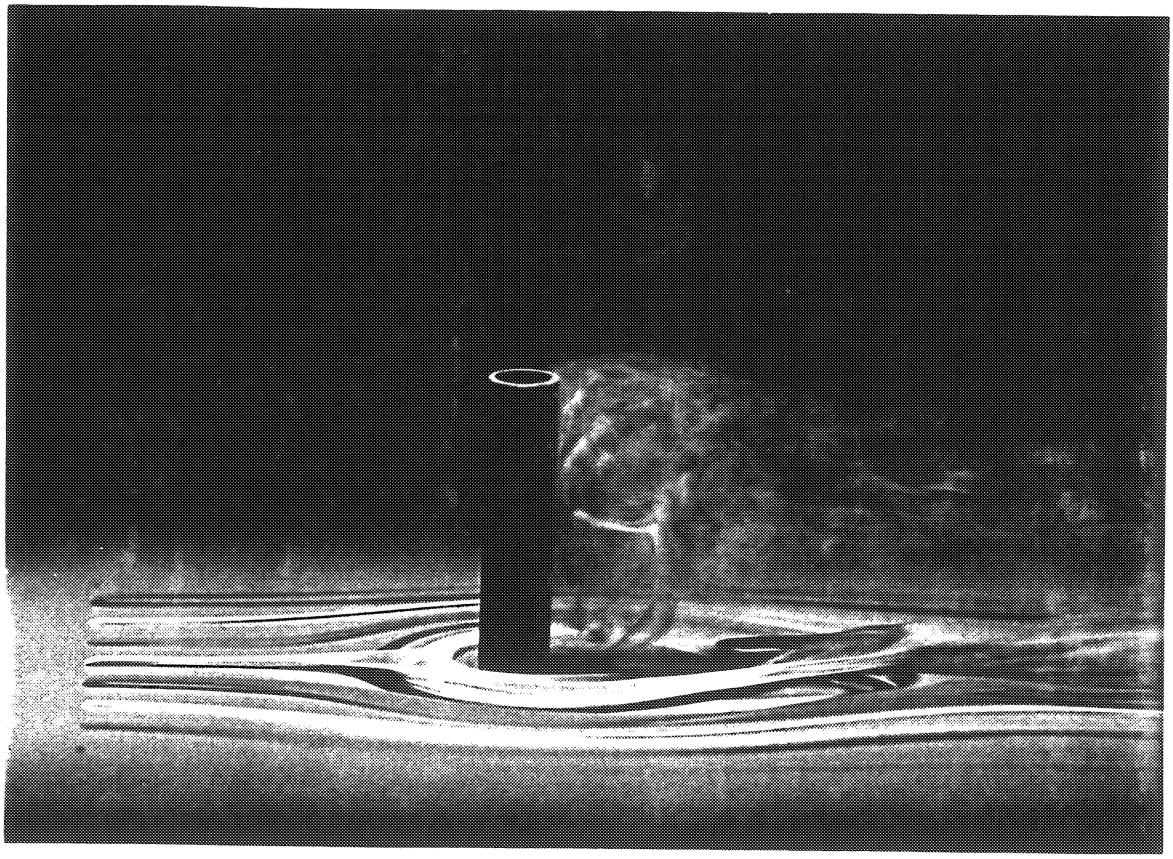

WAKE BEHIND A CYLINDER

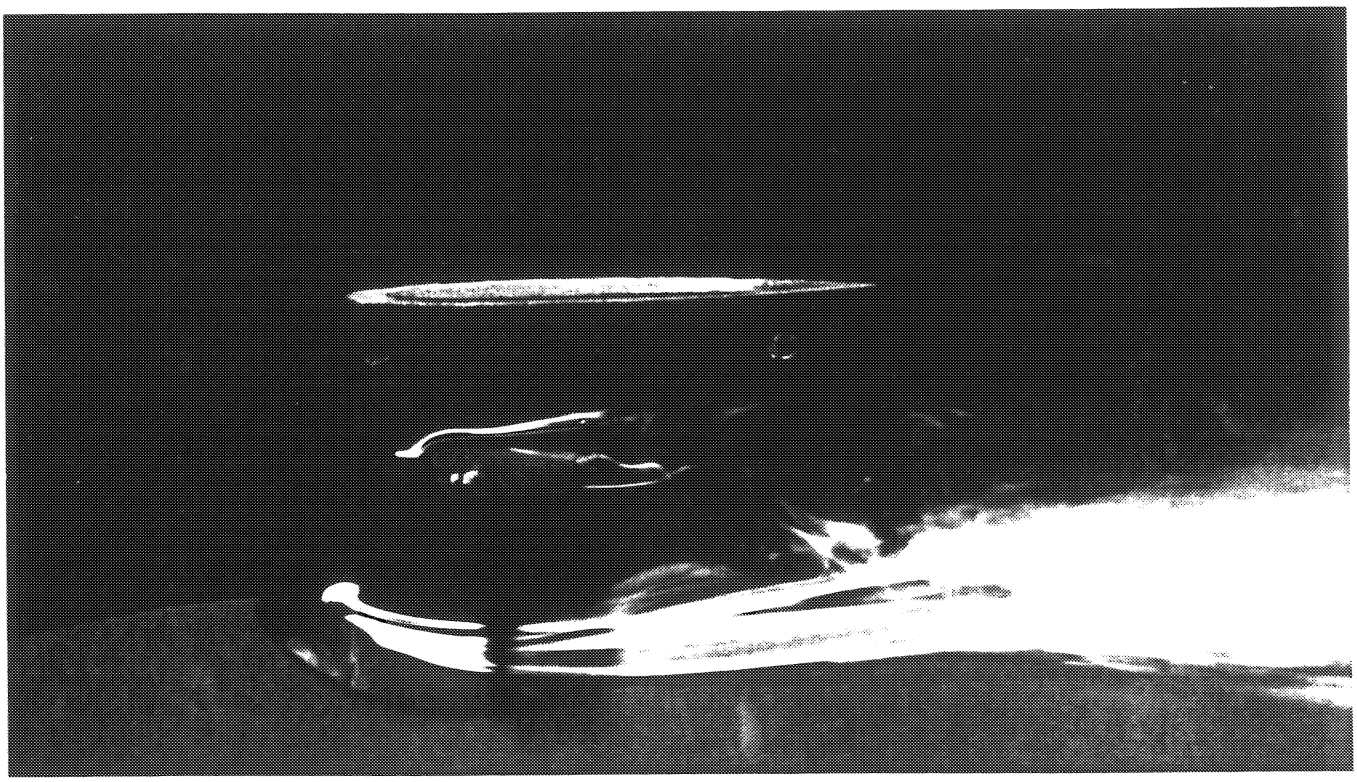

WAKE BEHIND A SUBMARINE

(SHIH ONERA)
Laboratory experiments
by Henri Werlé

CHANNEL FLOW

Multiscale Analysis of Turbulent Flow

Turbulent Channel Flow

Direct Numerical Simulation 196 x 96 x 192

$$
\begin{aligned}
\mathbf{u}_t + \nabla \cdot (\mathbf{u} \otimes \mathbf{u}) &= \mathbf{f} - \nabla p + \nu \Delta \mathbf{u} \\
\nabla \cdot \mathbf{u} &= 0 \\
Re_H &= 3000 \\
\text{domain} &= [0, L] \times [-H, H] \times [0, B] \\
\text{periodic b.c.} &: \text{stream-, spanwise} \\
\text{no slip} &: \text{upper,lower wall} \\
\text{grid} &: 192 \times 96 \times 192
\end{aligned}
$$

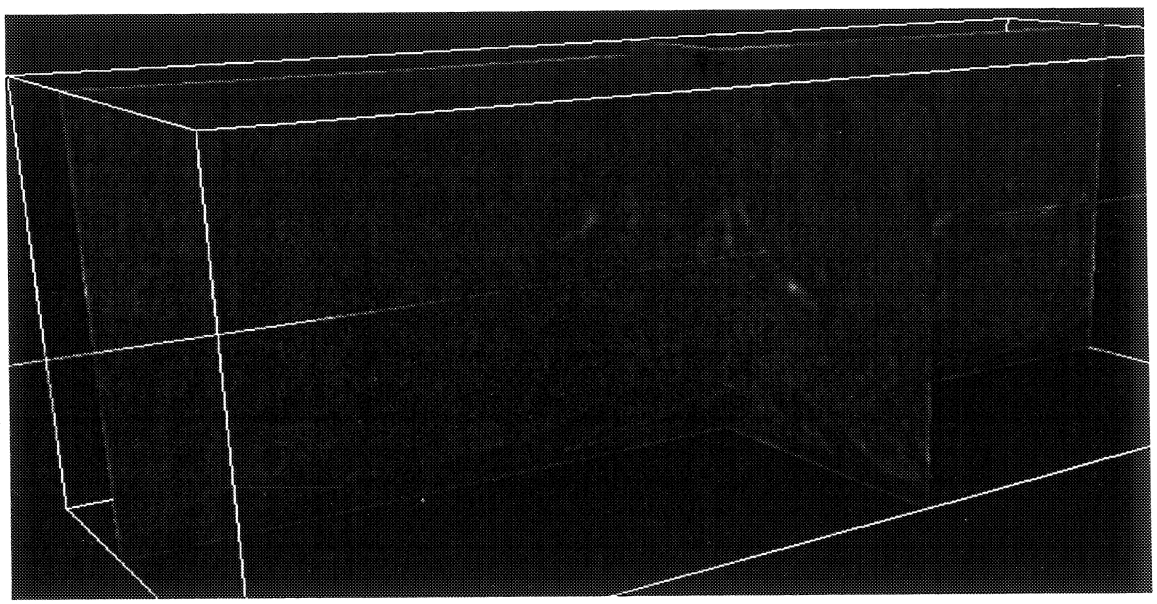

modulus of vorticity

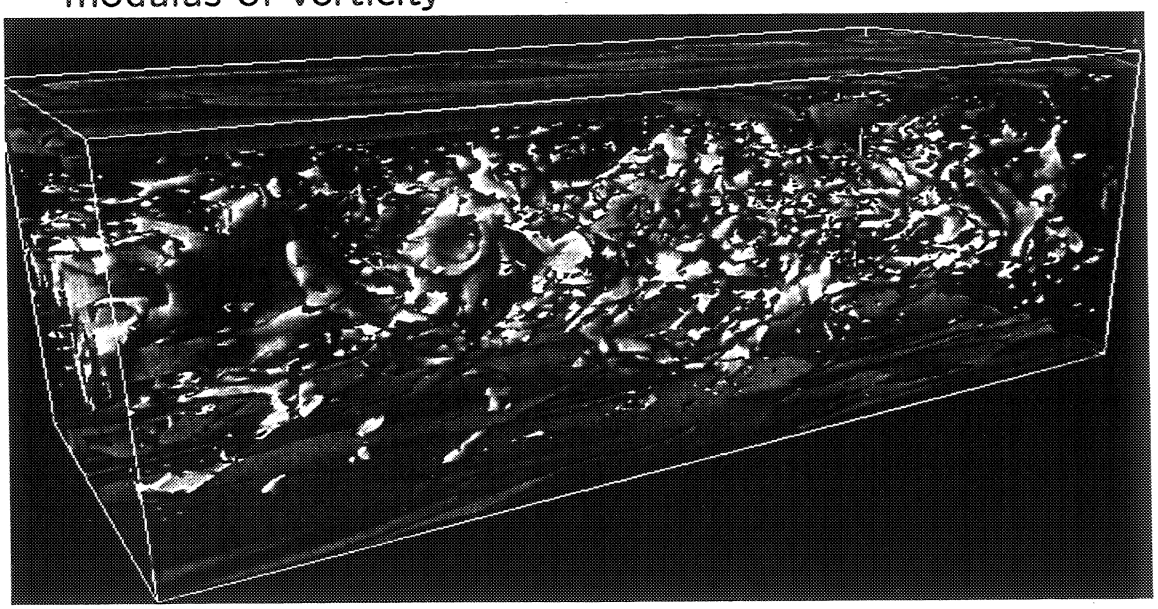

isosurfaces of modulus of vorticity (green, yellow: $|\omega| \approx 10,\ 0.1$)

Kaltenbach (Berlin) & Griebel, Koster (Bonn)

STATISTICAL THEORY OF HOMOGENEOUS AND ISOTROPIC TURBULENCE

for 2D and 3D flows

- Statistical ensembles
- Statistical equilibrium
- Kolmogorov's theory
- Intermittency correction
- Experimental verifications in Laboratory and numerical experiments
- Critics of Kolmogorov's theory by Robert Kraichnan
- Direct Numerical Simulation of 3D forced turbulence (homogeneous and isotropic flow)
- Wavelet analysis of 3D turbulent flows (Mixing layer and Channel flow)

STATISTICAL ENSEMBLES

Microcanonical ensemble
One considers all the states allowed by the macroscopic data and assumes that each state occurs with equal probability. This recipe is suitable for an isolated system.

Canonical ensemble
The probability of a microscopic state is proportional to $\exp(-\beta E_s)$ where E_s is the energy of that state and β is a parameter.

Principle of "equivalence of ensembles"
The two ensembles are equivalent in the sense that, when the parameter β is properly chosen, and the system has many degrees of freedom, average properties calculated in either ensemble are equal

Lacroix temperature
$\beta = \frac{1}{T}$, in a more abstract way, β is the parameter that makes the two ensembles equiva

In fluid mechanics
β is correlated to what one
normally calls the temperature
because fluid motions are
decoupled from molecular
vibrations. But standard
thermodynamics survives when
one uses this less intuitive
notion of temperature.

Phase transition in fluids
Chorin constructs an ensemble of
discrete vortex filaments living on a
lattice with mesh length h, with
length L, energy E and circulation Γ.

If $\Lambda = \frac{L\sqrt{E}}{\Gamma}$ small the filaments
break up Γ into a collection of
isolated vortex loops

If $\Lambda = \frac{L\sqrt{E}}{\Gamma}$ large the filaments
coexist as a dense collection
of smooth vortex lines.

If $\Lambda \cong \Lambda_c$, transition point then
fluctuations become large, $\frac{\partial E}{\partial \beta}$ large,
correlation length large,
$\exists$ scaling laws, e.g. Kolmogorov's spectrum

STATISTICAL EQUILIBRIUM IN FLUID MECHANICS

A fluid mechanical system can be described macroscopically or microscopically.

A macroscopic description requires just a few global parameters, such as energy per unit of mass or the rate of energy dissipation per unit of mass.

A microscopical description provides much of the details of the system. As many microscopical descriptions are compatible with a single macroscopical picture, a microscopical description consists of an ensemble of possible realizations, all compatible with a fixed macroscopical picture, and each occuring with a certain probability.

To find a statistical equilibrium, one fixes the large scale parameters, and, having waited for the system to settle down, one observes the resulting

microscopic states and the probabilities of their occurence.

In hydrodynamical incompressible turbulence one assumes that the hydrodynamical motion and the vibrations of molecules are decoupled.

Hypothesis for a statistical theory of turbulence:

- there exists an intermediate range of scales, between the scales on which the turbulence is stirred and those at which turbulence is dissipated by viscosity, which are near a statistical equilibrium that is well-described as a canonical or microcanonical equilibrium ensemble
- this equilibrium is characterized by values of macroscopical parameters such as energy or enstrophy by unit of mass.
- this inertial range is assumed to be approximately isolated, i.e. the motion on the inertial range has enough time to settle down to an equilibrium before little energy is added or substracted.

HOMOGENEOUS AND ISOTROPIC TURBULENCE

- If turbulence is characterized by strain $S_{ij} = \frac{1}{2}\left(\frac{\partial v_i}{\partial x_j} + \frac{\partial v_j}{\partial x_i}\right)$ unit s^{-1}

or rotation $\Omega_{ij} = \frac{1}{2}\left(\frac{\partial v_i}{\partial x_j} - \frac{\partial v_j}{\partial x_i}\right)$ s^{-1}

at a constant rate in space it remains homogeneous but is no more isotropic.

- If the rate of strain or the rate of rotation varies in space, turbulence is no more homogeneous. This is the case near walls.

Kolmogorov's theory

- 1st hypothesis:
dissipation rate ε is constant independent on ν and on Re unit: $m^2 s^{-3}$

$$\varepsilon = \nu \int_0^\infty k^2 E(k,t)\,dk = \nu \mathcal{Z}$$

Therefore the spectral energy density $E(k)$ $m^2 s^{-2}$ / m^{-1} varies as:

$$E(k) = f(\varepsilon, k) \propto \varepsilon^\alpha k^\beta$$

$$m^3 s^{-2} = C\,(m^2 s^{-3})^\alpha\,(m^{-1})^\beta \quad \rightarrow \beta = -5/3$$

s: $-2 = -3\alpha \rightarrow \alpha = 2/3$ m: $3 = 2\alpha - \beta$, $3 = 4/3 - \beta$

Therefore:

$$E(k) = C_k \varepsilon^{2/3} k^{-5/3}$$

2nd hypothesis:

- Viscosity ν $m^2 s^{-1}$ determines how small the smallest vortex filaments must be in order to dissipate energy that has been passed from large scales to small scales

Therefore the Kolmogorov dissipation scale depends only on ν and ε

$$\ell_D = f(\nu, \varepsilon) \propto \nu^\alpha \varepsilon^\beta$$
$$m = (m^2 s^{-1})^\alpha (m^2 s^{-3})^\beta$$

$$s: \; 0 = -\alpha - 3\beta \Rightarrow \alpha = -3\beta$$
$$m: \; 1 = 2\alpha + 2\beta \Rightarrow -3\beta + \beta = \frac{1}{2}$$
$$\Rightarrow \alpha = \frac{3}{4}, \quad \beta = -\frac{1}{4}$$

Therefore: $\ell_D = \left(\frac{\nu^3}{\varepsilon}\right)^{1/4}$

- 3rd hypothesis: of velocity PDF skewness $S \neq 0$ constant, independent on ℓ. Namely the flow is slightly non Gaussian due to nonlinear interactions (Karman-Howarth equation)

Therefore: $C_k = \frac{-4}{55}$

KOLMOGOROV'S THEORY
1941

- 1st hypothesis:

  Statistical homogeneity and isotropy of ensemble averages.

- 2nd hypothesis:

  Inertial range where energy is transferred from large scales (production scales) to small scales (dissipation scales) in a conservative manner at a rate ε constant independent on ν and on Re

  $$\varepsilon = \nu \int_0^\infty k^2 E(k,t)\,dk = \nu Z \qquad (m^2 s^{-3})$$

  $\Rightarrow$ spectral energy density $E(k)$ $(m^3 s^{-2})$

  $$E(k) = f(\varepsilon, k) = C_k\, \varepsilon^{2/3} k^{-5/3}$$

- 3rd hypothesis:

  Viscosity ν $(m^2 s^{-1})$ determines the kolmogorov dissipation scale (m)

  $$\ell_k = f(\nu, \varepsilon) = \left(\frac{\nu^3}{\varepsilon}\right)^{1/4}$$

STATISTICAL THEORY OF 3D TURBULENCE

The problem

- How does Navier-Stokes equations distribute energy among the different degrees of freedom of the flow?
- But here we have an open irreversible thermodynamical system $\Rightarrow$

energy is not conserved

HYPOTHESES

1. Energy is injected only in the large scales, L_I integral scale, and dissipated only in the small scales, L_D Kolmogorov scale, therefore for the intermediate range of scales, so called inertial scale, ℓ energy is conserved and is only

transfered from large scales to small scales at a constant rate of energy transfer

ε.

This hypothesis is only valid for Gibbs ensemble averages and not for an given realization of the flow.

$Re \gg 1 \iff L_0 \ll \ell \ll L_I$

2. The flow is
supposed to be
statistically,
i.e. for GCSs
ensemble averages,

- homogeneous
  i.e. translation invariant,
- isotropic
  i.e. rotation invariant,
- self-similar
  i.e. dilation invariant.

3. The

skewness S,

departure from

Gaussianity,

of the velocity

probability

distribution

is constant.

PREDICTION

Scaling law for the 2-point velocity structure function

$$\langle |v(x+\ell) - v(x)|^2 \rangle$$

Dimensional analysis

$t = \frac{\ell}{u}$ eddy turn over time

$\varepsilon = \frac{u^3}{\ell}$ energy transfer rate

$\Longrightarrow \quad u = C \varepsilon^{1/3} \ell^{1/3}$

$$\langle (v(x+\ell) - v(x))^2 \rangle$$

$$\sim C \varepsilon^{2/3} \ell^{2/3}$$

with $C = -\frac{4}{5S}$

Kolmogorov constant

$$E(k) = \frac{1}{2} \iiint_{-\infty}^{+\infty} \hat{v}^2(\vec{k}) d^3\vec{k}$$

$$= \frac{1}{2} \int_0^{\infty} E(k) dk$$

$$\sim C \varepsilon^{2/3} k^{-2/3} dk$$

$\Longrightarrow$

$$E(k) \sim C \varepsilon^{2/3} k^{-5/3}$$

INTERMITTENCY

G. I. Taylor, 1938
'The spectrum of turbulence,
Proc. Roy. Soc. London A 164, 476

'The fact that small quantities of very high frequency disturbances appear, and increase as the speed increases seems to confirm the view frequently put forward by the author (G.I.), that the dissipation of energy is due chiefly to the formation of very small regions where the vorticity is very high.'

⇒ intermittency

≡ spottiness of the vorticity spatial distribution (rare events)

Conjecture: $Re \to \infty$ spot area $\to 0$

⇒ no need for intermittency corrections for 2nd order moments, Kolmogorov's theory do not work for high order moments

INTERMITTENCY

Laboratory experiments

Batchelor & Townsend 1949

Anselmet, Gagne, Hopfinger
& Antonia 1984

and numerical
experiments show
that the spectral
slopes are steeper
than those predicted

To explain this discrepancy we suppose that the flow is intermittent, namely that the regions of the flow which transfer energy or enstrophy are not densely distributed in space and time

From this intermittency hypothesis several corrections to the spectral slope have been proposed

in 3D: $\ln\left(\frac{L_I}{\ell}\right)^{p}$ Kolmogorov 1961 (Stochastic argument)

$(k L_I)^{-(3-D/3)}$ Parisi and Frisch 1985 (multi-fractal hypothesis)

in 2D: $(\ln L_I k)^{-1/3}$ Kraichnan 1971 (non locality of enstrophy transfers in Fourier space)

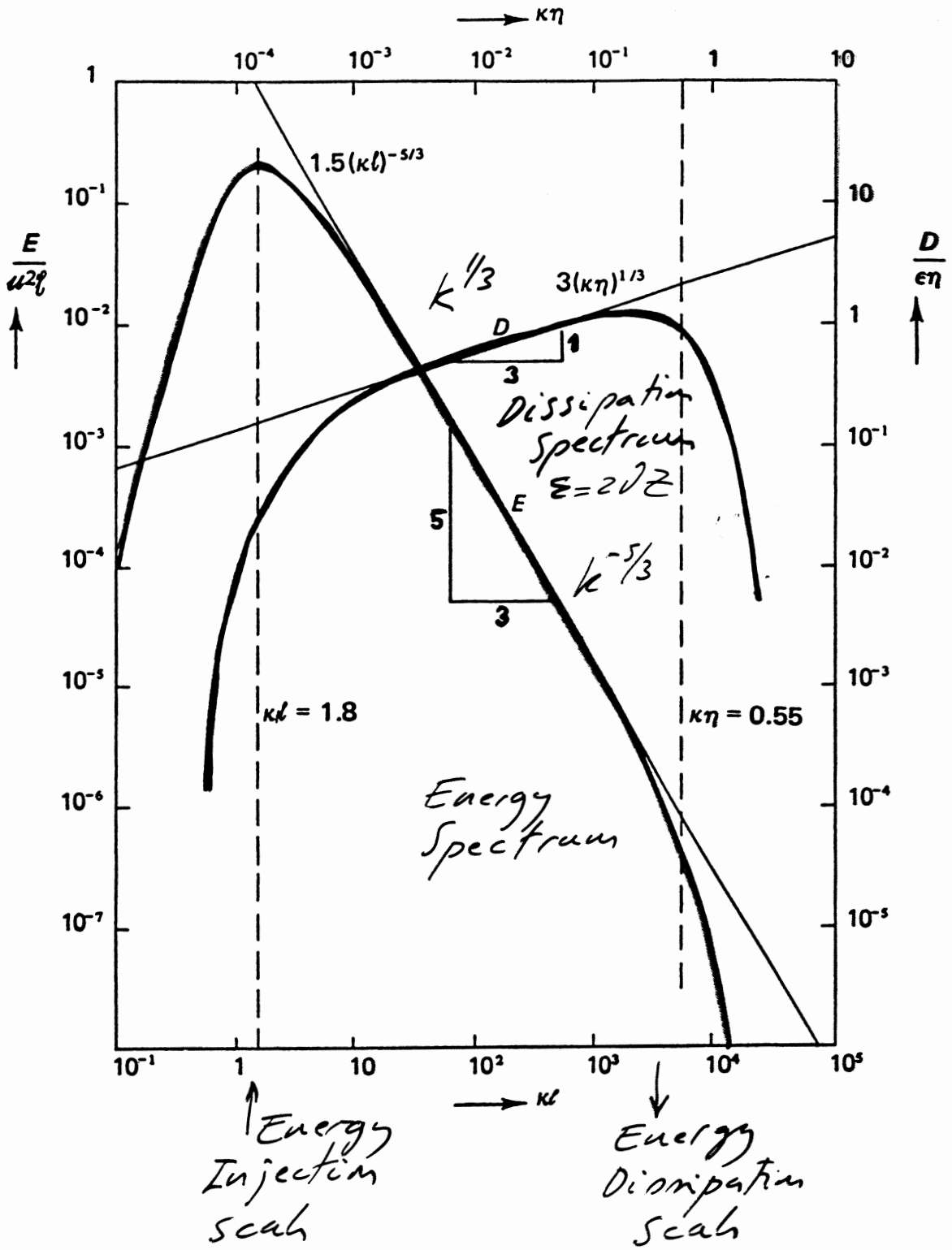
κη
10⁻⁴
10⁻³
10⁻²
10⁻¹
1
10
1.5(κl)^-5/3
E/νε
D/εη
k^1/3
3(κη)^1/3
D
1
3
Dissipation Spectrum
ε=2νΣ
E
5
3
k^-5/3
κl = 1.8
κη = 0.55
Energy Spectrum
10⁻¹
1
10
10²
10³
10⁴
10⁵
κl
Energy Injection scale
Energy Dissipation scale

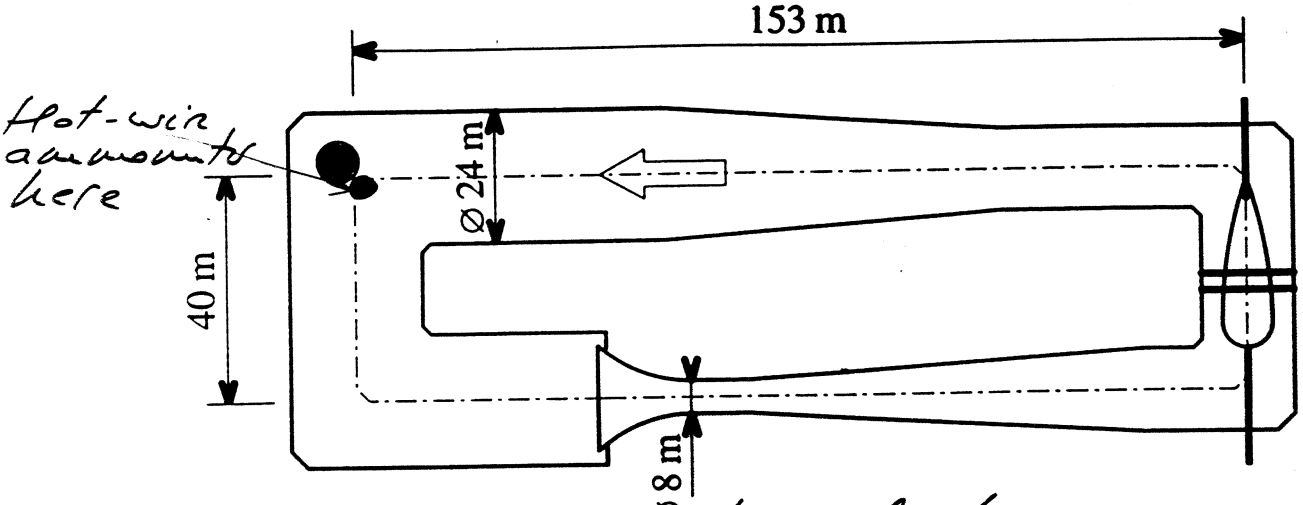

S1 wind tunnel of ONERA in Modane

2nd order structure function in the time domain

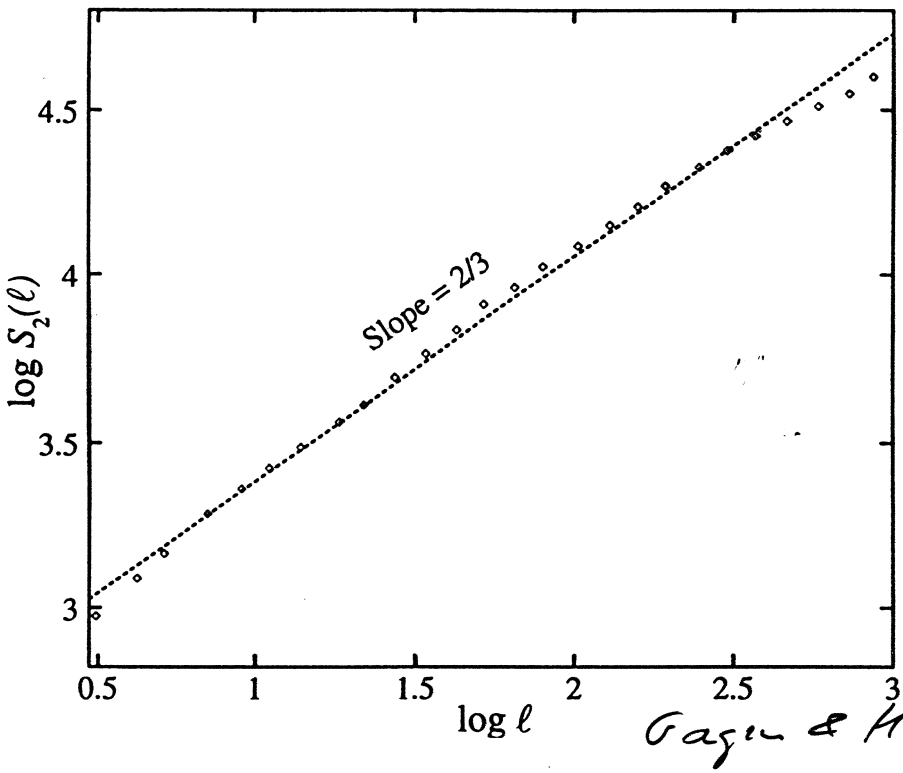

Gagne & Hopfinger

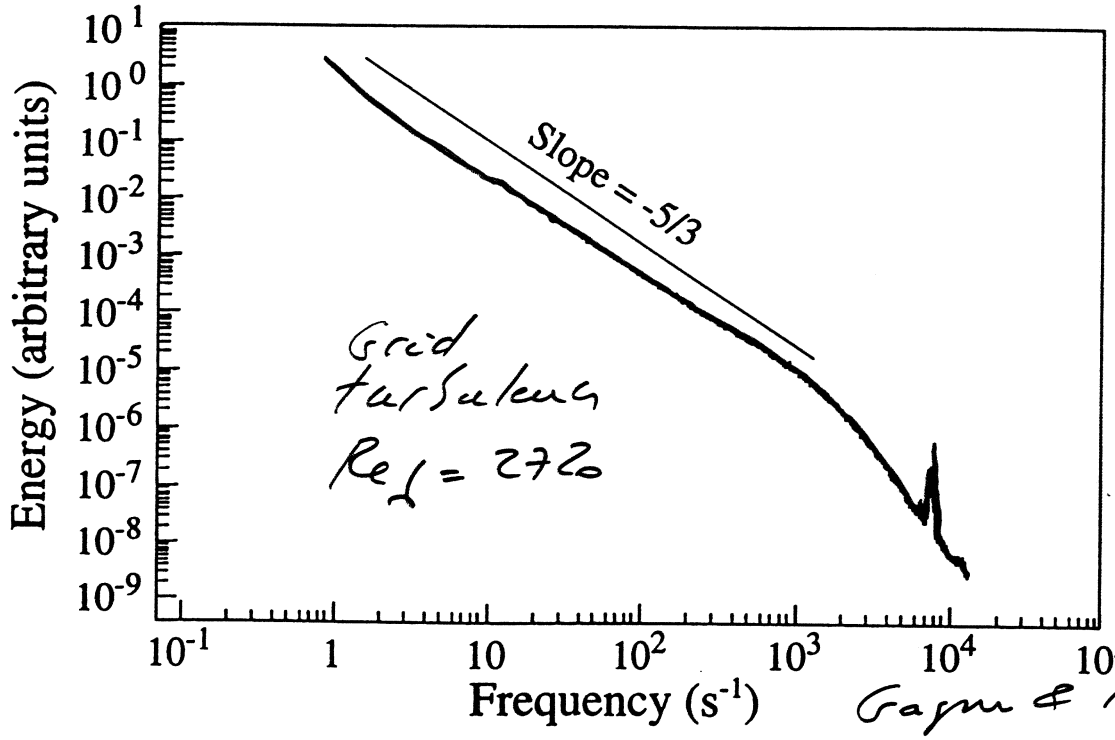

Gagne & Marchand

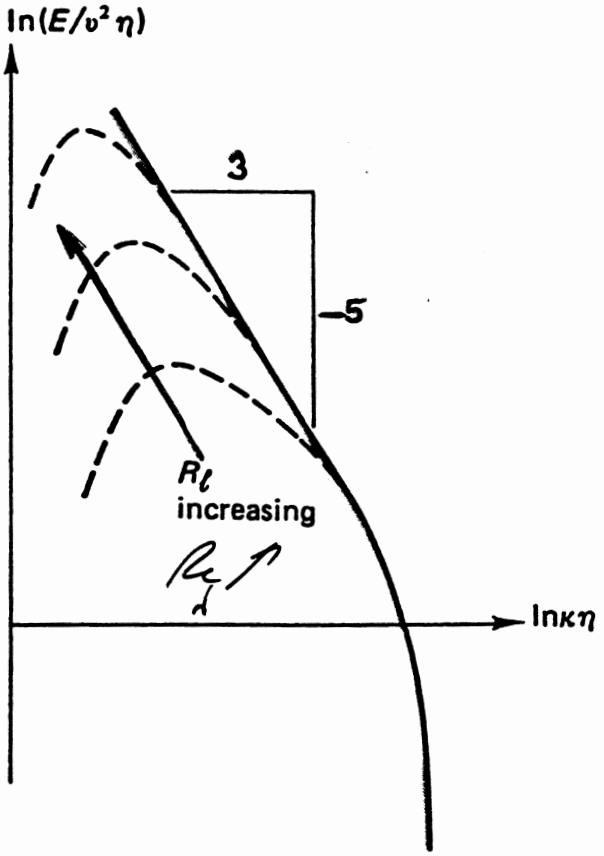
ln(E/υ² η)
3
5
Rl
increasing
lnκη

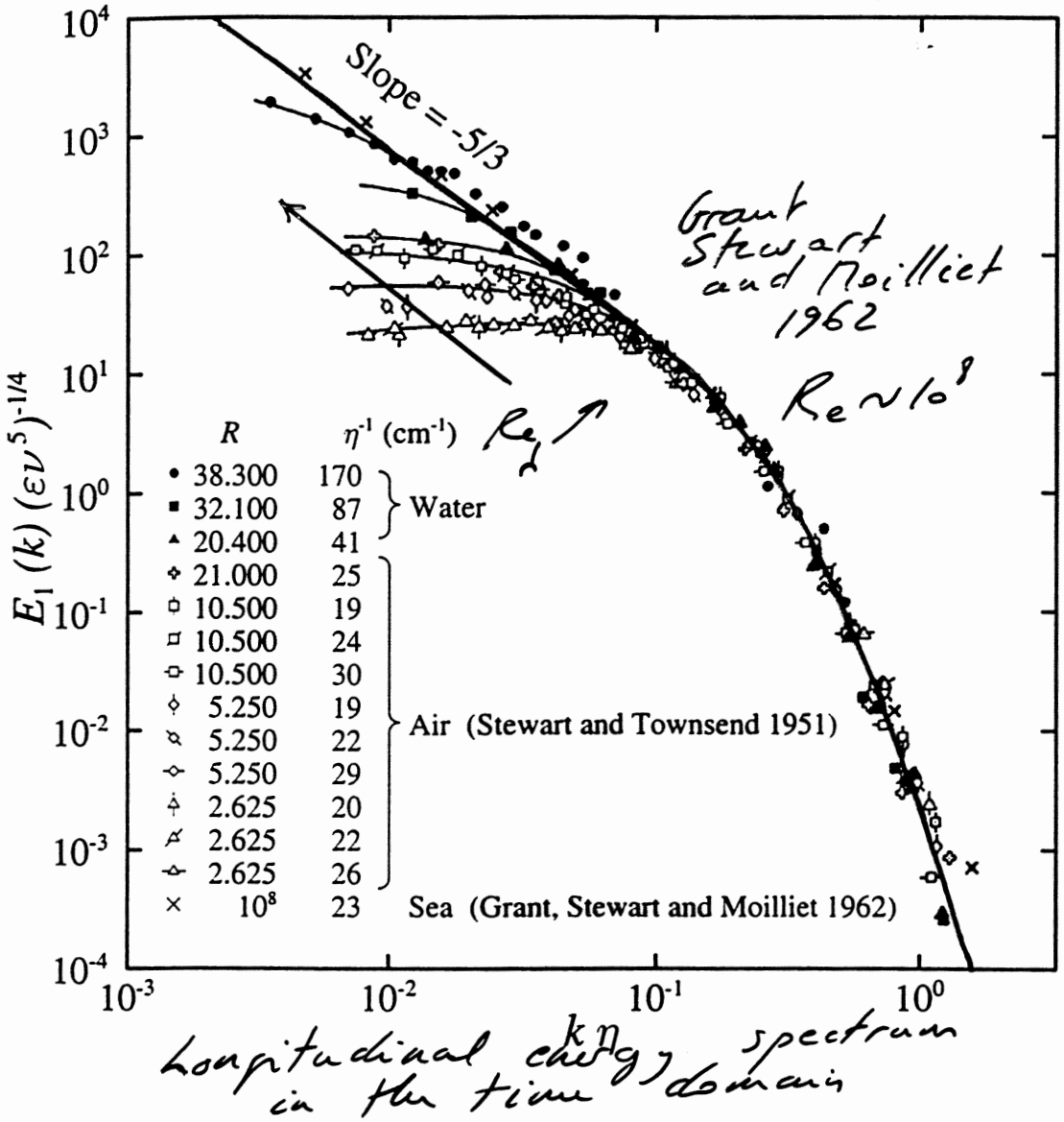
Slope = -5/3
Grant Stewart and Moilliet 1962
Re ~ 10⁸
R
η⁻¹ (cm⁻¹)
38.300 170
32.100 87
20.400 41
Water
21.000 25
10.500 19
10.500 24
10.500 30
5.250 19
5.250 22
5.250 29
2.625 20
2.625 22
2.625 26
Air (Stewart and Townsend 1951)
10⁸ 23
Sea (Grant, Stewart and Moilliet 1962)
E₁ (k) (εν⁵)⁻¹/⁴
kη
Longitudinal energy spectrum in the time domain

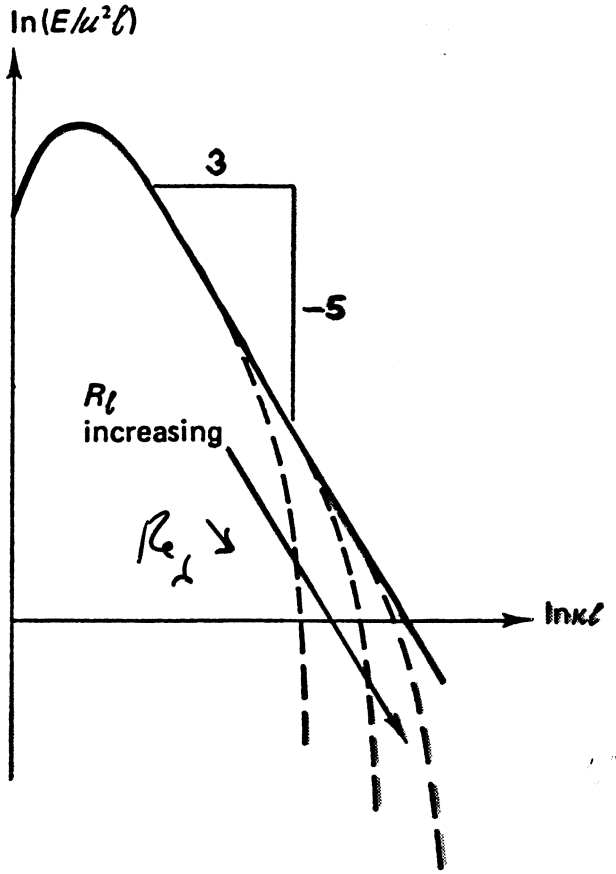

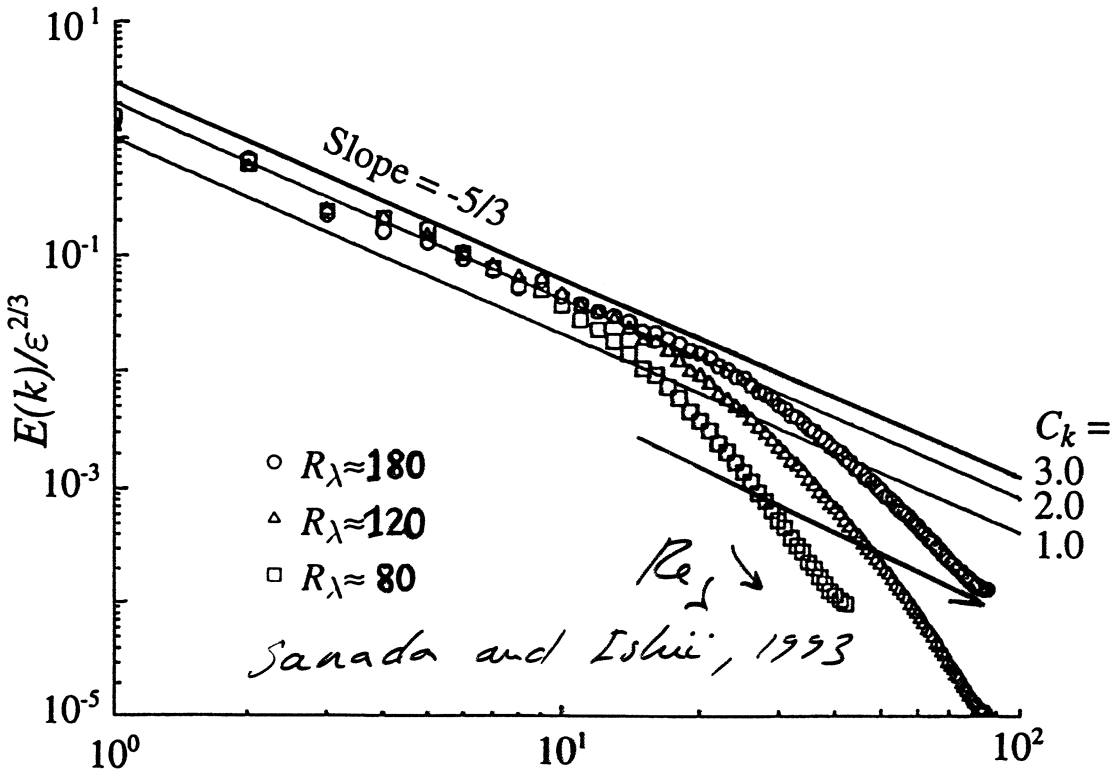

Energy spectrum in the space domain

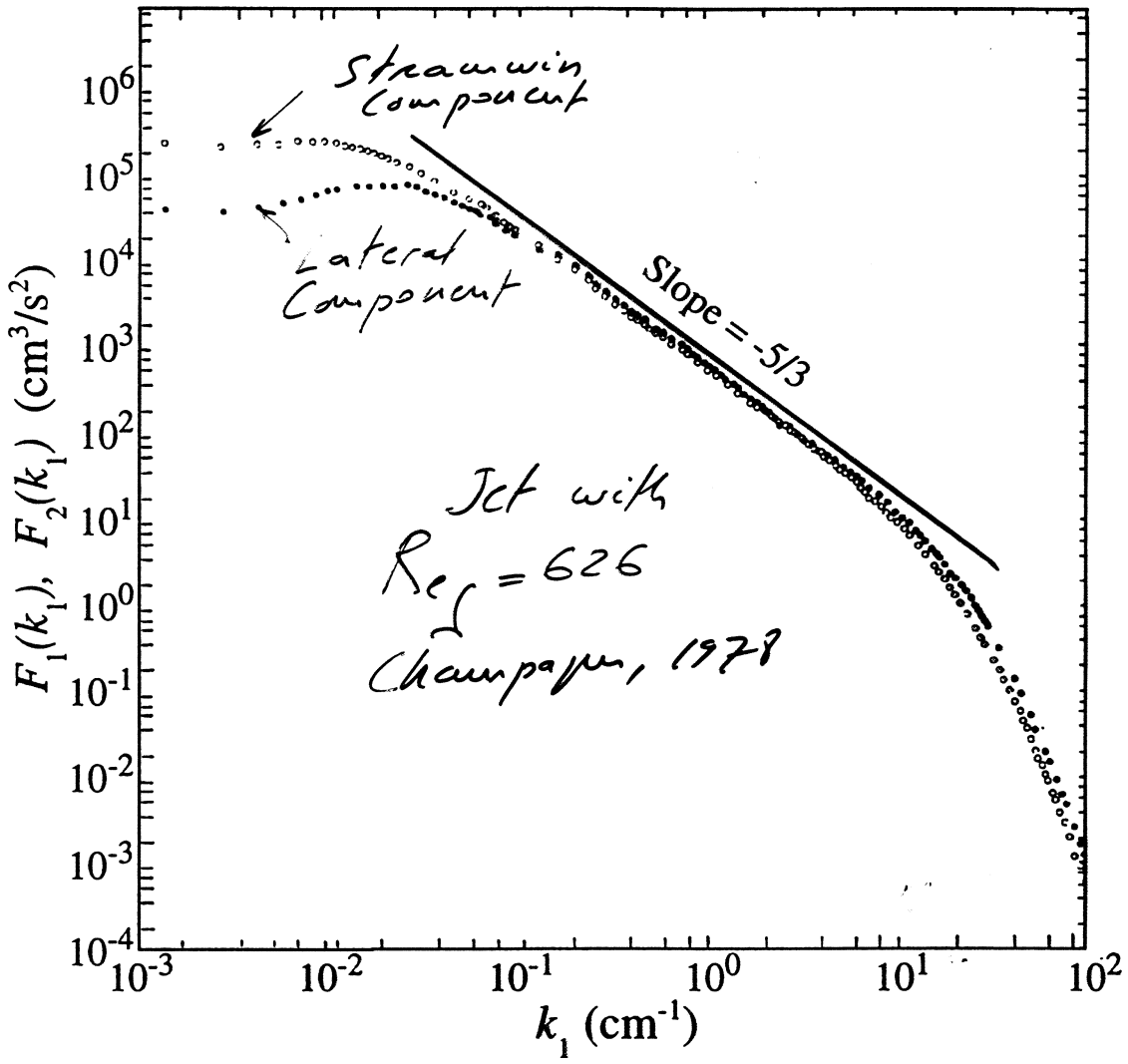
Streamwise Component
Lateral Component
Slope = -5/3
Jet with
$Re_\lambda = 626$
Champagne, 1978
$F_1(k_1)$, $F_2(k_1)$ (cm^3/s^2)
k_1 (cm^{-1})

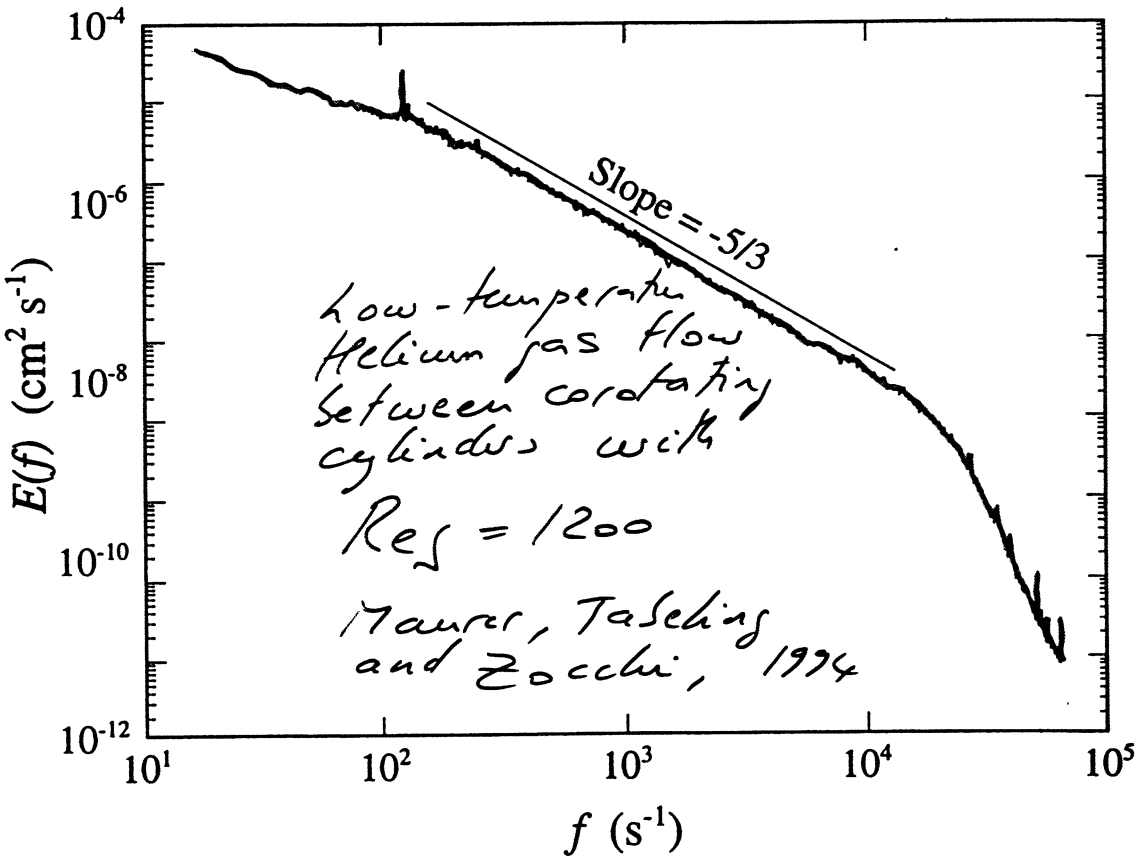
Slope = -5/3
Low-temperature Helium gas flow between corotating cylinders with
$Re_\lambda = 1200$
Maurer, Tabeling and Zocchi, 1994
$E(f)$ (cm^2 s^{-1})
f (s^{-1})

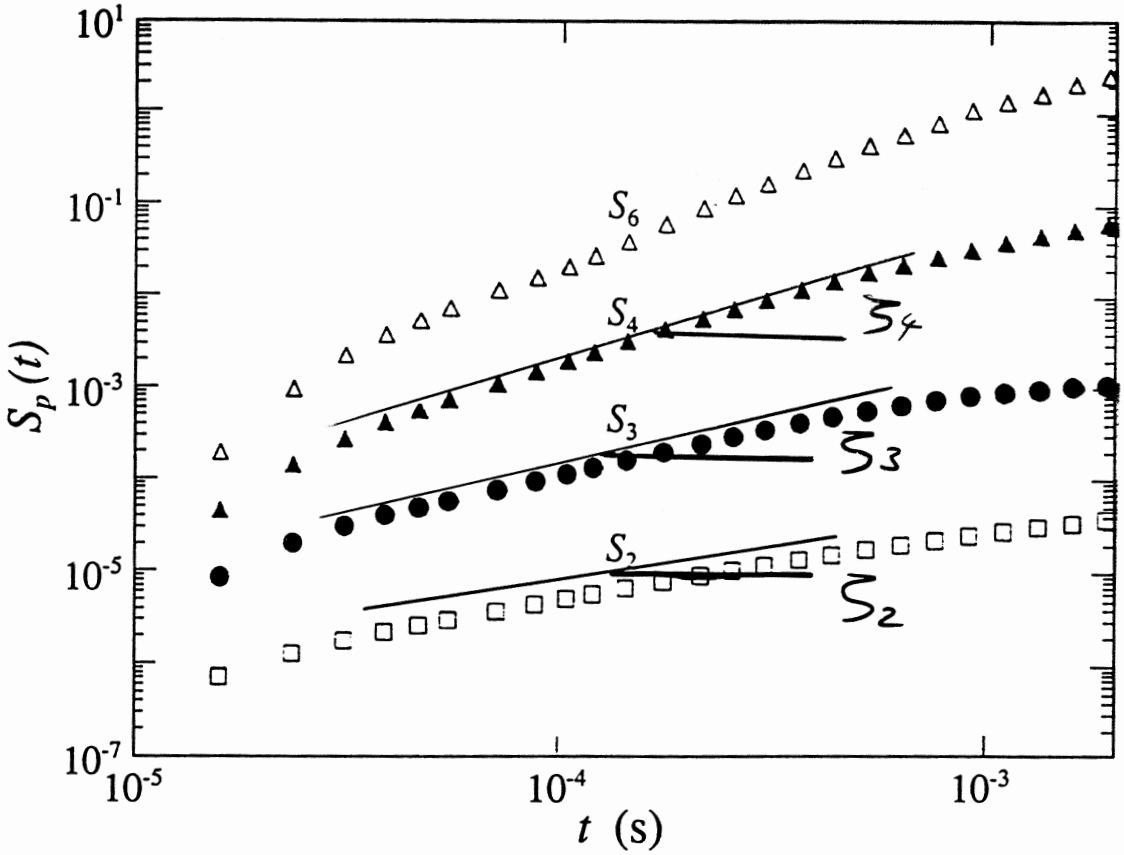
10^1
10^{-1}
10^{-3}
10^{-5}
10^{-7}
$S_p(t)$
S_6
S_4
ζ_4
S_3
ζ_3
S_2
ζ_2
10^{-5}
10^{-4}
10^{-3}
t (s)

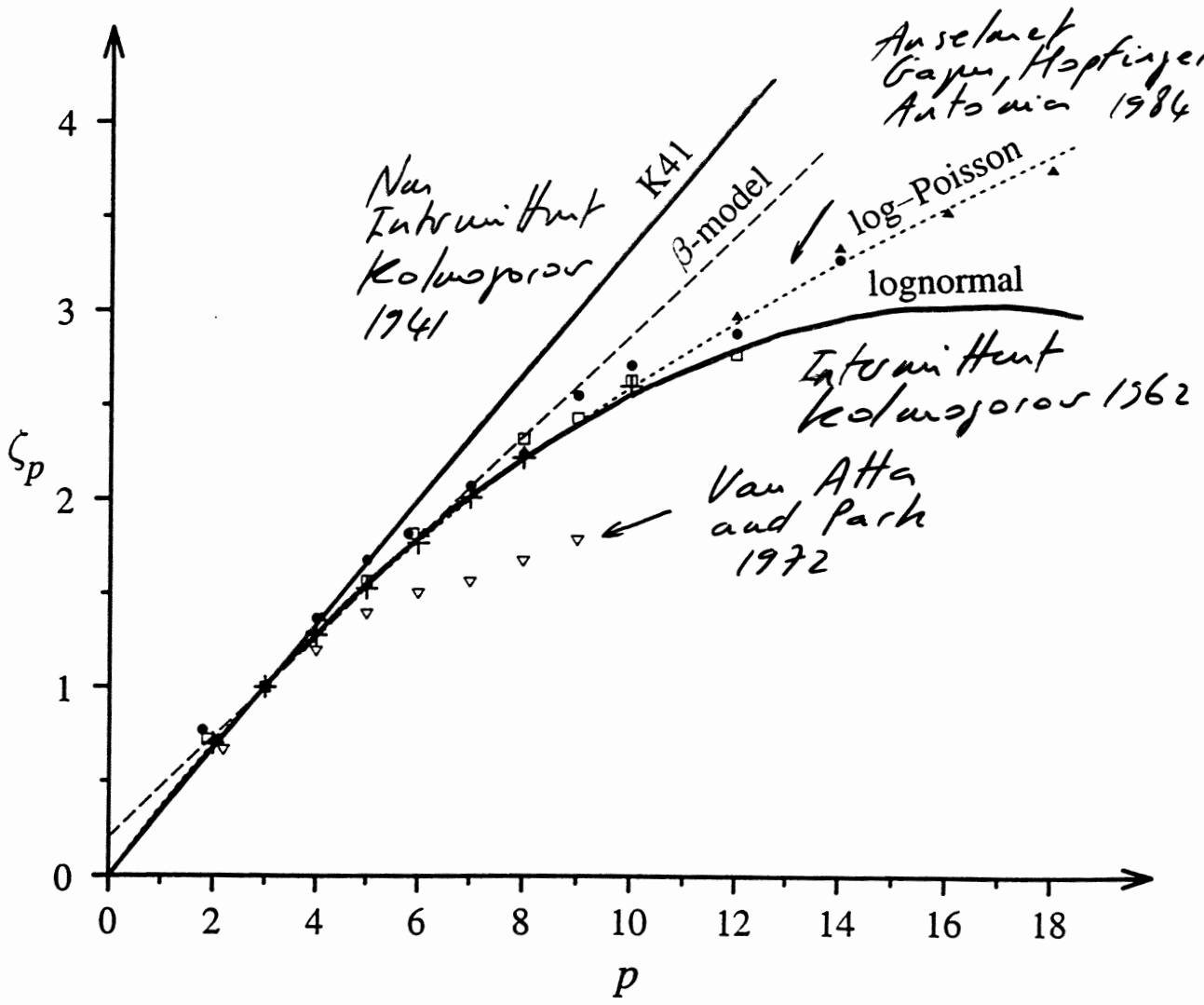
Anselmet Gagne, Hopfinger, Antonia 1984
Van Intermittent Kolmogorov 1941
K41
β-model
log-Poisson
lognormal
Intermittent Kolmogorov 1962
Van Atta and Park 1972
ζ_p
p
0
1
2
3
4
0
2
4
6
8
10
12
14
16
18

CRITICS OF KOLMOGOROV'S THEORY

KRAICHNAN 1974

'On Kolmogorov's inertial range theories' JFM 62 pp. 305-330

'Kolmogorov's 1941 theory has achieved an embarrassment of success. The $k^{-5/3}$ spectrum has been found not only when it reasonably could be expected, but also at Reynold's numbers too small for a distinct inertial range to exist as in boundary layers and shear flows where there are substantial departures from isotropy, and such strong effects from the mean shearing motion that the stepwise cascade appealed to by Kolmogorov is dubious.'

KRAICHNAN 1974

'On Kolmogorov's inertial range theories' JFM 62

'Our basic point is that the inertial-range cascade represents strong statistical disequilibrium. This carries two implications. First, that analogies with equilibrium and near-equilibrium phenomena are unjustified. Second, that the structure of the inertial range depends on the actual magnitude of the coefficients coupling the degrees of freedom and not just on their overall symmetries and invariance properties. This is because cascade is a transport process and the coefficient magnitudes affect the rate of transport.'

'The terms 'scale of motion' or 'eddy of size l' appear repeatedly in treatments of the inertial range. One gets an impression of little, randomly distributed whirls in the fluid, with the cascade process consisting of the fission of the whirls into smaller ones, after the fashion of Richardson's poem. This picture seems drastically in conflict with what can be inferred about the qualitative structure of high-Reynolds number turbulence from laboratory visualization techniques and from plausible application of the Kelvin circulation theorem.'

KRAICHNAN 1974

'On Kolmogorov's inertial range theories' JFM 62

'The stretching mechanism has led a number of authors to conjecture that the small-scale structure should consist typically of extensive thin sheets of vorticity drawn out by the stirring action of their own shear field (Townsend 1951, Batchelor 1953, Kraichnan 1959, Corrsin 1962, Saffman 1968, Tennekes 1968). In this picture, the randomness lies in the distribution of thickness and extension of the thin sheets and vortices, and in the way they are folded and tangled through the fluid. A typical small-scale structure is thought to be small in one or two dimensions only, not in the third.'

KRAICHNAN 1974

'On Kolmogorov's inertial range theories' JFM 62

Once the 1941 theory is abandoned, a Pandora's box of possibilities is open. The 1962 theory of Kolmogorov seems arbitrary, from an a priori viewpoint.

We make the point that even in the general framework of some kind of self-similar cascade, and of intermittency which increases with the number of cascade steps, the 1962 theory is only one of many possibilities!

'The 1941 theory is by no means logically disqualified merely because the dissipation rate fluctuates. On the contrary, we find that at the level of crude dimensional analysis and eddy-mitosis picture the 1941 theory is as sound a candidate as the 1962 theory.

This does not imply that we espouse the 1941 theory. On the contrary, the theory is made implausible by the basic physics of vortex stretching. The point is that this question cannot be decided a priori; SOME KIND OF NON-TRIVIAL USE MUST BE MADE OF THE NAVIER-STOKES EQUATION.

If the Kolmogorov law $E(k) \propto k^{-5/3-\mu}$ is asymptotically valid, it is argued that THE VALUE μ DEPENDS ON THE DETAILS OF THE NON-LINEAR INTERACTION EMBODIED IN THE NAVIER-STOKES EQUATIONS AND CANNOT BE DEDUCED FROM OVERALL SYMMETRIES, INVARIANCES AND DIMENSIONALITY.'

3D FORCED HOMOGENEOUS TURBULENT FLOW

Numerical simulation
by Vincent & Meneguzzi
JFM 91 & JFM 93

$$\begin{cases} \dfrac{\partial \vec{v}}{\partial t} = \vec{v} \times \vec{\omega} - \vec{\nabla}(P + \tfrac{1}{2} v^2) + \nu \nabla^2 \vec{v} + \vec{F} \\ \vec{\nabla} \cdot \vec{v} = 0 \\ \text{Periodic Boundary Conditions} \\ \text{Random initial velocity} \\ \text{Deterministic forcing} \end{cases}$$

$$\frac{\partial \hat{\vec{v}}_k}{\partial t} = \hat{\vec{\vec{P}}}(k) \cdot (\hat{\vec{v}} \times \hat{\vec{\omega}})_k - \nu k^2 \hat{\vec{v}}_k + \hat{\vec{F}}_k$$

P projector on the space of solenoidal fields $\quad P_{ij}(k) = \delta_{ij} - \dfrac{k_i k_j}{k^2}$

δ_{ij} Kronecker symbol

- Pseudo-spectral scheme for space integration without desaliasing,
- For time integration exact integration for the linear dissipation term and Adams-Bashforth scheme for the nonlinear advection term.

FORCED 3D TURBULENT FLOW

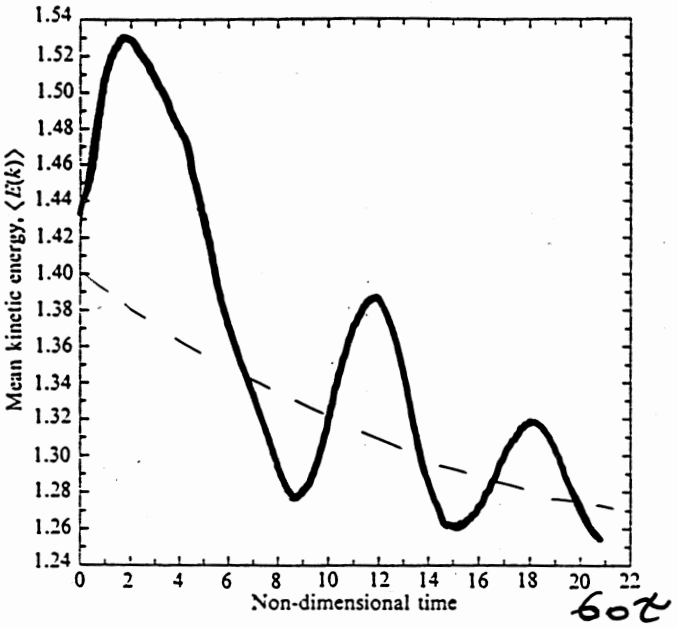

$E = \langle v^2 \rangle$

Time evolution of the total kinetic energy

240^4 Cray 2 - 4 proc.

t

FIGURE 1. Mean kinetic energy per unit mass versus time. The turnover time is 0.35.

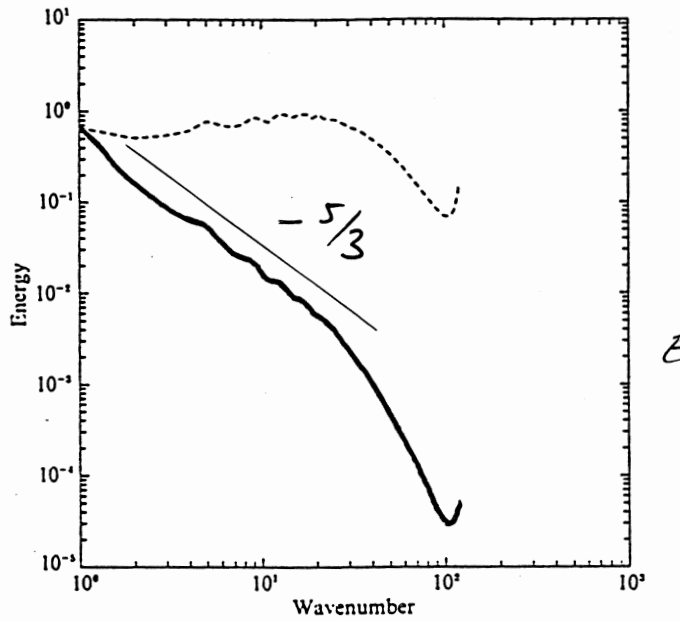

$\log E$

Energy spectrum

$E(k) = \frac{1}{2} \sum |\hat{v}_k|^2$

$k - \frac{1}{2} < |\vec{k}| \leq k + \frac{1}{2}$

$\log k$

FIGURE 2. Energy spectrum at a given time (continuous curve). Same energy spectrum multiplied by $k^{\frac{5}{3}}$ (dashed curve).

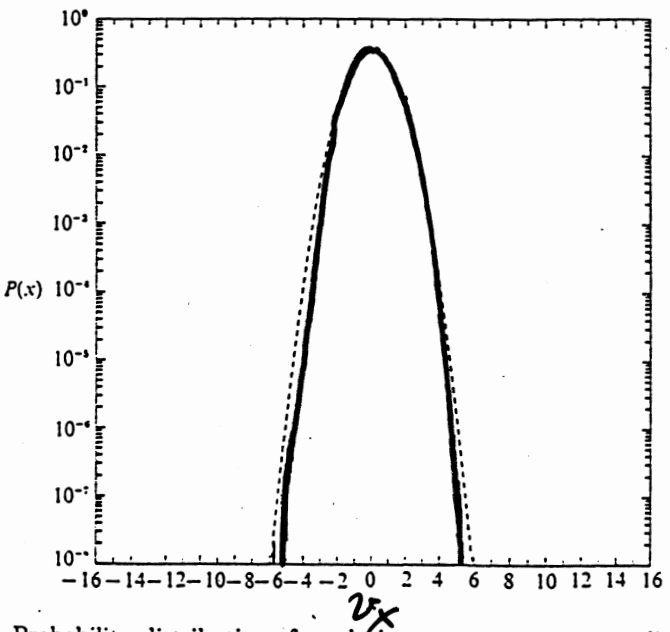

$\log P(v_x)$

Probability Distribution Function of the 1st component of velocity

FIGURE 4. Probability distribution of a velocity component v_x, normalized so that $\sigma = 1$, shown together with a Gaussian distribution (dashed line).

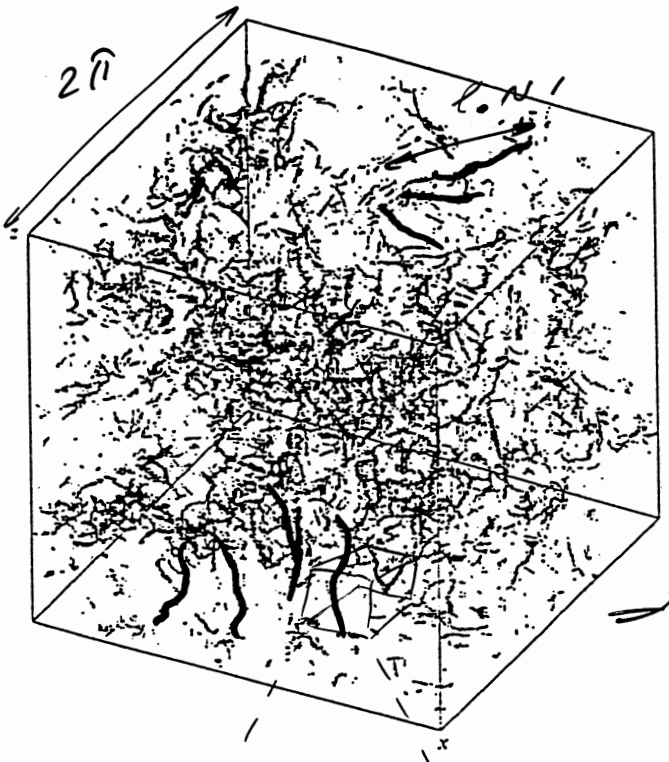

Integral scale

$$l_0 = \frac{\int_0^\infty k^{-1} E(k)\,dk}{\int_0^\infty E(k)\,dk}$$

$$v_0 = (\langle v^2 \rangle)^{1/2}$$

$$\Rightarrow R_e = \frac{v_0 l_0}{\nu} = 1000$$

FIGURE 13. View of the vorticity field, represented by a vector of length proportional to the vorticity amplitude at each grid point. Only vectors larger than a given threshold value are shown.

Vorticity field

240

3

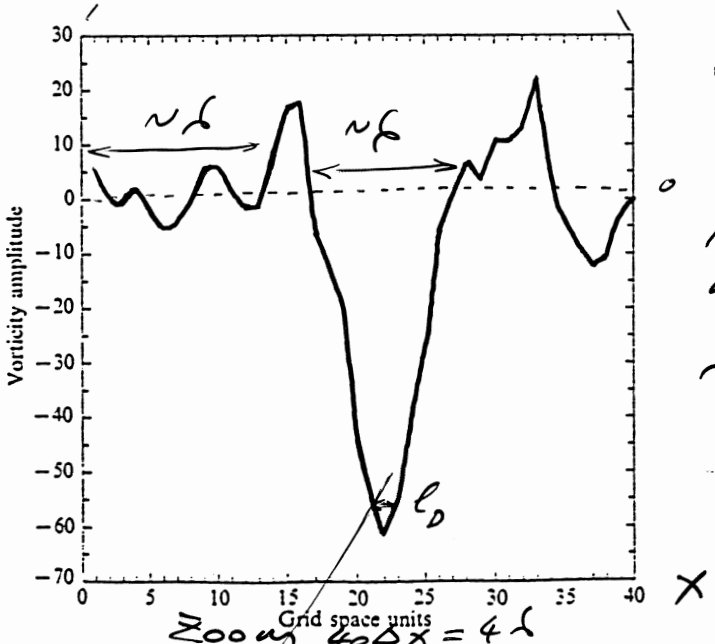

Does λ characterize vortex width or vortex spacing?

ω

Taylor microscale

$$\lambda = \sqrt{\frac{\epsilon}{\nu}} = 10\,\Delta x$$

Kolmogorov dissipative scale

FIGURE 15. Cut through a typical vorticity tube along a direction perpendicular to its axis.

$$l_D = \left(\frac{\nu^3}{\epsilon}\right)^{1/4} = 1\Delta$$

Vortex cor

$$\Rightarrow R_\lambda = \frac{\lambda v_0}{\nu} = 150$$

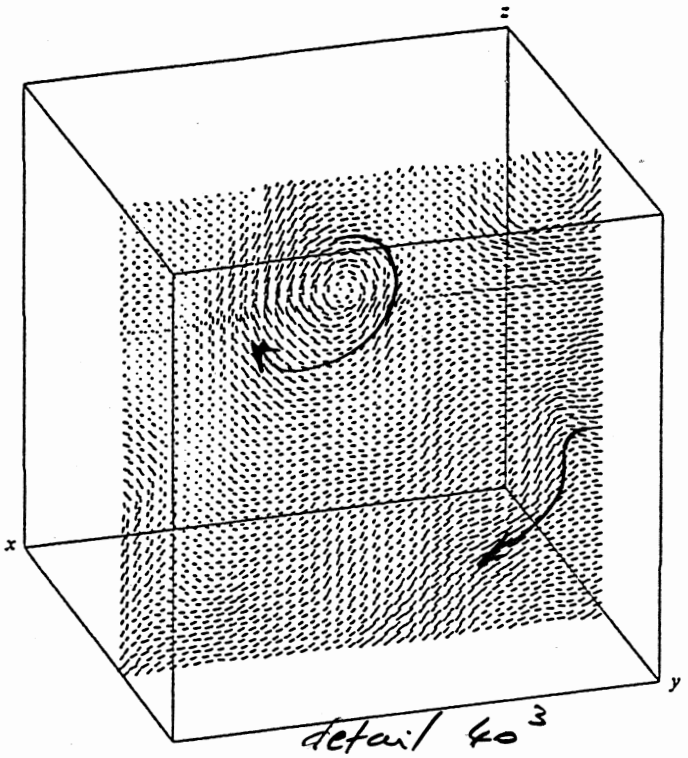

FIGURE 18. Projection of the velocity field on a plane perpendicular to a particular vorticity tube.

2D cut of the velocity field

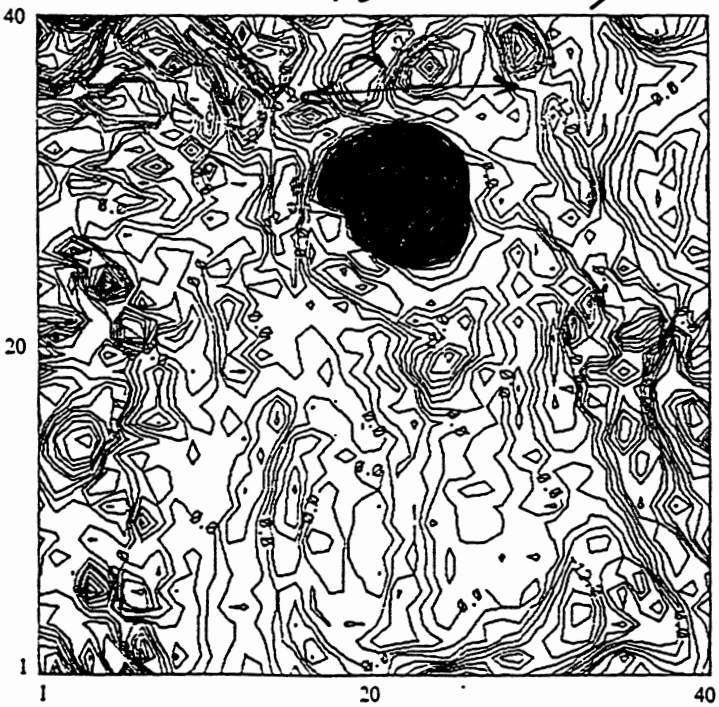

No evidence of spiral structure of vorticity as suggested by Lundgren 1982

FIGURE 19. Curves of constant vorticity in a plane perpendicular to a selected vorticity tube.

2D cut of the vorticity modulus 40^2

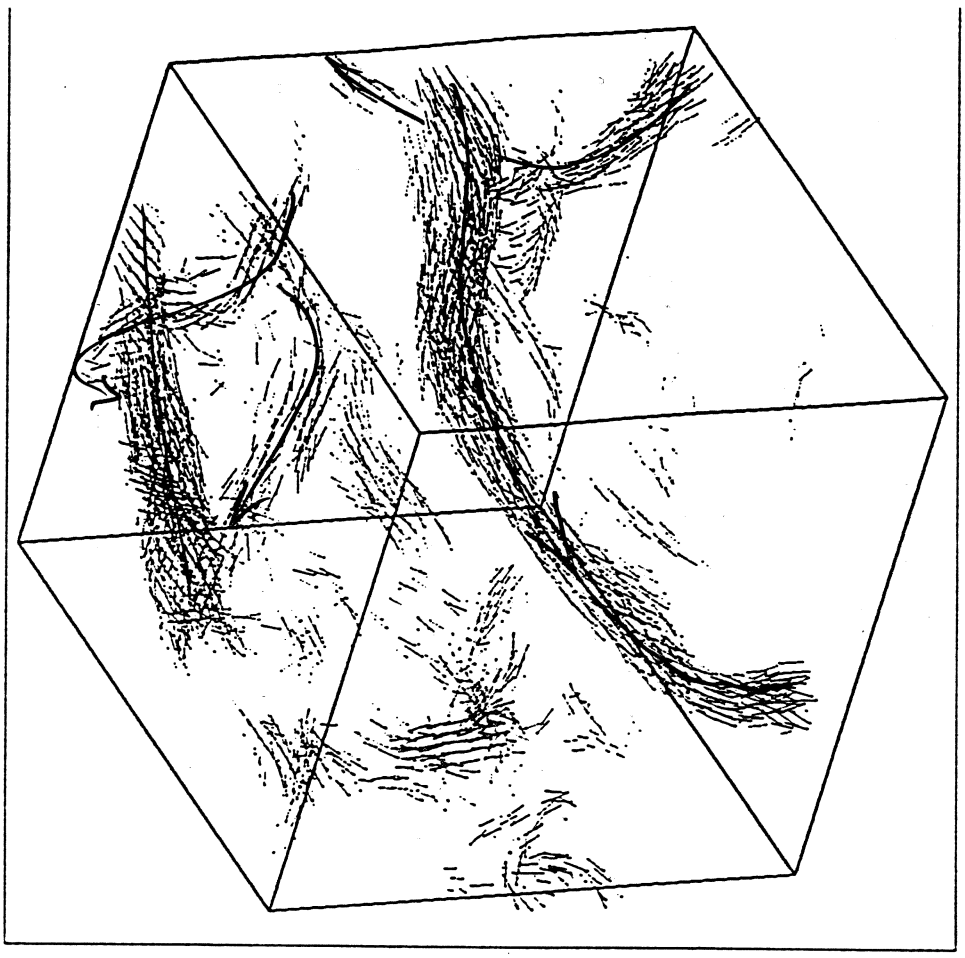

FIGURE 16. Detail of the vorticity field, showing a sub-cube of size one sixth of the complete cube, i.e. 40 grid points in each direction.

Detail of the vorticity field 40^3

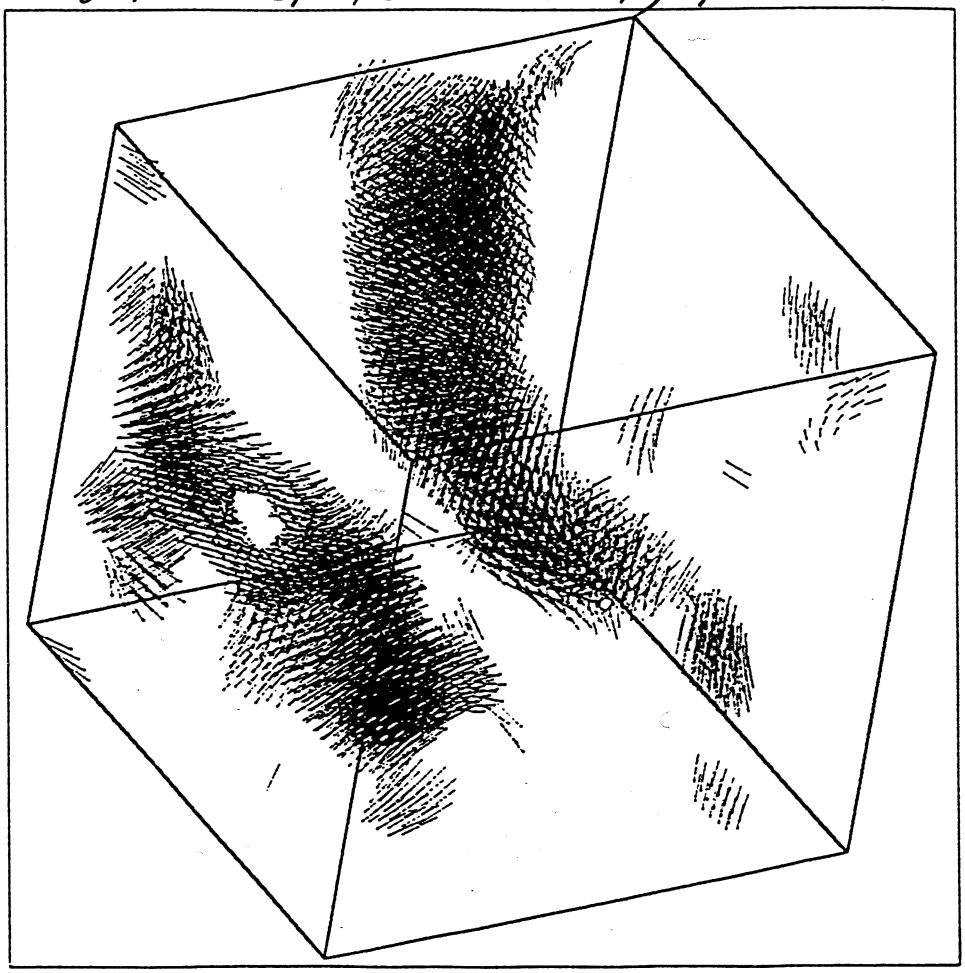

FIGURE 17. Same vorticity tube as in figure 6, but showing only inertial-subrange scales. Dissipation and energy-injection scales have been removed by filtering in Fourier space.

Detail of the vorticity field filtered to retain only the inertial scales 40^3

Probability Distribution function (PDF) of the horizontal gradients of velocity $\partial u_x/\partial x$

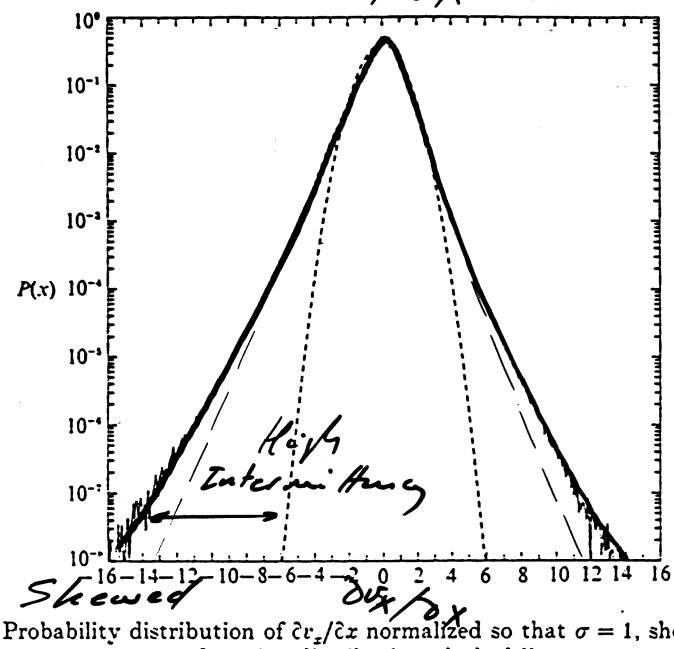

$\log P(\partial u_x/\partial x)$

$S = -0.5$

$F = 5.9$

S independent of R_λ comparing with Tennekes 1968 turbulence model of a collection of vorticity tubes

Similar to the Cauchy's distribution predicted by Min & Negzic 1996

FIGURE 5. Probability distribution of $\partial v_x/\partial x$ normalized so that $\sigma = 1$, shown together with a Gaussian distribution (dashed line).

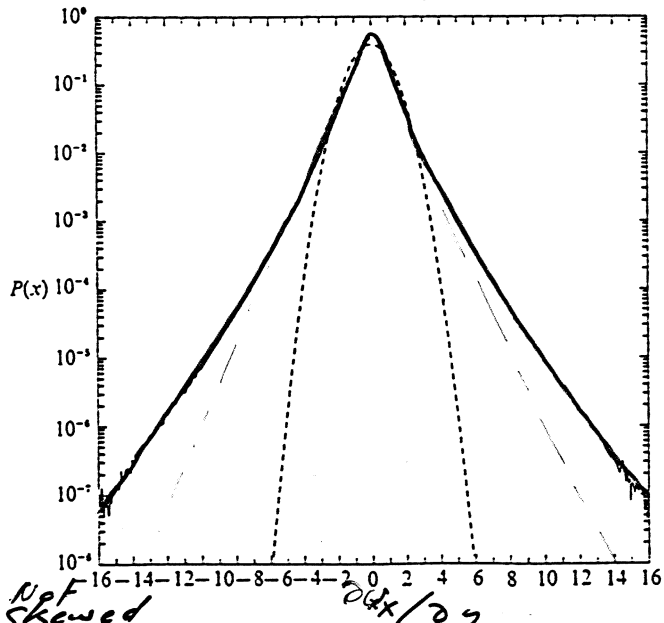

$\log P(\partial u_x/\partial y)$

$S = -0.04$

$F = 8$

Similar to experiment by Castaing, Gagne & Hopfinger 1990

FIGURE 6. Probability distribution of $\partial v_x/\partial y$ normalized so that $\sigma = 1$, shown together with a Gaussian distribution (dashed line).

Probability Distribution function (PDF) of the lateral gradients of velocity $\partial u_x/\partial y$

Probability Distribution Function (PDF) of the velocity differences, $\delta u_x(r) = u_x(x+r) - u_x(x)$

For $r = 0.05$ dissipative scales

$\log P(\delta u_x(r))$

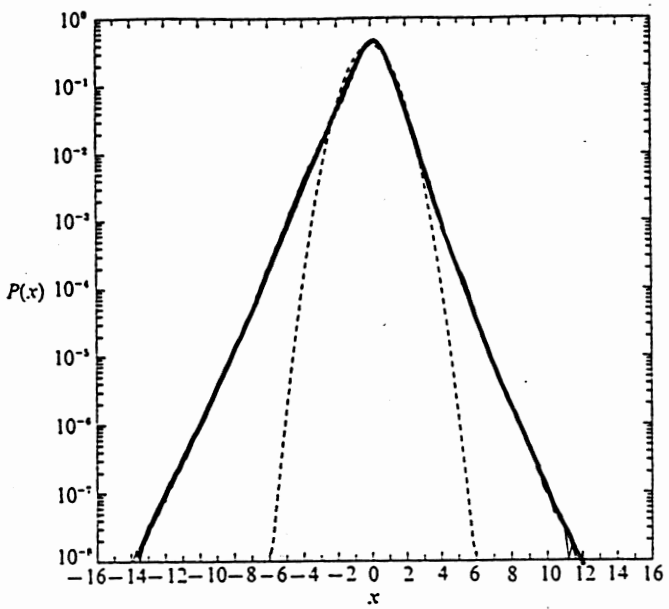

Exponential distribution similar to experiment by Van Atta & Chen 1970

FIGURE 7. Probability distribution of $\delta v_x(r) = v_x(x+r) - v_x(x)$ for $r = 0.05$ (a dissipation scale), normalized so that $\sigma = 1$, shown together with a Gaussian distribution (dashed line).

For $r = 0.39$ inertial scales

$\log P(\delta u_x(r))$

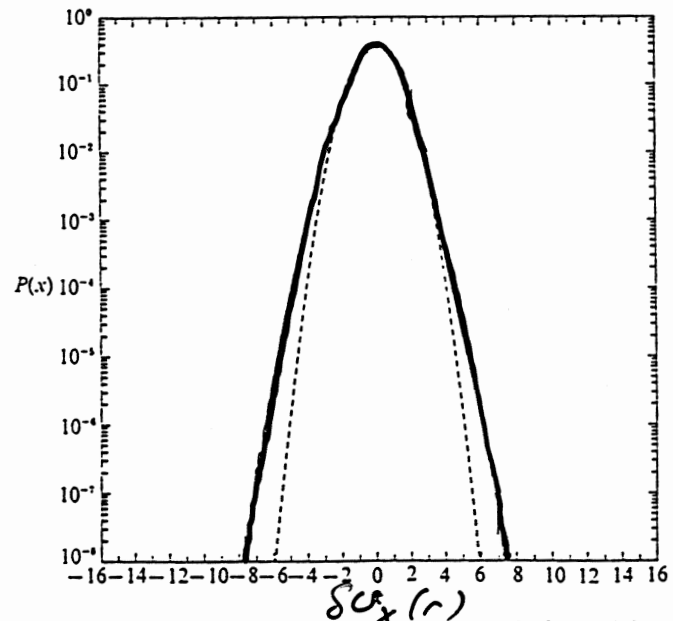

FIGURE 8. Same as figure 7 with $r = 0.39$, a typical inertial-range scale.

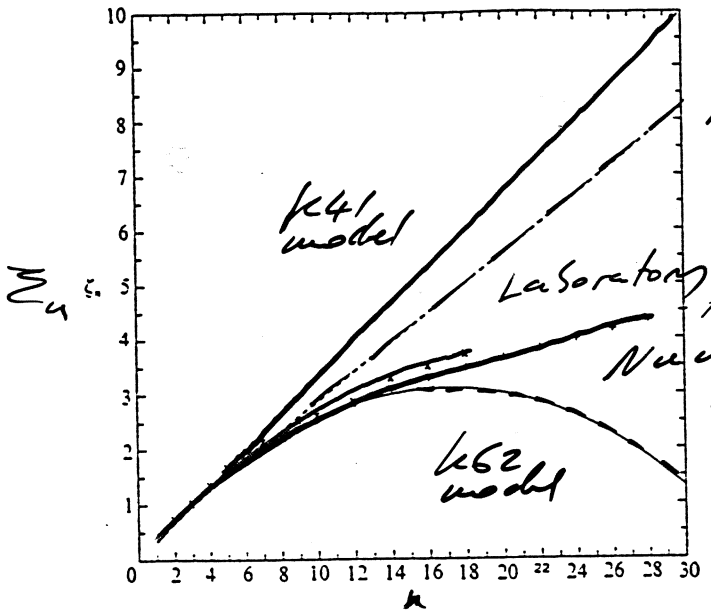

FIGURE 10. Power-law exponent ζ_n of the structure functions $F_n(r) \sim r^{\zeta_n}$ as a function of n. ---, prediction of the Kolmogorov (1941) theory; ----, β-model; ——, Kolmogorov (1962) model; +, values from our simulation; ×, experimental values of Anselmet *et al.* (1984) for $R_\lambda = 852$.

$F_n(r) \sim r^{\zeta_n}$

ζ_n exponent of the structure function of order n

F_6

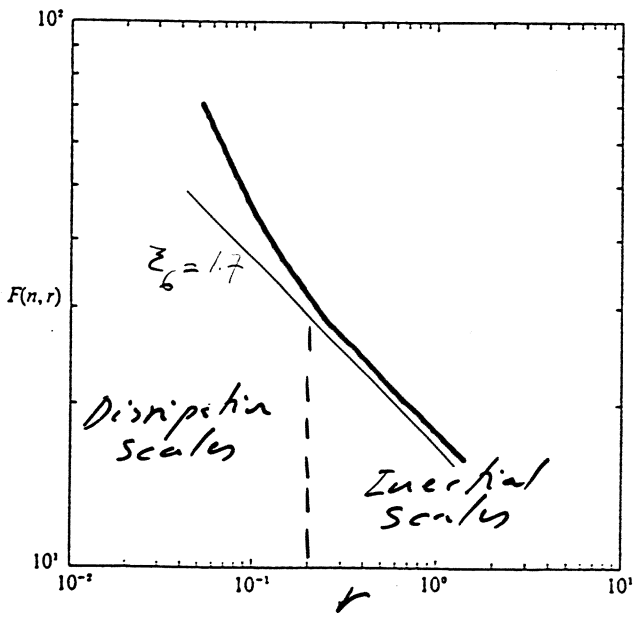

FIGURE 9. Structure function of order 6, $F_6(r) = \langle [\delta v_x(r)]^6 \rangle$ as a function of r. Note the power-law form for r in the inertial range ($r > 0.2$).

Velocity structure function of order 6

$F_6(r) = \langle (\delta v_x(r))^6 \rangle$

sample: 1.4×10^9 values

Dissipation-rate correlation $\langle \varepsilon(x+r)\,\varepsilon(x) \rangle$

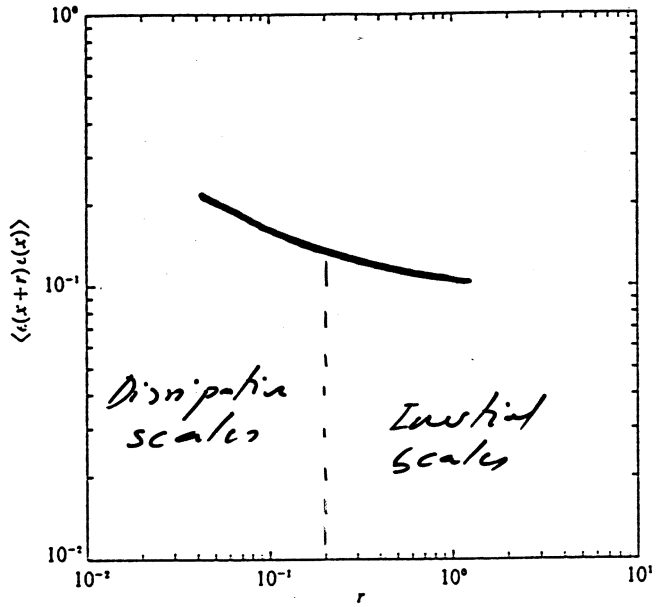

FIGURE 11. Energy dissipation correlation $\langle \epsilon(x+r)\epsilon(x) \rangle$ versus r at the end of our calculation.

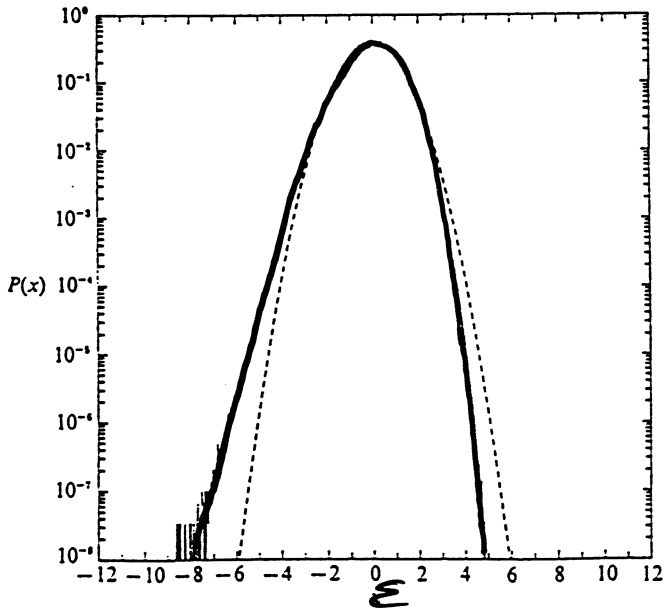

$\log P(\varepsilon)$

Different from the Gaussian distribution assumed by Kolmogoros 1962 model

FIGURE 12. Probability distribution of $\log \epsilon(x)$, where ϵ is the energy dissipation per unit mass, normalized so that $\sigma = 1$, shown together with a Gaussian distribution (dashed line).

Probability Distribution function (PDF) of the energy dissipation

θ_i, ANGLE CHARACTERIZING THE ALIGNEMENT BETWEEN $\vec{e}_i$ of $\overrightarrow{\overrightarrow{S_{ij}}}$ and $\vec{\omega}_i$

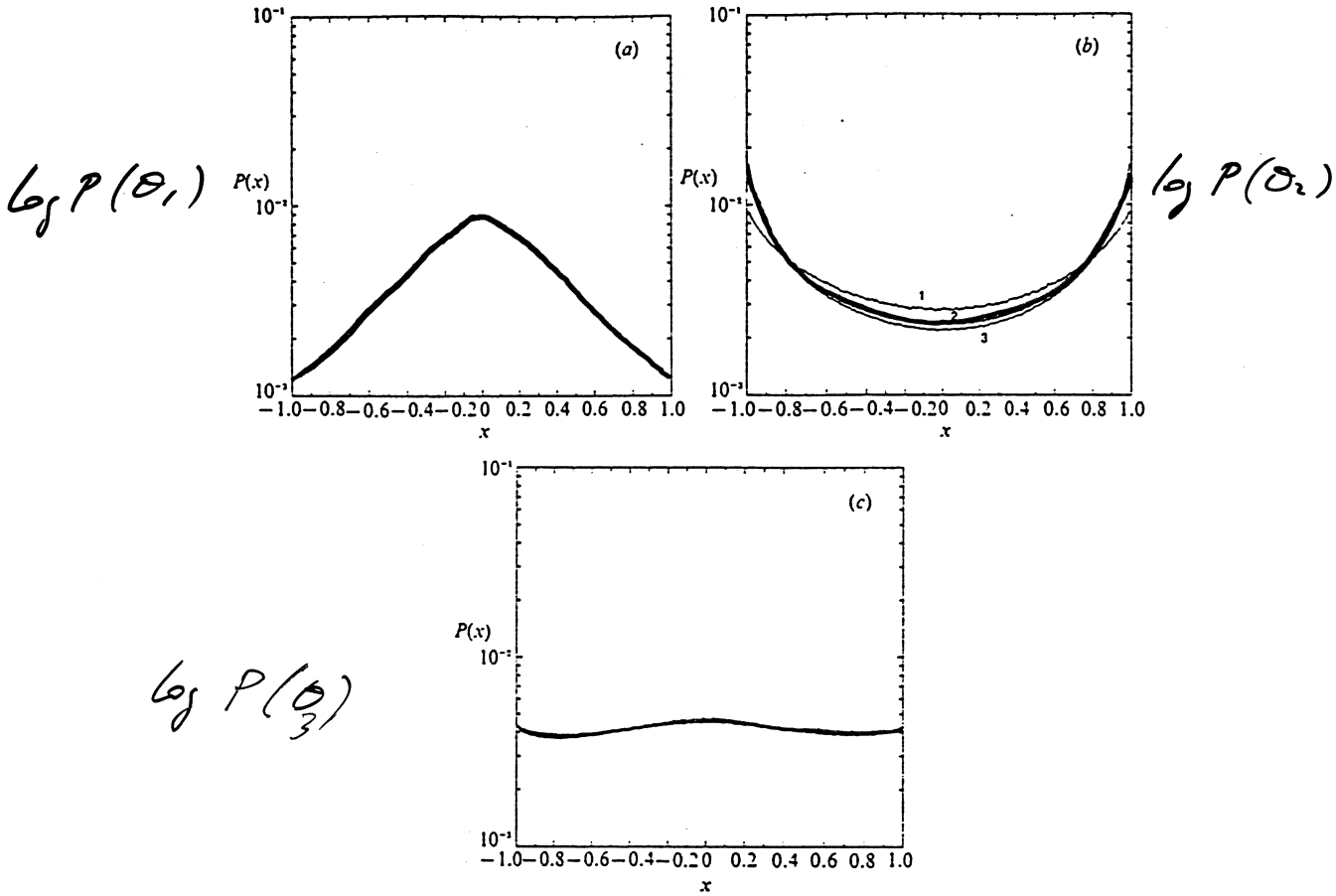

log P(θ1)

log P(θ2)

log P(θ3)

FIGURE 23. Distribution of the angle between the vorticity field and the rate of strain eigenvectors: (*a*) eigenvector e_1, associated with the smallest eigenvalue λ_1 (always negative); (*b*) eigenvector e_2, associated with the intermediate eigenvalue λ_2 (curve 1 for $\lambda_2 < 0$, curve 2 for all λ_2 values, curve 3 for $\lambda_2 > 0$); (*c*) eigenvector e_3, associated with the largest eigenvalue λ_3 (always positive).

$\lambda_1 < 0$, λ_2, $\lambda_3 > 0$ & $\vec{e}_1$, $\vec{e}_2$, $\vec{e}_3$ eigenvalues of the rate-of-strain tensor $S_{ij} = \frac{1}{2}(\partial_i v_j + \partial_j v_i)$

$\lambda_1 < 0$, $\vec{e}_1$ contraction direction

$\lambda_2 > 0$ or < 0, $\vec{e}_2$ aligned with $\vec{\omega}$ confirming Kerr 1985

$\lambda_3 > 0$, $\vec{e}_3$ stretching direction

$\vec{\nabla}\cdot\vec{v} = 0$ implies $\lambda_1 + \lambda_2 + \lambda_3 = 0$

FORCED 3D TURBULENT HOMOGENEOUS FLOW

Vincent & Meneguzzi
JFM 91 & JFM 93

- The flow is organized in very elongated vorticity tubes
  Cantwell Rogallo 81, Kerr 85, She et al. 90, Douady et al. 91.
  $Re = 90\,000$
- This involves all inertial scales from l_0 to few l_0.
- Vorticity is produced by the rolling up of vorticity sheets due to shear instability and then amplified by vortex stretching. Betchov 76
  No Richardson's cascade.
- Dissipation occurs near vortex tubes but outside their core.
- Energy spectrum $k^{-5/3+\mu}$
  $\mu \neq$ from predicted by intermittency corrections.

DIRECT NUMERICAL SIMULATION
OF HOMOGENEOUS 3D TURBULENCE

PSEUDO-SPECTRAL CODE
(DECAYING CASE)

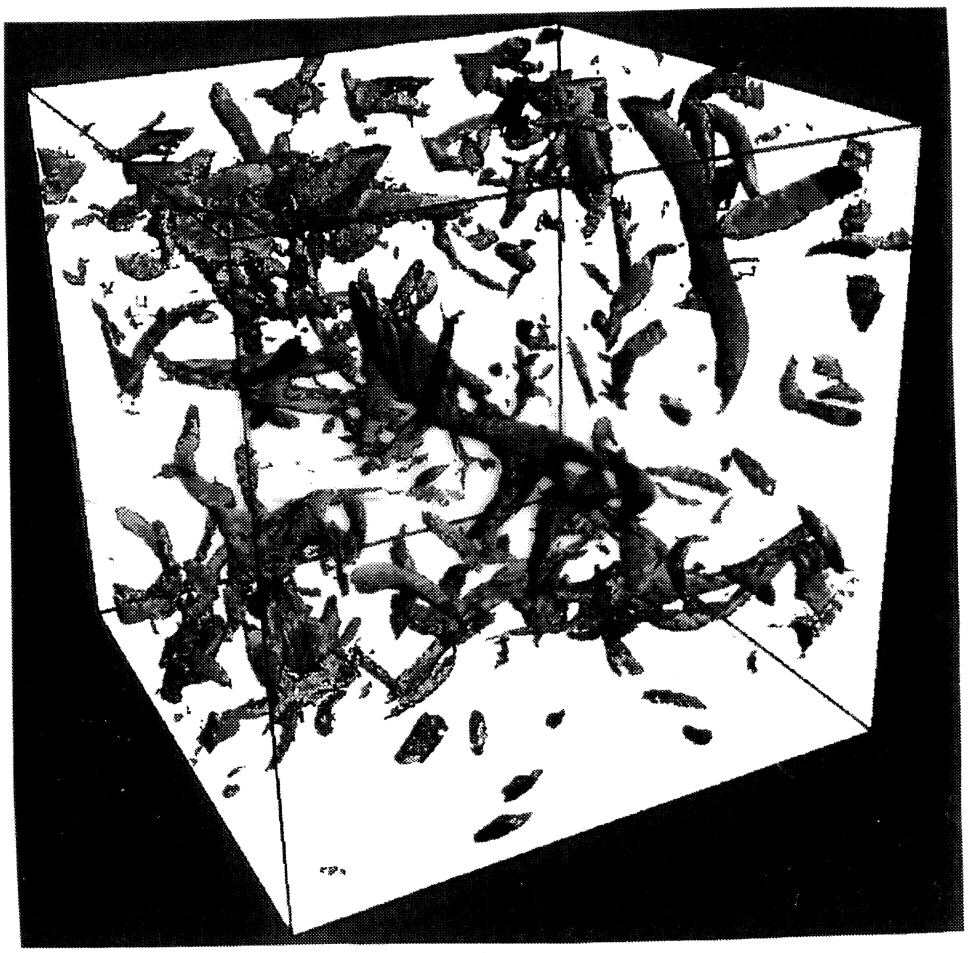

Vorticity
Numerical Simulation
512^3
Shu and Jackson

Kiyoshi YAMAMOTO, NAL, Tokyo, 1995

FREELY DECAYING 3D HOMOGENEOUS TURBULENT FLOW

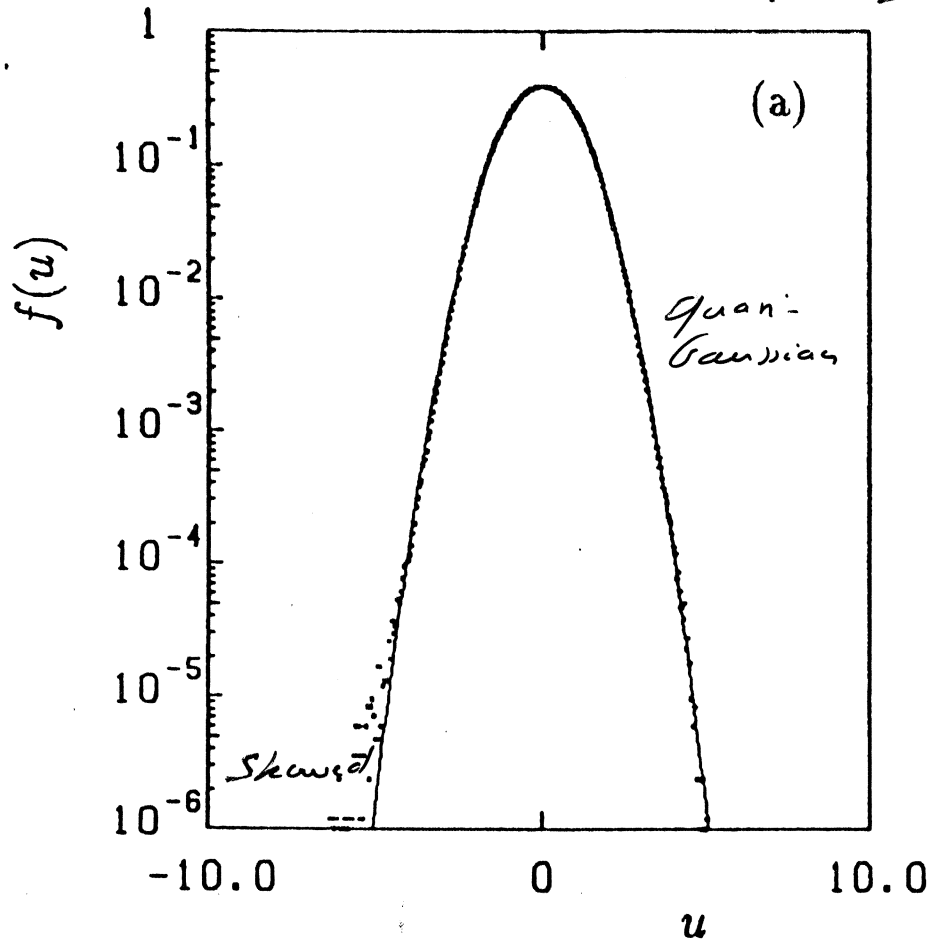

PDF of u_x

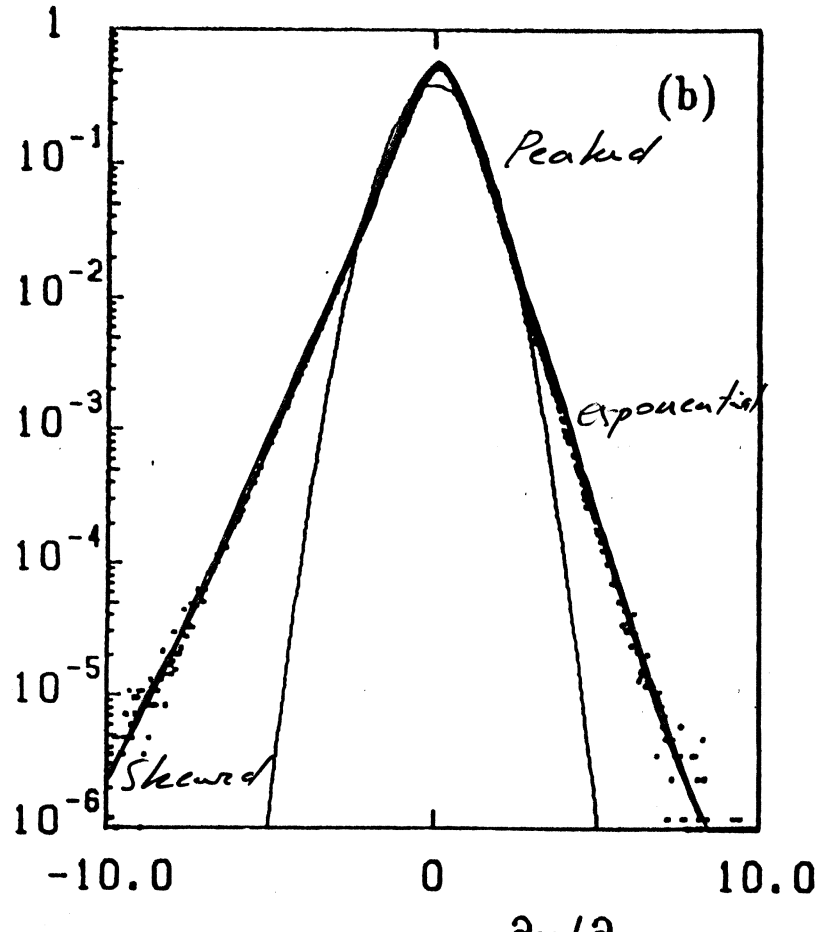

PDF of $\partial u_x/\partial x$

$Re = 2000$, $R_\lambda = 134$, 512^3

Decaying 3D Turbulence

Kiyoshi YAMAMOTO, NAL, Tokyo, 1995

FREELY DECAYING 3D HOMOGENEOUS TURBULENT FLOW

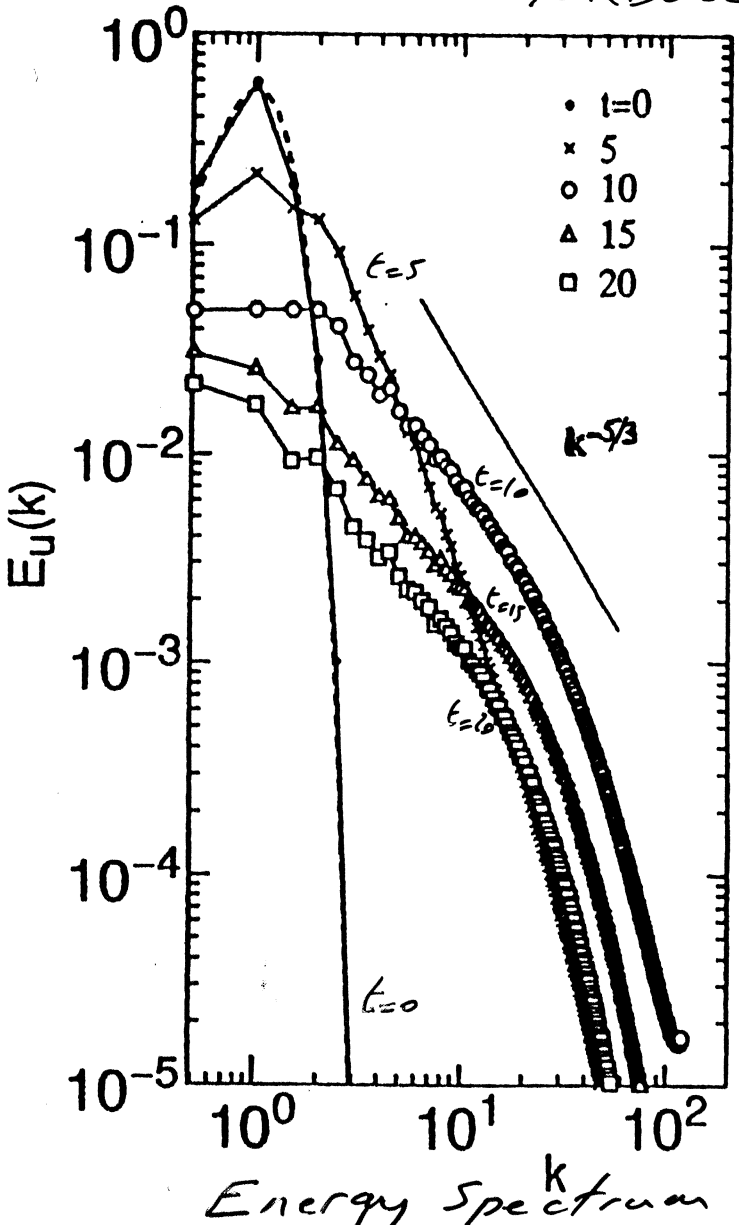

Energy Spectrum

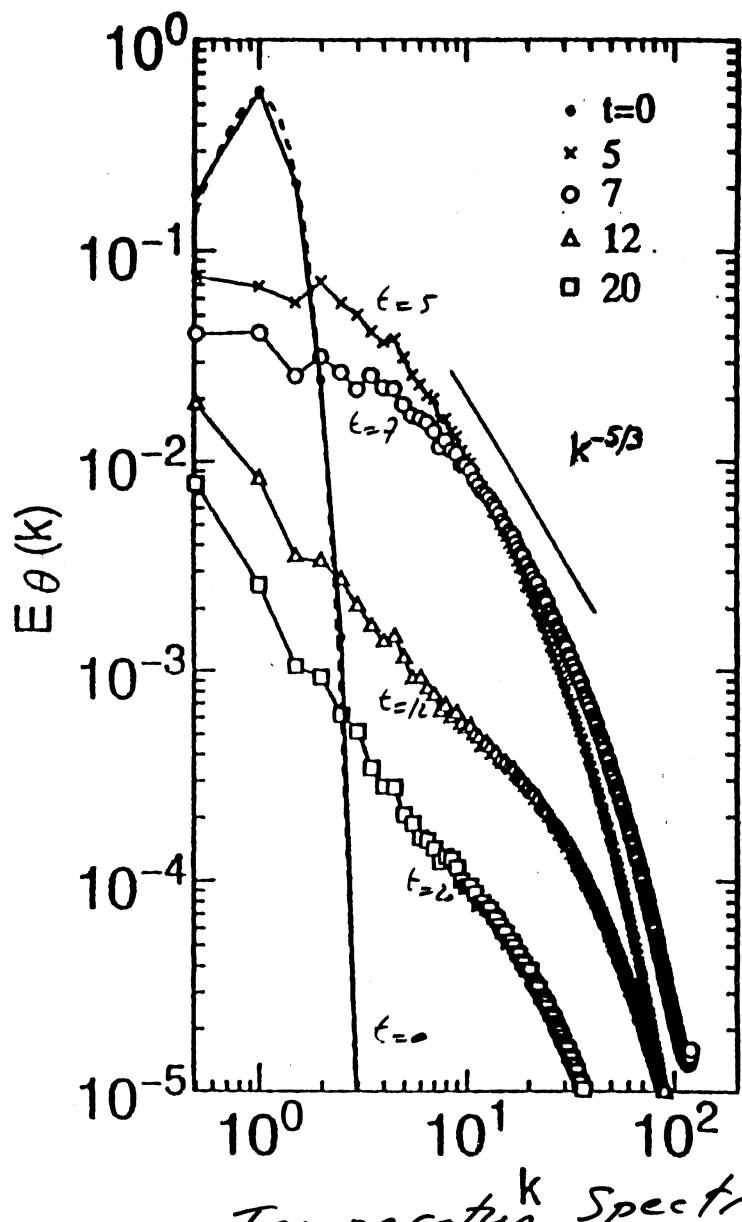

Temperature Spectrum

$Re = 2000$, $R_\lambda = 134$, 512^3

Decaying 3D Turbulence

SOME ESSENTIAL QUESTIONS ABOUT TURBULENCE

1. What is the dynamical role of coherent structures in terms of small scales generation? Is there intermittency?

2. What is the local scaling behaviour of coherent structures and how does it relate to the energy spectrum?

3. Where and what are the scales when dissipation acts? What is their spatial support?

INTERMITTENCY FACTOR

Where are the small scales?
How intermittent are they?

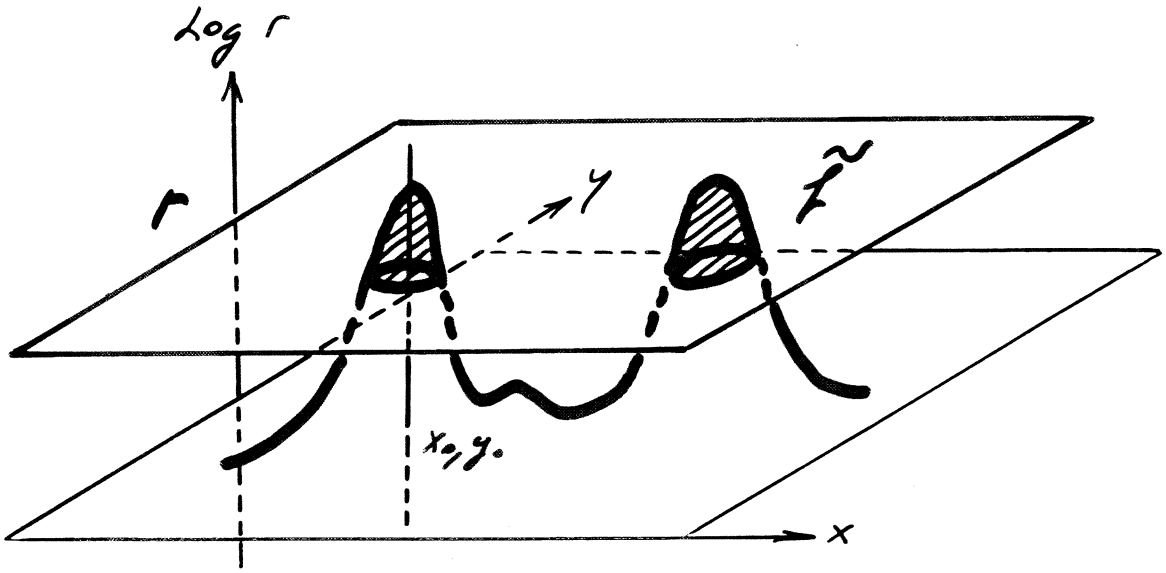

$$I(r,\vec{x}) = \frac{|\tilde{f}(r,\vec{x})|^2}{\langle |\tilde{f}(r,\vec{x})|^2 \rangle_{\vec{x}}}$$

Therefore average energy is normalized to 1 at each scale

ECOULEMENT CANAL

Analyse en ondelettes

2D

Canal, Re = 180, Pr = 0.7, y+ = 10

Couleur --> Temperature, Contour --> Vitesse normale

CONTOUR LEVELS

0.60000
0.61000
0.62000
0.63000
0.64000
0.65000
0.66000
0.67000
0.68000
0.69000
0.70000
0.71000
0.72000
0.73000
0.74000
0.75000
0.76000
0.77000
0.78000
0.79000
0.80000
[illegible]
[illegible]
[illegible]
0.87000
0.88000
0.89000
0.90000
0.91000
0.92000
0.93000
0.94000
0.95000
0.96000
0.97000
0.98000
0.99000
1.00000

KIM and MOIN
NASA - Ames
1989

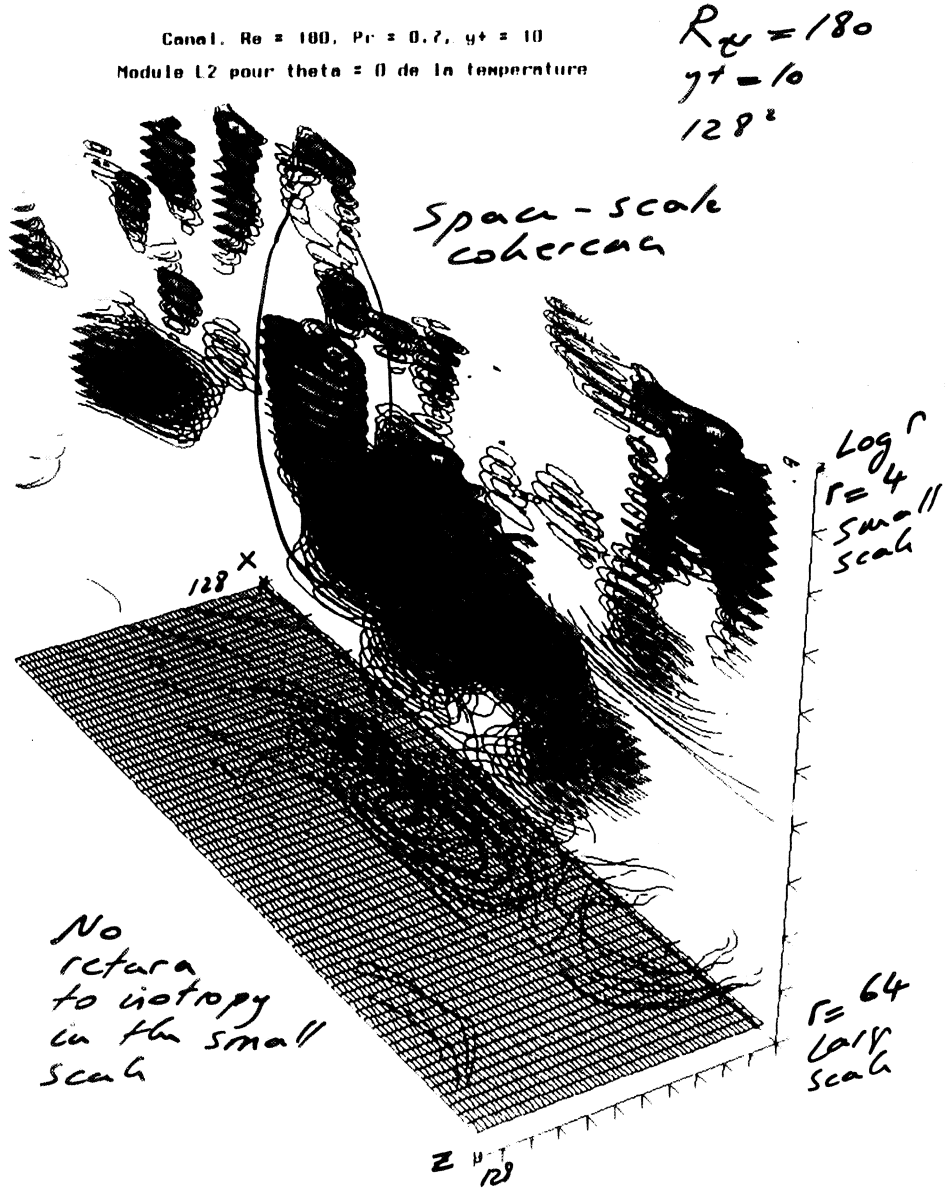

Canal, Re = 100, Pr = 0.7, y+ = 10

Module L2 pour theta = 0 de la temperature (echelles 20 a 10)

CONTOUR LEVELS
2.00000
2.50000
3.00000
3.50000
4.00000
4.50000
5.00000
5.50000
6.00000
6.50000
7.00000
7.50000
8.00000
8.50000
9.00000
9.50000
10.00000
10.50000
11.00000
11.50000
14.00000
14.50000
15.00000
15.50000
16.00000
16.50000
17.00000
17.50000
18.00000
18.50000
19.00000
19.50000
20.00000

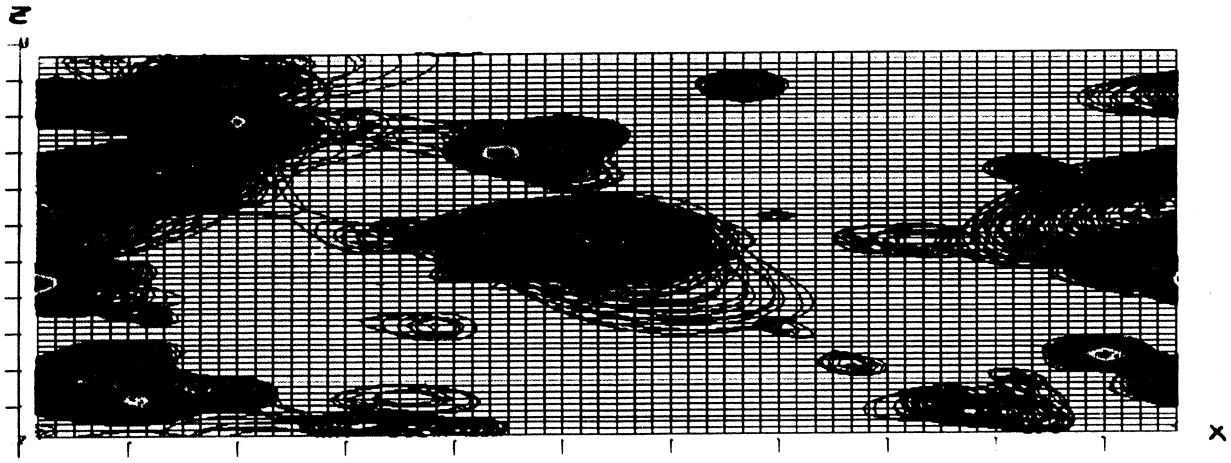

No return to isotropy

The active regions are correlated to the maxima of vertical velocity corresponding to ejections from the viscous sublayer (cf. Grégoire)

COUCHE DE MELANGE

Analyse en ondelettes 2D

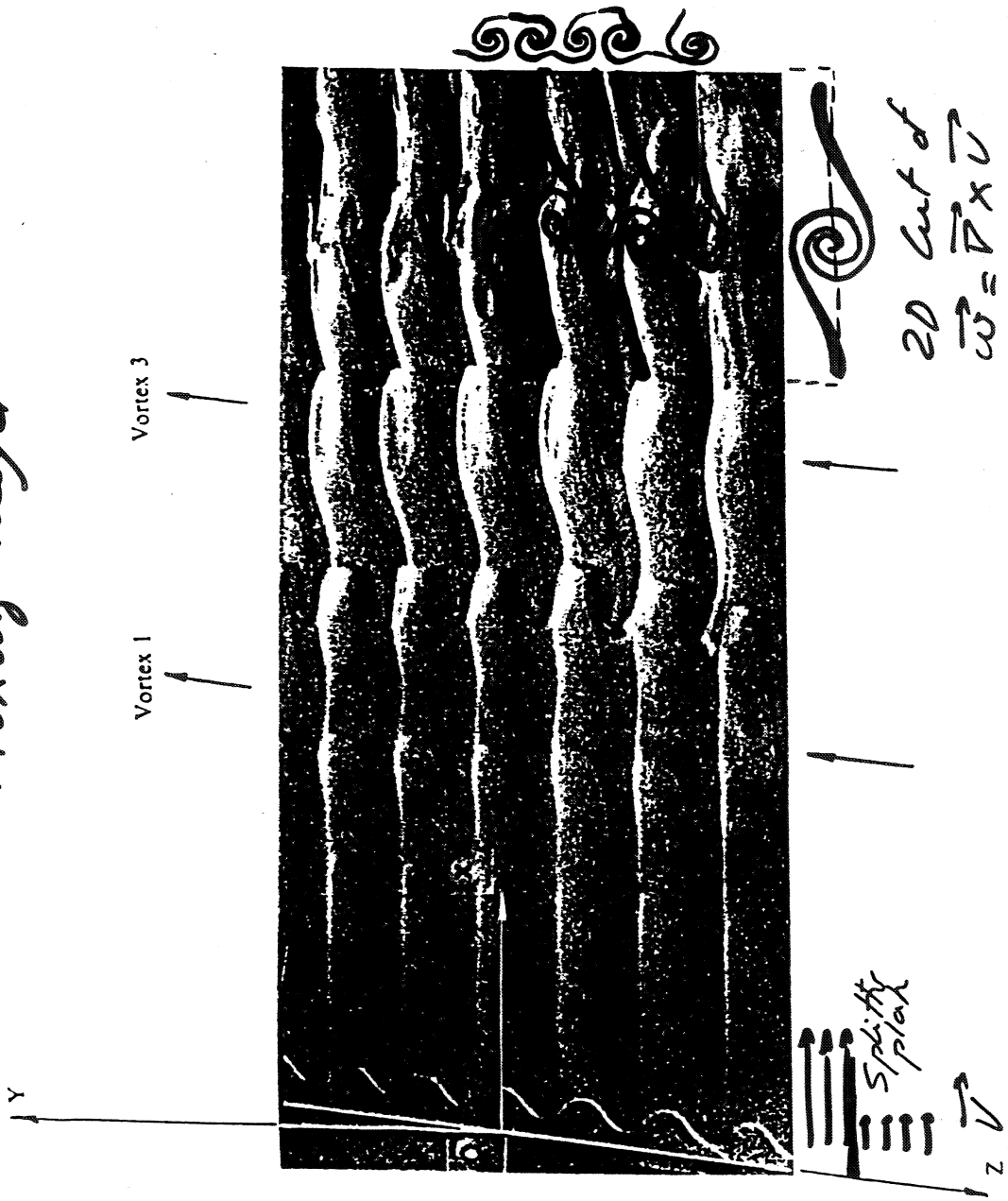

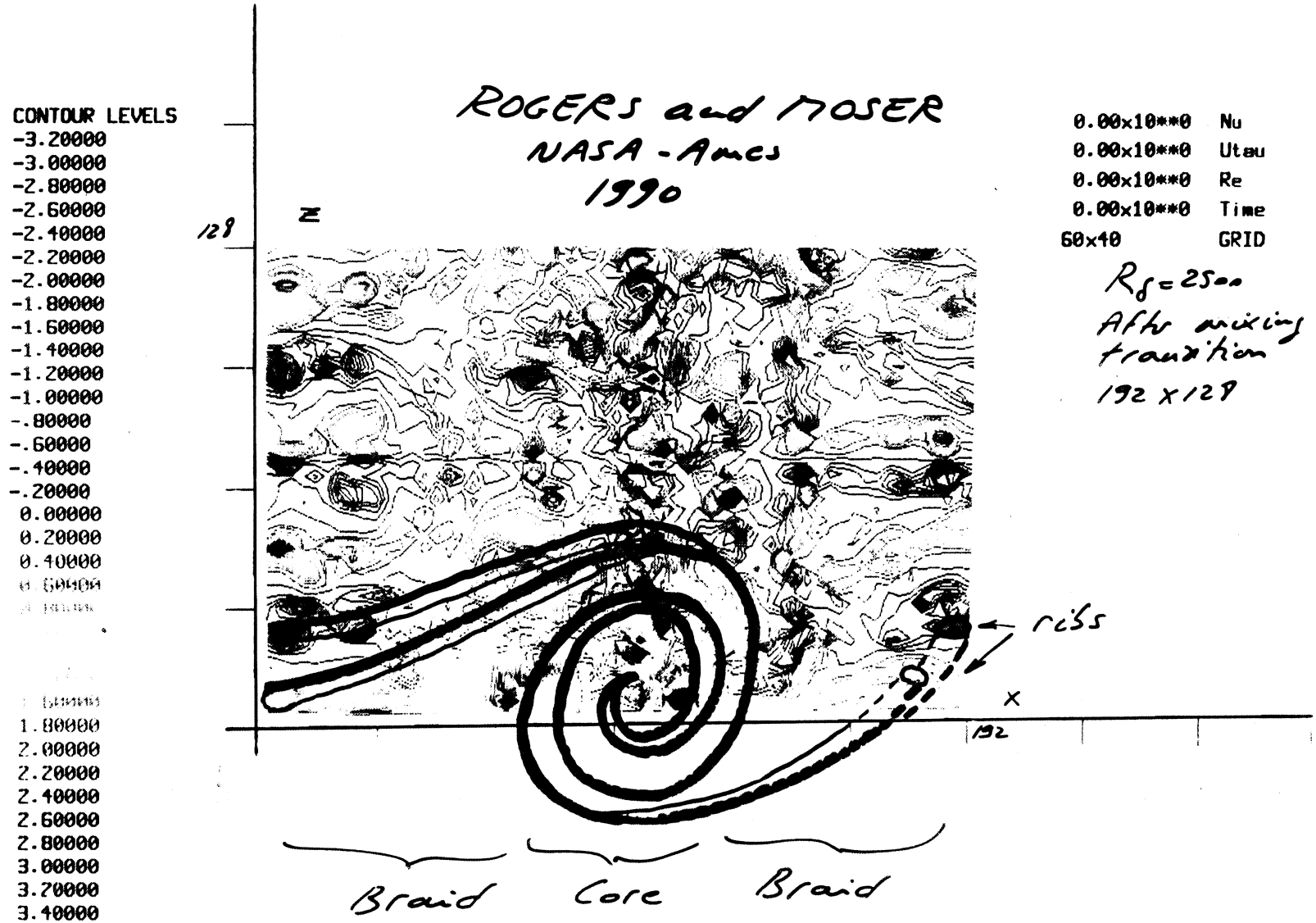
ROGERS and MOSER
NASA - Ames
1990
CONTOUR LEVELS
-3.20000
-3.00000
-2.80000
-2.60000
-2.40000
-2.20000
-2.00000
-1.80000
-1.60000
-1.40000
-1.20000
-1.00000
-.80000
-.60000
-.40000
-.20000
0.00000
0.20000
0.40000
1.80000
2.00000
2.20000
2.40000
2.60000
2.80000
3.00000
3.20000
3.40000
0.00x10**0 Nu
0.00x10**0 Utau
0.00x10**0 Re
0.00x10**0 Time
60x40 GRID
128
Z
X
192
$R_\delta = 250$
After mixing transition
192 x 128
rolls
Braid
Core
Braid

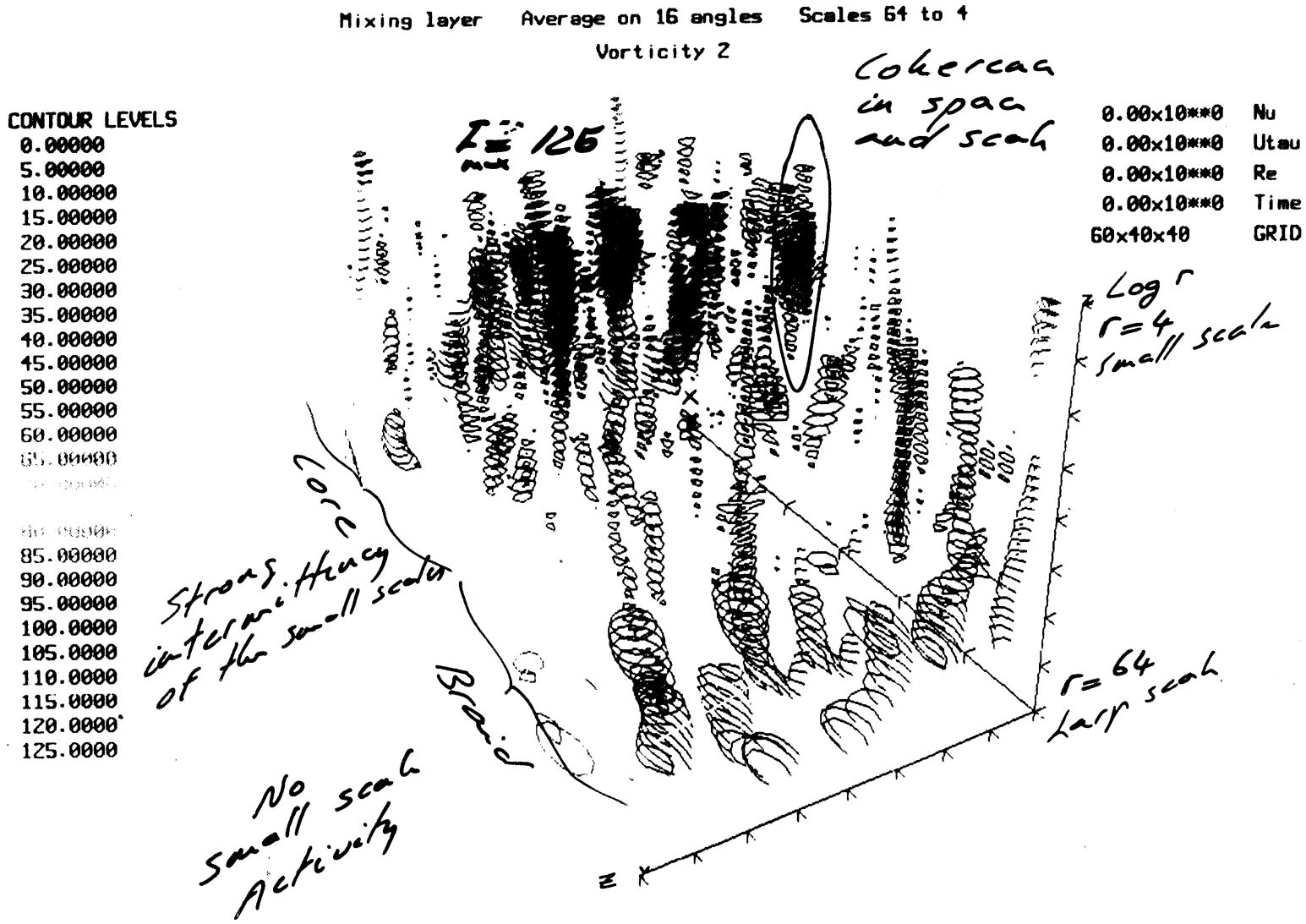
Mixing layer Average on 16 angles Scales 64 to 4
Vorticity 2
CONTOUR LEVELS
0.00000
5.00000
10.00000
15.00000
20.00000
25.00000
30.00000
35.00000
40.00000
45.00000
50.00000
55.00000
60.00000
85.00000
90.00000
95.00000
100.0000
105.0000
110.0000
115.0000
120.0000
125.0000
0.00x10**0 Nu
0.00x10**0 Utau
0.00x10**0 Re
0.00x10**0 Time
60x40x40 GRID
Coherence in space and scale
Log r
r=4 small scale
r=64 Large scale
Core
Strong intermittency of the small scales
Braid
No small scale activity
Z

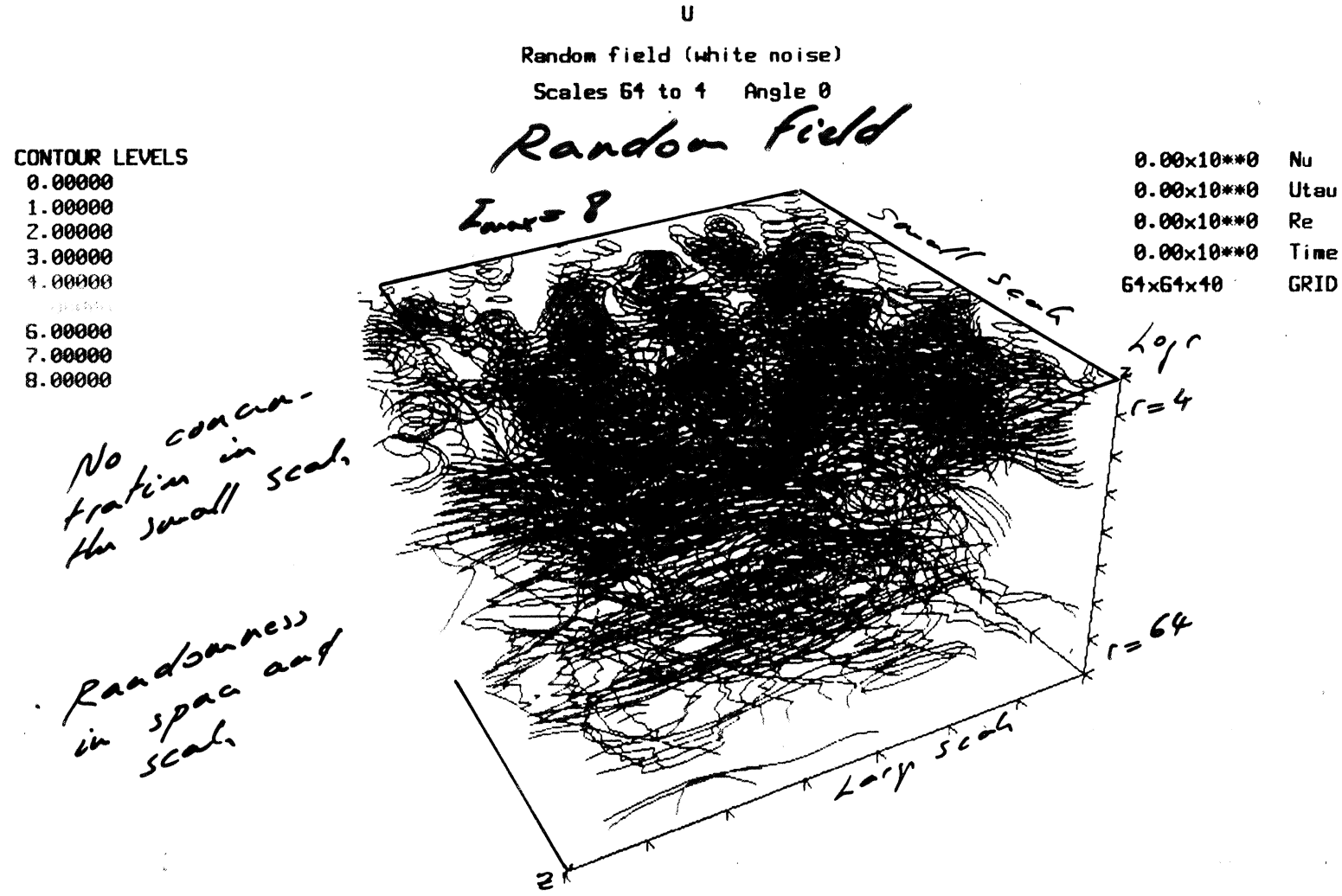
U
Random field (white noise)
Scales 64 to 4 Angle 0
Random field
CONTOUR LEVELS
0.00000
1.00000
2.00000
3.00000
4.00000
6.00000
7.00000
8.00000
0.00x10**0 Nu
0.00x10**0 Utau
0.00x10**0 Re
0.00x10**0 Time
64x64x40 GRID
Imax=8
Small scale
Log r
r=4
r=64
Large scale
Z
No concentration in the small scale
Randomness in space and scale
Coherent Structures are not just turbulent fluctuations

Mixing layer Average on 16 angles Scales 64 to 4

Vorticity Z

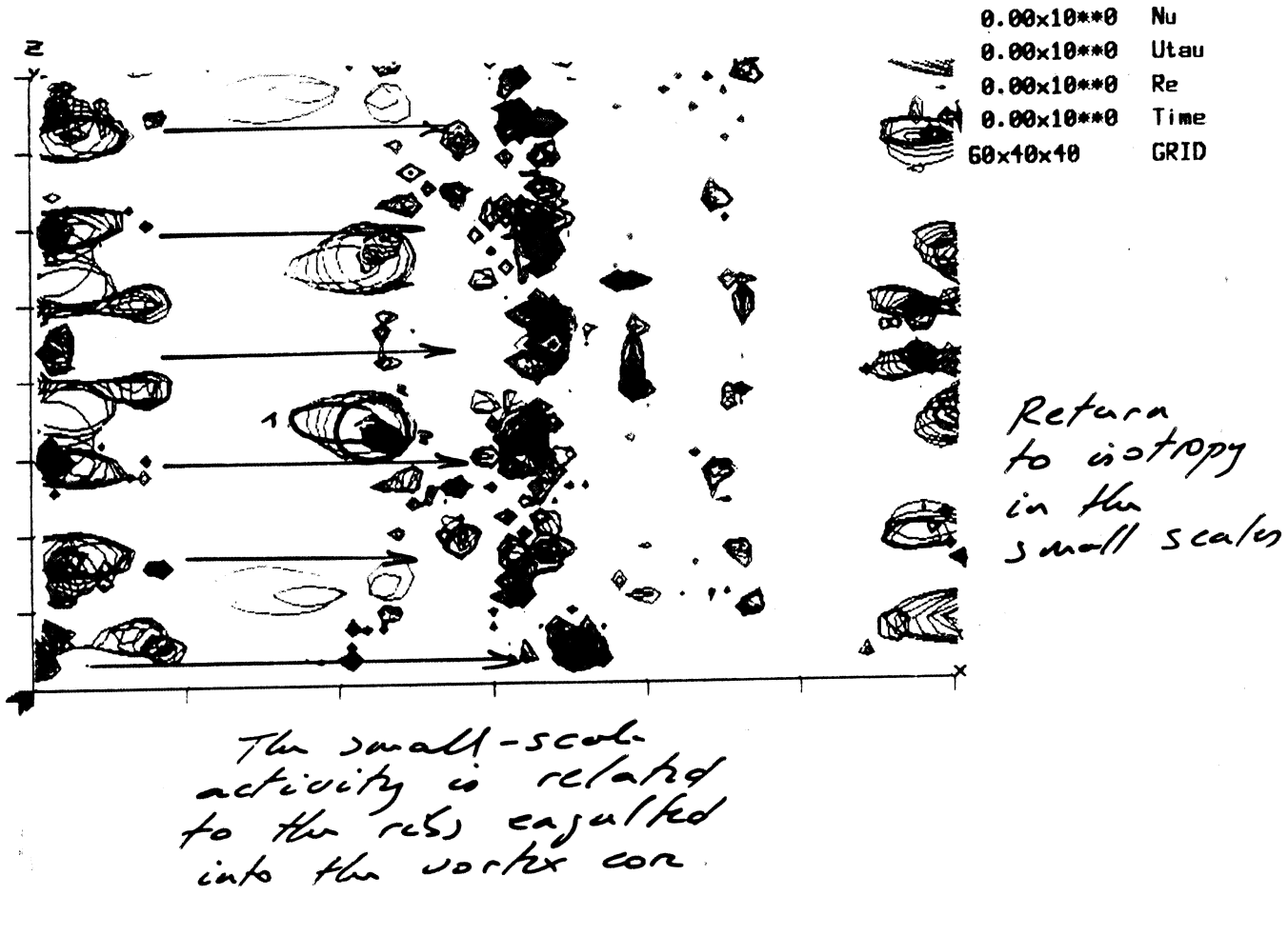

Return to isotropy in the small scales

The small-scale activity is related to the rolls ejected into the vortex core

LOCAL SPECTRA

What is the local scaling behavior of coherent structures? Is it very different from one structure to another? How does it relate to the Fourier spectrum?

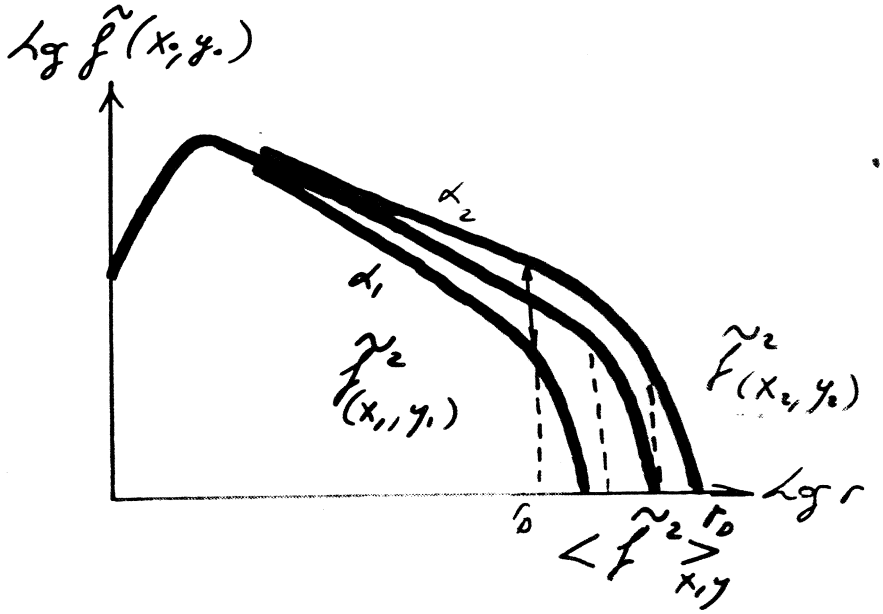

We can compare the local spectrum of the most excited region of the flow with the one of the less excited.

omega y of mixing layer

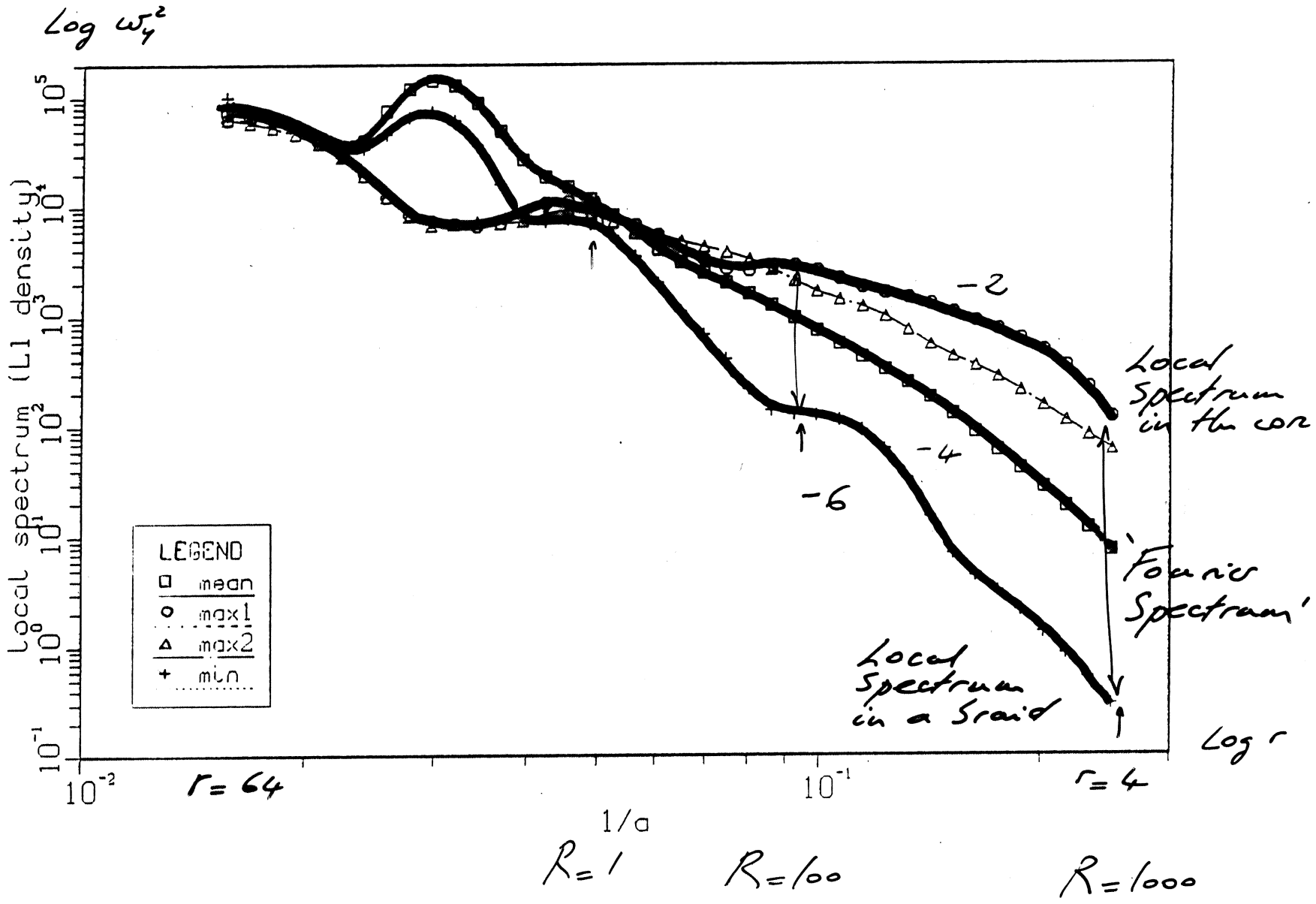

LOCAL (IN SPACE AND SCALE) REYNOLDS NUMBER

What is the topology of the dissipation manifold ($R_e=1$)?
What is its scale extension?

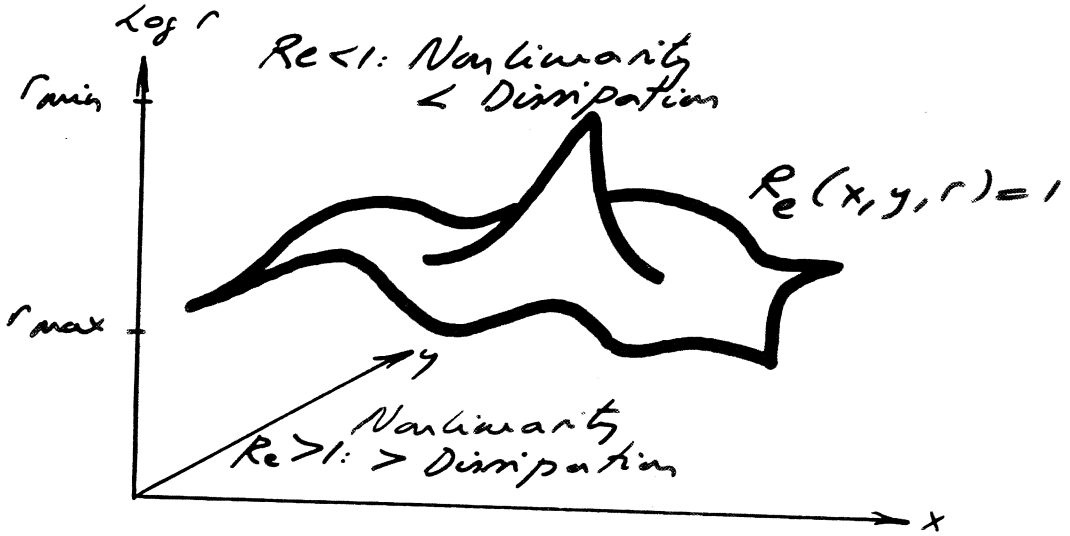

$$Re(x,y,r,\theta) = \frac{r}{\nu}\sqrt{\frac{\xi_i\left[\tilde{v}_i(x,y,r,\theta)\right]^2}{3\,C_\psi}}$$

We can therefore measure the local Kolmogorov scale and its spatial variability.

Iso-Reynolds surface

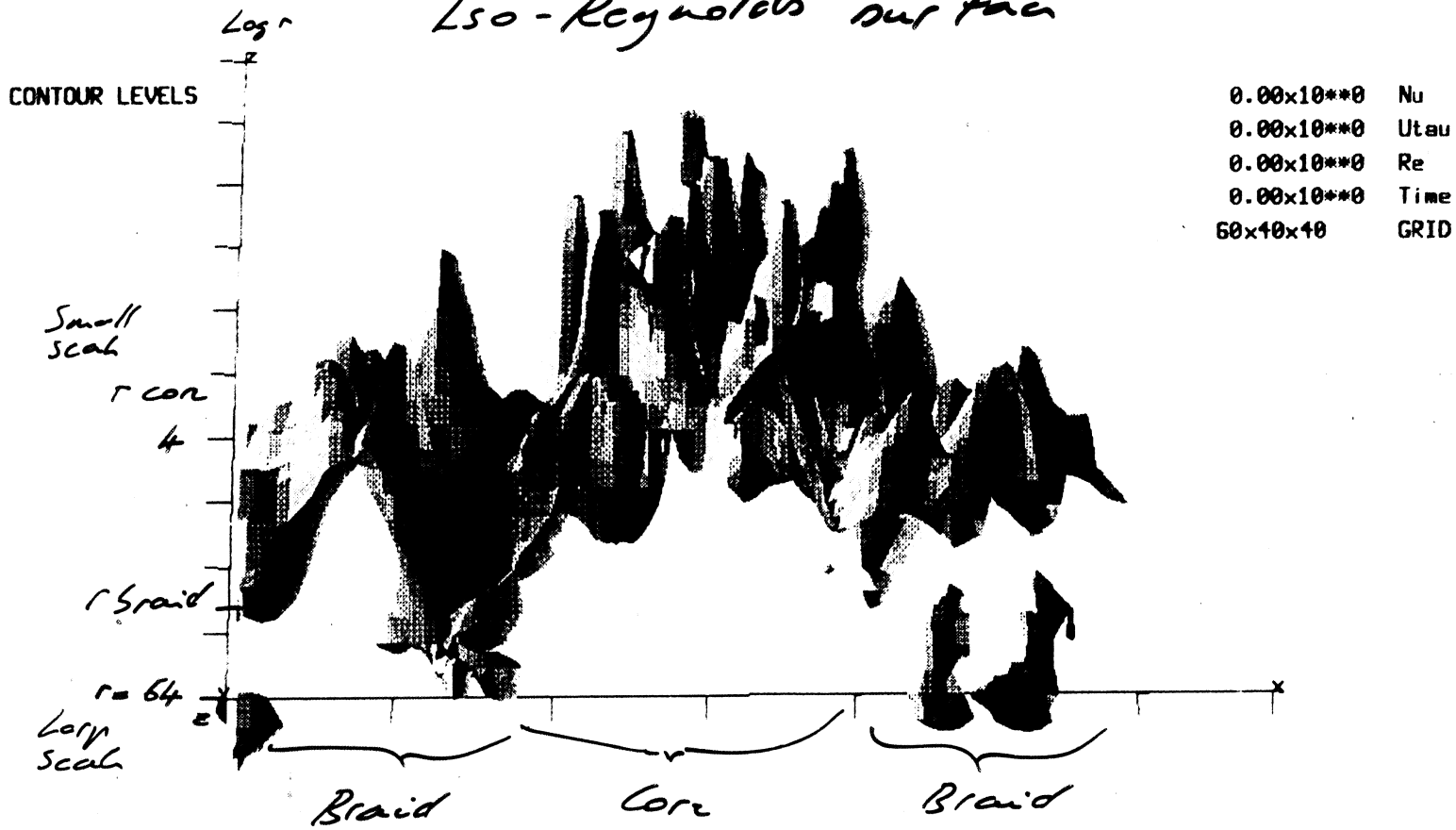

The nonlinearity is stronger in the vortex core

CONCLUSION

Strong intermittency in the small scales:

Some very localized small-scale structures contain 100 times more energy than the Fourier spectrum.

Coherence in both space and scale:

the same coherent structure contributes significantly to the energy for a wide range of scales.

Spatial variability of the Kolmogorov scale:

e.g. for the mixing layer it is much smaller in the vortex core than in the braids.

TURBULENCE CONTROL

'Probably the most important aspect of the existence of deterministic structure in turbulent flow is the possibility of turbulence control by direct interference with these large structure. Such control could lead to very significant technological advances!'

Hans Liepmann, 1979
'Rise and fall of ideas in turbulence'
American Scientist, 67

Wished effects:

Control of pressure fluctuations (sound),
Control of heat transfer,
Control of drag.

Possible methods:

Steady state or {dynamical} actions on the geometry (wall roughness, riblets or airfoils longitudinal or transversal, curvature), {need sensors & correct phasing} → Drag −20%

the fluid properties by additives (polymers, surfactants, microbubbles, fibers), → wall shear −80%

the boundary conditions (pressure gradient, injection / suction, wall vibration, porosity), marginal effect

the compressibility (shocklets due to wall roughness) Turbulence intensity ×2, Drag ↗.

3. ECOULEMENTS TURBULENTS BIDIMENSIONNELS INCOMPRESSIBLES

Turbulence dans les écoulements géophysiques (météorologie et océanographie)

Ecoulements stratifiés et/ou en rotation : observés par satellite, dans des expériences de laboratoire et dans des expériences numériques effectuées par simulation directe

Théorie statistique de la turbulence bidimensionnelle homogène et isotrope

Intermittence et structures cohérentes bidimensionnelles

VORTICES ON 33 DECADES

Quantized vortices in liquid Helium — 10^{-10} m

Smallest turbulent eddies — 10^{-3} m

Vortices emitted behind insects, squids, fishes — 10^{-3} – 10^{-1} m

Whirlpools in tidal currents; Dust devils — 1–10 m

Waterspouts and whirlwinds; Convection clouds — 100–1000 m

Gulf-stream vortices; Hurricanes; Cyclon and anty cyclones — 100–2000 km

General circulation (oceans & atmosphere); Convection cells inside Earth — 2000–5000 km

Jupiter Red Spot; Vortices in Saturn; Sun spots — 5000–10^5 km

Rotation inside stars — 10^{10} m

Galaxies — 4–4000 k parsec

40 kps = 10^{21} m

10^{23} m

Vortices in the Mediterranean sea observed from the Shuttle Challenger



Vortices observed in 2D numerical simulation of Navier-Stokes



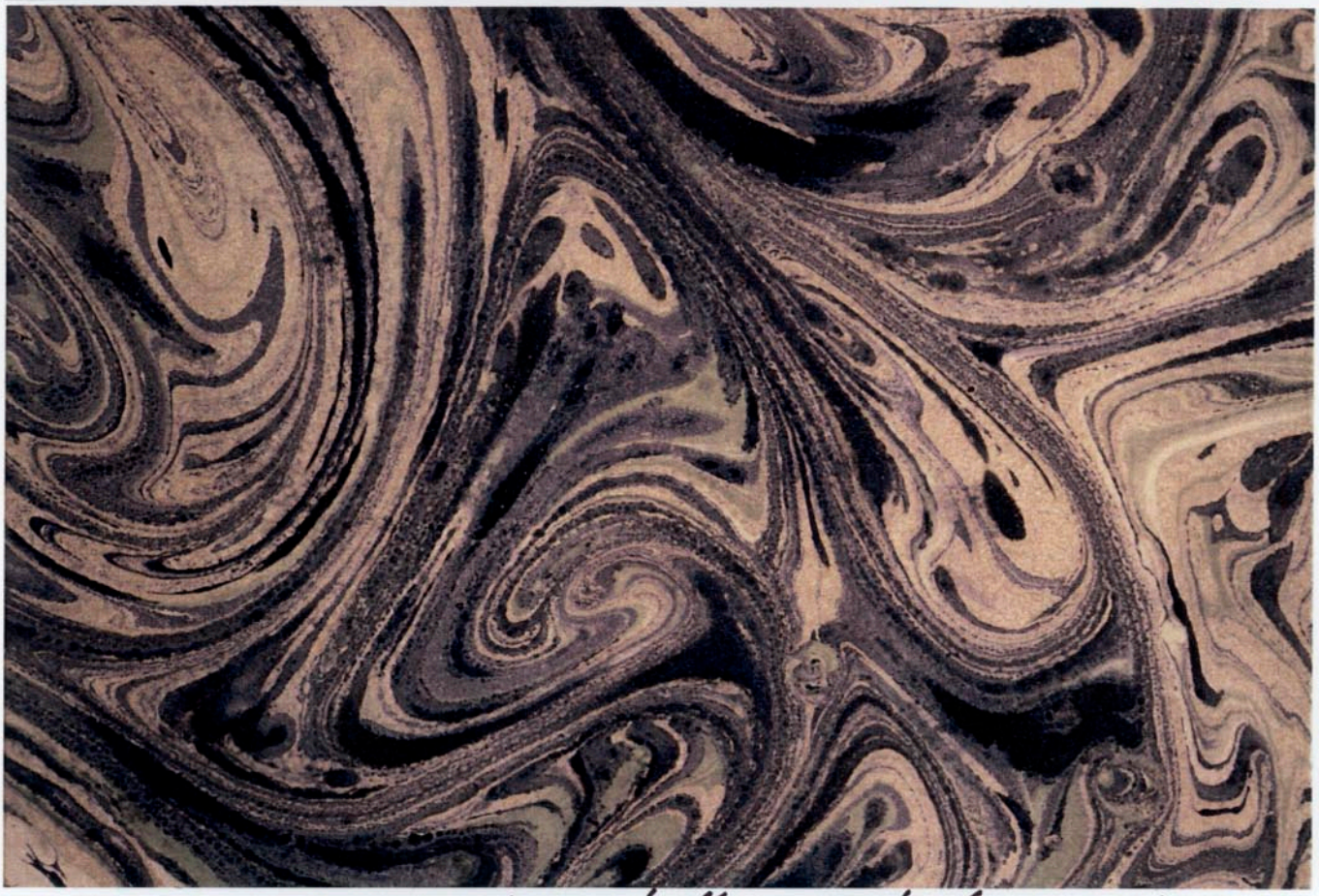

Vortices observed in a shallow water layer using ink tracers, similarly to the technique developed for marbled papers

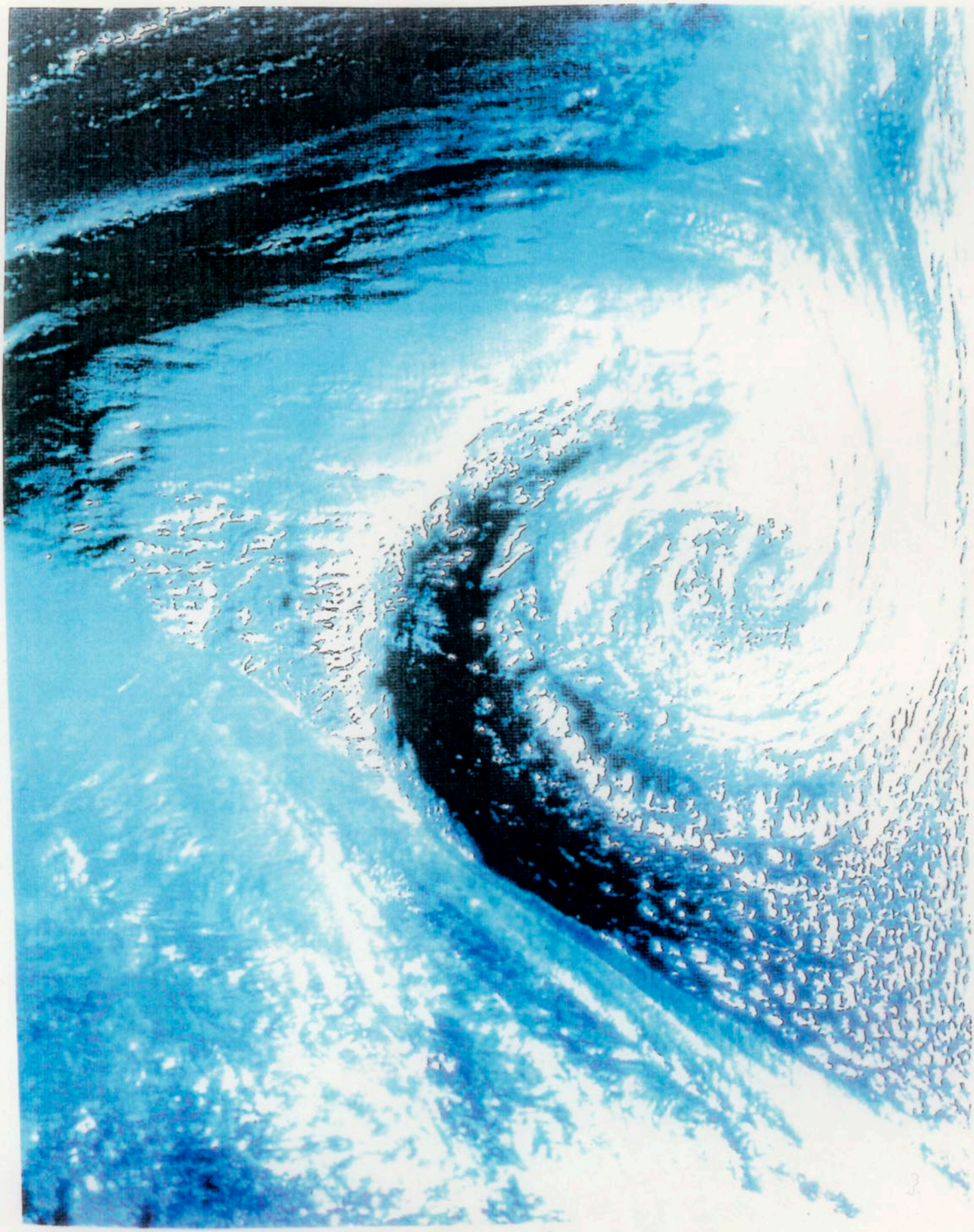

~ 1000 km

Cyclone in the Southern hemisphere

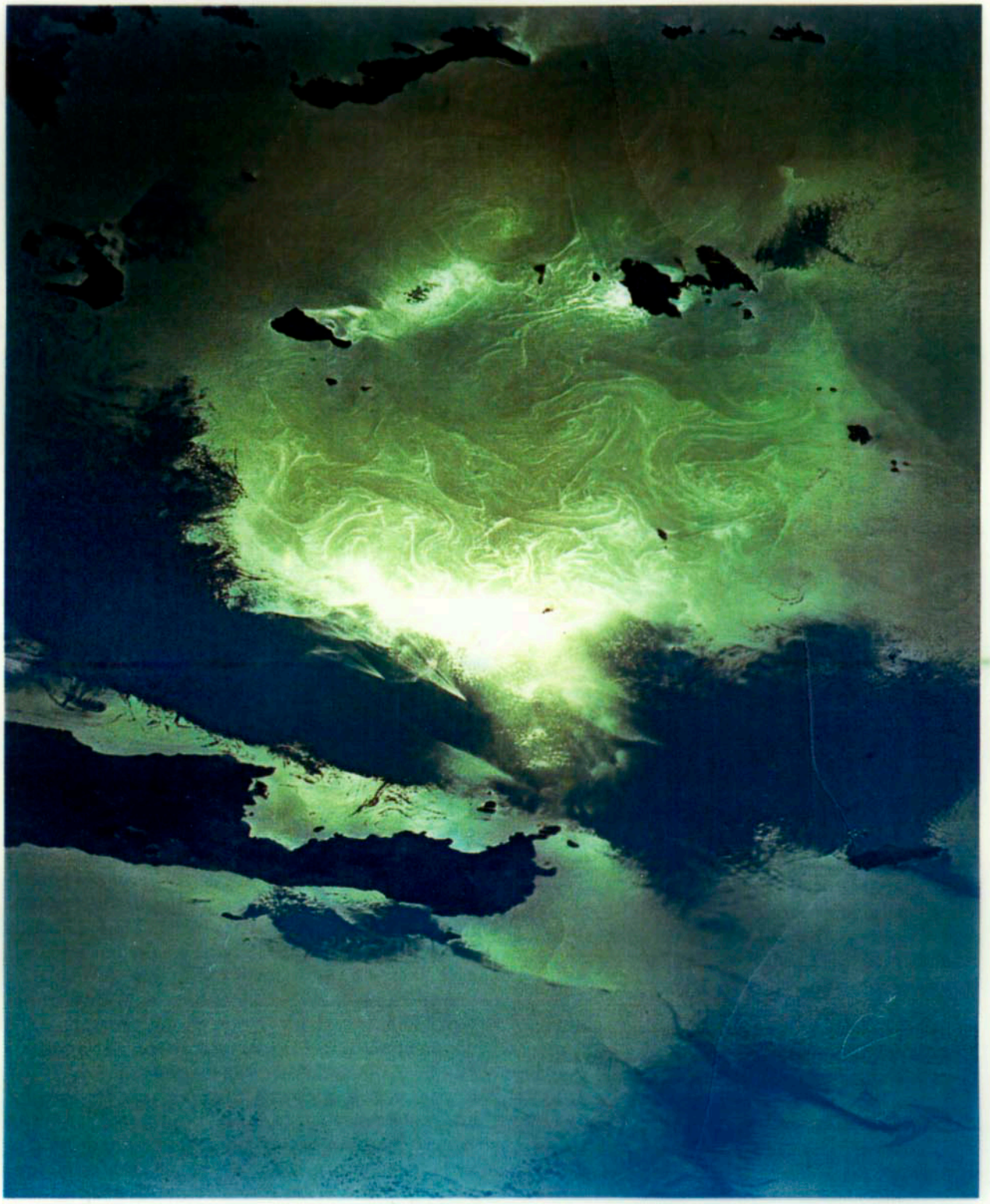

La circulation océanique et son couplage avec l'atmosphère restent actuellement une des principales difficultés de la modélisation du climat, en particulier la représentation des tourbillons océaniques qui se développent à l'échelle de quelques dizaines de kilomètres.

Vortices observed in the Mediterranean sea observed from Challenger shuttle

Jupiter's atmosphere observed by the satellite Voyager



Saturn's atmosphere observed by the satellite Voyager

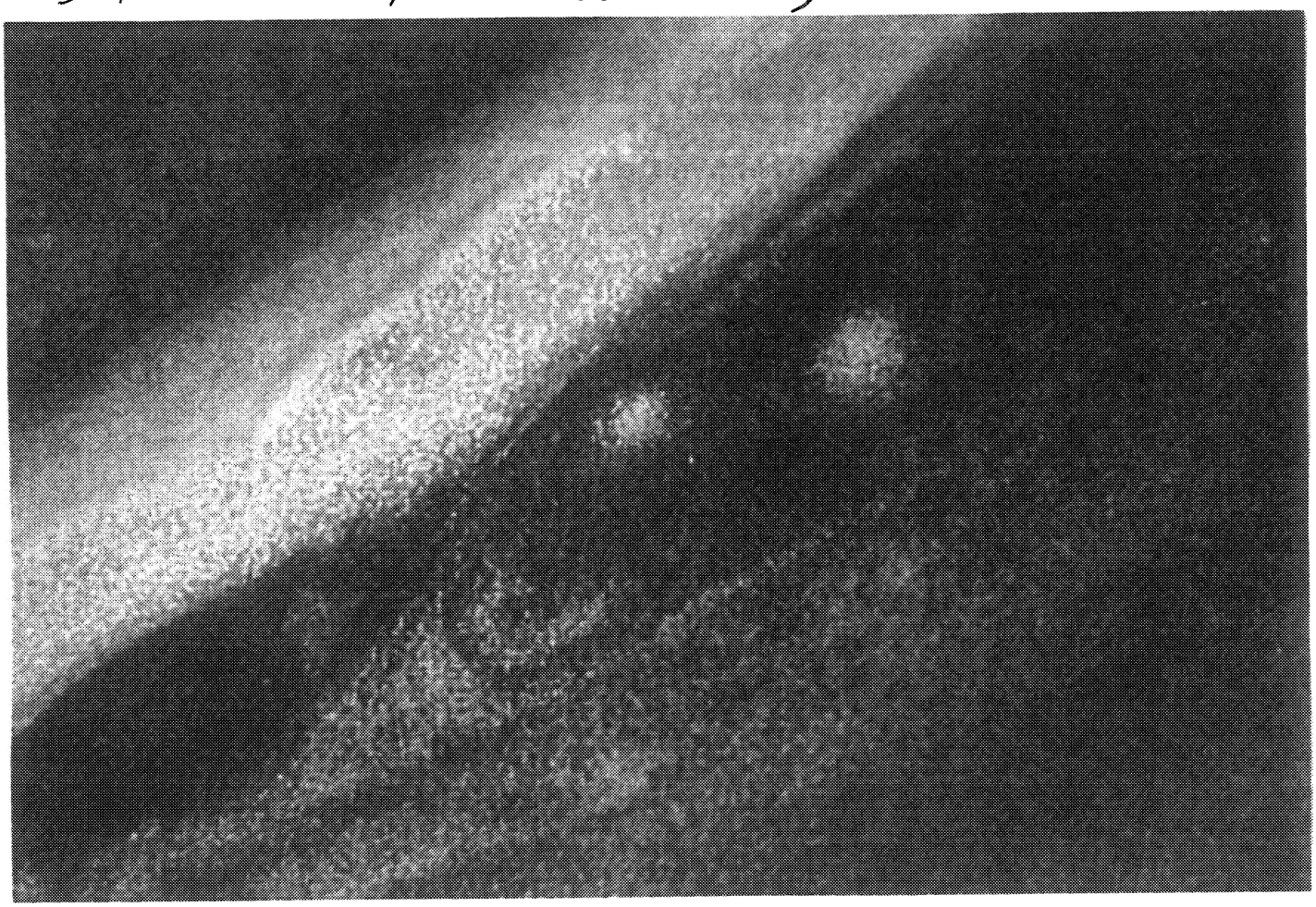

SIMILARITY IN ROTATING SYSTEMS

$$\text{Rossby} = \frac{\text{inertial force}}{\text{Coriolis force}} = \frac{U}{\Omega L}$$

$$\text{Ekman} = \frac{\text{frictional force}}{\text{Coriolis force}} = \frac{\nu}{\Omega L^2}$$

$$\text{Reynolds} = \frac{\text{Rossby}}{\text{Ekman}} = \frac{UL}{\nu}$$

			Rossby
Bathtub vortices	1 cm	0.1 m/s	10^5
Dust devils	3 m	10 m/s	3.10^4
Tornadoes	50 m	150 m/s	3.10^4
Hurricanes	500 km	50 m/s	1
Cyclone - anticyclones	1000 km	10 m/s	10^{-1}
Ocean circulation	3000 km	1.5 m/s	5.10^{-3}

HIÉRARCHIE DE MODÈLES

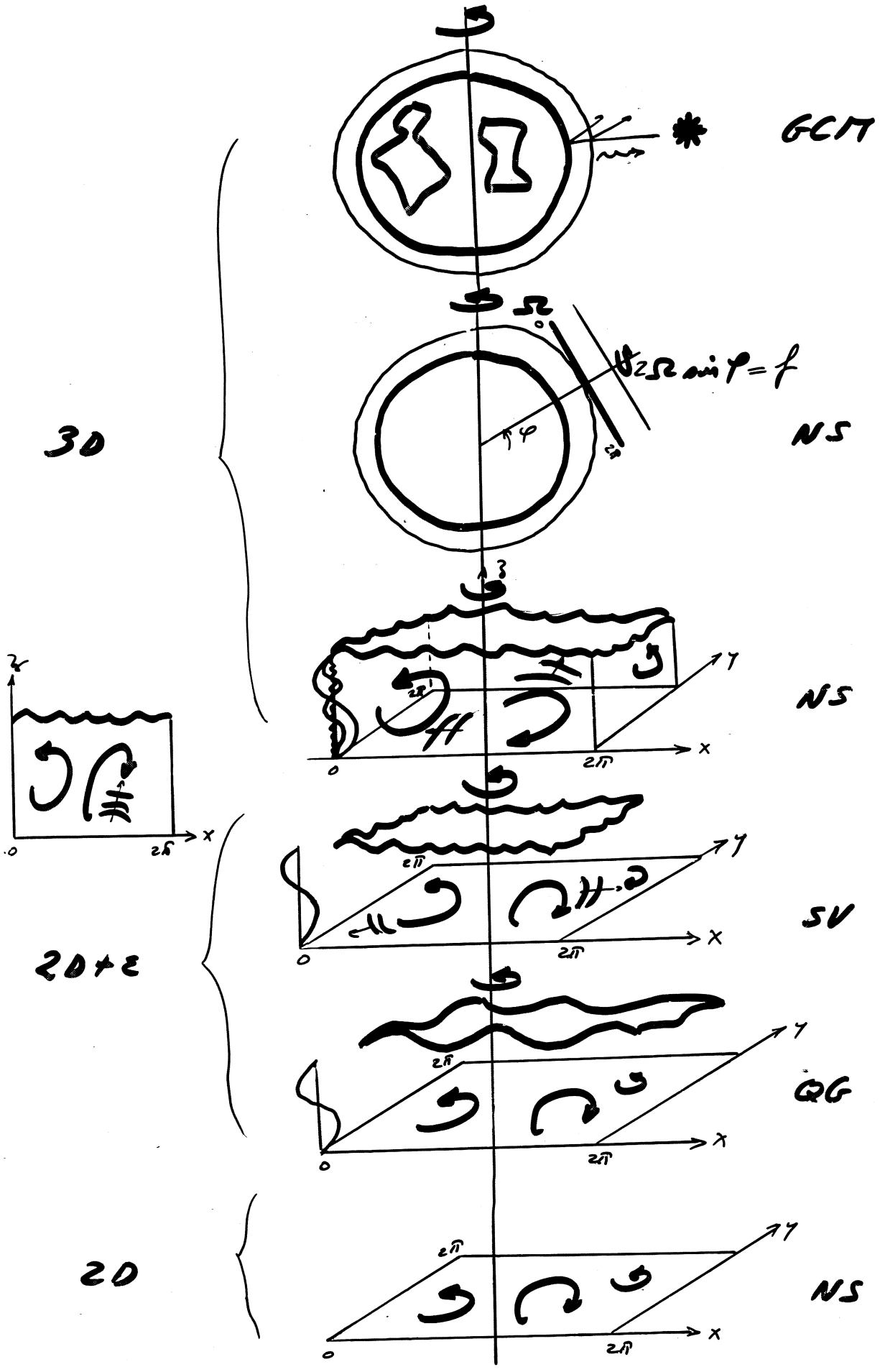

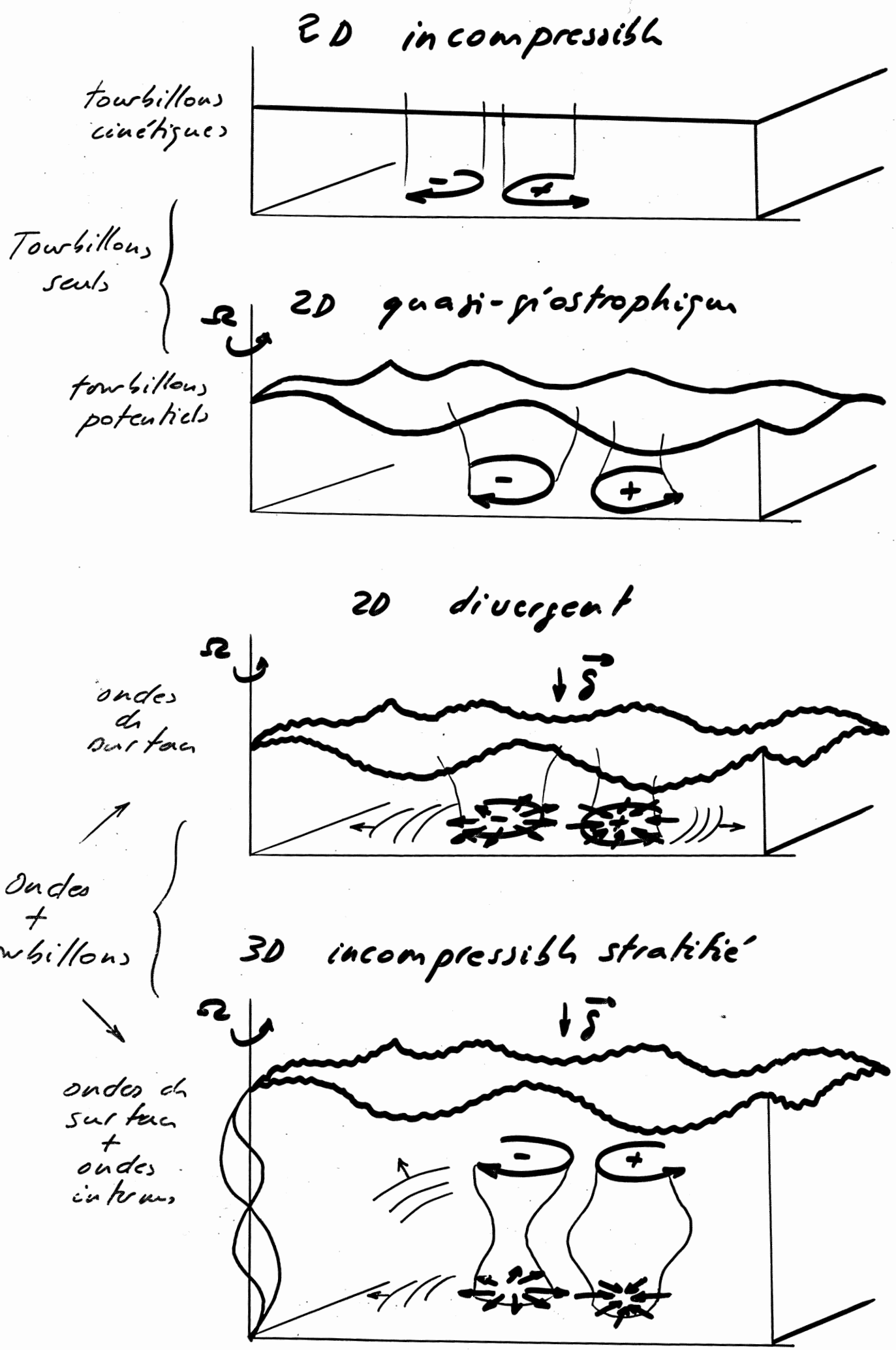
2D incompressible
tourbillons cinétiques
Tourbillons seuls
2D quasi-géostrophique
tourbillons potentiels
2D divergent
ondes de surface
Ondes + tourbillons
3D incompressible stratifié
ondes de surface + ondes internes

HYPOTHESES ET MODELES

Approximations

Euler	2D incompressible :	$\delta = 0$
Saint-Venant Réduit	2D faiblement divergent :	$\delta \ll \xi \ll f$, $\phi' \ll \bar{\phi}$
Saint-Venant	2D fortement divergent :	$\xi \ll f$

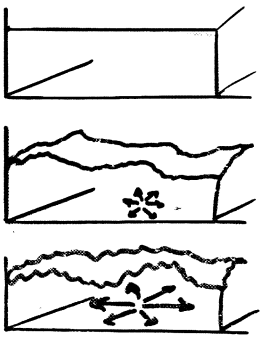

Equations conservatives

$$\frac{\partial \xi}{\partial t} + f\delta + J(\psi,\xi) + \vec{\nabla}\cdot(\xi\vec{\nabla}\chi) = 0$$

$$\frac{\partial \delta}{\partial t} - f\xi + J(\xi,\chi) - \vec{\nabla}\cdot(\xi\vec{\nabla}\psi) + \nabla^2\phi + \nabla^2\frac{V^2}{2} = 0$$

$$\frac{\partial \phi}{\partial t} + \bar{\phi}\delta + J(\psi,\phi) + \vec{\nabla}\cdot(\phi\vec{\nabla}\chi) = 0$$

Invariant lagrangien

$$\frac{d\Sigma}{dt} = 0 \qquad \hat{\xi} \equiv k^2\hat{\psi}$$

$$\frac{d\eta'}{dt} = 0 \qquad \eta' = \xi - \frac{f\phi'}{\bar{\phi}} = \xi - k_0^2\phi' \qquad k_0 = \frac{f}{\sqrt{\bar{\phi}}}$$

$$\hat{\phi} \equiv (k^2 + k_0^2)\hat{\psi} \quad \text{si } \phi' = f\psi$$

$$\frac{d\eta}{dt} = 0 \qquad \eta = \frac{\xi + f}{\phi}$$

Invariants eulériens

$$E_c = \langle V^2 \rangle \qquad \mathcal{E} = \langle \xi^2 \rangle$$

$$E' = \langle \bar{\phi}V^2 + \phi^2 \rangle \qquad S' = \langle (\bar{\phi}\xi - f\phi')^2 \rangle$$

$$E = \langle \phi V^2 + \phi^2 \rangle \qquad S = \frac{(\xi + f)^2}{\phi}$$

en pratique $\phi' \simeq 5\%\,\bar{\phi}$

ROTATING SHALLOW WATER EQUATIONS

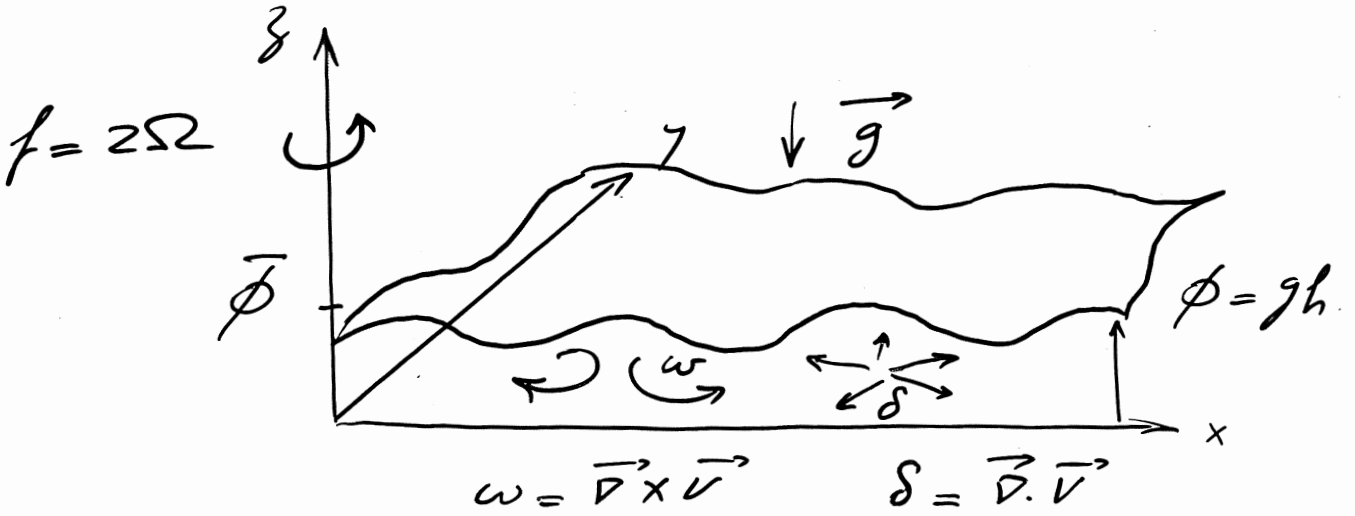

Initial value problem and periodic boundary conditions

$$\begin{cases} \dfrac{\partial \omega}{\partial t} + \vec{\nabla} \cdot \left[(\omega + f) \vec{v} \right] = D_\omega \\ \dfrac{\partial \delta}{\partial t} - \vec{\nabla} \times \left[(\omega + f) \vec{v} \right] + \nabla^2 \left(\phi + \dfrac{v^2}{2} \right) = D_\delta \\ \dfrac{\partial \phi}{\partial t} + \phi \delta + \vec{v} \cdot \vec{\nabla} \phi = D_\phi \end{cases}$$

Also called St Venant's equations

Invariants for $D_\omega = D_\delta = D_\phi = 0$:

Energy $E = \frac{1}{2} \iint (\phi^2 + \phi \bar{v}^2) \, dx \, dy$

Potential Enstrophy $\mathcal{Z} = \frac{1}{2} \iint \left(\frac{\omega^2}{\phi} \right) dx \, dy$

Reference: Farge and Sadourny, 1989 Wave-vortex Interactions in Rotating Shallow Water, J. Fluid Mech., 206, 433

RESOLUTION AND ANALYSIS

Pseudo-spectral
space integration
Leapfrog time integration

Physical parameters:

$L = 6400$ km

$f = 10^{-4}\,s^{-1}$ and $6.10^{-4}\,s^{-1}$

$\Rightarrow R_o = 0.03$ and 0.1

$v' \sim 10\ ms^{-1}$ à $30\ m\,s^{-1}$

$c = \sqrt{gh} = 300\ ms^{-1}$

$$\Rightarrow \begin{cases} Mach = \dfrac{v'}{c} = 0.03 \text{ à } 0.1 \\ k_{def} = \dfrac{f}{c} = 2 \text{ and } 12 \end{cases}$$

$k_{ex} = 3$

For the analysis we project onto the eigenvectors of the linearized equations:

Geostrophic modes { rotational, non-divergent

Inertio-gravitational modes { wave-like, dispersive, $f^2 = \phi(k^2 + k_{def}^2)$

Prévision à un jour pour mercredi 10 avril à 14 h :

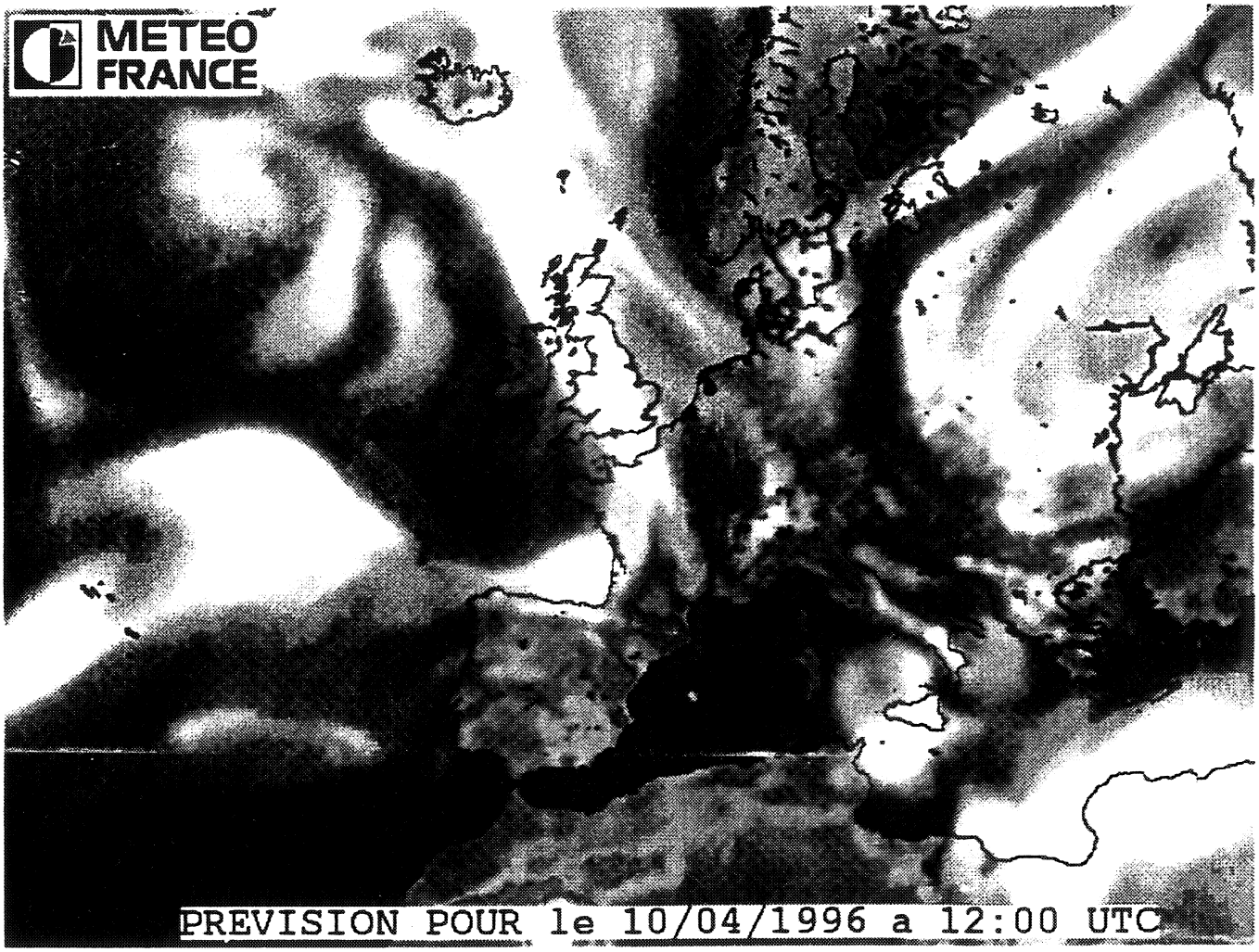

SENSITIVITY TO INITIAL CONDITIONS

t = 0

t = 2 jours

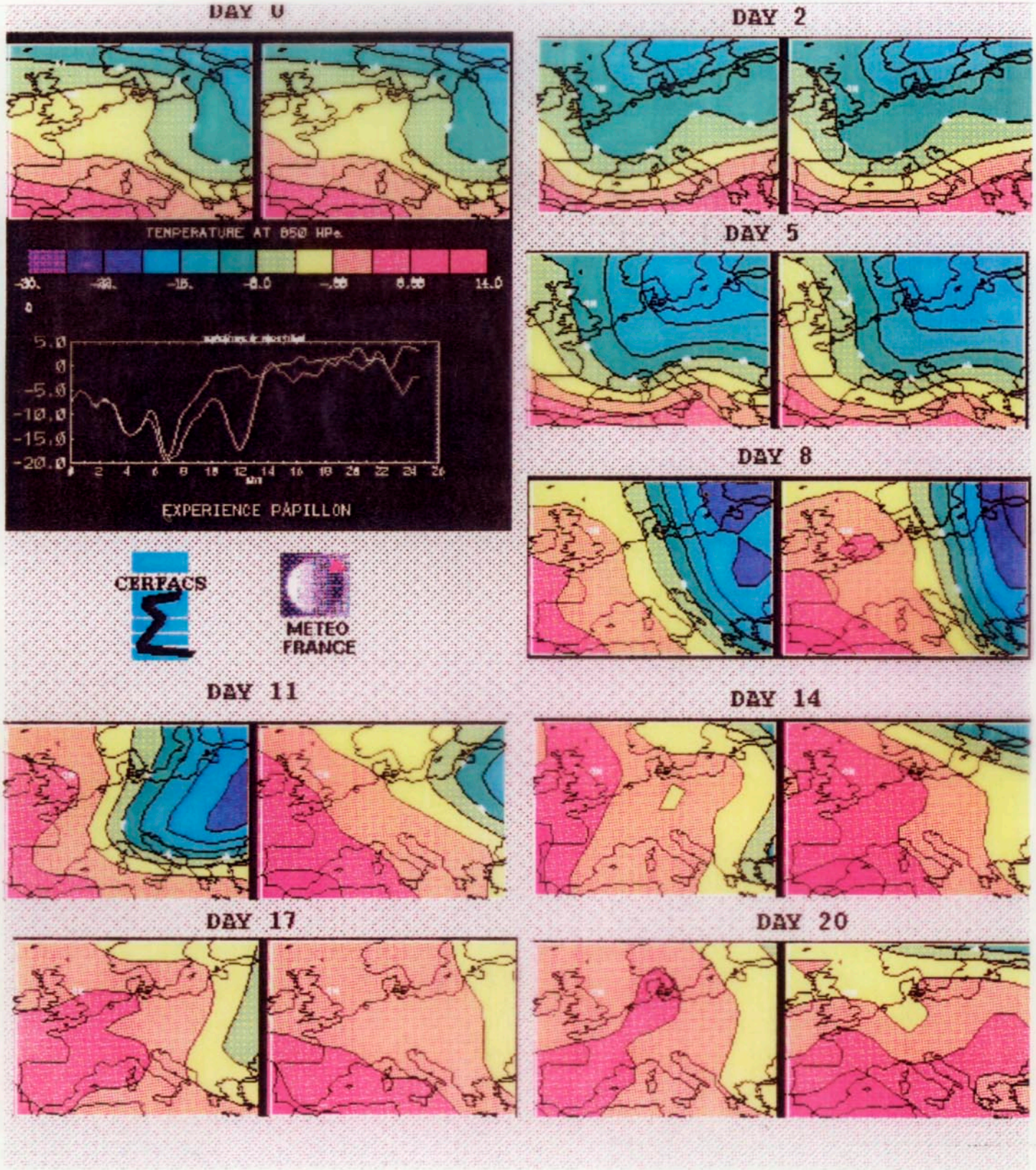

t = 17 jours

t = 20 jours

Resolution T42 (128 × 64)

Initial error : + 0.01°C in Bordeaux

⇒

Separation of the 2 solutions after 6 days

Vorticity at $t = 0$

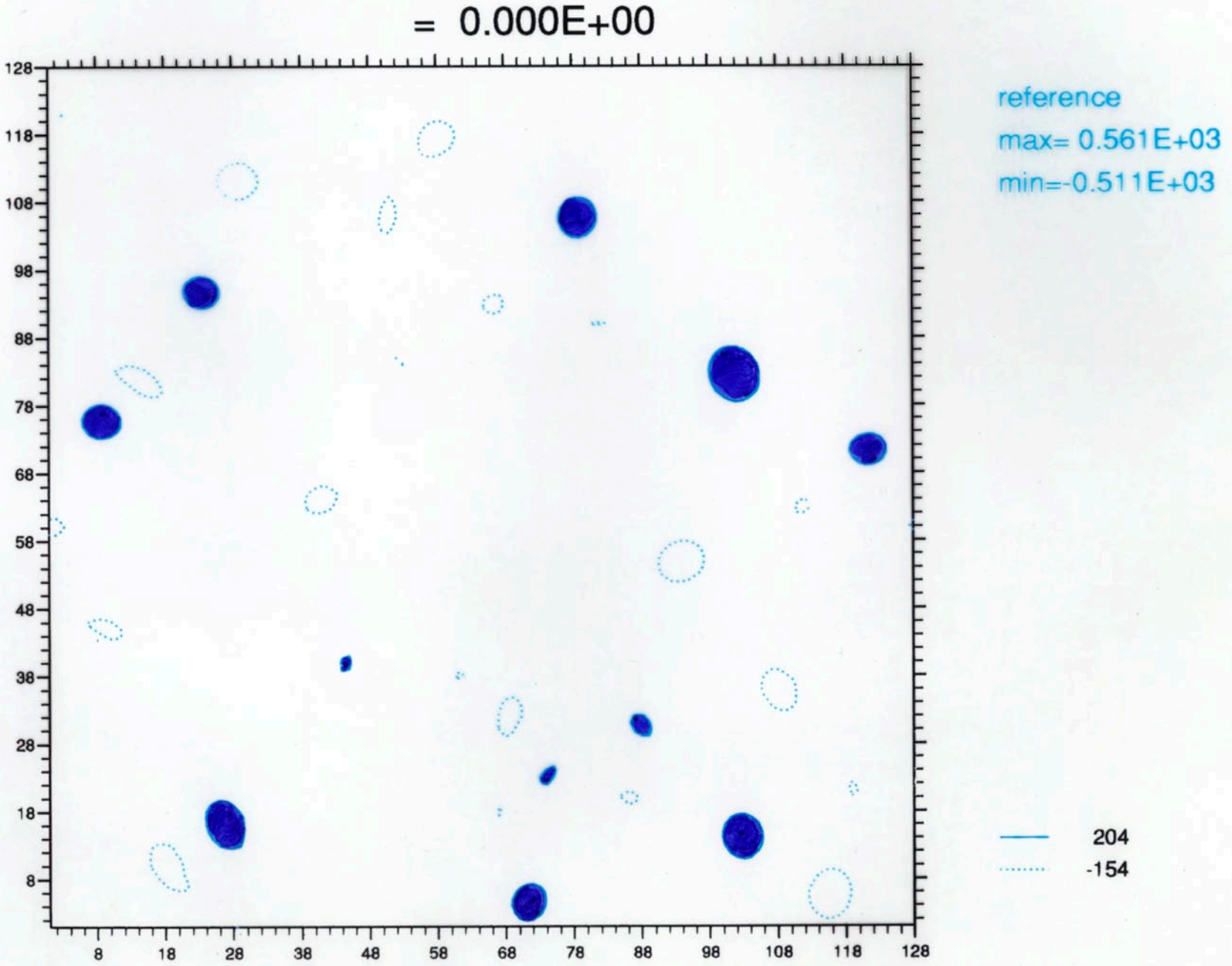

Vorticity after 1000 time steps

Unfiltered field

Initially filtered field

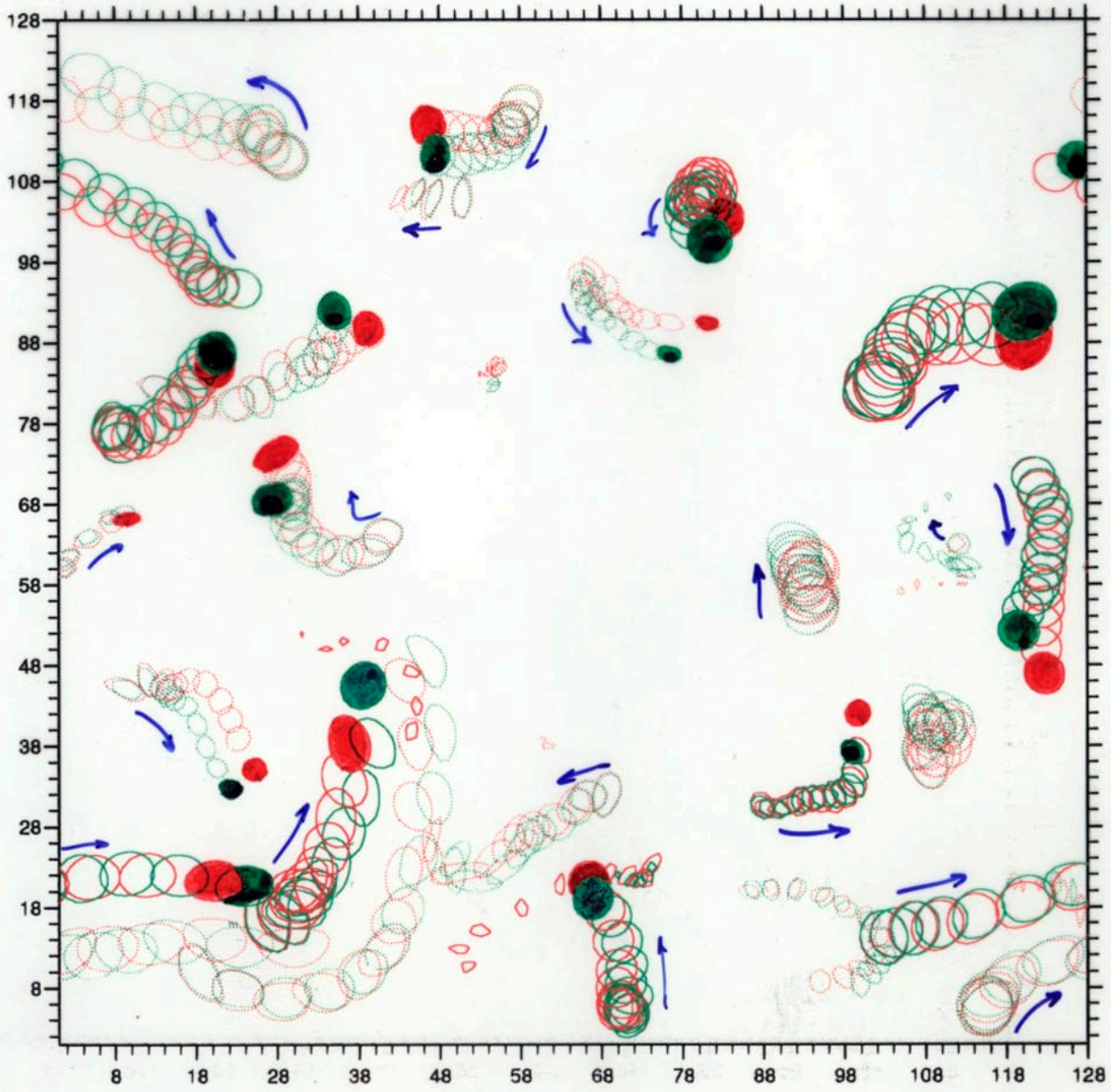

204 204

-154 -154

CLIMATIC PREDICTION
FOR CO_2 CONCENTRATION
DOUBLING

Average temperature WINTER increase for Dec-Jan-Feb.

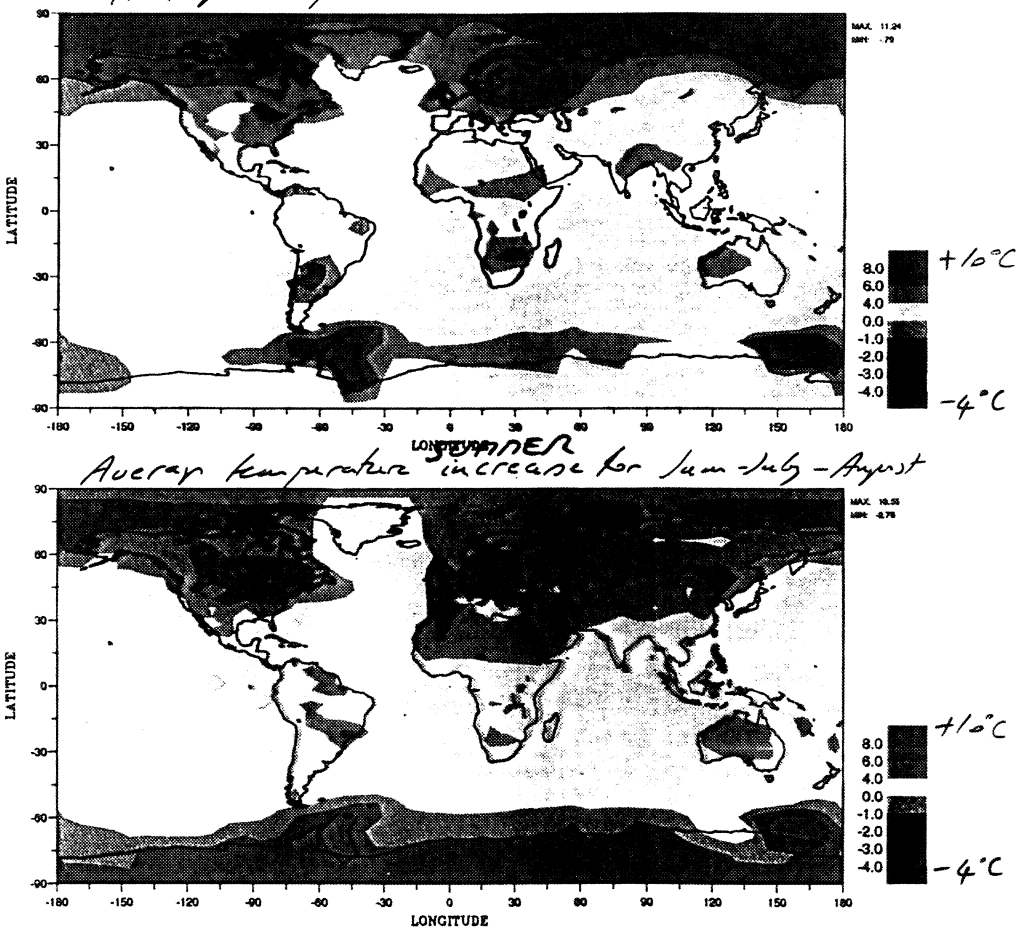

Average temperature SUMMER increase for June-July-August

Tous les modèles de simulation numérique du climat prévoient un réchauffement en cas de doublement de la concentration de gaz carbonique. Les régions les plus touchées seraient les hautes latitudes polaires pendant l'hiver, avec une augmentation de la température pouvant atteindre 10 °C, comme le montrent les cartes de variations de température obtenues pour décembre-janvier-février et juin-juillet-août à partir du modèle du Laboratoire de météorologie dynamique (CNRS).

G.C.M. of C.N.D.

CLIMATIC PREDICTION FOR CO_2 CONCENTRATION DOUBLING

WINTER
Averap rainfall variation for Dec-Jan-Feb.

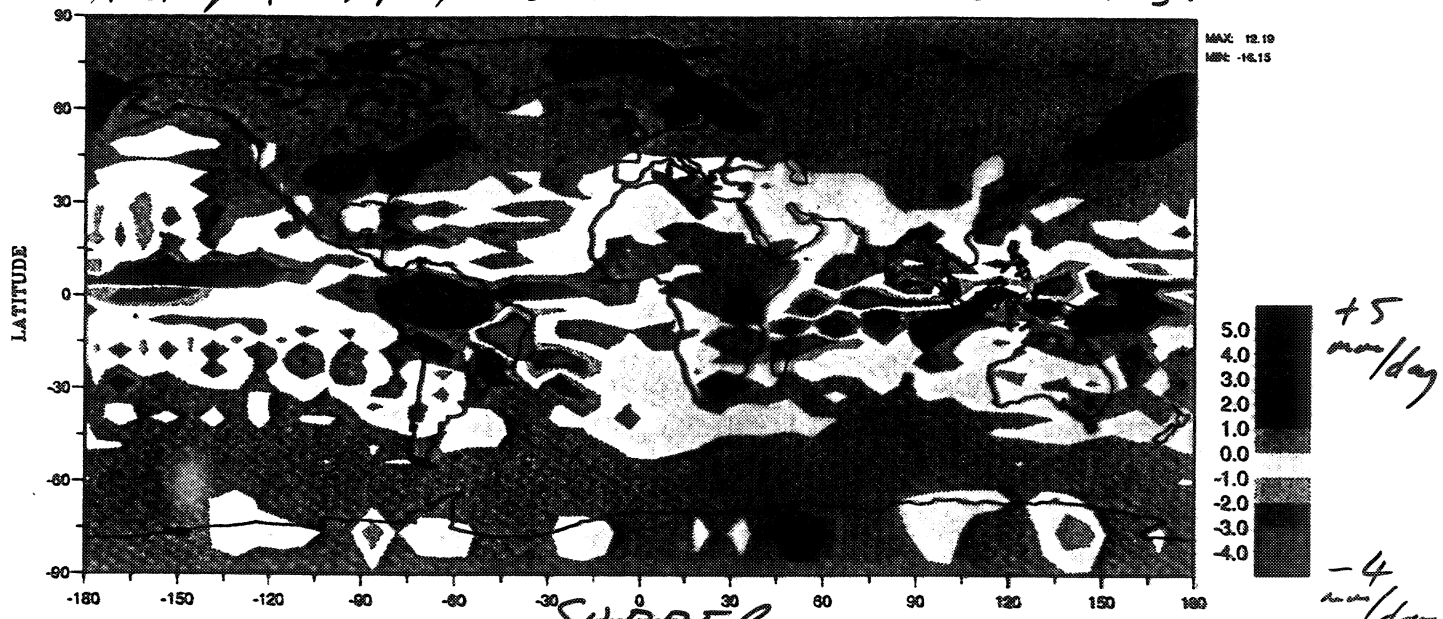

SUMMER
Averap rainfall variation for June-July-August

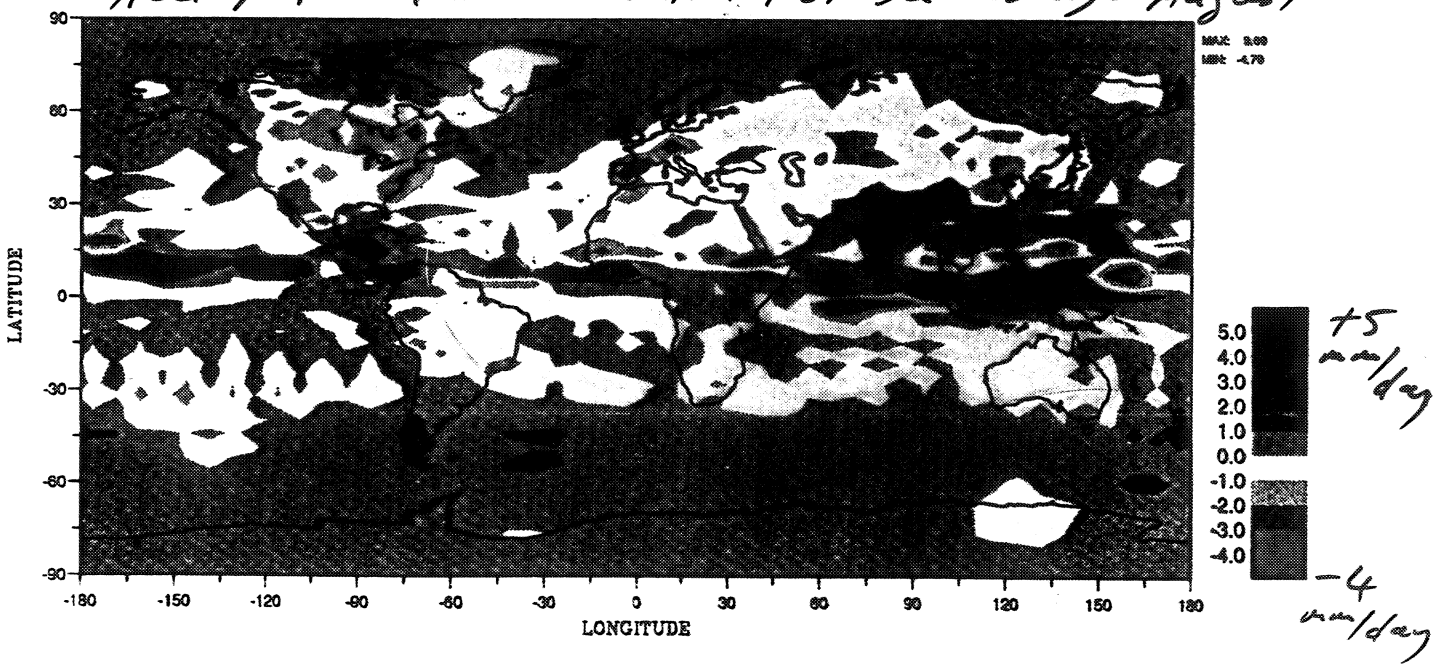

Le réchauffement du climat prévu en cas de doublement de la concentration de gaz carbonique s'accompagnerait inévitablement de modifications importantes des précipitations, comme le montrent les changements estimés (en millimètres par jour) pour décembre-janvier-février et juin-juillet-août à partir du modèle du Laboratoire de météorologie dynamique (CNRS).

G.C.M. of L.M.D.

CLIMATIC PREDICTION FOR CO_2 CONCENTRATION DOUBLING

Average temperature WINTER increase for Dec-Jan-Feb.

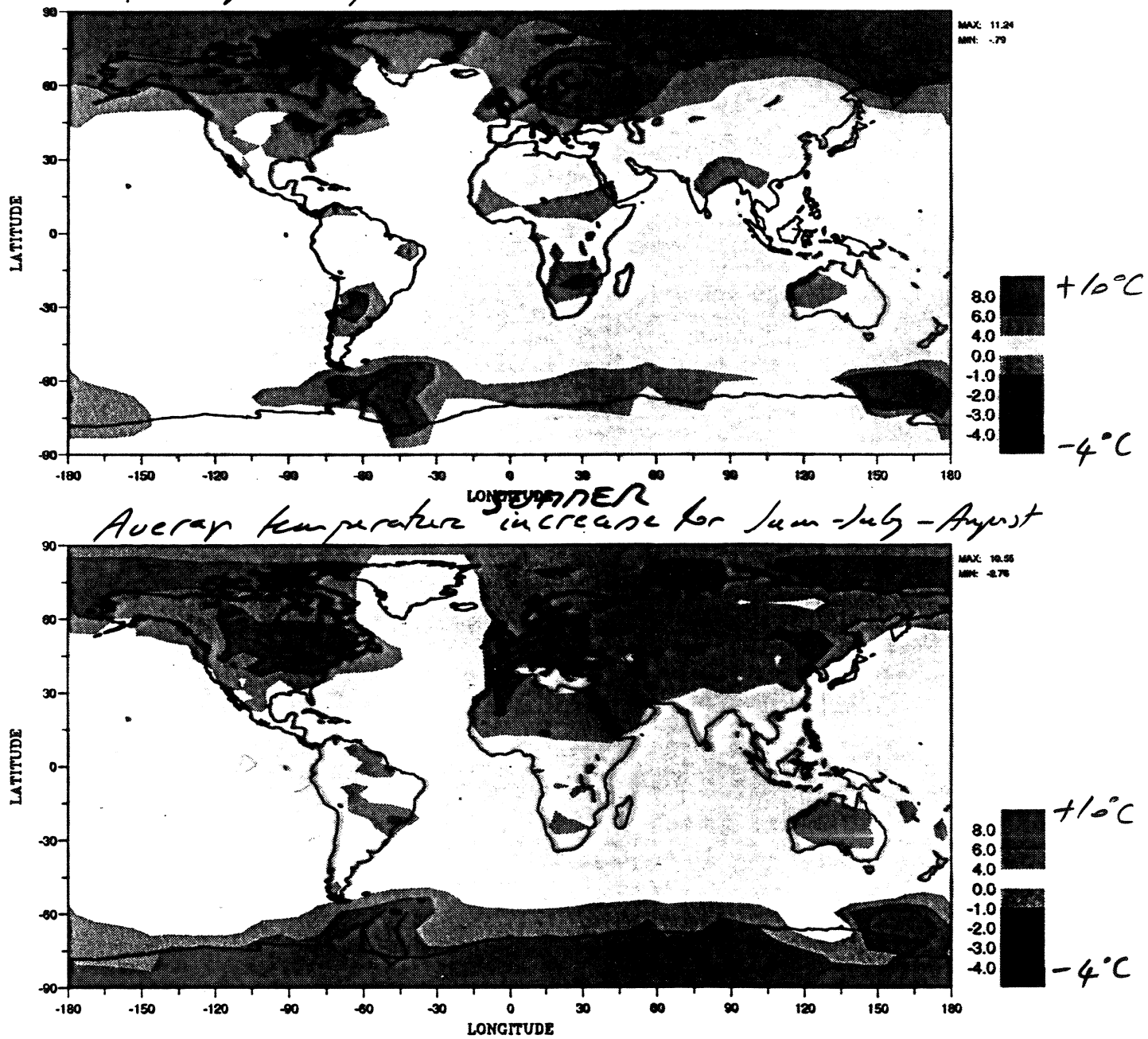

Tous les modèles de simulation numérique du climat prévoient un réchauffement en cas de doublement de la concentration de gaz carbonique. Les régions les plus touchées seraient les hautes latitudes polaires pendant l'hiver, avec une augmentation de la température pouvant atteindre 10 °C, comme le montrent les cartes de variations de température obtenues pour décembre-janvier-février et juin-juillet-août à partir du modèle du Laboratoire de météorologie dynamique (CNRS).

G.C.M. of L.M.D.

SEA-SURFACE TEMPERATURE

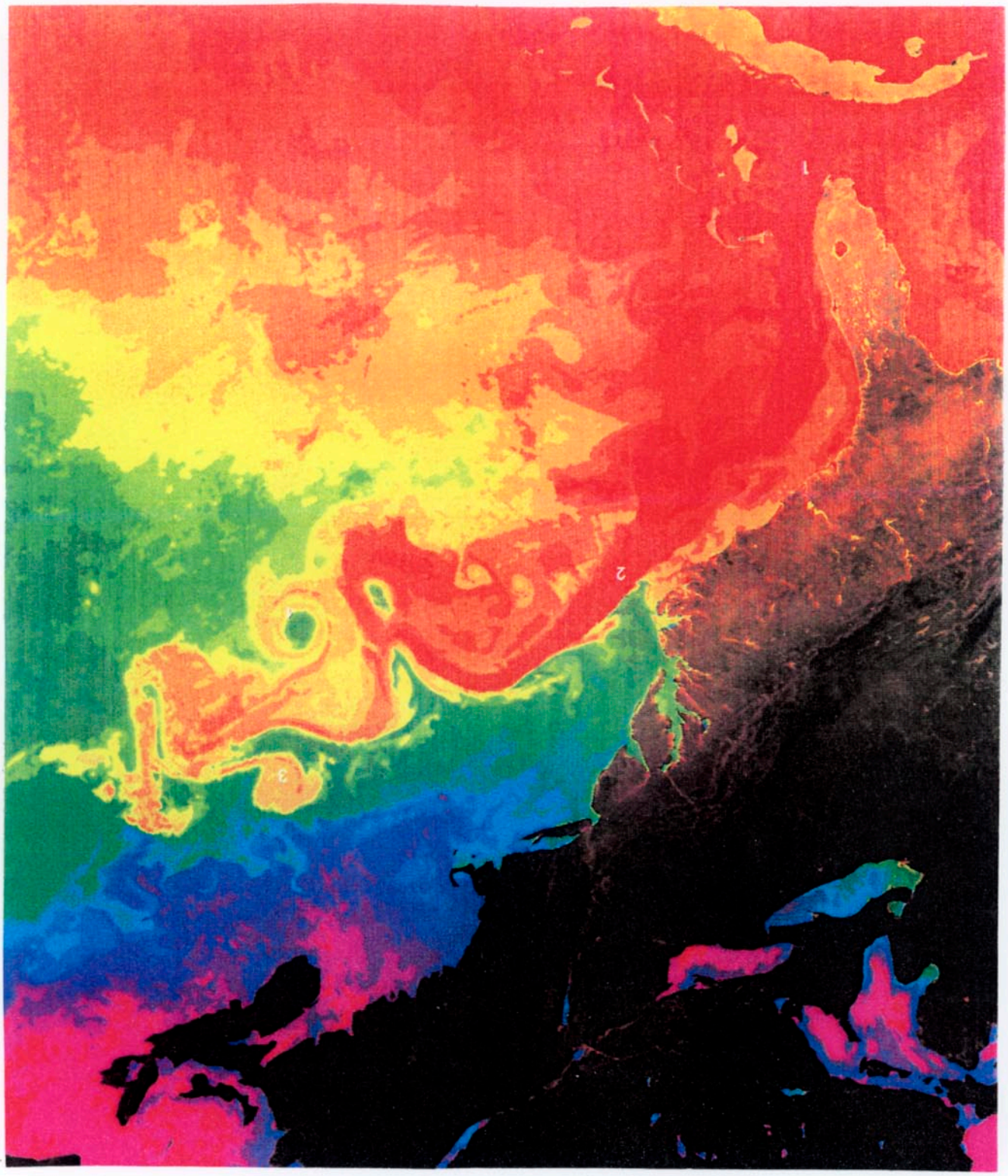

SATELLITE OBSERVATION

General Circulation Model
(G.C.M.) for Ocean
Dynamics
Los Alamos Code
1995

Seasurface
temperature
(S.S.T)

Comparison
between
numerical
experiment
and satellite
observation



DATA ASSIDILATION IN OCEAN GENERAL CIRCULATION MODELS

FOR ANNUAL SEA SURFACE TEMPERATURE & WIND

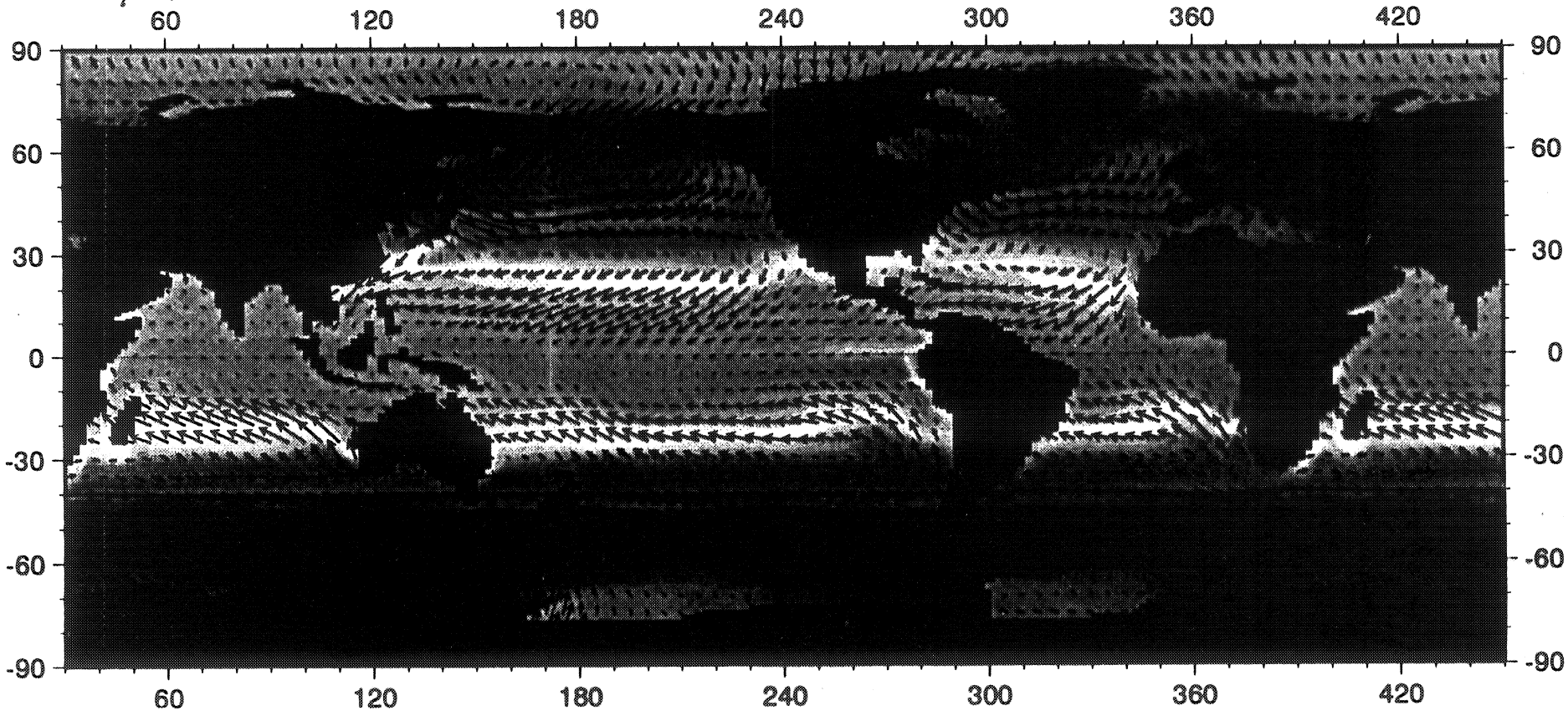

→ OPERATIONAL OCEANOGRAPHIC PREDICTIONS

Project MERCATOR (CERFACS, CNES, CNRS, Météo-France)
Coupled Model ARPEGE-OPA

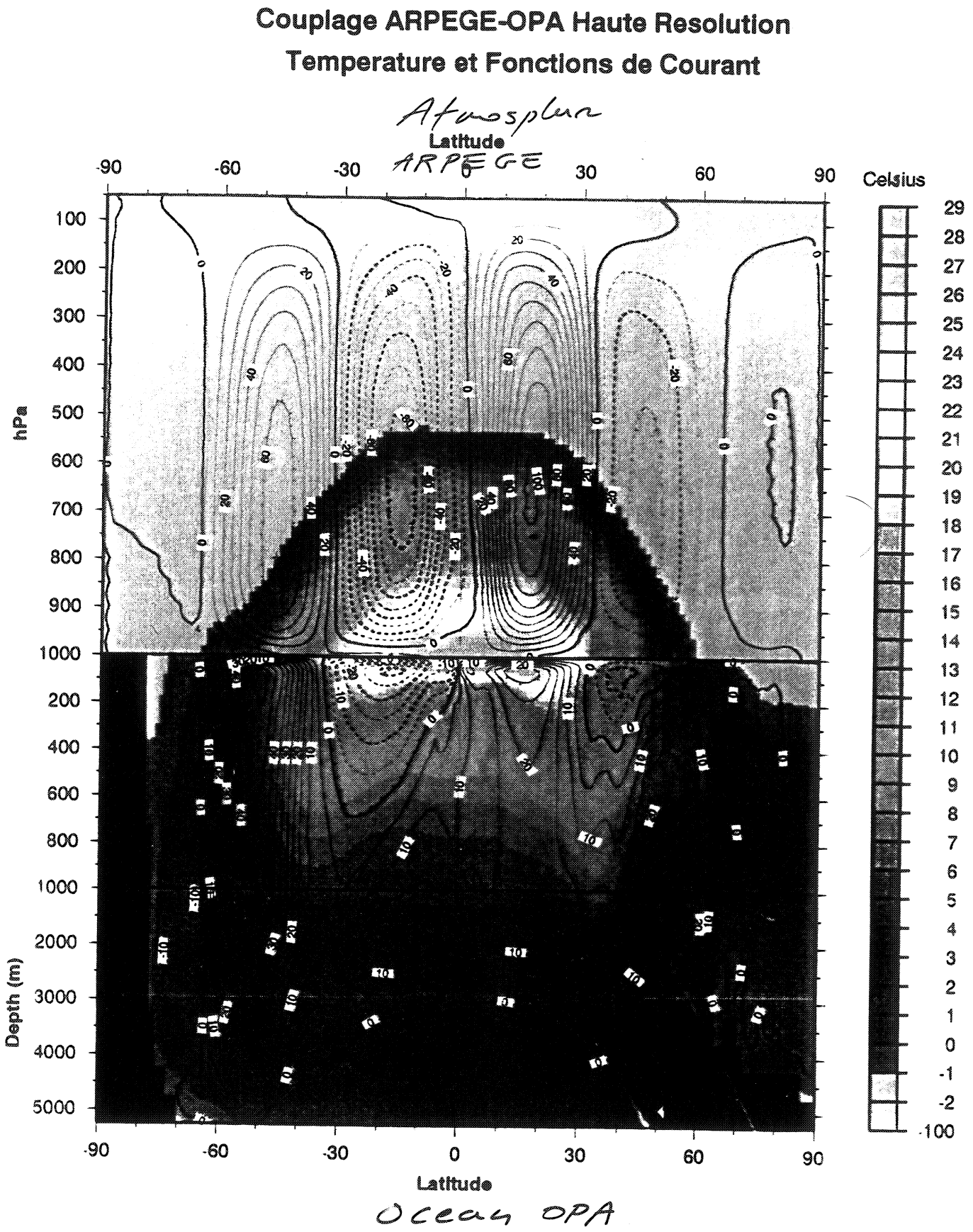

Figure 1 : Moyenne zonale du champ de température (champ coloré) et de la fonction de courant de la moyenne zonale du champ de vitesse (isocontours) dans l'océan et l'atmosphère. Champs issus des 25 ans de simulation couplée avec le modèle haute résolution ARPEGE/OASIS/OPA global. Intervalle entre les contours 10 Sverdrup pour l'océan, 10^9 kg/s pour l'atmosphère

ZONAL MEANS FOR 25 years coupled Simulations: TEMPERATURE & STREAMFUNCTION

April Mean SST (°C)

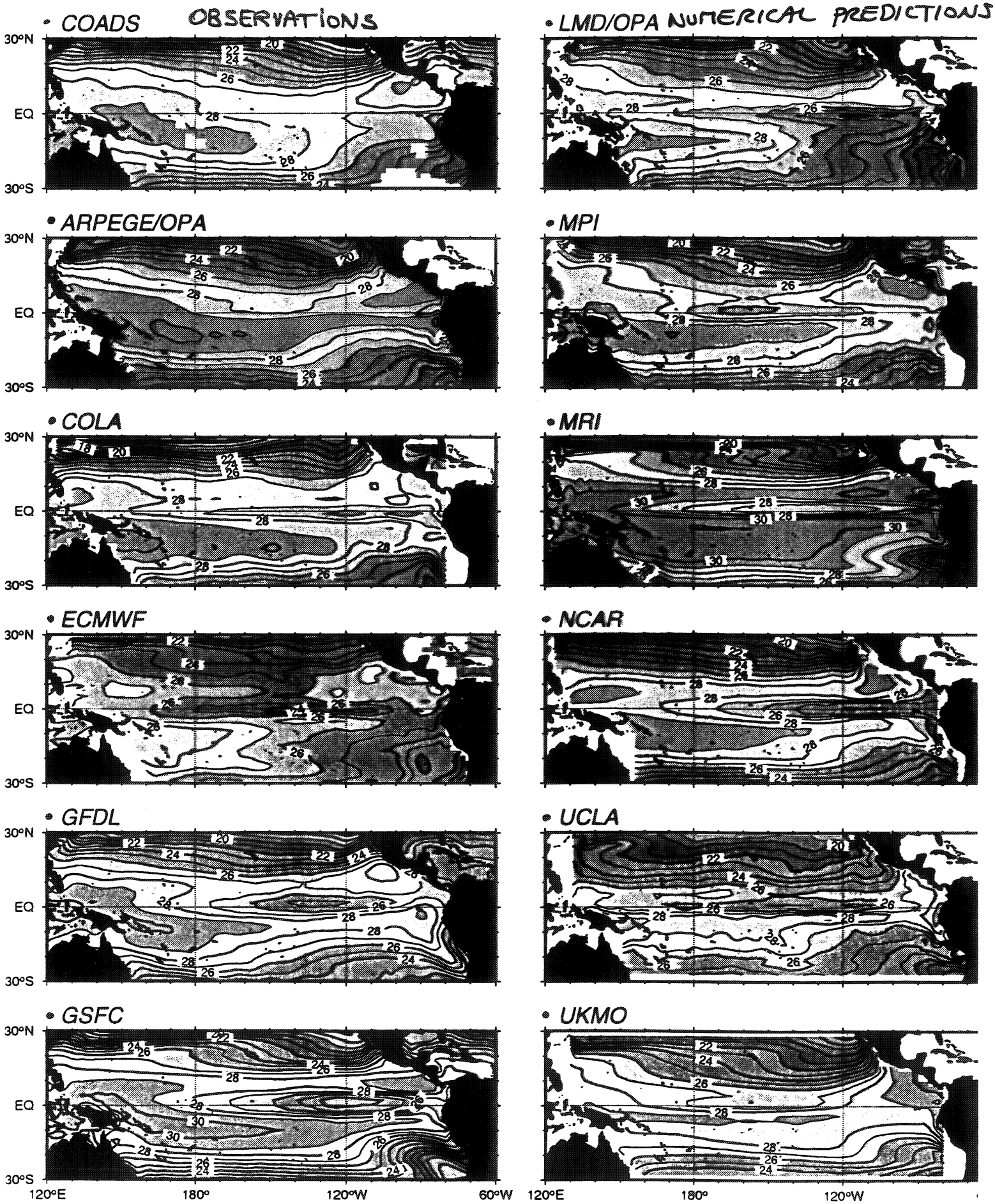

APRIL SEA SURFACE TEMPERATURE

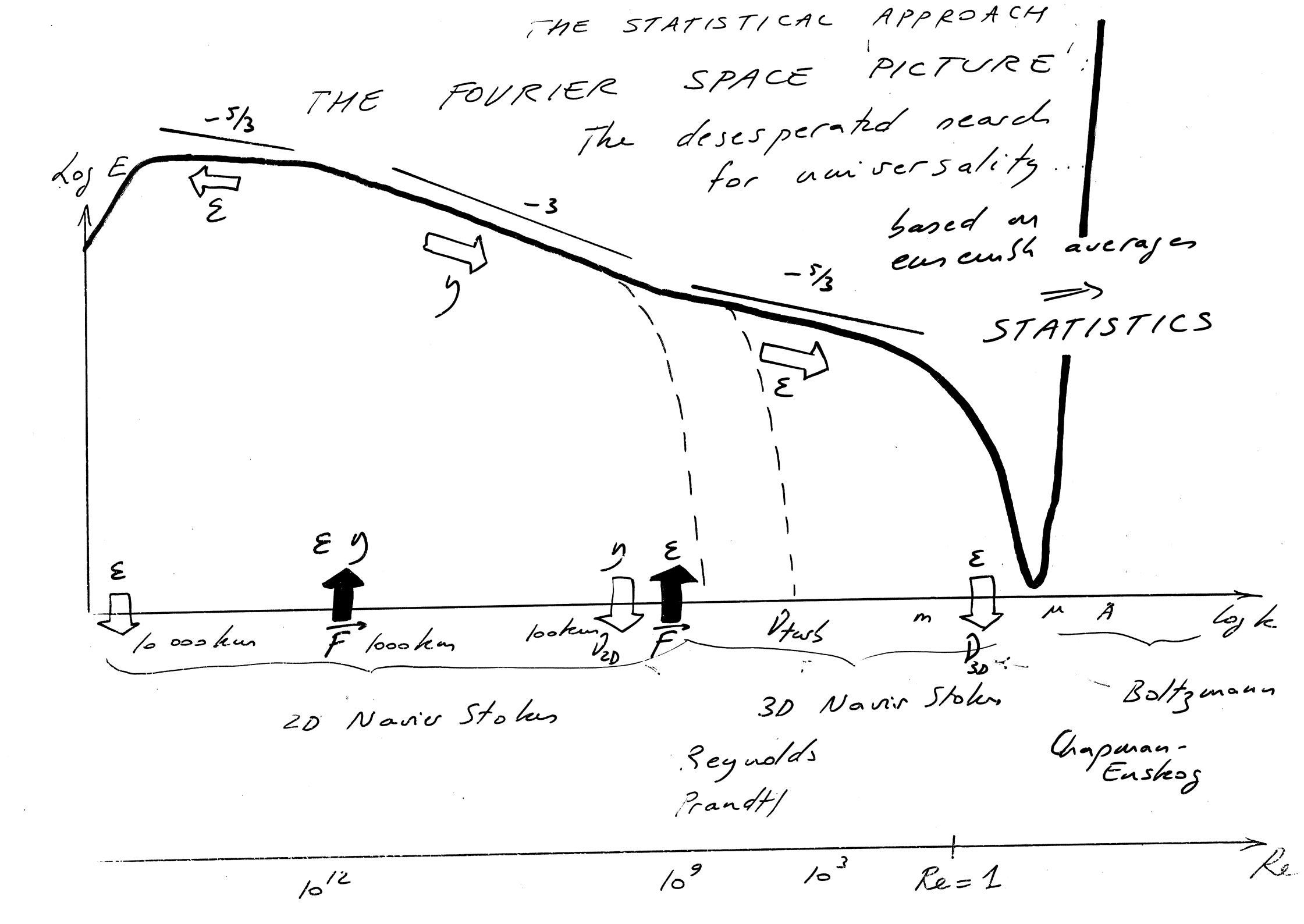
THE STATISTICAL APPROACH
THE FOURIER SPACE 'PICTURE':
The desesperated search for universality...
based on ensemble averages
STATISTICS
Log E
-5/3
-3
-5/3
ε
η
ε
ε η
η ε
ε
10 000 km
F 1000 km
100 km
ν2D
F
νturb
m
ν3D
μ
Å
Log k
2D Navier Stokes
3D Navier Stokes
Boltzmann
Reynolds
Prandtl
Chapman-Enskog
10^12
10^9
10^3
Re = 1
Re

STATISTICAL THEORY OF 2D TURBULENCE

- Ensemble average of a large number of uncorrelated realizations
  ⇒ homogeneity and isotropy,
- Forcing in the low-wavenumbers k_F
  Dissipation in the high-wavenumbers k_D
  to try to recover a conservative nonlinear dynamics in the inertial range,
- Hypothesis: constant rate of transfer in the inertial range for $k_D \ll k \ll k_F$.

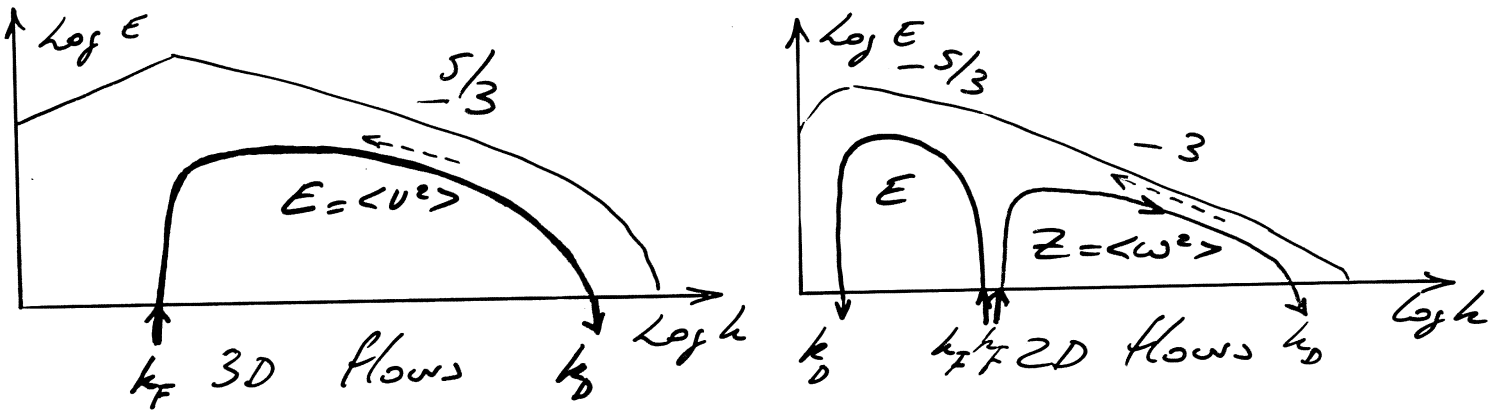

PROBLEMS

- No ensemble average ⇒ inhomogeneity of each realization
- Steeper spectral slopes
- Back-scattering
- No spectral gap:
  no decoupling between
  low-wavenumber dynamics
  and high-wavenumber dynamics

TURBULENT FLOW COMPUTATION

The limit $Re \to \infty$ implies an ∞ number of degrees of freedom.

- In practice we have to split the flow into:

Active components to be computed + Passive components to be modelled

Our goal is to find the representation presenting the fewest active components

Most classical methods split the flow into

low wavenumbers + high wavenumbers

assuming a spectral gap and no inverse cascade

TURBULENT FLOW COMPUTATION

The numerical discretization consists of selecting the most significant coefficients $\tilde{f}_>$, which discarding the others $\tilde{f}_<$.

Dirac basis

(Finite elements, finite differences, vortex methods)

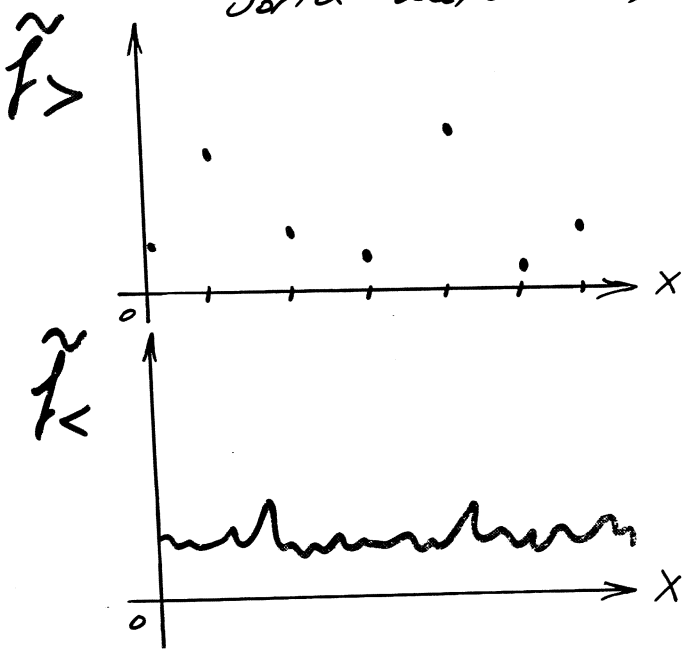

Fourier basis

(spectral methods)

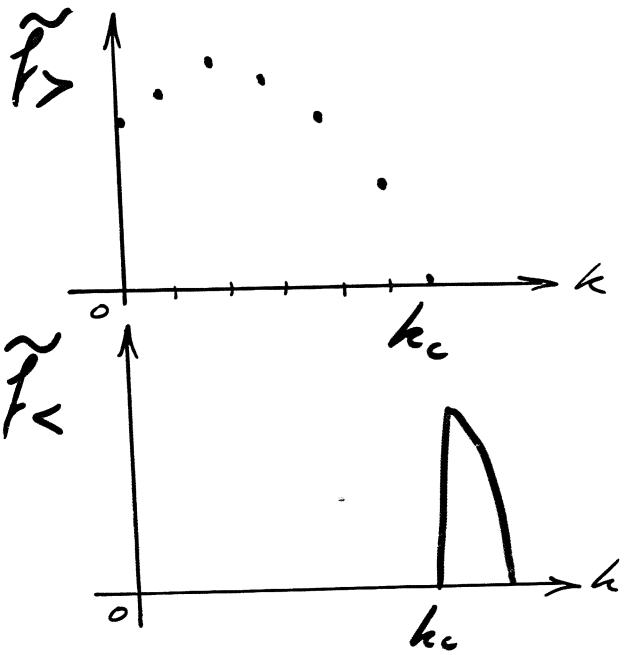

Only the time evolution of $\tilde{f}_>$ is computed and $\tilde{f}_<$ is discarded or modeled by an adhoc subgrid scale model.

NUMERICAL SIMULATION 2D TURBULENT FLOWS

Direct Numerical Simulation

Navier-Stokes

$$\begin{cases} \dfrac{\partial \vec{V}}{\partial t} + \vec{V}\cdot\vec{\nabla}\vec{V} + \dfrac{1}{\rho}\vec{\nabla}P = \nu\nabla^2\vec{V} \\ \vec{\nabla}\cdot\vec{V} = 0 \end{cases} \quad + \text{B.C} \;\&\; \text{I.C.}$$

$$\begin{cases} \omega = \vec{\nabla}\times\vec{V} = \nabla^2\psi \\ \dfrac{\partial \omega}{\partial t} + \vec{V}\cdot\vec{\nabla}\omega = \nu\nabla^2\omega \end{cases} \quad + \text{B.C} \;\&\; \text{I.C.}$$

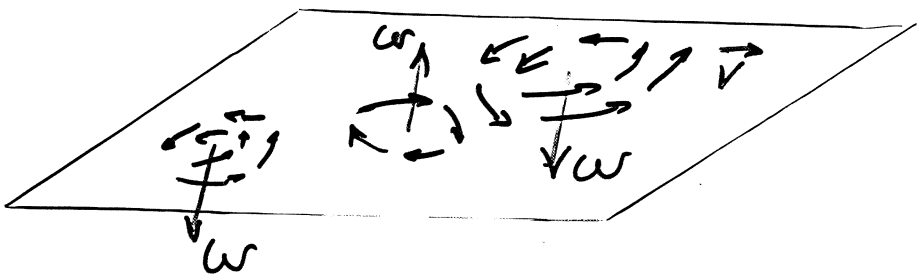

Laminar flows
$Re \sim 1$

Turbulent flows
$Re \to \infty$

Reynolds Number

$$Re = \frac{UL}{\nu} = \frac{L}{\delta} \qquad \delta = \frac{\nu}{U}$$

number grid points $\propto Re$

2D NAVIER-STOKES
PSEUDO-SPECTRAL CODE
2D DECAYING TURBULENCE

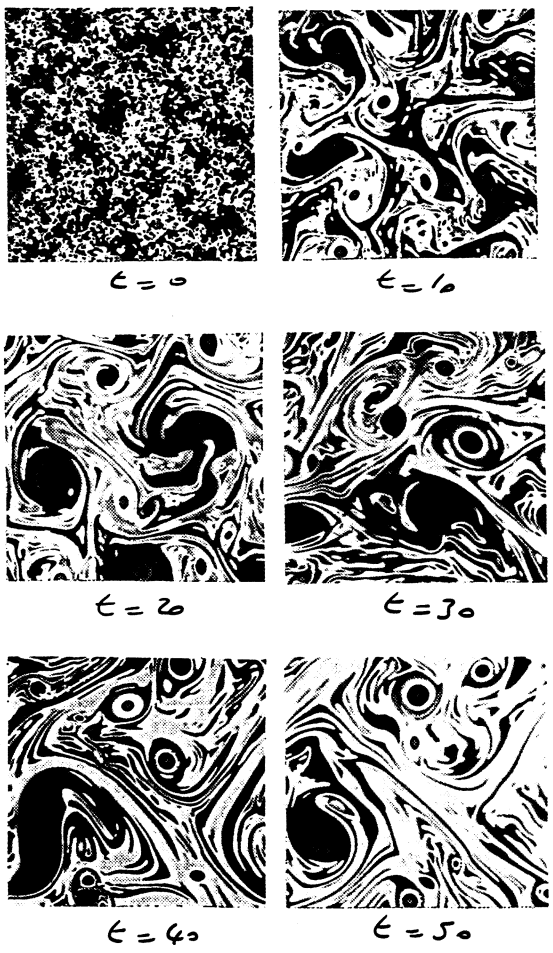

Formation of
Coherent Structures
from an initial
random distribution of
vorticity ($\omega = \vec{\nabla} \times \vec{v}$)

(Marie FARGE,
1982)

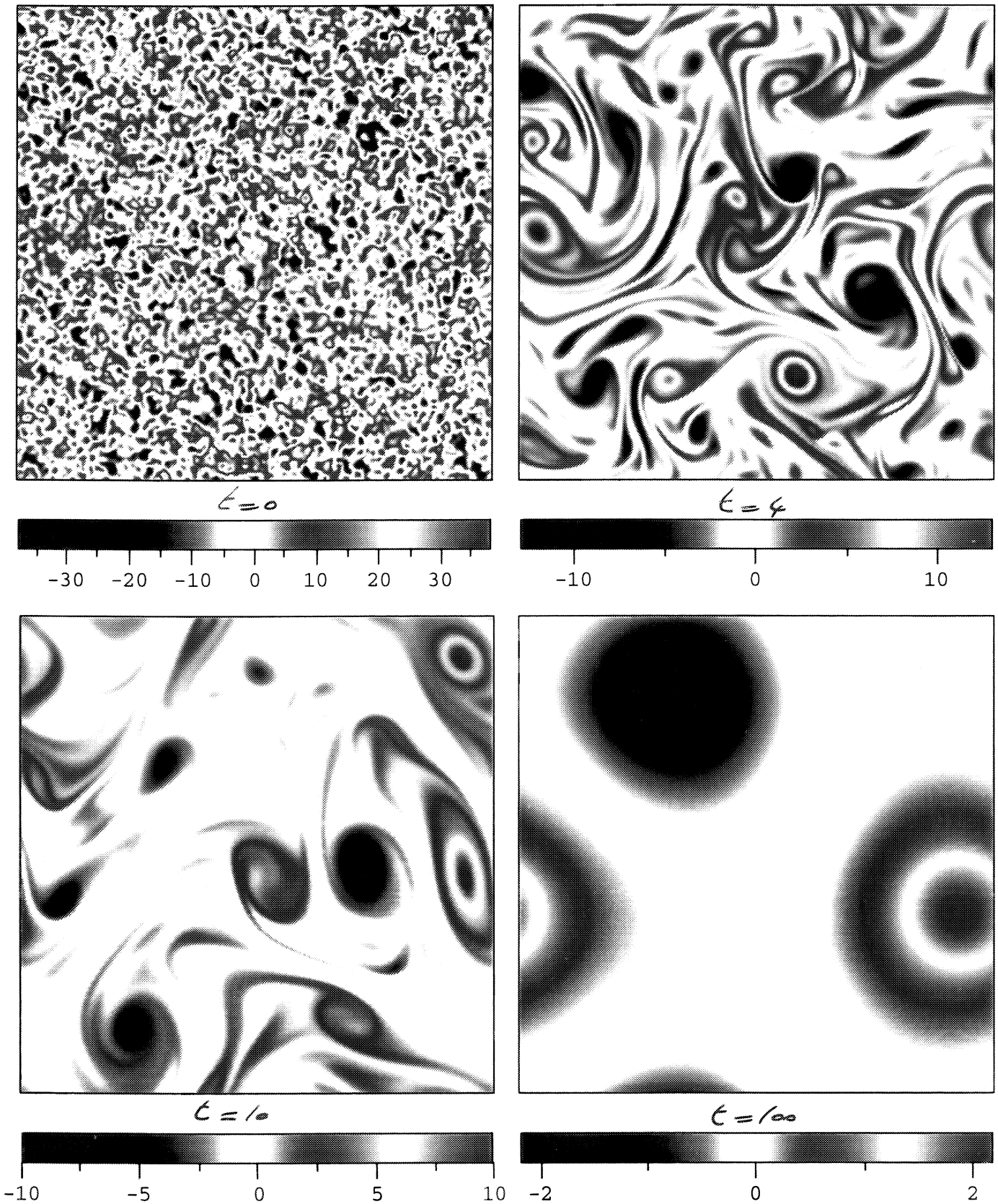

Decaying turbulence: Resolution N=256, $\nu = 9.910^{-4}$.
Top: Vorticity field at t=0, t=4.
Bottom: Vorticity field at t=10, t=100.

Decaying 2D turbulence
Pseudo spectral code
(Kai SCHNEIDER, 1997)

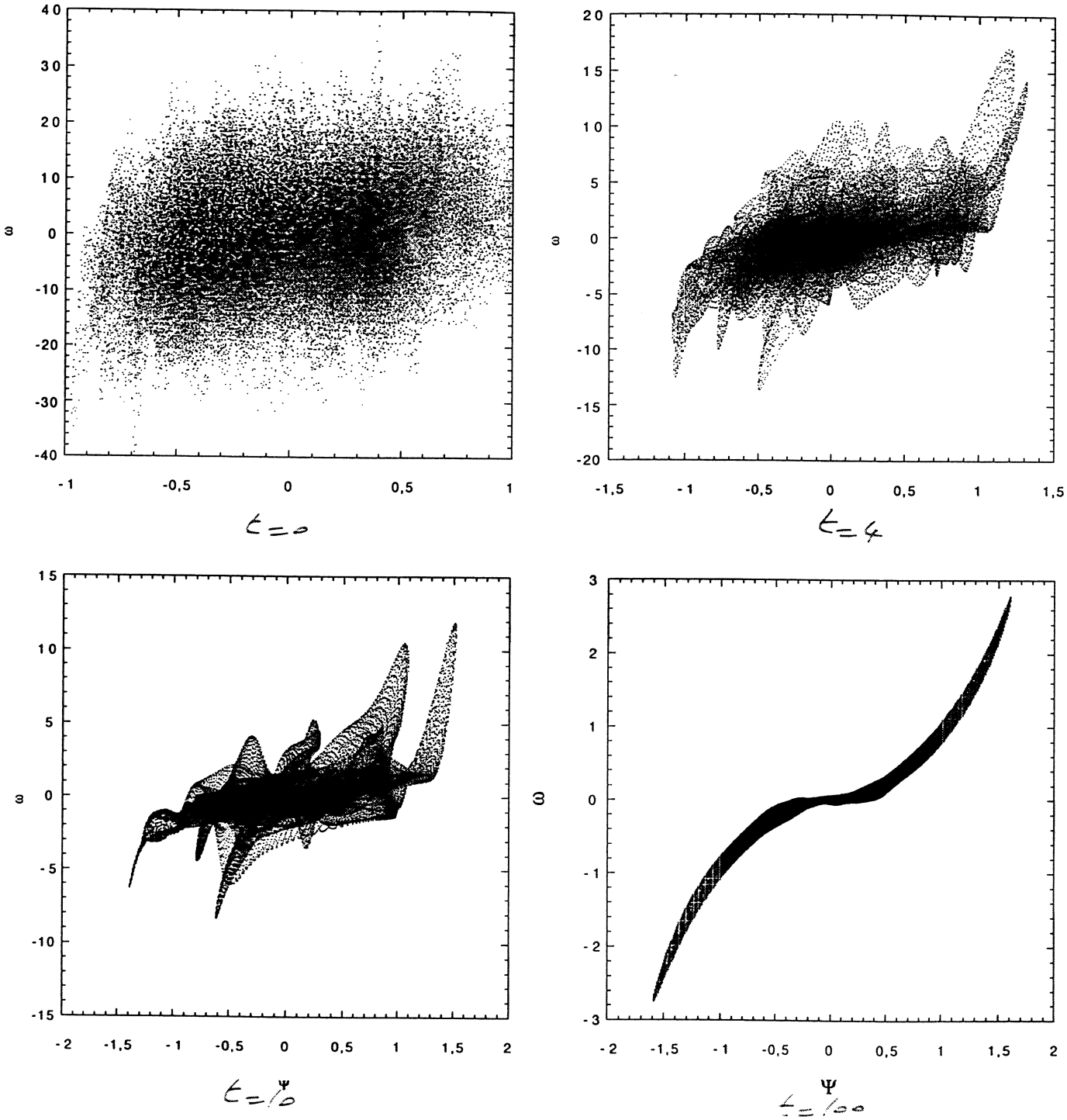

Decaying turbulence: Resolution N=256, $\nu = 9.910^{-4}$.
Top: Scatter plot at t=0, t=4.
Bottom: Scatter plot at t=10, t=100.

Coherent scatter-plot

$\omega = F(\psi)$

Decaying 2D turbulence 256^2

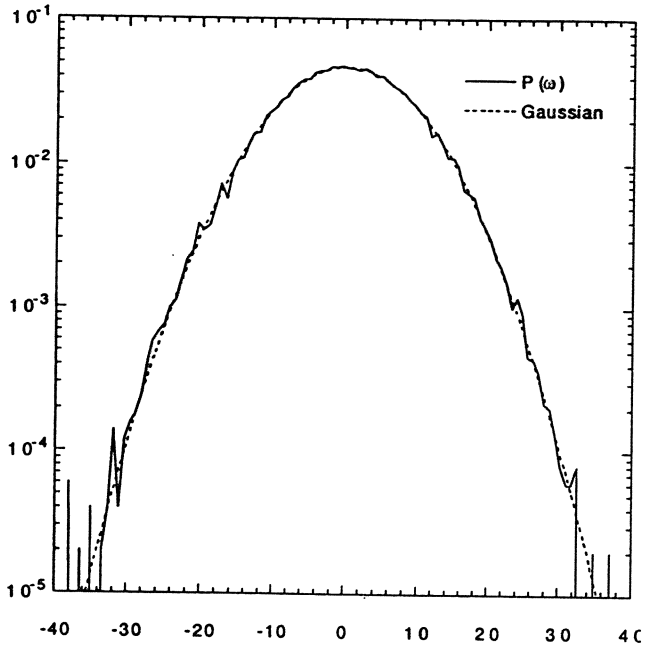

t=0

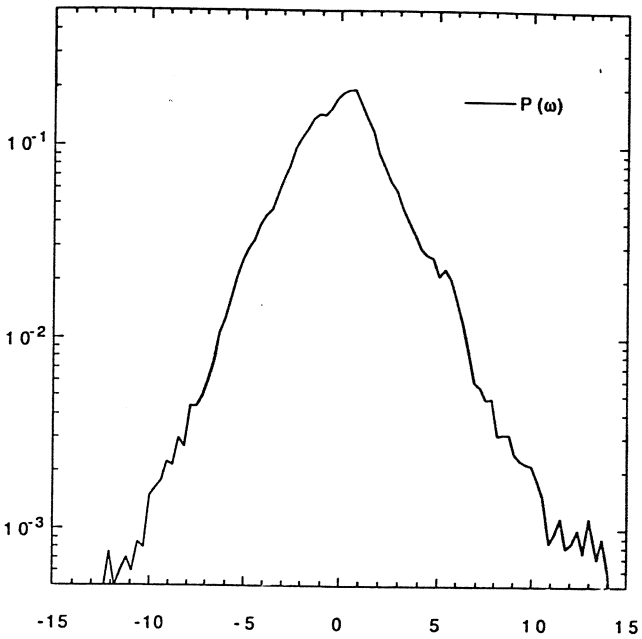

t=4

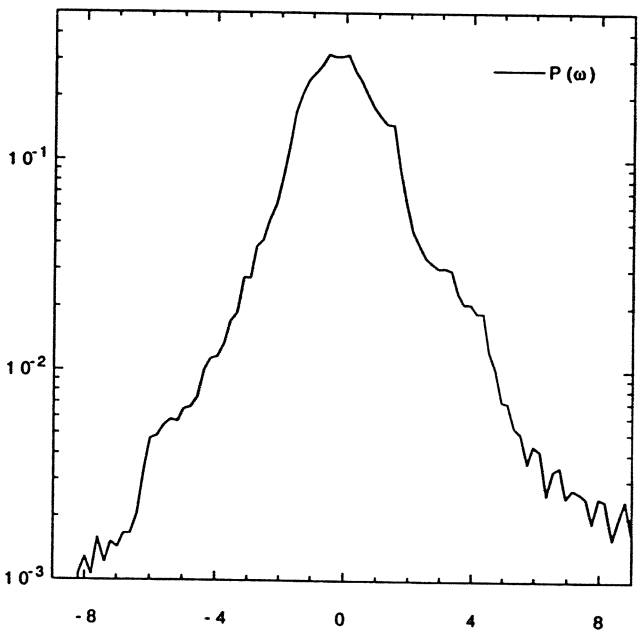

t=10

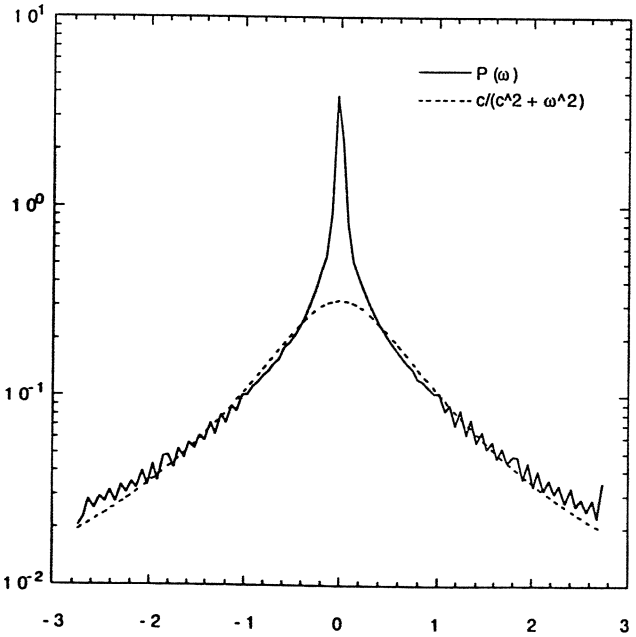

t=100

Decaying turbulence: Resolution N=256, $\nu = 9.910^{-4}$.
Top: PDFs of vorticity at t=0, t=4.
Bottom: PDFs of vorticity at t=10, t=100.

Probability Density Function of Vorticity

Decaying 2D turbulence 256^2

SPECTRA

Energy

E(K)

Non Forcé
No forcing

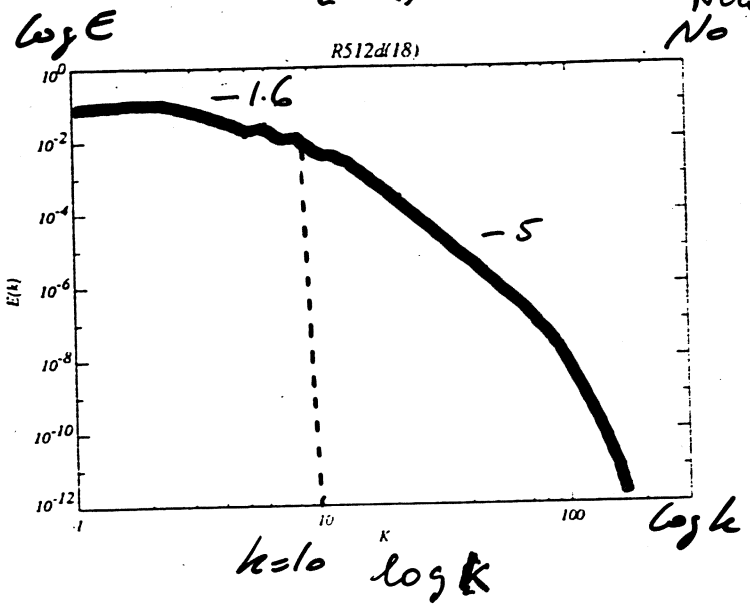

Enstrophy

Z(k)

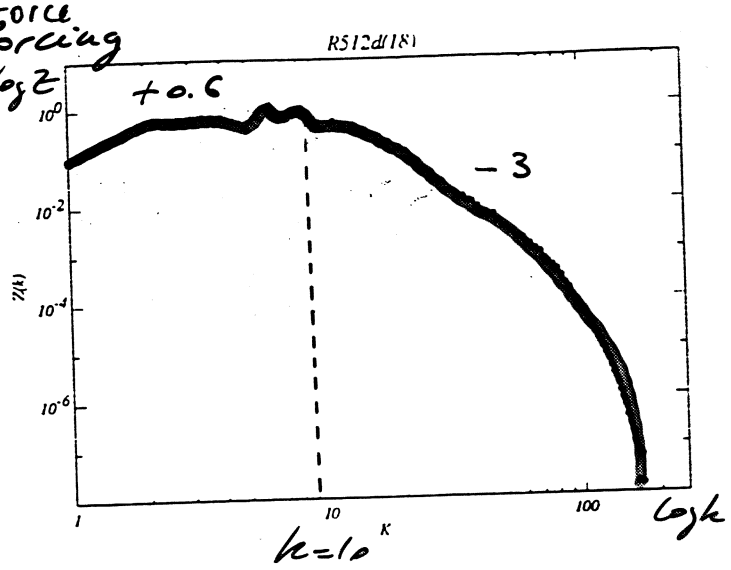

Forcé K=40
Forcing at k=40

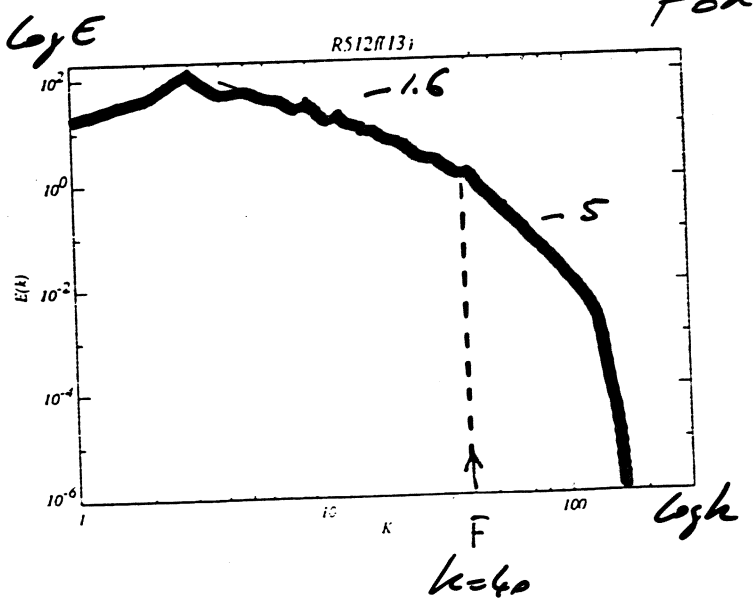

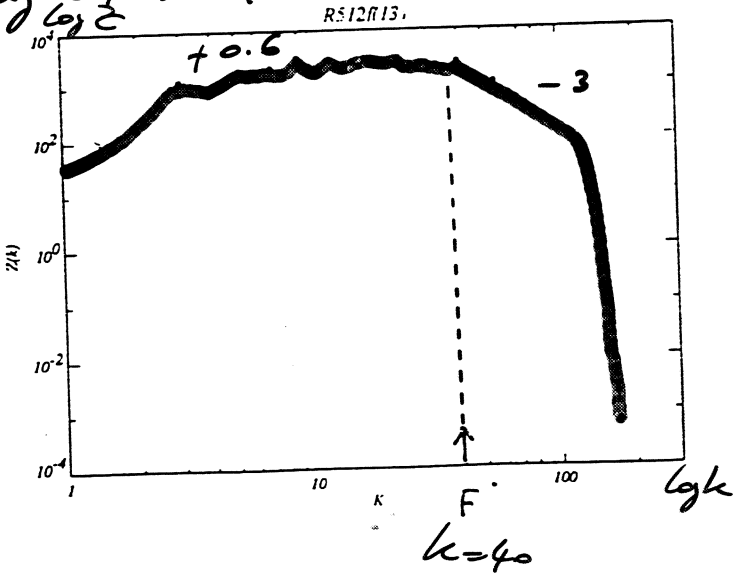

We show that if we randomize the phase of the vorticity we obtain the same energy spectrum although the spatial structure is destroyed

Vorticité
with random phase

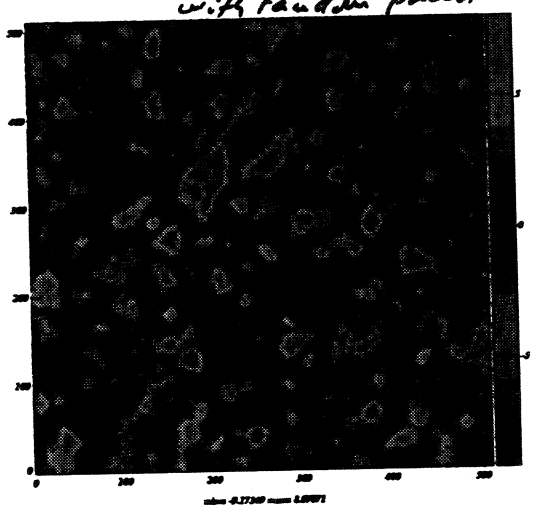

← PHASE ALÉATOIRE pour la transformée de Fourier

Vorticité
with coherent phase

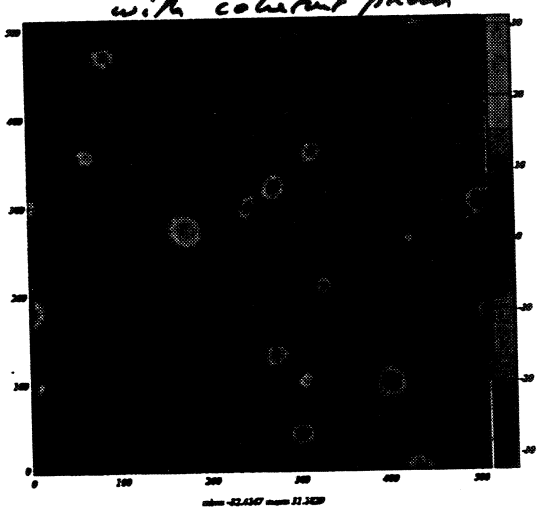

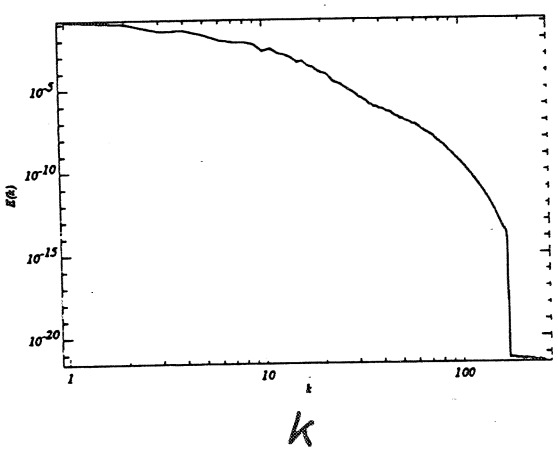

Spectre d'énergie.

We obtain the same energy spectrum for the 2 fields

(512^2 - Non forcé)

COHERENT STRUCTURES

- Localized accumulations of vorticity, which concentrate most of the enstrophy in a small fraction of the spatial domain and which persist on time scales much larger than the eddy-turn over time $\tau = \frac{1}{\sqrt{Z}}$.

- Elliptical regions of the flow where rotation dominates deformation / $\Theta = \omega^2 - s^2 < 0$ (Weiss 1992).

- Maximum entropy solutions of Navier-Stokes equations (coarse-grained Euler equations) characterized by a point-wise relation $\omega(\vec{x}) = F\,\psi(\vec{x})$ between vorticity ω and streamfunction ψ (Montgomery & Joyce 1973, Robert & Sommeria 1992, Miller 1992).

A KEY QUESTION

Is there a generic shape for coherent structures?

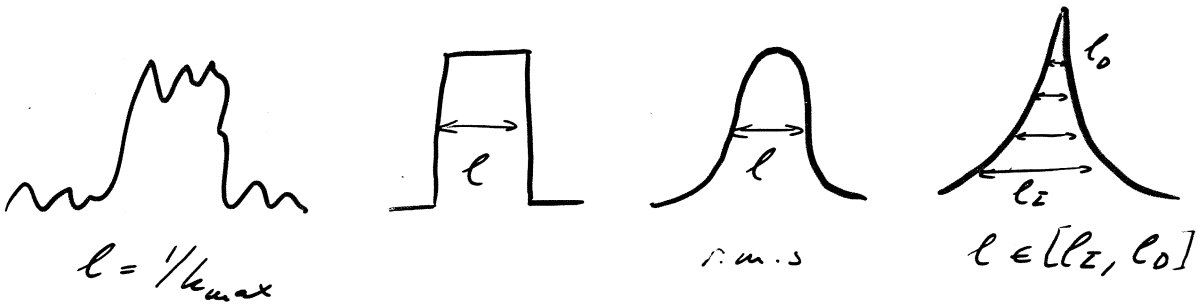

$l = 1/k_{max}$ r.m.s $l \in [l_1, l_0]$

Our a priori model of coherent structures conditions the notion of vortex scale, vortex area, circulation ...

A priori in statistical analysis are as essential as hypotheses in modelling

$\Rightarrow$

we should state our a priori's clearly, otherwise our results will be meaningless.

The problem is the same for 3D turbulent flows when coherent structures are vorticity tubes.

COHERENT STRUCTURES DYNAMICS

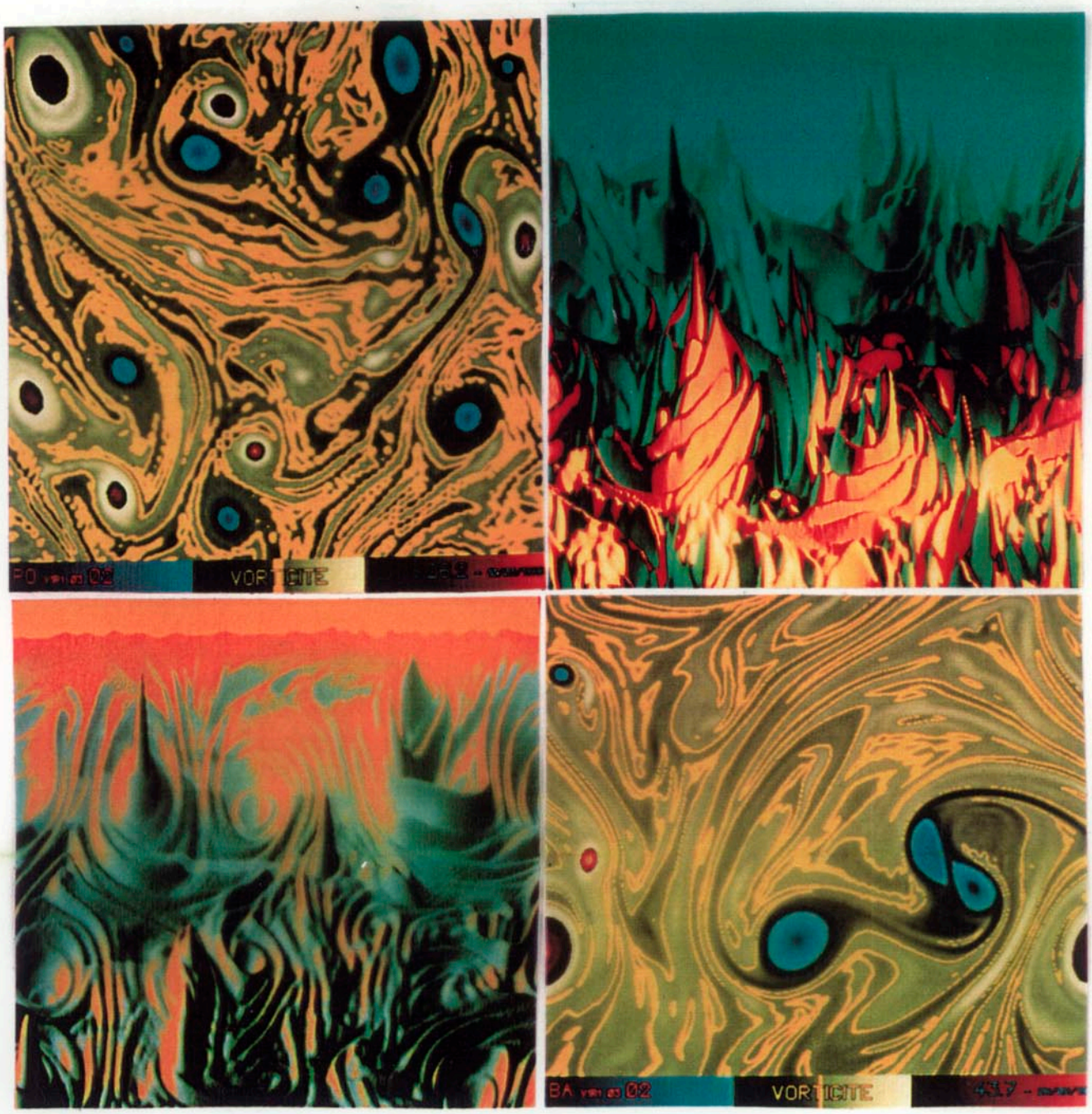

Ground State

1. if Same sign:

Weak Interaction

Strong Interaction



$d > \lambda_w$



$\lambda_w > d > \lambda_s$



$\lambda_s > d$

$\vec{\nabla} V \nearrow$

Etude des structures cohérentes en turbulence bidimensionnelle

Straining

Les quatre réalisations du champ de vorticité ci-contre nous permettent d'illustrer les différents types d'interactions entre structures cohérentes:

- fusion de deux tourbillons de même signe,
- liaison sous forme de modon de deux tourbillons de signes opposés,
- émission de filaments de vorticité sous l'effet de la déformation par les structures voisines,
- relaxation vers une forme axisymétrique en l'absence d'interaction .

Merging + filamentation

Nous observe également la présence de certaines structures cohérentes quasi-singulières en forme de cusp, correspondant à une distribution affine de vorticité, dont la présence expliquerait, d'après Farge et Holschneider, le comportement en loi de puisssance du spectre d'énergie.

2. if opposite sign:

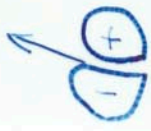

$\lambda_c > d$ $\vec{V} \nearrow$ Binding

Coherent Vortices
observed in 2D tur-
bulent flows

(Farge, 1984)

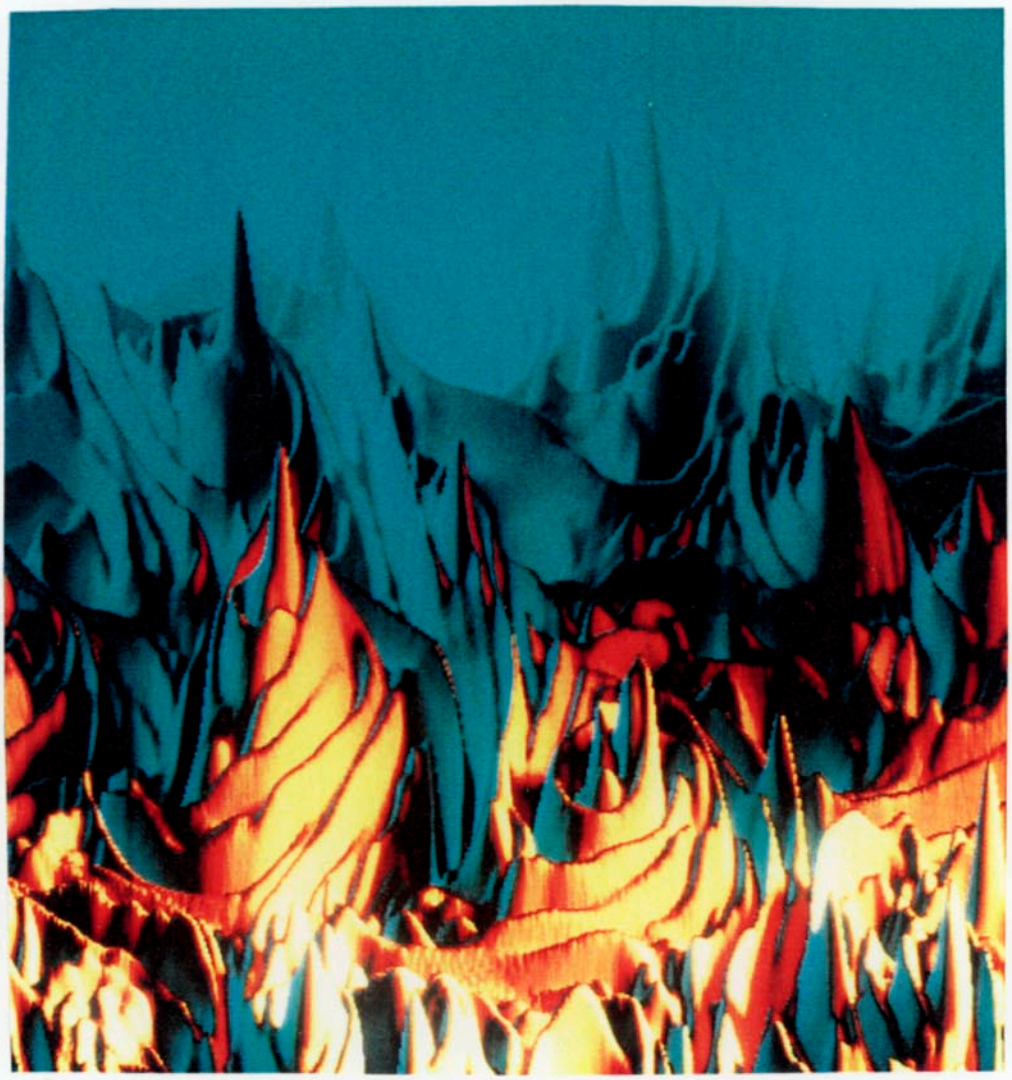

Time evolution of
coherent vortices in
2D turbulent flows
(Farge et Coury, 1986)

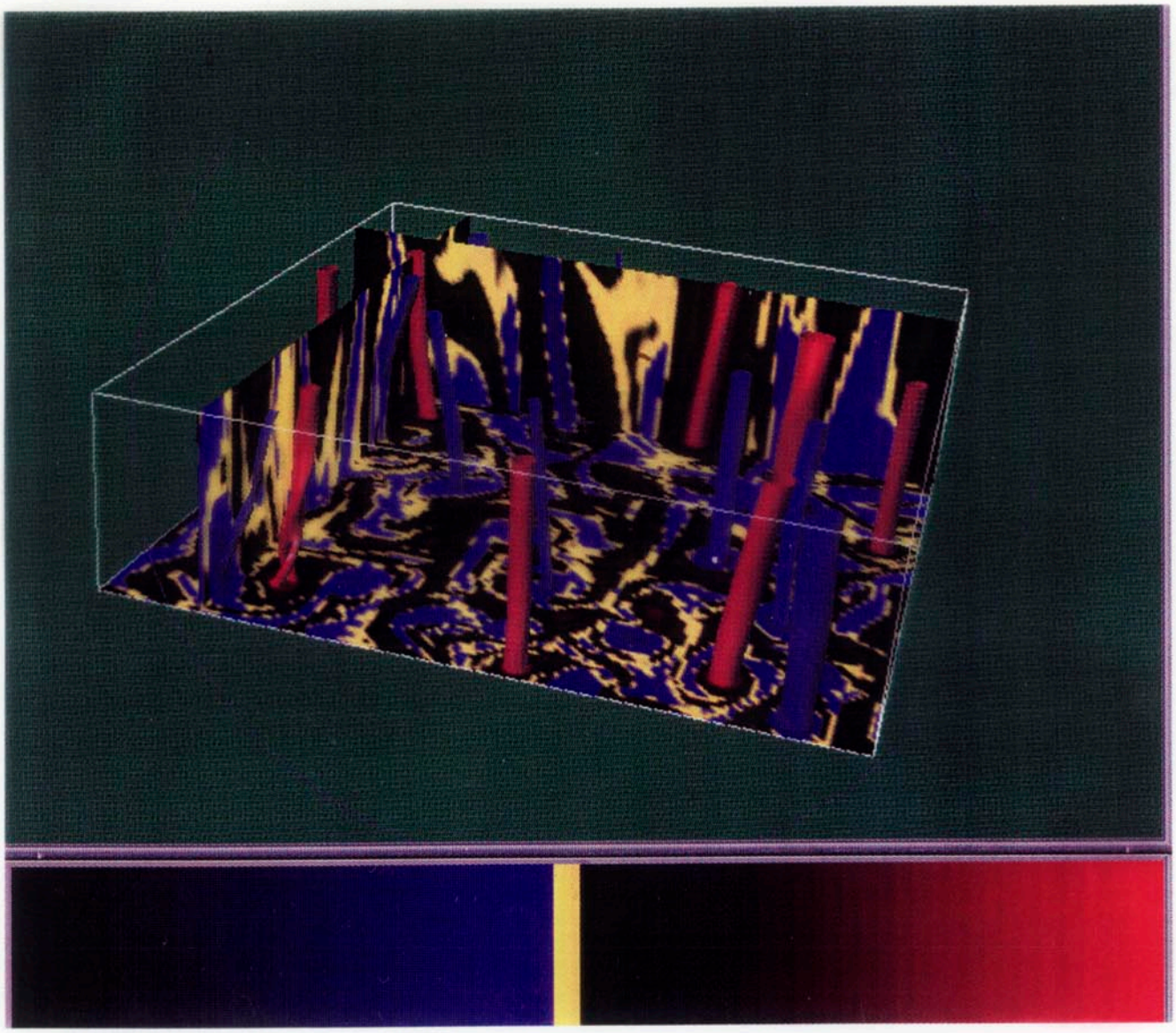

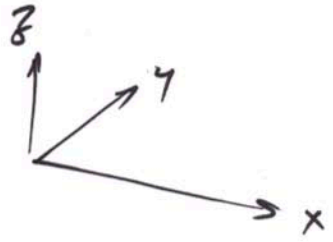

WHICH ARE THE DYNAMICALLY ACTIVE COMPONENTS OF TURBULENT FLOWS?

Need for a physical intuition from observations ⇒

1. ANALYSIS using the continuous wavelet transform.

Need to compute the flow evolution with a reduced number of degrees of freedom (active components) ⇒

2. COMPRESSION and
3. COMPUTATION using orthogonal wavelets.

TURBULENT FLOW ANALYSIS

Turbulent flows are described by continuous fields f:

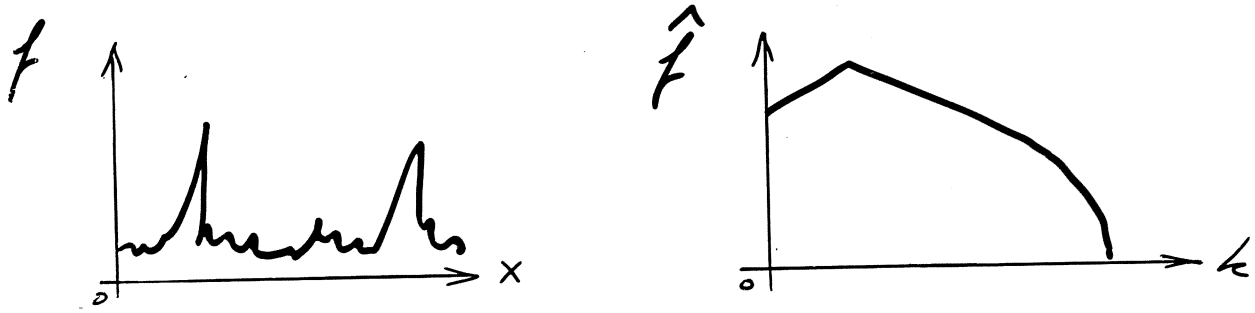

To measure and analyse them, we project them onto orthogonal bases described by analysing functions ψ_μ:

$$\hat{f}(\mu) = \int_{R^n} f(x)\, \psi_\mu(x)\, dx$$

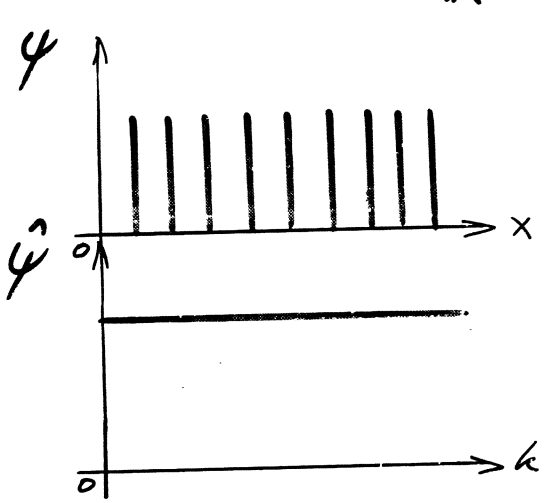

Grid-points or Dirac basis

$$\psi_{x_0}(x) = \delta(x - x_0)$$

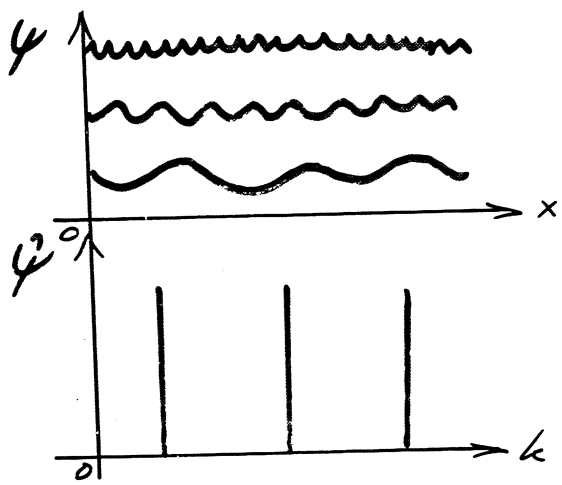

Wavenumbers or Fourier basis

$$\psi_k(x) = e^{-2i\pi k \cdot x}$$

TWO-DIMENSIONAL WAVELET ANALYSIS OF TURBULENT FIELDS

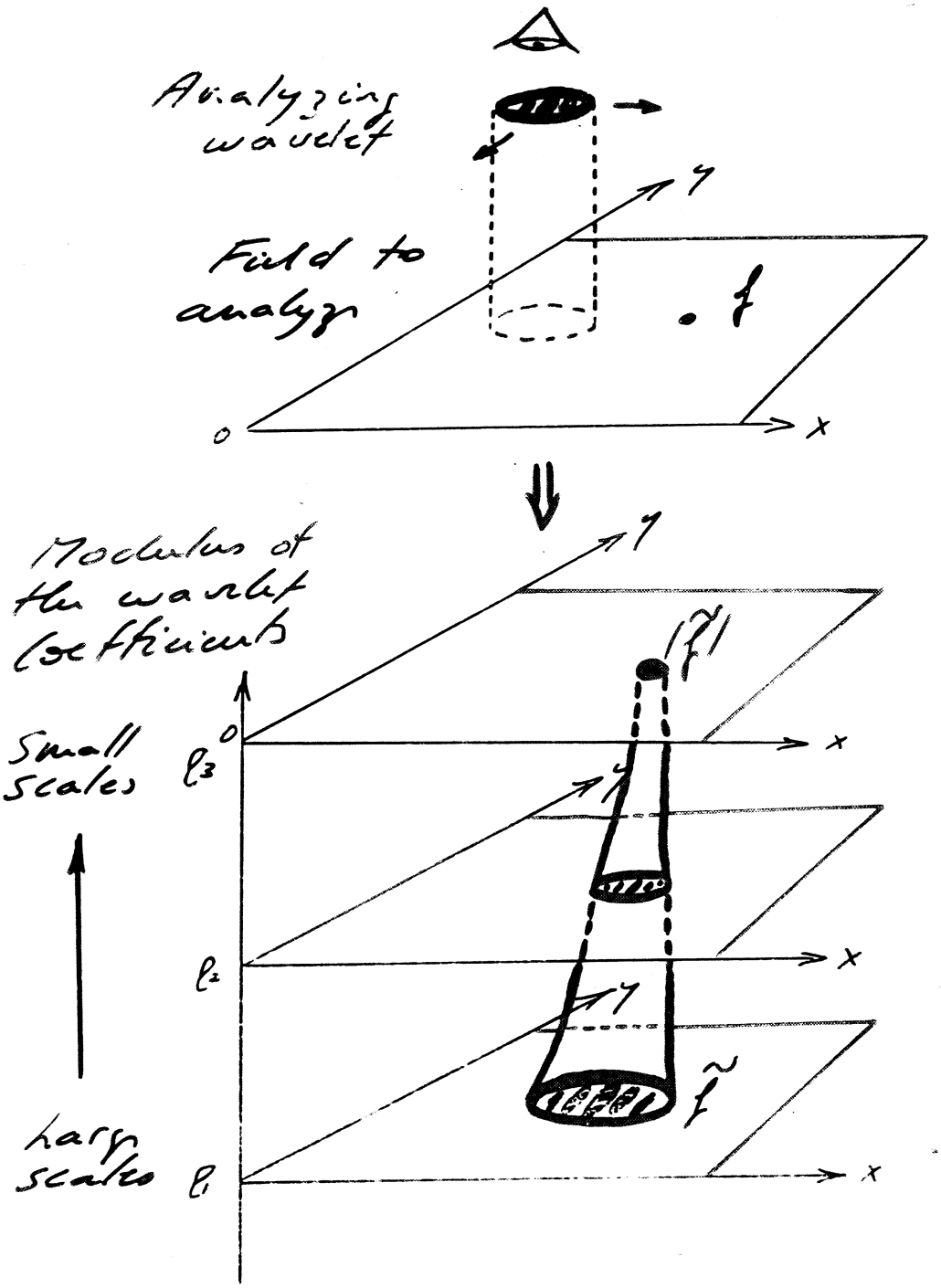

CONTOUR LEVELS
-.85000
-.80000
-.75000
-.70000
-.65000
-.60000
-.55000
-.50000
-.45000
-.40000
-.35000
-.30000
-.25000
-.20000
-.15000
-.10000
-.05000
0.00000
0.05000
0.10000

0.40000
0.45000
0.50000
0.55000
0.60000
0.65000
0.70000
0.75000
0.80000

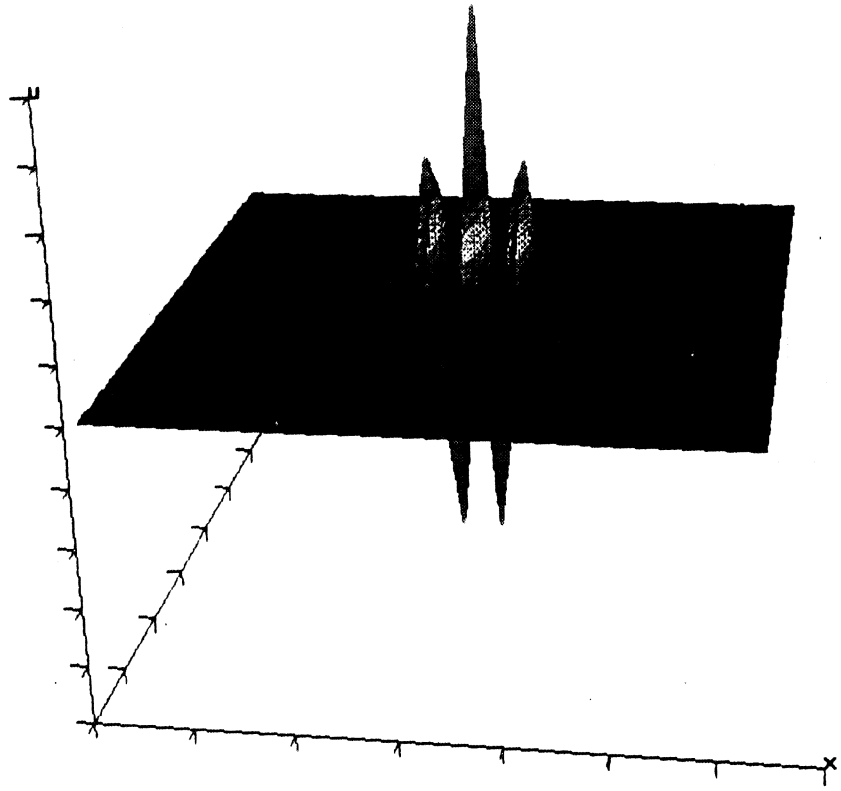

0.00x10**0 Nu
0.00x10**0 Utau
0.00x10**0 Re
0.00x10**0 Time
64x64 GRID

Topological Fluid Dyn., 1993
Farge, Holschneider & Glowna

2D Wavelet Analysis of Vorticity

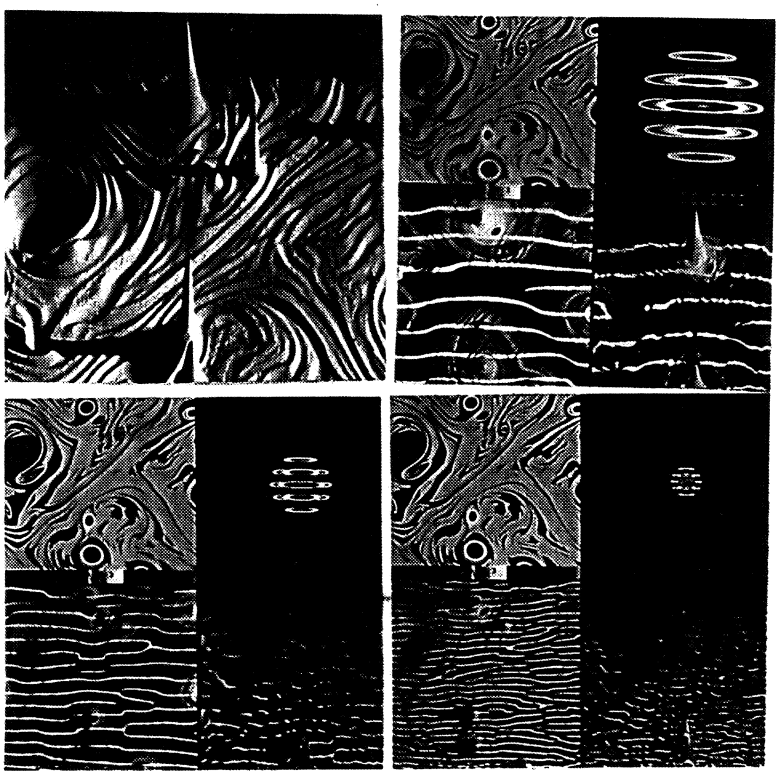

Strong wavelet coefficients correspond to coherent structures
Weak wavelet coefficients correspond to background flow

Analyses en ondelettes de champs turbulents

La transformée en ondelettes est une nouvelle technique d'analyse de signal, et nous avons été les premiers à l'utiliser pour étudier la turbulence. Nous avons écrit le premier code de transformée en ondelettes bidimensionnelles et nous l'avons utilisé pour analyser les sttructures cohérentes dans les écoulements turbulents, à deux et trois dimensions, résultats qui ont fait l'objet d'une dizaine de publications.

Sur la figure est représentée l'analyse en ondelettes de Morlet bidimensionnelles (montrées en haut à droite de chaque vue) d'un champ turbulent (montré en haut à gauche) à trois échelles différentes. Pour cela nous avons superposé le champ (en vue cavalière), le module des coefficients d'ondelettes (en couleur) et leur phase (l'isoligne blanche correspondant à la phase zéro).

Coherent structures condensate enstrophy ($<\omega^2>$) on a wide range of scales

COHERENT STRUCTURES FILTERING & ANALYSIS

1. By wavelet influence cones

$$\psi_{\ell x' \theta}(\vec{x}) = \ell^{-1} \psi\left[\mathcal{R}^{-1}(\theta) \frac{\vec{x} - \vec{x}'}{\ell} \right]$$

$$\tilde{\omega}(\ell, \vec{x}', \theta) = \langle \psi_{\ell x' \theta} / \omega \rangle$$

$$\omega_>(\vec{x}) = C_\psi^{-1} \int_0^\infty \iint_{-\infty}^{+\infty} \int_0^{2\pi} \tilde{\omega}(\ell, \vec{x}', \theta) \psi_{\ell x' \theta}(\vec{x}) \frac{d\ell\, d^2x}{\ell^3} d\mu(\theta)$$

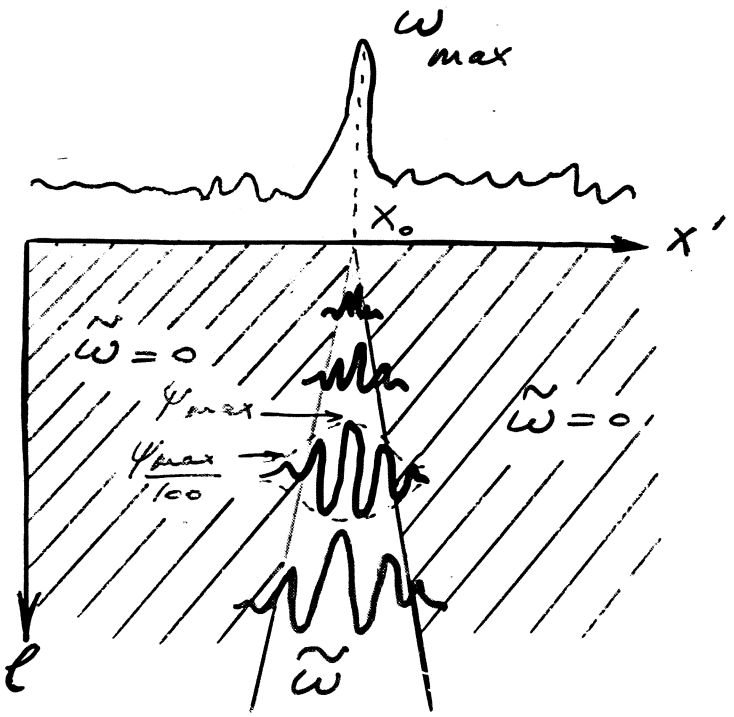

2. By thresholding in L^2 wavelet coefficients space

keep $\tilde{\omega}^2(\ell, \vec{x}', \theta) > \varepsilon$

discard $= 0$ if $\leq \varepsilon$

Then reconstruct $\omega_>(\vec{x})$

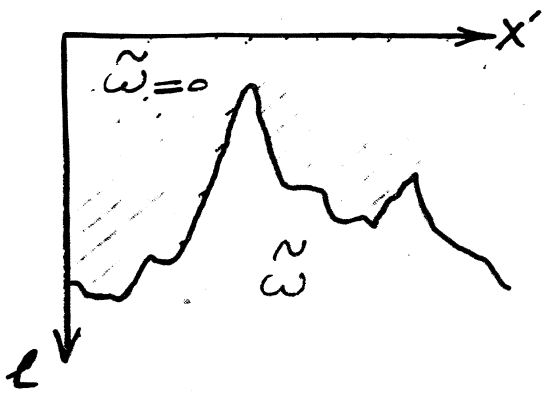

Filtrage d'1 structure par cône d'influence

le tourbillon à isoler

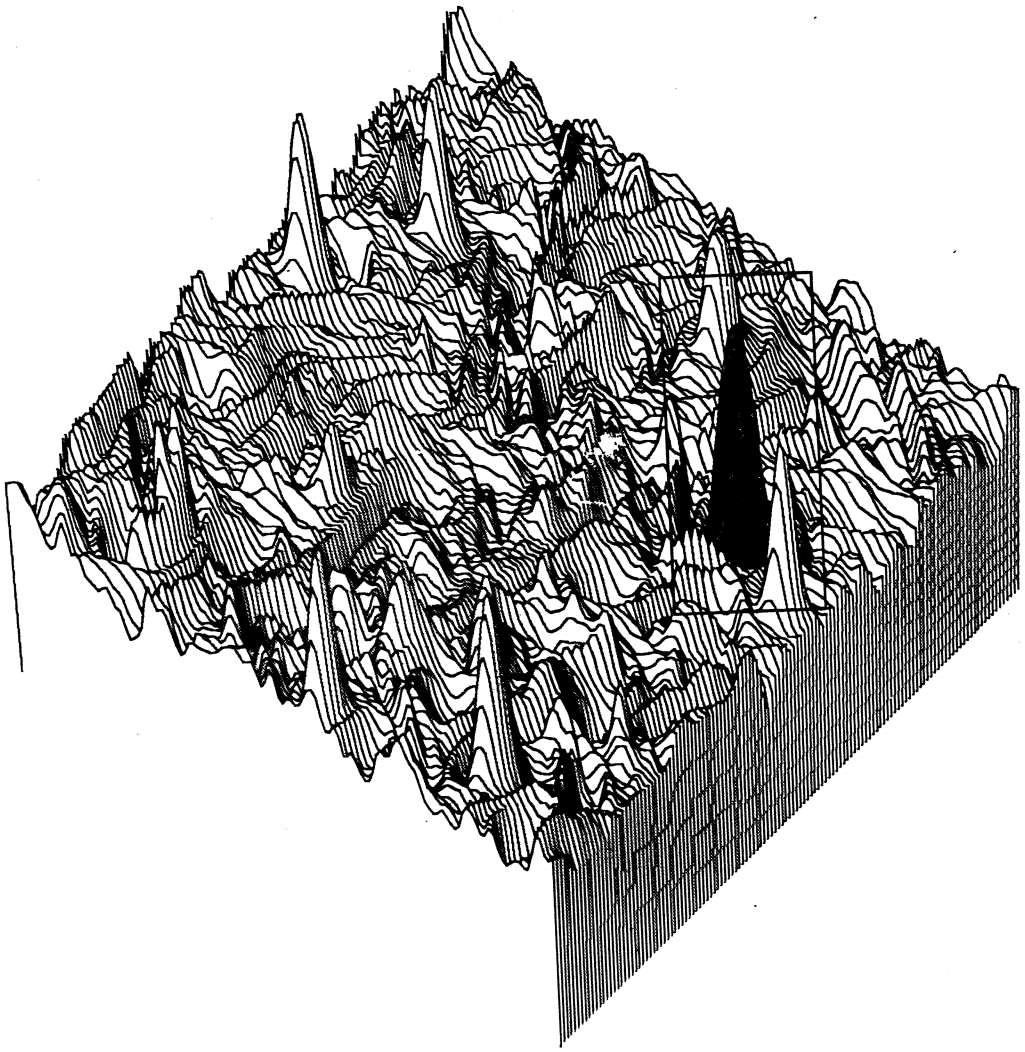

Filtrage d'une structure par cône d'influence

tourbillon isole

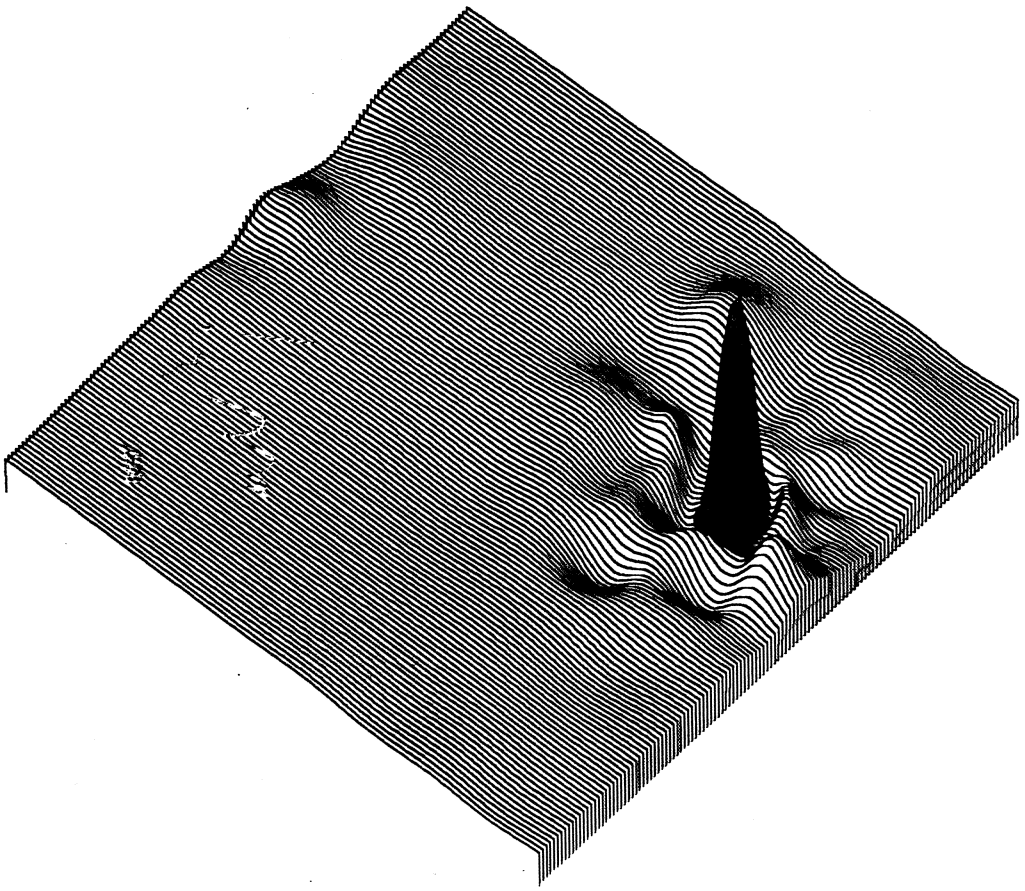

Filtrage d'1 structure
par cône d'influence

champ sans le tourbillon

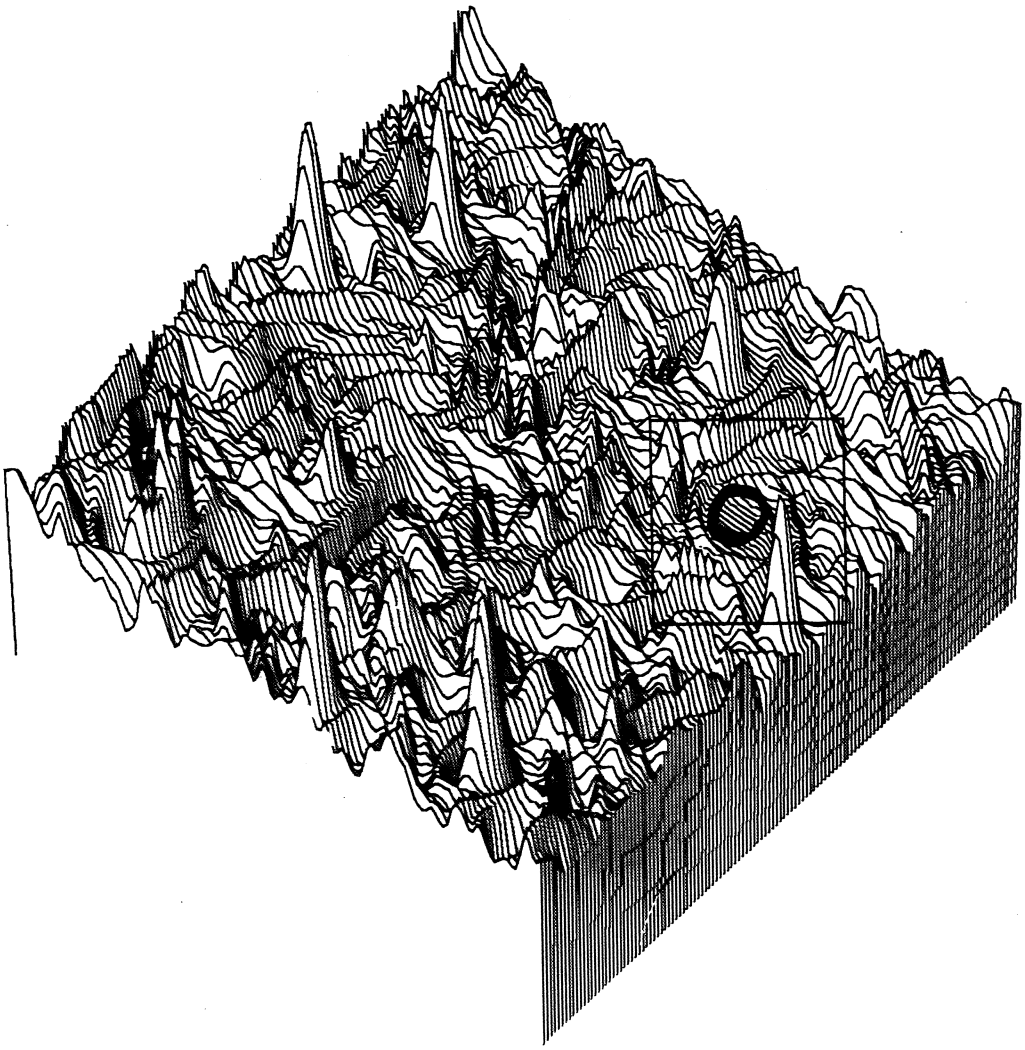

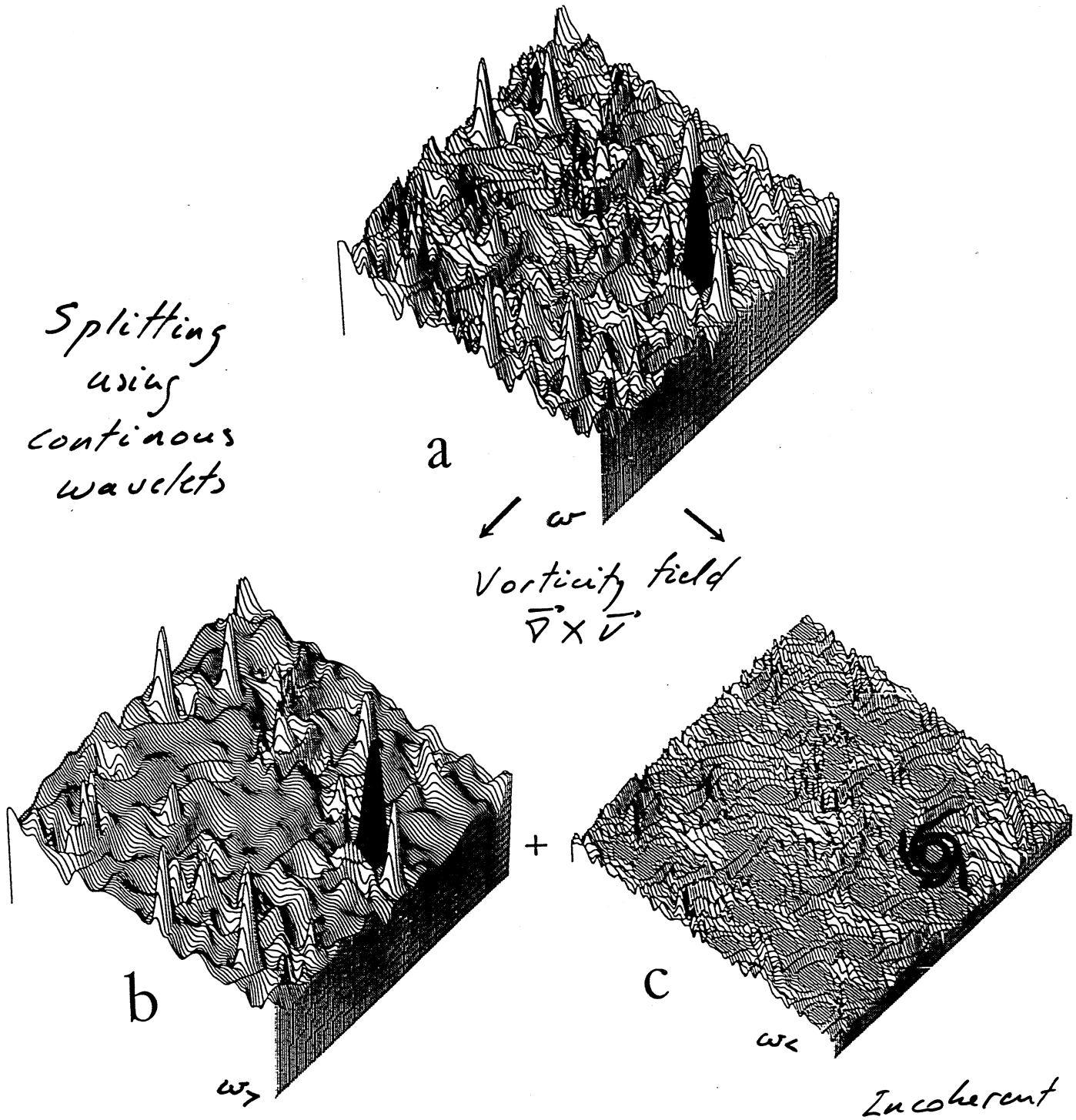
Splitting using continous wavelets
a
ω
Vorticity field
$\vec{\nabla} \times \vec{v}$
b
+
c
$\omega_>$
$\omega_<$
Coherent flow of vortices
Incoherent background flow
SPECTRE D'ENERGIE
E(K)
K
Pente : -4.6
Pente : -2.6
Pente : -5.9
−5
−3
−6
d
Dynamically 'active' elliptic regions: rotation >> strain
Passively advected hyperbolic regions: strain >> rotati

Figure 1

Filtrage d'1 structure par cône d'influence

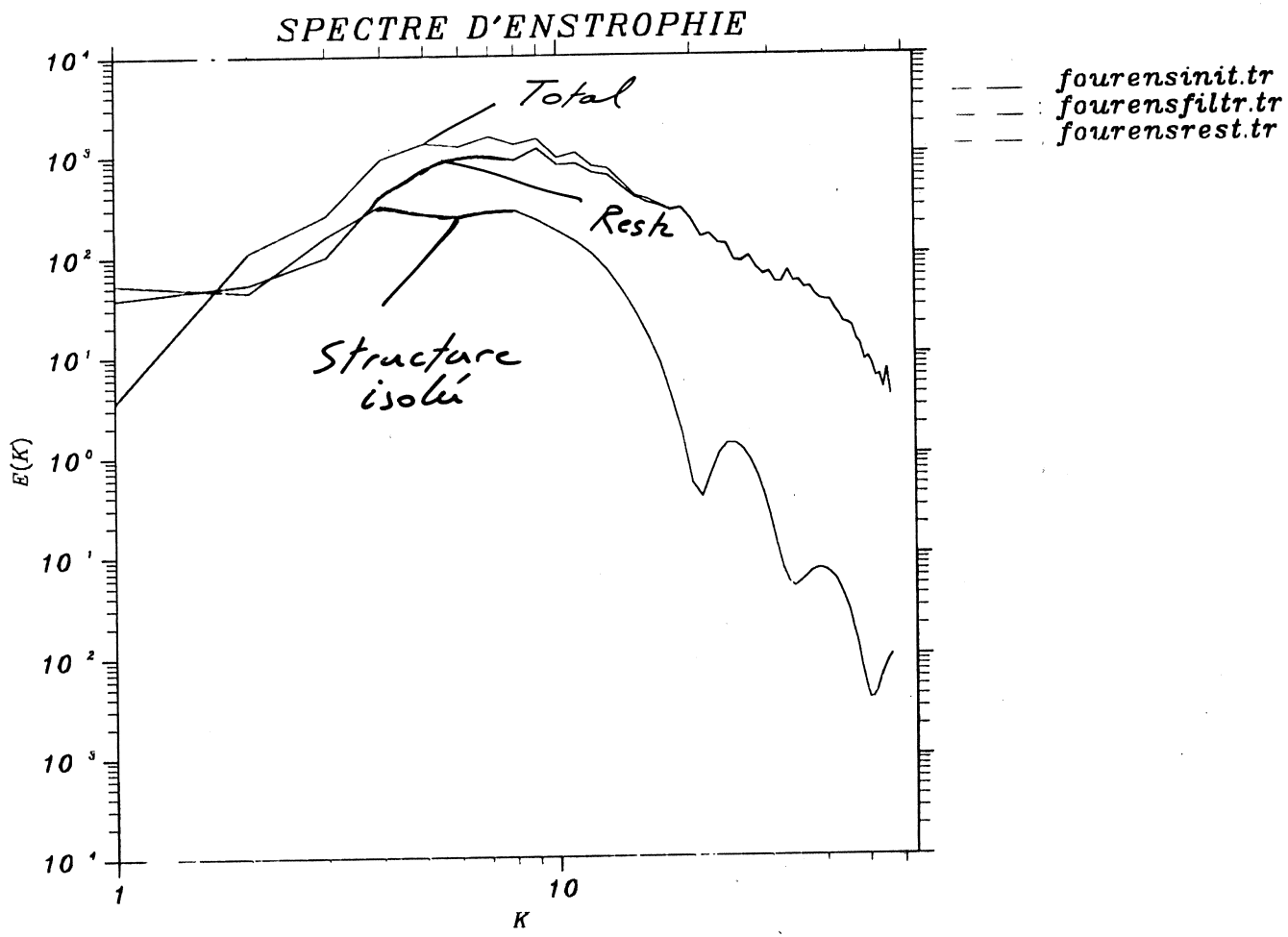

COMPRESSION

IN FOURIER MODES:

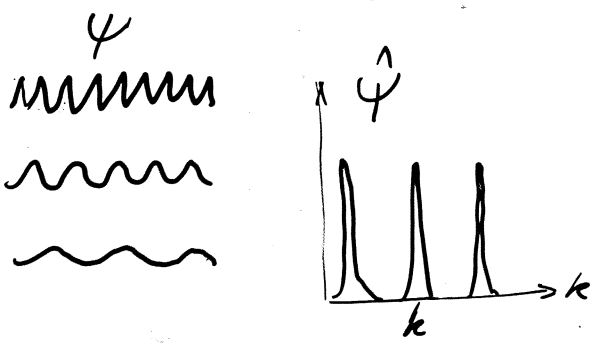

$$\hat{\omega}(k) = \langle \psi_k | \omega \rangle$$

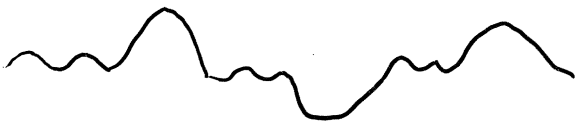

$$\omega_> = |\hat{\omega}_>\rangle\langle\psi|$$

Smooth the coherent vortices
⇒ loss of coherent enstrophy

&

Spurious oscillations in the background due to the loss of phase information

$$\omega_< = |\hat{\omega}_<\rangle\langle\psi|$$



non homogeneous background ⇒ cannot be modelled

IN WAVELET MODES:

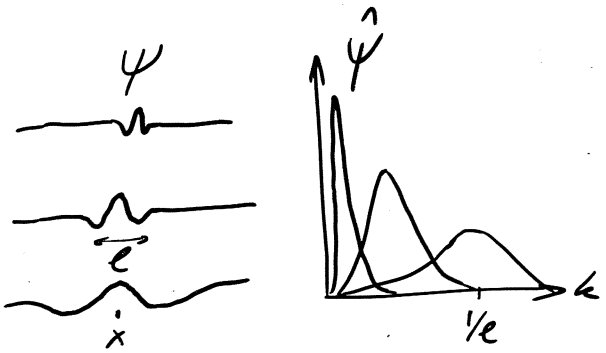

$$\tilde{\omega}(\ell, x) = \langle \psi_{\ell,x} | \omega \rangle$$



$$\omega_> = |\tilde{\omega}_>\rangle\langle\psi|$$

Respect the quasi-singularity of vortices ⇒ no loss of coherent enstrophy

&

no spurious oscillations in the background

$$\omega_< = |\tilde{\omega}_<\rangle\langle\psi|$$



homogeneous background ⇒ can be modelled

COMPRESSION OF VORTICITY FIELD IN 2D TURBULENT FLOWS

Linear Fourier compression

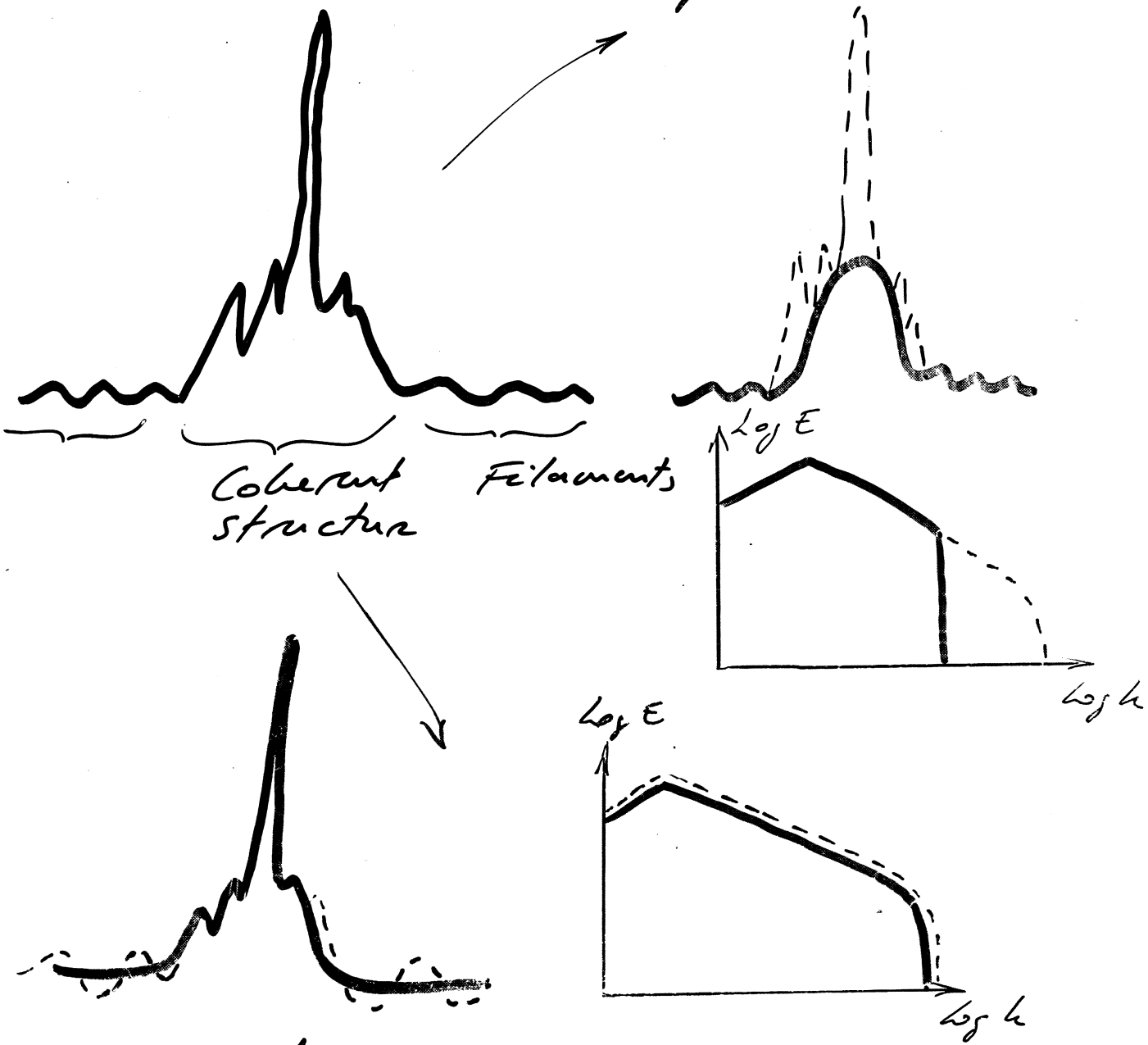

Non linear Wavelets compression

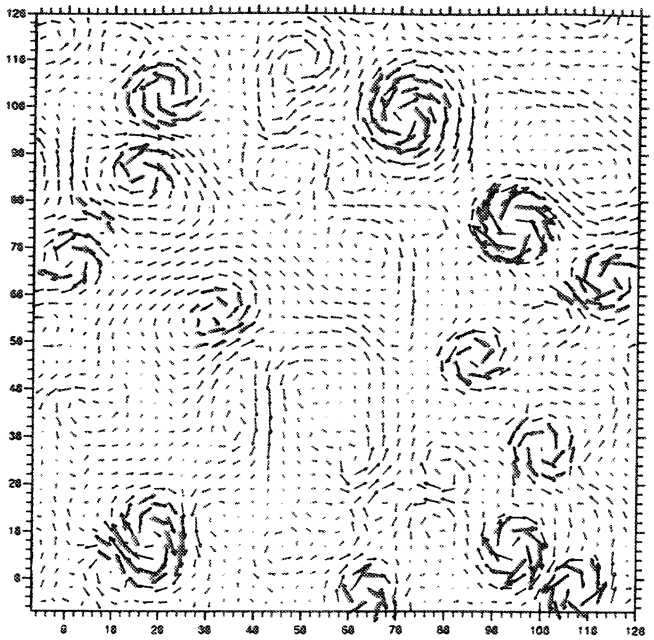

(a) Velocity

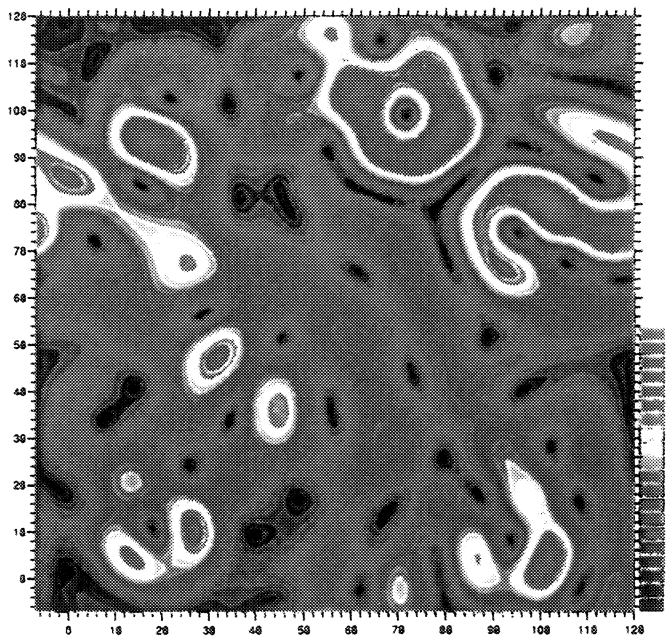

(b) Scale 64 Δx

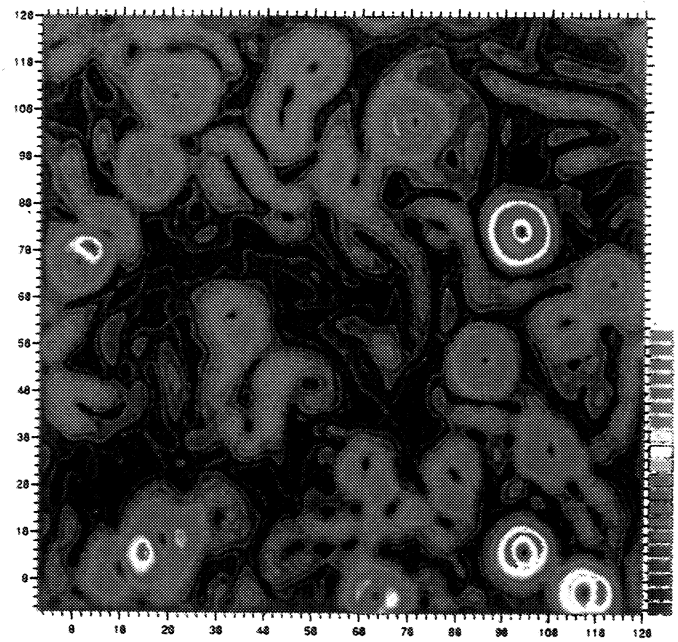

(c) Scale 20 Δx

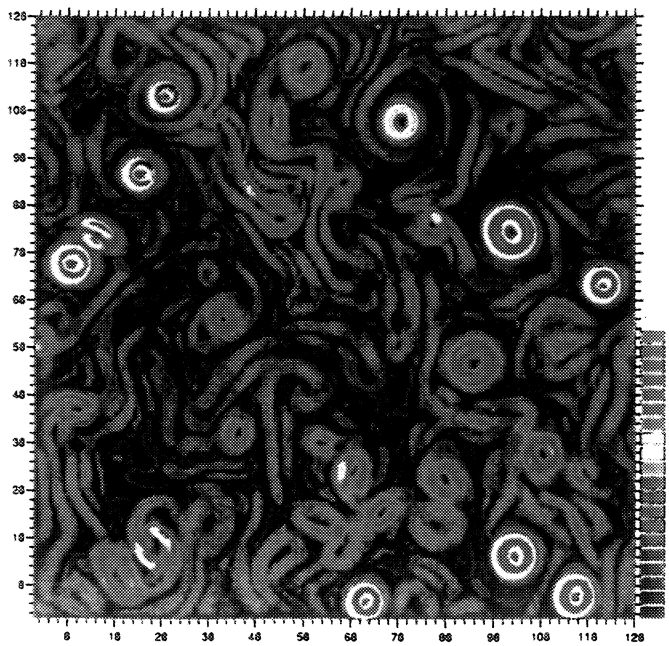

(d) Scale 8 Δx

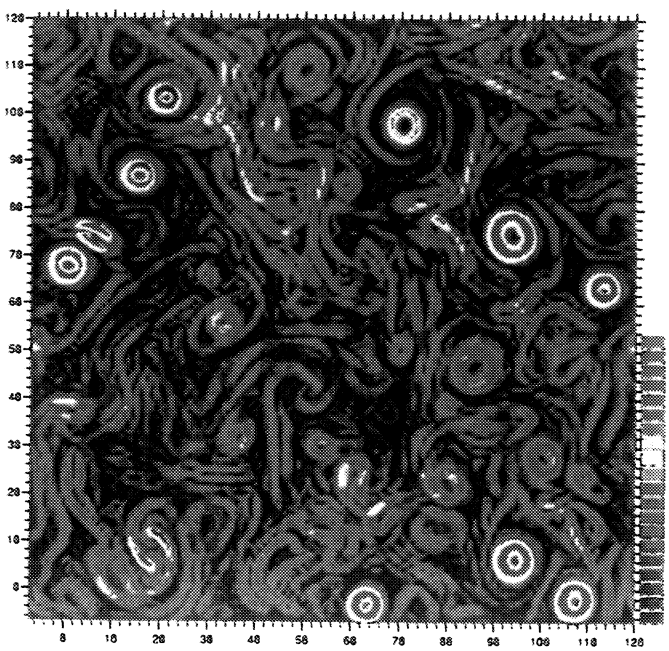

(e) Scale 2 Δx

Figure 5
Wavelet Reynolds number

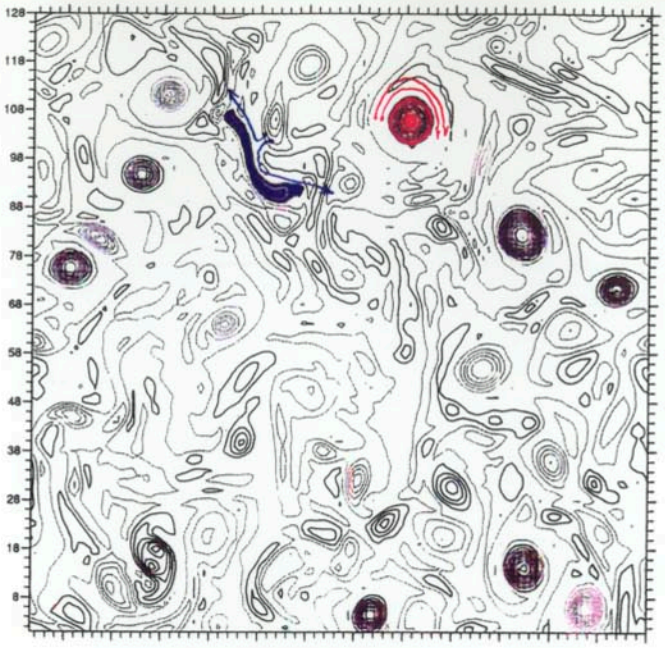

(a) Vorticity field

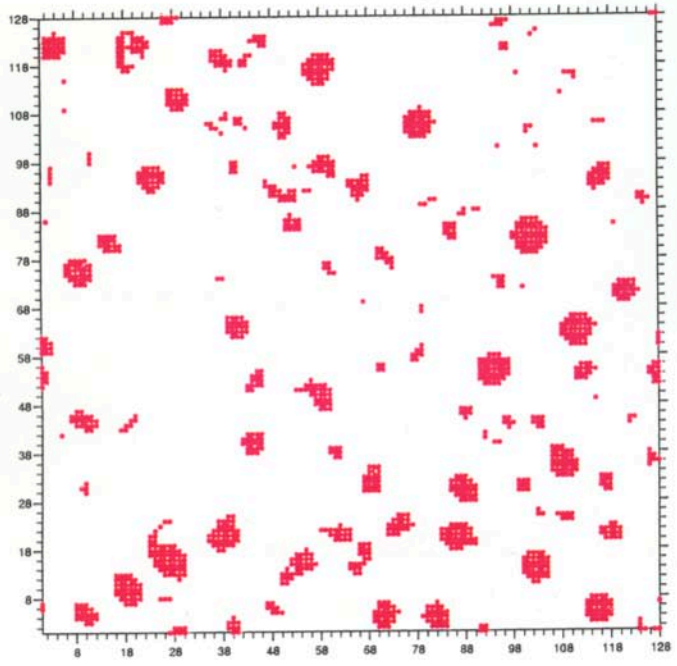

(b) Coherent vortices

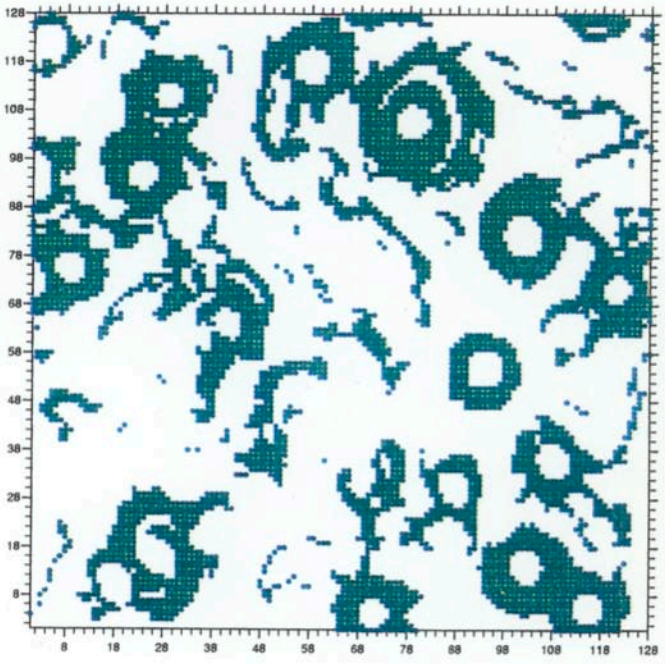

(c) Shear layers

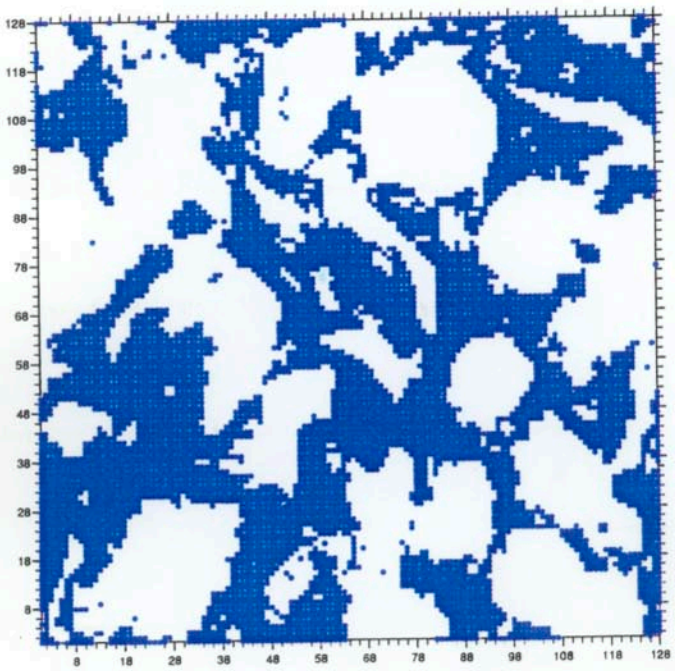

(d) Background flow

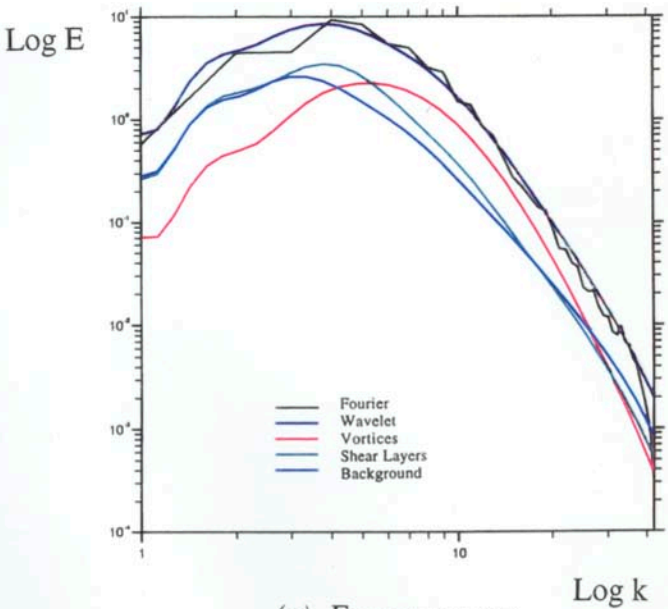

(e) Energy spectra

Figure 2
Conditional wavelet spectra

Wavelet Reynolds Number:

$$\tilde{Re}(\ell,\vec{x}) = \frac{\tilde{u}(\ell,\vec{x})\,\ell}{\nu}$$

with

$$\tilde{u}(\ell,\vec{x}) = \left[\frac{1}{3C_4}\sum_{i=1}^{3}|\tilde{u}_i(\ell,\vec{x})|^2\right]^{1/2}$$

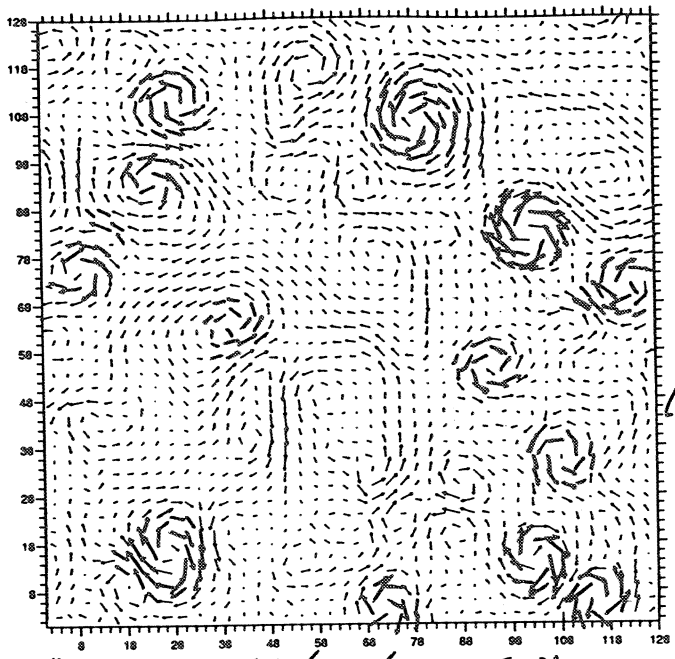

Velocity $\vec{u}(\vec{x})$

64 Δx

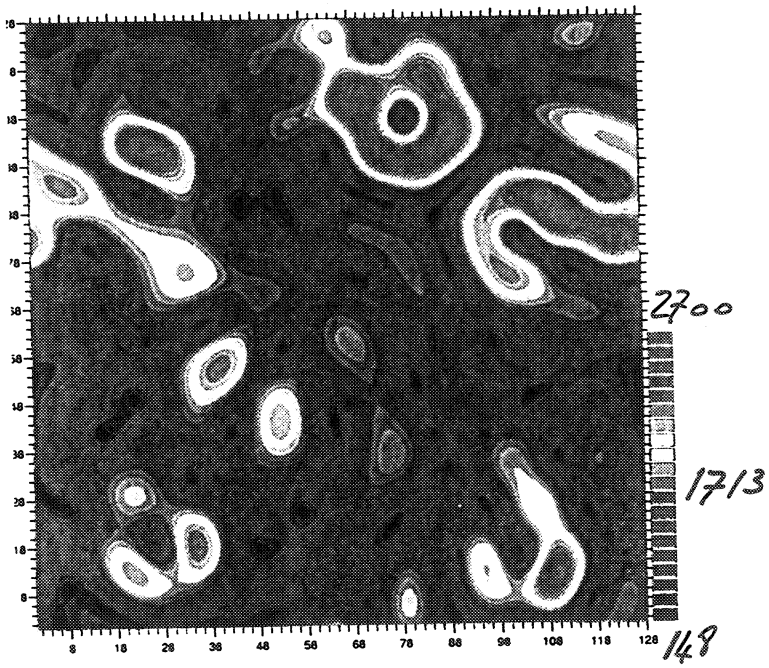

20 Δx

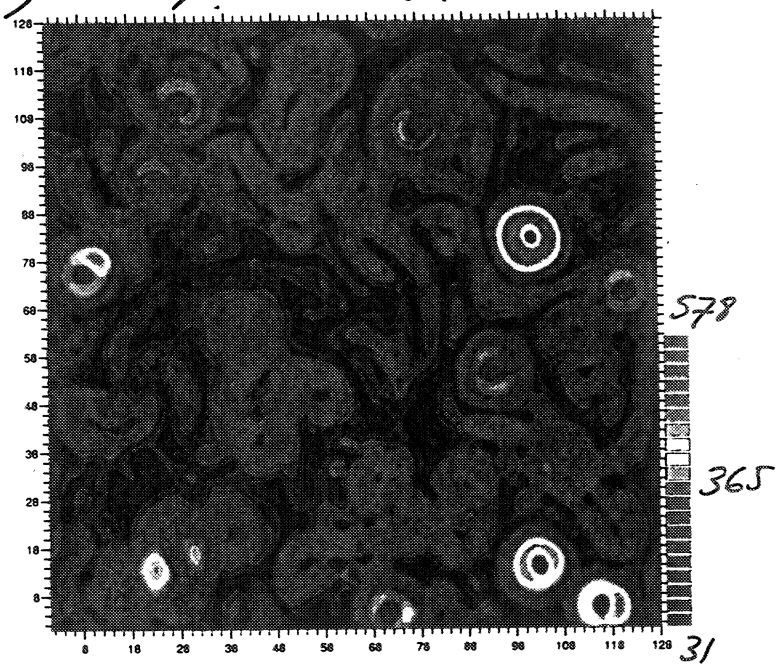

8 Δx

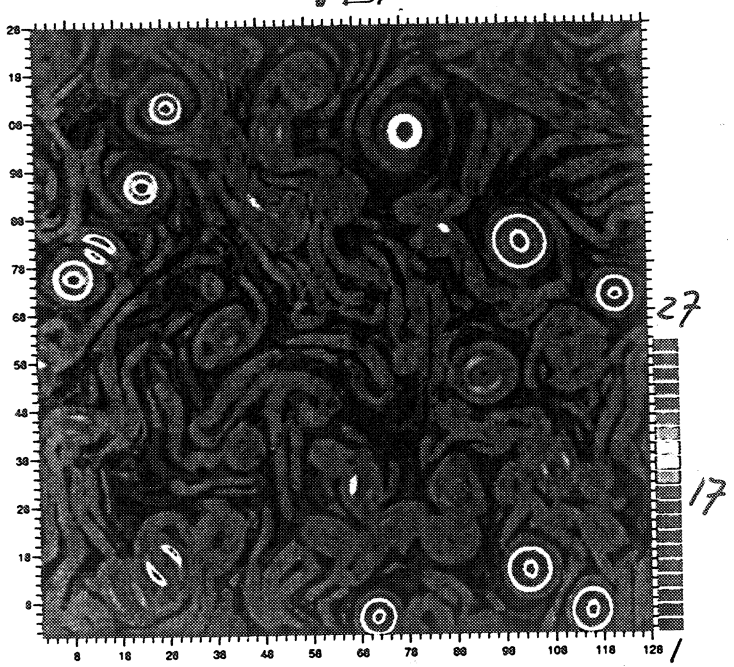

2 Δx

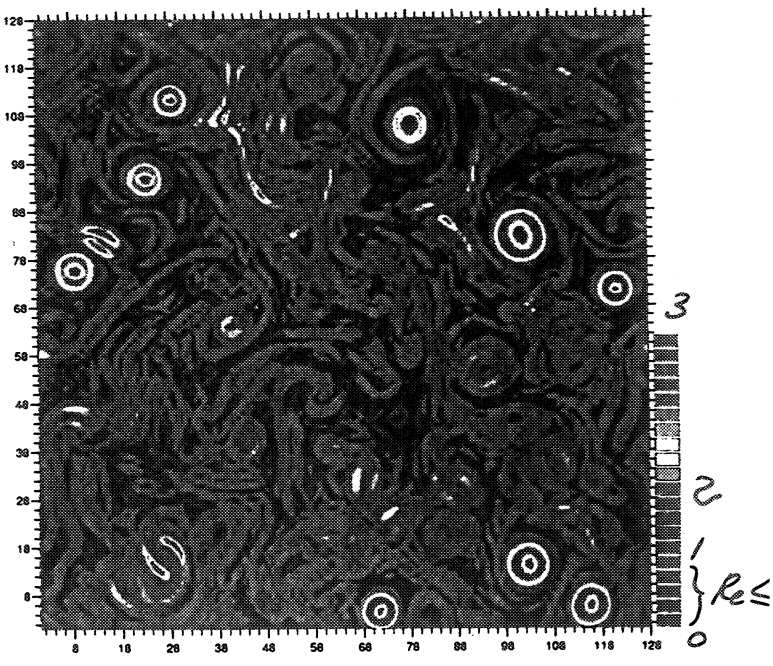

(Collaboration with Thierry Philipovitch)
1992



(a) Uncompressed vorticity field



(b) Vorticity compressed in a wavelet packet basis

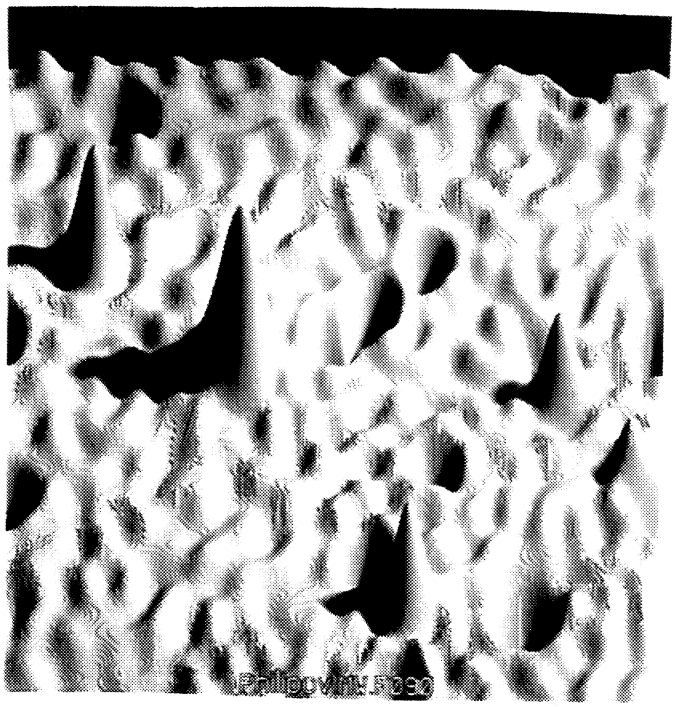

(c) Vorticity compressed in an adapted local cosine basis

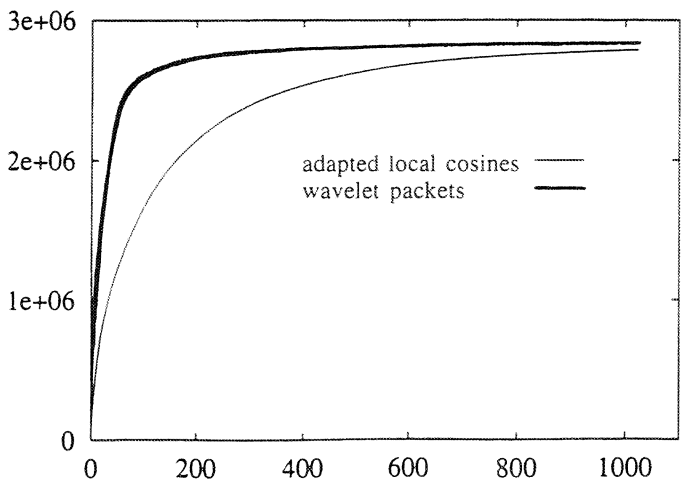

(d) Amount of enstrophy retained for each compression

Figure 4
Comparison between wavelet packet and adapted local cosine compression

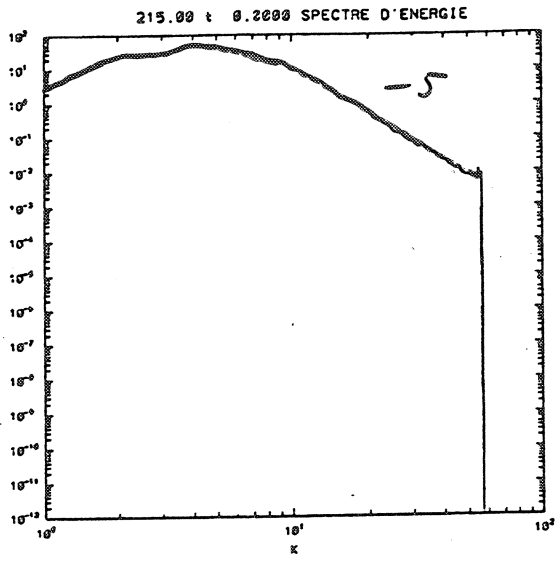



Vorticity field

Compression by 2

ω_1 50%

ω_2 50%

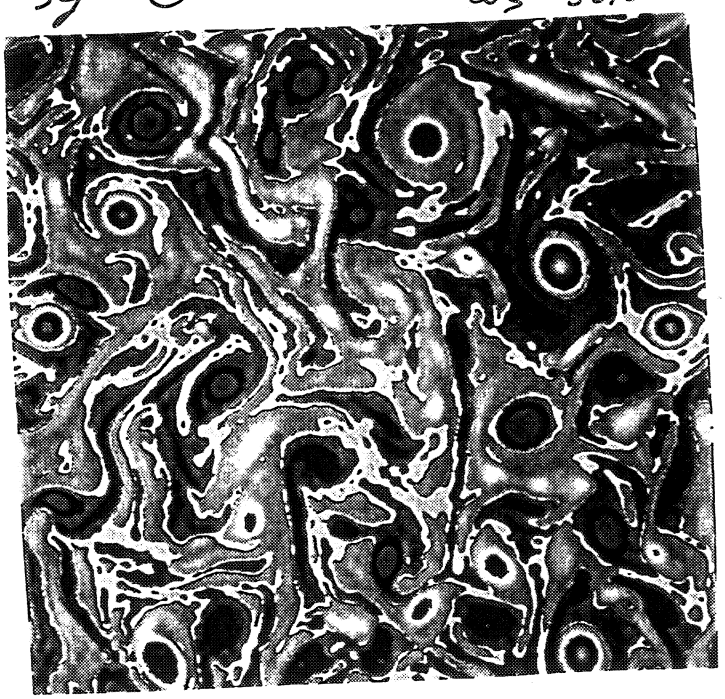

+

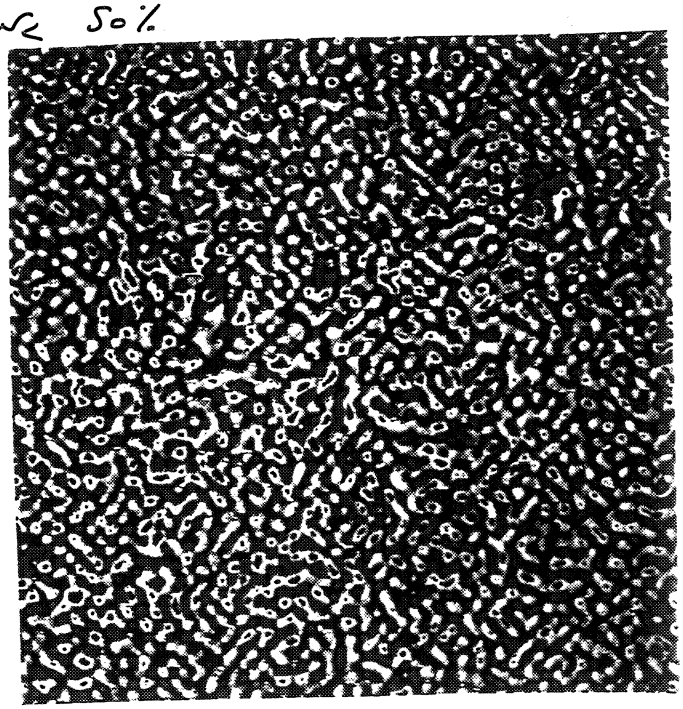

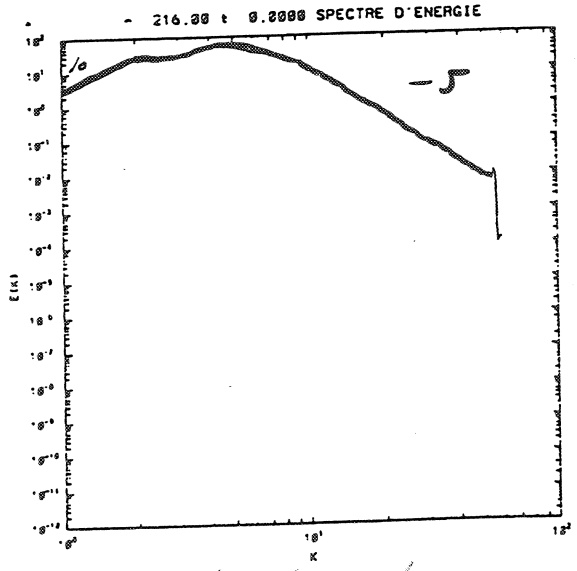

Splitting using orthonormal wavelet packets

99.96%

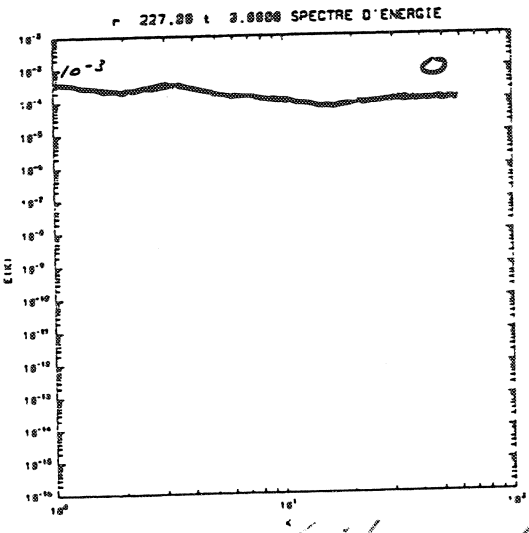

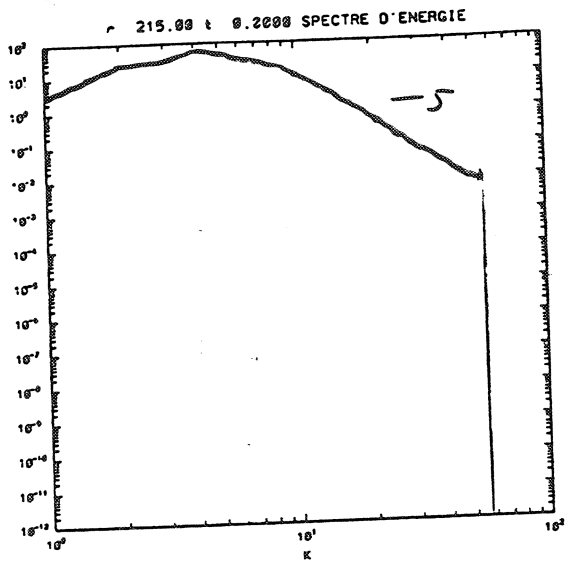

Vertical field



ω 100%

Compression by 2

$\omega_>$ 50%

$\omega_<$ 50%

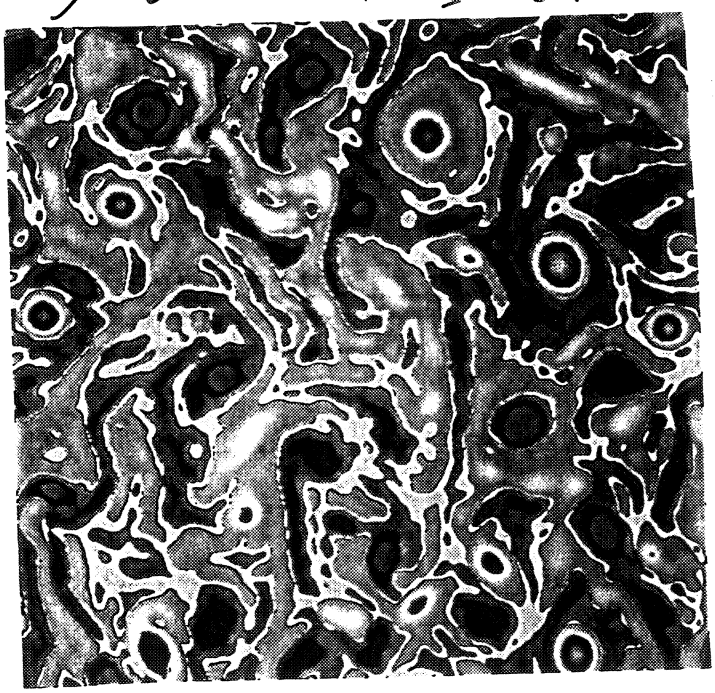

+

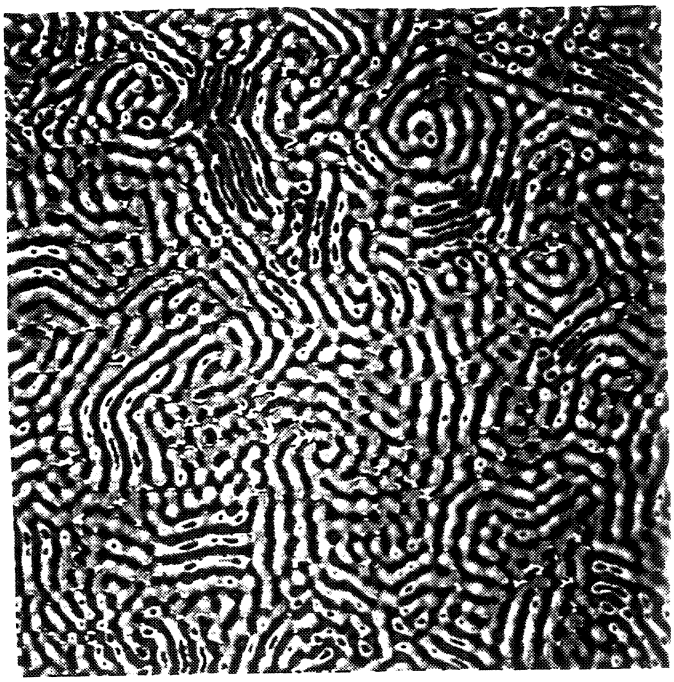

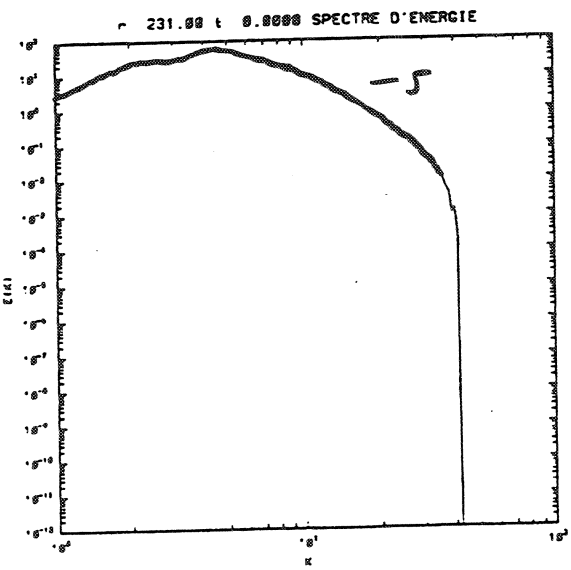

Low wavenumbers

Splitting using orthonormal Fourier modes

97%

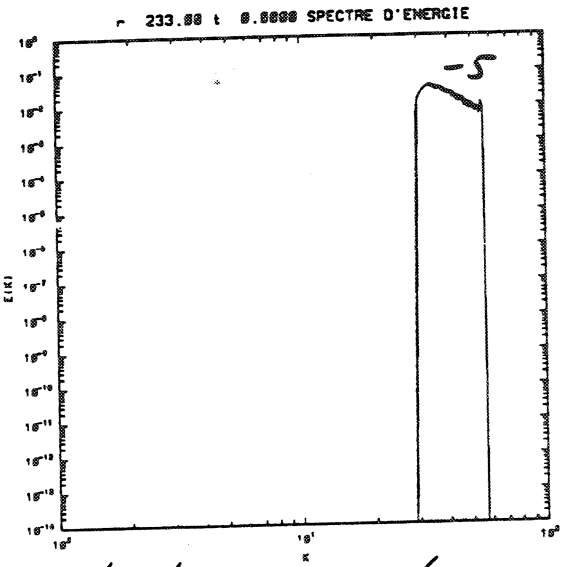

high wavenumbers

The uncompressed vorticity field and its Fourier spectrum

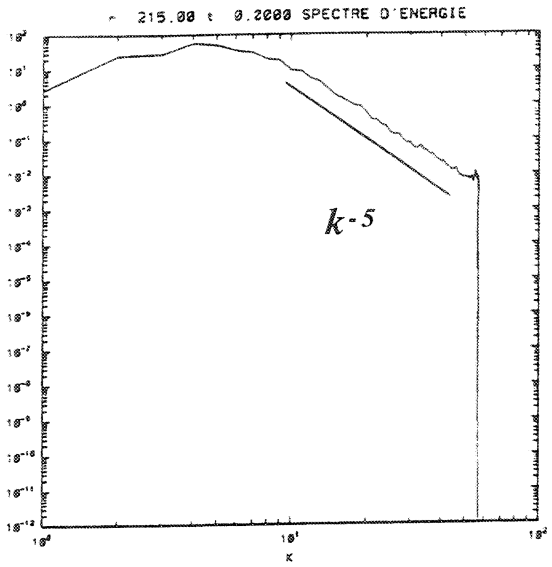



(a)

The vorticity field reconstructed from the 5% strongest wavelet packet coefficients

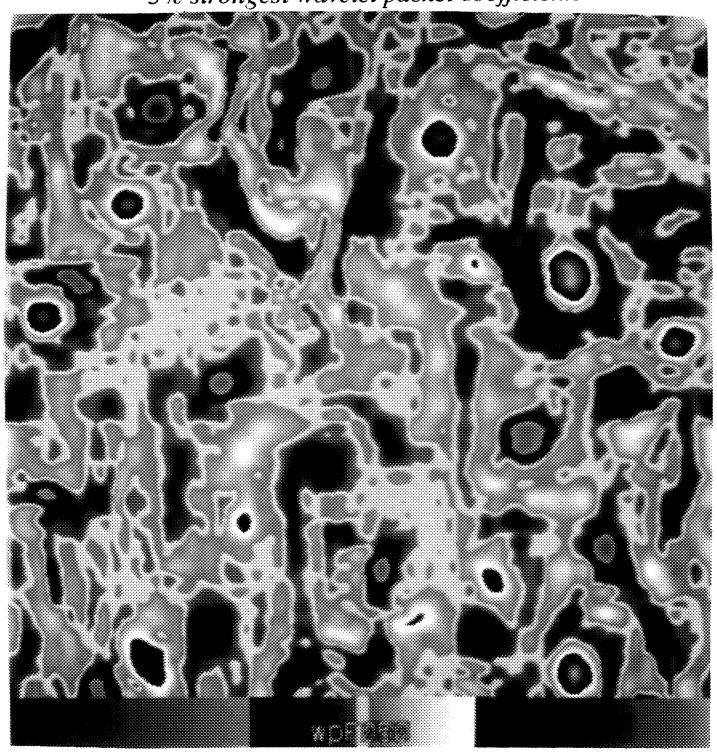

(b)

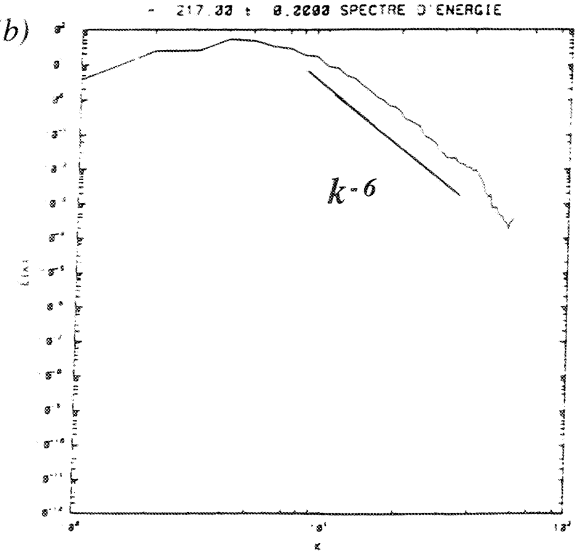

The vorticity field reconstructed from the 95% weakest wavelet packet coefficients

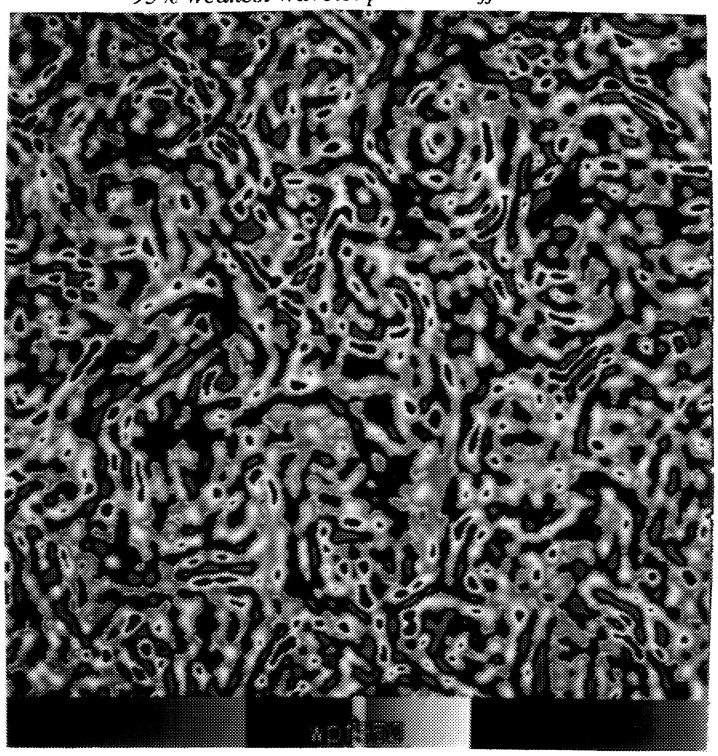

(c)

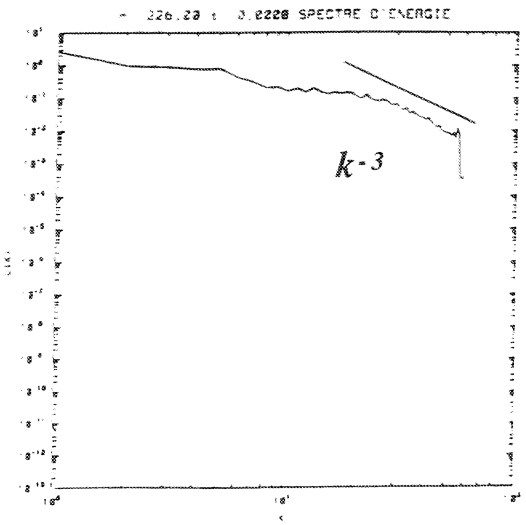

Figure 3 Wavelet packet compression of vorticity

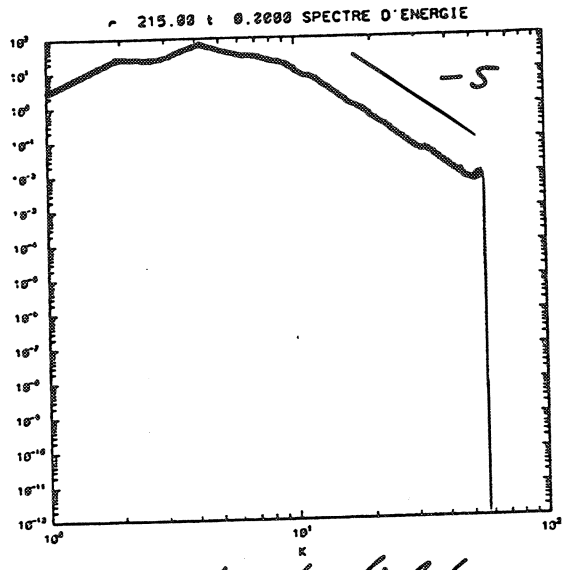

Vorticity field

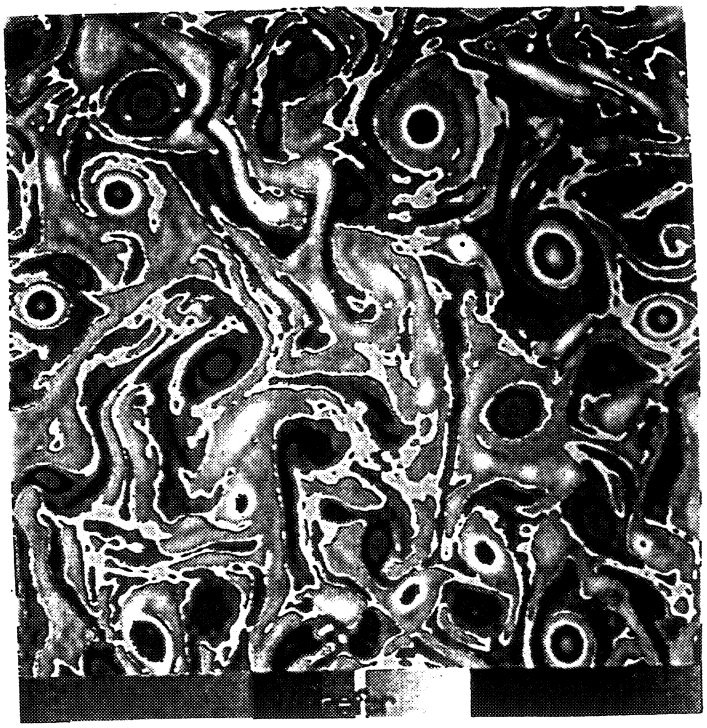

ω 100%

Compression by 2

ω_1 5%

ω_2 95%

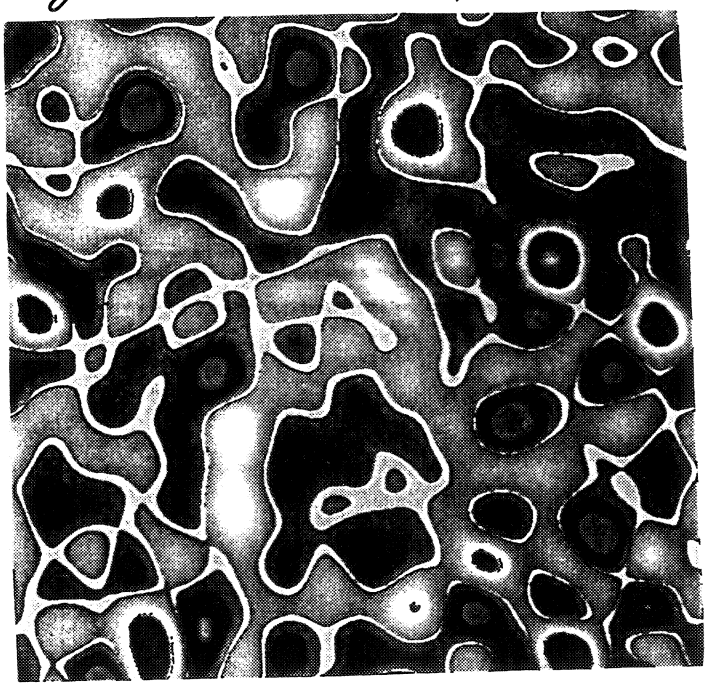

+

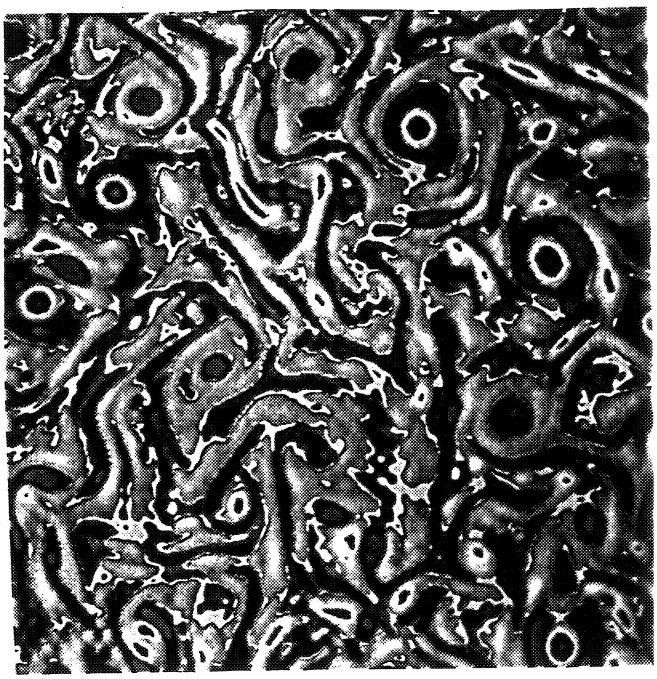

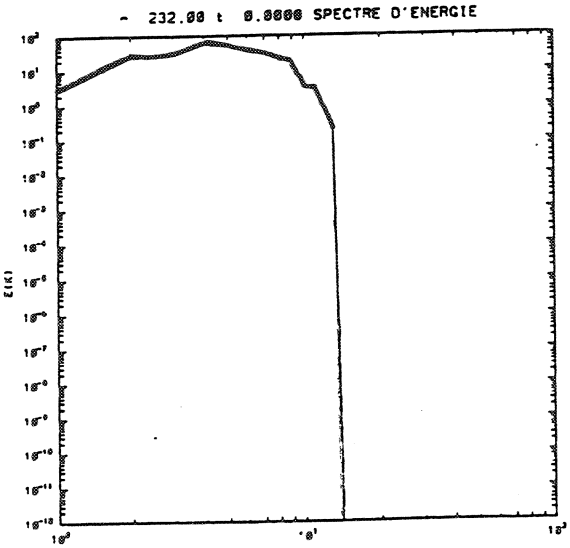

Low-wavenumber modes

Splitting using Fourier modes

58%

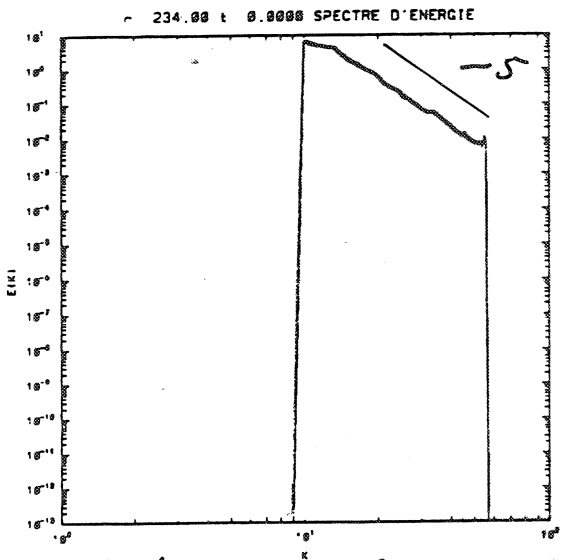

High-wavenumber modes

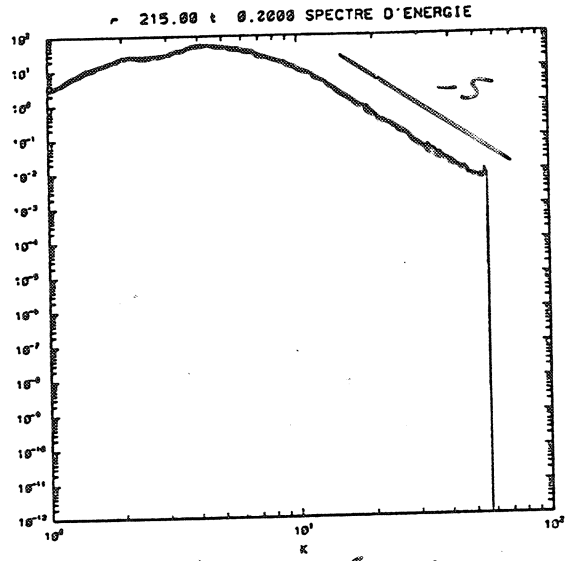

Vorticity field



ω 100%

Compression by 200

$\omega_>$ 0.5%

$\omega_<$ 99.5%

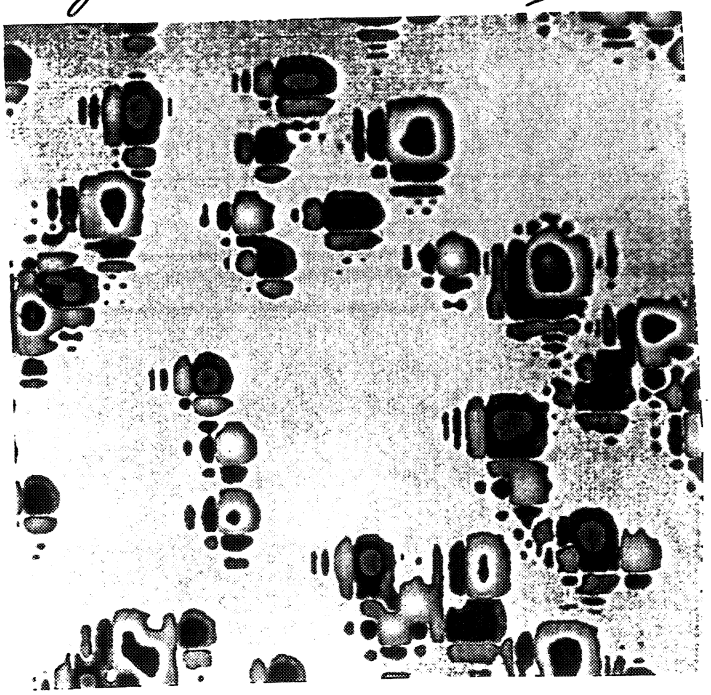

+



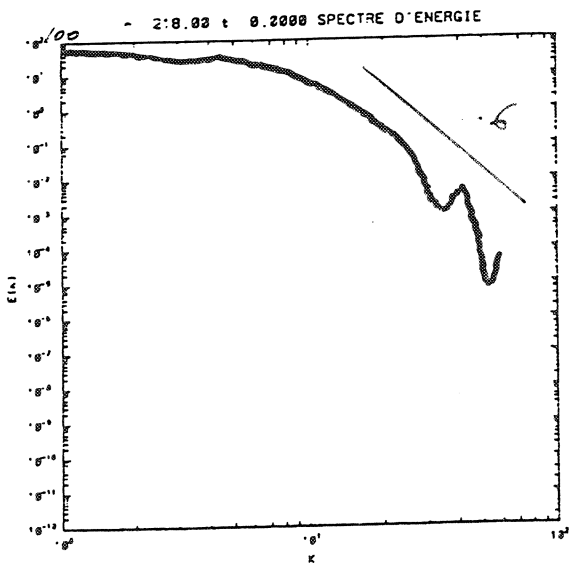

Splitting using orthonormal wavelet packets

55%

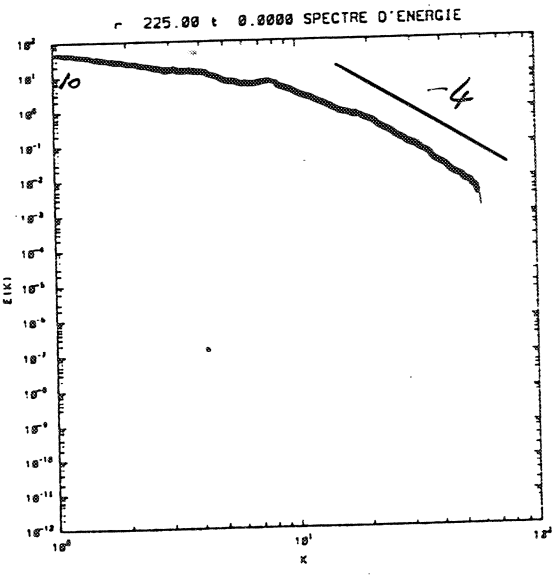

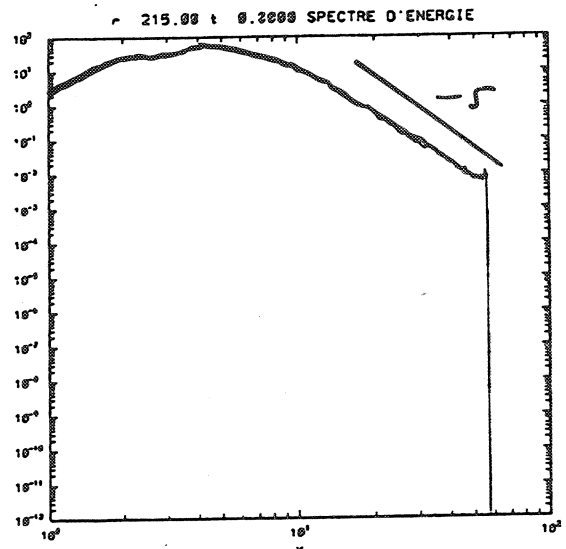

Vorticity field

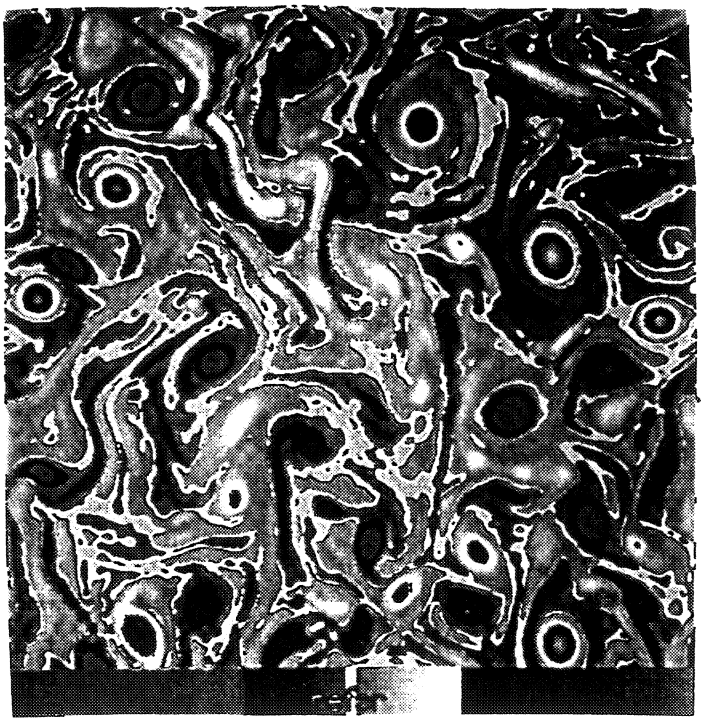

ω 100%

Compression by 200

$\omega_>$ 0.5%

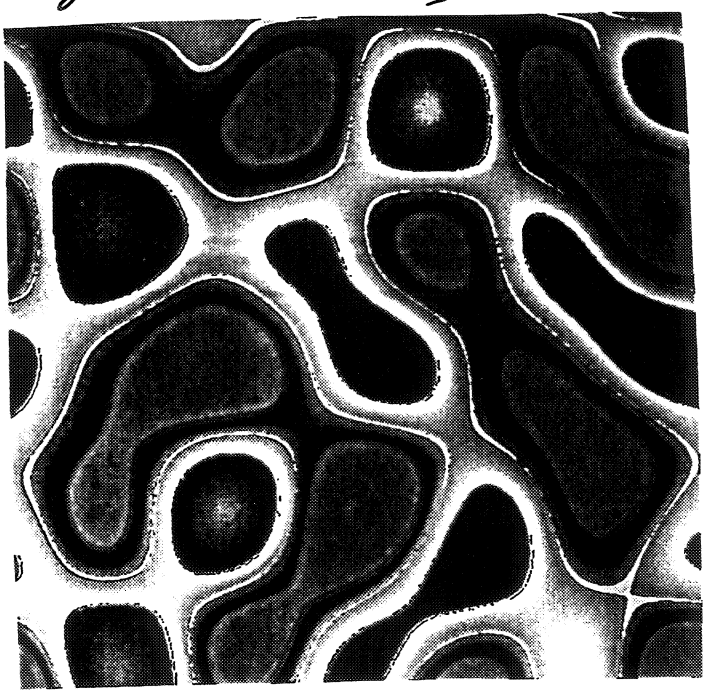

+

$\omega_<$ 99.5%

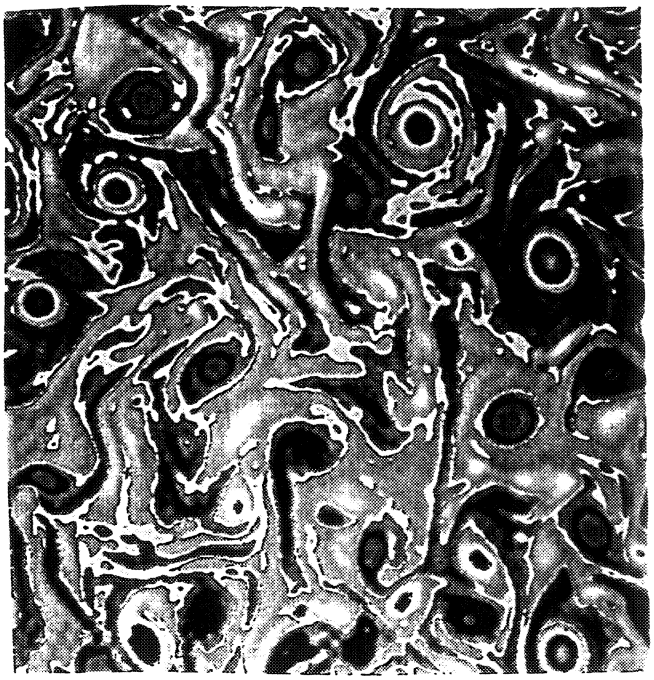

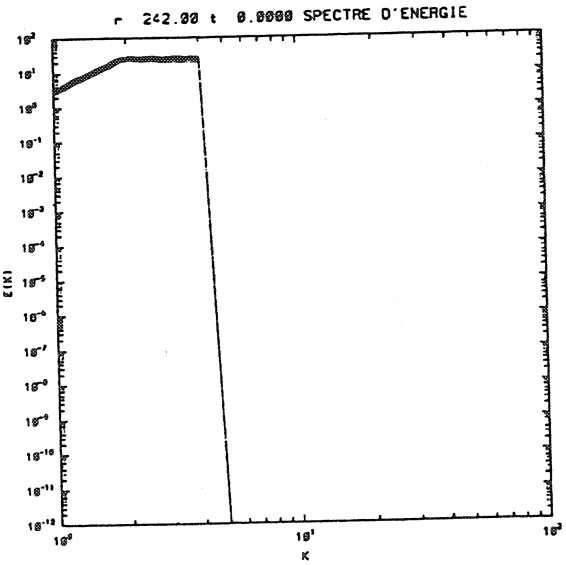

Splitting using orthonormal Fourier modes

5%

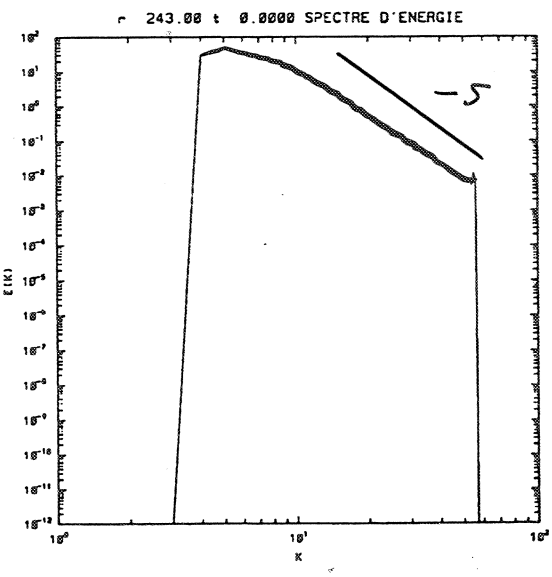

CONJECTURE

There are universal scalings in 2D turbulent flows depending on the regions:

1. elliptic regions k^{-6}
2. parabolic regions k^{-4}
3. hyperbolic regions k^{-3}

Then we may explain the observed variation of the spectral slop, which depends on both initial conditions and forcing:

it varies from k^{-6} to k^{-3} depending on the density of coherent structures and on their mean free-path between strong interactions

$\Rightarrow$

we have to define new statistics in terms of coherent structures

CONJECTURE

Non universality of the spectral laws observed in numerical simulations

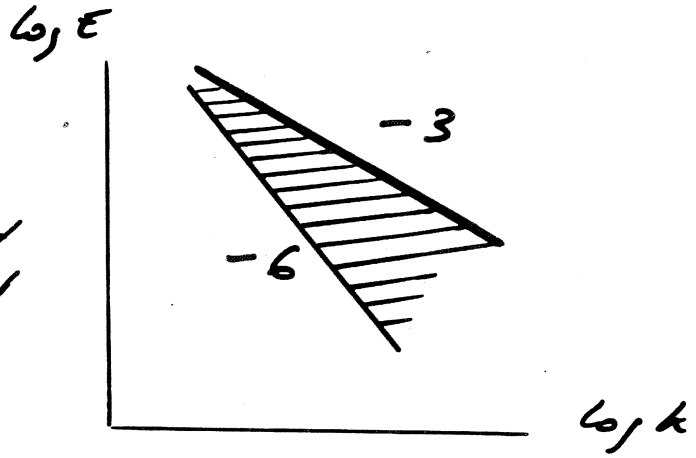

α

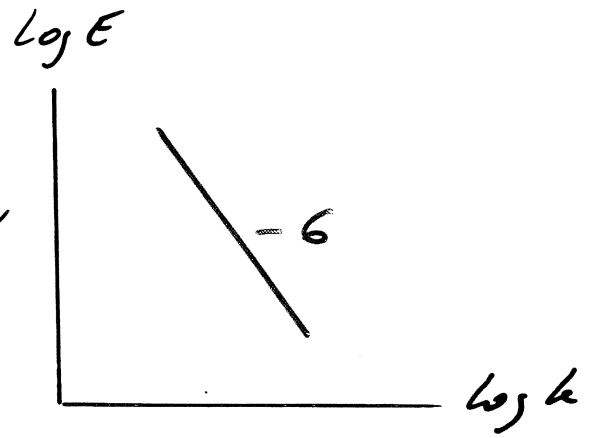

Possible universal law for the vortices scaling ?

+ β

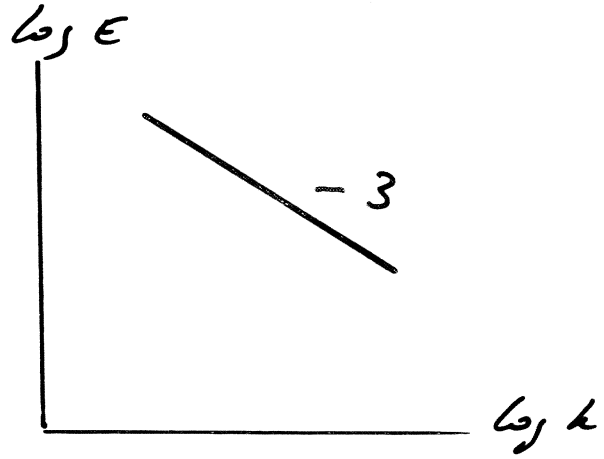

Universality law ('à la kraichnan') for the incoherent flow

with α and β depending on the probability density of vortices

CONCLUSION

Batchelor - Kraichnan hypotheses:

after averaging (in ensemble) 2D turbulent flows are generically homogeneous, the whole vorticity field participates to the direct enstrophy cascade, dissipation location is clear in space.

Our hypotheses:

2D turbulent flows are generically inhomogeneous and we should only perform conditional averaging.

they are compound of multi-scale coherent vortices embedded in a random quasi-irrotational flow,

enstrophy cascade and dissipation happen only in the shear layers surrounding strongly interacting vortices.

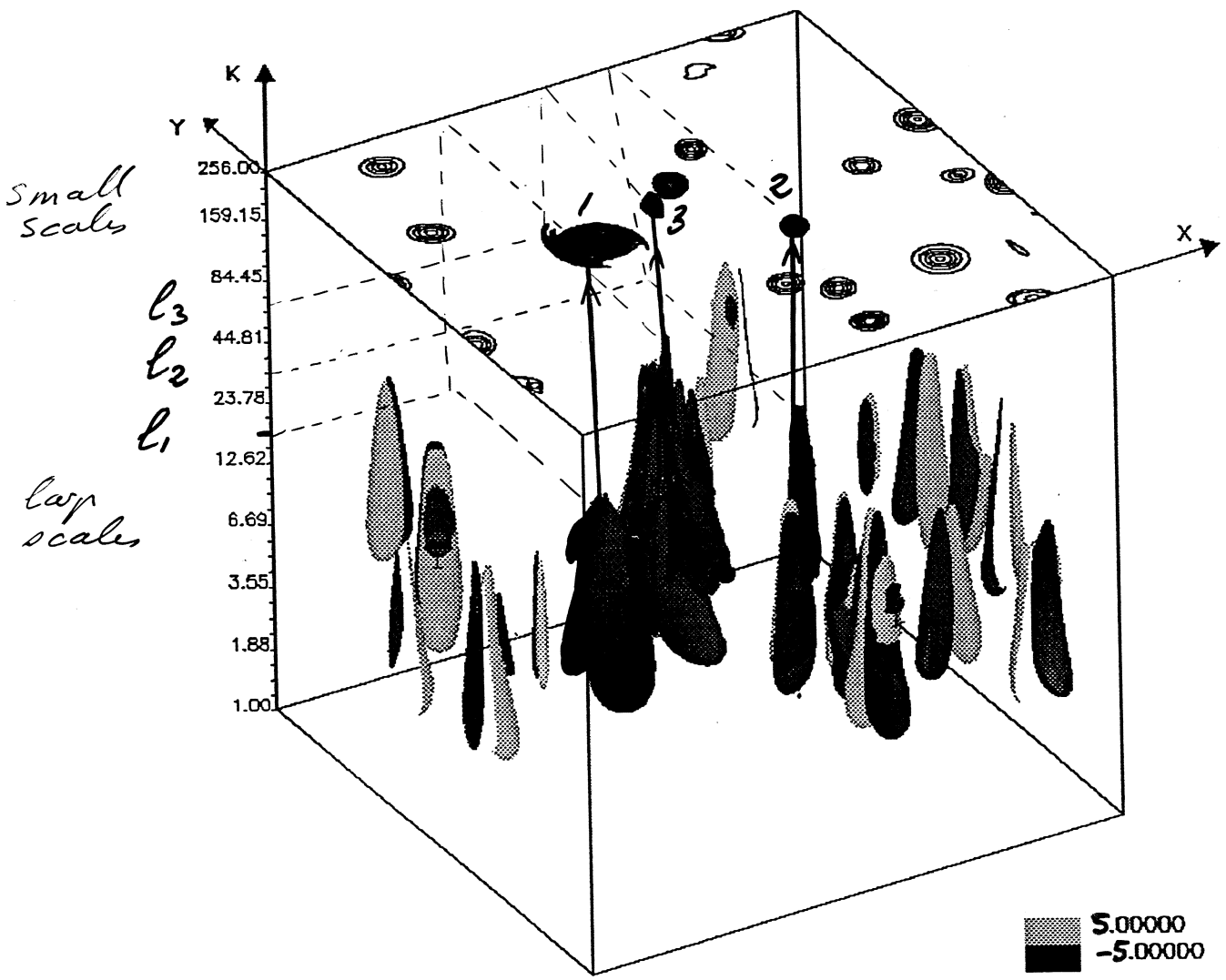

FIG. 4.94 - *Champ:R512d-38.(h_4). Transfert locaux d'enstrophie. Isosurface:±5.*

Local transfers of enstrophy $\widetilde{\omega \frac{\partial \omega}{\partial t}}$

THE ESSENTIAL QUESTION

Which are the dynamically active components of turbulent flows that we need to compute?

Namely, which are the 'leaders' and which are the 'followers'?

Method to identify them:

$w(t)$ { 1. Compute a 'reference' evolution with everyone, leaders + followers,

$w_1(t)$ { 2. Compute a 'compressed' evolution with only the leaders, check that this evolution is similar to the 'reference',

$w_2(t)$ { 3. Compute a 'residual' evolution with only the followers, check how the followers behave when the leaders are gone.

PREDICTABICITY

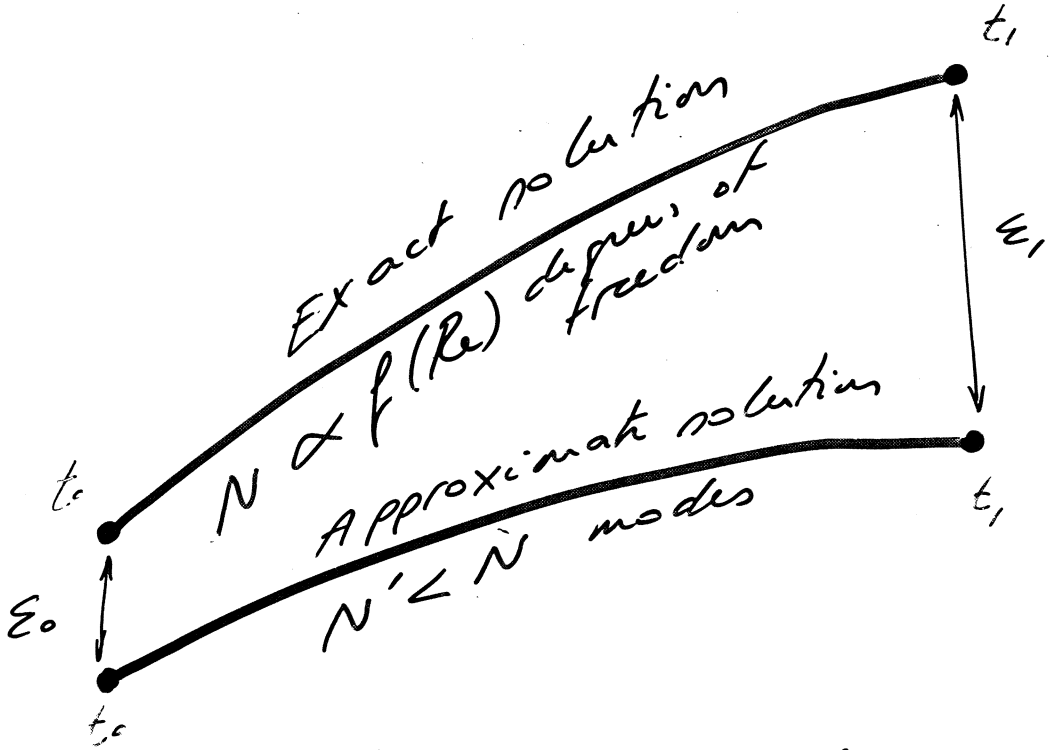

Find a projection of the initial flow which minimizes ε_0

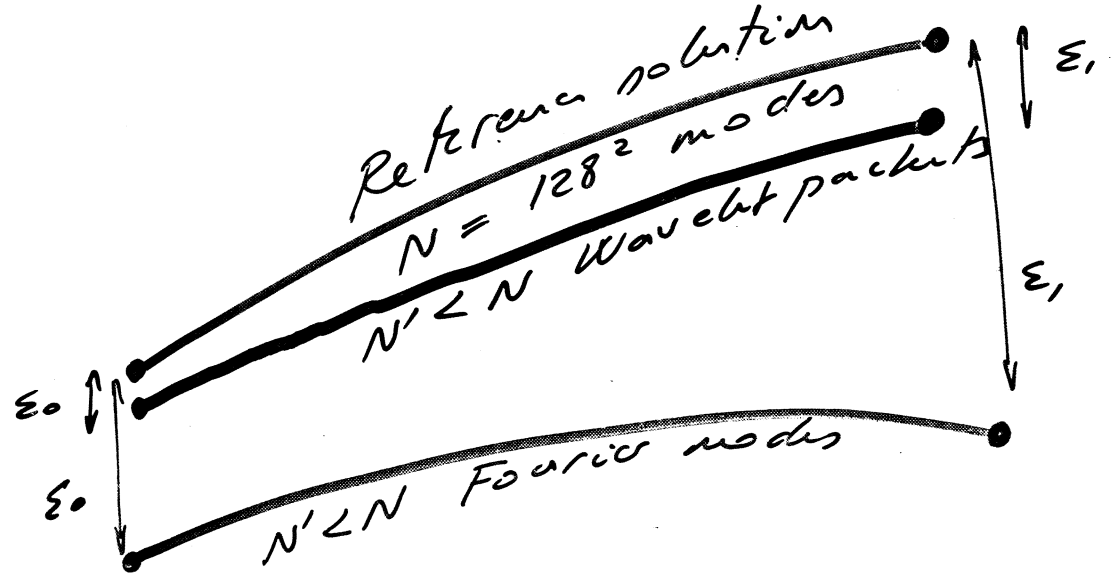

Bootstrap

Next step, compute flow evolution in the best basis

RESULTS

We compute the time evolution during 6000 time steps of different initially compressed flows using a 128^2 pseudo-spectral code with an hyperdissipation.

We compare their predictability

2 types of compressions:

1. Linear in Fourier basis,
2. Nonlinear in Wavelet Packet 'Best basis'.

f

$\tilde{f}$

$f_>$: 50%, 5% and 0.5% of the strongest coefficients (if non linear) or of the lowest wavenumbers (if linear)

then

$f_<$: 50%, 95% and 99.5% of the weakest coefficients (if non linear) or of the highest wavenumbers (if linear).



t = 0
Reference

Wavelet Packets

Fourier





50% WP 99.96% E

50% Fourier 97% E

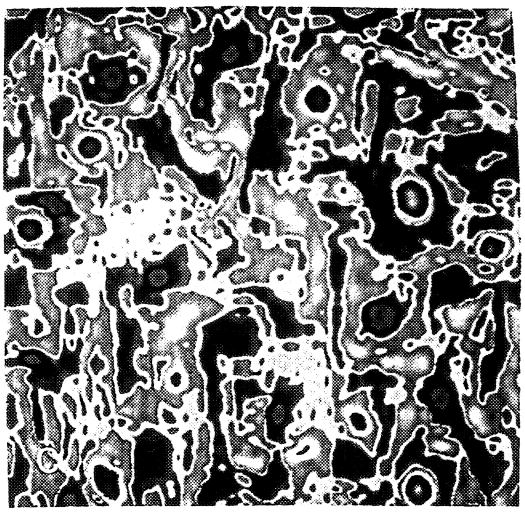

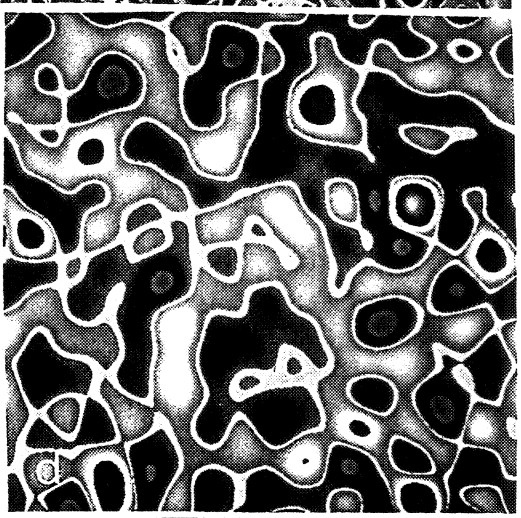

5% WP 89% E

5% Fourier 58% E

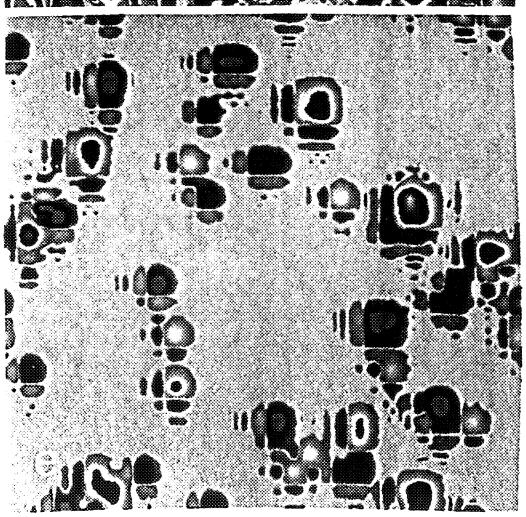

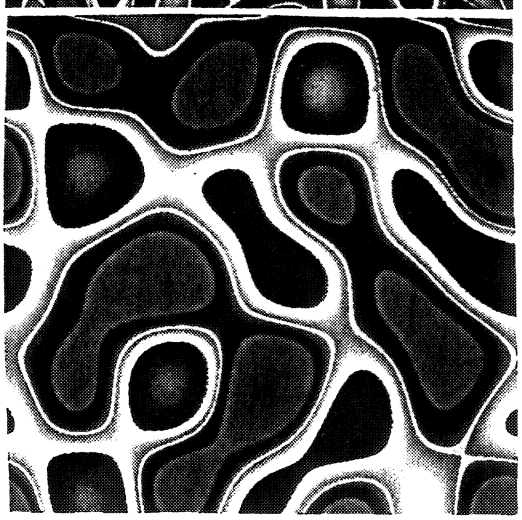

0.5% WP 55% E

0.5% Fourier 5% E

(Collaboration with Eric Goirand)
Fluid Dyn. Res., 1992

t = 6000
Reference

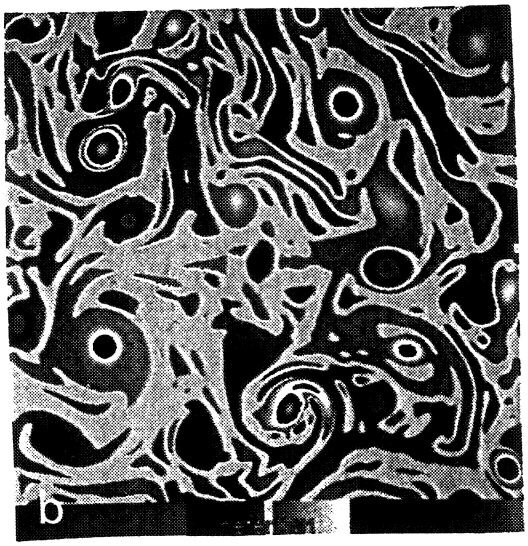

Wavelet Packets

Fourier

50% WP



50% Fourier

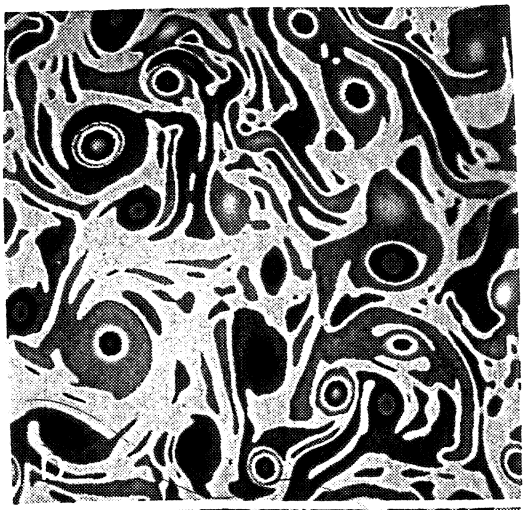

5% WP



5% Fourier



0.5% WP

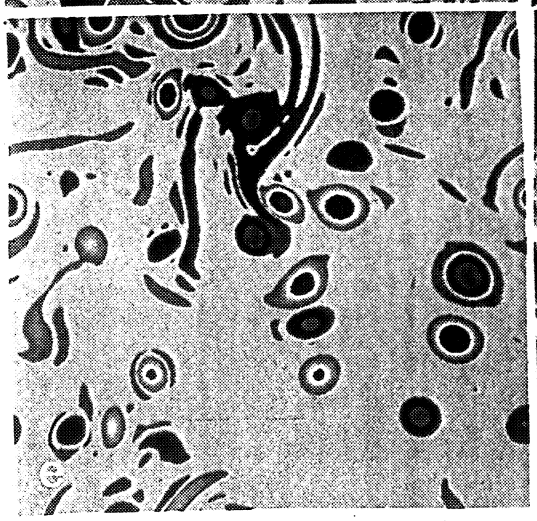

0.5% Fourier



Nicholas KEVLAHAN

Marie FARGE

JFM 77

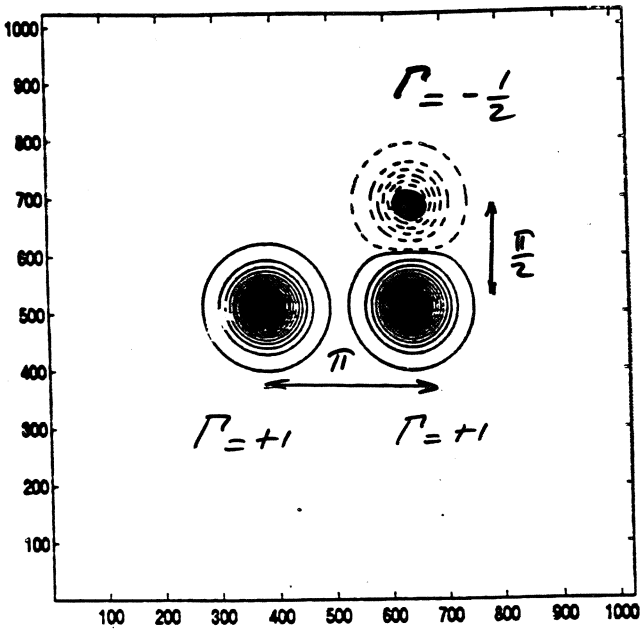

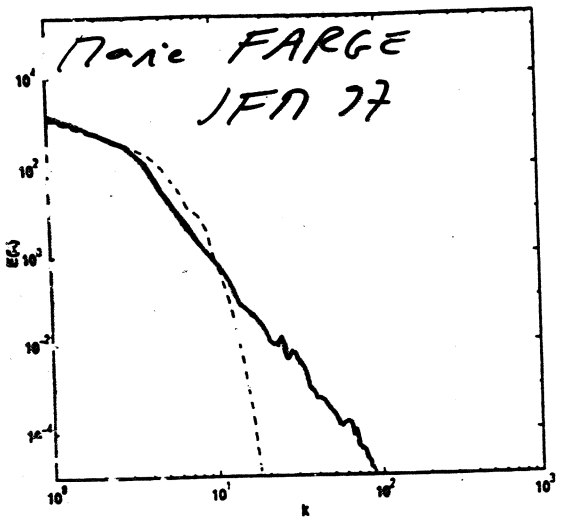

$N = 1024^2$

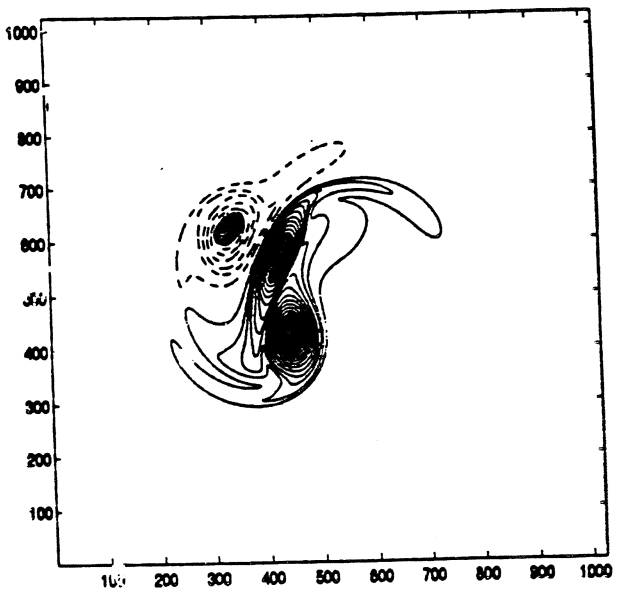

(a) $t = 10$

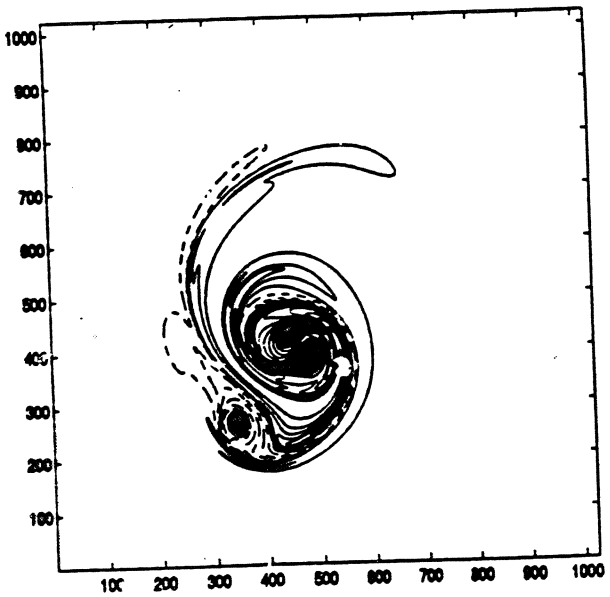

(b) $t = 20$

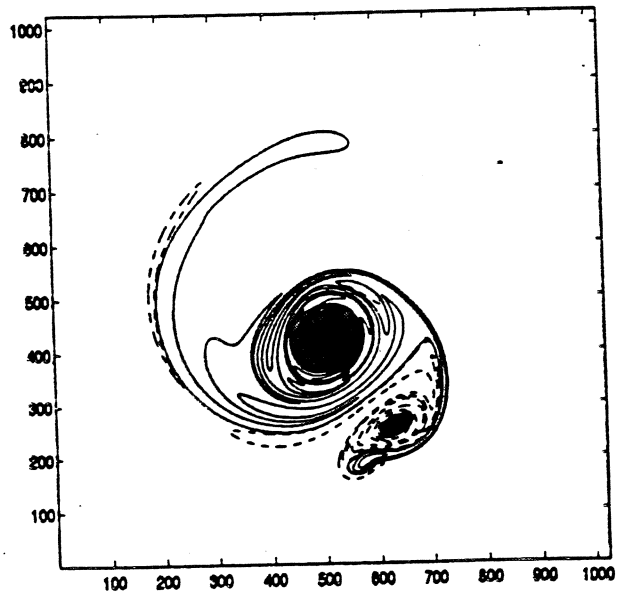

(c) $t = 30$

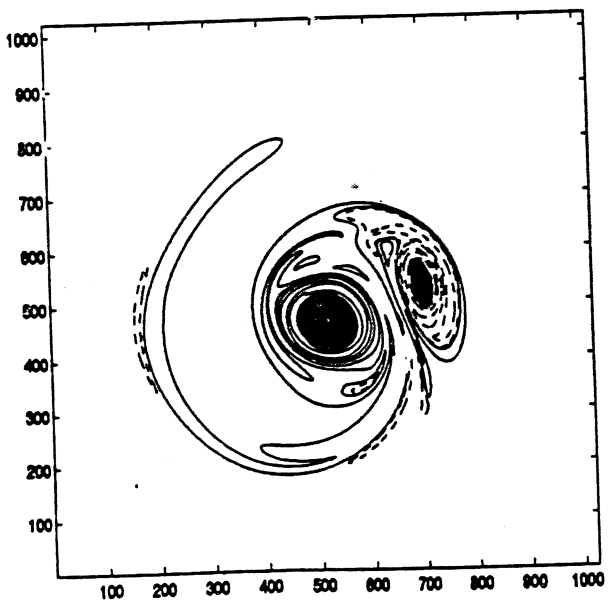

(d) $t = 40$

Pseudo-Fourier



$t = 29$
with
hyperdissi-
pation
$D = 40(-\nabla^2)^8$
Resolution
1024^2

Direct
Numerical
Simulation
of 2D
Navier-
Stokes
equations

(Farge et
Kevlahan,
1997, JFM)

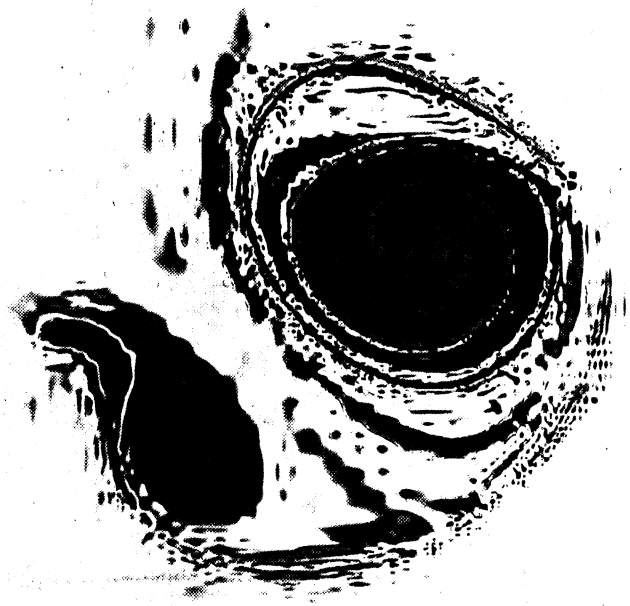



95%
eustroply

928
strong WP
coefficients

Compression
Sy 400



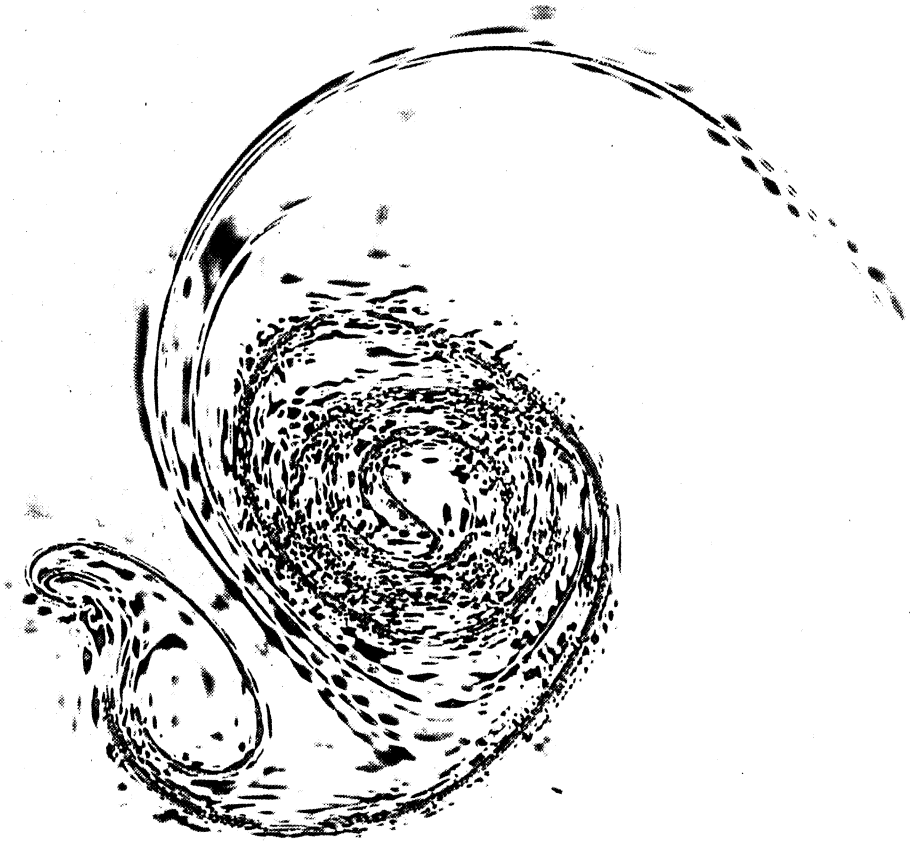

+4.0e+00

5% enstrophy

932 573 weak WP coefficients

+0.0e+00

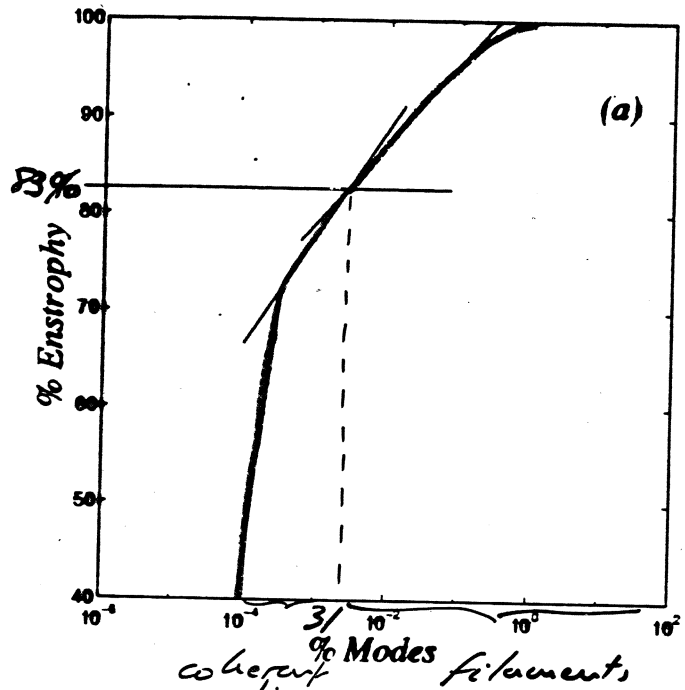

coherent vortices filaments

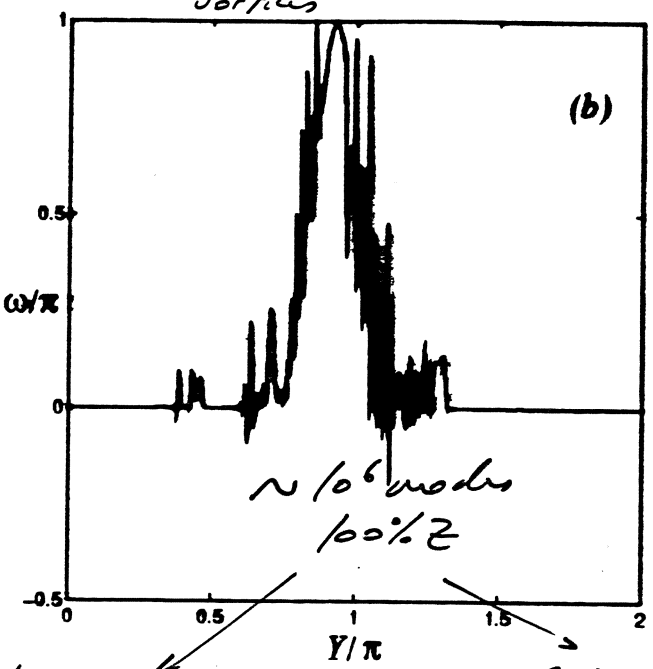

~ 10^6 modes
100% Z

Coherent vortices

filaments

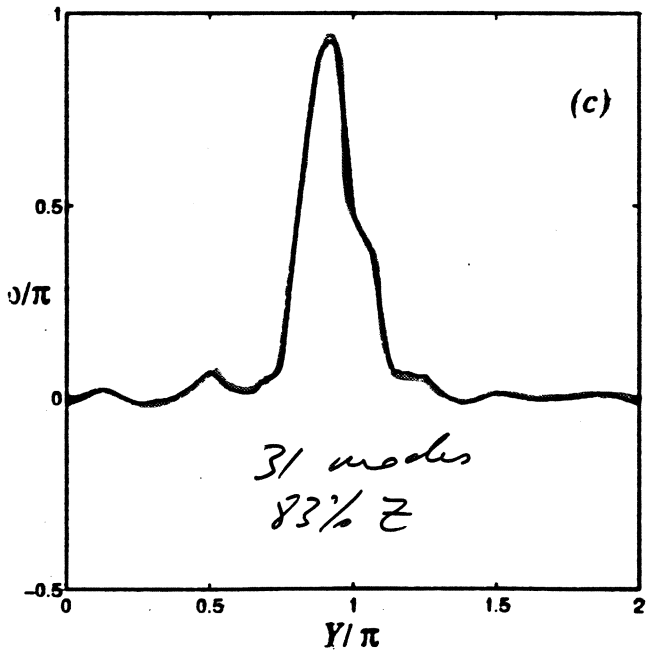

31 modes
83% Z

+

~ 10^6 modes
17% Z

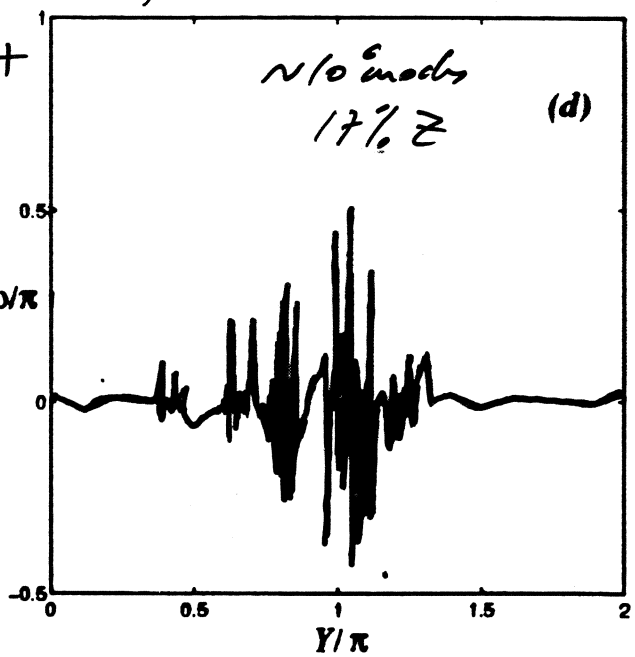

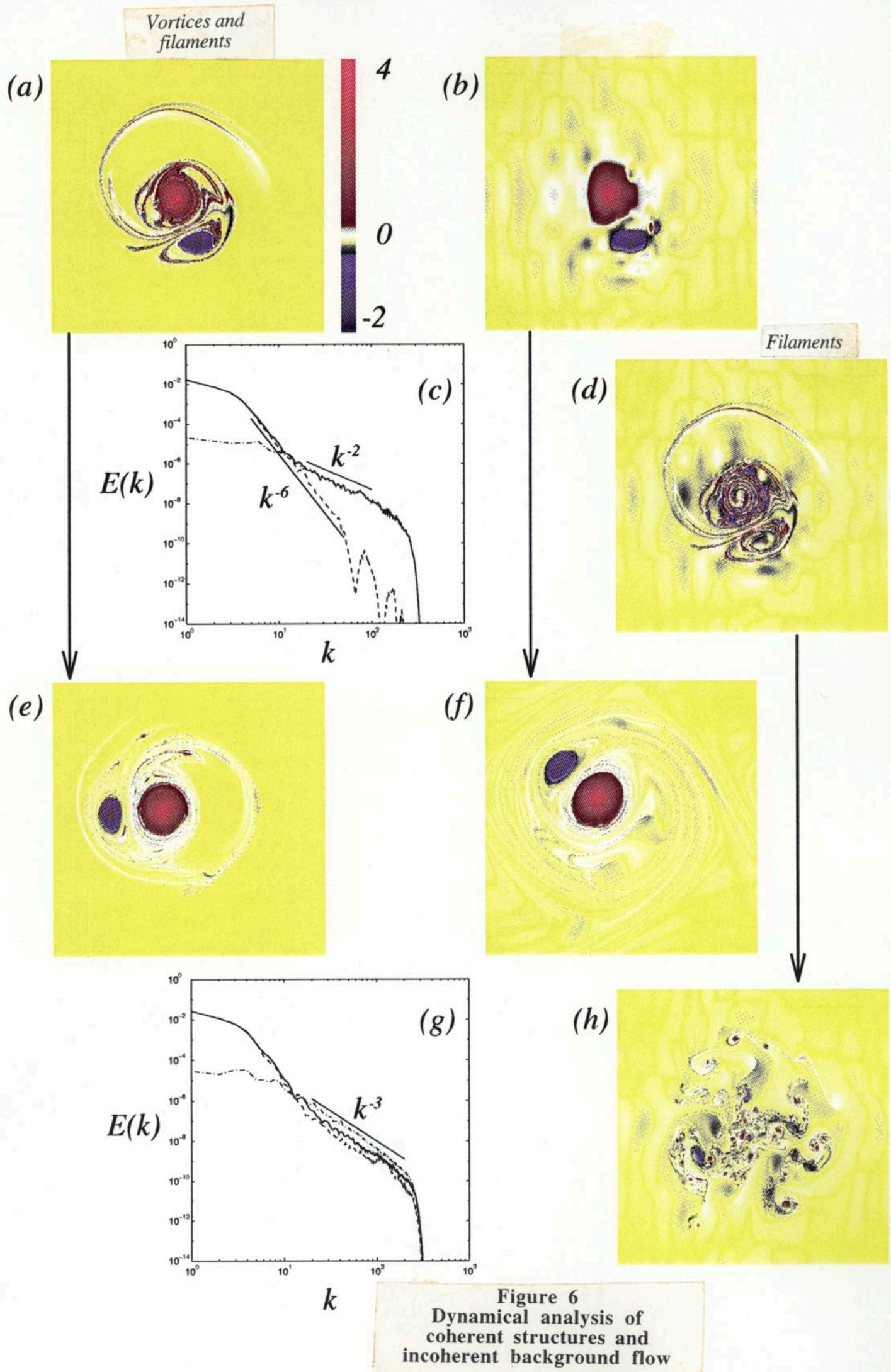

Figure 6
Dynamical analysis of coherent structures and incoherent background flow

CONJECTURE

We have observed that the strain imposed by the coherent vortices inhibits the nonlinear instabilities to grow in the background

$\Rightarrow$

Wavelet gap

{ the background flow is aligned to the coherent vortices and there is no backscatter from the background to the coherent vortices

$\Rightarrow$

We propose to model the background flow by a Gaussian (with a k^{-1} scaling) stochastic process.

CONCLUSION

For 2D turbulent flows
there is no spectral gap
in Fourier space.

There exists a dynamical
gap in wavelet packet
phase-space
between:

1. Coherent Vortices,
quasi-singular elliptic regions,
which correspond to the
strongest WP coefficients,
having non-Gaussian statistics.
Background flow,
well-mixed hyperbolic regions,
which correspond to the
weakest WP coefficients,
having Gaussian statistics.

low-dimensional deterministic system out of statistical equilibrium

2. high-dimensional stochastic background in statistical equilibrium

This gives some hope for
drastically reducing the number
of degrees of freedom to compute
Large Reynolds 2D flows.

4. TRANSPORT ET MELANGE PAR LA TURBULENCE

Equation d'advection - diffusion

Nombres de Péclet, de Prandtl et de Schmidt

Equation de Corrsin

Loi de Richardson

Diffusion de particules par un écoulement turbulent (bidimensionnel)

Diffusion de concentration par un écoulement turbulent (bidimensionnel)

Transport et mélange turbulents par les vortex polaires et formation de trous d'ozone

ADVECTION-DIFFUSION EQUATION

Passive scalar hypothesis

We suppose that the variations of the scalar field do not react back upon the turbulent velocity

Linear PDE with variable coefficients

for temperature:

$$\frac{\partial T}{\partial t} + \vec{V}.\vec{\nabla}T = K\nabla^2 T$$

K thermal diffusivity

for scalar concentration

$$\frac{\partial c}{\partial t} + \vec{V}.\vec{\nabla}c = D\nabla^2 c$$

D scalar diffusivity

Non-dimensional characteristic numbers

for temperature:

$$Prandtl = \frac{\nu}{K} = Pr$$

$$Péclet = \frac{UL}{K} = Pr.Re = Pe$$

for scalar concentration:

$$Schmidt = \frac{\nu}{D} = Sc$$

CORRSIN'S EQUATION

We study the influence of $\vec{v}\cdot\vec{\nabla}\theta$ on the statistics of the scalar field $\theta(\vec{x},t)$.

The turbulent velocity $\vec{v}(\vec{x},t)$ is supposed to be a random field having homogeneous, isotropic and Gaussian statistics and mean zero $\langle \theta(\vec{x},t)\rangle = 0$.

The two-point correlation of θ is:

$$C(\vec{r}) = \langle \theta(\vec{x})\,\theta(\vec{x}+\vec{r})\rangle$$

and we take its Fourier transform:

$$E_\theta(\vec{k}) = \int C(\vec{r})\, e^{-i\vec{k}\cdot\vec{r}}\, d\vec{r}$$

Using Navier-Stokes we obtain Corrsin's equation (1951):

$$\left(\frac{\partial}{\partial t} + 2K k^2\right) E_\theta(\vec{k}) = T(\vec{k})$$

T nonlinear transfer term

similar to Karman-Howarth equation: (1938)

$$\left(\frac{\partial}{\partial t} + 2\nu k^2\right) E(\vec{k}) = T(\vec{k})$$

PASSIVE SCALAR SPECTRUM

Characteristic scales

Kolmogorov dissipation scale for kinetic energy

$$\ell_k = \left(\frac{\nu^3}{\varepsilon}\right)^{1/4}$$

Corrsin dissipation scale for scalar concentration

$$\ell_c = \left(\frac{K^3}{\varepsilon}\right)^{1/4}$$

The temperature variance spectrum will depend on the Prandtl number

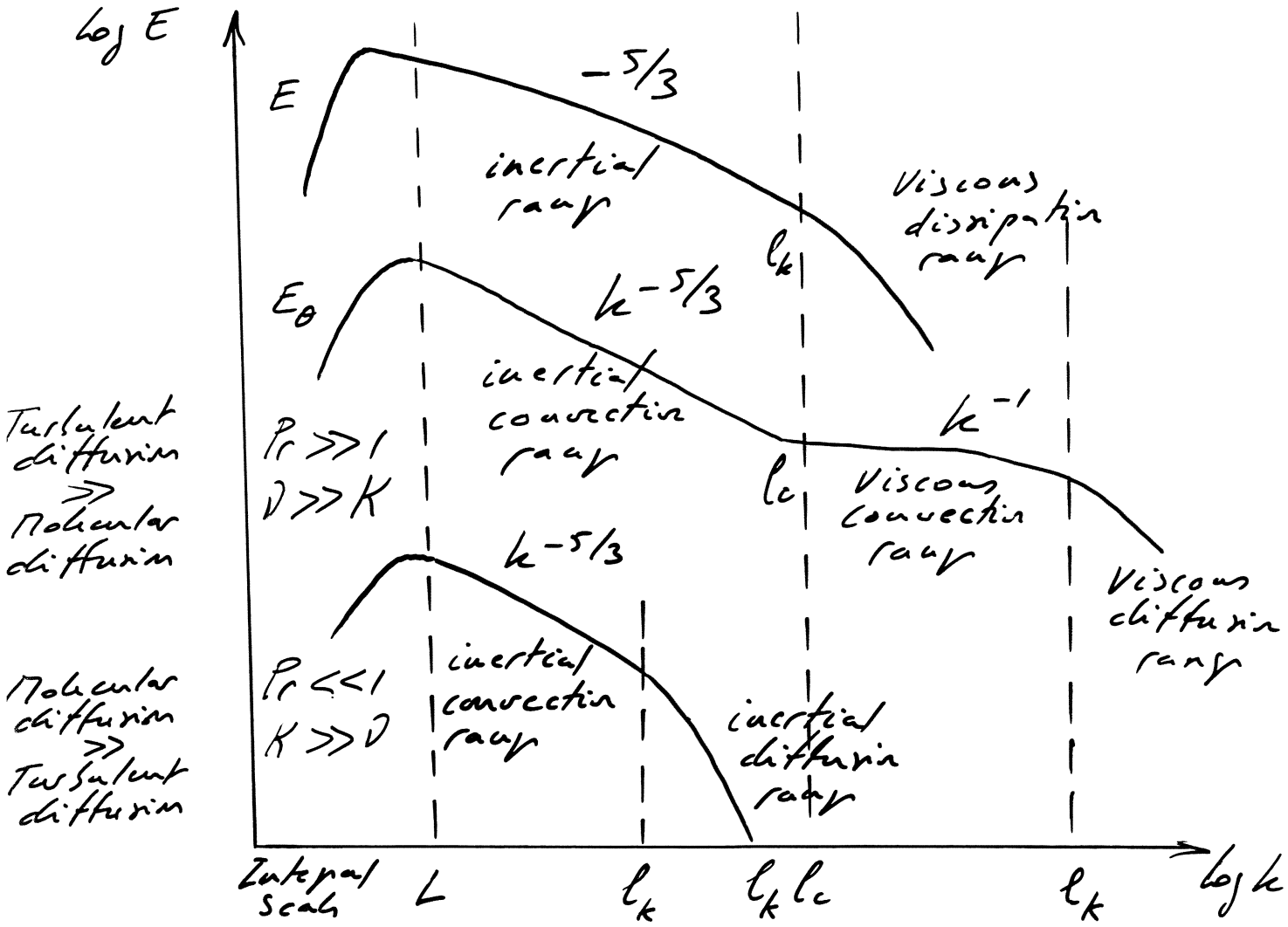

RICHARDSON'S LAW (1929)

We consider two particles having the same position at $t=0$ and we study the time evolution of their mean quadratic distance $D(t)$.

- For $D \gg L$ integral scale the motions of the 2 particles are decorrelated

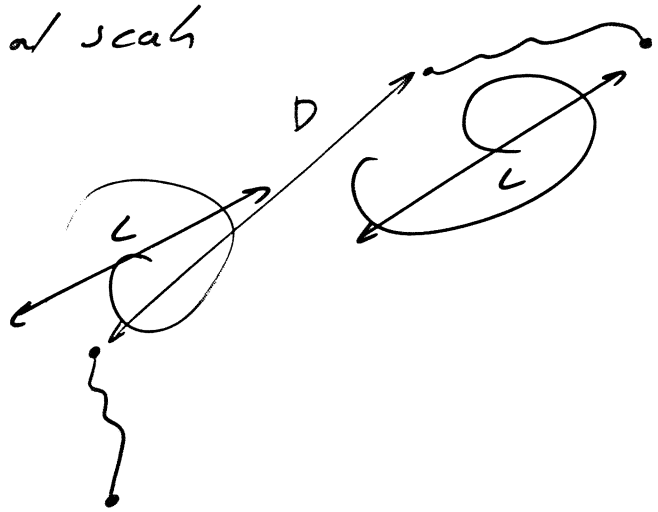

$$\Rightarrow D(t) = C_D \varepsilon^{1/2} t$$

C_D diffusion constant

- For $\ell_c < D \ll L$ the particles are trapped in the same turbulent motion correlated according to $E(k) \sim C_k \varepsilon^{2/3} k^{-5/3}$ $\Rightarrow$



$$D(t) = C_R \varepsilon^{1/2} t^{3/2}$$

C_R Richardson's constant

PARTICLE DIFFUSION BY A STRAINED 2D VORTEX (1)

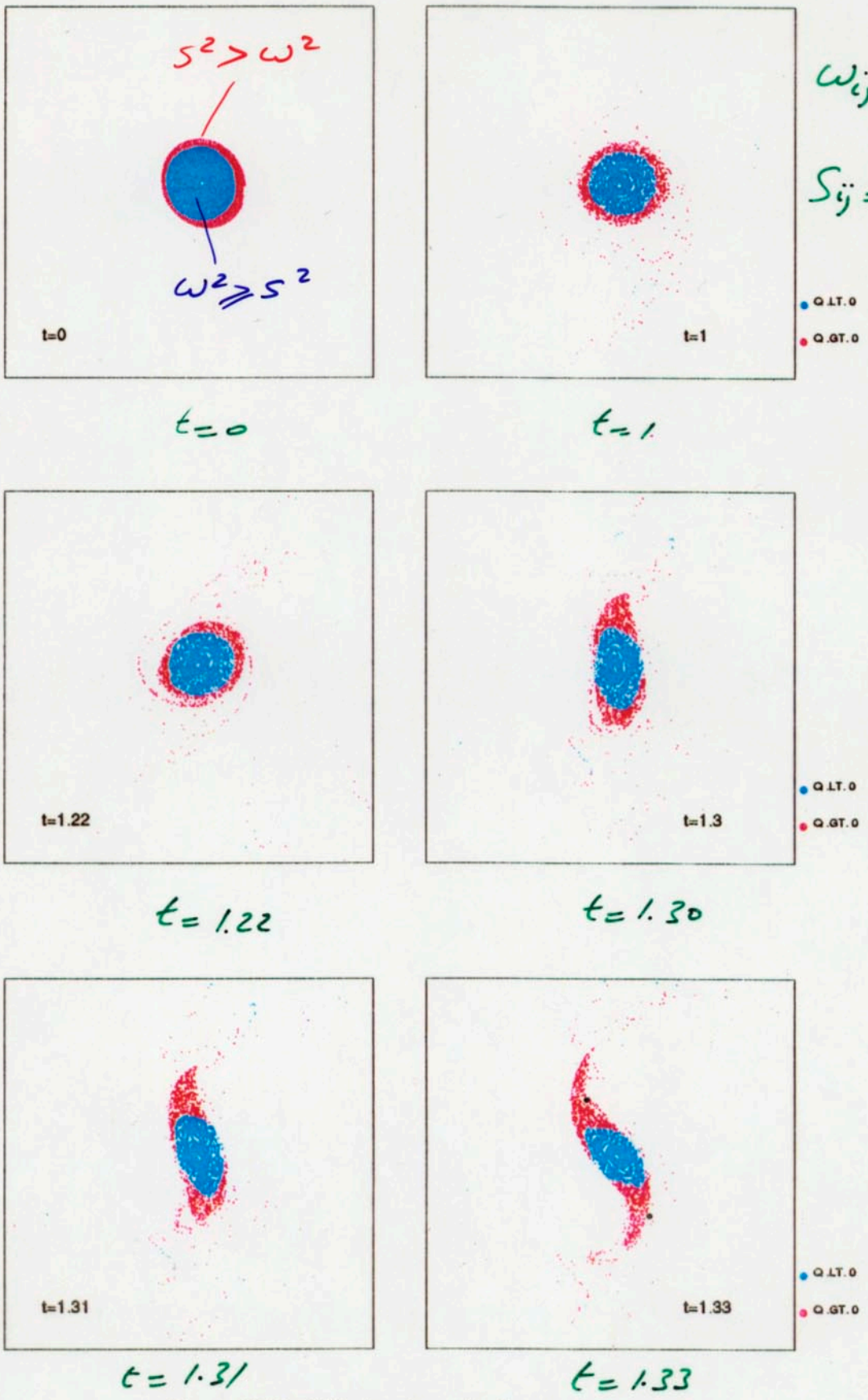

$$\omega_{ij} = \frac{1}{2}\left(\frac{\partial v_i}{\partial x_j} - \frac{\partial v_j}{\partial x_i}\right)$$

$$S_{ij} = \frac{1}{2}\left(\frac{\partial v_i}{\partial x_j} + \frac{\partial v_j}{\partial x_i}\right)$$

Figure III.9: Diffusion à partir d'un vortex:
en bleu: Q≤0; en rouge: Q>0. Numerical experiment

Dalila Elmaidi & Armando Babiano

PARTICLE DIFFUSION BY A STRAINED 2D VORTEX (2)

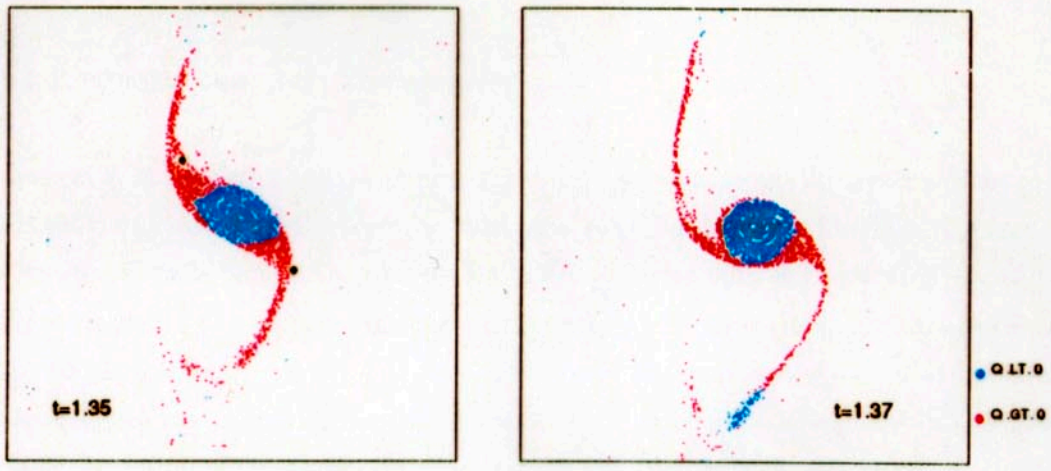

t = 1.35 t = 1.37

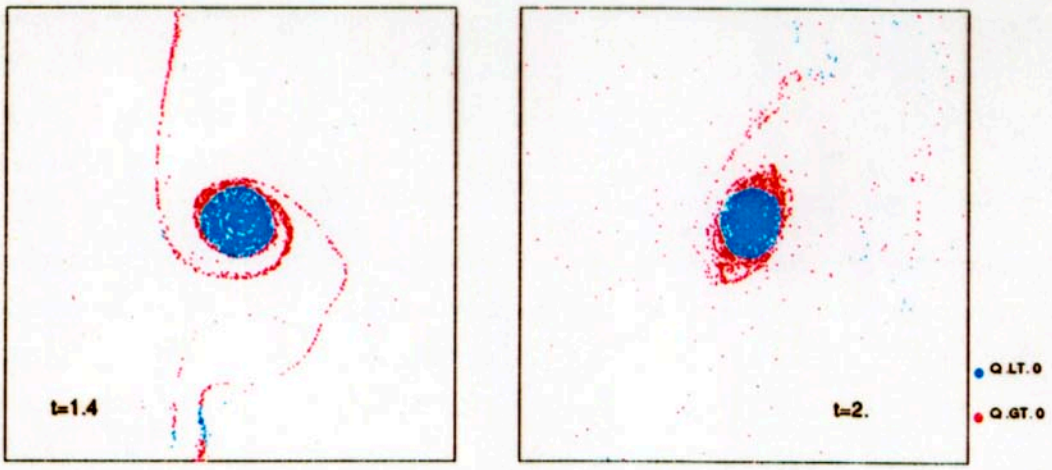

t = 1.4 t = 2

Suite de la figure III.9.

Numerical experiment

Dalila Elmaichi & Armando Babiano

PARTICLE DIFFUSION BY 2D VORTEX MERGING (1)

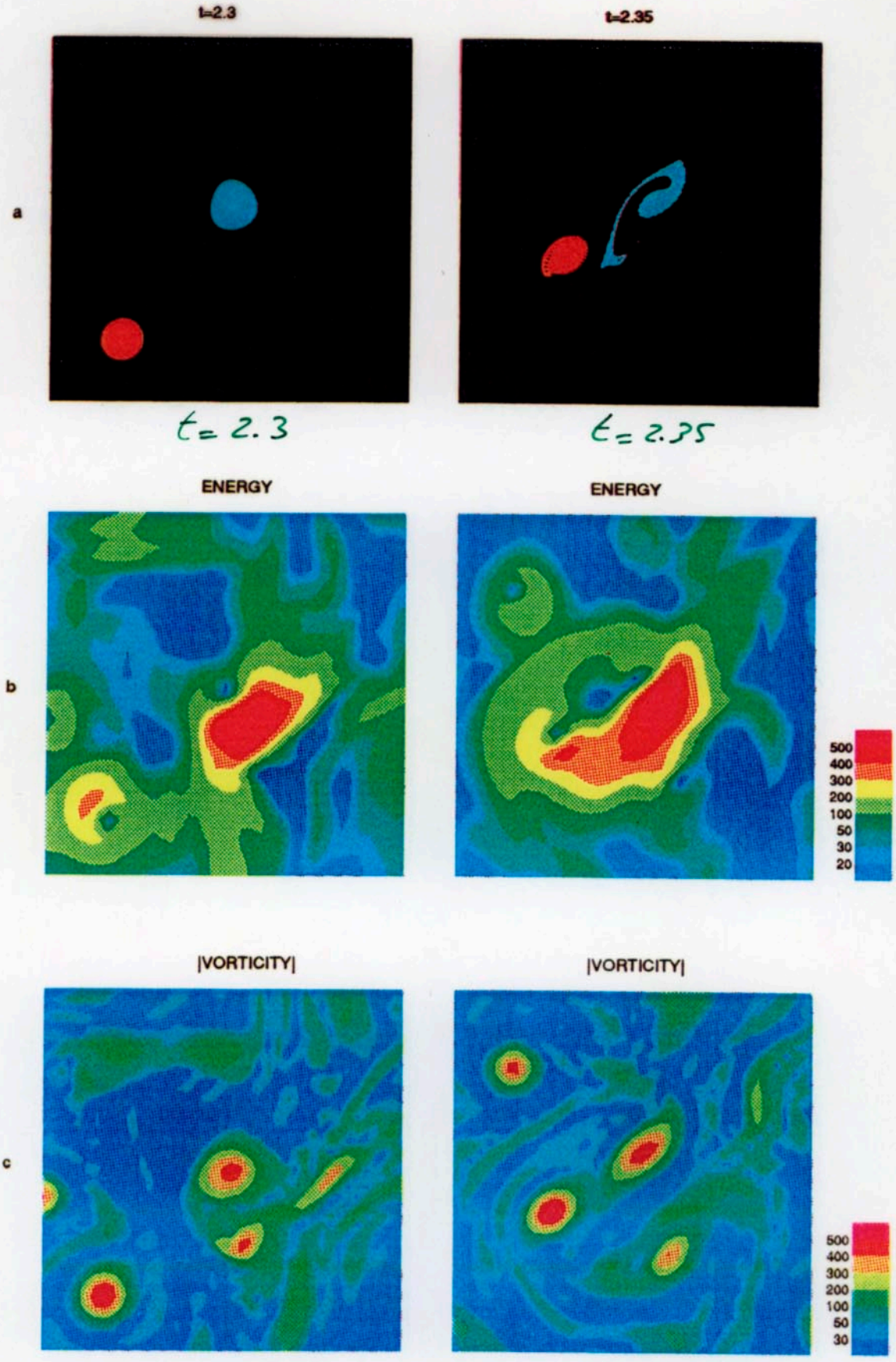

Figure III.16: Interaction de deux vortex de même signe et d'intensités différentes.
a) Positions des particules; b) énergie; c) |vorticité|.

Numerical experiment
Dalila Elmaidi & Armando Babiano

PARTICLE DIFFUSION BY 2D VORTEX MERGING (2)

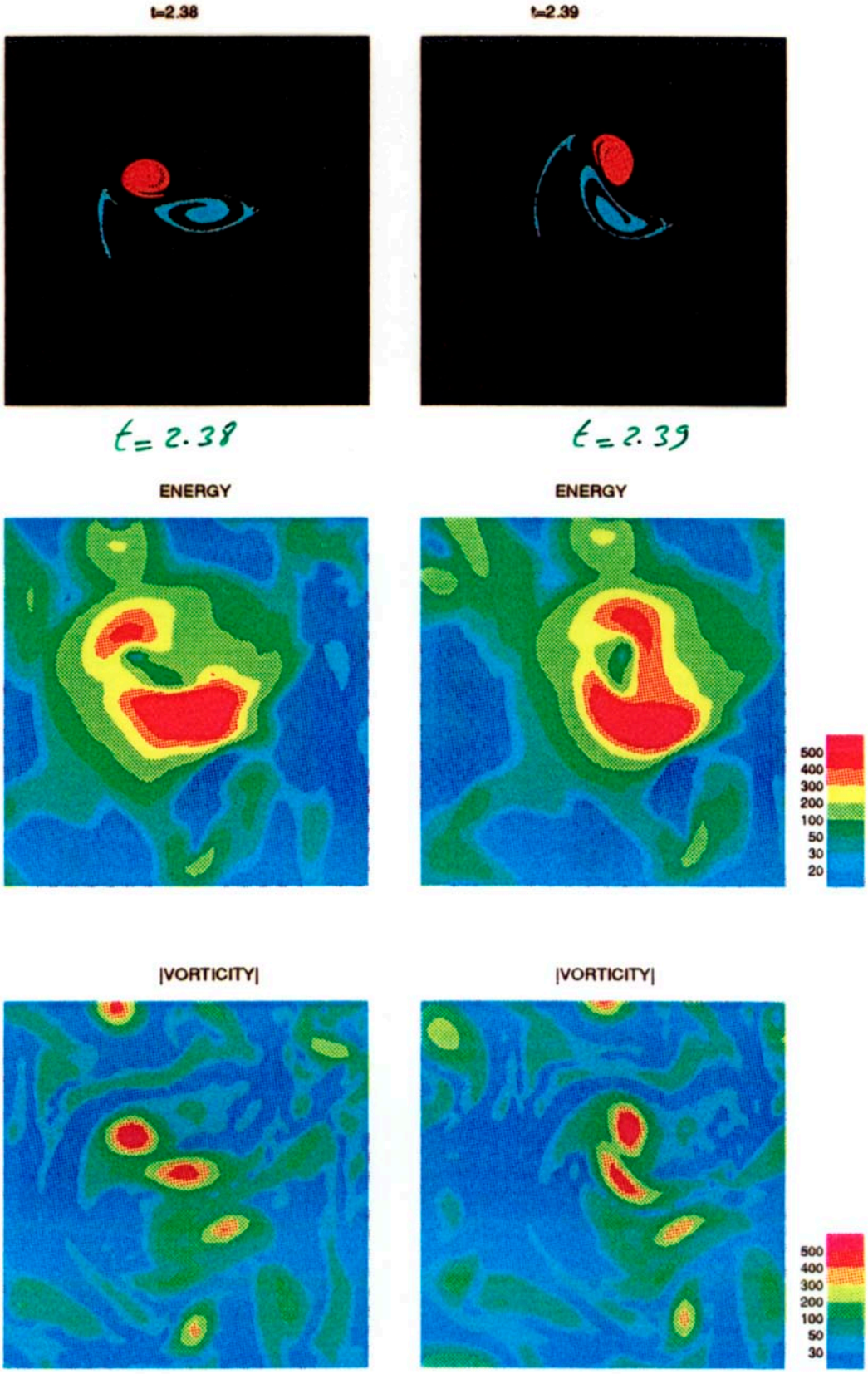

Suite de la figure III.16.

Numerical experiment
Dalila Elmaidi & Armando Bassano

PARTICLE DIFFUSION BY 2D VORTEX MERGING (3)

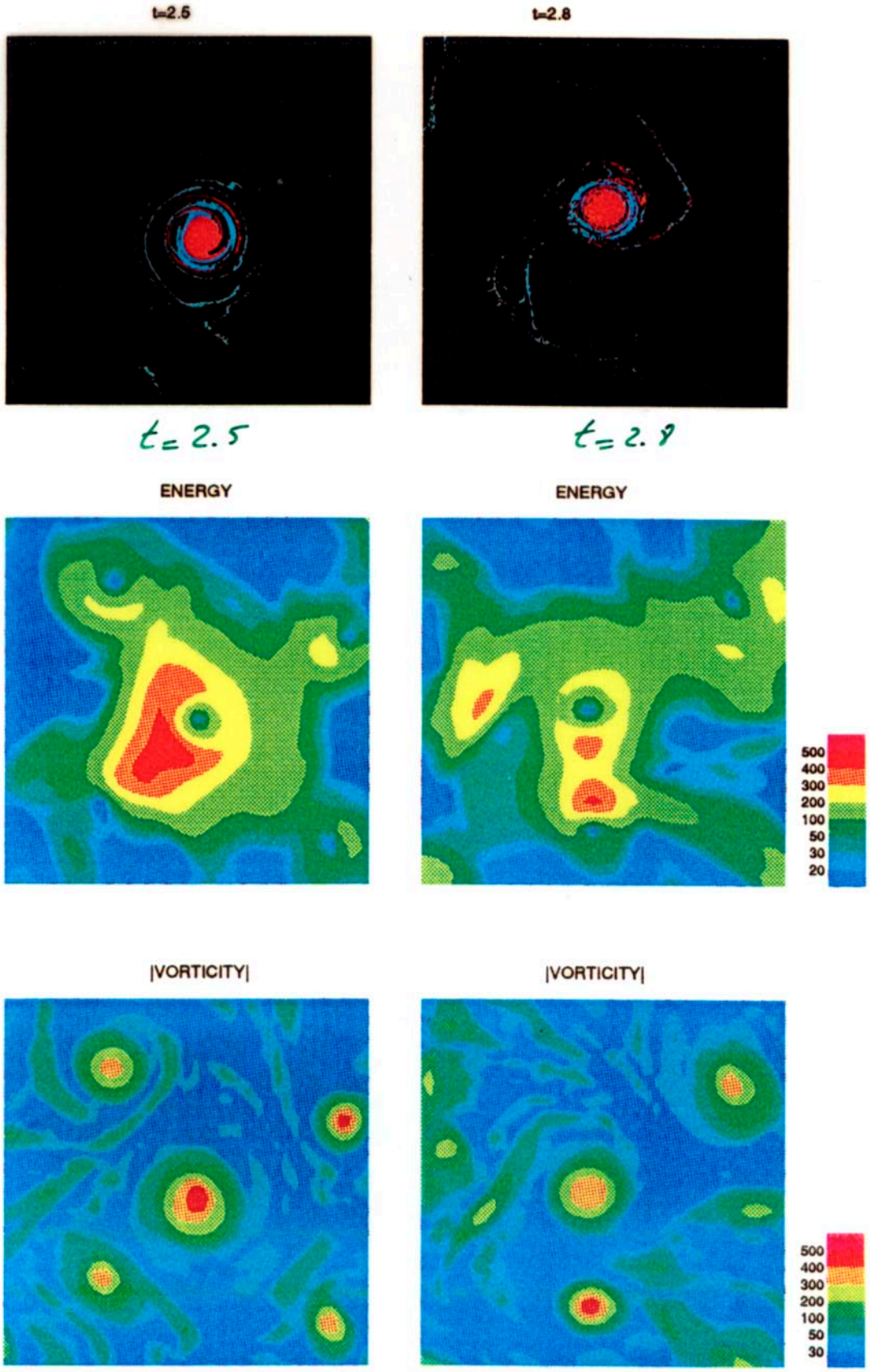

Suite de la figure III.16.

Numerical experiment

Dalila Elmaidi & Armando Bosciano

MIXING BY
ONE GAUSSIAN VORTEX

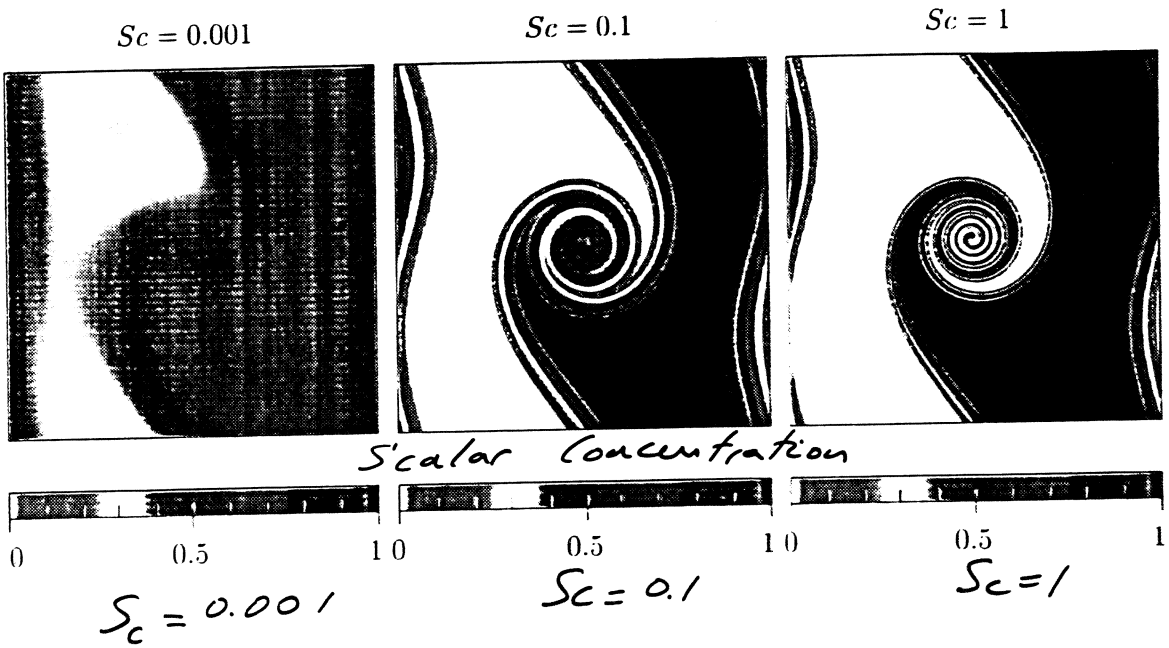

Abbildung 5.17: Konzentrationsfelder von A zur Zeit $t = 20$ für Schmidt-Zahlen von $Sc = 0.001$, 0.1 und 1.

$$Sc = \frac{\text{kinematic viscosity}}{\text{scalar diffusion}}$$

PASSIVE SCALAR MIXING BY TWO GAUSSIAN VORTICES
Numerical experiment

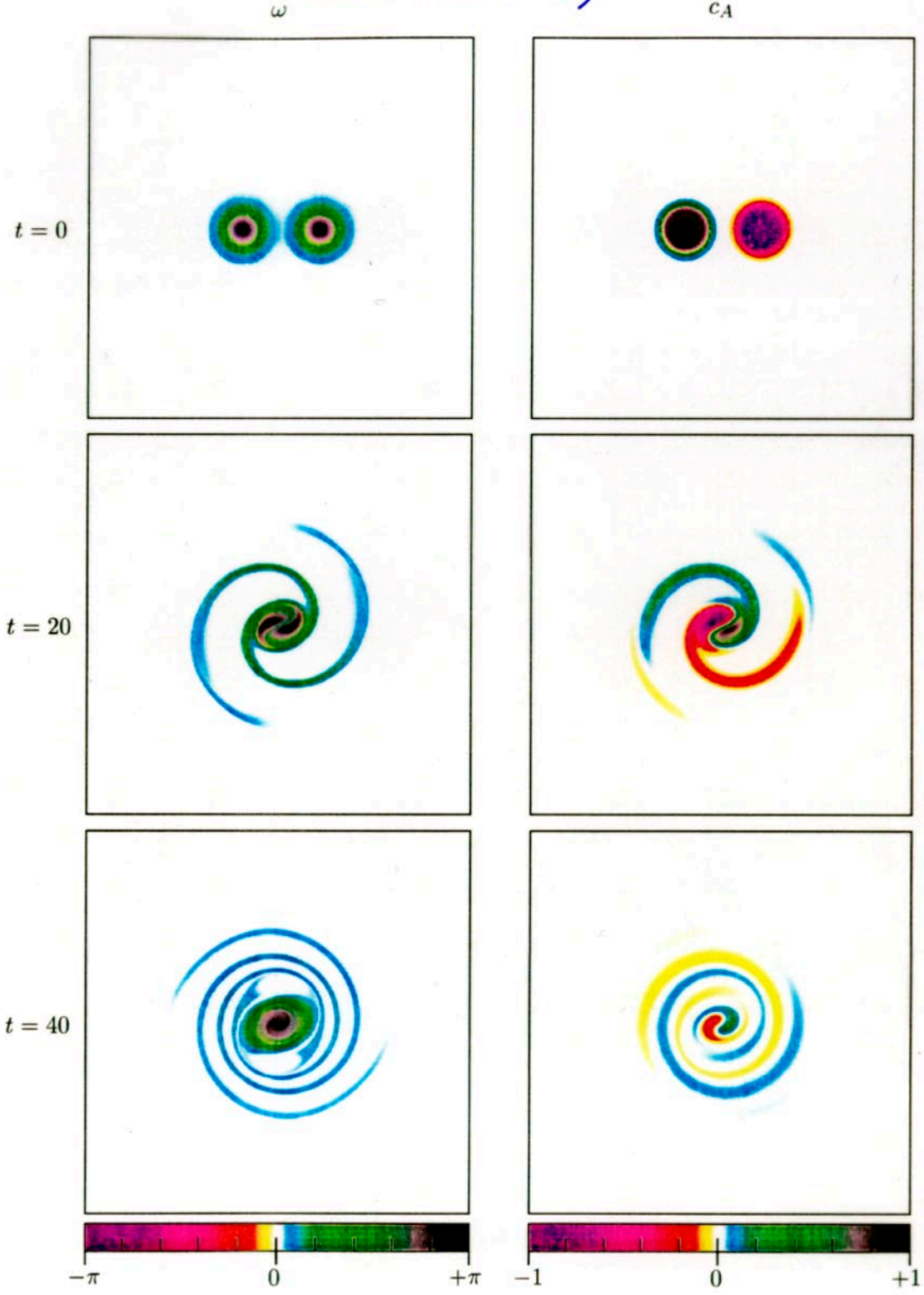

Abbildung 6.4: Zeitliche Entwicklung der Wirbelstärke (links) und der Konzentration von A (rechts) bei einer Schmidt-Zahl von $Sc = 0.1$ für einen homostrophen Dipol.

Vorticity
Scalar Concentration
Sc=0.1
Kai Schneider & Wolfgang Gerlinger

PASSIVE SCALAR

MIXING BY THREE
INITIALLY GAUSSIAN VORTICES

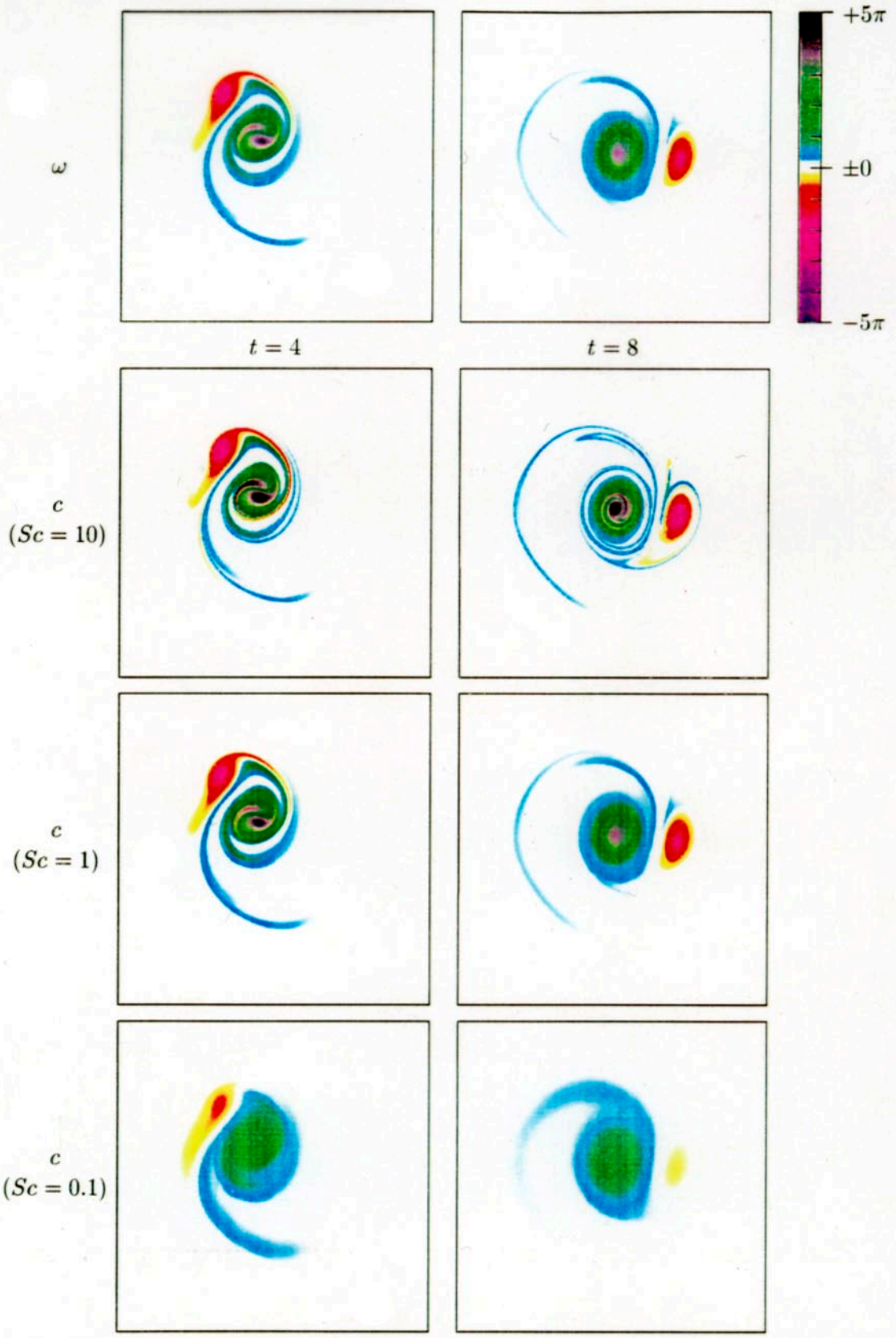

Abbildung 6.1: Zeitliche Entwicklung der Wirbelstärke ω (oben) und der Konzentration c für Schmidt-Zahlen von Sc=0.1, 1 und 10 für die Anfangsbedingung dreier zweidimensionaler Gaußfunktionen für ω und c.

Numerical experiment
Kai Schneider & Wolfgang Gerlinger

MIXING BY THREE VORTICES

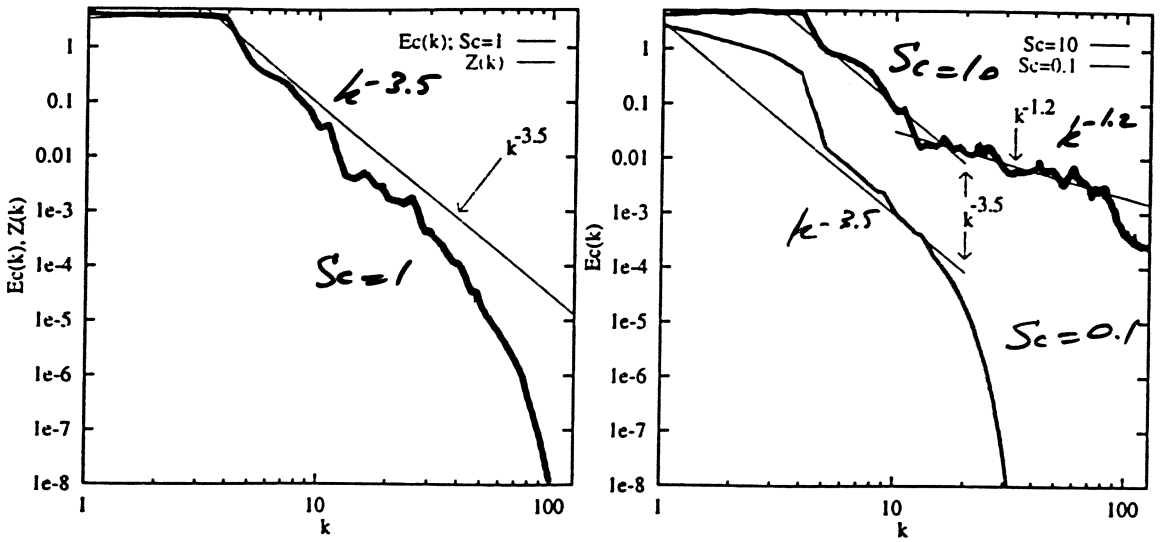

Scalar Concentration Spectrum

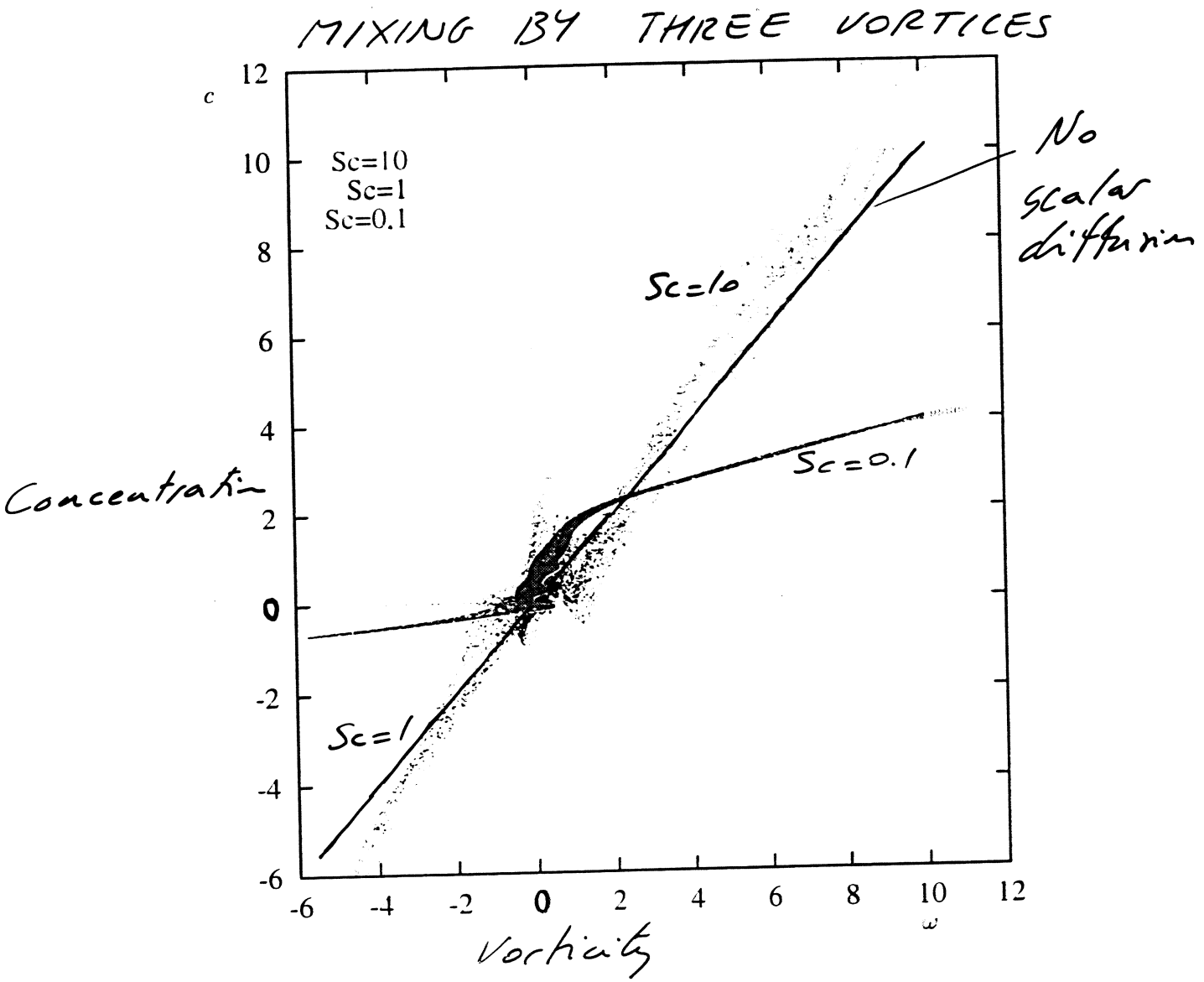

Abbildung 6.3: Auftragung der Wirbelstärke gegen die Konzentration in jedem Punkt des Datenfeldes für drei Simulationen mit Schmidt-Zahlen von $Sc = 10, 1$ und 0.1 nach 40 Zeiteinheiten.

DECAYING 2D TURBULENCE

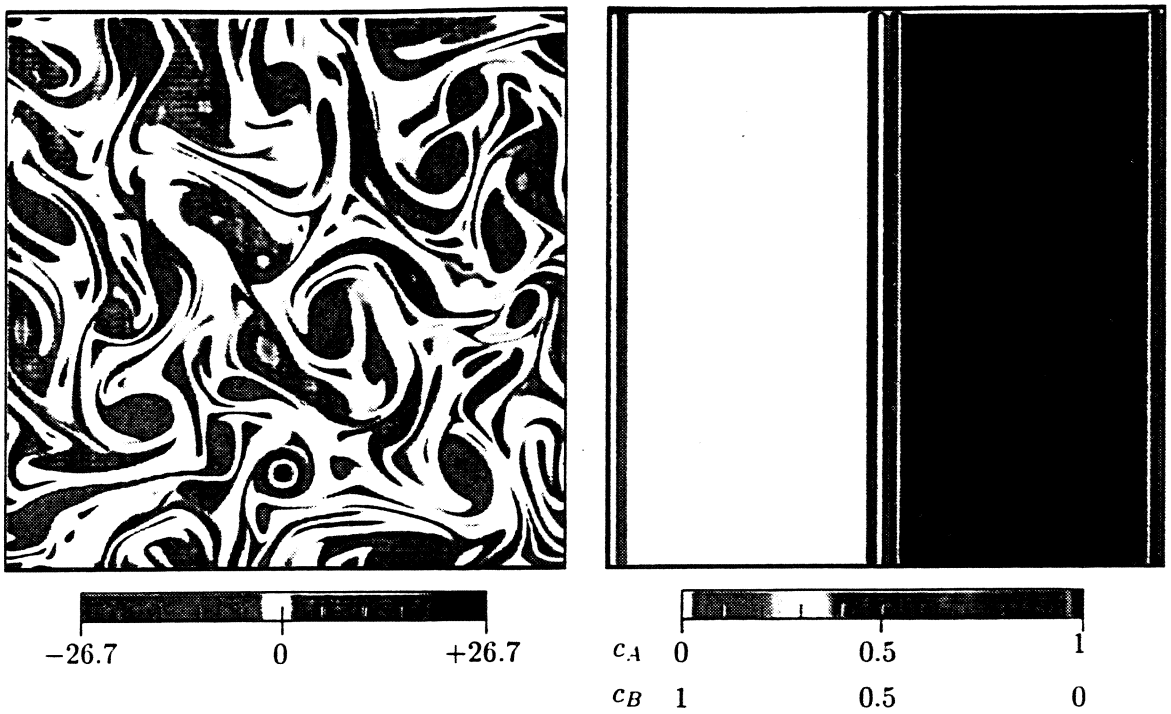

Abbildung 7.1: Anfangsbedingung für die Konzentration und Wirbelstärke zur Simulation abklingender Turbulenz.

Vorticity at t=0

Scalar Concentration at t=0

TURBULENT MIXING IN DECAYING 2D TURBULENCE

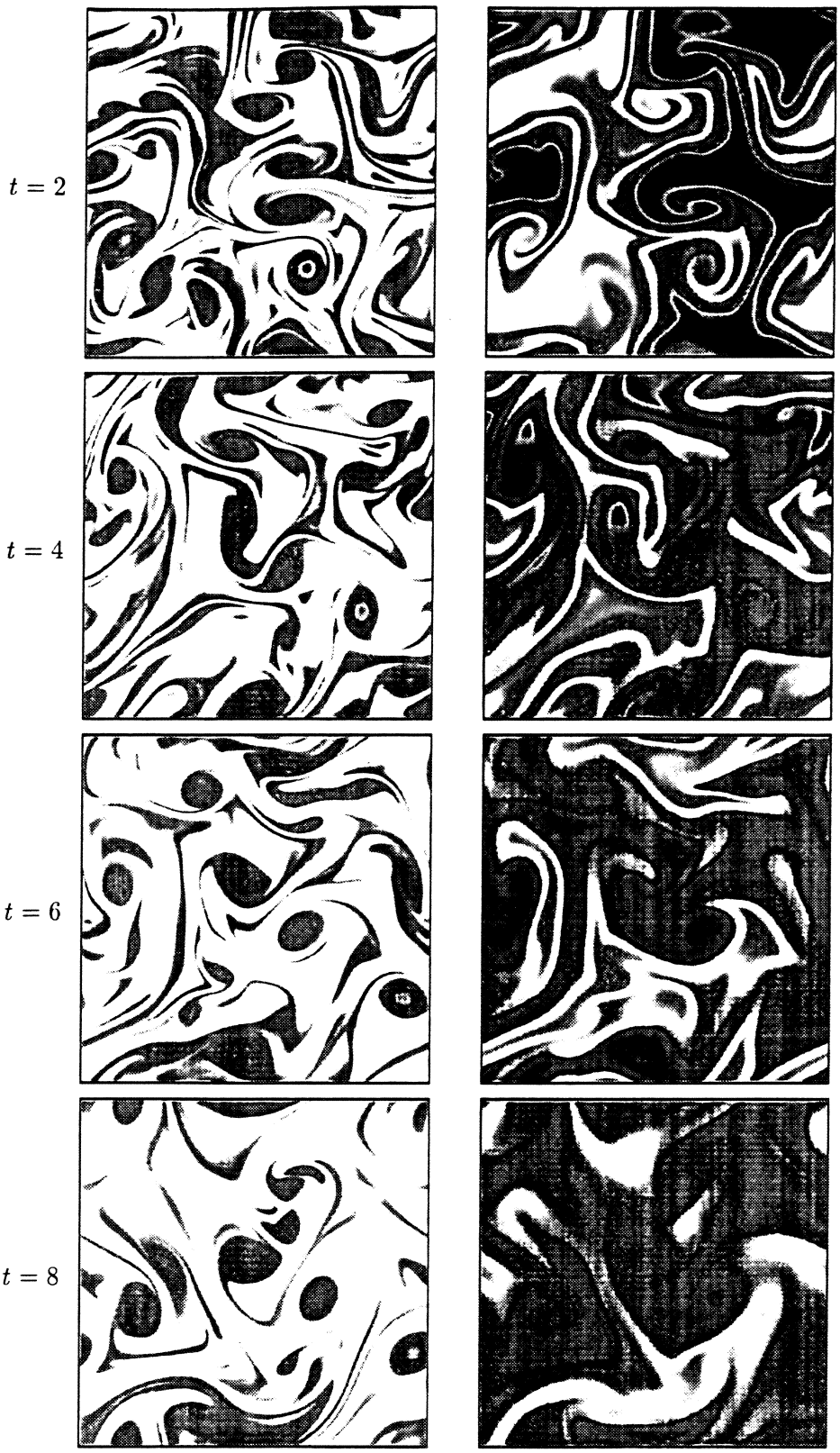

Abbildung 7.2: Zeitliche Entwicklung der Wirbelstärke (links) und der Konzentration von A (rechts) bei einer Schmidt-Zahl von $Sc = 0.1$. Die Anfangsbedingungen und Farbskalierungen sind in Abbildung 7.1 dargestellt.

Vorticity Scalar Concentration

TURBULENT MIXING IN DECAYING 2D TURBULENCE

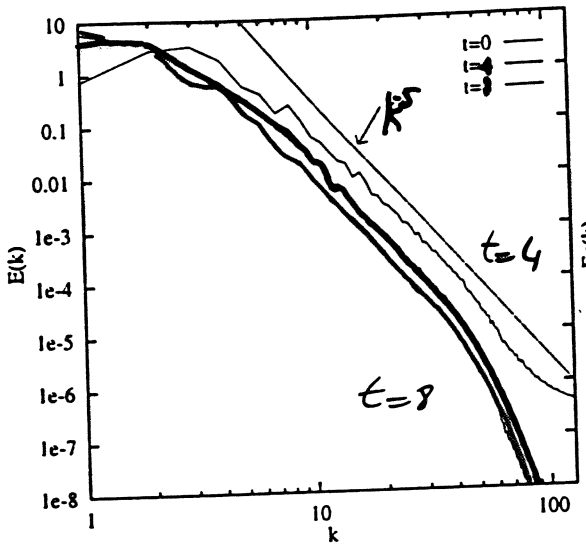

Energy Spectrum

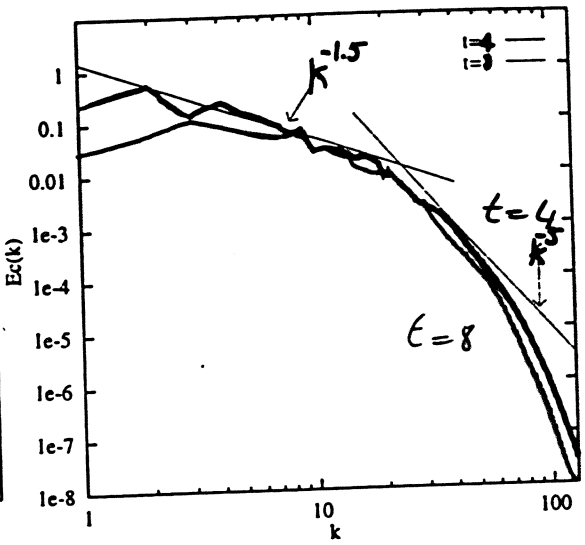

Scalar concentration spectrum

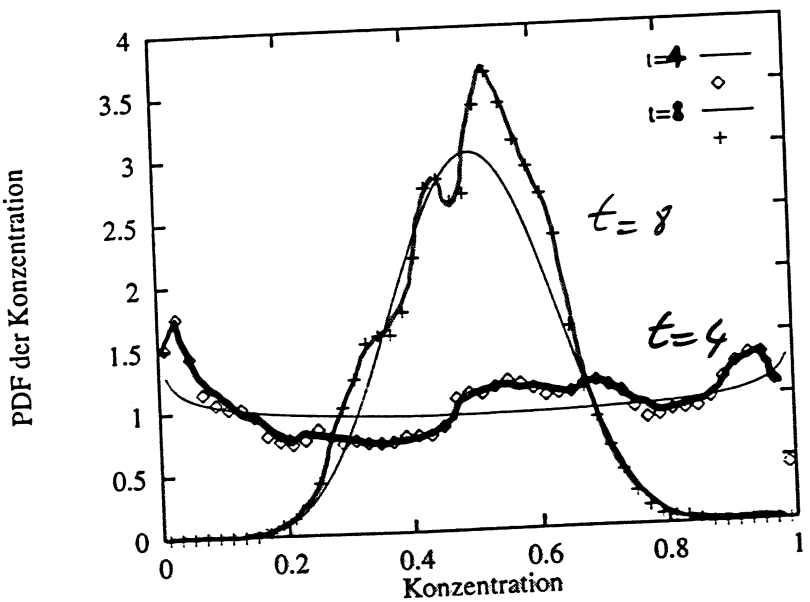

PDF of scalar concentration

OBSERVATION OF THE OZONE HOLE ASSOCIATED TO THE POLAR VORTEX

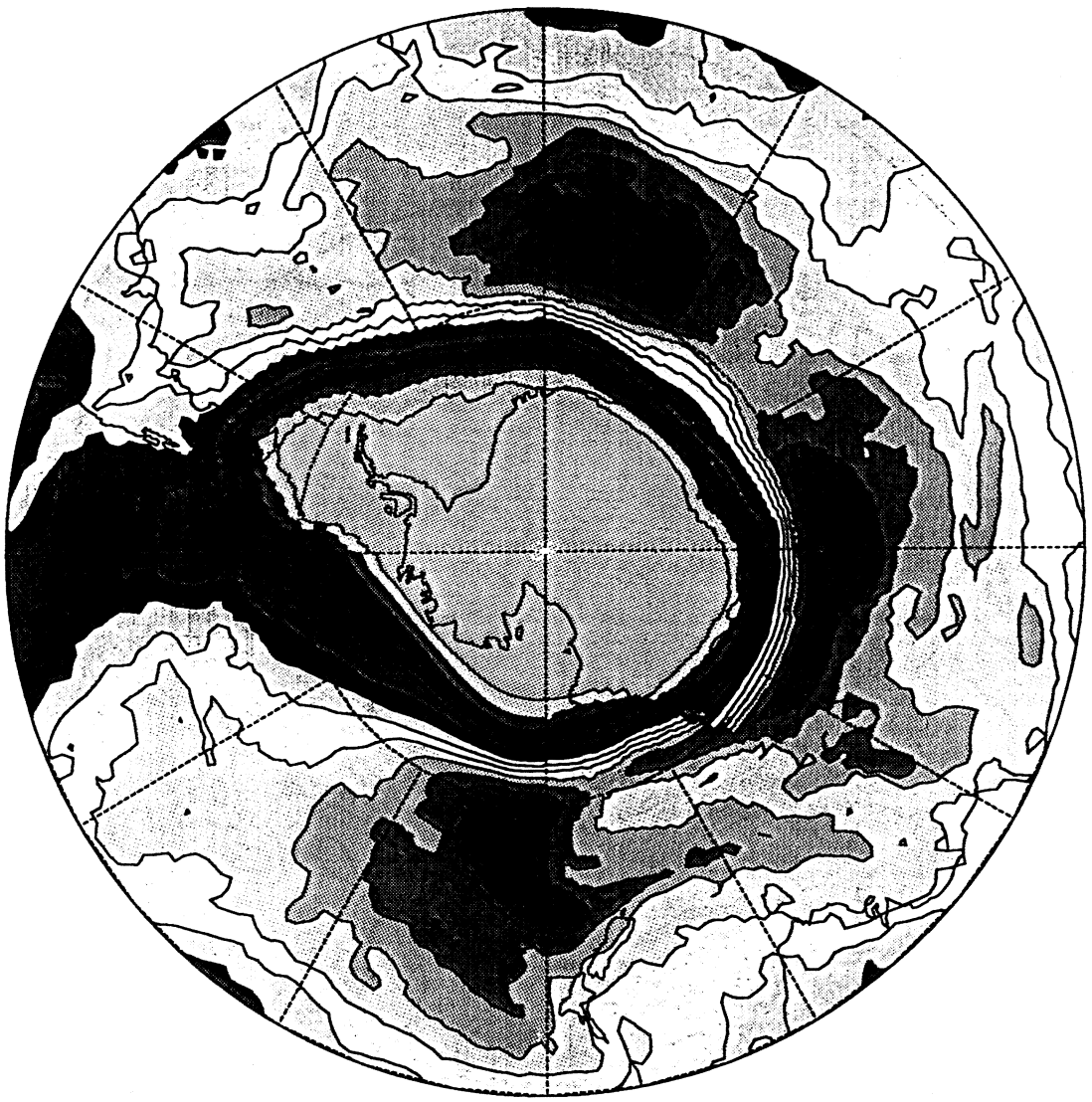

180. 200. 220. 240. 260. 280. 300. 320. 340. 360. 380. 400.

Ozon Concentration

27 Sep 1993 DU

TOMS TOTAL OZONE

Observation of the ozone hole

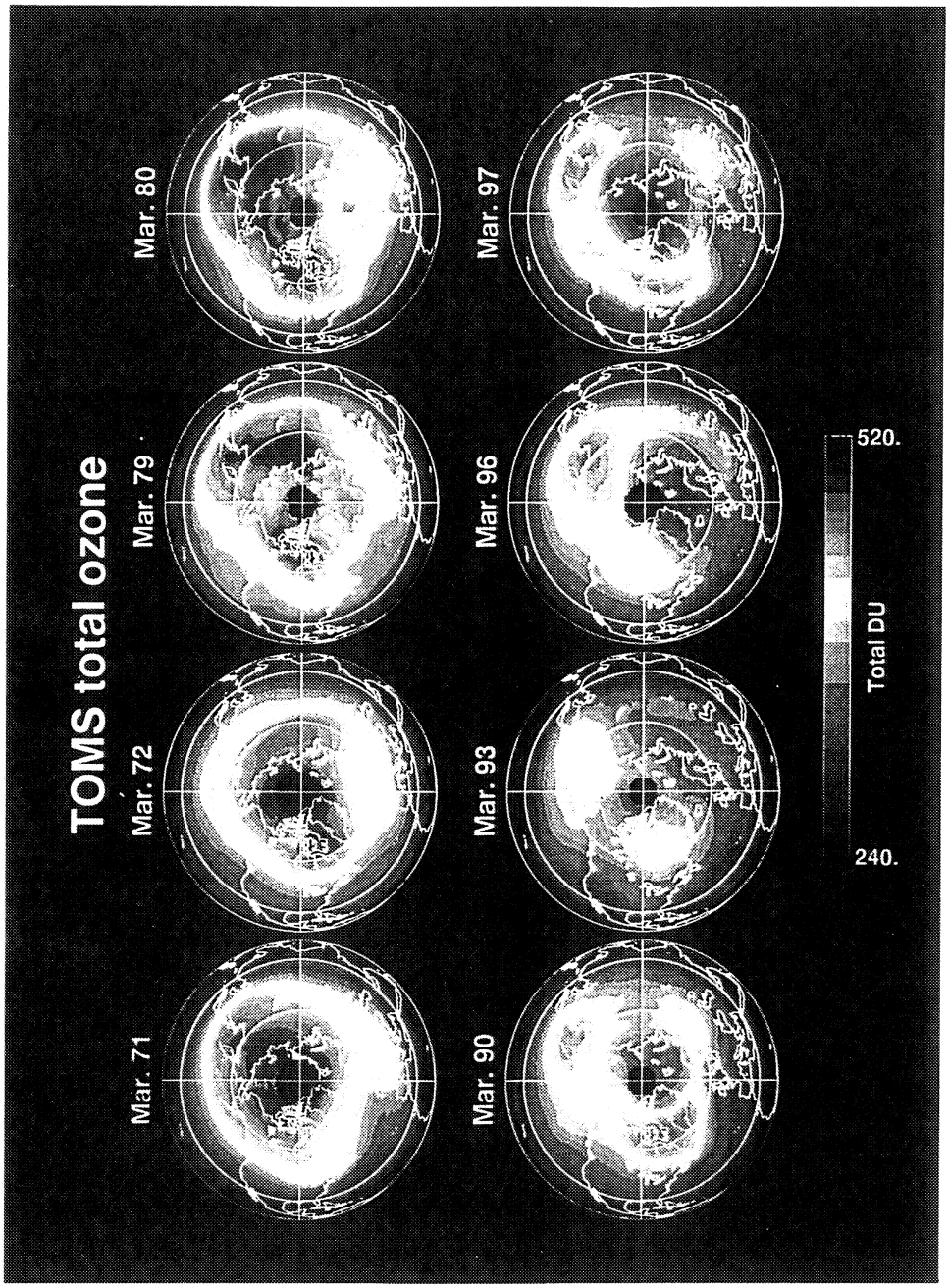

Observation of Mr Ozan Koh

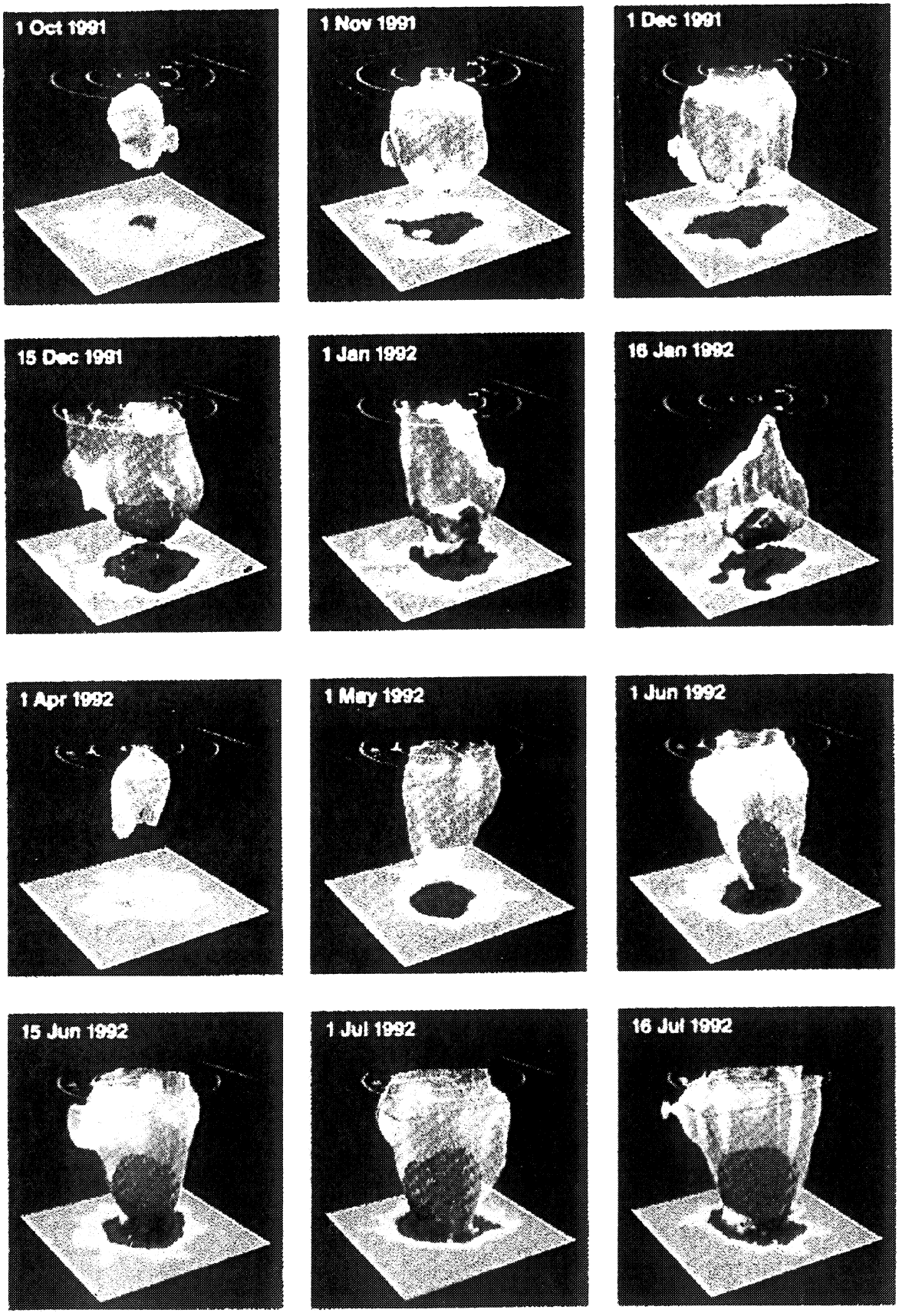

MIXING BY ONE GAUSSIAN VORTEX

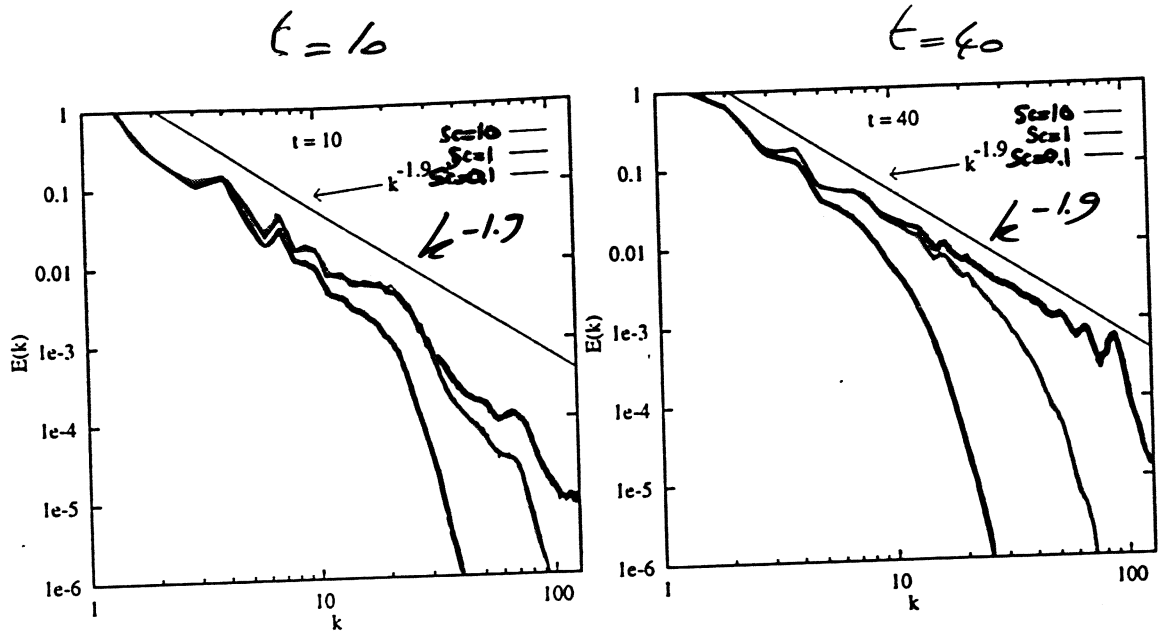

Scalar concentration Spectrum

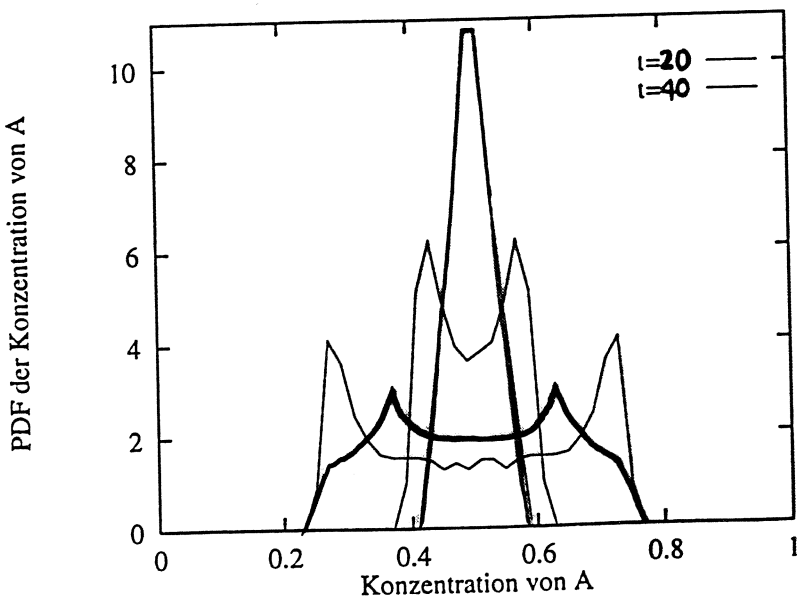

PDF of Scalar Concentration

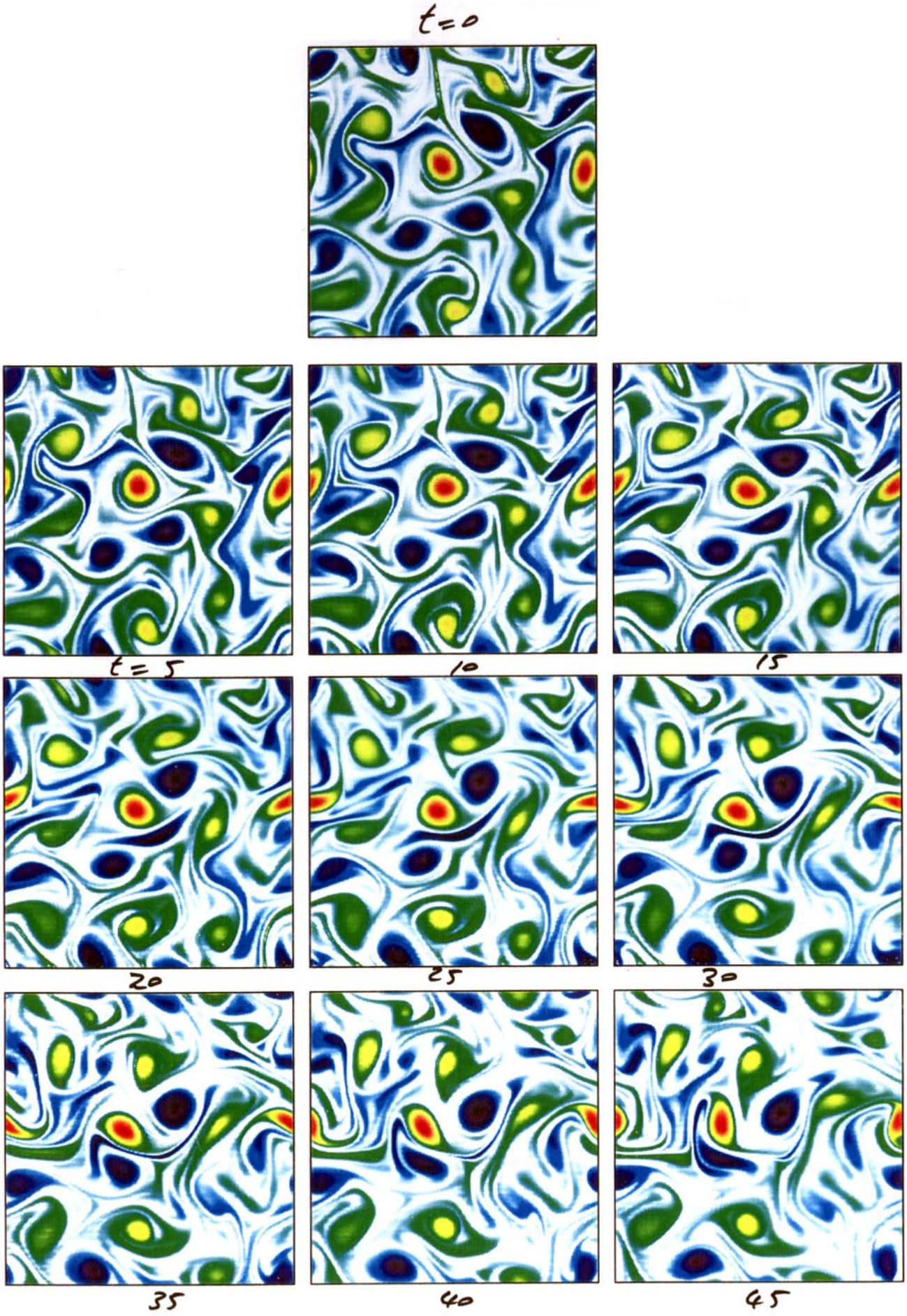

Evolution of vorticty, $t = 0, 5, 10, ..., 45$ (decaying turbulence 256^2).

20 Decaying turbulence
(Kai SCHNEIDER)

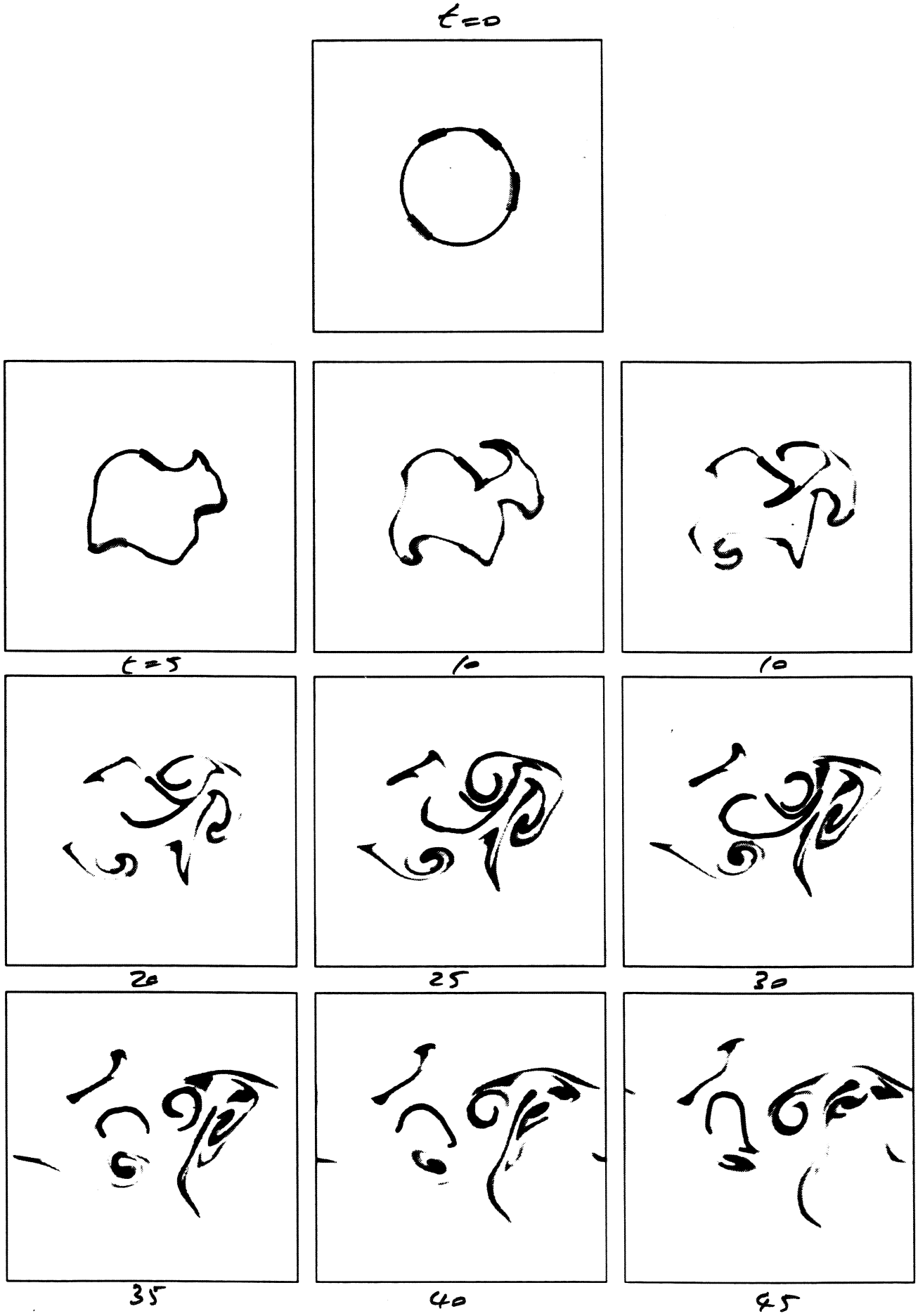

Evolution of Concentration, $t = 0, 5, 10, \ldots, 45$ in decaying turbulence.

5. MODELISATION DE LA TURBULENCE

Définition de la moyenne : moyenne temporelle, moyenne spatiale, moyenne d'ensemble

Hypothèse ergodique et hypothèse de Taylor

Equations moyennées de Reynolds

Modèle de Smagorinsky

Modèle k-ε

Simulation des grandes échelles (LES)

Simulation des structures cohérentes (SSC)

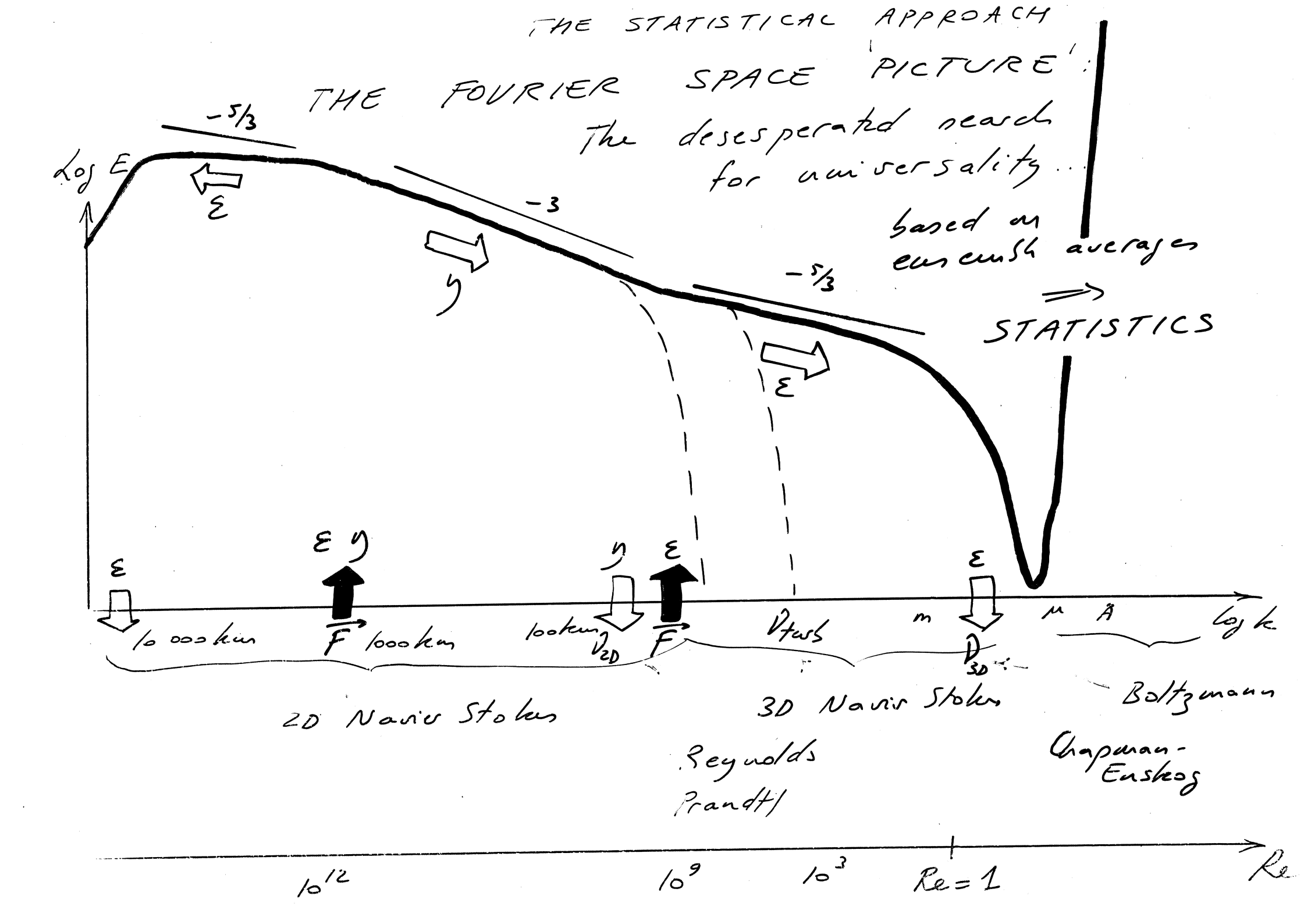
THE STATISTICAL APPROACH
THE FOURIER SPACE 'PICTURE':
The desesperated search for universality...
based on ensemble averages
⟹ STATISTICS
-5/3
-3
-5/3
Log E
ε
η
ε
ε η
η ε
ε
10 000 km
F
1000 km
100 km
ν_{2D}
F
ν_{turb}
m
D_{3D}
μ λ
Log k
2D Navier Stokes
3D Navier Stokes
Boltzmann
Reynolds
Prandtl
Chapman-Enskog
10^{12}
10^{9}
10^{3}
Re = 1
Re

THE DETERMINISTIC APPROACH

THE PHYSICAL SPACE 'PICTURE':

based on each flow realization ⇒ The Zoo! DYNAMICS

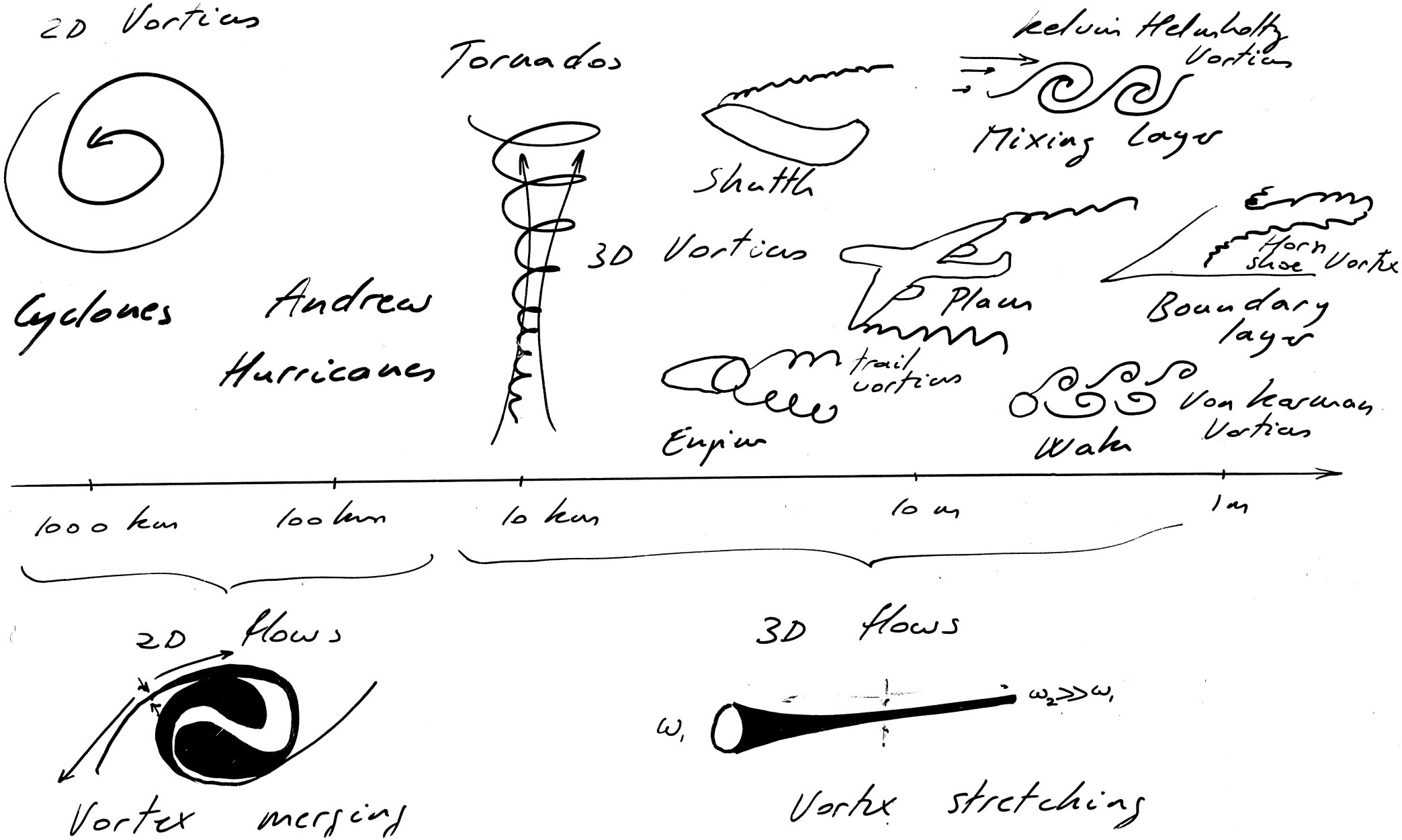

HISTOIRE DES MOYENNES EN TURBULENCE

Jean Boussinesq en 1872 dans son 'Essai sur la théorie des eaux courantes' distingue deux régimes le premier 'bien continu' et le second 'tumultueux et tourbillonnant'.

Dans ce deuxième régime, 'les vitesses vraies' sont 'rapidement ou même brusquement variables d'un point à l'autre' et il propose de 'choisir pour équations du mouvement, non pas les relations qui expriment à un moment donné l'équilibre dynamique des divers volumes élémentaires du fluide, mais les moyennes de ces relations pendant un temps assez court, ou ce que l'on peut appeler les équations de l'équilibre dynamique moyen des particules fluides qui passent successivement en un même point'.

Pour étudier les mouvements caractérisés par des 'changements fréquents et rapides, mais assujettis à une sorte de périodicité irrégulière'

Boussinesq introduit au lieu du liquide étudié réellement, un fluide fictif dont les vitesses auraient pour composantes suivant les axes en chaque point et à chaque instant

$$\bar{u}_i(\vec{x}, t) = \frac{1}{T}\int^{t+T} \vec{V}_i(\vec{x}, \tau)\, d\tau$$

où T désigne t un temps assez petit

Boussinesq a vu très clairement que pour écrire les équations du mouvement moyen du fluide il fallait faire dépendre les actions moyennes exercées à travers un élément plan fixe, non seulement des vitesses moyennes locales ou plutôt de leurs dérivées du premier ordre qui mesurent les glissements relatifs moyens des couches fluides, mais encore de l'intensité en chaque point de l'agitation tourbillonnaire qui y règne.

Boussinesq suppose que les forces de viscosité turbulente traduisant l'action du mouvement tourbillonnaire sur le mouvement moyen s'écrivent $\varepsilon\left(\frac{\partial \bar{V}_i}{\partial x_j} + \frac{\partial \bar{V}_j}{\partial x_i}\right)$

$\varepsilon(\vec{x}, t)$ scalaire

KAMPÉ DE FERIÉT

La notion de moyenne dans la théorie de la turbulence

Seminario Mat. e Fis. di Milano
vol. XXVII, 8 May 1956

La définition de la moyenne sur un ensemble de solutions des équations de Navier résout toutes les difficultés du passage des équations de Navier aux équations de Reynolds, tant qu'on demeure sur un plan abstrait; mais dès qu'on veut préciser $\mathcal{R}$ et μ, pour obtenir le mouvement moyen dans un problème concret de la théorie de la turbulence, on se heurte aux conséquences de notre ignorance des propriétés générales des équations de Navier. La définition statistique de la moyenne, pour devenir un instrument de recherche vraiment efficace dans la théorie de la turbulence, exige donc encore, croyons-nous, sur la théorie de l'intégration des équations de Navier [illegible] de très substantiels progrès.

AVERAGES USED IN TURBULENCE

- If the flow is statistically steady, one uses time average:

$$\bar{f}^T(\vec{x}) = \lim_{T\to\infty} \frac{1}{2T} \int_{-T}^{+T} f(\vec{x}, t)\, dt$$

- If the flow is statistically homogeneous, one uses space average:

$$\bar{f}^V(t) = \lim_{V\to\infty} \frac{1}{V} \int_V f(\vec{x}, t)\, d^n x$$

n space dimension

- If the flow is neither statistically steady nor homogeneous, one uses ensemble average:

$$\bar{f}^E(\vec{x}, t) = \lim_{N\to\infty} \frac{1}{N} \sum_{n=1}^{N} f^{(n)}(\vec{x}, t)$$

- If the flow is ergodic and statistically steady then: $\bar{f}^T = \bar{f}^E$

or and statistically homogeneous then: $\bar{f}^V = \bar{f}^E$

TAYLOR'S HYPOTHESIS

It is much easier to measure $V_{x_0}(t)$ in one point x_0 than $V_{t_0}(x)$ in many points x at the same time t_0.

If the flow moves very fast over the probe, one assumes that the velocity field does not change appreciably during the time of measurement, this is called the frozen-turbulence approximation.

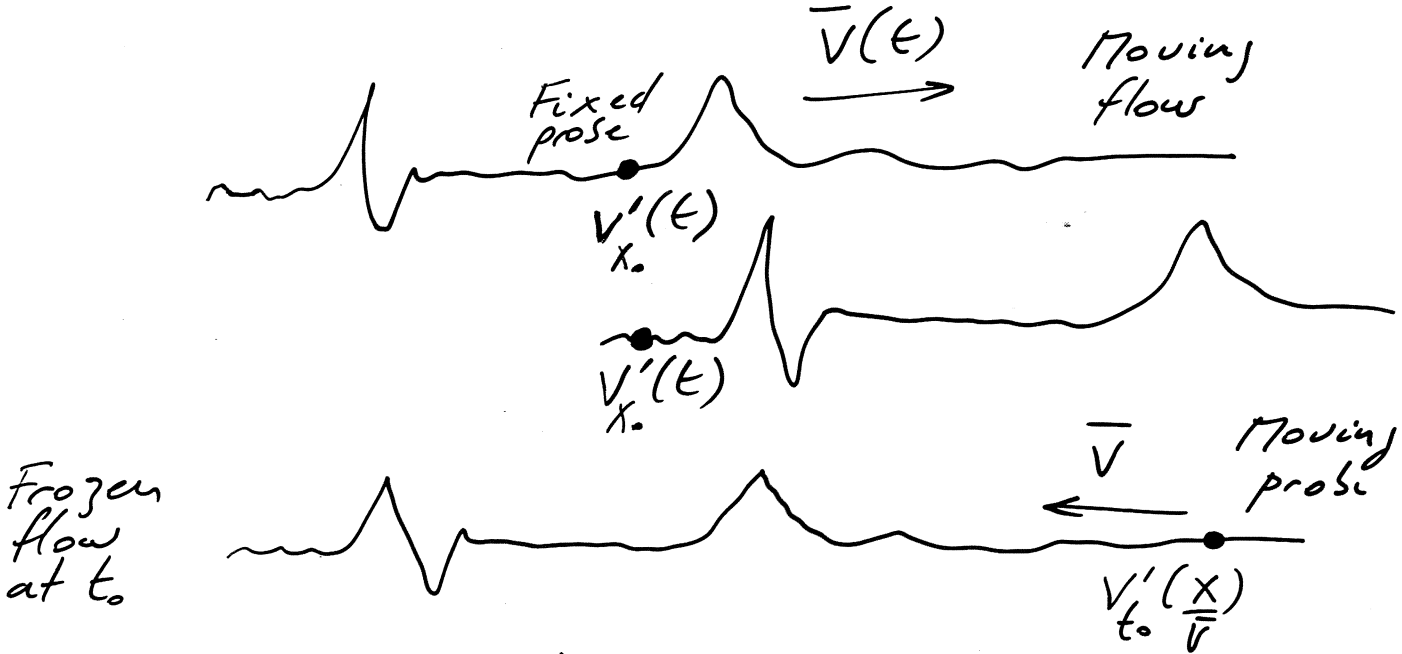

$V'_{x_0}(t) \equiv V'_{t_0}(\frac{x}{\bar{V}})$ only if $V' << \bar{V}$.

REYNOLDS EQUATIONS

$V = \bar{V} + V'$ $\qquad P = \bar{P} + P'$

We substitute in Navier Stokes equations to get $N.S.(\bar{V}, \bar{P}) = f(V', P')$.

Reynolds averaging conditions

$$f = \bar{f} + f'$$

Fluctuations $\bar{f'} = 0$

Average $\bar{\bar{f}} = \bar{f}$

Linearity: $\begin{cases} \overline{f+g} = \bar{f} + \bar{g} \\ \overline{\alpha f} = \alpha \bar{f} \\ \overline{\partial f} = \partial \bar{f} \end{cases}$

Product: $\overline{f \cdot g} = \bar{f} \cdot \bar{g} + \overline{f' g'}$

$\overline{\bar{f} \cdot g} = \bar{f} \cdot \bar{g}$

Averaged Navier-Stokes equations

$$\frac{\partial \bar{V}_i}{\partial t} + \bar{V}_j \frac{\partial \bar{V}_i}{\partial x_j} + \frac{1}{\rho} \frac{\partial \bar{P}}{\partial x_i} = \nu \nabla^2 \bar{V}_i - \frac{\partial}{\partial x_j} \tau_{ij}$$

with $\tau_{ij} = \overline{V_i' V_j'}$ Reynolds stress tensor

$\frac{\partial \bar{V}_i}{\partial x_i} = 0$ 2 equations

3 unknowns: $\bar{V}_i, \bar{P}, \tau_{ij}$

HOW TO COMPUTE THE REYNOLDS STRESS?

Fluctuating momentum equations

$$\frac{\partial v_i'}{\partial t} + \bar{v}_j \frac{\partial v_j'}{\partial x_j} + v_j' \frac{\partial v_i'}{\partial x_j} + v_j' \frac{\partial \bar{v}_i}{\partial x_j} + \frac{1}{\rho}\frac{\partial p'}{\partial x_i}$$

$$= -\nu \nabla^2 v_i' - \frac{\partial}{\partial x_j}(v_i' v_j')$$

$$\frac{\partial v_i'}{\partial x_i} = 0$$

$\Rightarrow$ equation for $\overline{v_i' v_j'} = f(\overline{v_i' v_j' v_k'})$

equation for $\overline{v_i' v_j' v_k'} = f(\overline{v_i' v_j' v_k' v_e'}$

$\vdots$

equation for the nth order moments $= f[(n+1)^{th}$ order moments$]$

$\vdots$

ad infinitum

There are always more unknowns than equations to solve them $\Rightarrow$

CLOSURE PROBLEM

Modèle RANS
Modèle de Boussinesq avec viscosité turbulente

MODELES DE TURBULENCE

— $\boxed{\text{au 1er ordre}}$

Avantage

Stabilité des schémas numériques car la viscosité turbulente amortit de nombreux mécanismes physiques non linéaires, en particulier les instabilités donnant lieu aux structures cohérentes.

Inconvénients

Cas d'écoulements où la loi linéaire de Boussinesq est toujours en défaut :

- voisinage des points d'arrêt,
- distorsions rapides,
- décollements,
- surfaces courbes,
- mouvement secondaires,
- configurations 3D ...

Le comportement de l'agitation turbulente (modélisée par la loi linéaire de Boussinesq) n'est pas identique à l'agitation moléculaire (modélisée par la loi linéaire de Newton)

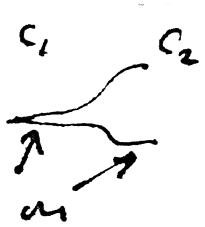

On doit ajuster les constantes de façon différente et on ne peut pas avoir de bons résultats partout.

MODELES DE TURBULENCE

- **au 2nd ordre:** modèle $k-\varepsilon$
résolution des équations de transport des contraintes turbulentes

Avantages

La modélisation au 2nd ordre simule mieux les aspects non-linéaires et les instabilités conduisant aux structures cohérentes. Elle prend en échange local et actuel de l'énergie du mouvement fluctuant vers le mouvement moyen. Elle est capable de simuler la relaminarisation des écoulements instationnaires.

30% de temps de calcul en plus.

Inconvénients

La divergence du tenseur des contraintes n'apparaît plus sous la forme de diffusion, mais sous la forme de terme source $\Rightarrow$ caractère hyperbolique des équations (la forme de diffusion moléculaire étant négligeable) $\Rightarrow$ nécessité de mettre une viscosité numérique sinon le modèle diverge.

→ une loi de comportement tenant compte uniquement de la partie symétrique du tenseur des gradients de vitesse moyenne est incomplète. Pour remédier à cela il faut supposer que le tenseur d'anisotropie doit être également fonction de S et de Ω : $A = \overline{u_i u_j} - \frac{2}{3} k$

(Pope, 1975)

$$S = S_{ij} = \frac{\partial U_i}{\partial x_j} + \frac{\partial U_j}{\partial x_i}$$

$$-\rho \overline{u_i u_j} = C_\mu(S, \Omega) \frac{k^2}{\varepsilon} \left[S + f(S, \Omega) \right]$$

appelée loi de comportement non linéaire dans laquelle les constantes varient avec les propriétés locales de l'écoulement (varient avec les fonctions de structures analogues à celles proposées par Rotta & Lesieur et par Cousteix).

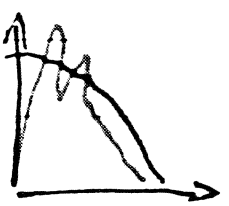

Modèle semi déterministe

$$F(X,t) = \underbrace{\overline{F(X)}}_{\text{déterministe}} + \underbrace{F(X,t)}_{\text{aléatoire}} + \underbrace{f(X,t)}_{\text{aléatoire}}$$

Moyenne d'ensemble

REYNOLDS AVERAGED NAVIER-STOKES RANS MODEL

Moyenne $\langle\rangle$

$$\langle u \rangle = \lim_{n\to\infty} \frac{1}{n} \sum_{l=1}^{n} u_l$$

Moyenne d'ensemble

$$u'_i = u_i - \langle u \rangle$$ Fluctuation

$\langle u' \rangle = 0$

$\langle u'^2 \rangle = \sigma^2$

$\Rightarrow$ taux de turbulence $I = \left(\frac{\sigma}{\langle u \rangle}\right)^2$

$\left(\frac{\text{Variance}}{\text{moyenne}}\right)^2$

Propriétés exactes de l'opérateur de moyenne d'ensemble

linéarité $\langle u+v \rangle = \langle u \rangle + \langle v \rangle$

$\langle au \rangle = a\langle u \rangle, a \in \mathbb{R}$

$\langle Du \rangle = D\langle u \rangle$

Distributivité de + par rapport à $\times$

$\langle \langle u \rangle v \rangle = \langle u \rangle \langle v \rangle$

$\langle \langle u \rangle \rangle = \langle u \rangle$.

$\langle u' \rangle = 0$ exact

Equations de NS moyennées

$$\partial_t \langle u_i \rangle + \partial_{x_j} \langle u_i u_j \rangle + \partial_{x_i} \langle p \rangle = \nu \partial^2_{x_i x_j} \langle u_i \rangle$$

$\partial_{x_i} \langle u_i \rangle = 0$ exact

On décompose le terme non linéaire moyenné et on obtient le tenseur de Reynolds :

$$\langle u_i u_j \rangle = \langle (\langle u_i \rangle + u'_i)(\langle u_j \rangle + u'_j) \rangle$$

car $u = \langle u \rangle + u'$

$$= \langle \langle u_i \rangle \langle u_j \rangle \rangle$$

$$+ \langle \langle u_i \rangle u'_j \rangle \quad \text{nul car} = \langle u_i \rangle \underbrace{\langle u'_j \rangle}_{=0}$$

$$+ \langle u'_i \langle u_j \rangle \rangle \quad \text{nul car} = \underbrace{\langle u'_i \rangle}_{=0} \langle u_j \rangle$$

$$+ \langle u'_i u'_j \rangle$$

$$= \langle u_i \rangle \langle u_j \rangle + \langle u'_i u'_j \rangle$$

tenseur de Reynolds

car $\langle \langle u_i \rangle \langle u_j \rangle \rangle = \langle \langle \langle u_i \rangle \rangle u_j \rangle$

$$= \langle \langle u_i \rangle u_j \rangle = \langle u_i \rangle \langle u_j \rangle$$

exact

Modélisation du tenseur de Reynolds (hypothèse de Boussinesq)

Modélisé

$$\boxed{\begin{array}{l} \langle u'_i u'_j \rangle \sim L\,(\nabla \bar{u} + \nabla \bar{u}^T) \\ k - \varepsilon : \quad L \sim (\nabla \bar{u}, k, \varepsilon) \end{array}}$$

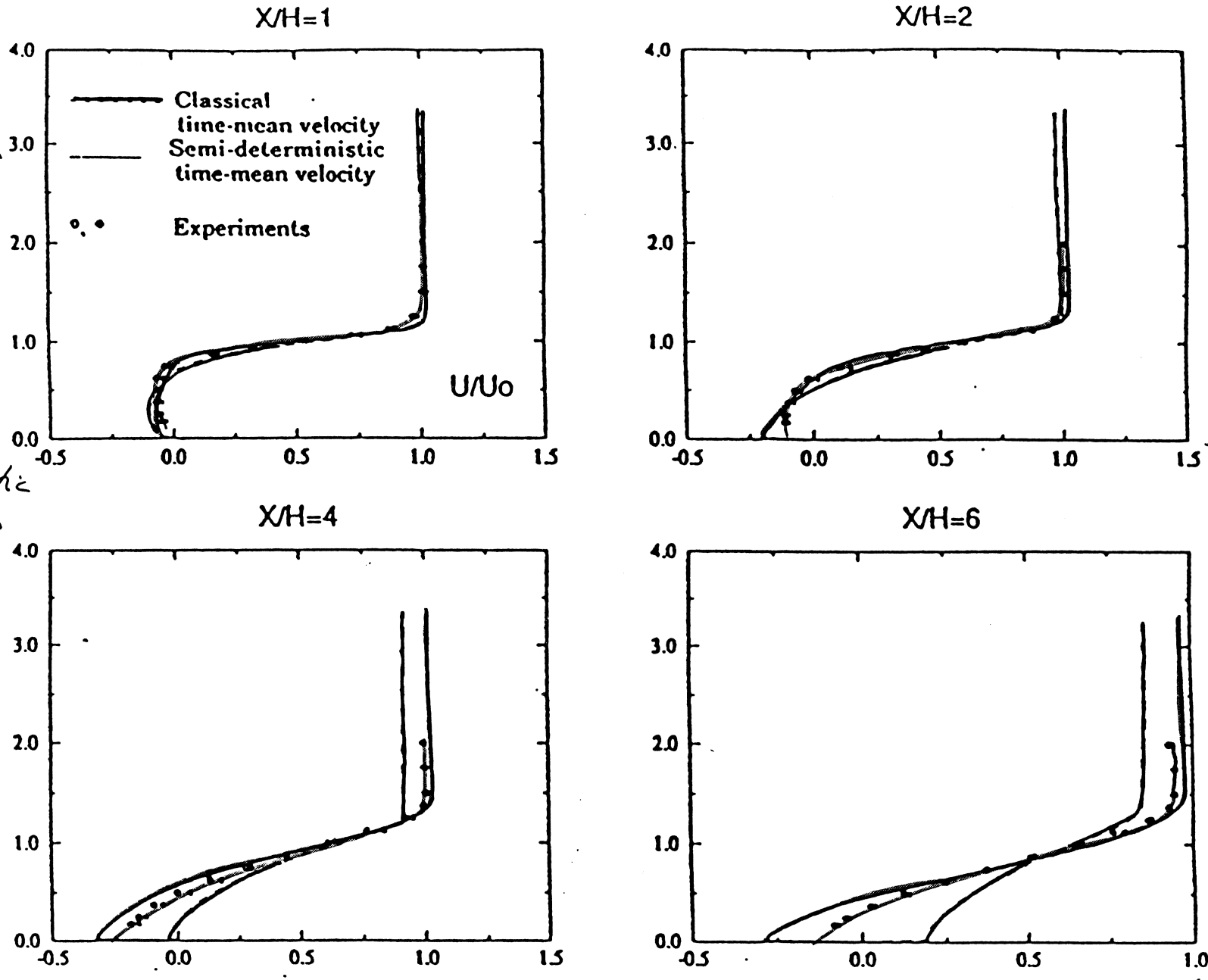

expérience en Laboratoire

k-ε simulation

Semi-déterministe simulation (Ha Minh 93)

COMPARAISON ENTRE PREDICTION NUMERIQUE AVEC UN MODELE DE TURBULENCE ET EXPERIENCE DE LABORATOIRE

Mean velocity profile of a flow behind a step

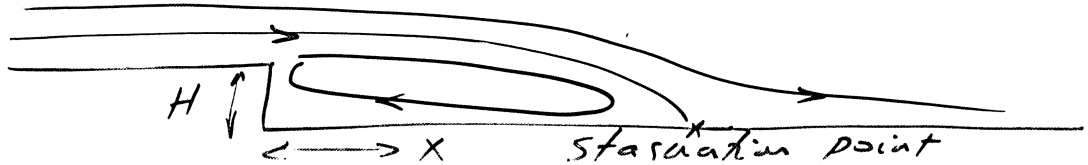

LARGE EDDY SIMULATION

LES MODEL

On considère un filtre F qui sépare les grandes échelles

$$\boxed{\bar{u} = F * u}$$

des petites échelles ou l'écoulement

$$\boxed{u' = u - \bar{u} = (1-F) * u}$$

$*$ opérateur de convolution

Propriétés du filtre

linéarité : $\begin{cases} \overline{u+v} = \bar{u} + \bar{v} \\ \overline{au} = a\bar{u}, \ a \text{ cste} \\ \overline{Du} = D\bar{u}, \ D \text{ opérateur différentiel} \end{cases}$

Mais en général F n'est pas un projecteur

$$\bar{\bar{u}} = F^2 * u \neq \bar{u} = F * u$$

$$\Rightarrow \boxed{\bar{\bar{u}} \neq \bar{u}}$$

Le filtrage par F n'est pas orthogonal

$$\Rightarrow \boxed{\bar{u'} \neq 0} \quad \text{car } \bar{u'} = F(1-F)*u = F*u - F^2*u$$

et $F^2 \neq F$

Equations de Navier-Stokes filtrées

$$\partial_t \bar{u_i} + \partial_{x_j}(\bar{u_i}\bar{u_j}) + \partial_{x_i}\bar{P} = \partial\,\partial_{x_j}(\partial_{x_j}\bar{u_i} + \partial_{x_i}\bar{u_j})$$

$$\partial_{x_i}\bar{u_i} = 0 \qquad \text{exact}$$

On décompose le terme non linéaire final (Décomposition de Léonard) :

$$\overline{u_i u_j} = \overline{\bar{u}_i \bar{u}_j} + \overline{\bar{u}_i u_j'} + \overline{u_i' \bar{u}_j} + \overline{u_i' u_j'}$$

exact

car $u = \bar{u} + u'$

Ici les termes $\overline{\bar{u}_i u_j'}$ et $\overline{u_i' \bar{u}_j}$ ne s'annulent plus car $\overline{u'} \neq 0$.

Modélisation du tenseur de Léonard

Deux approches sont possibles :

1. $\partial_t \bar{u}_i + \partial_{x_j}(\overline{\bar{u}_i \bar{u}_j}) + \partial_{x_i} \bar{P} - \partial_{x_j} \tau_{ij}$
$= \nu \partial_{x_j}(\partial_{x_j} \bar{u}_i + \partial_{x_i} \bar{u}_j)$

Terme non linéaire moyenné : $\partial_{x_j}(\overline{\bar{u}_i \bar{u}_j}) - \partial_{x_j} \tau_{ij} = \partial_{x_j} \overline{u_i u_j}$)

ou supposon $\tau = \tau(\bar{u})$

τ indépendant de u'

Tenseur des contraintes sous-maille

$$\tau_{ij} = C_{ij} + R_{ij} = \overline{u_i u_j} - \overline{u_i}\,\overline{u_j}$$

tenseur croisé (Interaction échelles résolues / échelles sous maille)

tenseur de Reynolds sous-maille

$\tau_{ij} = C_{ij} + R_{ij} = \overline{u_i u_j} - \bar{u}_i \bar{u}_j$

Tenseur d'interaction — Décomposition double

$C_{ij} = \bar{u}_i u_j' + \bar{u}_j u_i'$

Tenseur de Reynolds sous-maille

$R_{ij} = u_i' u_j'$

(2.) $\overline{\bar{u}_i \bar{u}_j}$ n'est pas calculable directement

$$\overline{\bar{u}_i \bar{u}_j} = \overline{\bar{u}_i \bar{u}_j} \underbrace{- \bar{u}_i \bar{u}_j + \bar{u}_i \bar{u}_j}_{- \quad +}$$

$$= L_{ij} + \bar{u}_i \bar{u}_j$$

$L_{ij} = \overline{\bar{u}_i \bar{u}_j} - \bar{u}_i \bar{u}_j$

tenseur de Leonard qui décrit les interactions entre les échelles résolues.

Navier-Stokes moyennés deviennent :

$$\partial_t \bar{u}_i + \partial_{x_j}(\bar{u}_i \bar{u}_j) - \partial_{x_j} \tau_{ij} + \partial_{x_i} \bar{p}$$

$$= \nu \partial_{x_j}(\partial_{x_j} \bar{u}_i + \partial_{x_i} \bar{u}_j)$$

avec $\tau_{ij} = L_{ij} + C_{ij} + R_{ij} = \overline{u_i u_j} - \bar{u}_i \bar{u}_j$

Décomposition triple

CLASSIFICATION OF TURBULENCE MODELS

Multi-scale models

2-scale models

steady state

1. Reynolds Stress Models & 1 point closures to calculate 1 point first and second moments (mean velocity, turbulent kinetic energy ...). Only shady state without intermittency. Handle walls and complex geometry. Ex. k-ε Spalding-Launder 1972

2. Subgrid scale models for LES DNS for large scales and the effect of small scales is modeled. Only simple geometry. No strong inhomogeneity, therefore problems near walls. Handle intermittency. Ex. Deardoff 73

Time evolution

3. Spectral models & 2 point closures to calculate the 2 point velocity correlation tensor and the energy spectrum. Homogeneous flows only. No walls. Ex. EDQNM Orszag 1970

4. PDF models to calculate the joint PDFs. No walls. Homogeneous flows only. Ex. Pope 1985

5. Vorticity transport models & CS^2 DNS for coherent vorticity and the effect of incoherent vorticity is modelled. Simple geometry. Inhomogeneity & intermittency, wa

ONE-POINT CLOSURES WITH ZERO EQUATION MODELS

Turbulence models consist of arbitrarily closing the hierarchy of Reynolds equations by modelling either the second order moments (Reynolds stress tensor) $\Rightarrow$ one-point closures or the nth order moments $\Rightarrow$ n-point closures.

The model should respect: realizability (i.e. $E > 0$) and frame invariance (i.e. Galilean).

SMAGORINSKY'S MODEL 1963

$$\ldots = \nu \nabla^2 \overline{V_i} - \frac{\partial}{\partial x_j} \tau_{ij}$$

$$= \nu \nabla^2 \overline{V_i} + \nu_T \nabla^2 \overline{V_i}$$

with eddy viscosity $\equiv \dfrac{\ell_0^2}{t_0} = C_S (\Delta x)^2 \overline{S_{ij}}$

Rate-of-strain tensor $\overline{S_{ij}} = \frac{1}{2}\left(\dfrac{\partial \overline{V_i}}{\partial x_j} + \dfrac{\partial \overline{V_j}}{\partial x_i}\right)$ and $C_S \approx 0.01$ Smagorinsky's constant

ONE-POINT CLOSURE WITH TWO EQUATIONS MODELS

Two separate modeled transport equations are solved based on a turbulent length scale ℓ_0 and a turbulent time scale t_0.

For the k-ε model:

$$\ell_0 \sim \frac{k^{3/2}}{\varepsilon} \quad \text{and} \quad t_0 \sim \frac{k}{\varepsilon}$$

with $k = \frac{1}{2}\overline{v_i v_i}$ turbulent kinetic energy

and $\varepsilon = \nu \overline{v_{i,j} v_{i,j}}$ turbulent dissipation rate

Other characteristic scales:

turbulent velocity $v = \sqrt{\frac{2}{3}k}$

Taylor microscale $\lambda = \sqrt{\frac{15\nu}{\varepsilon}}$

Kolmogorov dissipative scale $\ell_D = \left(\frac{\nu^3}{\varepsilon}\right)^{1/4}$

K-ε MODEL

One-point closure model having two equations to compute turbulent kinetic energy k and dissipation rate ε (Launder & Spalding 1974):

$$\tau_{ij} = \overline{v_i' v_j'} = \frac{2}{3} k \delta_{ij} - \nu_T \left(\frac{\partial \bar{v}_i}{\partial x_j} + \frac{\partial \bar{v}_j}{\partial x_i} \right)$$

$$\nu_T = C_\mu \frac{k^2}{\varepsilon}$$

$$\frac{\partial k}{\partial t} + \bar{v}_i \frac{\partial k}{\partial x_i} = -\tau_{ij} \frac{\partial \bar{v}_i}{\partial x_j} - \varepsilon + \frac{\partial}{\partial x_i} \left(\frac{\nu_T}{\sigma_k} \frac{\partial k}{\partial x_i} \right) + \nu \nabla^2 k$$

$$\frac{\partial \varepsilon}{\partial t} + \bar{v}_i \frac{\partial \varepsilon}{\partial x_i} = -C_{\varepsilon 1} \frac{\varepsilon}{k} \tau_{ij} \frac{\partial \bar{v}_i}{\partial x_j} - C_{\varepsilon 2} \frac{\varepsilon^2}{k} + \frac{\partial}{\partial x_i} \left(\frac{\nu_T}{\sigma_\varepsilon} \frac{\partial \varepsilon}{\partial x_i} \right) + \nu \nabla^2 \varepsilon$$

with the 5 constants:

$C_\mu = 0.09$ $\quad \sigma_k = 1.0$ $\quad C_{\varepsilon 1} = 1.44$

$\sigma_\varepsilon = 1.3$ $\quad C_{\varepsilon 2} = 1.92$

which have been identified from physical experiments on equilibrium turbulent boundary layers and the decay of isotropic turbulence.

To take care of walls some ad hoc damping should be added.

Lewis Fry RICHARDSON
and J. Arthur GAUNT

'Diffusion regarded as a compensation for smoothing'
Memoirs of the Royal Meteorological Society, 1930

'Diffusion is a compensation for neglect of detail. By an arbitrary choice we try to divide motions into two classes:
(a) Those we treat in detail.
(b) Those which we smooth away by some process of averaging.
Unfortunately these two classes are not always mutually exclusive!

'The law of diffusion depends entirely upon the arbitrarily chosen method of averaging, which is always implied when diffusion or viscosity are mentioned!

We must expect to find a different law of diffusion for each different type of smoothing.

1) The mean over the whole of a spreading cluster. Then exists no differential eq.

2) Means taken over long time or means over many occasions distributed at random. Such means convert weather into climate.

The relation between the diffusivities appropriate to the long-time mean and those appropriate to other sorts of mean is at present the inner mystery of non-Fickian diffusion.

3) Mean over space-time cells The appropriate law of diffusion is then a difference equation. A differential equation would require apology if used here.

A-PRIORI MODELS OF TURBULENCE

What to keep? to compute? Which components are active?

/ What to discard? to model? Which components are passive?

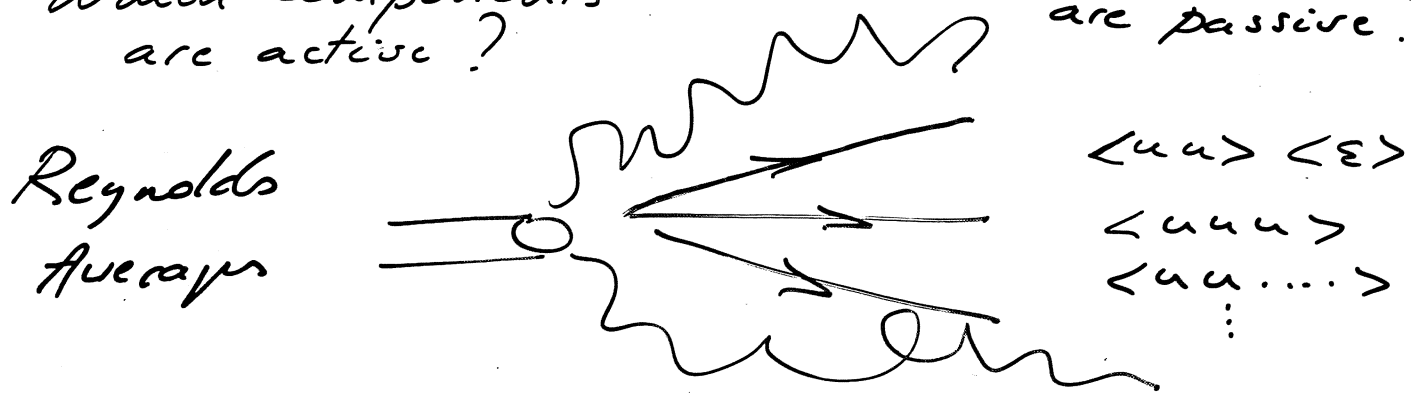

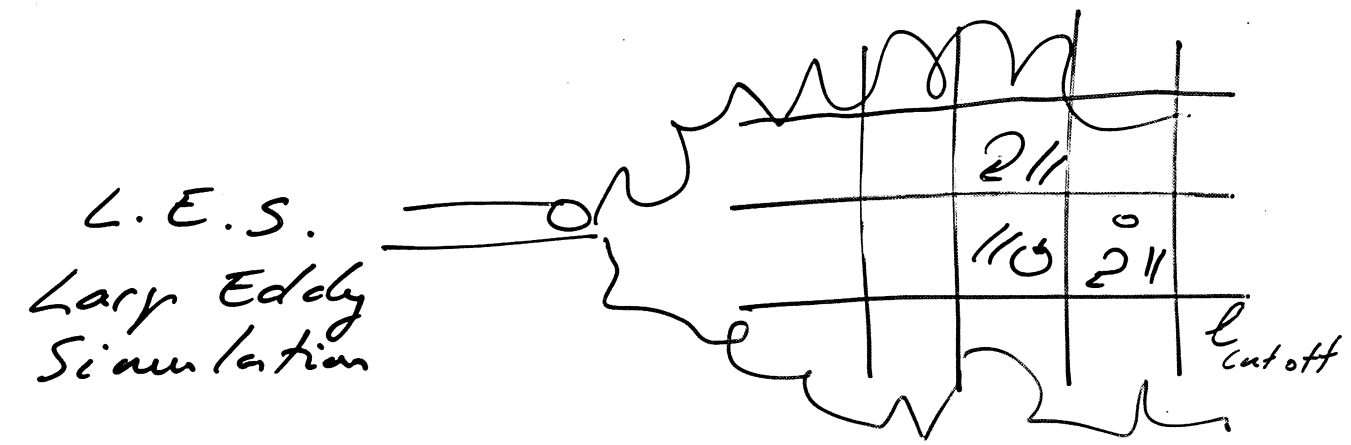

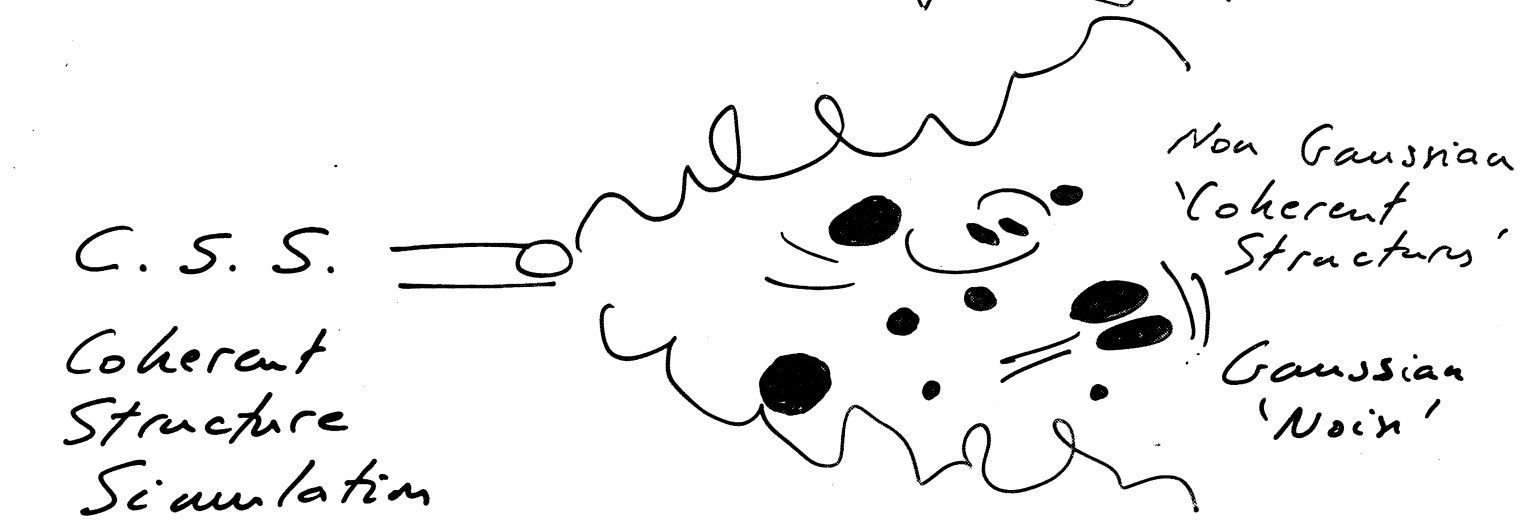

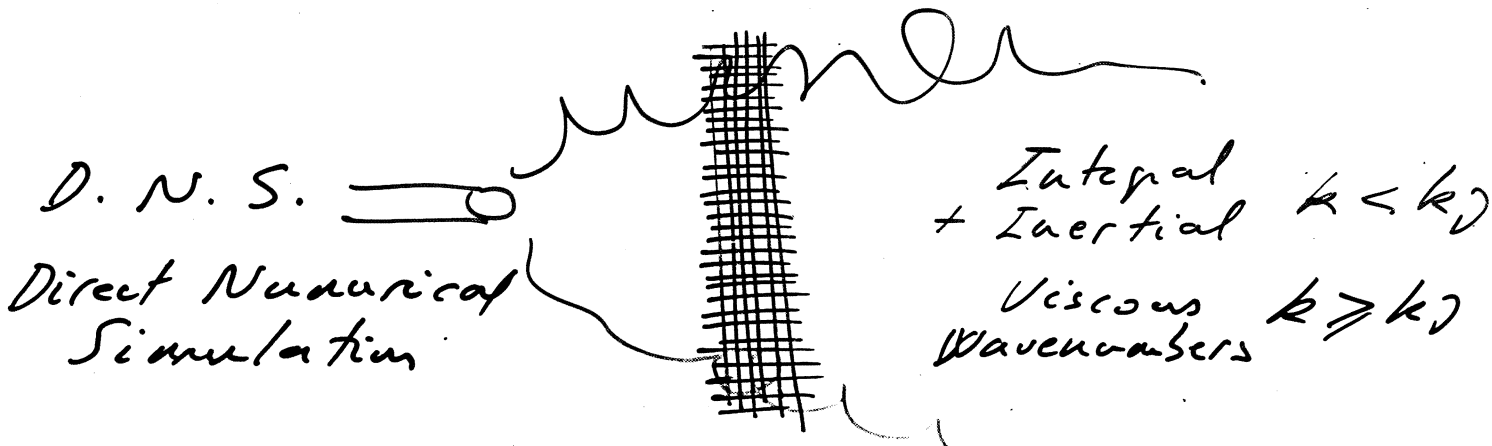

TURBULENCE MODELLING WITH L.E.S.

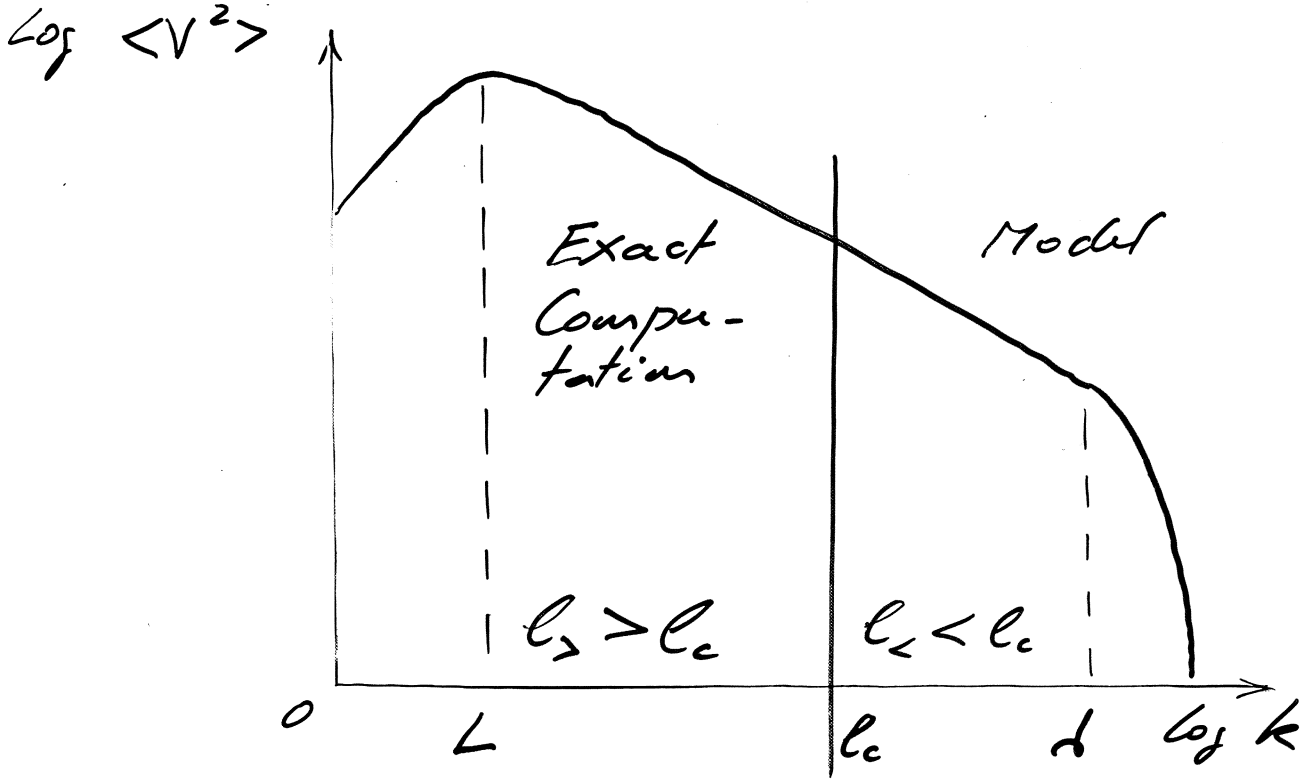

Energy spectrum

$$\vec{V} = \vec{V}_> + \vec{V}_<$$

Reynolds Averaged Equations

$$\frac{\partial \vec{V}_{>i}}{\partial t} + \vec{V}_j \frac{\partial \vec{V}_{>i}}{\partial x_j} + \frac{\partial}{\partial x_i}\frac{P_>}{\rho} = \frac{\partial}{\partial x_j}\left(\nu \frac{\partial \vec{V}_{>i}}{\partial x_j} - \vec{V}_{<i}\vec{V}_{<j}\right)$$

$$\frac{\partial V_{>i}}{\partial x_i} = 0$$

PROPOSED METHOD FOR COHERENT STRUCTURE SIMULATION (CS^2)

To model or compute turbulent flows we have to perform some averaging procedure

$\Longrightarrow$

We propose to split the vorticity field into:

- inhomogeneous organized components, out of thermal equilibrium, having non-Gaussian statistics $\Rightarrow$ Coherent Vortices
- $+$
- homogeneous random components in thermal equilibrium, having Gaussian Statistics $\Rightarrow$ Background flow

Both are multi-scale, with different scalings $\Rightarrow$ neither Fourier nor grid-point representations can discriminate them.

COHERENT STRUCTURE SIMULATION RESEARCH PROGRAM

The description of turbulent flows in terms of a mean plus random fluctuations is eroded, since they are a superposition of deterministic coherent structures moving in the random background flow their interactions have produced.

Although coherent structures play an essential role in the flow dynamics, classical averaging procedures (ensemble, time, space) do not see them.

They are correlated in space (phase locking) ⇒ we need wavelet representation,

they are rare events ⇒ we need conditional averaging procedures.

NO MEAN PROFILE

The description of turbulent flows in terms of a mean profile $\bar{f}$ plus random fluctuations f' is eroded since the mean profile is a superposition of deterministic coherent structures moving within a random background.

In this case the classical averaging procedures are blind to these coherent structures which are essential to the dynamics.

We need to find new averaging methods about to retain the local information attached to coherent structures.

$\Rightarrow$ local functions such as WAVELETS

NO WAVENUMBER SEPARABILITY

The non separability of the turbulent flow dynamics between low wavenumbers and high wavenumbers is a major obstacle which any mathematical modelling of turbulence is facing.

We propose to analyze turbulent flows in different functional bases to find some ash to separate the flow dynamics between action and plasma modes, both being multiscale.

$\Rightarrow$ multiscale bases such as WAVELET BASES

NO THERMAL EQUILIBRIUM

Navier-Stokes equations can be deduced from Boltzmann equation (Chapman-Enskog) because the molecular velocities responsible for the transport and mean fields are reasonably decoupled ⇒

Universality of the transport coefficients: the diffusion coefficient D is related to molecular interactions by treating the flow as a perturbation of a thermal equilibrium state (Maxwell).

But there do not seem to be such an 'equilibrium state' in the turbulent regime from which a similar perturbation scheme can be derived.

⇒ CONDITIONAL AVERAGING distinguishing components in thermal equilibrium and out of equilibrium

HOW TO COMBINE THE DYNAMICAL AND THE STATISTICAL APPROACHES?

To compute 2D turbulent flows we propose to split the problem into:

DYNAMICAL SYSTEM
non Gaussian
elliptical regions
non ergodic
inhomogeneous

1. Compute the evolution of a low-dimensional deterministic system of vortices out of statistical equilibrium,

STATISTICAL MODEL
Gaussian
hyperbolic regions
ergodic
homogeneous

2. Model the statistics of a high-dimensional background flow in statistical equilibrium by an Gaussian stochastic process having k^{-3} energy spectrum.

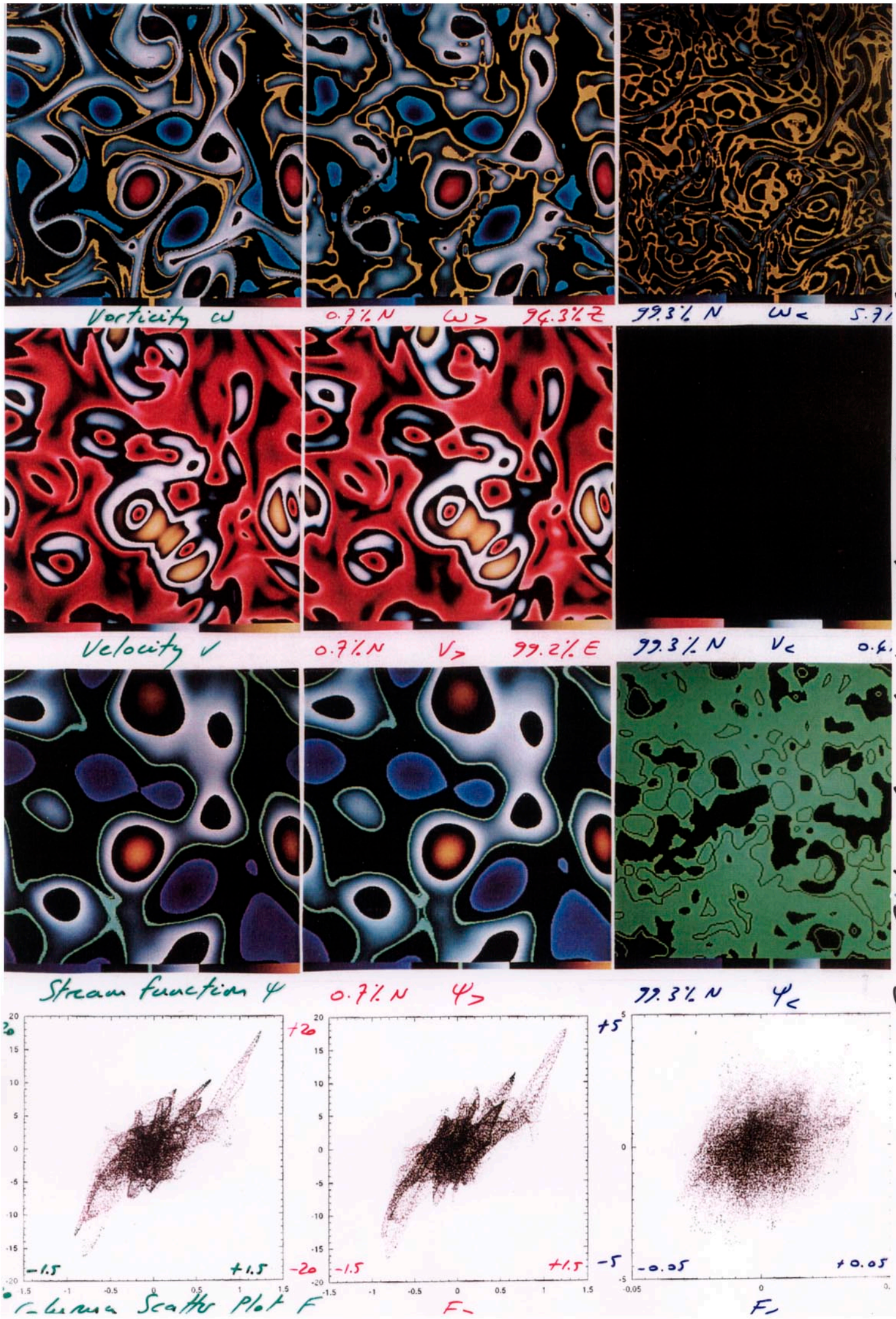

Farp Schneider and Keulahan, Physics of Fluids, 1999

For 2D turbulent flows
Separation between coherent (>)
and incoherent (<) components

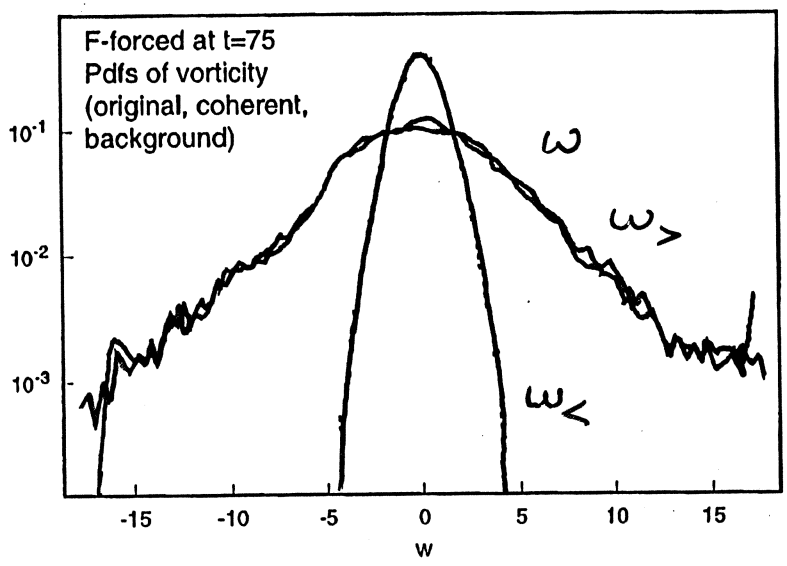

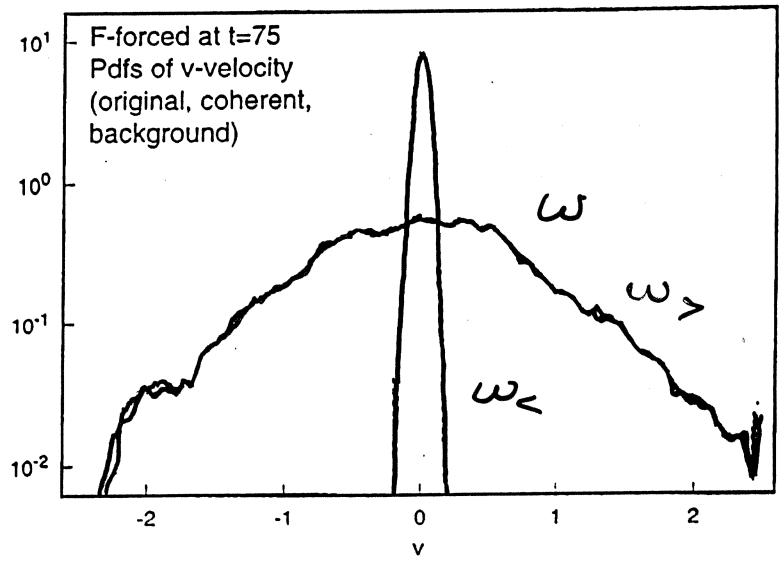

ω vorticity
N Number of samples
$N = 256^2$

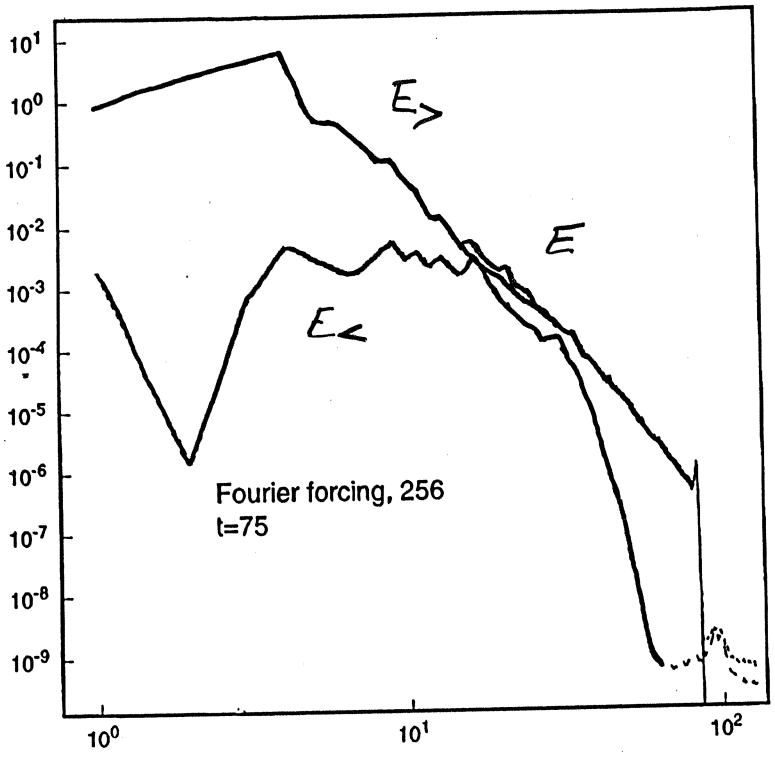

cf. Physics of Fluids - August 93
Farge, Schneider and Kevlahan

$$\tilde{\omega} = \langle \omega | \psi \rangle$$

$$\tilde{\omega}_T = \left(2 \langle \omega^2 \rangle \log_{10} N \right)^{1/2}$$

$\tilde{\omega}_> > \tilde{\omega}_T$

$\omega_> = |\psi\rangle\langle\tilde{\omega}_>| +$
Coherent vorticity
0.7% N

$\tilde{\omega}_< \leq \tilde{\omega}_T$

$\omega_< = |\psi\rangle\langle\tilde{\omega}_<|$
Incoherent vorticity
99.3% N

For 3D turbulent flows
separation between coherent (>)
and incoherent (<) components

Total Vorticity

DNS 512^3 by Meneguzzi

$|\vec{\omega}'|$

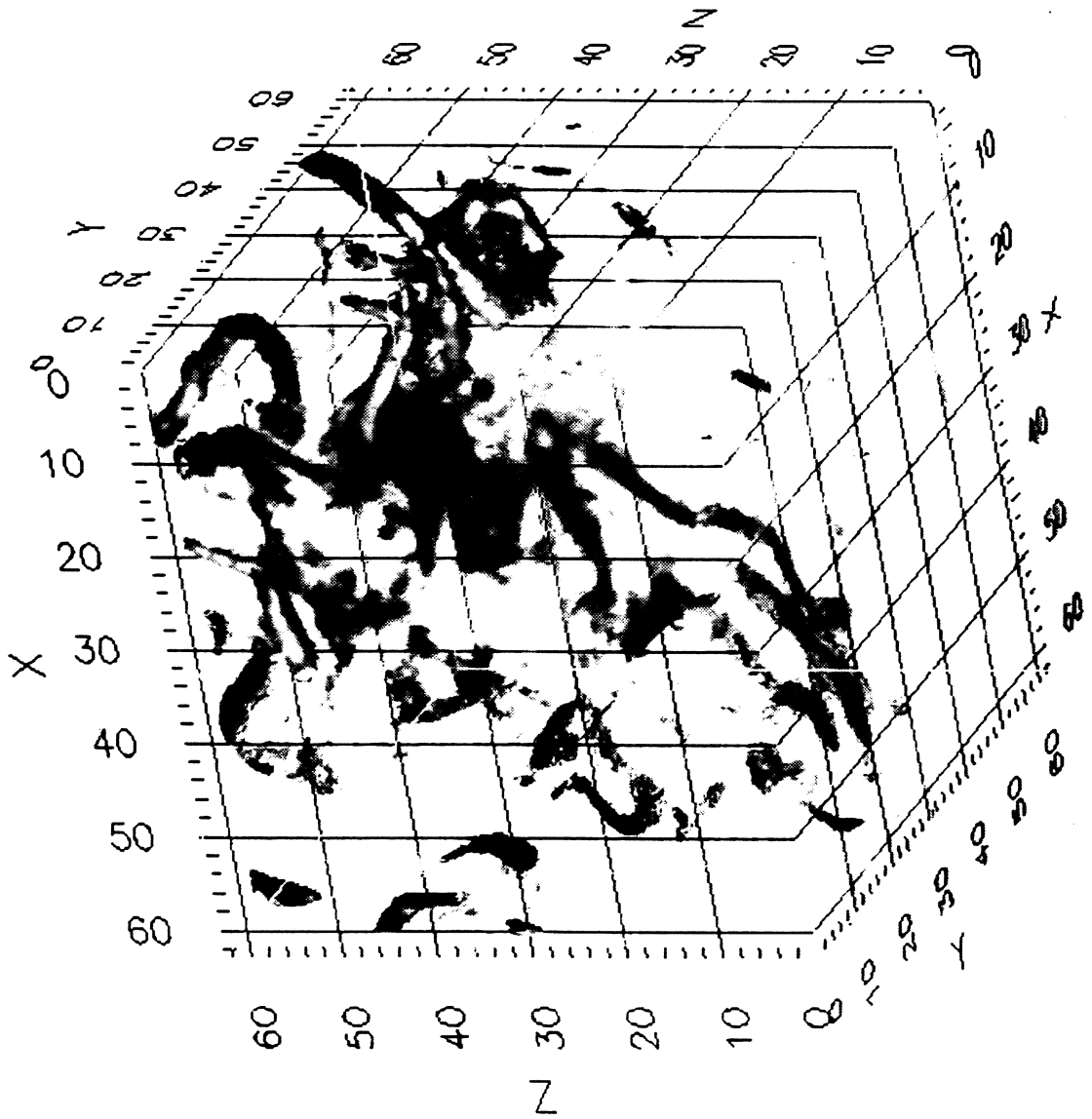

Coherent Vorticity

3% N retains 84% Z

$|\vec{\omega}|$

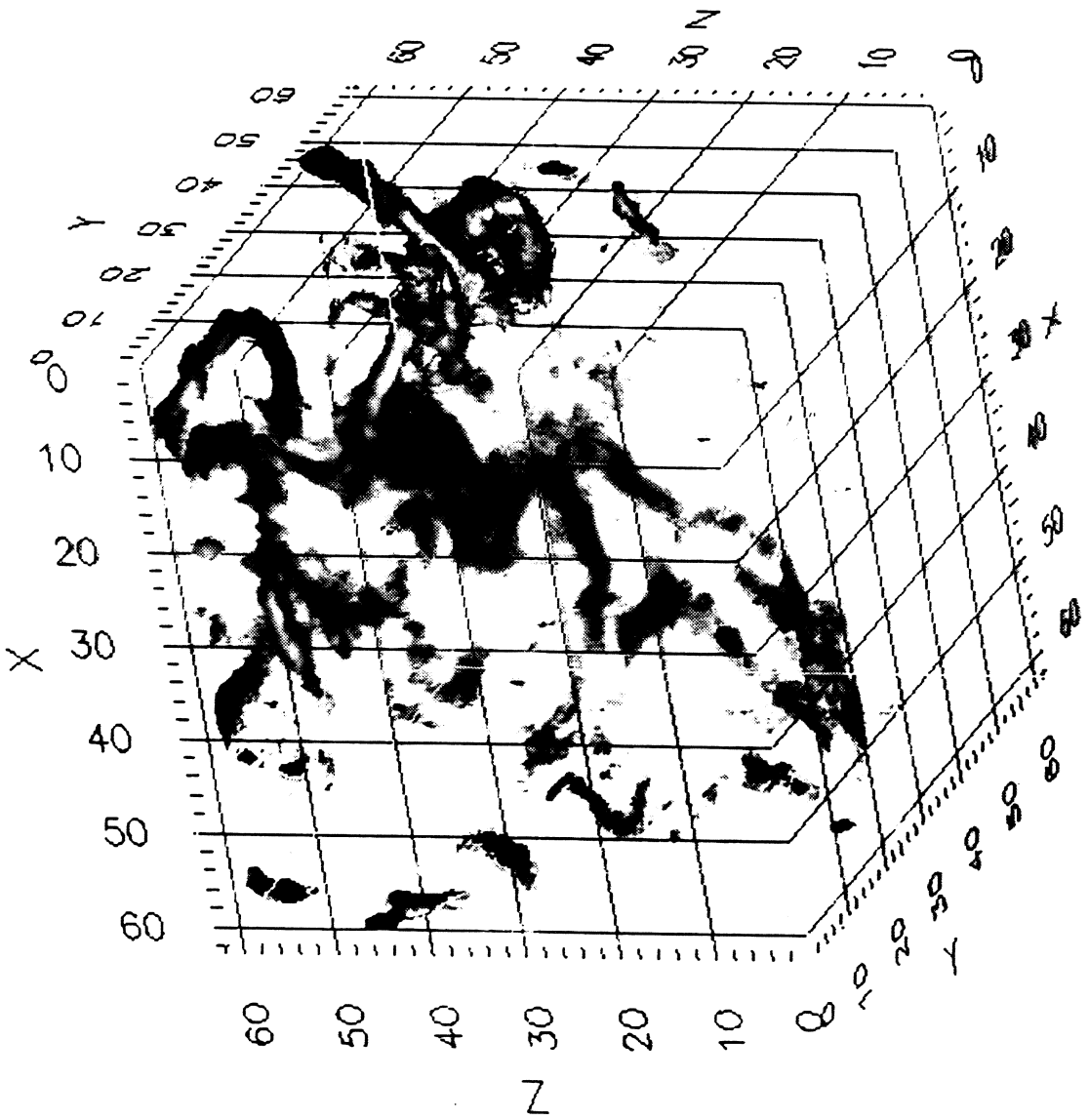

Background Vorticity

77% N retains 16% Z

$\bar{\omega}_z$

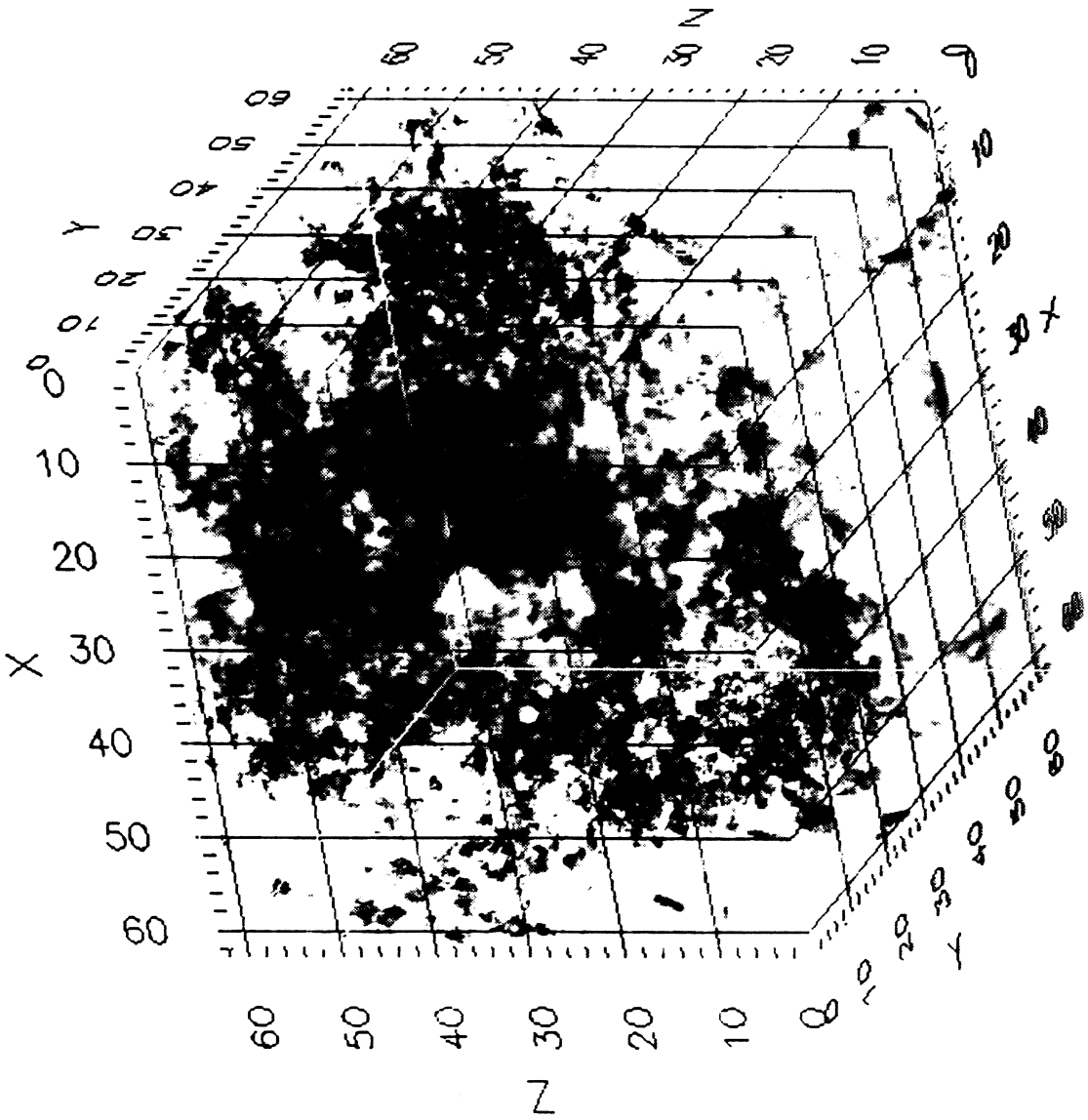

Vorticity PDF
in lin-log

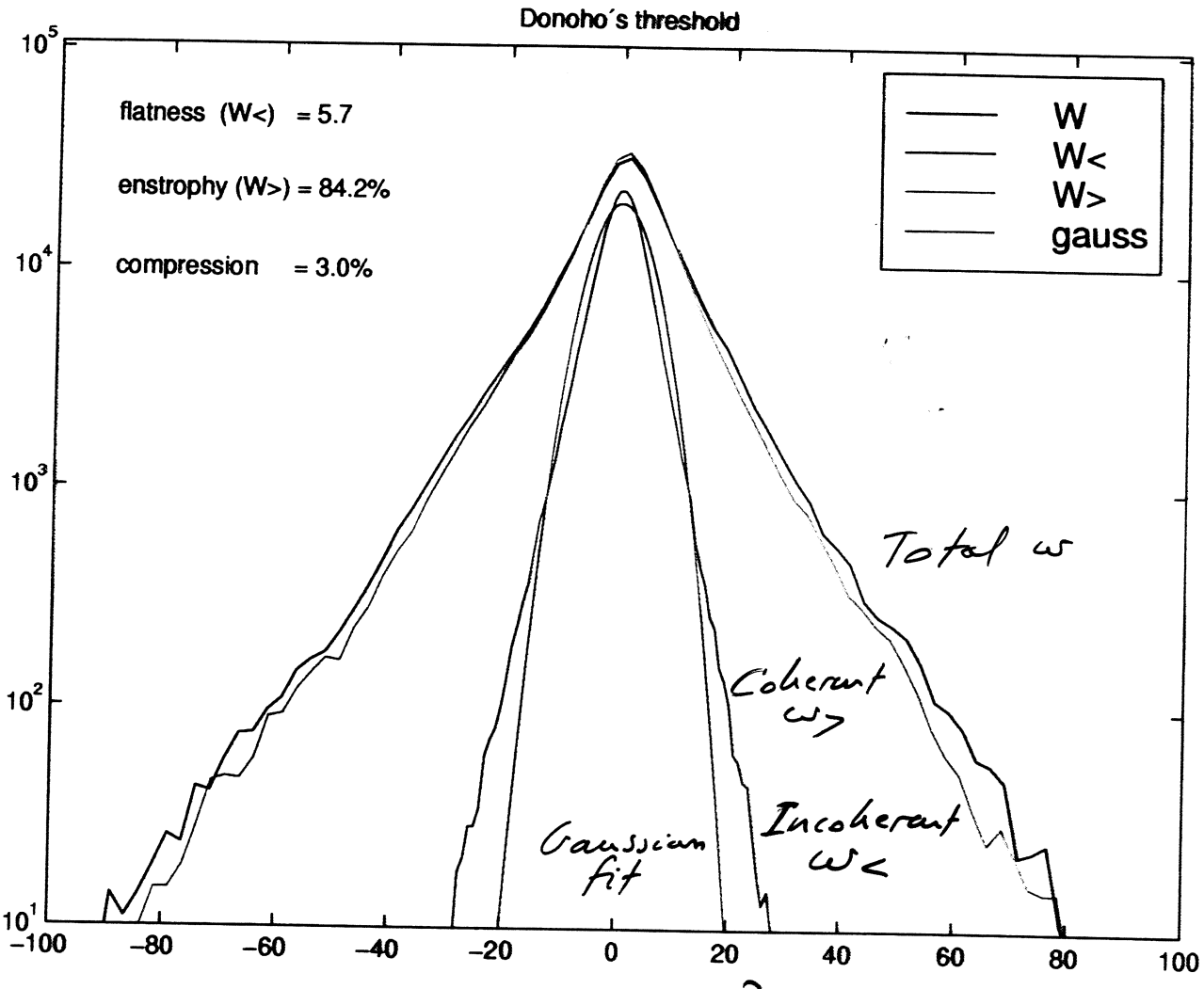

$DNS\ 512^3$

Donoho's threshold

Incoherent $\omega_<$: 97% N retains 16% Z

Coherent $\omega_>$: 3% N retains 84% Z

Energy Spectrum
in Log - Log

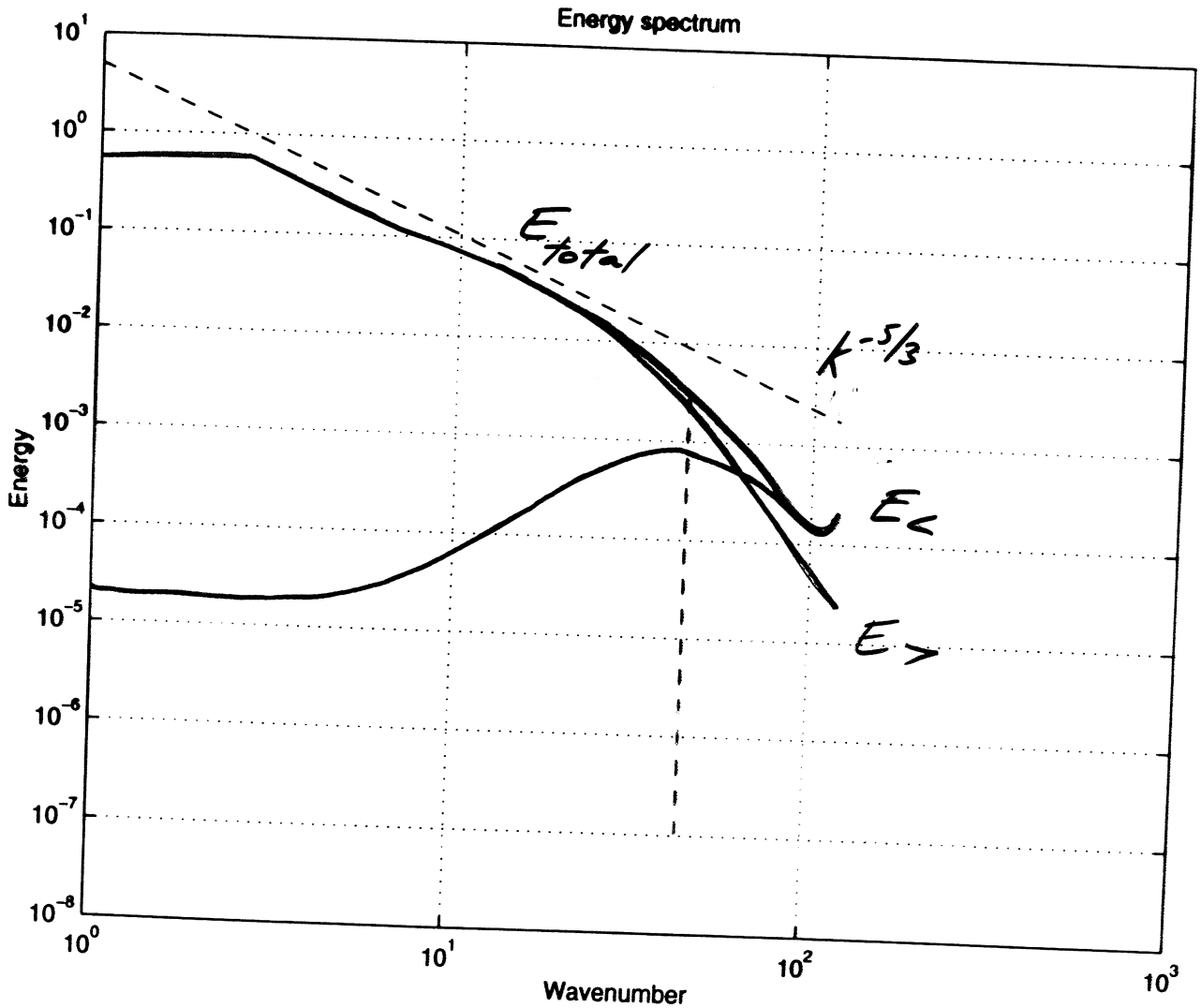

DNS 512^3

Donoho's threshold

Incoherent $w_<$: 97% N retains 16% Z

Coherent $w_>$: 3% N retains 84% Z

INTERPRETATION

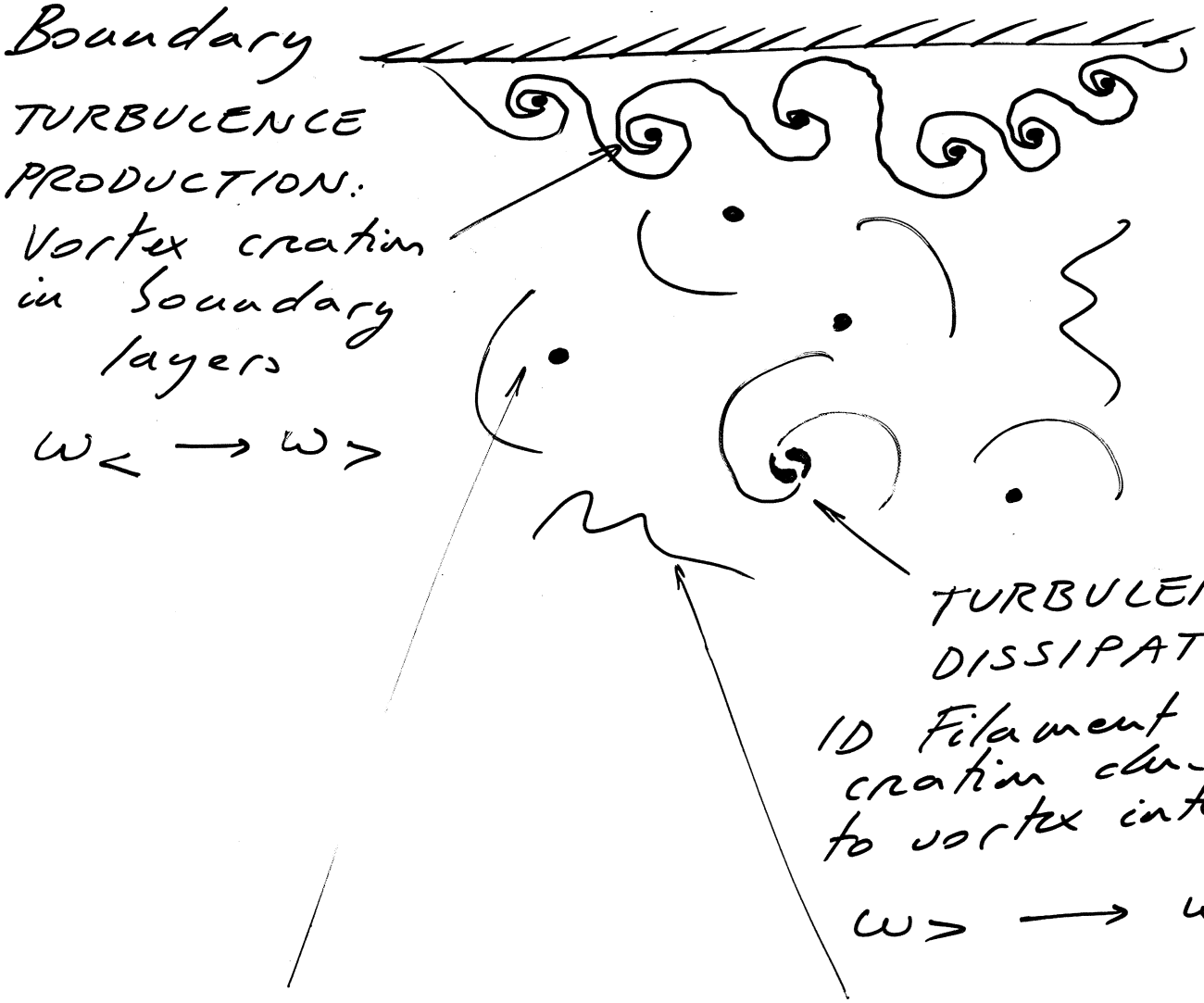

COHERENT VORTICITY:

- 2D vortices or 3D vortex tubes rare in space & time
  ⇒ disappear in the total energy spectrum,
- Non Gaussian PDF
  ⇒ dominates the total PDF,
- Small number of degrees of freedom $N_>$
  ⇒ non equilibrium stat.

INCOHERENT VORTICITY:

- 1D vorticity filaments dense in space & time
  ⇒ dominate the total energy spectrum,
- Gaussian PDF
  ⇒ disappears in the total PDF,
- large number of degrees of freedom $N_<$
  ⇒ equilibrium stat

RESOLUTION OF 2D NAVIER-STOKES IN WAVELETS

We want to solve:

$$\begin{cases} \dfrac{\partial \omega}{\partial t} + J(\psi, \omega) = \nu \nabla^2 \omega \\ \omega = \nabla^2 \psi \end{cases}$$

We choose an appropriate wavelet or wavelet packet basis $|\psi^t>$ adapted for time t and we project onto it:

$$<\left[\frac{\partial}{\partial t}\tilde{\omega}_> + J(\nabla^{-2}\tilde{\omega}_>, \tilde{\omega}_>)\right] | \psi^{t+1}> = F^{t+1}$$

$\tilde{\omega}_>$ are the strongest wavelet coef.

F random phase forcing term such that $|F| = <\omega_<^2> (1-D)$ and $\hat{F} = |F| e^{i\theta}$, θ random

$0 \leq D \leq 1$ turbulent diffusion parameter $\left(Re \propto \frac{1}{D} \right)$.

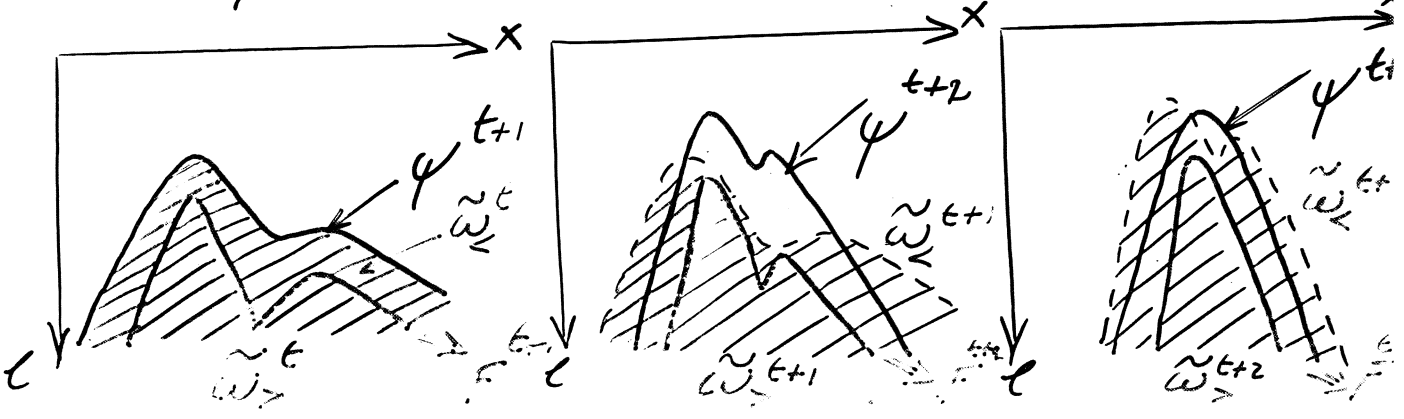

Schneider, Farge, Kevlahan
(Theoretical & Computational Fluid Dynamics)

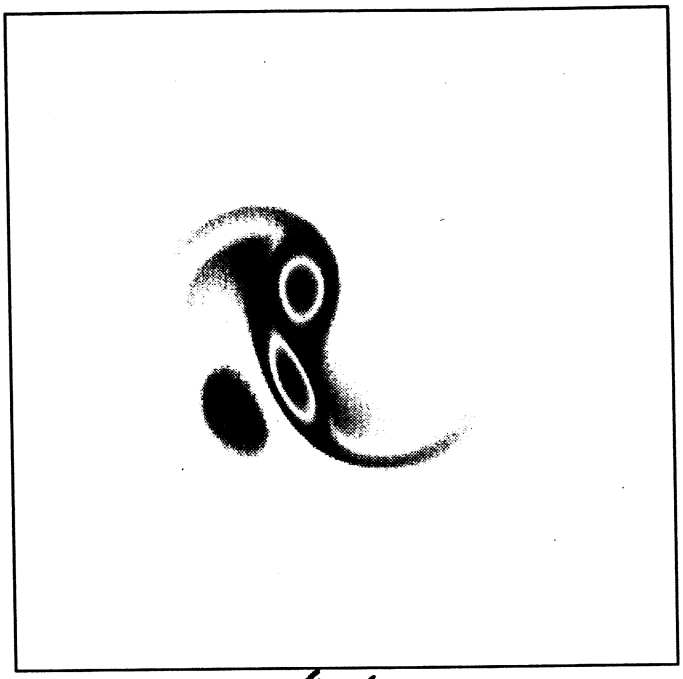

$t = 10$

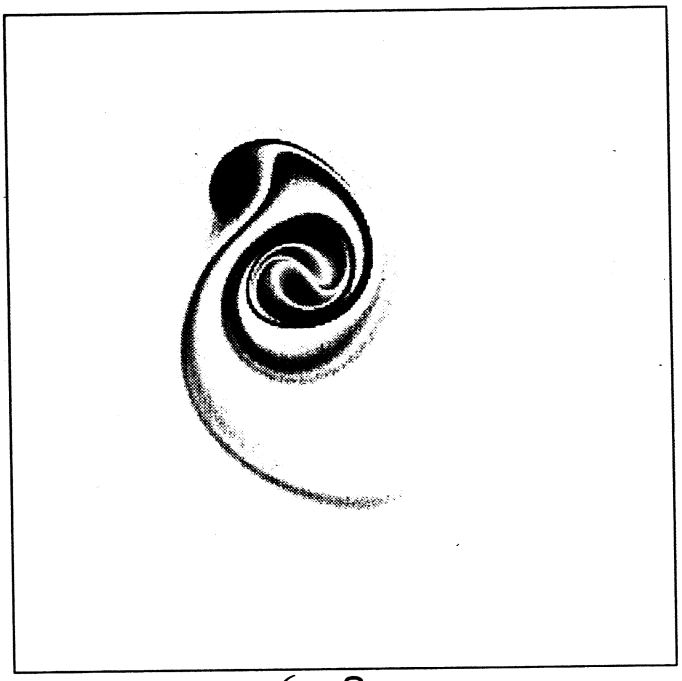

$t = 20$

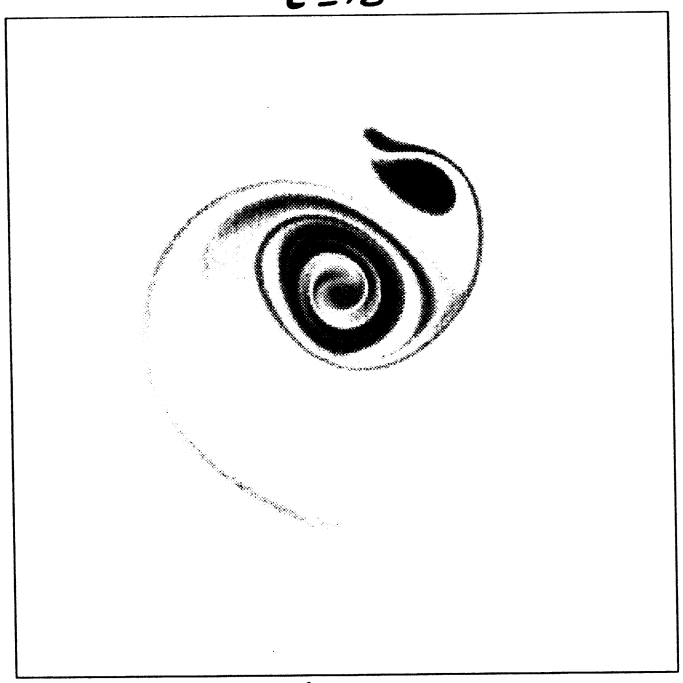

$t = 30$

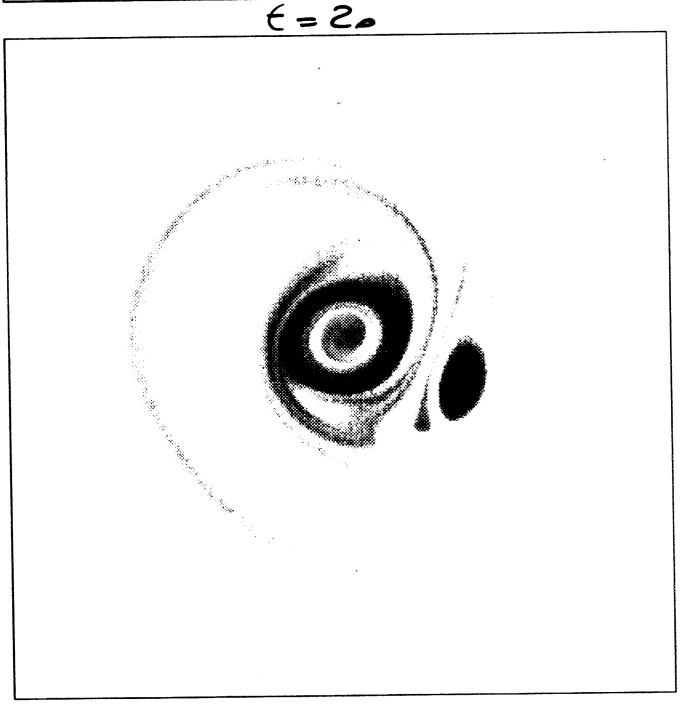

$t = 40$

$N = 256^2$

Interaction of 3 vortices: Spectral method with resolution N=256.
Top: Vorticity field at t=10, t=20. $dt = 2.5\ 10^{-3}$
Bottom: Vorticity field at t=30, t=40. $\nu = 5\ 10^{-5}$

Pseudo-Wavelet
Scheme
Vk^2

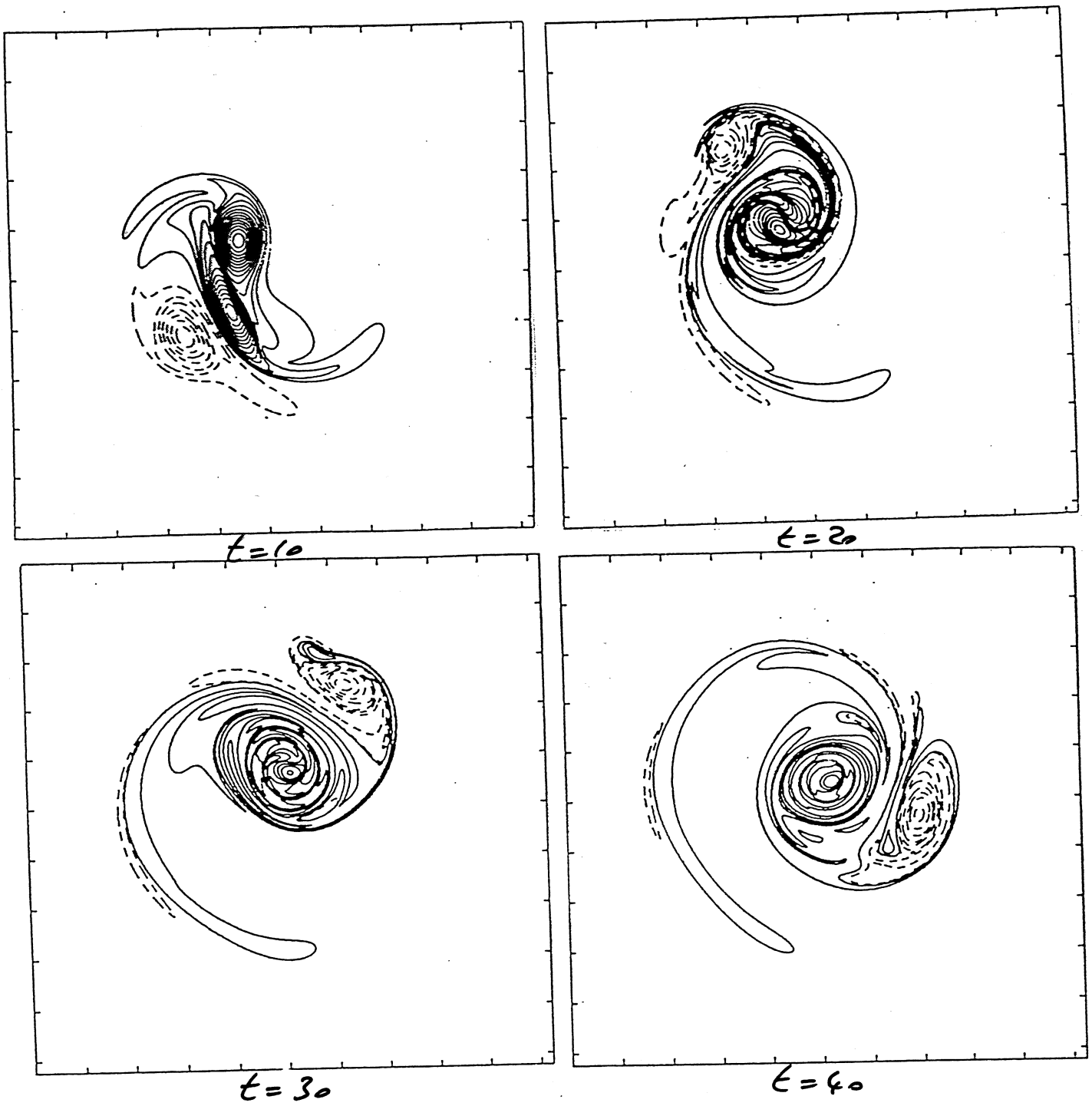

$N = 1024^2$

Pseudo-Fourier
Scheme

Vk^{16}

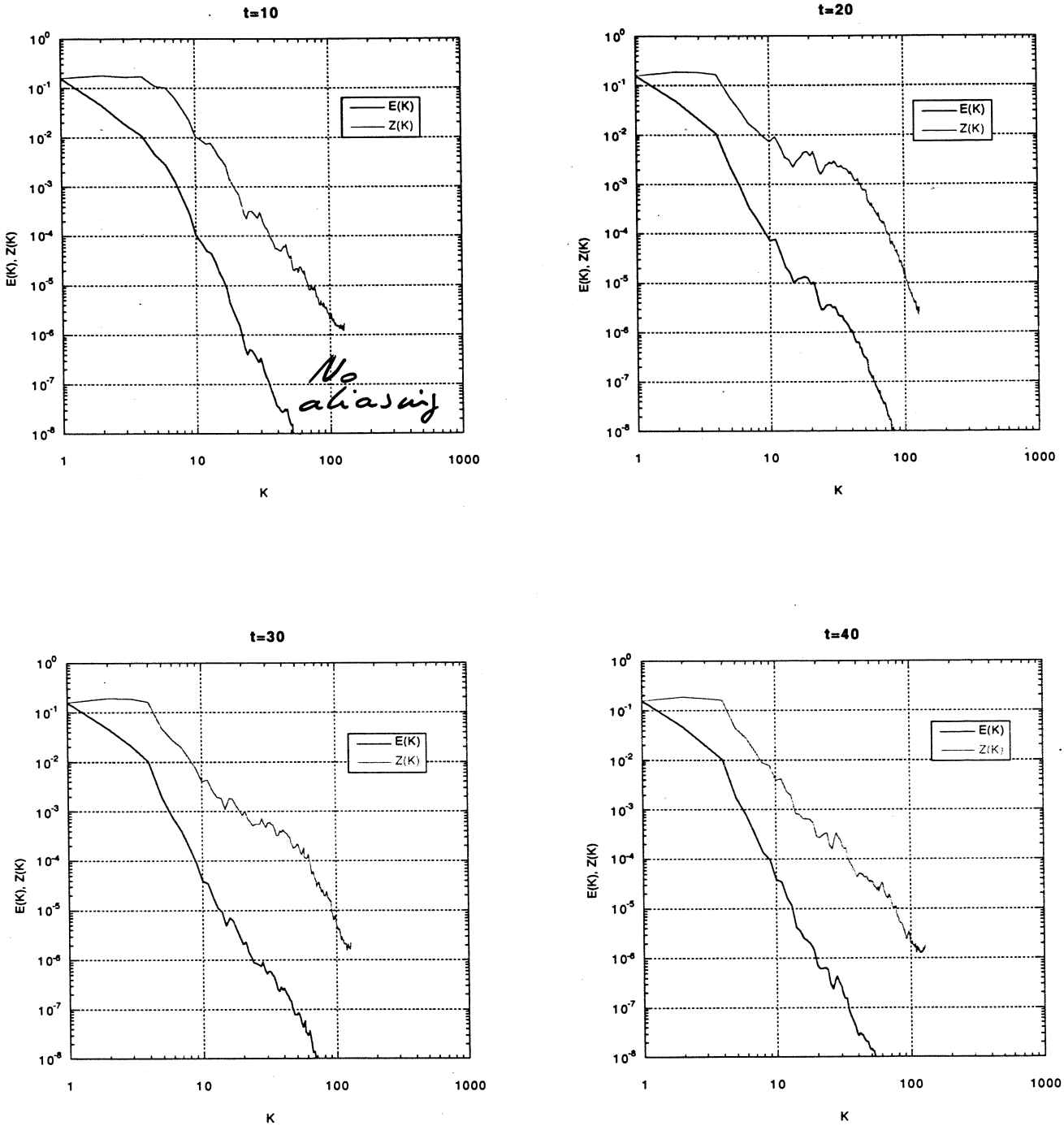

$N = 256^2$

Interaction of 3 vortices: Wavelet method [Fröhlich & Schneider 95] with $\epsilon = 1E-6$, quadratic truncation (40/30) and resolution $J = 8 (N = 256)$.
Energy and Enstrophy spectra.
Top: at t=10, t=20. Threshold $\varepsilon = 10^{-6} s^{-1}$
Bottom: at t=30, t=40.

Pseudo-Wavelet Scheme

Nk^2

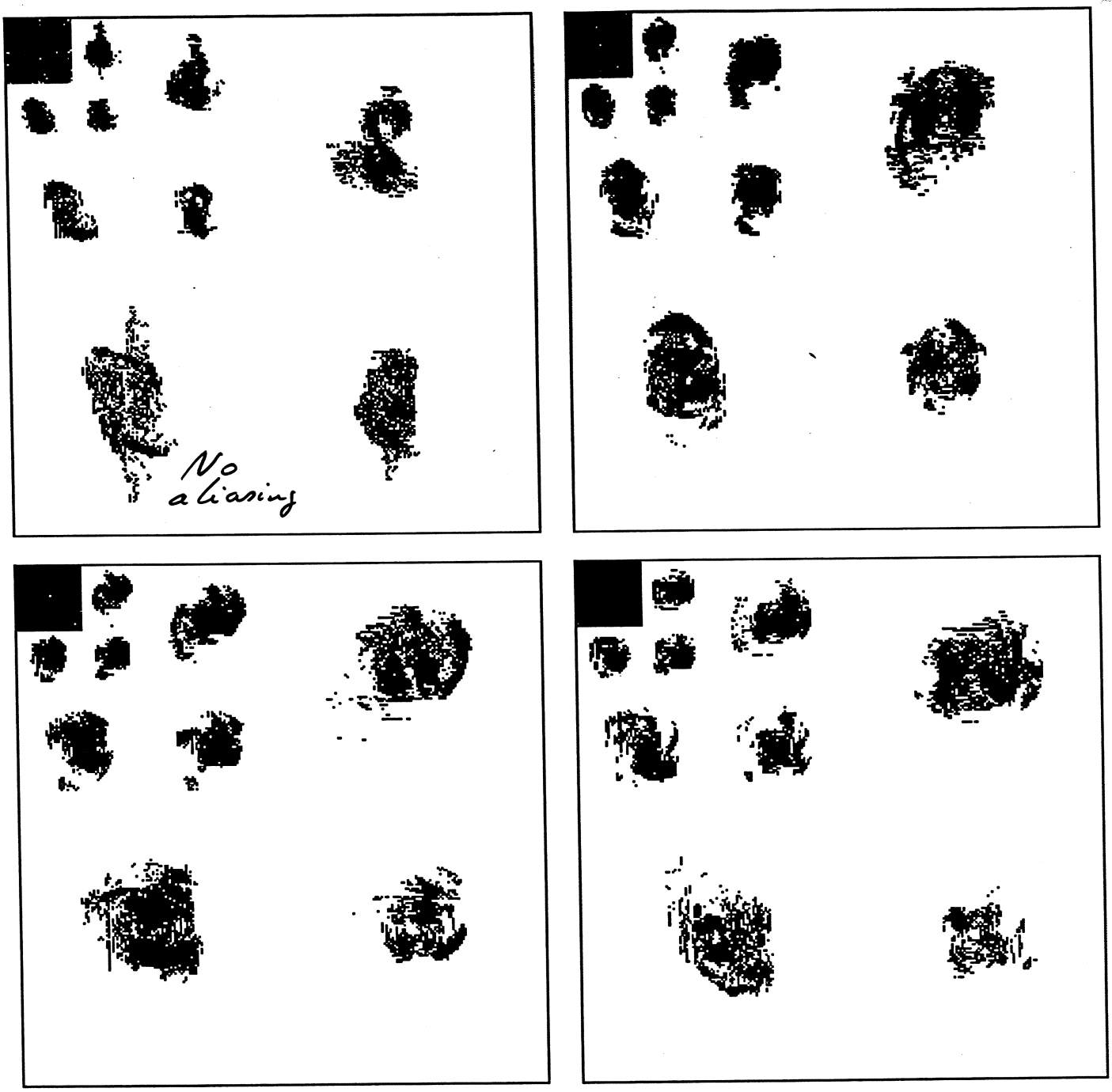

$N = 256^2$

Interaction of 3 vortices: active Wavelet coefficients above ϵ=1E-6, resolution $J = 8(N = 256)$, quadratic truncation.
Top: at t=10, t=20.
Bottom: at t=30, t=40.

Threshold $10^{-6} s^{-1}$

Pseudo-Wavelet
Scheme
Vk^2

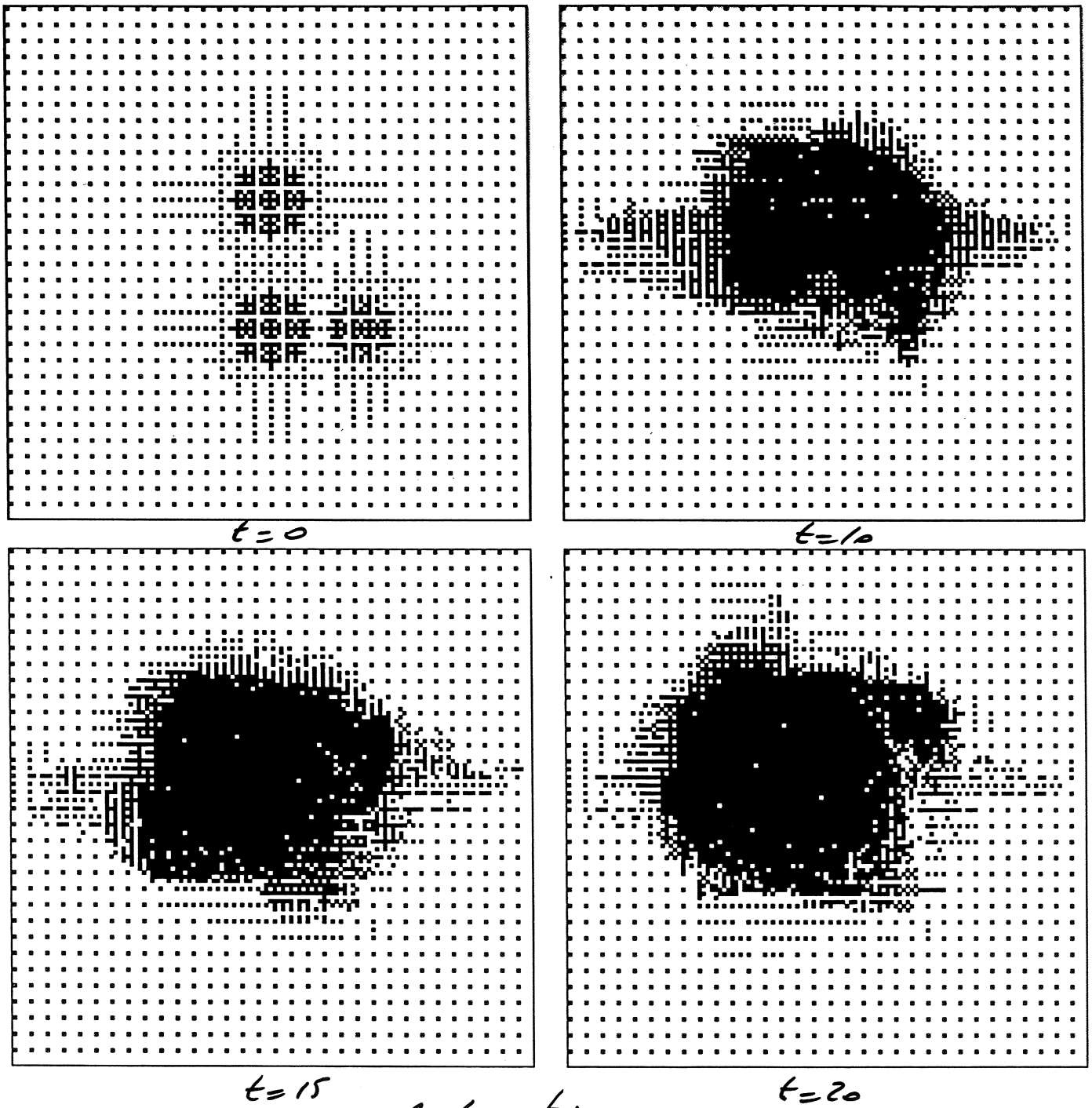

Fig.4 Interaction of 3 vortices: Wavelet method [Fröhlich & Schneider 95] with ϵ=1E-6, resolution $J = 7(N = 128)$.

Top: Associated grid at t=0, t=10. Bottom: Associated grid at t=15, t=20.

$N = 128^2$
Prend6 - wavelet
Threshold $\varepsilon = 10^{-5}$

Figure 9
Merging of three vortices

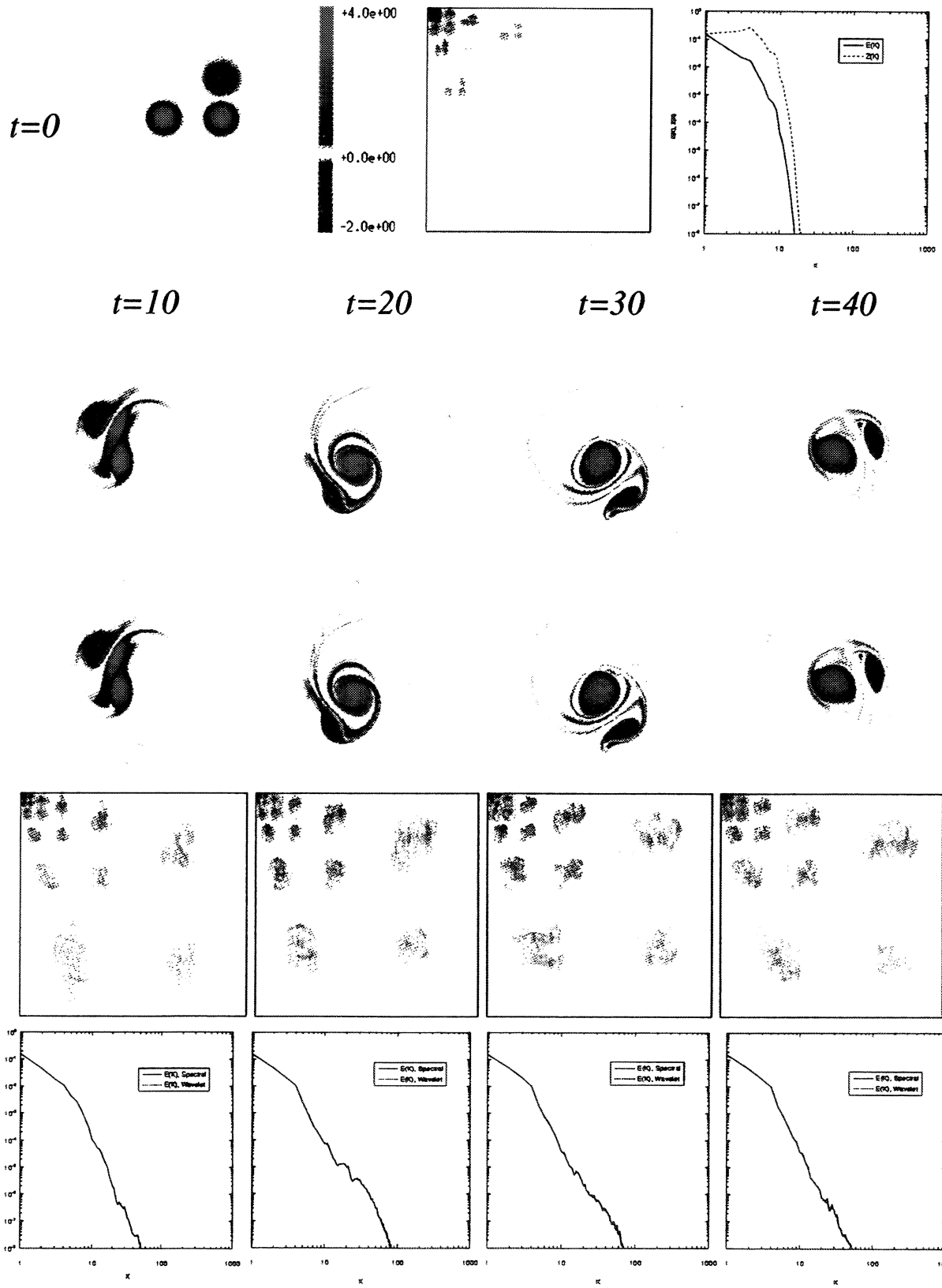

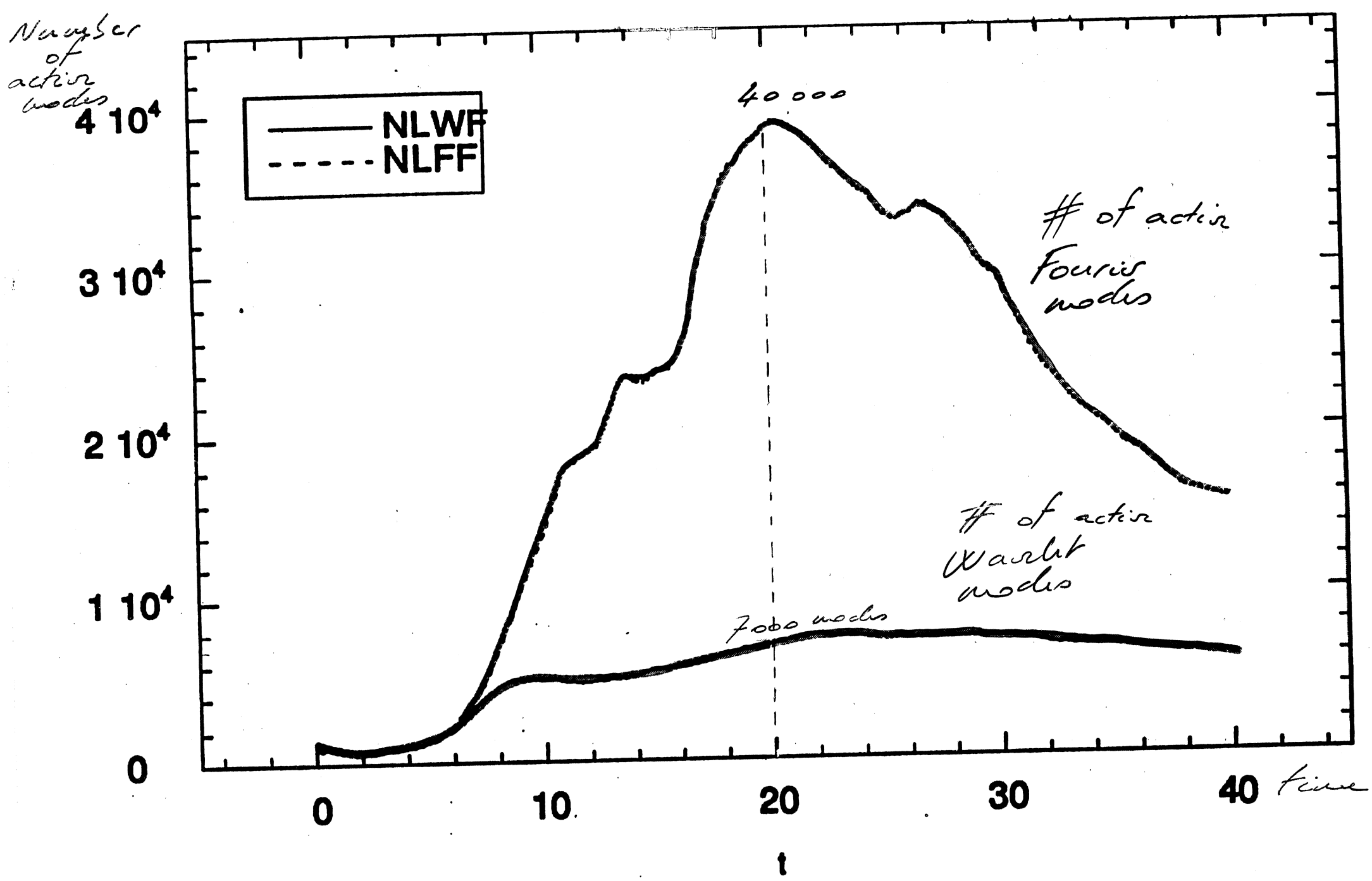
Number of active modes
NLWF
NLFF
40 000
# of active Fourier modes
# of active Wavelet modes
7000 modes
4 10^4
3 10^4
2 10^4
1 10^4
0
0
10
20
30
40
time
t

ATOMIC DECOMPOSITION OF ENSTROPHY DURING VORTEX MERGING

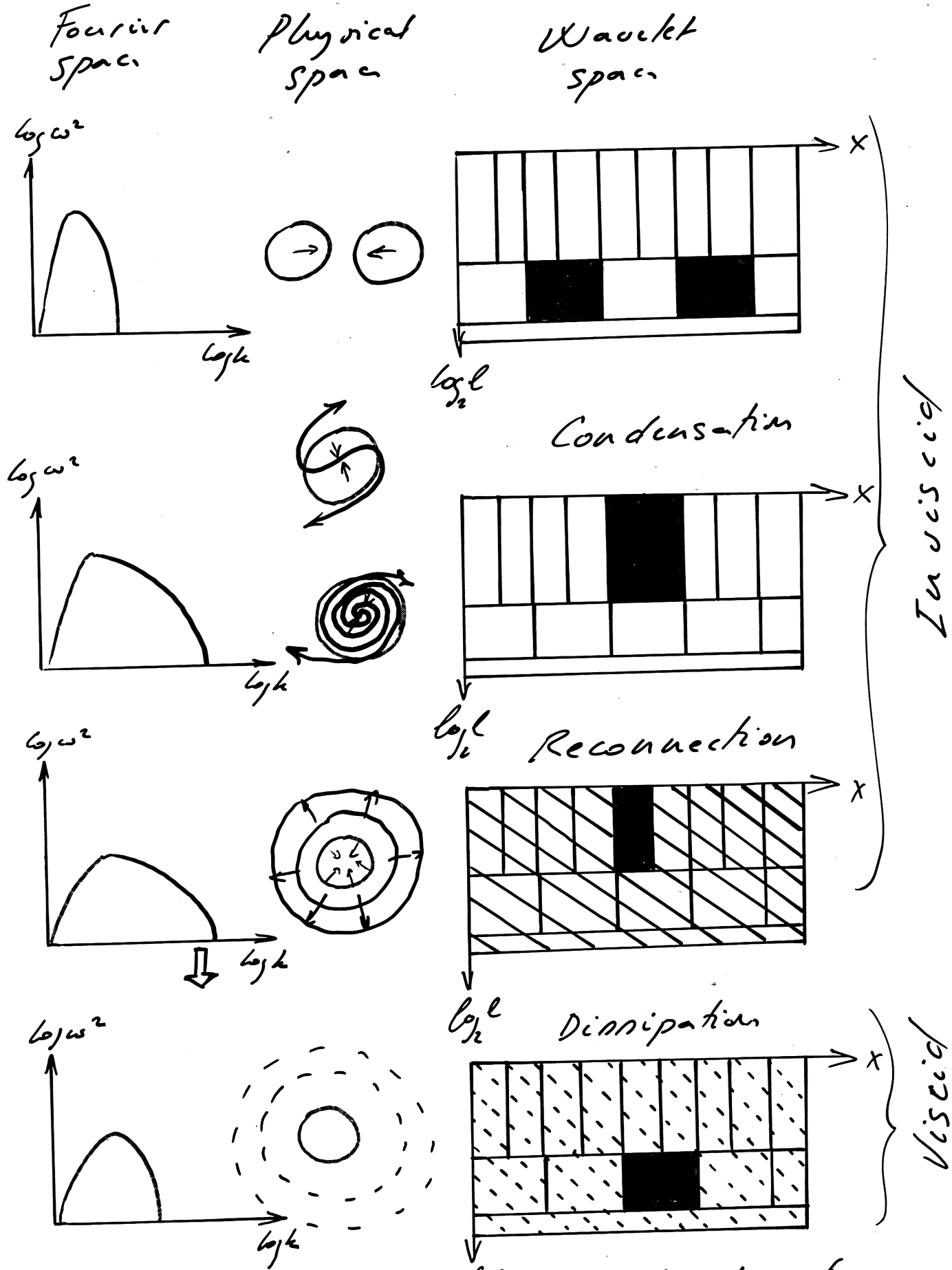

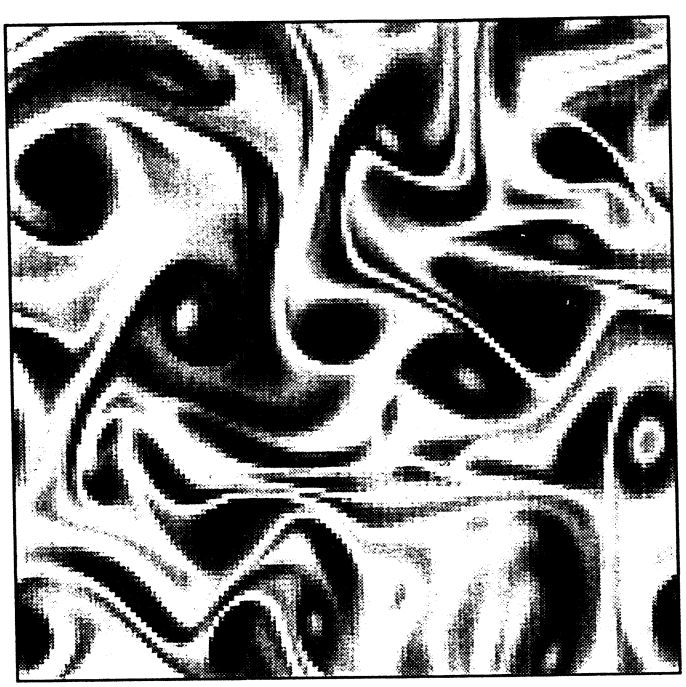



t=4

t=8

Freely Decaying 2D Turbulence

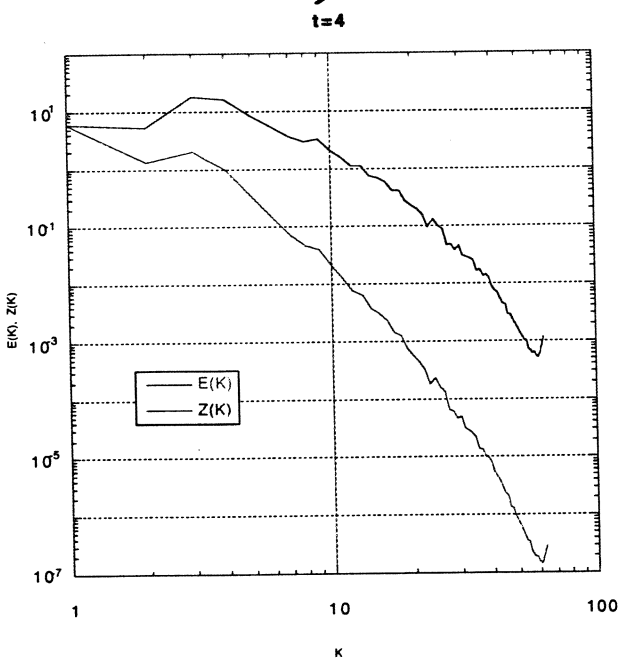

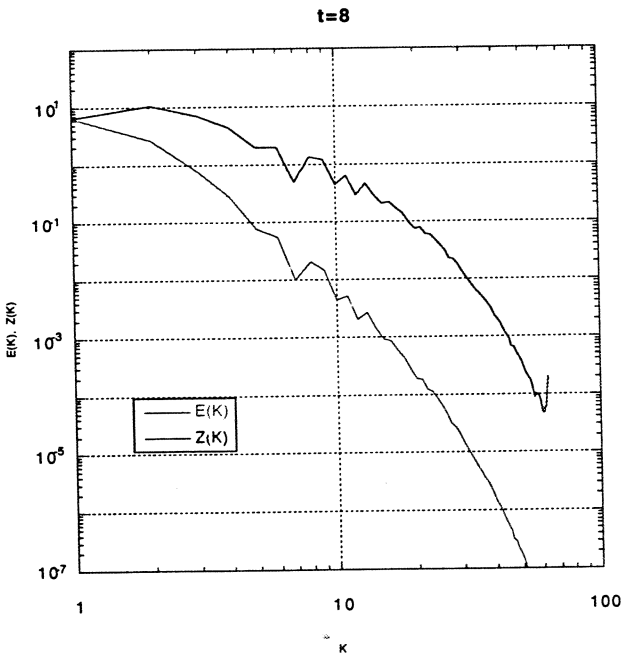

Spectral method with resolution N=128 without forcing/compression as reference method, same initial condition.
Top: Vorticity field at t=4, t=8.
Bottom: Spectra at t=4, t=8.

$N = 128^2$

Pseudo-Fourier Scheme

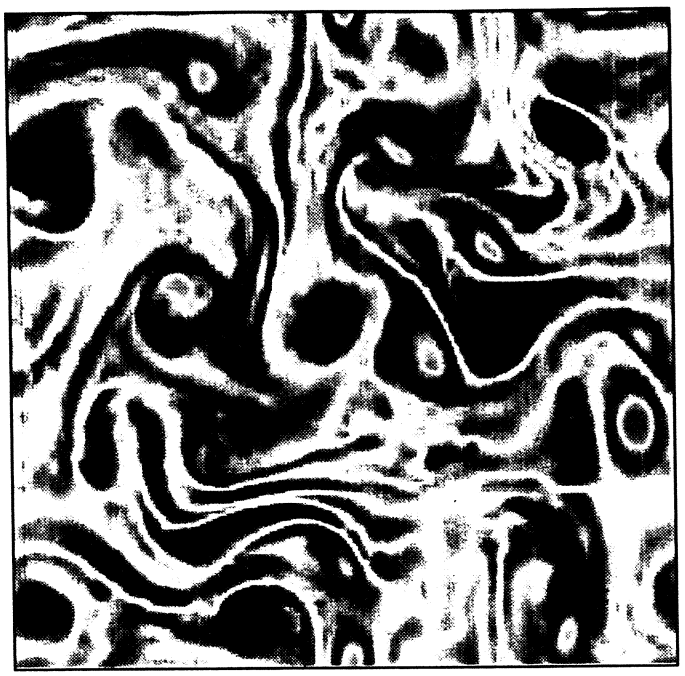



t=4 t=8

Wavelet Forced 2D Turbulence

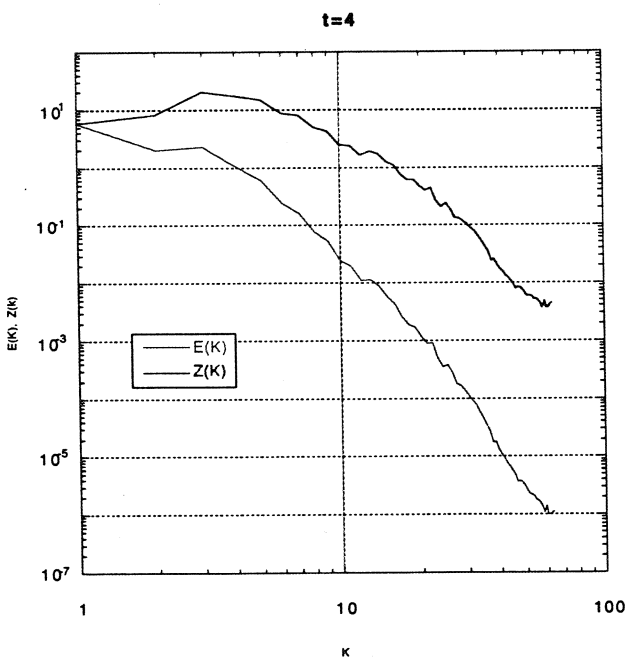

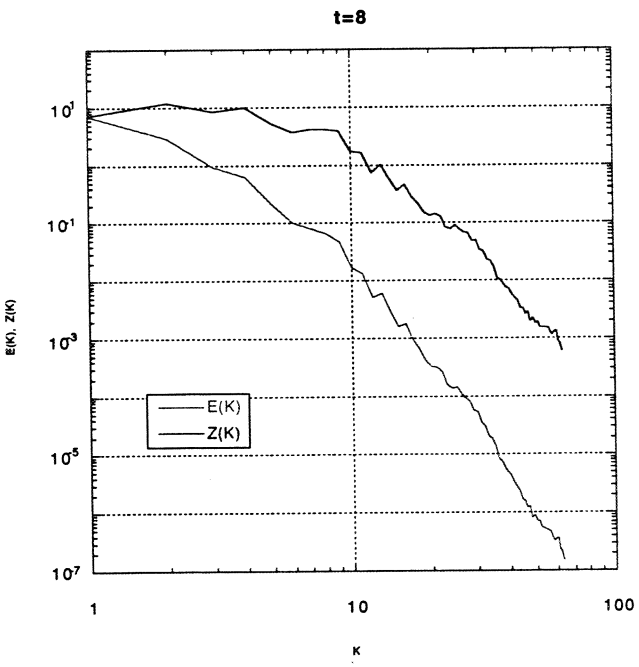

Nonlinear forcing in wavelet space down to scale $j = 3$:
Spectral method with resolution N=128 and wavelet compression in each time step with $\epsilon = 1.e-4$. Threshold $\varepsilon = 10^{-4}$
Top: Vorticity field at t=4, t=8.
Bottom: Spectra at t=4, t=8.

$N = 128^2$
Pseudo-Wavelet Scheme

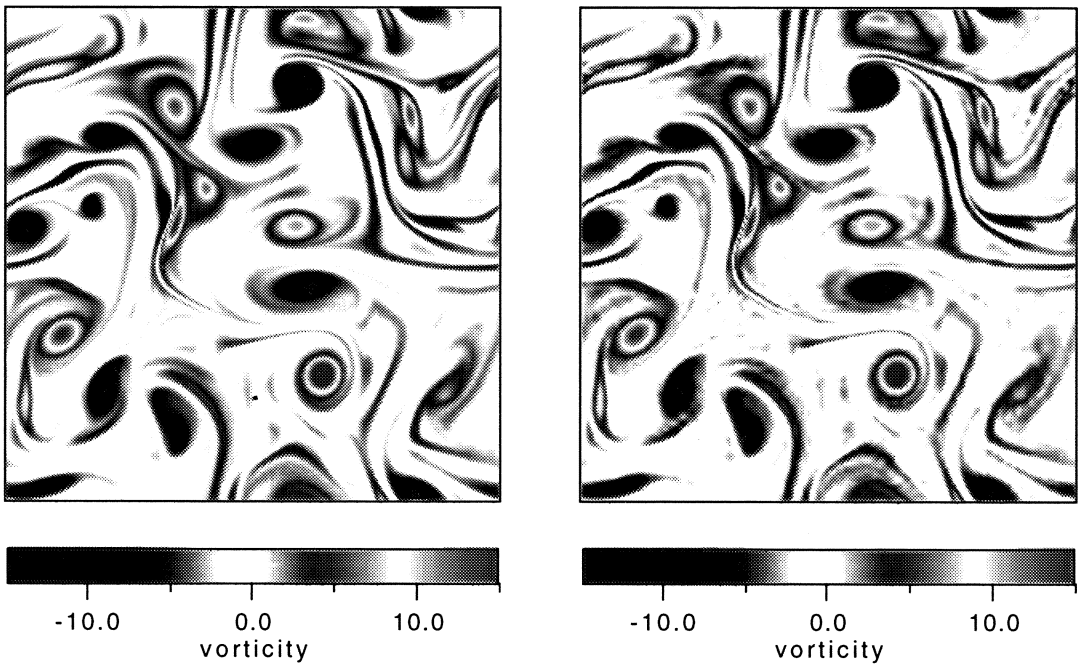

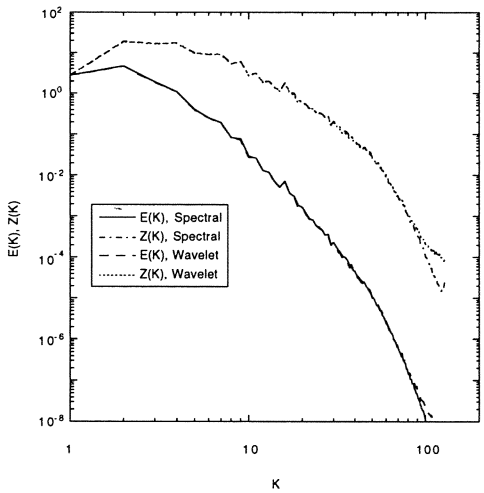

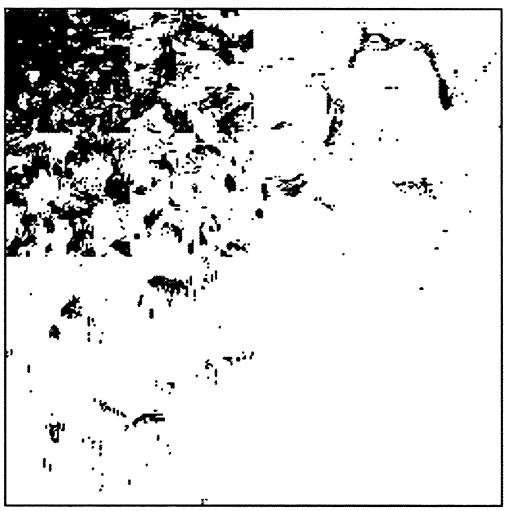

Decaying turbulence, resolution 256^2:
Top: vorticity field at t=2, spectral method (left), adaptive wavelet method (right)
Bottom: energy and enstrophy spectra (left), active wavelet coefficients (right).

WAVELET FORCING OF 2D TURBULENT FLOW

2D Navier-Stokes equations:

$$\partial_t \omega + \vec{v} \cdot \vec{\nabla} \omega = \nu \nabla^2 \omega + \alpha \psi + \vec{\nabla} \times \vec{F}$$

$\omega = \vec{\nabla} \times \vec{v}$, $\psi = \nabla^{-2} \omega$, ν kinematic viscosity and α friction strength.

Periodic boundary conditions,
Pseudo-spectral scheme,
Normal dissipation.

At each time step, we project ω into a wavelet basis and we keep only the strongest wavelet coefficients $\tilde{\omega}_> > \tilde{\omega}_c$. The weakest coefficients are set to zero: $\tilde{\omega}_< = 0$.

We then form the flow, such that:

$$\vec{\nabla}^\perp \times \vec{F} = c\, \tilde{\omega}_>(x,y)$$

We adjust c and α in order to reach a statistically steady state.

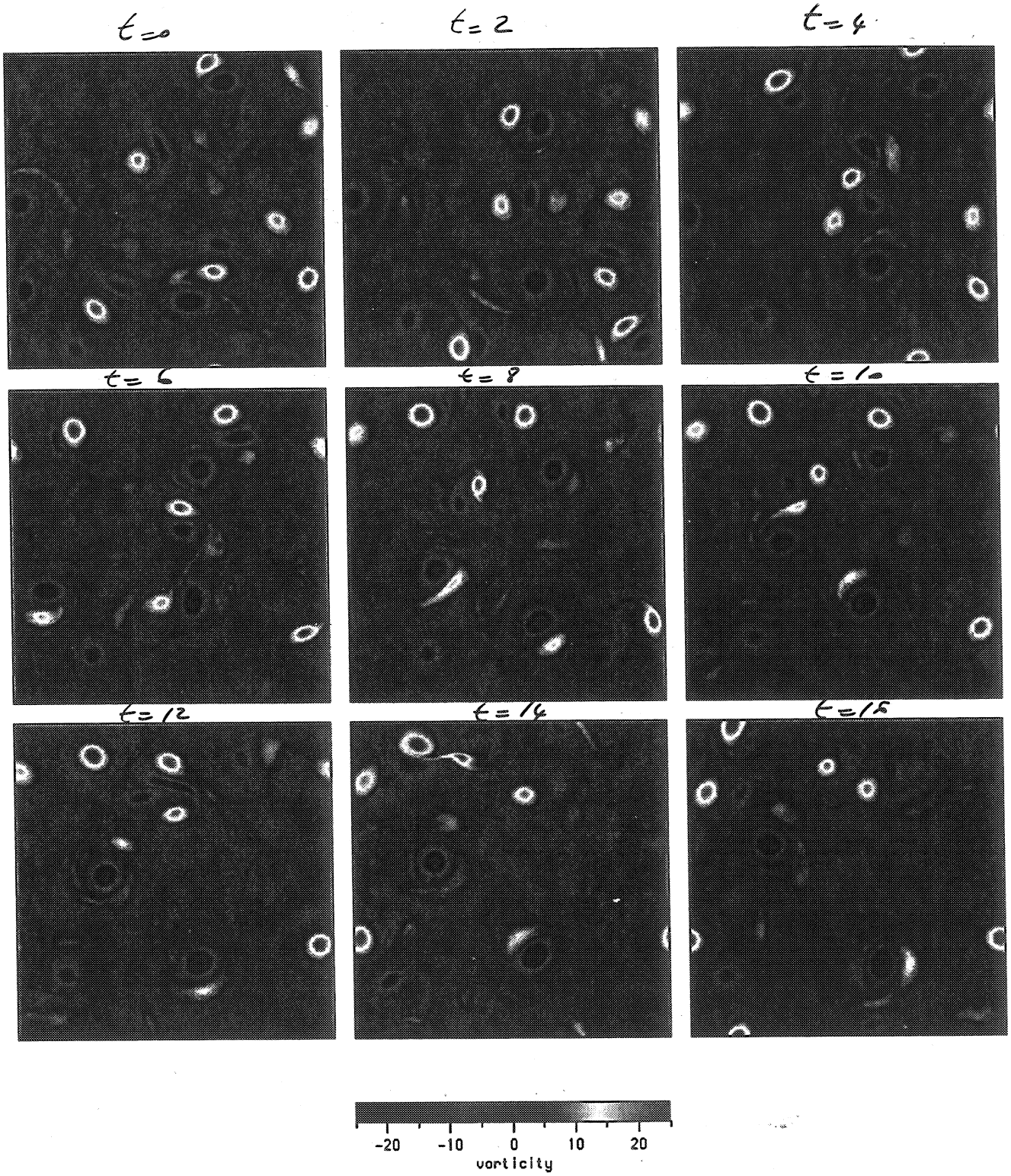

Wavelet forcing, $N = 128$. Vorticity field at $t = 0, 2, ..., 16$.

Wavelet Forcing
Vorticity field
Time evolution

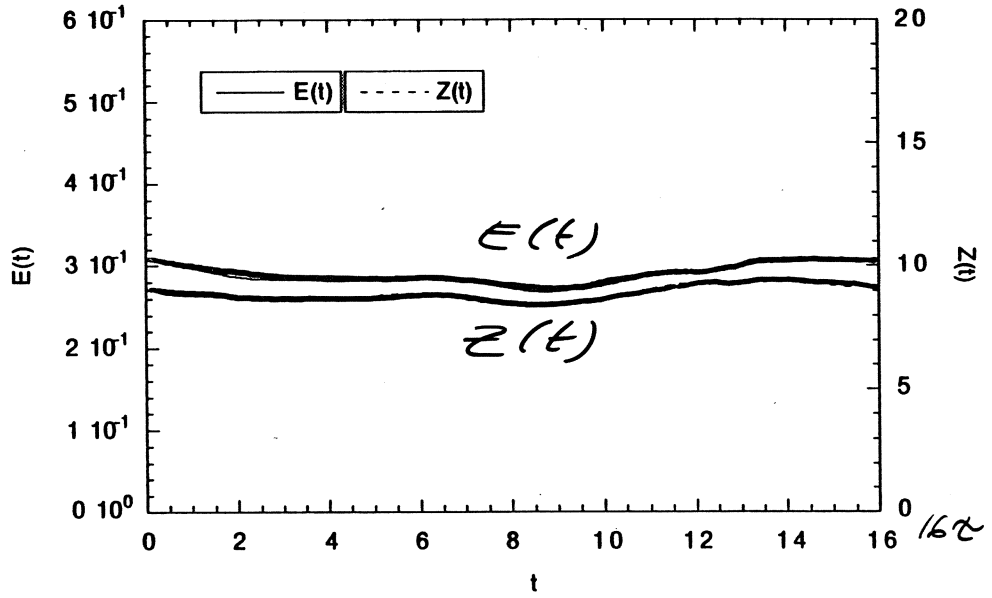

Figure 1: Evolution of energy and enstrophy.

Energy
Enstrophy
Time evolution

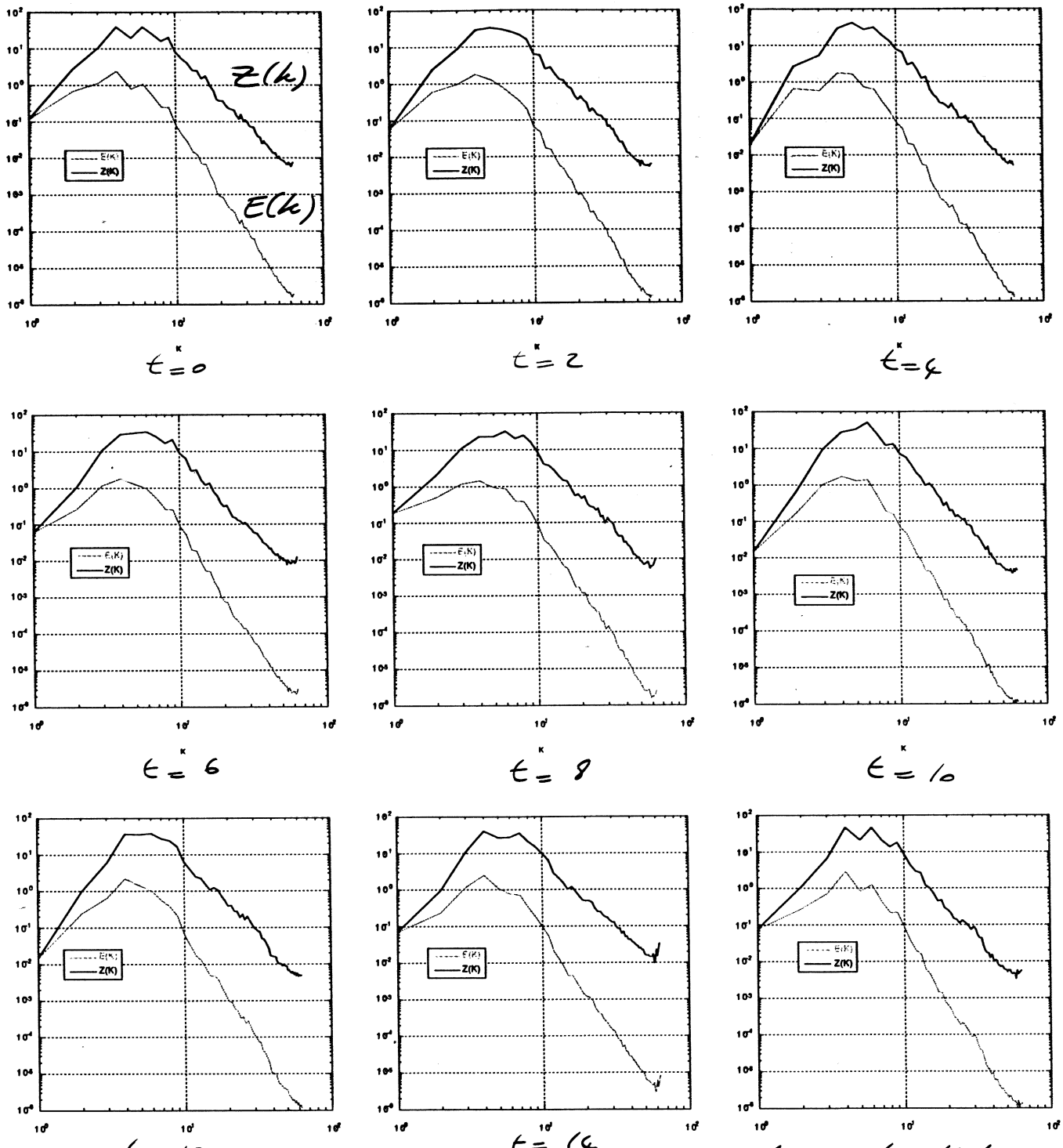

Wavelet forcing, $N = 128$. Spectra at $t = 0, 2, ..., 16$.

Energy
Enstrophy
1D Spectrum

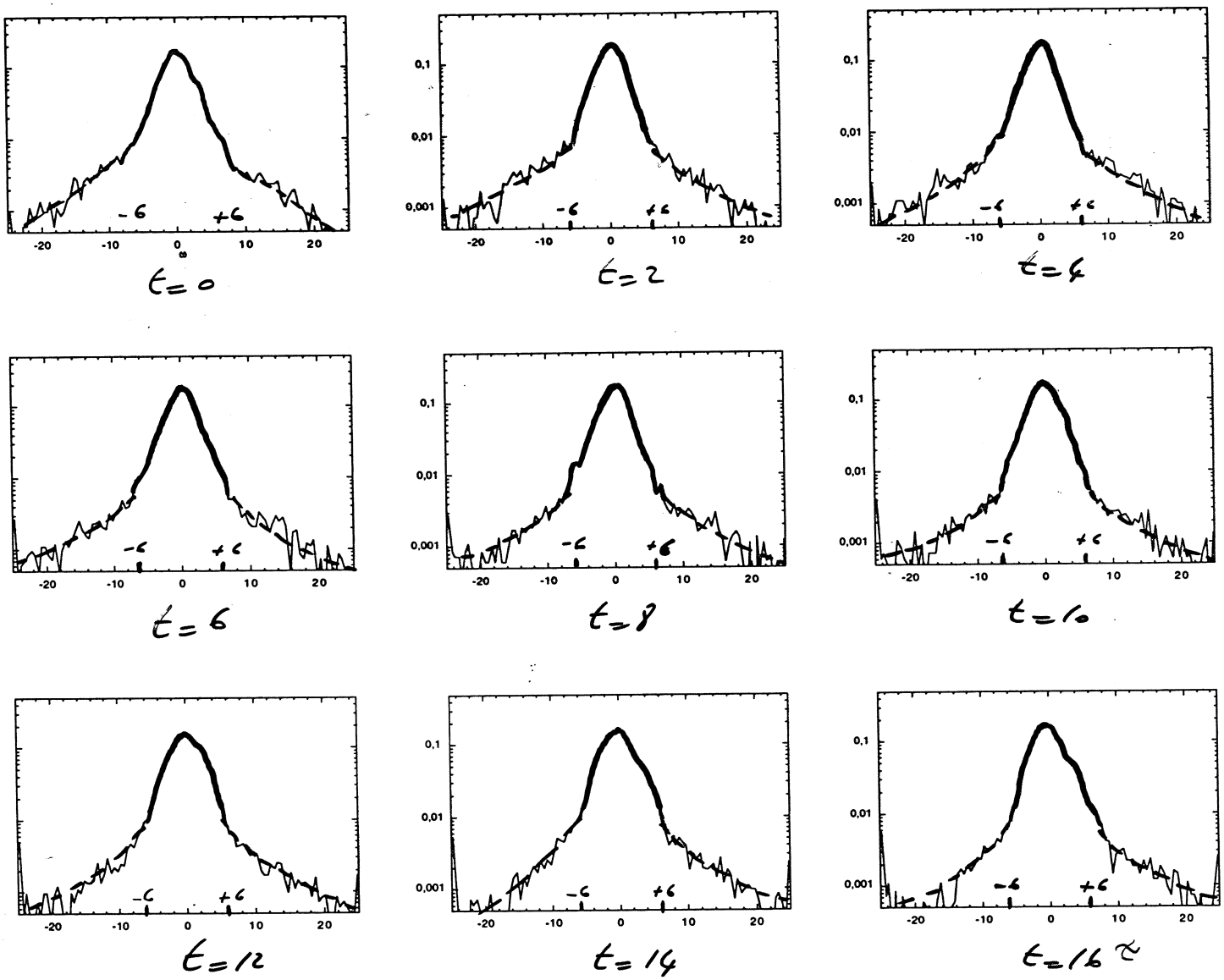

Wavelet forcing, $N = 128$. PDFs of the vorticity at $t = 0, 2, ..., 16$ in logarithmic scale.

Probability distribution Function of vorticity

Gaussian distribution for the weak values

Heavy tails for the strong values

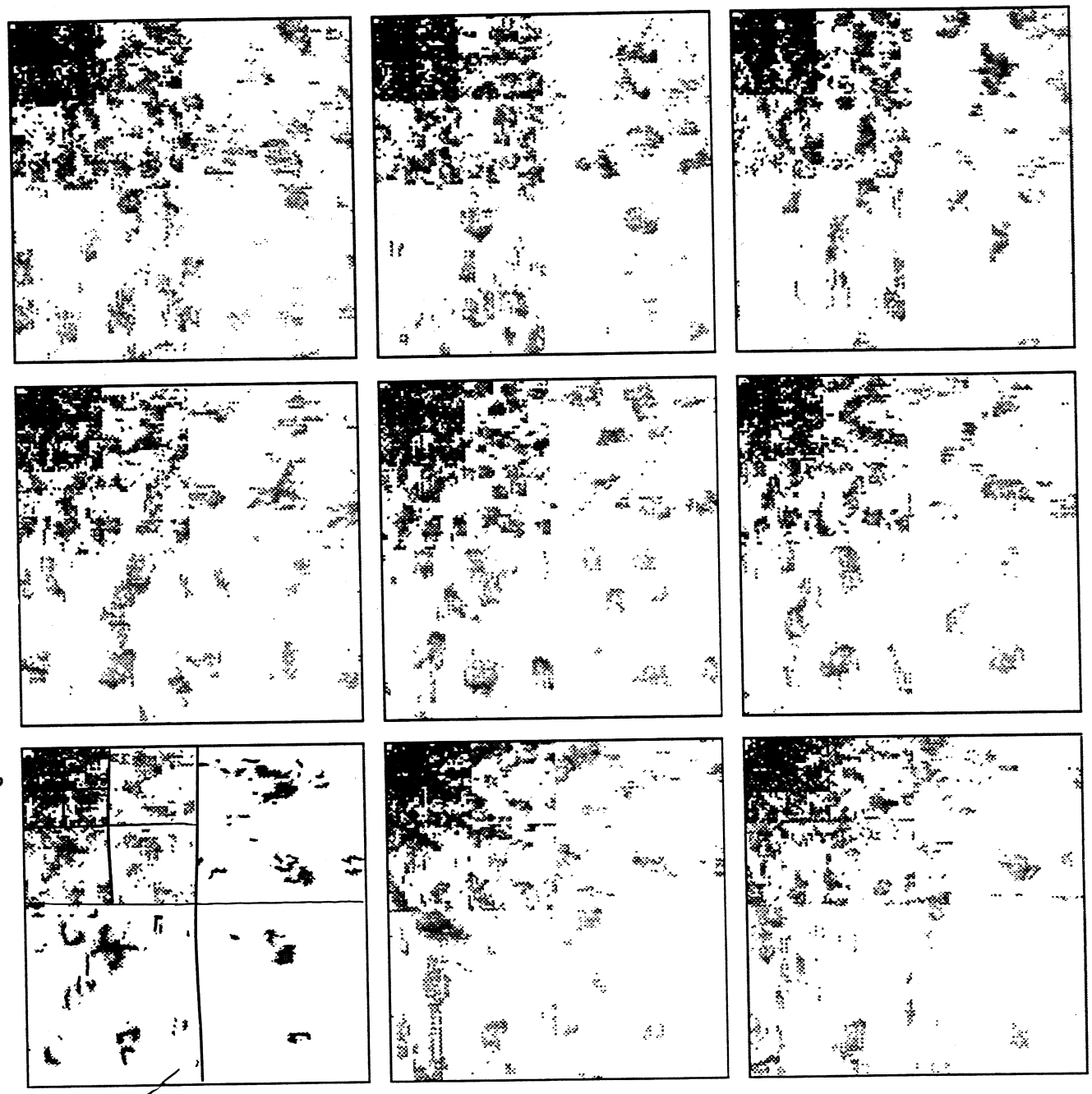

Wavelet forcing, $N = 128$. Active wavelet coefficients at $t = 0, 2, ..., 16$.

Intermittency
$\Rightarrow$ sparsity
of the small
scale wavelet
coefficients

Enstrophy

2D Wavelet Coefficients

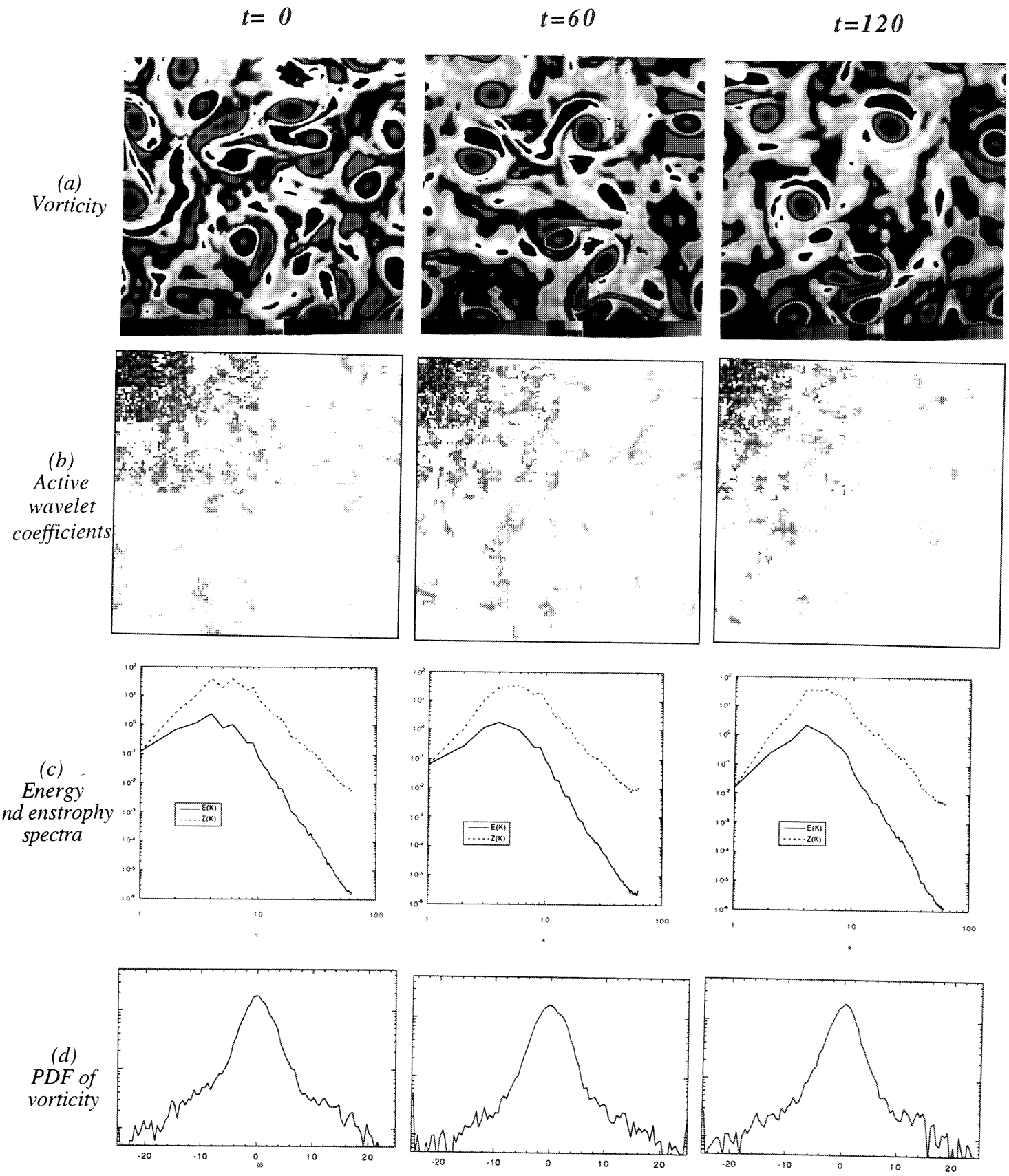

Figure 11
Wavelet-forced turbulence simulation
resolution 128^2

Marie Farge, Kai Schneider & Nicholas Kevlahan 'Dynamics of Shear Vortices' Cambridge University Press, 1997

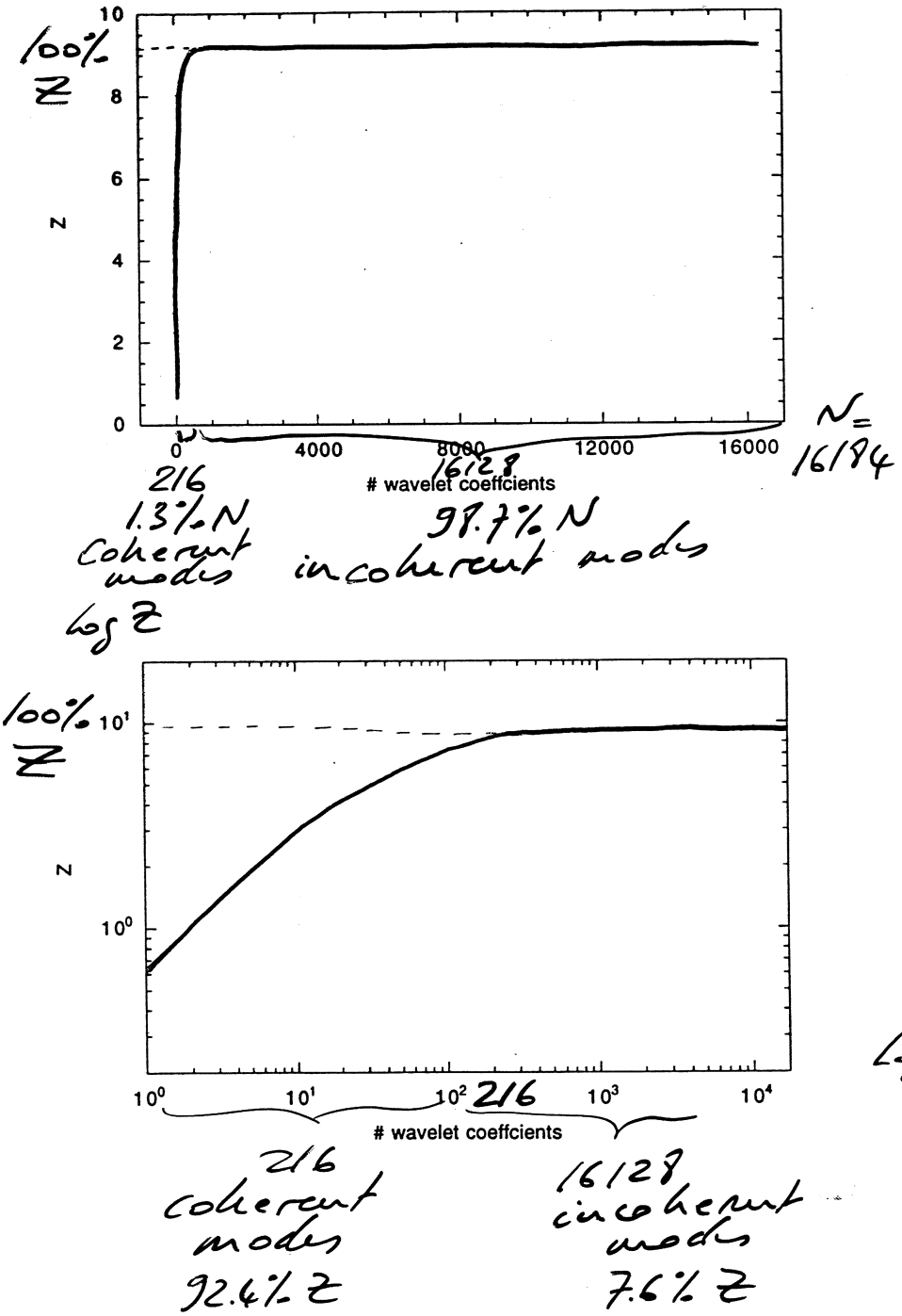

Figure 2. Compression rate: enstrophy versus the number of wavelet coefficents.

WAVELET FORCED
2D TURBULENT FLOW
$t = 16$
$N = 128^2$

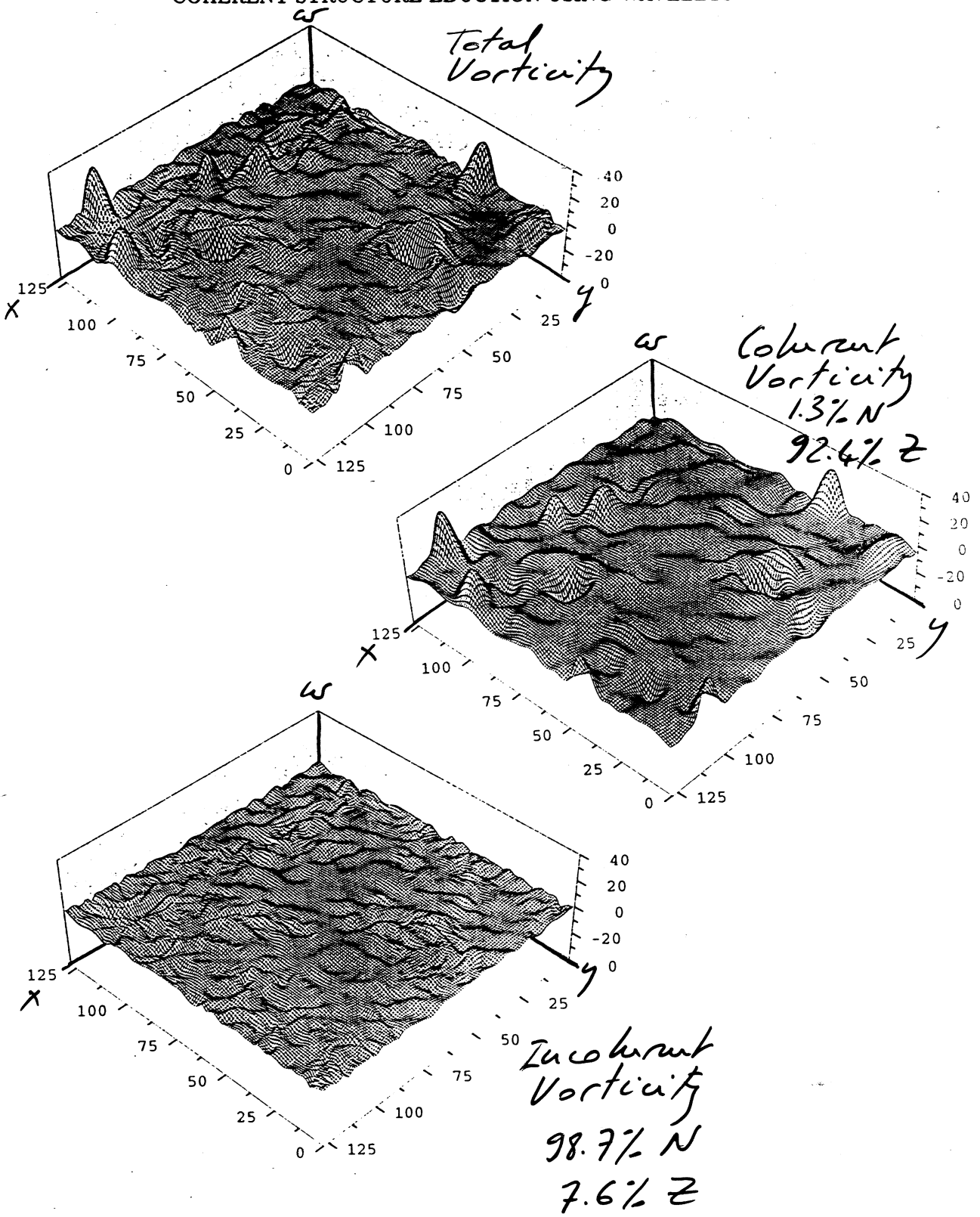

Figure 3. Surface plots of the vorticity fields ω (top), $\omega_>$ (middle) and $\omega_<$ (bottom).

ω

Total Vorticity having variance $\langle \omega^2 \rangle = 16 \longrightarrow$

$\tilde{\omega}_T = (2 \langle \omega^2 \rangle \log N)^{1/2} = 12^3$

(Threshold chosen from Donoho's Wavelet Shrinkage Method, 1992)

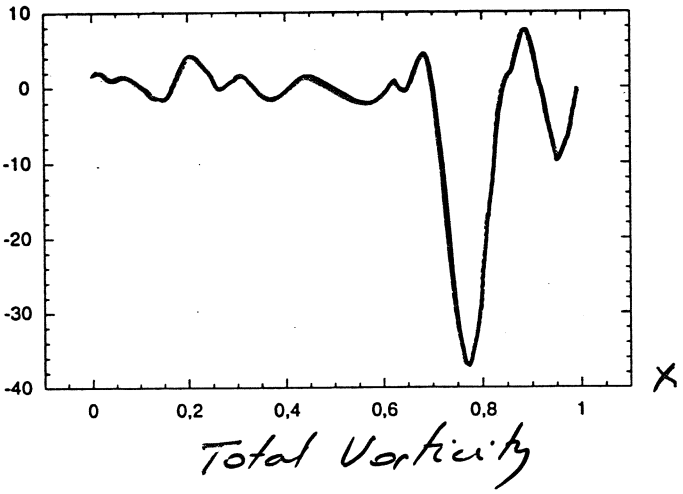

100% N
100% Z

$\omega_>$

Coherent Vorticity reconstructed from the strongest wavelet coefficients $\tilde{\omega} > \tilde{\omega}_T$

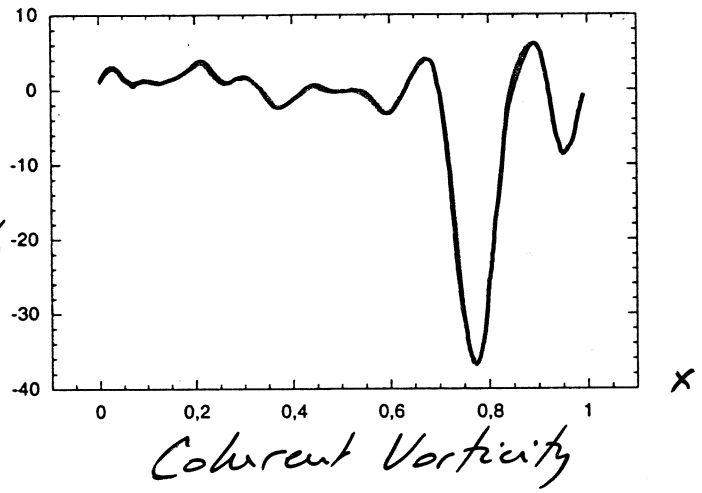

1.3% N
92.4% Z

$\omega_<$

Background Vorticity reconstructed from the weakest wavelet coefficients $\tilde{\omega} \leq \tilde{\omega}_T$

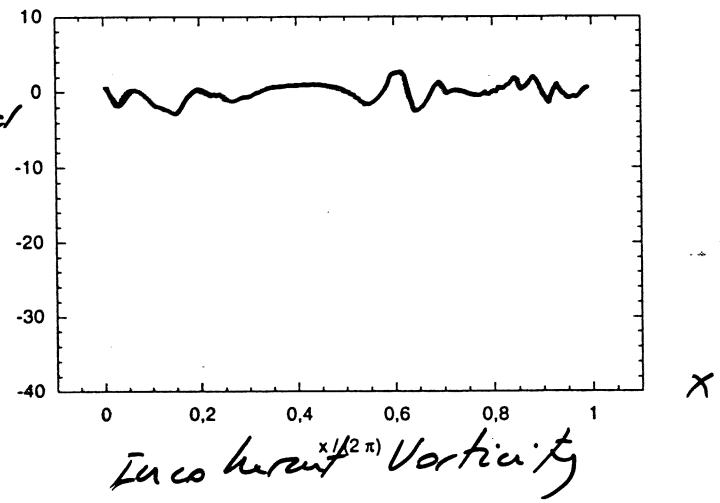

99.7% N
7.6% Z

Figure 4. Cuts of the vorticity fields ω (top), $\omega_>$ (middle) and $\omega_<$ (bottom) at $y = 2\pi 77/128$.

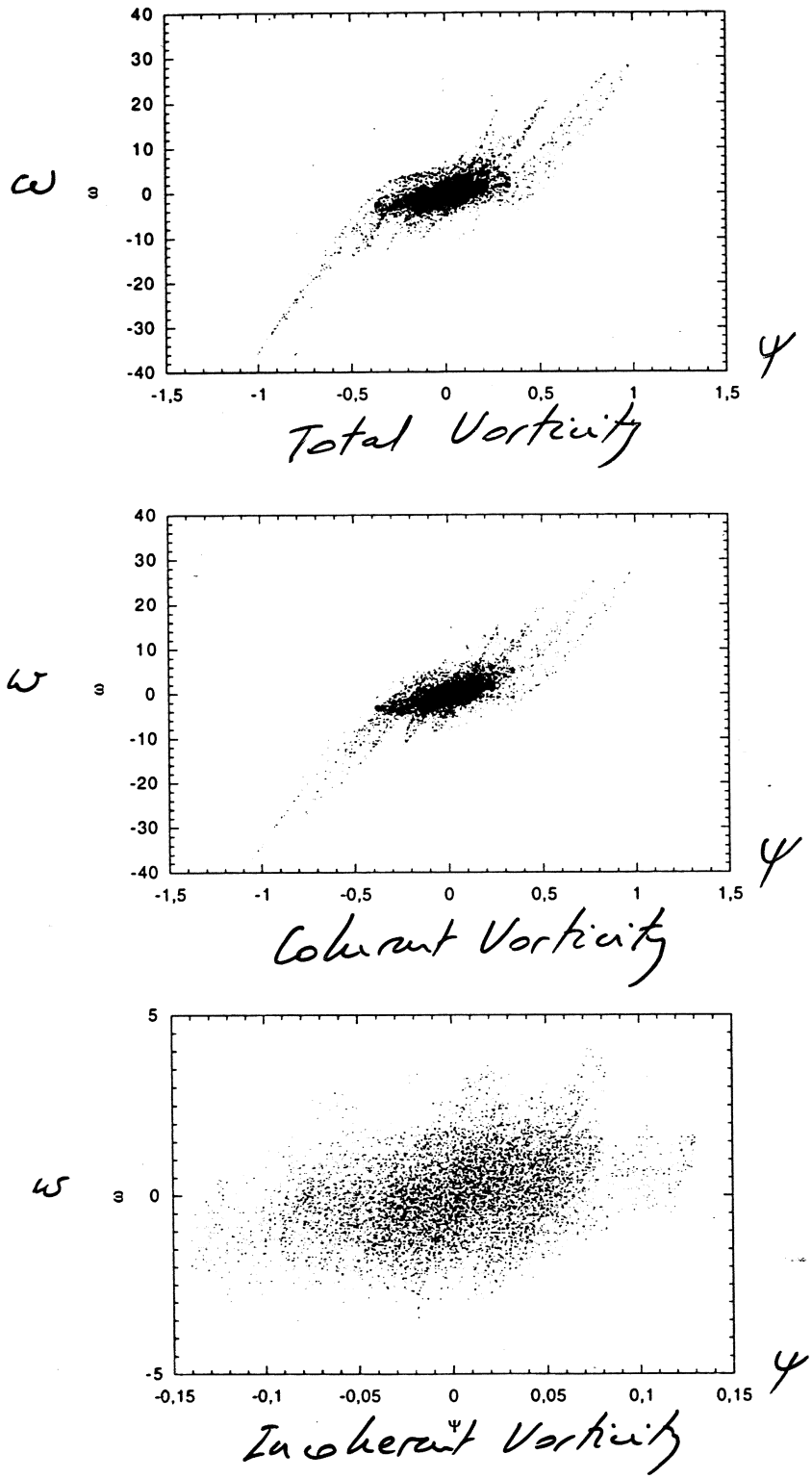

Figure 7. Scatter plots of the vorticity fields ω (top), $\omega_>$ (middle) and $\omega_<$ (bottom) versus the corresponding stream functions Ψ, $\Psi_>$ and $\Psi_<$.

Skewness $S = \frac{\langle \omega^3 \rangle}{\langle \omega^2 \rangle^{3/2}}$

Flatness $F = \frac{\langle \omega^4 \rangle}{\langle \omega^2 \rangle^2}$

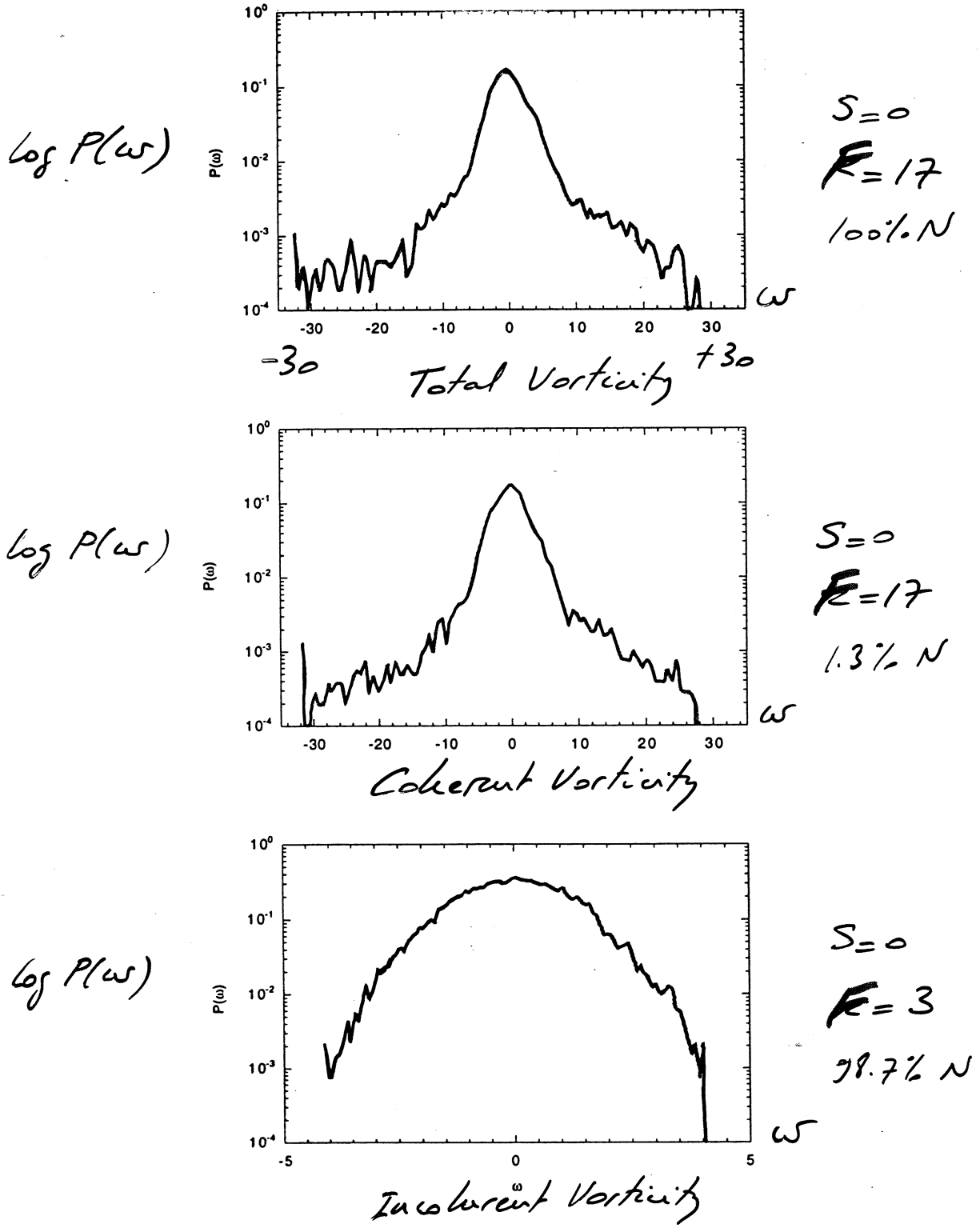

Figure 6. Probability density functions (histograms using 100 bins) of the vorticity fields ω (top), $\omega_>$ (middle) and $\omega_<$ (bottom).

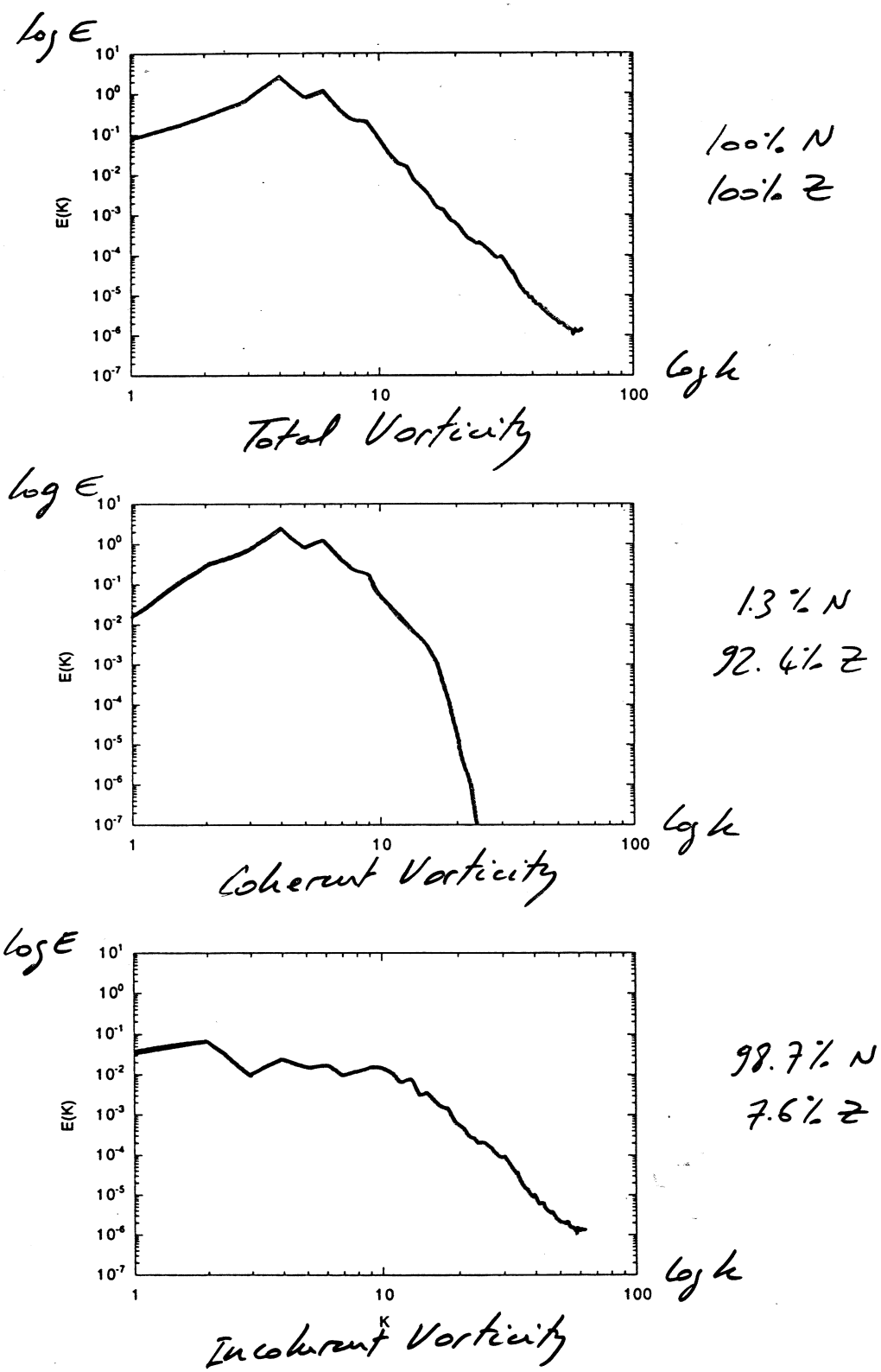

Figure 5. Energy spectra of the vorticity fields ω (top), $\omega_>$ (middle) and $\omega_<$ (bottom).

FLOW ALONG A SMOOTH PLANE

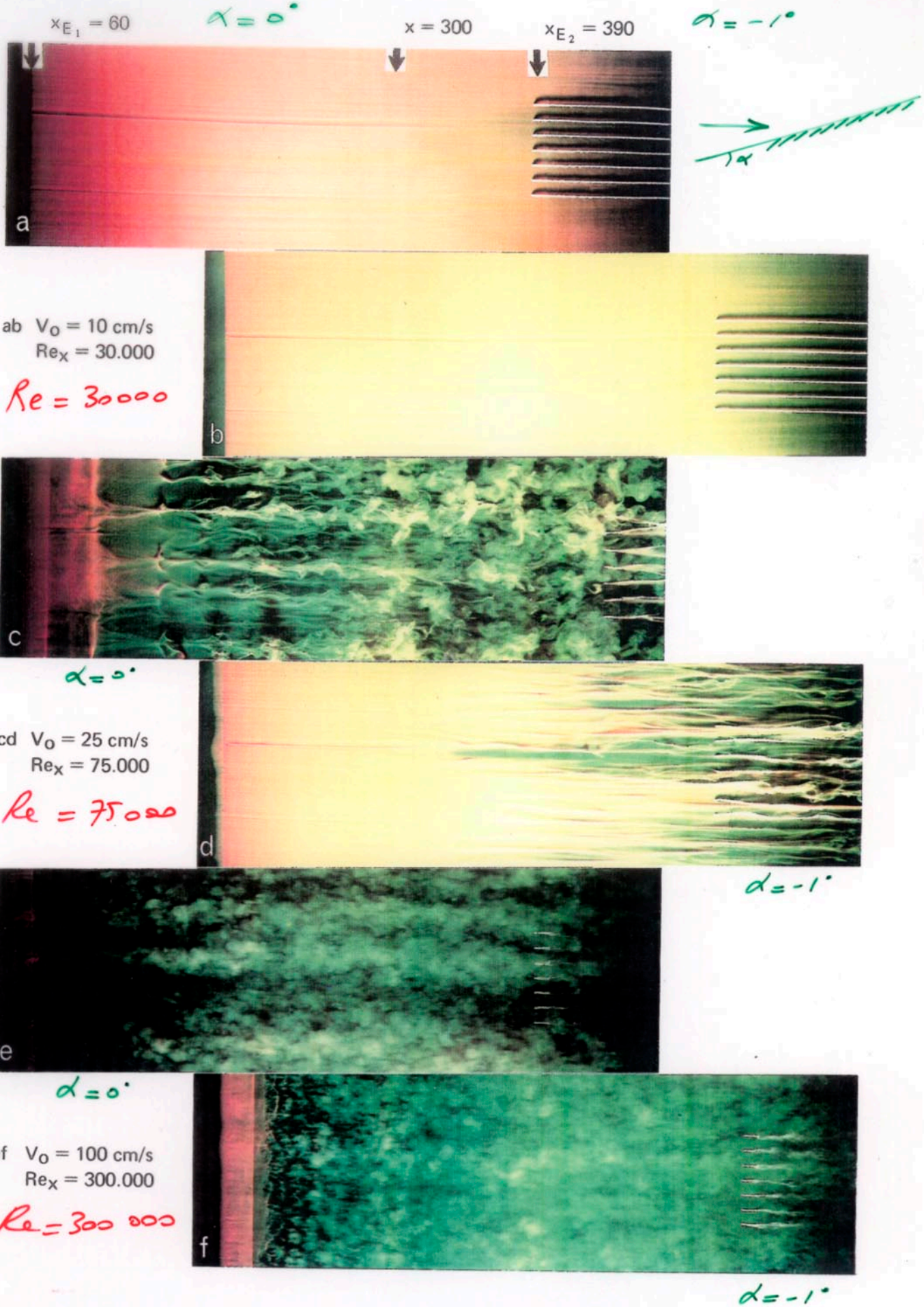

Henri WERLE, 1987

FLOW ALONG A CORRUGATED CYLINDER

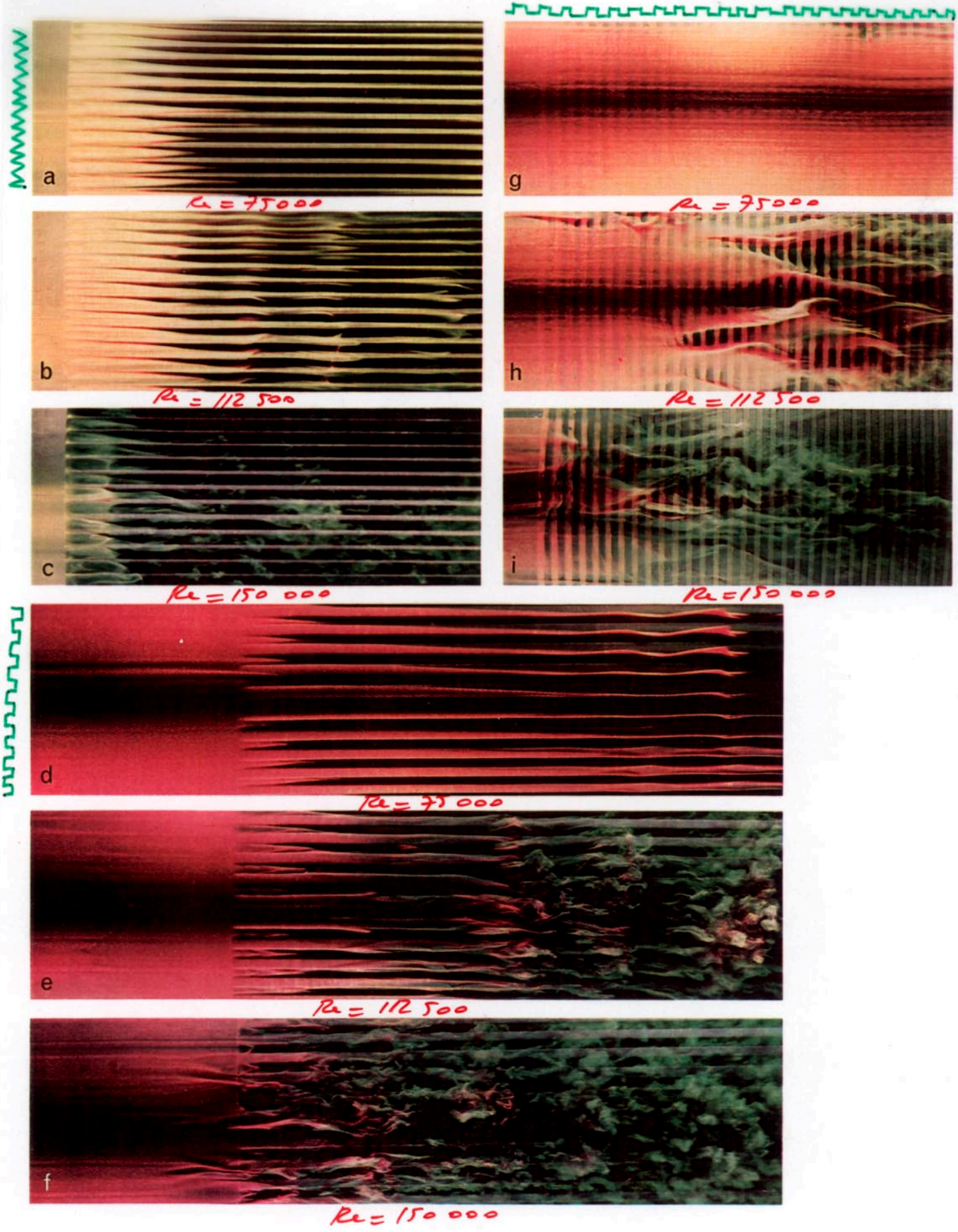

Henri WERLE, 1987

CONTROL OF TURBULENCE (cf. Bartosz Protas) Warsaw University & ESPCI, Paris

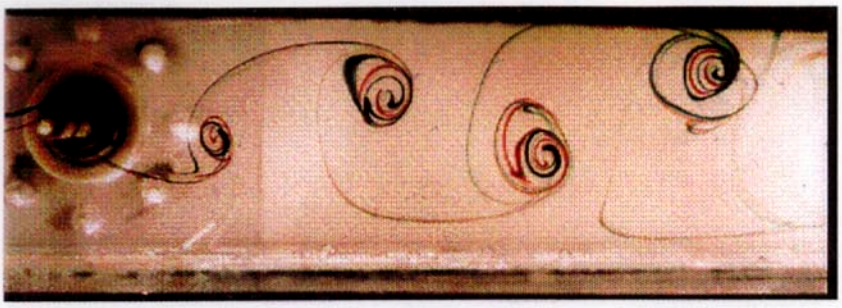

(A_e) $Re = 96$, $\frac{St}{St_{nat}} = 0.5$, $\Omega = 2.0$ - Laboratory experiment [6]

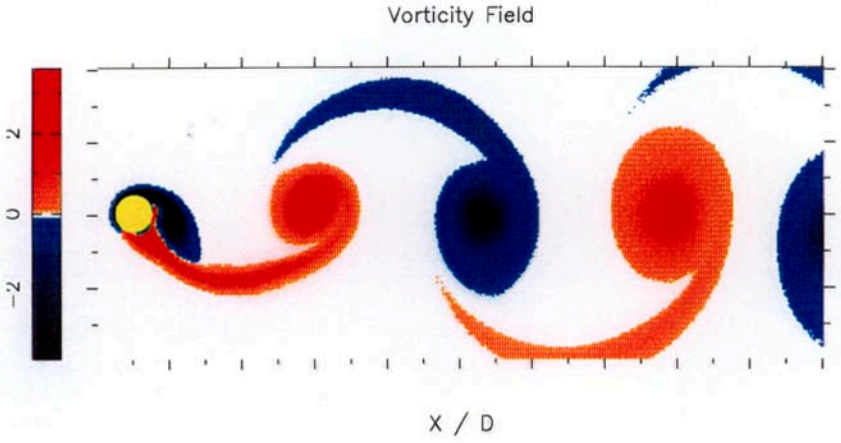

(A) $Re = 150$, $St = 0.09(0.5)$, $\Omega = 2.0$, $t = 33.75$

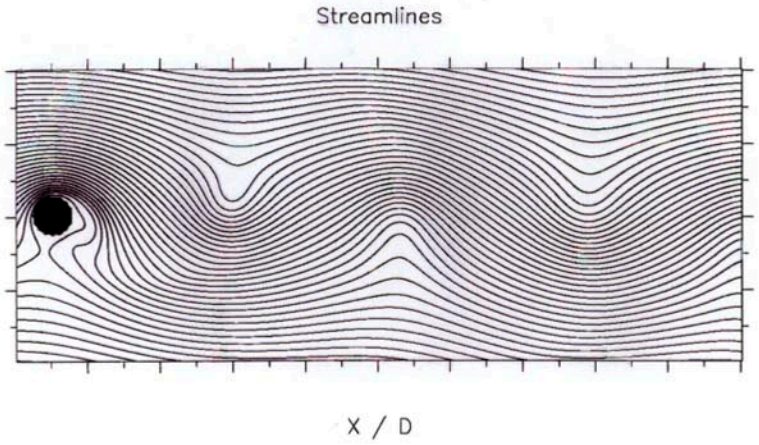

Figure 2.2: Visulalization of streaklines (laboratory experiment), vorticity field and streamlines (numerical simulation) for the forcing conditions A_1.



(B_e) $Re = 96$, $\frac{St}{St_{nat}} = 0.9$, $\Omega = 2.0$ - Laboratory experiment [6]

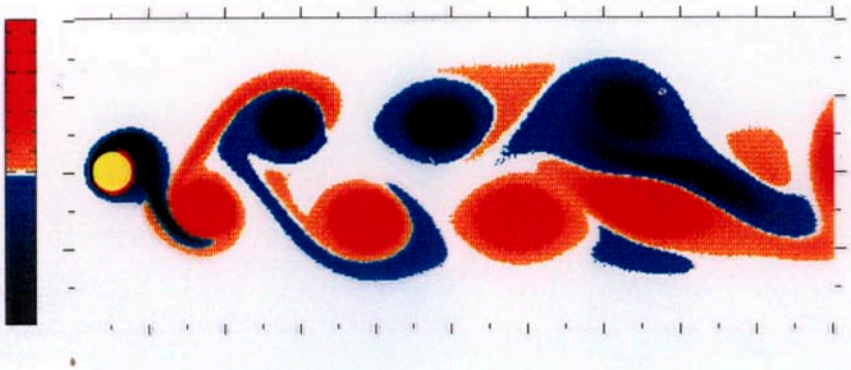

(B) $Re = 150$, $St = 0.16(0.89)$, $\Omega = 2.0$, $t = 46.25$

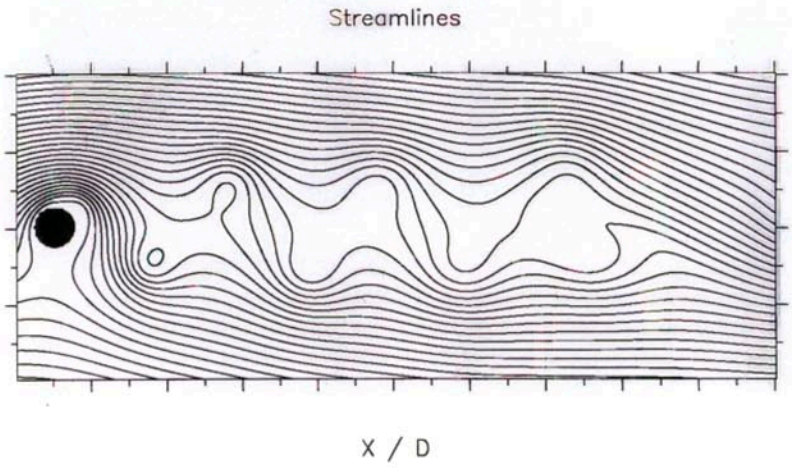

Figure 2.2: Visulalization of streaklines (laboratory experiment), vorticity field and streamlines (numerical simulation) for the forcing conditions B_1.



(C_e) $Re = 96$, $\frac{St}{St_{nat}} = 1.0$, $\Omega = 2.0$ - Laboratory experiment [6]

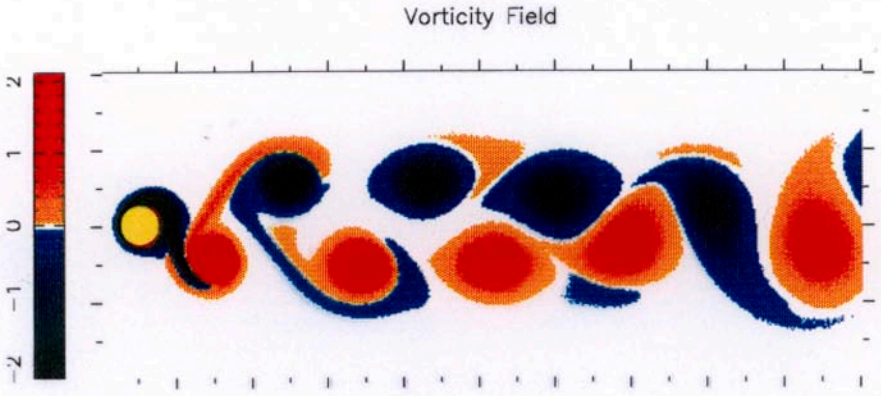

(C) $Re = 150$, $St = 0.18(1.0)$, $\Omega = 2.0$, $t = 35.0$

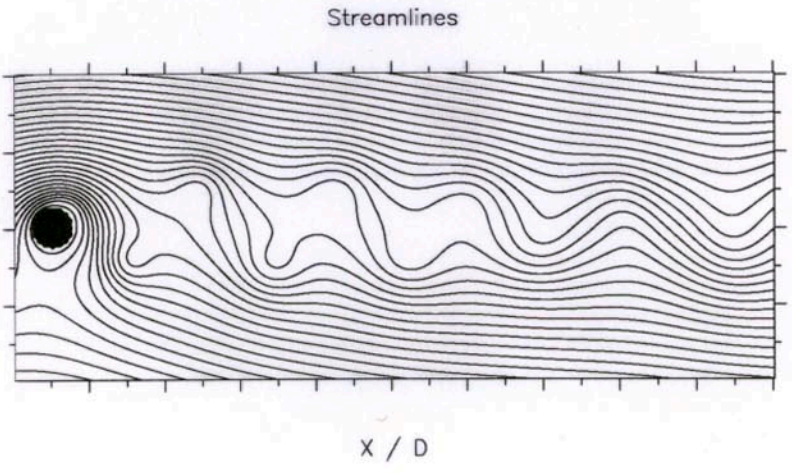

Figure 2.2: Visulalization of streaklines (laboratory experiment), vorticity field and streamlines (numerical simulation) for the forcing conditions C_1.



(G_e) $Re = 96$, $\frac{St}{St_{nat}} = 5.0$, $\Omega = 2.0$ - Laboratory experiment [6]

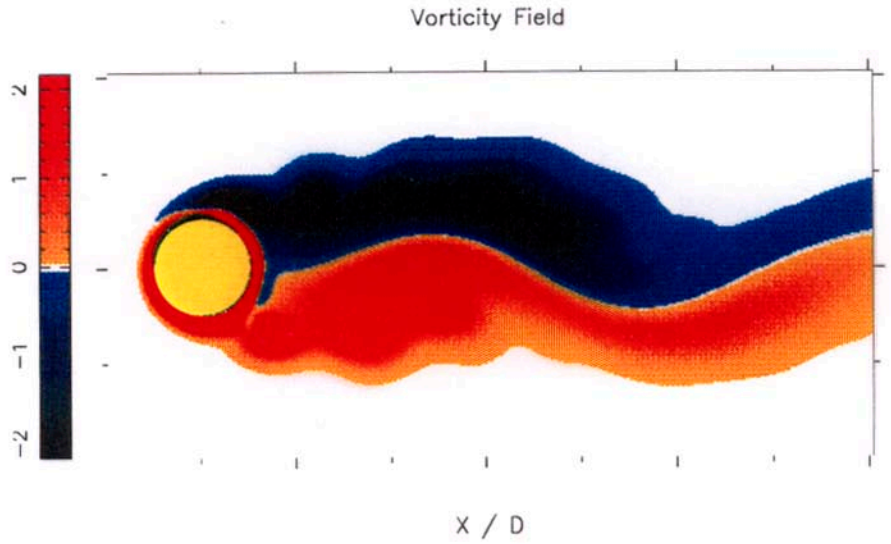

(G) $Re = 150$, $St = 1.00(5.56)$, $\Omega = 2.0$, $t = 10.9375$

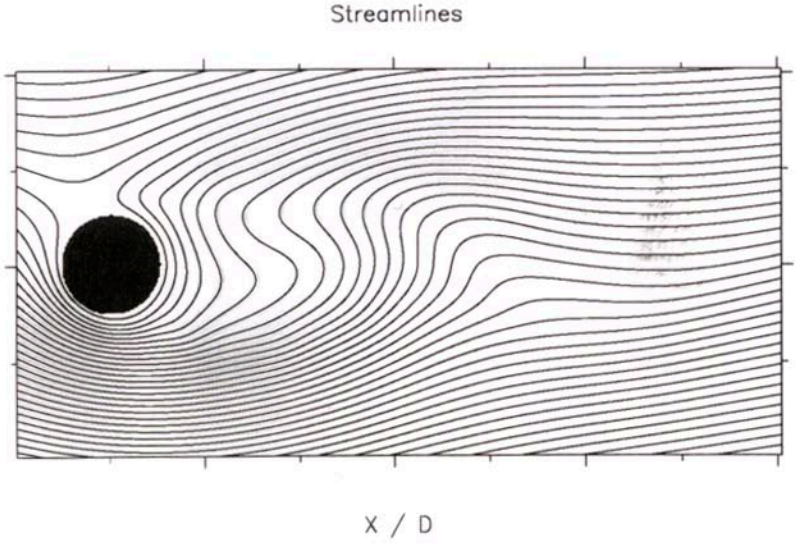

Figure 2.2: Visulalization of streaklines (laboratory experiment), vorticity field and streamlines (numerical simulation) for the forcing conditions G_1.

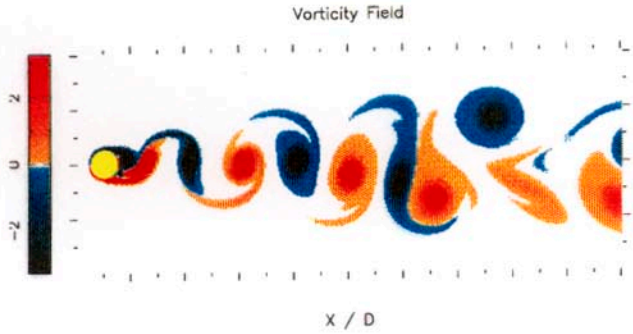

$Re = 500,\ t = 31.25$, no control

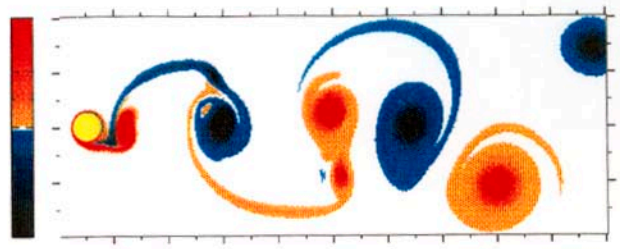

$Re = 500,\ St = 0.11(0.5),\ \Omega = 2.0,\ t = 25.0$

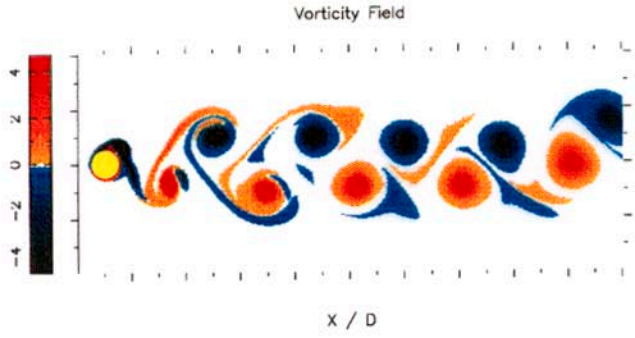

$Re = 500,\ St = 0.20(0.91),\ \Omega = 2.0,\ t = 32.5$

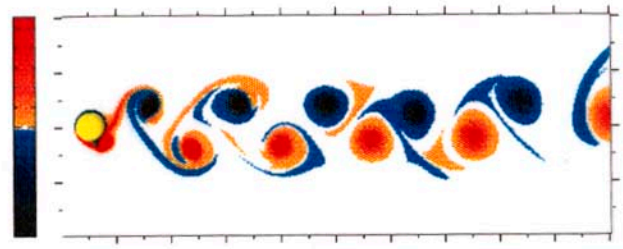

$Re = 500,\ St = 0.22(1.0),\ \Omega = 2.0,\ t = 27.5$

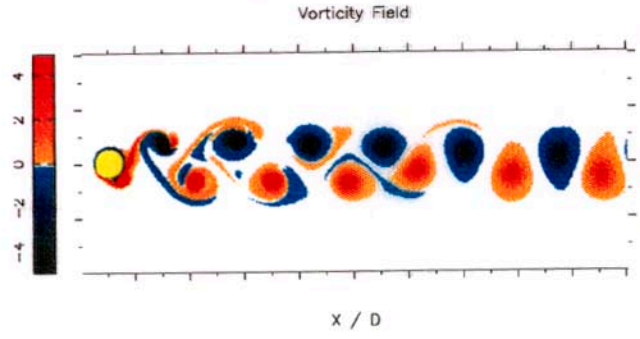

$Re = 500,\ St = 0.25(1.14),\ \Omega = 2.0,$
$t = 36.25$

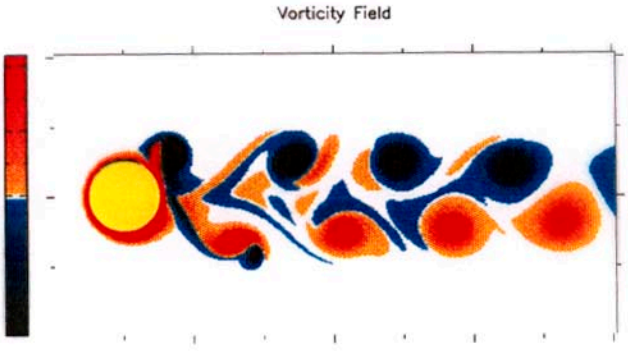

$Re = 500,\ St = 0.44(2.0),\ \Omega = 2.0,$
$t = 15.625$

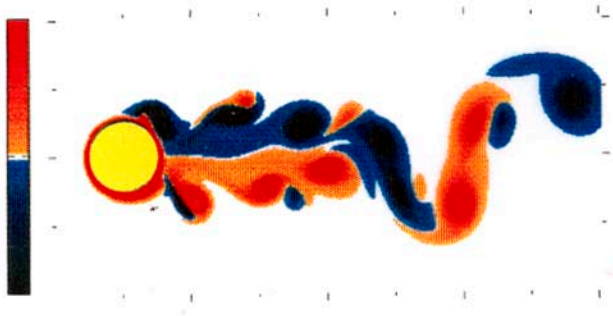

$Re = 500,\ St = 0.70(3.18),\ \Omega = 2.0,$
$t = 8.4375$

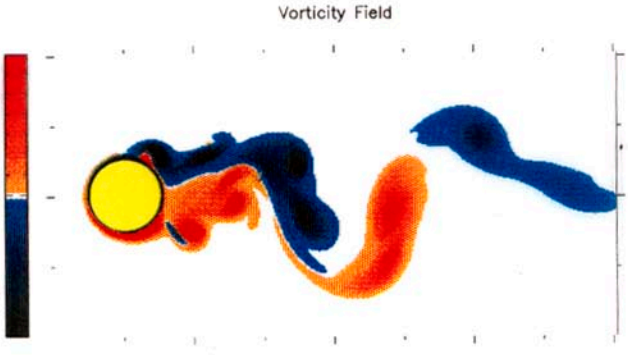

$Re = 500,\ St = 1.00(4,54),\ \Omega = 2.0,$
$t = 8.125$

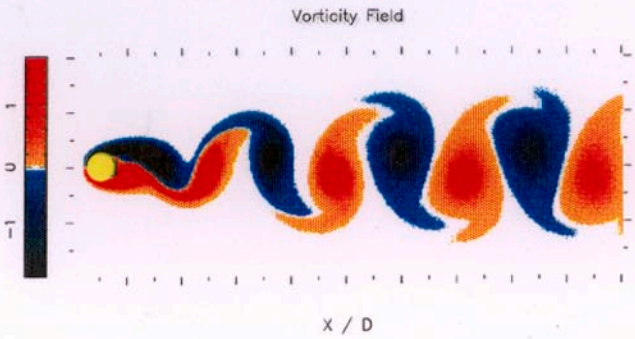

$Re = 150$, $t = 70$, no control

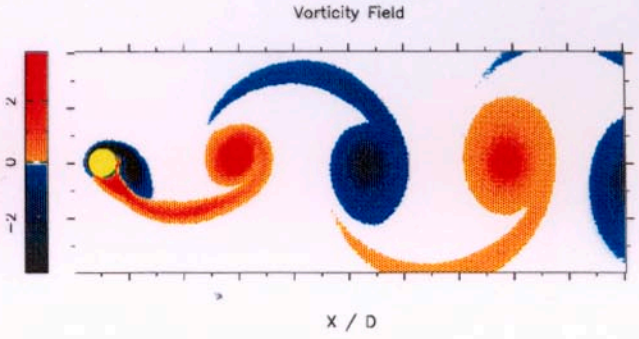

$Re = 150$, $St = 0.09(0.5)$, $\Omega = 2.0$, $t = 33.75$

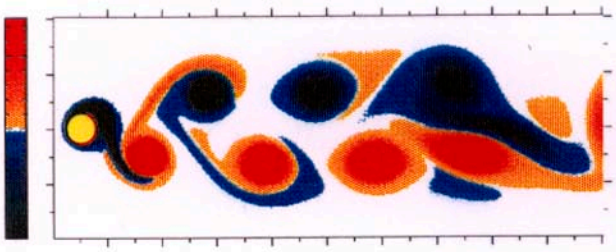

$Re = 150$, $St = 0.16(0.89)$, $\Omega = 2.0$, $t = 46.25$

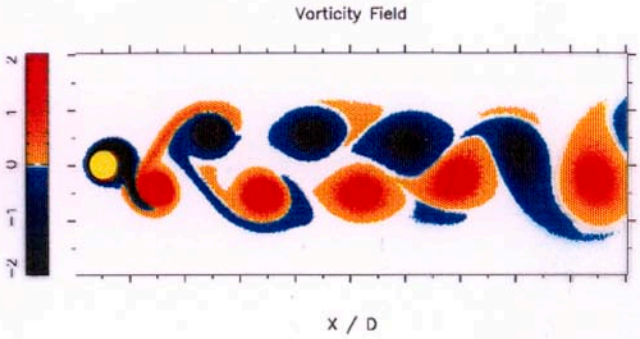

$Re = 150$, $St = 0.18(1.0)$, $\Omega = 2.0$, $t = 35.0$

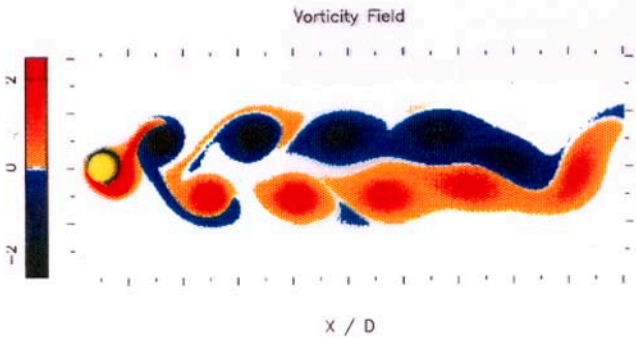

$Re = 150$, $St = 0.20(1.11)$, $\Omega = 2.0$, $t = 45.0$

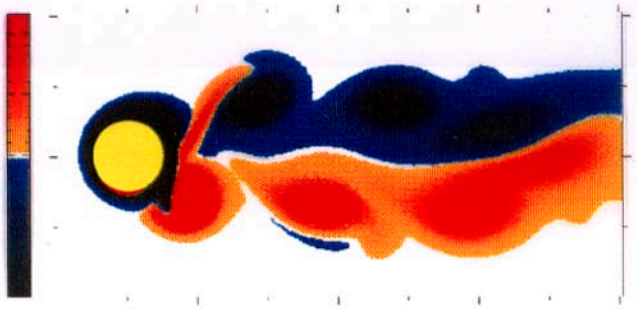

$Re = 150$, $St = 0.36(2.0)$, $\Omega = 2.0$, $t = 17.5$

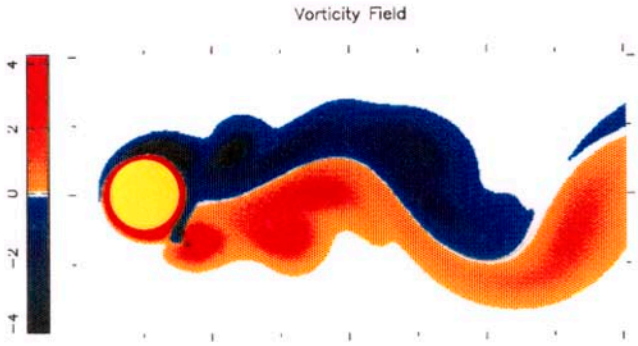

$Re = 150$, $St = 0.70(3.89)$, $\Omega = 2.0$, $t = 10.9375$

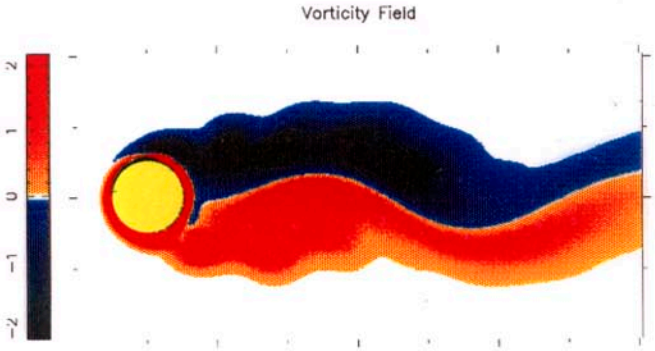

$Re = 150$, $St = 1.00(5.56)$, $\Omega = 2.0$, $t = 10.9375$

CONCLUSIONS

- Comment by Hermann Schlichting 1950
- Comment by Hans Liepmann 1961
- Comments by Hans Liepmann 1997

BOOK TO READ ON TURBULENCE

Hermann SCHLICHTING

1950

Introduction to his book

'Boundary Layer Theory'

'In discussing turbulent flows use has been made essentially only of the semi empirical theories which derive from Prandtl's mixing length. It is true that according to present views these theories possess a number of shortcomings but nothing superior has so far been devised to take their place, nothing, that is, which is useful for the engineer. Moreover, the older theories give answers to very many problems which are entirely satisfactory. No account of the statistical theories of turbulence has been included because they have not yet attained any practical significance for engineers. [...] essential progress is not made through an accumulation of extensive experimental results but rather through a small number of fundamental experiments backed by theoretical considerations.'

HANS LIEPMANN'S THOUGHTS

1st International Conference on Turbulence
Marseille, 1961
(cf. Mécanique de la turbulence ed. Favre, Dunod, 1962)

'It is clear that the essence of turbulent motion is vortex interaction. In the particular case of homogeneous isotropic turbulence this fact is largely masked, since the vorticity fluctuations appear as simple derivations of the velocity fluctuations. In general this is not the case, and a Fourier representation is probably not the ultimate answer. The proposed detailed models of an eddy structure represent, I believe, a groping for an eventual representation of a stochastic rotational field, but none of the models proposed so far has proven useful except in the description of a single process.'

HANS LIEPMANN'S THOUGHTS

Santa Barbara Workshop on
'Dynamical Systems and Statistical Mechanics Methods for Coherent Structures in Turbulent Flows'
12 & 13 February 1993

'Kolmogorov's theory has been counter-productive. It is OK for light or sound scattering by turbulent flows, but it is unuseful for the main lines of turbulence'

⇒ need for a new statistical theory

'Turbulent flows are not stationary but fluctuations which are limited remain limited'

⇒ study non stationary processes

HANS LIEPMANN'S THOUGHTS

'In turbulence you have long range forces, and it is difficult to extrapolate from Boltzmann's gas, which has short range forces. Therefore I am uneasy about Reynolds equations

⇒ study long range dependence

'Ask mathematicians. Like for transonic flows, can we prove that smooth solutions do not exist? Because if they do not exist, we do not have to look for them!'

⇒ study the possibility of finite time singularities

HANS LIEPMANN'S THOUGHTS

Santa Barbara, 12th February 97

'As long as we will not be ask to predict the drag on a sphere or the pressure drop in a pipe from continuous, incompressible and Newtonian assumptions without any other complications (first principle), we will not have made it!'

⇒ study the production of vorticity at the boundaries and in shear layers



production of vortices

Interaction of vortices

well-mixed region

REFERENCES A CONSULTER

- H. Tennekes and J.L. Lumley
  A first course in turbulence
  The MIT Press, 1972

- M. Lesieur
  Turbulence in Fluids
  Kluwer, 1990

- U. Frisch
  Turbulence
  Cambridge University Press, 1995

- A.S. Monin and A.M. Yaglom
  Statistical Fluid Mechanics
  The MIT Press, 1965

- B. Mohammadi and O. Pironneau
  Analysis of the k-ε turbulence model
  Wiley and Masson, 1993

- B. Burbe Hubbard
  Ondes et ondelettes
  Pour la science, Belin, 1995